

Normal Brain

Exhibition Hall

Monday, May 9, 2016: 10:45 - 12:45

1158

Impact of acquisition parameters on cortical thickness and volume derived from Multi-Echo MPRAGE scans
Ross W. Mair^{1,2}, Martin Reuter^{2,3}, and Andre J. van der Kouwe²

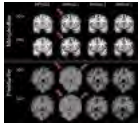


¹Center for Brain Science, Harvard University, Cambridge, MA, United States, ²A.A. Martinos Center for Biomedical Imaging, Massachusetts General Hospital, Charlestown, MA, United States, ³Department of Mechanical Engineering, Massachusetts Institute of Technology, Cambridge, MA, United States

The multi-echo MPRAGE (MEMPRAGE) sequence was implemented to reduce signal distortion by acquiring at a higher bandwidth and averaging multiple echoes to recover SNR while providing additional T_2^* information that can enhance cortical segmentation. A rapid 2-minute MEMPRAGE protocol has been implemented for large multi-center studies. Here, we investigate the impact on morphometric results for the cortex by systematically varying all the parameters modified between the rapid 2-minute scan and a conventional 6-minute structural scan. Small but significant differences in cortical thickness and gray matter volume result from a combination of the use of partial fourier acquisition and lowering the spatial resolution to 1.2mm.

1159

Quantitative comparison of MP2RAGE skull-stripping strategies



Pavel Falkovskiy^{1,2,3}, Bénédicte Maréchal^{1,2,3}, Shuang Yan⁴, Zhengyu Jin⁴, Tianyi Qian⁵, Kieran O'Brien^{6,7}, Reto Meuli², Jean-Philippe Thiran^{2,3}, Gunnar Krueger^{2,3,8}, Tobias Kober^{1,2,3}, and Alexis Roche^{1,2,3}

¹Advanced Clinical Imaging Technology (HC CMEA SUI DI BM PI), Siemens Healthcare AG, Lausanne, Switzerland, ²Department of Radiology, University Hospital (CHUV), Lausanne, Switzerland, ³LTSS, École Polytechnique Fédérale de Lausanne, Lausanne, Switzerland, ⁴Department of Radiology, Peking Union Medical College Hospital, Peking Union Medical College, Chinese Academy of Medical Sciences, Beijing, China, People's Republic of, ⁵MR Collaborations NE Asia, Siemens Healthcare, Beijing, China, People's Republic of, ⁶Centre for Advanced Imaging, University of Queensland, Brisbane, Australia, ⁷Siemens Healthcare Pty Ltd, Brisbane, Australia, ⁸Siemens Medical Solutions USA, Boston, MA, United States

The MP2RAGE pulse sequence exhibits higher grey-matter/white-matter contrast compared to standard MPRAGE acquisitions and provides images with greatly reduced B1 bias. In theory, these qualities of MP2RAGE should lead to more accurate morphometric results. However, a major hindrance to MP2RAGE morphometric processing is the salt-and-pepper noise in the background and cavities. This poses a major problem for the skull-stripping stage of most automated morphometry algorithms. We investigated three skull-stripping strategies using the MorphoBox prototype and FreeSurfer automated-morphometry software packages and compared them to results obtained using the gold-standard MPRAGE contrast.

1160

Synthetic Quantitative MRI through Relaxometry Modelling for Improved Brain Segmentation



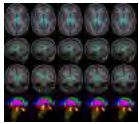
Martina F Callaghan¹, Siawoosh Mohammadi^{1,2}, and Nikolaus Weiskopf^{1,3}

¹Wellcome Trust Centre for Neuroimaging, UCL Institute of Neurology, London, United Kingdom, ²Department of Systems Neuroscience, University Medical Center Hamburg-Eppendorf, Hamburg, Germany, ³Department of Neurophysics, Max Planck Institute for Human Cognitive and Brain Sciences, Leipzig, Germany

Here we exploit the inter-dependence of quantitative MRI (qMRI) parameters via relaxometry modelling to generate synthetic quantitative maps of magnetisation transfer saturation. The utility of the new concept of synthetic quantitative data is demonstrated by improving image segmentation of deep gray matter structures for neuroimaging applications.

1161

Evaluation of Pairwise and Groupwise Templates-based Approaches for Automated Segmentation of Structures in Brain MR Images



Subrahmanyam Gorthi¹ and Srikrishnan Viswanathan¹

¹Samsung R&D Institute, Bangalore, India

This work presents a detailed investigation of two multiple-templates based fusion approaches for automated segmentation of structures in the brain MR images: (i) fusion based on direct pairwise registrations between each template and the target image, and (ii) fusion based on an intermediate groupwise template, requiring only a single onsite registration. The key finding from these evaluations is that, if computational time for automated segmentations is a major concern, then groupwise-template based registration followed by fusion is an optimal choice; if time is not a major constraint, then multiple pairwise registrations followed by fusion provides more accurate segmentations.

1162

DR-TAMAS: Diffeomorphic Registration for Tensor Accurate alignMent of Anatomical Structures



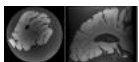
Mustafa Okan Irfanoglu^{1,2}, Amritra Nayak^{1,2}, Jeffrey Jenkins^{1,2}, Elizabeth B Hutchinson^{1,2}, Neda Sadeghi¹, Cibu P Thomas^{1,3}, and Carlo Pierpaoli¹

¹NICHD, NIH, Bethesda, MD, United States, ²Henry Jackson Foundation, Bethesda, MD, United States, ³CNRM, Bethesda, MD, United States

Spatial alignment of diffusion tensor MRI data is of fundamental importance for voxelwise statistical analysis and creation of population specific atlases of diffusion MRI metrics. In this work, we propose DR-TAMAS, a novel diffusion tensor imaging registration method which uses a spatially varying metric to achieve accurate alignment not only in white matter but also in gray matter and CSF filled

regions. Our tests indicate that DR-TAMAS shows excellent overall performance in the entire brain, while being equivalent to the best existing methods in white matter.

1163

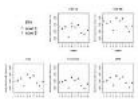


High resolution anatomical imaging of the human occipital lobe with a large ex-vivo 9.4T RF coil
Shubharthi Sengupta¹, Ron Hellenbrand², René Finger², Chris Wiggins³, and Alard Roebroeck¹

¹Dept. of Cognitive Neuroscience, Faculty of Psychology and Neuroscience, Maastricht University, Maastricht, Netherlands, ²Lab Engineering & Instrumentation Department, Maastricht University, Maastricht, Netherlands, ³Scannexus, Maastricht, Netherlands

Small-bore animal scanners or spectroscopy systems have often been used for the investigation of small post-mortem human brain samples. These studies use the high field strengths and strong gradients, but are inherently limited to very small sample sizes. In this abstract, we discuss the acquisition of very high resolution anatomical images (100µm isotropic) of a full occipital sample as large as 80x80x80 mm³, using a customised RF receive coil-array in a large-bore 9.4 T human scanner.

1164

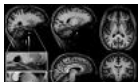


Cross-validation of a CSF MRI sequence for calculating brain volume by comparison with brain segmentation methods
Lisa A. van der Kleij¹, Jeroen de Bresser¹, Esben T. Petersen², Jeroen Hendrikse¹, and Jill B. De Vis¹

¹Department of Radiology, UMC Utrecht, Utrecht, Netherlands, ²Danish Research Centre for Magnetic Resonance, Centre for Functional and Diagnostic Imaging and Research, Copenhagen University Hospital Hvidovre, Hvidovre, Denmark

We recently introduced a CSF MRI sequence to automatically measure intracranial volume (ICV) and brain parenchymal volume (BPV). This sequence with short imaging time (0:57 min) and fast post processing correlates well with qualitative brain atrophy scores. This study demonstrates that the low resolution and high resolution CSF MRI sequences perform well in the assessment of BPV and ICV, with a precision similar to the conventional brain segmentation methods FSL, Freesurfer and SPM. The CSF MRI sequence showed a good to very good correlation with the conventional segmentation methods for ICV and BPV.

1165



A 7T Human Brain Microstructure Atlas by Minimum Deformation Averaging at 300µm
Andrew L Janke¹, Kieran O'Brian², Steffen Bollmann¹, Tobias Kober³, and Markus Barth¹

¹Centre for Advanced Imaging, University of Queensland, Brisbane, Australia, ²Siemens Healthcare Pty Ltd, Brisbane, Australia, ³Advanced Clinical Imaging Technology, Siemens Healthcare AG, Lausanne, Switzerland

7T provides a method to see detailed image contrast in the human brain; the MP2RAGE sequence allows 500µm acquisition resolution.

1166



Evaluating the variability of multicenter and longitudinal hippocampal volume measurements.

Stephanie Bogaert¹, Michiel de Ruiter², Sabine Deprez^{3,4}, Ronald Peeters³, Pim Pullens^{5,6}, Frank De Belder⁶, José Belderbos⁷, Sanne Schagen², Dirk De Rysscher^{8,9}, Stefan Sunaert^{3,4}, and Eric Achten¹

¹Radiology, Ghent University Hospital, Ghent, Belgium, ²Psychosocial Research and Epidemiology, Netherlands Cancer Institute, Amsterdam, Netherlands, ³Radiology, Leuven University Hospital, Belgium, ⁴Imaging and Pathology, KU Leuven, Belgium, ⁵Radiology, University of Antwerp, Belgium, ⁶Radiology, Antwerp University Hospital, Belgium, ⁷Radiation Oncology, Netherlands Cancer Institute, Amsterdam, Netherlands, ⁸Radiation Oncology, MAASTRO clinic Maastricht, Netherlands, ⁹Respiratory Oncology, Maastricht University Medical Center, Netherlands

Longitudinal multicenter MRI studies require stable and comparable measurements. We scanned two subjects in six different scanners (two vendors) at different time points and assessed hippocampal volumes manually and automatically.

Intrascanner CV was <2.62% for both techniques; Freesurfer is a good alternative for manual delineation for longitudinal studies.

Intervendor variability was sometimes lower than intrascanner variability for the manual technique, which suggests only a modest effect of hardware differences across vendors. Freesurfer results were systematically higher for vendor B compared to A; it is not recommended to compare cross-sectional Freesurfer results between vendors in this multicenter study.

1167



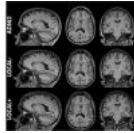
Evaluation of 3D T1-weighted imaging at 3 T across scanner vendors and models

Sjoerd B Vos^{1,2}, M Jorge Cardoso¹, Marzena Wylezinska-Arridge³, David L Thomas^{1,3}, Enrico De Vita^{3,4}, Marios C Yiannakas⁵, David Carmichael⁶, John S Thornton^{3,4}, Olga Ciccarelli⁵, John S Duncan^{2,7}, and Sébastien Ourselin¹

¹Translational Imaging Group, University College London, London, United Kingdom, ²MRI Unit, Epilepsy Society, Chalfont St Peter, United Kingdom, ³Neuroradiological Academic Unit, Department of Brain Repair and Rehabilitation, UCL Institute of Neurology, London, United Kingdom, ⁴Lysholm Department of Neuroradiology, National Hospital for Neurology and Neurosurgery, London, United Kingdom, ⁵Department of Neuroinflammation, UCL Institute of Neurology, London, United Kingdom, ⁶Institute of Child Health, University College London, London, United Kingdom, ⁷Department of Clinical and Experimental Epilepsy, UCL Institute of Neurology, London, United Kingdom

Volumetric analyses of 3D T1-weighted images has become an integral part of the clinical work-up and research studies. Variation between scanners, in both vendors and models, is a major confound in combining imaging-derived biomarkers across sites. In this work, we analyse test-retest data from different days on six 3 T scanners from three vendors to quantify this inter-scanner variability compared to intra-scanner variability. Contrast-to-noise ratios as well as volumetric analyses are performed showing between-scanner variation in total brain volumes – indicating different scanner calibrations – but also tissue-specific differences – possibly arising from different effective contrasts.

1168



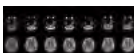
Basic MR sequence parameters systematically bias automated brain volume estimation

Sven Haller^{1,2,3,4}, Pavel Falkovskiy^{5,6,7}, Reto Meuli⁶, Jean-Philippe Thiran⁷, Gunnar Krueger⁸, Karl-Olof Lovblad^{1,9}, Alexis Roche^{5,6,7}, Tobias Kober^{5,6,7}, and Bénédicte Maréchal^{5,6,7}

¹Faculty of Medicine of the University of Geneva, Geneva, Switzerland, ²Affidea Centre de Diagnostique Radiologique de Carouge CDRC, Geneva, Switzerland, ³Department of Surgical Sciences, Radiology, Uppsala University, Uppsala, Sweden, ⁴Department of Neuroradiology, University Hospital Freiburg, Freiburg, Germany, ⁵Advanced Clinical Imaging Technology (HC CMEA SUI DI BM PI), Siemens Healthcare AG, Lausanne, Switzerland, ⁶Department of Radiology, University Hospital (CHUV), Lausanne, Switzerland, ⁷LTS5, École Polytechnique Fédérale de Lausanne, Lausanne, Switzerland, ⁸Siemens Medical Solutions USA, Inc., Boston, MA, United States, ⁹University Hospitals of Geneva, Geneva, Switzerland

Standard MR parameters, notably spatial resolution, contrast and image filtering, systematically bias results of automated brain MRI morphometry by up to 4.8%. This is in the same range as early disease-related brain volume alterations, for example in Alzheimer's disease. Automated brain segmentation software packages should therefore require strict MR parameter selection or include compensatory algorithms to avoid MR-parameter-related bias of brain morphometry results.

1169



Distortion correction in diffusion weighted imaging of the brain: a quantitative comparison of four correction approaches

Ileana Hancu¹, Ek Tsoon Tan¹, Luca Marinelli¹, Nathan White², Dominic Holland², Tim Sprenger³, and Jonathan Sperl³

¹GE Global Research Center, Niskayuna, NY, United States, ²University of California San Diego, San Diego, CA, United States, ³GE Global Research Center, Munich, Germany

The performance of four distortion correction algorithms was investigated in a cohort of normal volunteers. While all approaches reduced distortion, it was found that the reversed polarity gradient methods were inherently better than registration or B0-mapping approaches. It was likely that the limited degrees of freedom of the registration approach could not account for localized magnetic field inhomogeneity. The extrapolation of B0 maps in the distorted EPI space introduced errors that decreased the overall performance of the B0-mapping method.

1170



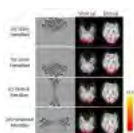
3D FLASH Optimization with Improved Contrast Efficiency and Image Inhomogeneity Correction

Jinghua Wang¹, Lili He², and Zhong-Lin Lu¹

¹The Ohio State University, Columbus, OH, United States, ²Center for Perinatal Research, Nationwide Children's Hospital, Columbus, OH, United States

The 3D FLASH sequence is frequently used in structural imaging of the brain. Tissue contrast inhomogeneity, resulting from inhomogeneous transmit field and receiver sensitivity, significantly affects quantitative structural brain analyses such as classification and quantification of brain tissues in voxel-based morphometry and detection of pathological brain changes in clinical studies. It is important to optimize the sequence to jointly improve contrast efficiency and image homogeneity. In this work, we propose optimal imaging parameters and present methods to improve contrast efficiency and reduce or eliminate image inhomogeneity.

1171



The Neural Basis of Visual Field Asymmetry in Human Visual System by Functional MRI

Caitlin O'Connell¹, Leon Ho^{2,3}, Matthew Murphy², Yolandi van der Merwe^{1,2}, Ian Conner^{1,2}, Gadi Wollstein^{1,2}, Joel Schuman^{1,2}, Rakie Cham¹, and Kevin Chan^{1,2}

¹Department of Bioengineering, University of Pittsburgh, Pittsburgh, PA, United States, ²UPMC Eye Center, Eye and Ear Institute, Ophthalmology and Visual Science Research Center, Department of Ophthalmology, University of Pittsburgh, Pittsburgh, PA, United States, ³Department of Electrical and Electronic Engineering, The University of Hong Kong, Pokfulam, Hong Kong

Human visual performance has been observed to exhibit superiority in the lower visual field and horizontal meridian compared to the upper visual field and vertical meridian, respectively, in response to many classes of stimuli, but the underlying neural mechanisms remain unclear. This study determines if processing of visual information is dependent on the location of stimuli in the visual field using functional MRI. The results show stronger brain responses and larger activation volumes upon flickering visual stimulation to the lower hemifield compared to upper hemifield, while only the activation size differed between visual presentations to the horizontal and vertical meridians.

1172



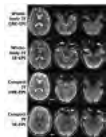
Synthetic MRI: an old concept becomes practical

Christina Andica¹, Akiyumi Hagiwara^{1,2}, Misaki Nakazawa^{1,3}, Masaaki Hori¹, Saori Shiota¹, Mariko Yoshida¹, Kanako Sato¹, Yuko Takahashi¹, Kanako Kumamaru¹, Michimasa Suzuki¹, Atsushi Nakanishi¹, Kouhei Tsuruta^{1,3}, Ryo Ueda^{1,3}, and Shigeki Aoki¹

¹Department of Radiology, Juntendo University School of Medicine, Tokyo, Japan, ²Department of Radiology, Graduate School of Medicine, The University of Tokyo, Tokyo, Japan, ³Department of Radiological Sciences, Graduate School of Human Health Sciences, Tokyo Metropolitan

Synthetic magnetic resonance imaging (MRI) is a technique which can be used to synthesize contrast-weighted images based on quantification of the longitudinal T1 relaxation, the transverse T2 relaxation, the proton density (PD), and the amplitude of the local radio frequency B1 field. Synthetic MRI images were useful in the evaluation of brain disorders. With Synthetic MRI, echo time (TE), repetition time (TR), and inversion time (TI) of the contrast-weighted image can be freely adjusted retrospectively to optimize image quality. Limitation of synthetic MRI is the partial volume effect.

1173



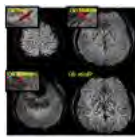
Towards Higher Spatial Resolution Echo-Planar-Imaging With A Compact Head 3T System

Ek T Tan¹, Seung-Kyun Lee¹, Paul Weavers², Matthew Middione³, Matt A Bernstein², John Huston², and Thomas KF Foo¹

¹GE Global Research, Niskayuna, NY, United States, ²Mayo Clinic, Rochester, MN, United States, ³GE Healthcare, Menlo Park, CA, United States

It is challenging to increase spatial resolution (≤ 1.5 mm) in whole-brain, single-shot echo-planar-imaging (ss-EPI) on conventional whole-body systems due to EPI distortion and limited SNR. A compact head 3T system with an asymmetric head gradient coil capable of high gradient amplitude and 3.5 times the slew rate of whole-body systems can enable ss-EPI acquisition with high spatial resolution and reduced spatial distortion, simultaneously. This work compares spin-echo and gradient-recalled-echo ss-EPI between the compact and whole-body systems, showing substantially reduced distortion and signal dropout, and shorter echo-times. Results with the high performance gradient were also demonstrated in multi-band-accelerated, high b-value diffusion-imaging.

1174



Susceptibility Weighted Imaging in Different Regions of Human Brain at 7T

Yeong-Jae Jeon^{1,2}, Sang-Woo Kim^{1,2}, Joo-Yeon Kim¹, Young-Seok Park³, and Hyeon-Man Baek^{1,2}

¹Bio-Imaging Research Team, Korea Basic Science Institute, Ochang, Korea, Republic of, ²Bio-Analytical Science, University of Science & Technology, Daejeon, Korea, Republic of, ³College of Medicine, Chungbuk National University, Cheongju-si, Korea, Republic of

The purpose of this study was to investigate contrast enhancement difference of SWI from human brain regions at 7T, and to compare contrast enhancement between cortical, anterior septal, and hippocampal veins. Five healthy volunteers (mean \pm SD, 24.4 ± 1.67 years) participating in this study were scanned on 7T. The observation in this work was the significant difference of contrast enhancement of cortical and other veins, and no significant contrast enhancement difference between anterior septal and hippocampal veins. In conclusion, contrast enhancement of human brain at 7T depends on the regions giving higher cortical vein contrast with respect to anterior septal and hippocampal veins.

1175



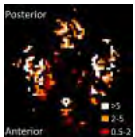
The cerebrovascular response to a single session of exercise

Jessica Steventon¹, Catherine Foster¹, Daniel Helme², Monica Busse³, and Kevin Murphy¹

¹CUBRIC, Cardiff University, Cardiff, United Kingdom, ²School of Medicine, Cardiff University, Cardiff, United Kingdom, ³School of Healthcare Sciences, Cardiff University, Cardiff, United Kingdom

Here we examine the acute effects of a single exercise session on cerebrovasculature using a multi-TI arterial spin labelling (ASL) sequence to measure cerebral blood flow (CBF), and a dual-echo ASL sequence with hypercapnia to measure cerebrovascular reactivity (CVR). We show that contrary to previous smaller studies, 20-minutes of aerobic exercise does not affect CBF or CVR in the 60-minute period after exercise. Despite this, changes in CBF after exercise were related to individually-determined systemic physiological changes associated with exercise intensity, informing on moderators of cerebral autoregulation.

1176



Vessel-size dependent response of human cerebral arteries to hyperoxia

Esther AH Warnert¹, Ian D Driver¹, Joseph Whittaker¹, and Kevin Murphy¹

¹Cardiff University Brain Research Imaging Centre, Cardiff University, Cardiff, United Kingdom

Due to the potential of using hyperoxia as a treatment for cerebral ischemic diseases, including stroke, it is important to fully understand the effects of hyperoxia on the cerebrovasculature. Although it is known that breathing of 100% O₂ leads to a decrease in cerebral blood flow, it is unclear where along the cerebral arterial tree vasoconstriction occurs. Here we show that, while there is expected constriction of the large arteries, smaller and more distal arteries actually show vasodilation upon hyperoxia.

Traditional Poster

Neuro: Clinical Studies

Exhibition Hall

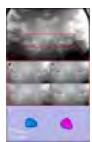
Monday, May 9, 2016: 10:45 - 12:45

1177

An Investigation of Lateral Geniculate Nucleus(LGN) Volume in Patients with Glaucoma using 7T MRI

Hyun Jin Jeong¹, Jong Yeon Lee², Jong Hwan Lee², Yu Jeong Kim², Eung Yeop Kim³, Young Yeon Kim⁴, Zang-Hee Cho¹, and Young-Bo Kim¹

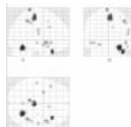
¹Neuroscience Research Institute, Incheon, Korea, Republic of, ²Gil Hospital, Department of Ophthalmology, Incheon, Korea, Republic of, ³Gil Hospital, Department of Radiology, Incheon, Korea, Republic of, ⁴Korea University College of Medicine, Department of Ophthalmology, Seoul,



Korea, Republic of

To investigate lateral geniculate nucleus (LGN) volume of glaucoma patients compared with age-matched normal controls using ultra-high field 7.0-T magnetic resonance imaging (MRI). On high-resolution 7.0-T MRI, LGN volumes in POAG patients are significantly smaller than those of healthy subjects. Furthermore, in patients, LGN volume was found to be significantly correlated with ganglion cell layer and inner plexus layer (GC-IPL) thickness of the contralateral eye.

1178



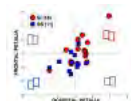
Regional Brain Iron Mapping in Patients with Obstructive Sleep Apnea Syndrome

Sudhakar Tummala¹, Daniel W Kang², Bumhee Park¹, Ruchi Vig¹, Mary A Woo³, Ronald M Harper^{4,5}, and Rajesh Kumar^{1,5,6,7}

¹Anesthesiology, University of California at Los Angeles, Los Angeles, CA, United States, ²Medicine, University of California at Los Angeles, Los Angeles, CA, United States, ³UCLA School of Nursing, Los Angeles, CA, United States, ⁴Neurobiology, University of California at Los Angeles, Los Angeles, CA, United States, ⁵Brain Research Institute, University of California at Los Angeles, Los Angeles, CA, United States, ⁶Radiological Sciences, University of California at Los Angeles, Los Angeles, CA, United States, ⁷Bioengineering, University of California at Los Angeles, Los Angeles, CA, United States

OSA subjects show brain injury in multiple areas, which may contribute to accumulation of iron in those sites. Deposition of iron in OSA subjects is unclear. We examined regional iron deposition using T2*-relaxometry procedures; R2* values were significantly increased in insular, parietal, cingulate and cingulum bundle, temporal, and cerebellar areas. The increased iron depositions in OSA subjects may result from neural and white matter injury, including myelin and glial dysfunction, with iron potentially accelerating tissue degeneration. These data suggest that interfering with the iron action may reduce the exacerbation of injury in OSA.

1179



Measurement of Brain Asymmetry on 3D Magnetic Resonance (MR) Images Obtained for 16 Subjects with Situs Inversus

X. Li¹, Neil Roberts¹, M. Perrins¹, and G. Vingerhoets²

¹University of Edinburgh, Edinburgh, United Kingdom, ²Department of Experimental Psychology, Ghent University, Ghent, Belgium

The human brain is structurally asymmetric and typically described as if it has been subject to a rotational moment about the vertical axis of the body, the so-called "Yakovlevian Torque". In subjects with situs inversus totalis (SI) the internal organs of the body are transposed and it has been obvious to question whether in these subjects brain torque is also reversed? We recruited 16 subjects with SI and 16 age, sex and education matched controls (SS) and applied state of the art image analysis techniques to investigate the extent to which brain asymmetry is reversed on 3D MR images in these subjects. Analysis of the frontal and occipital petalia has confirmed previous reports of significant reversal of the latter but not the former on average in SI, and has also shown that reversed asymmetry is not present in all individuals with SI.

1180



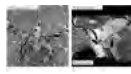
QUANTITATIVE MEASURES OF BRAIN CHANGES IN CHILDREN WHO DO JUDO ON MRI

Tina Seah¹, Tang Phua Hwee¹, Toh Zhe Han¹, Gu Qing Long², and Wong Weng Hang²

¹Diagnostic Imaging, KK women's and children's hospital, singapore, Singapore, ²singapore, Singapore

Quantitative study of the brain changes between young judo athletes and normal children who do not do judo, using diffusion tensor imaging (DTI) and magnetic resonance spectroscopy (MRS). Study shows significant increased fractional anisotropy (FA) of the major white matter tracks (corpus callosum, corticospinal tracks, superior longitudinal fasciculus) with slight increase in N-Acetylaspartate to Creatine (NAA/Cr) ratio in the parietal white matter bilaterally. The increased FA and NAA/Cr ratios support structural changes involving grey matter volumes in the cortical cerebral grey matter described in published literatures on athletes.

1181



Visualization of the pituitary gland region's perforating branch artery before transsphenoidal surgery using a high-spatial-resolution three-dimensional fast spin echo sequence

Keiya Hirata¹, Osamu Tachibana², Chihiro Watari¹, Tatsunori Kuroda¹, Nanako Miyamoto¹, Saeko Tomida¹, Masaru Takahashi¹, Tomokazu Oku¹, Shigeo Miyazaki¹, Masahiro Kawashima¹, Naoko Tsuchiya³, Ichiro Toyota³, Mariko Doai³, and Hisao Tonami³

¹Division of radiology, Kanazawa medical university, Uchinada, Japan, ²Department of neurosurgery, Kanazawa medical university, Uchinada, Japan, ³Department of radiology, Kanazawa medical university, Uchinada, Japan

Transsphenoidal surgery is performed in the surgery of the pituitary region. The perforating branch which performs a nutrient of optic nerve and a mamillary body is present in the cistern around the pituitary gland. We can reduce complications of the surgery if we can identify a perforating branch before surgery. We try to visualize the perforating branch as black blood MRA using the high spatial resolution 3D-FSE sequence. We examined the optimal conditions at phantoms and normal volunteers. The optimal condition was a combination of TR2400msec/2shots, and the imaging time was 20 min and 45 s.

1182



Subtractionless MR Angiography of the Neck Using Dixon-based MRI

Ivan E Dimitrov^{1,2}, Qing Yuan³, Sepand Salehian³, Gaurav Khatri³, Marco Pinho³, and Ivan Pedrosa^{2,3}

¹Philips Medical Systems, Cleveland, OH, United States, ²Advanced Imaging Research Center, UT Southwestern Medical Center, Dallas, TX, United States, ³Radiology, UT Southwestern Medical Center, Dallas, TX, United States

We investigated the ability of dynamic contrast-enhanced (DCE) dual-echo multi-peak Dixon-based imaging to generate MR angiography of the neck, without the need of subtraction thus eliminating the possibility of errors due to motion. In six patients with multiple

sclerosis, DCE MRA based on subtraction of pre-contrast from post-contrast images was compared with MRA generated solely from the post-contrast data where fat suppression was achieved using Dixon-based water imaging. While high levels of vessel-to-background contrast was observed in both methods, the subtractionless DIXON-MRA resulted in higher overall contrast for the aortic arch, the brachiocephalic arteries, and the carotid bifurcation.

1183



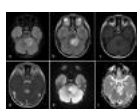
Are Negative BOLD Responses Induced by Acupuncture Associated with Neural Inhibitory Effects? : an MRS & BOLD Functional MRI Study
Jiliang Fang¹, Yanping Zhao¹, Sinyeob Ahn², Guiyong Liu¹, Caixia Fu³, Jin Yang¹, Xiaoling Wang¹, Bo Hou⁴, Feng Feng⁴, and Tianyi Qian⁵

¹*Radiology, Guang An Men Hospital, China Academy of Chinese Medical Sciences, Beijing, China, People's Republic of*, ²*MR Collaboration, Siemens Healthcare, San Francisco, CA, United States*, ³*APPL, Siemens Shenzhen Magnetic Resonance Ltd., Shenzhen, China, People's Republic of*

⁴*Radiology, Peking Union Medical College Hospital, Beijing, China, People's Republic of*, ⁵*MR Collaborations NE Asia, Siemens Healthcare, Beijing, China, People's Republic of*

This study investigates the neurotransmitter basis of the negative response in the medial prefrontal cortex induced by acupuncture stimulus. The MEGA-PRESS 1H-MRS sequence was used to detect the gamma-aminobutyric acid (GABA) and Glutamine (Glu) concentration before and after acupuncture stimulation in normal subjects. The result showed that the GABA concentrations were decreased, while the Glu/Gln concentrations were increased. The task-fMRI data acquired during acupuncture stimulation showed deactivation in the same area. These results suggest that the deactivated BOLD response induced by acupuncture might be associated with the neural inhibition effects.

1184



MR and Proton MR Spectroscopy Findings of a Pediatric Case with Solitary Intracranial Rosai-Dorfman Disease in the Posterior Fossa
Sehnaz Tezcan¹, Muhtesem Agildere¹, Taner Sezer², Ozge Ozturk¹, and Aydin Sav³

¹*Radiology, Baskent University Hospital, Ankara, Turkey*, ²*Pediatrics, Division of Neurology, Baskent University Hospital, Ankara, Turkey*

³*Pathology, Acibadem Maslak Hospital, Istanbul, Turkey*

Rosai-Dorfman disease (RDD) is a histioproliferative disorder, rarely affects central nervous system. A 5-year old boy presented with ptosis, diplopia. MR revealed enhancing mass in the cerebellar peduncle and pons. MR Spectroscopy (MRS) of the lesion showed increased Choline/N-acetyl aspartate ratio and lactate peak. Histopathology was compatible with RDD. Although intracranial RDD generally presents as dural based lesions and supratentorial in location, intraparenchymal lesions may be seen. In this case report a rare form of RDD, posterior fossa parenchyma involvement presented with particular interest to brain MR, MRS and diffusion findings.

1185



Cervical spondyloarthropathy due to the dialysis-related amyloidosis: magnetic resonance imaging findings
Hale Turnaoglu¹, Kemal Murat Haberal¹, Ozlem Isiksacan Ozen², and Ahmet Muhtesem Agildere¹

¹*Radiology, Baskent University, Faculty of Medicine, Ankara, Turkey*, ²*Pathology, Baskent University, Faculty of Medicine, Ankara, Turkey*

Dialysis-related amyloidosis that occurs secondarily to the deposition of amyloid fibrils containing beta-2-microglobulin, is a type of amyloidosis affecting patients undergoing long-term hemodialysis. It involves the osteoarticular system predominantly. Destructive spondyloarthropathy, which frequently involves the cervical spine, have been reported only sporadically. CT is the best modality for detecting osseous erosion or small areas of osteolysis in cortical bone. MRI shows the extent and distribution of osseous, articular, spinal cord and soft-tissue involvement and indicates amyloid deposits in the intervertebral disk, synovium of apophyseal joints, and ligaments. The gold standard of the diagnosis is the histological identification of beta-2-microglobulin.

1186



Increased Glutamate in Frontal Lobe of HIV Infected Patients with CNS involvement: 3T MRS Study

Virendra Kumar¹, Devender Bairwa², Surabhi Vyas³, Achal Srivastava⁴, Bimal K Das⁵, R. M. Pandey⁶, S. K. Sharma², Sanjeev Sinha², and N. R. Jagannathan¹

¹*Department of NMR, All India Institute of Medical Sciences, New Delhi, India*, ²*Department of Medicine, All India Institute of Medical Sciences, New Delhi, India*, ³*Department of Radiology, All India Institute of Medical Sciences, New Delhi, India*, ⁴*Department of Neurology, All India Institute of Medical Sciences, New Delhi, India*, ⁵*Department of Microbiology, All India Institute of Medical Sciences, New Delhi, India*, ⁶*Department of Biostatistics, All India Institute of Medical Sciences, New Delhi, India*

We investigated the effect of HIV infection status on brain metabolites in HIV patients with CNS involvement and asymptomatic HIV patients. 71 subjects were studied including HIV patients with CNS involvement, asymptomatic HIV patients and healthy controls. Single voxel MRS was carried out at 3.0 Tesla MR scanner and metabolite concentrations were determined from three brain regions; left frontal, left basal ganglia and lesion in case of HIV patients with CNS involvement. Glx (Glu+Gln) and creatine were significantly increased in HIV patients in frontal region compared to healthy controls. The concentration of N-acetylaspartate in basal ganglia showed a significant decrease in HIV patients.

1187



Regional Brain Myelin Mapping in Patients with Obstructive Sleep Apnea

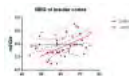
Sudhakar Tummala¹, Bumhee Park¹, Ruchi Vig¹, Mary A Woo², Daniel W Kang³, Ronald M Harper^{4,5}, and Rajesh Kumar^{1,5,6,7}

¹*Anesthesiology, University of California at Los Angeles, Los Angeles, CA, United States*, ²*UCLA School of Nursing, Los Angeles, CA, United States*

³*Medicine, University of California at Los Angeles, Los Angeles, CA, United States*, ⁴*Neurobiology, University of California at Los Angeles, Los Angeles, CA, United States*, ⁵*Brain Research Institute, University of California at Los Angeles, Los Angeles, CA, United States*, ⁶*Radiological Sciences, University of California at Los Angeles, Los Angeles, CA, United States*, ⁷*Bioengineering, University of California at Los Angeles, Los Angeles, CA, United States*

Obstructive sleep apnea (OSA) patients show gray matter injury in multiple brain areas based on various MRI techniques, which can accompany subcortical and white matter myelin integrity loss in the condition. However, the extent of regional myelin changes in OSA is unclear. We examined regional myelin integrity in newly-diagnosed, treatment-naïve OSA patients, and found decreased values, probably resulting from hypoxic/ischemic processes, in critical autonomic, cognitive, respiratory, and mood control sites, functions that are deficient in the condition. These findings show that myelin mapping, based on the ratio of T1- and T2-weighted images, is useful in assessing regional myelin alterations.

1188



Investigation of 1H MRS changes in the brain of osteoarthritis patients in relation to perceived pain
Franklyn Arron Howe¹, Olakunbi Harrison², Thomas Richard Barrick¹, and Nidhi Sofat²

¹Neuroscience Research Centre, St George's, University of London, London, United Kingdom, ²Institute for Infection and Immunity, St George's, University of London, London, United Kingdom

Chronic pain from osteoarthritis (OA) may be aggravated by "central sensitisation", whereby pain-processing pathways become sensitised by inflammatory and degenerative disease processes. 1H MRS was used to investigate biochemical changes in pain processing brain areas of hand OA patients (n=32) compared to controls (n=14). There were no differences between controls and patients in the anterior cingulate gyrus, nor age related changes. In the insula cortex ml/Glx correlated with the pain score ($R^2 = 0.52$, $p = 0.018$) after co-varying for age. High ml/Glx in the insula cortex was associated with high pain and may reflect inflammatory effects or neurological changes.

1189



Brain bioenergetics as markers of vigilance failure in obstructive sleep apnoea

Caroline D Rae¹, Haider Naqvi², Andrew Vakulin^{2,3}, Angela D'Rozario², Michael Green¹, Hannah Openshaw², Keith Wong^{2,4}, Jong-Won Kim⁵, Delwyn J Bartlett⁶, Doug McEvoy⁷, and Ronald R Grunstein⁶

¹The University of New South Wales, Randwick, Australia, ²NHMRC Centers of Research Excellence, CIRUS and NeuroSleep, Woolcock Institute of Medical Research, The University of Sydney, Sydney, Australia, ³Adelaide Institute for Sleep Health: A Flinders Centre of Research Excellence, School of Medicine, Flinders University, Adelaide, Australia, ⁴Sydney Medical School, The University of Sydney, Sydney, Australia, ⁵School of Physics, The University of Sydney, Sydney, Australia, ⁶NeuroSleep and Woolcock Institute of Medical Research, The University of Sydney, Sydney, Australia, ⁷Adelaide Institute for Sleep Health: A Flinders Centre of Research Excellence, School of Medicine, Flinders University, Adelaide, Australia

Here, we investigated the potential for MRS/MRI markers to differentiate between phenotypes of obstructive sleep apnea patients who are vulnerable, versus resistant to vigilance failure, an indicator of driving impairment and accident risk. Vulnerable patients (N = 15) and resistant patients (N = 30) were differentiated on the basis of left orbito-frontal glutamate and aspartate and also anterior cingulate glutathione levels. There was a trend towards lower orbitofrontal creatine levels in vulnerable OSA subjects, but no group differences in brain volumes.

1190

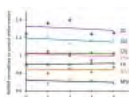


A Diffusional Kurtosis Imaging Study of the White Matter Abnormalities in Type-2 Diabetic Brain
YING XIONG^{1,2}, Shun Zhang¹, Qiang Zhang³, and Wenzhen Zhu¹

¹Radiology Department, Tongji Hospital, Tongji Medical College, Huazhong University of Science and Technology, Wuhan, China, People's Republic of, ²Certe for MR Research, University of Illinois at Chicago, Chicago, IL, United States, ³Neurology Department, Tongji Hospital, Tongji Medical College, Huazhong University of Science and Technology, Wuhan, China, People's Republic of

This study aims at investigating brain microstructural changes in white-matter (WM) of type 2 diabetes mellitus (T2DM) patients using diffusional kurtosis imaging (DKI), and making a comparison with diffusion tensor metrics. Thirty T2DM patients and 28 healthy controls were recruited and imaged on a 3 Tesla scanner. It was found that in the whole-brain and atlas-based analysis, mean kurtosis (MK) detected more regions with WM alterations than fractional anisotropy (FA), especially in some regions including crossing fibers. DKI can complement conventional DTI and provide more information to characterize and pinpoint brain microstructural changes in WM of T2DM patients.

1191



Hematopoietic stem cell transplantation in late-onset Krabbe disease halts demyelination and axonal loss: A 4 year longitudinal case study
Cornelia Laule^{1,2}, Elham Shahinfard¹, Burkhard Maedler¹, Jing Zhang¹, Irene Vavasour¹, Ritu Aul³, David K.B. Li^{1,4}, Alex L. MacKay^{1,5}, and Sandra Sirrs⁶

¹Radiology, University of British Columbia, Vancouver, BC, Canada, ²Pathology & Laboratory Medicine, University of British Columbia, Vancouver, BC, Canada, ³Medical Genetics, North York General Hospital, Toronto, ON, Canada, ⁴Medicine (Neurology), University of British Columbia, Vancouver, BC, Canada, ⁵Physics & Astronomy, University of British Columbia, Vancouver, BC, Canada, ⁶Medicine (Endocrinology), University of British Columbia, Vancouver, BC, Canada

Late-onset Krabbe disease is a very rare demyelinating leukodystrophy. We found hematopoietic stem cell transplantation in Krabbe disease halts demyelination and axonal loss up to 4 years post-allograft. Abnormalities far beyond those visible on conventional imaging were detected, suggesting a global pathological process occurs in Krabbe disease with adult onset etiology, with myelin being more affected than axons. However, the degree of Krabbe abnormality did not increase over time for any advanced MR metrics, which supports hematopoietic stem cell transplantation as an effective treatment strategy for stopping progression associated with late-onset Krabbe disease.

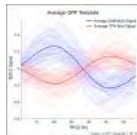
Connectomics

Exhibition Hall

Monday, May 9, 2016: 10:45 - 12:45

1192

Phase of quasi-periodic patterns in the brain predicts performance on psychomotor vigilance task in humans
Anzar Abbas¹, Waqas Majeed², Garth Thompson³, and Shella Keilholz⁴



¹Neuroscience Program, Emory University, Atlanta, GA, United States, ²School of Science and Engineering, Lahore University of Management Sciences, Lahore, Pakistan, ³Radiology and Biomedical Imaging, Yale University, New Haven, CT, United States, ⁴Biomedical Engineering, Emory University and Georgia Institute of Technology, Atlanta, GA, United States

Functional organization of brain networks plays an important role in behavior. Analysis of the dynamics of two functional networks – the default mode (DMN) and task positive (TPN) networks – has shown a dependency of task performance on relative network activation. Fluctuations between these two networks have been seen to occur in humans in a continuous, quasi-periodic fashion. However, the nature of these quasi-periodic patterns (QPPs) and their effect on behavior is not well understood. We show that QPPs do not differ between resting state and task-based scans and that the phase of these QPPs can serve as predictors of performance on the psychomotor vigilance task (PVT).

1193

Reduced low frequency band power in resting state activity predicts symptom severity in mild traumatic brain injury (mTBI)
Radhika Madhavan¹, Suresh E Joel¹, Sumit Niogi², John A Tsioris², Luca Marinelli³, and Teena Shetty²



¹GE Global Research, Bangalore, India, ²Hospital for special surgery, New York, NY, United States, ³GE Global Research, Niskayuna, NY, United States

mTBI diagnosis is controversial since although the brain appears normal on CT/MRI scans, a significant proportion of patients display persistent cognitive impairments up to 6 months post-injury. We recorded rs-fMRI in mTBI patients longitudinally over 3 months, to track functional changes in the brain as patients recovered. Symptom scores were negatively correlated with fractional power in the low-frequency band (0.01-0.1 Hz) of rs-fMRI, and this correlation was most significant in the higher visual, salience and sensorimotor networks. We suggest that low frequency power of rs-fMRI can be used as a biomarker for predicting severity of cognitive impairment in brain injury.

1194

Modular changes in functional connectivity associated with clinical symptoms in mild traumatic brain injury (mTBI)

Radhika Madhavan¹, Hariharan Ravishankar¹, Suresh E Joel¹, Rakesh Mullick¹, Sumit Niogi², John A Tsioris², Luca Marinelli³, and Teena Shetty⁴



¹GE Global Research, Bangalore, India, ²Weill Cornell Medical College, New York, NY, United States, ³GE Global Research, Niskayuna, NY, United States, ⁴Hospital for Special Surgery, New York City, NY, United States

Although most mTBI patients recover by 3-6 months, they suffer serious short and long term effects. Additionally, multiple mTBIs may have serious long-term consequences. Here, we correlated brain network-level connectivity features derived from resting state functional magnetic resonance imaging (rs-fMRI) with clinical symptoms, in order to identify neuroimaging biomarkers of mTBI as patients recover over 3 months. We used a machine-learning framework to select connectivity features associated with symptoms and identified functional regions with altered connectivity. These modular network-level features can be used as diagnostic tools for predicting disease severity and recovery profiles.

1195

Disruption of the Relationship between Default Mode Network Connectivity and Task-related Deactivation in Patients with Mild Traumatic Brain Injury

David Yen-Ting Chen^{1,2}, Yi-Tien Li^{1,3}, Chien-Yuan Eddy Lin^{4,5}, Chi-Jeng Chen¹, and Ying-Chi Tseng¹



¹Department of Radiology, Shuang-Ho Hospital, Taipei Medical University, New Taipei City, Taiwan, ²Brain and Consciousness Research Center, Taipei Medical University, Taipei City, Taiwan, ³Institute of Biomedical Engineering, National Taiwan University, Taipei City, Taiwan, ⁴GE Healthcare, Taipei City, Taiwan, ⁵MR Advanced Application and Research Center, GE Healthcare, Beijing City, China, People's Republic of

Mild traumatic brain injury (MTBI) may cause disruption of default mode network (DMN) in patients. We found differences in both resting state DMN connectivity and task-related deactivation between MTBI patients and healthy controls. Although no significant within-network difference was found in the DMN connectivity between patients and controls, there was increased extra-network connection to the left inferior frontal gyrus in the patients. Significantly more profound task-related deactivation was found in the patients, especially in bilateral IPCs. Increased task-related deactivation may imply the patients need more attention on performing the WM tasks. Furthermore, significant correlation between resting state connectivity and task-related deactivation of DMN was found in healthy controls and this rest-task correlation was disrupted in the patients.

1196

mTBI symptom severity is associated with functional connectivity of specific networks

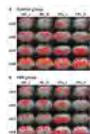
Suresh Emmanuel Joel¹, Radhika Madhavan¹, Rakesh Mullick¹, Sumit Niogi², John A Tsioris², Luca Marinelli³, and Teena Shetty⁴



¹Diagnostic Imaging and Biomedical Technologies, General Electric Global Research, Bangalore, India, ²Weill Cornell Medical College, New York, NY, United States, ³Diagnostic Imaging and Biomedical Technologies, General Electric Global Research, Niskayuna, NY, United States, ⁴Hospital for Special Surgery, New York, NY, United States

Patients who suffer from mild traumatic brain injury (mTBI) have cognitive and behavioral deficits though MR and CT appear normal. Functional neuroimaging has high promise to provide biomarkers which may enable better prognosis and therapy of mTBI. The work here shows in a large sample (78 mTBI patients and 26 controls in 3 sessions spanning 3 months from injury), significant correlation between functional connectivity in visual, motor and default mode networks and self-reported symptom scores. Given this association, functional connectivity stands to be an important contributor to predict mTBI outcome.

1197

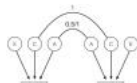


Resting-state functional connectivity reveals age-related difference in Valproate-induced rat autism model
Hsin-Yi Lai¹, Hui-Ching Lin^{2,3}, Hui-Yu Wang⁴, Jun-Cheng Weng⁵, Han-Fang Wu², and You-Yin Chen⁴

¹Interdisciplinary Institute of Neuroscience and Technology (ZIINT), Zhejiang University, Hangzhou City, China, People's Republic of, ²Department and Institute of Physiology, National Yang-Ming University, Taipei, Taiwan, ³Brain Research Center, National Yang Ming University, Taipei, Taiwan, ⁴Department of Biomedical Engineering, National Yang-Ming University, Taipei, Taiwan, ⁵Department of Medical Imaging and Radiological Sciences, Chung Shan Medical University, Taichung, Taiwan

This study demonstrates changes of functional connectivity in motor related brain areas and it is age-related different in Valproate-induced rat autism model. Our results indicate that the motor cortex and striatum may be crucial areas for treatment and evolution of ASD. rsfMRI has potential to explore functional connectivity in the brain and monitor functional plasticity changes in a specific neuroanatomical pathway *in vivo*.

1198



The heritability of structural brain network

Xiaopei Xu¹, Pek-Lan Khong¹, Nichol M. L. Wong^{2,3}, Rainbow T. H. Ho⁴, C. Mary Schooling⁵, Pui-sze Yeung⁶, Tatia M. C. Lee^{2,3,7,8}, and Edward S Hui¹

¹Department of Diagnostic Radiology, The University of Hong Kong, Hong Kong, Hong Kong, ²Laboratory of Neuropsychology, The University of Hong Kong, Hong Kong, Hong Kong, ³Laboratory of Social Cognitive Affective Neuroscience, The University of Hong Kong, Hong Kong, Hong Kong, ⁴Department of Social Work and Social Administration, The University of Hong Kong, Hong Kong, Hong Kong, ⁵School of Public Health, The University of Hong Kong, Hong Kong, Hong Kong, ⁶Faculty of Education, The University of Hong Kong, Hong Kong, Hong Kong, ⁷Institute of Clinical Neuropsychology, The University of Hong Kong, Hong Kong, Hong Kong, ⁸The State Key Laboratory of Brain and Cognitive Science, The University of Hong Kong, Hong Kong, Hong Kong

To better understand the importance of education, genetic, and environmental influences on brain structural connectivity, we used DTI-based tractography and brain network analysis to investigate the thereof in twin pairs. The correlation between network properties and education was also studied in both twin and non-twin participants. We showed significant correlations between twin pairs for the topology of brain network and the nodal characteristics of brain hubs. Nodal characteristics of hubs were also significantly correlated with education level. These findings suggested that brain topology and cognitive capacity are heritable, and brain network analysis is of potential value in intelligence assessment.

1199



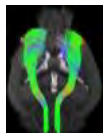
Impaired small-world structural brain network in patients with neuropsychiatric systemic lupus erythematosus

Xiaopei Xu¹, Henry KF Mak¹, MY Mok², CS Lau², and Edward S Hui¹

¹Department of Diagnostic Radiology, The University of Hong Kong, Hong Kong, Hong Kong, ²Department of Medicine, The University of Hong Kong, Hong Kong, Hong Kong

To better understand the underlying mechanisms for various neuropsychiatric symptoms in patients with neuropsychiatric systemic lupus erythematosus (NPSLE), we used DTI-based tractography and graph theory approaches to investigate the change in the global configuration and nodal characteristics of the structural brain network in NPSLE and SLE patients. Our results showed impaired small-world structural network and diminished role of several brain regions as hubs in NPSLE patients, indicating the disruption of brain architecture underlying multiple neuropsychiatric manifestations present in NPSLE. Our results demonstrated that brain network analysis is a reliable method to study systemic disease like NPSLE.

1200



Tractography Study of Brain Asymmetries in a Genetic Mouse Model

Alexandra Petiet^{1,2}, Gonçalo C Vilhais-Neto^{3,4}, Daniel Garcia-Lorenzo¹, Stéphane Lehéricy^{1,2}, and Olivier Pourquié^{3,4,5,6,7}

¹Center for Neuroimaging Research, Brain and Spine Institute, Paris, France, ²UPMC/Inserm UMR1127 / CNRS UMR7225, Paris, France, ³Institut de Génétique et de Biologie Moléculaire et Cellulaire, Illkirch, France, ⁴Stowers Institute for Medical Research, Kansas City, MO, United States, ⁵Howard Hughes Medical Institute, Kansas City, MO, United States, ⁶Department of Anatomy and Cell Biology, University of Kansas Medical Center, Kansas City, MO, United States, ⁷Department of Genetics, Harvard Medical School and Department of Pathology, Brigham and Woman's Hospital, Boston, MA, United States

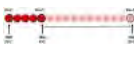
While humans show clear preference for right hand usage (90%), normal mice show consistent right or left paw usage (50%). We used a Rere-deficient mouse model (*Rere*^{+/-}) that shows clear right paw usage preference (80%) compared to wild-type (WT) mice (40%) to evaluate structural connectivity changes in the cortico-spinal tract (CST) using diffusion-based tractography. Our results showed significantly reduced and more asymmetric FA along the CST of the dominant hemisphere in the dextral mutant group compared to the WT group. These results show Rere-dependent structural connectivity changes in the brain that could be clinically relevant to human pathologies.



Thalamocortical network alteration in Children and Adolescents with Idiopathic Generalized Epilepsy
Tijiang Zhang¹, Wuchao Li¹, Quanzhong Zhou¹, Ganjun Song¹, Cong Tian¹, Zhen Zeng¹, and Xingyu Wang¹

¹Department of Radiology, Affiliated hospital of Zunyi Medical College, Zunyi, China, People's Republic of

The aim of this study is to investigate FC alterations of thalamocortical network using resting-state fMRI, and correlation FC alterations with Intelligence Quotient (IQ). 19 patients and 19 healthy volunteers took part in this research. The thalamocortical FC seeding at the left thalamus in the IGE patients showed a significant increase in left inferior temporal gyrus and right supramarginal gyrus, but decrease in left anterior cingulate, bilateral posterior cingulate, bilateral dorsolateral frontal gyrus, whereas, seeding the right thalamus as seed showed increase in right cerebellum, right supramarginal gyrus, but decrease in bilateral dorsolateral frontal gyrus, bilateral PCC and right supramarginal gyrus. Correlation analysis revealed that IQ positively correlated with FC strength between thalamus and left anterior cingulate, left dorsolateral superior frontal gyrus. The alteration of FC may reflect the progress of long-term destruction of functional architecture, and may be served as a potential biomarker to examine subtle brain abnormalities in children and adolescence with IGE.



Network centrality insights into the effects of Dexamethasone on brain function in healthy subjects

Fatima Nasrallah^{1,2,3}, Bernice OH⁴, Trina Kok², Mary Stephenson², Tony Chin-lan Tay⁴, Edwin Kean-Hui Chiew⁴, Jiesen Wang⁵, Alexandre Schaefer⁵, Adriana Benzoic⁵, Johnson Fam⁴, and Allen Eng-Juh Yeoh⁴

¹Clinical Imaging Research Centre, NUS/A*STAR, St Lucia, Australia, ²Clinical Imaging Research Centre, NUS/A*STAR, Singapore, Singapore,

³Queensland Brain Institute, Queensland, Australia, ⁴National University Hospital, Singapore, Singapore, ⁵Clinical Imaging Research Centre, NUS, Singapore, Singapore

Dexamethasone is a glucocorticoid which has demonstrated clinical improvement in acute lymphoblastic leukaemia patients but has been associated with diminished memory and executive function. Because it is normally administered as a cocktail of drugs during the treatment regimen, understanding its main mechanism of action has been hindered. We investigate the effect of dexamethasone on brain function in healthy volunteers using resting state fMRI connectivity



Altered structural network connectivity in non-neuropsychiatric systemic lupus erythematosus: a graph theoretical analysis
Man Xu¹, Xiangliang Tan², Patrick Peng GAO³, Ed.X. Wu^{3,4}, Yingjie Mei^{1,5}, Xixi Zhao², Yikai Xu², and Yanqiu Feng^{1,3,4}

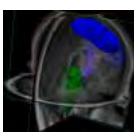
¹School of Biomedical Engineering and Guangdong Provincial Key Laboratory of Medical Image Processing, Southern Medical University,

Guangzhou, China, People's Republic of, ²Department of Medical Imaging Center, Nanfang Hospital, Southern Medical University, Guangzhou,

China, People's Republic of, ³Laboratory of Biomedical Imaging and Signal Processing, The University of Hong Kong, Hong Kong SAR, China,

People's Republic of, ⁴Department of Electrical and Electronic Engineering, The University of Hong Kong, Hong Kong SAR, China, People's Republic of, ⁵Philips Healthcare, Guangzhou, China, People's Republic of

The character of the brain structural connectivity in patients with non-neuropsychiatric systemic lupus erythematosus (non-NPSLE) has not been well studied. The aim of the study was to investigate the alterations of the topological metrics in non-NPSLE networks and to identify the regions in which the metrics were significantly different. A structural connectivity matrix was constructed for each subject using PANDA toolbox. Then graph theoretical analysis was applied to investigate the alteration of the metrics. The results revealed that the non-NPSLE group exhibited a trend of decreased global network properties and changed betweenness and degree in several brain regions.

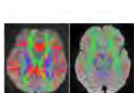


White matter parcellation on the basis of probabilistic fiber pathway reconstructions

Patrick Schiffler¹ and Jan-Gerd Tenberge¹

¹University of Münster, Münster, Germany

We present an approach that permits a fiber association based definition of white matter regions of interest, which offers region specific analysis of the white matter.



Quality Control measures for Constrained Spherical Deconvolution MR diffusion tractography in clinical use.

Donald W McRobbie^{1,2} and Marc Agzarian¹

¹Medical Imaging, Flinders Medical Centre, Adelaide, Australia, ²Surgery, Imperial College, London, United Kingdom

Quality Control (QC) methods for clinical MR tractography using whole-brain Constrained Spherical Deconvolution (CSD) in individual patients are used to assess the quality of the acquired data. Clinical scoring of the resulting tractograms demonstrates robust depiction of anatomically realistic tracts over a range of MR scanners, acquisitions, and with varying raw image quality. Whole brain CSD shows potential for clinical use subject to suitable QC measures.



Gray matter networks in the mouse brain

Marco Pagani^{1,2}, Angelo Bifone¹, and Alessandro Gozzi¹

Structural covariance MRI (scMRI) has highlighted robust gray matter networks encompassing known neuroanatomical systems of the human brain. The application of scMRI in the mouse can provide insights on the elusive neurobiological determinants underlying the emergence of this phenomenon. We show that the mouse brain contains robust inter-hemispheric anatomical covariance networks recapitulating anatomical features observed in humans. Our findings pave the way to the use of mouse genetics to investigate the biological underpinnings of scMRI networks and their aberration in brain disorders.

1207



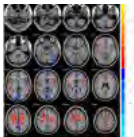
Altered Default Mode Network in Developmental Stages of ADHD Rats

Sheng-Min Huang¹, Kun-I Chao¹, Kung-Chu Ho², and Fu-Nien Wang¹

¹Department of Biomedical Engineering and Environmental Sciences, National Tsing Hua University, Hsinchu, Taiwan, ²Division of Nuclear Medicine, Chang Gung Memorial Hospital, Taoyuan, Taiwan

We investigated the DMN in ADHD rats of different ages. A major difference of DMN between SHR and WKY rats was found in caudate putamen area. As age increasing, the striatal activation presented in the DMN of 6-week SHR started to decrease at 8-week and tend to fade out at 10-week. Since the volume difference of striatal region between SHR and WKY rats has been reported, our result may suggest that the structural development is followed by persisted functional network alteration. The correlation of development of striatal volume and striatal resting state activity both suggest that the timing is important.

1208



Changes in brain Connectivity and Its Correlation with idiopathic complex partial seizures epilepsy Patients: Evidence from Resting-State fMRI

Peng-fei Qiao¹, Guang-ming Niu¹, Yang Gao¹, and Ai-shi Liu¹

¹Affiliated Hospital of Inner Mongolia Medical University, HOHHOT, China, People's Republic of

In order to detect the resting state fMRI (rfMRI) change of the complex partial seizures(CPS) epilepsy patients by employing the regional homogeneity(ReHo)、 the amplitude of low frequency fluctuation (ALFF) and the functional connectivity(FC) techniques. And we found there were important values to study epilepsy using 3 above techniques at the resting state.

1209



Graph-Theoretical Analysis of BOLD-fMRI Using Nociceptive Stimuli Unravels Characteristics of Pain Chronification

Isabel Wank¹, Silke Kreitz¹, and Andreas Hess¹

¹Institute of Pharmacology and Toxicology, University of Erlangen-Nuremberg, Erlangen, Germany

Pain is a warning sign and a highly potent modulator of behavior. This naturally very useful mechanism evolves into a central healthcare problem, when pain becomes chronic and highly impacting the patient's daily life. By means of fMRI and modern graph theoretical analyses, we surveyed dynamic changes of functional connectivity within the mouse brain evoked within 7 sessions of noxious thermal stimulation of the hind paw. With no evidence of peripheral hyperalgesia, we found noticeable alterations of connectivity especially within cognitive and associative-evaluative brain structures. We hypothesize that these findings reflect profound changes that central sensitization impresses on the brain.

Traditional Poster

Traumatic Brain Injury

Exhibition Hall

Monday, May 9, 2016: 10:45 - 12:45

1210



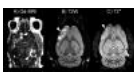
Quantitative sodium MRI in traumatic brain injury (TBI): Pilot study

Guillaume Madelin¹, Jonathan M Silver², Tamara Bushnik³, and Ivan I Kirov¹

¹Department of Radiology, New York University Langone Medical Center, New York, NY, United States, ²Department of Psychiatry, New York University Langone Medical Center, New York, NY, United States, ³Department of Rehabilitation Medicine, New York University Langone Medical Center, New York, NY, United States

In this pilot quantitative sodium MRI study, 4 patients in the chronic stage after traumatic brain injury (TBI) and 6 controls were scanned at 3 T. Intracellular sodium concentration (C_1) and extracellular volume fraction (α_2) were calculated in lesions, as well as in whole grey and white matters. Global C_1 skewness and kurtosis showed significant differences between patients and controls, and regional measurements in lesions presented large increases of C_1 and α_2 compared to normal tissue. The results indicate that quantitative sodium MRI shows promise as an imaging biomarker of cell death in chronic TBI.

1211



GluCoCEST matches 18F-FDG PET on a pulse focus ultrasound induced traumatic brain injury

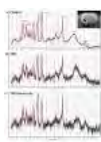
Tsang-Wei Tu¹, Zsofia I. Kovacs¹, George Z. Papadakis¹, Neekita Jikaria¹, William Reid¹, Dima Hammoud¹, and Joseph A. Frank¹

¹Radiology and Imaging Sciences, National Institute of Health, Bethesda, MD, United States

¹⁸F-FDG positron emission tomography (PET) is used to non-invasively measure the glucose metabolism in the brain. However PET

imaging is also limited on the longitudinal monitoring of glucose due low spatial and anatomical resolution. This study compares the glucoCEST and ¹⁸F-FDG PET in detecting the glucose concentration in a new traumatic brain injury model using MRI guided pulsed focus ultrasound. Our data show that the glucoCEST could deliver comparable results with the ¹⁸F-FDG PET results in detecting the event of hypo-metabolism in the traumatized brain with greater higher image resolution as compared to PET scans.

1212



Therapeutic potential of mesenchymal stem cells after transplantation in traumatic brain injury mice: an in vivo 1H MRS and behavioural study
Sushanta Kumar Mishra^{1,2}, Subash Khushu¹, and Gurudutta Gangenahalli²

¹NMR Research Centre, Institute of Nuclear Medicine and Allied Sciences, Delhi, India, ²Division of Stem Cell and Gene Therapy Research, Institute of Nuclear Medicine and Allied Sciences, Delhi, India

Mesenchymal stem cells have been shown to be effective against neuronal degeneration through mechanisms that include both the recovery of neurometabolites and behavioural activity. This study demonstrates that intravenous administration of MSCs in traumatic brain injury mice alter the neurometabolic concentration at lesion site and improve the behavioural functional outcome. The concentrations of metabolites like phosphocholine and inositol were increased, while other metabolites like NAA, GABA, Cr+PCr, Glu+Gln and taurine were decreased at injury site after MSCs transplantation and become its normal concentrations. The functional activities like stress level, grip strength and depression index were improved in transplanted TBI mice.

1213



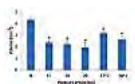
Effect of football position played on brain metabolite concentrations in retired NFL players

Alexander Lin¹, Jeffery K Cooper¹, Molly Charney¹, Huijun Liao¹, Benjamin C Rowland¹, Martha E Shenton², and Robert A Stern³

¹Radiology, Brigham and Women's Hospital / Harvard Medical School, Boston, MA, United States, ²Psychology, Brigham and Women's Hospital / Harvard Medical School, Boston, MA, United States, ³Chronic Traumatic Encephalopathy Center, Boston University School of Medicine, Boston, MA, United States

Repetitive brain trauma (RBT) from playing American football places athletes at risk for chronic traumatic encephalopathy (CTE). While all confirmed cases of CTE have had exposure to RBT, not all those exposed develop the disease, suggesting the importance of factors such as impact severity in its development. In this study we utilize magnetic resonance spectroscopy to measure brain chemistry levels in retired NFL players and compare differences in neurochemistry of different player positions and their related concussion burden. Results show significant changes in glutamate and creatine that provide a potential mode for understanding excitotoxic changes as a result of RBT.

1214



Characterization of white matter changes in a mouse model of mild blast traumatic brain injury

Sujith Sajja¹, Jiangyang Zhang¹, Jeff W.M. Bulte¹, Robert Stevens², Joseph Long³, Piotr Walczak^{1,4}, and Miroslaw Janowski^{1,5}

¹The Russell H. Morgan Department of Radiology and Radiological Science, Johns Hopkins University, Baltimore, MD, United States,

²Departments of Anesthesiology/Critical Care Medicine, Neurology, Neurosurgery, and Radiology, Johns Hopkins University, Baltimore, MD, United States, ³Walter Reed Army Institute of Research, Silver Spring, MD, United States, ⁴Department of Radiology, University of Warmia and Mazury, Olsztyn, Poland, ⁵NeuroRepair Department, Mossakowski Medical Research Centre PAS, Warsaw, Poland

White matter abnormalities in veterans with behavioral symptoms following blast exposure have been detected with diffusion tensor imaging (DTI) without changes in T1/T2-weighted anatomical MRI. Our aim was to reproduce the battlefield scenario in a mouse model. We observed no focal anatomical changes, while diffuse white matter abnormalities were observed with DTI, and CEST MRI. They coincided with behavioral abnormalities and post-mortem neuropathological changes. The use of MRI may facilitate non-invasive and longitudinal monitoring of blast injury, and aid in developing therapeutics aimed to minimize further damage progression.

1215



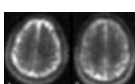
Volumetric analysis of structural brain changes in acute and sub-acute mild traumatic brain injury

Tianhao Zhang¹, Sumit Niogi², John A. Tsioris², Luca Marinelli³, and Teena Shetty⁴

¹GE Healthcare, Waukesha, WI, United States, ²Weill Cornell Medical Center, New York, NY, United States, ³GE Global Research, Niskayuna, NY, United States, ⁴Hospital for Special Surgery, New York, NY, United States

Mild traumatic brain injury (mTBI) is a heterogeneous disease with a variety of symptoms associated with brain function alterations after the trauma. There is still limited understanding of the relationship between physiological and structural changes and recovery rate. In this work, we aim to identify structural brain changes in a mTBI population at 4 time points. The analysis is in two folds: 1) correlation analysis between brain volumes and clinical scores; and 2) longitudinal analysis across different encounters. The results revealed significant brain volume changes over time, and at 3 months post-injury, volumes demonstrated significant negative correlations with clinical scores.

1216



Distribution of brain sodium after mild traumatic brain injury

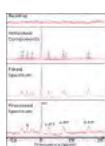
Yvonne W Lui¹, Yongxian Qian¹, Karthik Lakshmanan¹, Jacqueline Smith¹, Graham Wiggins¹, Steven Flanagan², and Fernando E Boada¹

¹Radiology, New York University, New York, NY, United States, ²Rehabilitation Medicine, New York University, New York, NY, United States

Mild traumatic brain injury (mTBI) is a growing public health problem with more than 1.5 million cases a year in the United States. The pathophysiological processes underlying mTBI are complex, including biomechanical injury induced stretching of the axons and depolarization of the normal resting voltage across the cell membrane. Sodium handling by the brain is critical to restore ionic

homeostasis after injury and disordered handling is implicated in the long-term pathophysiology of concussion. With state-of-the-art sodium (²³Na) MR imaging, one can obtain high quality sodium images in a clinical setting at 3T. Here we seek to observe patterns of total sodium distribution in brain in individuals with mTBI.

1217



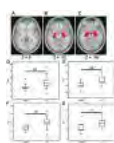
Assessment of mild traumatic brain injury due to blast overpressure in breachers: A ³¹P MRS Study.

Mary C Stephenson^{1,2}, Trina Kok¹, Fatima A Nasrallah¹, Pamela Boon Li Pun³, Melissa Ai Ling Teo³, Julie Su Li Yeo³, Lu Jia³, Benjamin A Thomas¹, Mary K Enci³, and John J Totman¹

¹Clinical Imaging Research Centre, A*STAR-NUS, Singapore, Singapore, ²Department of Medicine, NUS, Singapore, Singapore, ³Defense Science Organization, Singapore, Singapore

Traumatic Brain Injury (TBI) is identified as the signature injury of soldiers involved in the Iraq and Afghanistan wars. Mild TBI (mTBI) often goes undetected, meaning vital opportunities for early treatment are missed. In this study we use ³¹P MRS to investigate whether changes in ³¹P metabolites can be identified in soldiers at risk of mTBI due to blast overpressure. Measurements of brain volumes and ³¹P MRS are made at baseline and 1, 3, 7 and 28 days following training with low level explosives. We show a tendency for decreases in Pi/PCr ratio which reach significance 28 days after training.

1218



Quantitative Tissue Specific R2* Measurements detect mTBI related damage in brain areas without evident anatomical changes

Jie Wen¹, Serguei V. Astafiev², Kristina L. Zinn², Anne H. Cross², Dmitriy A. Yablonskiy¹, and Maurizio Corbetta²

¹Radiology, Washington University, Saint Louis, MO, United States, ²Neurology, Washington University, Saint Louis, MO, United States

In this study we used quantitative tissue specific R2* measurements to detect brain abnormalities in chronic subjects with mild traumatic brain injury (mTBI). mTBI patients demonstrated decreased R2* values in frontal pole and hippocampus. Reduced R2* values in the white matter of the hippocampus were strongly related to the reported memory problems typical for mTBI. Importantly, this R2* value reduction was not accompanied by decreased volume of white matter and grey matter inside those regions, suggesting that R2* values may detect mTBI related abnormalities before detectable anatomical changes appear.

1219



Single-subject level inference for volumetry features in mild traumatic brain injury using machine learning methods

Venkata Veerendranadh Chebrolu¹, Tianhao Zhang², Hariharan Ravishankar¹, Sumit Niogi³, John A Tsiouris³, and Luca Marinelli⁴

¹GE Global Research, Bangalore, India, ²GE Healthcare, Waukesha, WI, United States, ³Weill Cornell Medical Center, New York, NY, United States, ⁴GE Global Research, Niskayuna, NY, United States

The purpose of this work is to derive single-subject level inferences for volumetry features in mild traumatic brain injury (mTBI) at multiple time points after initial trauma using machine learning methods. 78 uncomplicated mTBI subjects were scanned three days (32 subjects), seven days (61 subjects), one month (56) and three months (42 subjects) post injury to derive volumetry features. 23 controls were also scanned. Logistic-regression models were used to identify important volumetry features that jointly describe the mTBI effects at single-subject level. Pallidus, supratentorial and whole-brain volumetry features together provide single-subject level signature for mTBI at multiple time-points after injury.

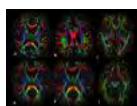
Traditional Poster

Neurodegeneration

Exhibition Hall

Monday, May 9, 2016: 10:45 - 12:45

1220



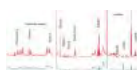
Periventricular Longitudinal Neural Tracts Are Implicated in Postural Instability Gait Disorder

Shawn Tan¹, Nicole Keong², Ady Thien², HuiHua Li¹, Helmut Rumpel¹, EK Tan², and Ling Chan¹

¹Singapore General Hospital, Singapore, Singapore, ²National Neuroscience Institute, Singapore, Singapore

Postural instability gait disorder (PIGD) is associated with predominant gait dysfunction compared to typical tremor dominant Parkinson's disease (PD). We evaluated the periventricular longitudinal neural tracts in PIGD using DTI compared to PD and controls, and examined their clinical correlates. We showed for the first time that these neural tracts are more affected in PIGD than PD or HC, and their DTI measures correlate with clinical gait severity. It has been postulated that disconnection of motor networks served by these tracts linking brain regions involved in executive function and visuoperception with those involved in gait control leads to gait decline.

1221



¹H NMR-based Metabolomics study of saliva samples in Patients with Parkinson's disease

Sadhana Kumari¹, Senthil S Kumaran¹, Vinay Goyal², Madhuri Behari², S N Dwivedi³, Achal Srivastava², and Naranamangalam R Jagannathan¹

¹Department of NMR and MRI Facility, All India Institute of Medical Sciences, New Delhi, India, ²Department of Neurology, All India Institute of Medical Sciences, New Delhi, India, ³Department of Biostatistics, All India Institute of Medical Sciences, New Delhi, India

NMR techniques play a major role in understanding the metabolic changes associated with neurological disorders. We used ¹H NMR spectra at 700 MHz for identification of biomarkers in PD from saliva samples. The data were processed using MestReNova software

(version 10.0) and PLS-DA multivariate analysis using MetaboAnalyst (version 3.0) software. We observed significantly elevated level of butyrate, glycine, phenyl alanine, tyrosine and decreased level of lactate, which may be attributed to poor intestinal absorption in PD patients.

1222



Quantitative Susceptibility Mapping (QSM) detects iron deposition and demyelination in mouse model of Huntington Disease

Xuan Vinh To¹, Hongjiang Wei², Reshma Rajendran¹, Marta Garcia-Miralles³, Ling Yun Yeow¹, Chunlei Liu², Hong Xin¹, Mahmoud A. Pouladi³, and Kai-Hsiang Chuang¹

¹Singapore Bioimaging Consortium, Agency for Science, Technology and Research (A*STAR), Singapore, Singapore, ²Brain Imaging and Analysis Center, School of Medicine, Duke University, Durham, NC, United States, ³Translational Laboratory in Genetic Medicine, Agency for Science, Technology and Research (A*STAR), Singapore, Singapore

This study looked at the potential for Quantitative Susceptibility Mapping (QSM) for longitudinal detection of demyelination and iron accumulation in YAC128 mouse model of Huntington disease. Control and YAC128 mice were scanned at 9, 12, and 15 months of age; with a number of mice sacrificed after each timepoint for histological validation and correlation (ongoing). Current results show the potential for QSM in detecting demyelination in several white matter regions and iron accumulation in grey matter.

1223



Tract-based Spatial Statistics of DTI Metrics in Parkinson's Disease

Yong Zhang¹, Hailong Luo², Changzheng Shi², and Li Guo³

¹GE Healthcare MR Research China, Beijing, China, People's Republic of, ²Medical Imaging Center, the First Affiliated Hospital of Jinan University, Guangzhou, China, People's Republic of, ³Neurology, the First Affiliated Hospital of Jinan University, Guangzhou, China, People's Republic of

Tract-based spatial statistics of average and directional DTI-derived metrics were analyzed between the Parkinson's patients and age-matched healthy controls. It was found that MD increased and FA decreased across WM in accordance with previous studies. The more widespread change of MD compared with FA suggests higher sensitivity of MD to WM degenerations. Besides, it was observed that the change of perpendicular diffusivity was more profound compared with that of axial diffusivity, suggesting the existence of demyelination in PD patients

1224



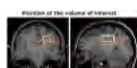
Identifying Brain Connectomic Alterations Specific to Mild Cognitive Impairment and Depression Co-morbid with Parkinson's Disease

Sinan Zhao¹, Peipeng Liang^{2,3,4}, and Gopikrishna Deshpande^{1,5,6}

¹AU MRI Research Center, Department of Electrical and Computer Engineering, Auburn University, Auburn, AL, United States, ²Department of Radiology, Xuanwu Hospital, Capital Medical University, Beijing, China, People's Republic of, ³Beijing Key Lab of MRI and Brain Informatics, Beijing, China, People's Republic of, ⁴Key Laboratory for Neurodegenerative Diseases, Ministry of Education, Beijing, China, People's Republic of, ⁵Department of Psychology, Auburn University, Auburn, AL, United States, ⁶Alabama Advanced Imaging Consortium, Auburn University and University of Alabama Birmingham, Auburn, AL, United States

Resting state fMRI has been used to investigate connectomic alterations in Parkinson's disease (PD). These studies used conventional connectivity analysis where connectivity is assumed to be stationary over time. However, recent work suggests that temporal variability of connectivity is sensitive to human behavior in health and disease. Therefore, we estimated static functional connectivity (SFC), dynamic FC (DFC) from: PD, PD subjects with mild-cognitive-impairment (PDMCI), Depressed PD subjects with MCI (DPDMCI) and Normal Controls (NC). We hypothesized that increased disease burden would lead to reduced strength of SFC and the variability of DFC. We provide evidence to support this hypothesis.

1225



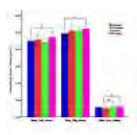
Cerebral diffusion-weighted spectroscopy in Duchenne muscular dystrophy patients shows higher diffusion in all intra-cellular metabolites compared to controls

Nathalie Doorenweerd^{1,2}, Ece Ercan¹, Melissa T Hooijmans¹, Jedrek Burakiewicz¹, Andrew Webb¹, Jos G.M. Hendriksen^{3,4}, Jan J.G.M. Verschuur², Erik H Niks², Hermien E. Kan¹, and Itamar Ronen¹

¹C.J. Gorter Center for High Field MRI, Leiden University Medical Center, Leiden, Netherlands, ²Neurology, Leiden University Medical Center, Leiden, Netherlands, ³Neurological Learning Disabilities, Kempenhaeghe Epilepsy Center, Heeze, Netherlands, ⁴Neurology, Maastricht University Medical Centre, Maastricht, Netherlands

Patients with Duchenne muscular dystrophy (DMD) suffer from behavioural or neurocognitive problems in addition to muscle weakness. Using DTI, we previously showed reduced white matter FA and increased ADC, especially radial diffusivity, in DMD patients indicating microstructural alterations. We now apply diffusion weighted spectroscopy in temporo-parietal white matter to study if these alterations are likely intracellular or extracellular. N-acetylaspartate, creatine and choline ADCs were higher in patients compared to controls. These results show higher diffusion both within cells and across membranes, irrespective of cell-type.

1226



Distinct atrophy of subcortical structures demonstrates gender-specific changes in ALS

Qiuli Zhang¹, Ming Zhang¹, Jingxia Dang², Jiaoting Jin², Fang Hu², Haining Li¹, Dandan Zheng³, and Yuchen Zhang⁴

¹Medical Imaging, the First Affiliated Hospital of Xi'an Jiaotong University, Xi'an, China, People's Republic of, ²Department of Neurology, the First Affiliated Hospital of Xi'an Jiaotong University, Xi'an, China, People's Republic of, ³GE Healthcare, MR Research China, Beijing, China, People's Republic of, ⁴Zonglian College, Xi'an Jiaotong University, Xi'an, China, People's Republic of

Clinical heterogeneity is a feature in ALS. Here we analyzed subcortical structure volume and executive function between male and

female ALS patients, compared with corresponding normal controls. Our results showed that male and female patients exhibited distinct subcortical structure atrophy. The linear regression results also indicated that compared with male patients, whose cognitive status was mostly related with age and education level, the executive dysfunction in female patients may be deteriorated by emotional disorder.

1227



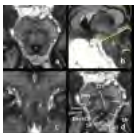
The Association Between Structural Brain Connectivity With Plasma APO-A1 Levels In Parkinson Disease: Connectometry Approach
Farzaneh Rahmani¹ and MohammadHadi Aarabi¹

¹Students' Scientific Research Center, Tehran University of Medical Sciences, Tehran, Iran

The basis of Parkinson disease (PD) pathology is accumulation of α -synuclein particles (Lewy bodies) in the presynaptic terminal and perikarya of neocortex, cerebellum, thalamus and SN.

Features of the lipid profile specially cholesterol levels are association with PD risk. However no such data exists on the association of these plasma markers with structural brain changes in PD. The primary site of PD pathology is the nigrostriatal tract which then progresses to the cingulum. The nigrostriatal tract is extensively damaged prior to PD onset. Lower plasma levels of apoA-I is associated with earlier onset of PD and greater putaminal DAT deficit and a more rapid motor decline in PD. However apoA-I levels have never been investigated regarding changes in structural brain connectivity. The our results show that apoA-I levels in drug_naïve patients are associated with structural changes in the even prior to pathologic involvement of cingulum.

1228

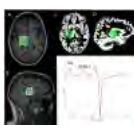


Direct visualization human pedunculopontine nucleus: validation and new coordinate establishing
Fei Cong¹, Jiawei Wang², Zhangyan Yang¹, Bo Wang¹, Yuqing Zhang², and Yan Zhuo¹

¹Institute of Biophysics, Chinese Academy of Science, Beijing, China, People's Republic of, ²Functional neurosurgery, Xuanwu Hospital, Capital Medical University, Beijing, China, People's Republic of

The pedunculopontine nucleus (PPN), as a potential Deep brain stimulation (DBS) target for the patients to improve gait and posture. Until now, only a few results of the location of PPN has been published. In this study, 7T ultra-high field MR system and high resolution MP2RAGE sequence were used to locate the PPN by a direct view, and a new coordinate designed for PPN location was introduced and tested. The boundary of PPN was displayed and a more consistency coordinate used for localizing PPN was presented.

1229

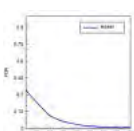


Comparison of Thalamic GABA and Glx Levels in Patients with Essential Tremor and Parkinson's Disease
Ruoyun Ma^{1,2}, Johnathan P Dyke³, Shalmali Dharmadhikari⁴, Nora Hernandez⁵, Elizabeth Zuerber⁶, Elan Louis^{5,7,8}, and Ulrike Dyak^{1,2}

¹School of Health Sciences, Purdue University, West Lafayette, IN, United States, ²Department of Radiology and Imaging Sciences, Indiana University School of Medicine, Indianapolis, IN, United States, ³Department of Radiology, Weill Cornell Medical College, New York, NY, United States, ⁴Radiology and Imaging Sciences, Emory University, Atlanta, GA, United States, ⁵Department of Neurology, Yale School of Medicine, New Haven, CT, United States, ⁶Department of Neurology, Indianapolis University School of Medicine, Indianapolis, IN, United States, ⁷Department of Chronic Disease Epidemiology, Yale School of Public Health, New Haven, CT, United States, ⁸Center for Neuroepidemiology and Clinical Neurological Research, Yale School of Medicine, New Haven, CT, United States

Essential tremor (ET) and Parkinson's disease (PD) are two most prevalent movement disorders. It was suggested that tremors in both diseases, though of different types, may be modulated by neuropathways involving the thalamus. We found a significant trend of elevated thalamic GABA levels from controls to ET patients to PD patients, which may be related to the increased risk of ET patients to develop PD, and thus suggesting thalamic GABA as imaging marker of preclinical parkinsonism. However, thalamic GABA is not associated with tremor of either type.

1230



Associations between Brain Microstructural and Motor Severity of Parkinsonian Symptoms in Elderly Parkinson Diseases
MohammadHadi Aarabi¹, Farzaneh Rahmani¹, Ahmad Shojaei², and Hamidreza Safabakhsh²

¹Students' Scientific Research Center, Tehran University of Medical Sciences, Tehran, Iran, ²Basir Eye Health Research Center, Tehran, Iran, Tehran, Iran

Parkinson's Disease (PD) is a progressive neurodegenerative disorder assumed to involve different areas of CNS and PNS. Thus, Diffusion Tensor Imaging (DTI) is used to examine the areas engaged in PD neurodegeneration. We studied the relationship between local connectome alterations obtained by connectometry approach and motor severity of elderly PD as measured with Unified Parkinson's disease 3. Our findings demonstrate the fornix and cingulum fibers in limbic system have association with motor severity in elderly PD patients in onset.

1231



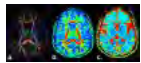
γ -aminobutyric acid spectroscopy of the thalamus in diabetic neuropathy

Iain D Wilkinson¹, Pillai Shillo¹, Marni Greig¹, Solomon Tesfaye¹, Richard A Edden², and Dinesh Selvarajah¹

¹Academic Radiology, University of Sheffield, Sheffield, United Kingdom, ²Kennedy Krieger Institute, Baltimore, MA, United States

The sensory system is affected in diabetic neuropathy (DN), a common ailment associated with diabetes mellitus. The thalamus is part of the brain's sensory pathway. This study applies MEGA-PRESS to assess thalamic GABA in-vivo in patients with and without DN. Differences in GABA/H₂O ratios were identified between those with and without DN, demonstrating potential differences in the

1232



Brain structural changes in type 2 diabetes mellitus: a DTI and VBM study

Qian Sun¹, YuChuan Hu¹, LinFeng Yan¹, Ying Yu¹, Xin-tao Hu², Yu Han¹, DanDan Zheng³, Xu-Feng Liu⁴, Wen Wang¹, and GuangBin Cui¹

¹Department of Radiology, Tangdu Hospital, Fourth Military Medical University, Xi'an, China, People's Republic of, ²Northwestern Polytechnical University, Xi'an, China, People's Republic of, ³MR Research China, GE Healthcare China, Beijing, China, People's Republic of, ⁴Department of Endocrinology, Tangdu Hospital, Fourth Military Medical University, Xi'an, China, People's Republic of

More than 20.4% of the elderly population have diabetes in China, among which Type 2 Diabetes Mellitus (T2DM) accounts for 90%. T2DM is a major risk factor for cardiovascular disease and has been consistently associated with an increased risk of incident dementia, as well as with cognitive deficits and increased brain atrophy. T2DM related cognitive decline may be partly due to neuroanatomical alterations revealed by structural MR. Diffusion tensor imaging (DTI) has been used to quantify microstructural alterations in white matter that may also impact cognition. Fractional anisotropy (FA) and average diffusion coefficient (DCavg) value derived from DTI reflect overall white matter health, maturation, and organization. Voxel-based morphometry (VBM), which reflects brain volume, can be used in early detecting brain structural abnormalities in T2DM patients. Our research aims to detect brain microstructure changes in T2DM patients both in white matter (WM) and gray matter (GM) based on global DTI and VBM.

1233



Regeneration of olfactory performance after sinus surgery correlates with white matter changes in cingulum bundle

Daniel Güllmar¹, Tabea Witting², Thomas Bitter², Orlando Guntinas-Lichius², and Jürgen R Reichenbach¹

¹Medical Physics Group / IDIR, Jena University Hospital - Friedrich Schiller University Jena, Jena, Germany, ²Department of Otolaryngology and the Institute of Phoniatry and Pedaudiology, Jena University Hospital - Friedrich Schiller University Jena, Jena, Germany

In this study we have investigated neuronal changes in a longitudinal study using anatomical and structural MRI before and after pansinus surgery. Neuronal changes measured by means of DTI before and after surgery were compared to changes in olfactory performance. The analysis was carried out using a tract specific analysis involving probabilistic tractography and subsequent alignment of control points along the cingulum bundles. Patients, which showed an improvement >10 in olfactory performance measure, showed also a significant increase in radial diffusivity in the middle segment of the left cingulum bundle.

1234



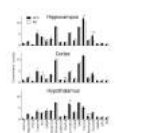
Increased slow diffusion in cortical gray matter is related with cognitive decline in severe white matter hyperintensity

Yerfan Jiaerken¹, Xinfeng Yu¹, and Minming Zhang¹

¹Radiology, The second affiliated hospital of Zhejiang university school of medicine, Hangzhou, China, People's Republic of

We used MRI IVIM technique to investigate how microstructure in cortical gray matter (CGM) affected by white matter hyperintensity (WMH), and how does it affect cognitive function. We found that diffusion in WMH is correlated with diffusion in CGM. And diffusion in CGM is connected with cognitive state, while diffusion in WMH isn't. This may suggest that CGM damage is secondary to microstructural damage in WMH. And CGM damage may lead to cognitive dysfunction, while WMH can only affect cognitive state by damaging gray matter.

1235



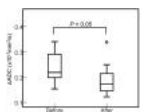
Regional specificity of obesity-induced neurochemical modifications measured in vivo by proton MRS at 14.1 T

João M.N. Duarte¹, Blanca Lizarbe¹, Rolf Gruetter^{1,2,3}, and Ana Francisca Soares¹

¹LIFMET, EPFL, Lausanne, Switzerland, ²UNIL, Lausanne, Switzerland, ³UNIGE, Geneva, Switzerland

Insulin resistance has deleterious effects on memory performance, brain morphology and the neurochemical profile of the cortex and hippocampus. We now investigated the neurochemical modifications in the hippocampus, cortex and hypothalamus of mice exposed to high-fat diet, a model of obesity-associated insulin resistance. In long-term high-fat diet-exposed mice, obesity-associated insulin resistance affects the neurochemical profiles of the hippocampus, cortex and hypothalamus in a region-specific manner.

1236



ΔADC in Idiopathic Normal Pressure Hydrocephalus After Shunt Surgery

Ryoko Yamamori¹, Toshiaki Miyati¹, Naoki Ohno¹, Mitsuhiro Mase², Tomoshi Osawa², Shota Ishida¹, Hiroto Kan³, Nobuyuki Arai³, Harumasa Kasai³, and Yuta Shibamoto³

¹Division of Health Sciences, Graduate School of Medical Sciences, Kanazawa University, Kanazawa, Japan, ²Department of Neurosurgery, Nagoya City University Graduate School of Medical Sciences, Nagoya, Japan, ³Department of Radiology, Nagoya City University Hospital, Nagoya, Japan

Apparent diffusion coefficient (ADC) in brain significantly changed during the cardiac cycle, and this change (ΔADC) in patients with idiopathic normal pressure hydrocephalus (iNPH) characterized by low intracranial compliance was significantly higher than those in control subjects. Shunt surgery is the most common treatment for iNPH. In this study, we determined and compared ΔADC values of the white matter in iNPH before and after shunt surgery. ΔADC in the frontal white matter decreases with the shunt surgery. ΔADC analysis makes it possible to noninvasively provide detailed information on change in the intracranial condition due to the shunt surgery.

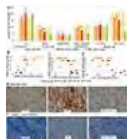
1237

Magnetic susceptibility in primary motor cortex correlates with iron concentration and upper motor neuron impairment in amyotrophic lateral sclerosis

¹Imago7, Pisa, Italy, ²University of Pisa, Pisa, Italy, ³IRCCS Stella Maris, Pisa, Italy

3D gradient-recalled multi-echo sequences were used on a 7 Tesla MR system for Quantitative Susceptibility Mapping (QSM) targeting M1 at high spatial resolution in patients with Amyotrophic Lateral Sclerosis (ALS) and Healthy Controls (HC). The magnetic susceptibility of the deep cortical layers of patients' M1 subregions corresponding to Penfield's areas of the hand and foot significantly correlated with the clinical scores of UMN impairment. QSM might therefore prove useful in measuring M1 iron concentration, as a possible in vivo biomarker of UMN burden and neuroinflammation in ALS patients.

1238



7T MR spectroscopy reflects disease severity in a large animal model of neurologic disease and the effects of gene therapy
Heather Gray-Edwards¹, Nouha Salibi², Anne Maguire¹, Taylor Voss¹, Lauren Ellis¹, Ashley Randle¹, Ronald Beyers¹, Miguel Sena-Esteves³, Thomas Denney¹, and Douglas Martin¹

¹Auburn University, Auburn, AL, United States, ²Siemens Healthcare, Malvern, PA, United States, ³University of Massachusetts, Worcester, MA, United States

GM1 gangliosidosis is a fatal neurodegenerative disorder of children and currently only palliative care is available to patients. Preclinical gene therapy experiments in the GM1 cat resulted in >5 fold increased lifespan, prompting human clinical trials, however objective markers are lacking. 7T MR spectroscopy reliably predicts feline GM1 neurodegeneration with several alterations occurring presymptomatically and worsening with disease progression. Gene therapy results in partial correction of several parameters and changes correlate with clinical assessment scores. Post-mortem analyses included assessment of microgliosis and demyelination, and these findings also correlated with MRS.

1239



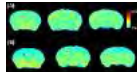
White matter connectome in patients with genetic dystonia

Silvia Basaia¹, Federica Agosta¹, Alexandra Tomic², Elisabetta Sarasso¹, Nikola Kresojević², Sebastiano Galantucci¹, Marina Svetel², Vladimir S. Kostic², and Massimo Filippi^{1,3}

¹Neuroimaging Research Unit, San Raffaele Scientific Institute, Vita-Salute San Raffaele University, Milan, Italy, ²Clinic of Neurology, Faculty of Medicine, University of Belgrade, Belgrade, Yugoslavia, ³Department of Neurology, San Raffaele Scientific Institute, Vita-Salute San Raffaele University, Milan, Italy

We investigated structural neural pathways in asymptomatic and symptomatic mutation carriers with several dystonia (DYT) genotypes using a network approach. Both symptomatic and asymptomatic mutation carriers showed an alteration of structural connectivity compared to controls, beyond the basal ganglia/sensorimotor cortex regions. No differences were found between symptomatic and asymptomatic DYT subjects. The structural connectome offered the possibility of identifying genotype-related trait characteristics, even in the preclinical phase of the disease, providing new insights into understanding DYT generation.

1240



MEMRI Detects Neuronal Loss in MPTP-Intoxicated Mice.

Aditya N Bade¹, Katherine Olson¹, Charles Schutt¹, Jingdong Dong², R Lee Mosley¹, Howard E Gendelman¹, Michael D Boska^{1,3}, and Yutong Liu^{1,3}

¹Department of Pharmacology and Experimental Neuroscience, University of Nebraska Medical Center, Omaha, Omaha, NE, United States,

²Second Affiliated Hospital, Dalian Medical University, Dalian, China, People's Republic of, ³Department of Radiology, University of Nebraska Medical Center, Omaha, Omaha, NE, United States

This study showed that neuronal loss in 1-methyl-4-phenyl-1,2,3,6-tetrahydropyridine (MPTP) injected mice as confirmed by immunohistology caused signal change in manganese-enhanced MRI (MEMRI). Both gliosis and neuronal loss occur in the progress of neurodegenerative diseases. Previous studies have shown that MEMRI signal is associated with gliosis in rodents. With the findings in this study, it is demonstrated the combined pathologic effects of neuronal damage and gliosis determine MEMRI results. The study suggested that MEMRI is an in vivo imaging tool to study the progress of neurodegenerative disease in rodents.

1241



Inline Morphometric Analysis of Temporal-Lobe Epilepsy Patients

Tianyi Qian¹, Yi Shan², Peipei Wang², Bénédicte Maréchal^{3,4,5}, Jie Lu², and Kuncheng Li²

¹MR Collaborations NE Asia, Siemens Healthcare, Beijing, China, People's Republic of, ²Radiology, Xuanwu Hospital, Capital Medical University, Beijing, China, People's Republic of, ³Advanced Clinical Imaging Technology (HC CMEA SUI DI BM PI), Siemens Healthcare, Lausanne, Switzerland,

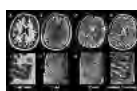
⁴Radiology, University Hospital (CHUV), Lausanne, Switzerland, ⁵LTS5, École Polytechnique Fédérale de Lausanne, Lausanne, Switzerland

Quantitative measurement of hippocampal volume using high-resolution MRI provides morphological and clinically relevant information in medial temporal lobe epilepsy with hippocampal sclerosis. In this study we applied an inline morphometry package in temporal-lobe HS epilepsy patients to investigate the degenerative patterns of this patient group. The volume computed by the inline segmentation tool could provide accurate information about the brain volume changes of temporal-lobe HS epilepsy patients. The tool also provided whole-brain structure volumetric information which was valuable for surgical or treatment planning.

1242

Clinical imaging at 7T: Initial results in epilepsy patients

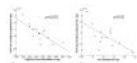
Se-Hong Oh¹, Irene Wang², Stephen E. Jones¹, and Mark J. Lowe¹



¹Imaging Institute, Cleveland Clinic Foundation, Cleveland, OH, United States, ²Epilepsy Center, Cleveland Clinic Foundation, Cleveland, OH, United States

This is an initial study of epilepsy patient scan using 7T. This study serves as a starting point toward 7T clinical scanning. In addition, it gives some insight as to current challenges and future work.

1243



Relationship between hippocampal volume, white matter and cognition in temporal lobe epilepsy

Amanda K.W. Buck^{1,2}, Lauren M. Severance², Benjamin N. Conrad¹, Bennett A. Landman^{1,3}, Adam W. Anderson^{1,2}, Bassel Abou-Khalil⁴, Monica L. Jacobs⁵, and Victoria L. Morgan^{1,2}

¹Institute of Imaging Science, Vanderbilt University, Nashville, TN, United States, ²Biomedical Engineering, Vanderbilt University, Nashville, TN, United States, ³Electrical Engineering and Computer Science, Vanderbilt University, Nashville, TN, United States, ⁴Neurology, Vanderbilt University, Nashville, TN, United States, ⁵Psychiatry, Vanderbilt University, Nashville, TN, United States

Temporal lobe epilepsy (TLE) is associated with changes in regional brain structure, function, and cognition. This study demonstrates an indirect link between right hippocampal volume reductions and extratemporal cognition in right TLE. As hippocampal volume decreases, the right uncinate fasciculus (RUF) axial diffusivity (AD) increases. This increase is correlated with verbal comprehension index (VCI) score decrease. Considering that VCI deficits are related to inferior frontal cortex lesions, these results imply that the RUF, which structurally connects the hippocampus to the frontal lobe, is the mediator of impairment between the seizure focus in the hippocampus and VCI deficits in right TLE.

1244



Arterial Spin Labelling perfusion measurements in Prion Disease: relation with restricted diffusion

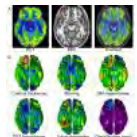
Enrico De Vita^{1,2}, Andrew Melbourne³, Marie-Claire Porter^{4,5}, David L Thomas⁶, Sebastien Ourselin³, Tarek Yousry^{1,2}, Xavier Golay², Rolf Jager^{1,2}, Simon Mead^{4,5}, and John S Thornton^{1,2}

¹Lysholm Department of Neuroradiology, National Hospital for Neurology and Neurosurgery, London, United Kingdom, ²Academic Neuroradiological Unit, Department of Brain Repair and Rehabilitation, UCL Institute of Neurology, London, United Kingdom, ³Medical Physics and Biomedical Engineering, University College London, London, United Kingdom, ⁴National Prion Clinic, National Hospital for Neurology and Neurosurgery, London, United Kingdom, ⁵MRC Prion Unit, Department of Neurodegenerative Diseases, UCL Institute of Neurology, London, United Kingdom, ⁶Dementia Research Centre, UCL Institute of Neurology, London, United Kingdom

Perfusion in Prion disease has only been explored with SPECT, except in 2 single-case studies.

We aimed to evaluate perfusion abnormalities with ASL-MRI in prion patients and compare the findings with clinically diagnostic high b-value diffusion weighted MRI. We observed high correlation between diffusion abnormalities and hypoperfusion. ASL-MRI could help to shed light non-invasively on the neurovascular aspects of prion disease

1245



Superior sensitivity to focal cortical dysplasia obtained by a multivariate analysis of MRI and PET image features

Hosung Kim¹, Yee-Leng Sung Tan², Tarik Tihan³, Anthony James Barkovich¹, Duan Xu¹, and Robert C Knowlton²

¹Radiology & Biomedical Imaging, University California San Francisco, San Francisco, CA, United States, ²Neurology, University California San Francisco, SAN FRANCISCO, CA, United States, ³Pathology, University California San Francisco, SAN FRANCISCO, CA, United States

Focal cortical dysplasia (FCD) is an epileptogenic developmental malformation. Identification of this lesion can lead to a successful surgery. We propose to analyze a combined feature-set extracted from MRI and PET. Studying 29 FCD patients and 23 controls, classification using the combined MRI and PET features demonstrated superior performance to the analysis of MRI as it resulted in a lower false positive (FP) rate in controls (1.3% lower) and a higher sensitivity in FCD (7% higher). Analysis of the combined MRI and PET revealed a larger FP rate in FCD compared to MRI-only, suggesting the presence of extralesional pathology.

1246

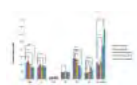
MR-based brain Morphometry Improves Localization of Focal Cortical Dysplasia at Individual Level

Xin Chen¹, Tianyi Qian², Bénédicte Maréchal^{3,4,5}, Nan Chen¹, and Kuncheng Li¹

¹Radiology, Xuanwu Hospital, Capital Medical University, Beijing, China, People's Republic of, ²MR Collaborations NE Asia, Siemens Healthcare, Beijing, China, People's Republic of, ³Advanced Clinical Imaging Technology (HC CMEA SUI DI BM PI), Siemens Healthcare AG, Lausanne, Switzerland, ⁴LTSS, Ecole Polytechnique Fédérale de Lausanne, Lausanne, Swaziland, ⁵Radiology, University Hospital (CHUV), Lausanne, Switzerland

In order to explore the potential of volume-based morphometry for computer-aided diagnosis on an individual level, we evaluated a volume-based morphometric MRI analysis prototype for detection of cortical abnormalities in individual focal cortical dysplasia (FCD) patients for whom no lesion was reported after routine MR exam. Using intracranial EEG as the gold standard, the results of a performed ROC analysis show good detection performance with AUC=0.882, sensitivity =93.88%, and specificity 79.57% at the optimal cut-off point. These results suggest that such automated methods provide additional value for MR-based diagnostics.

1247



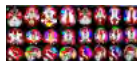
High-quality MRS detects metabolic changes in mice at different stages of prion disease

Eleni Demetriou¹, Mohamed Tachroud², Karin Shmueli³, Mark Farrow⁴, and Xavier Golay¹

¹Brain Repair and Rehabilitation, Institute of Neurology, London, United Kingdom, ²Brain repair and rehabilitation, Institute of Neurology, London, United Kingdom, ³Medical Physics and Biomedical Engineering, University College of London, London, United Kingdom, ⁴MRC prion unit,

The neurochemical profile of prion disease in mice at different disease stages was evaluated using high-quality MR spectra obtained in thalamus. Seven metabolites were measured in vivo and longitudinally providing substantial metabolic information. Metabolic changes were obtained throughout the disease course, however only glutamate and myo-inositol were significantly different at all stages of the disease. We conclude that MR spectroscopy provides additional information over previous histological studies [1].

1248



Alterations Of Functional Connectivity in Resting-State Networks Following Medial Temporal Lobectomy in Patients With Unilateral Hippocampal Sclerosis

Arzu Ceylan Has¹, Irsel Tezer², Burcak Bilginer³, Serap Saygi², and Kader Karli Oguz⁴

¹National Magnetic Resonance Research Center (UMRAM), Bilkent University, Ankara, Turkey, ²Department of Neurology, Hacettepe University, Ankara, Turkey, ³Department of Neurosurgery, Hacettepe University, Ankara, Turkey, ⁴Department of Radiology, Hacettepe University, Ankara, Turkey

Temporal lobe epilepsy with unilateral hippocampal sclerosis patients benefit from the medial temporal lobectomy. Since the hippocampus is involved in many cognitive tasks, we hypothesized that resting-state(rs) network alterations would occur in these patients following temporal lobectomy. All patients had pre- and post-operative neurocognitive tests, rs-fMRI and structural T1-weighted imaging. Post-operative studies were performed at 1-year-follow-up. Following temporal lobectomy, left- and right-HS patients showed significantly decreased and increased activations in default-mode-network and fronto-parietal-network. A pre-operative extent of tissue damage or dominancy of the epileptic hemisphere may be responsible for the different patterns of adaptation/change of brain networks after lobectomy.

1249



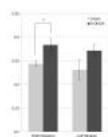
Investigation of the Healthy Nigrosome-1 for the Diagnosis of Parkinson's Disease using Multiple Susceptibility based MRI Techniques

Kyung Mi Lee¹ and Hyug-Gi Kim²

¹Radiology, Kyung Hee University Hospital, Seoul, Korea, Republic of, ²Biomedical Engineering, College of Electronic Information Engineering, Kyung Hee University, Gyeonggi-do, Korea, Republic of

Nigrosome-1 region that is affected to the loss of dopaminergic neurons is one of the important characteristics of Parkinson's disease (PD). To evaluate the early stage of PD and investigate the main mechanisms of nigrosome degeneration using MR images, the susceptibility based MRI techniques were performed: R2* (=1/T2*) map, SWI and QSM map in seven elderly healthy subjects that are reference subjects for PD.

1250



Structural and Functional Reorganization of the Rat Brain in the 6-OHDA Model of Parkinson's Disease

Vincent Perlberg^{1,2}, Benjamin Butler³, Justine Lambert³, Romain Valabregue³, Anne-Laure Privat³, Chantal François³, Stéphane Lehéricy^{4,5}, and Alexandra Petiet^{4,5}

¹Bioinformatics and Biostatistics Platform, Brain and Spine Institute, Paris, France, ²UPMC/Inserm UMR1146 / CNRS UMR7371, Paris, France, ³Brain and Spine Institute, Paris, France, ⁴Center for Neuroimaging Research, Brain and Spine Institute, Paris, France, ⁵UPMC/Inserm UMR1127 / CNRS UMR7225, Paris, France

Parkinson's disease (PD) is characterized by neurodegeneration of the dopaminergic neurons in the substantia nigra pars compacta (SNC), which can be recapitulated in the 6-hydroxydopamine (6-OHDA) rat model. To evaluate structural and functional cerebral reorganization after induction of the lesion, we performed a longitudinal study up to 6 weeks using diffusion and resting-state functional MRI. Our results showed increased fractional anisotropy in the striatum ipsilateral to the lesion and increased bilateral functional connectivity between the striatum, the globus pallidus and the sensorimotor cortex in the 6-OHDA group. These results will help improve our understanding of cerebral alterations and reorganization in PD pathology.

1251



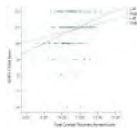
Towards Quantitation of Nerve Trauma Using SHINKEI Based MR Neurography of Brachial Plexus at 1.5T

Prashant Nair¹, Lalit Gupta², Rajagopal K.V.¹, Praveen Mathew¹, Rolla Narayana Krishna², and Indrajit Saha³

¹Radiodiagnosis and Imaging, KMCH, Manipal University, Manipal, India, ²Philips Healthcare, Bangalore, India, Bangalore, India, ³ Philips India Ltd., Gurgaon, India, Gurgaon, India

The purpose of this study was to make an image processing marker using 3D SHINKEI based MR Neurography images of brachial plexus to identify nerve conditions and establish the condition for normalcy and abnormality by extracting the contrast property from the second order gray level Co-occurrence Matrix. The images from fourteen healthy volunteers and three patients were studied. The contrast in perpendicular direction of nerve anatomy was twice as high as other contrasts among normal subjects, while in patients, there was no such difference. Our ongoing work has the potential to classify the severity of the detected nerve lesion.

1252



Neuropsychological Measures of Parietal Lobe Thickness

Christopher Bird¹, Sarah Banks¹, and Dietmar Cordes¹

¹Cleveland Clinic Lou Ruvo Center For Brain Health, Las Vegas, NV, United States

We report relationships between cortical thickness as assessed with Freesurfer, and performance on three tests: Judgment of Line Orientation (JLO), Brief Visuospatial Memory Test Copy Trial (BVMT-C), and Block Design (BD) in 122 consecutive memory clinic

patients. Geometric construction tests (BD) was more sensitive to right sided thickness, while judgment of angles and simple construction of shapes was more sensitive to the left parietal lobe.

1253



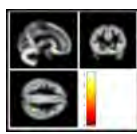
Conformity between Brain structures and Neuropsychological tests in Methamphetamine Abusers

Arpit Rodkong¹, Nuttawadee Intachai¹, Suwit Saekho^{1,2}, Apinun Aramrattana³, Kanok Uttawichai⁴, Mekkla Thomson⁵, Bangorn Sirirojn⁶, Daralak Thavornprasit⁶, Sineenart Taejaroenkul⁶, Kamolrawee Sintupat⁶, Victor Valcour⁷, Robert Paul⁸, and Napapon Sailasuta⁹

¹*Radiological Technology, Chiang Mai University, Chiang Mai, Thailand*, ²*Biomedical Engineering Center, Chiang Mai University, Chiang Mai, Thailand*, ³*Family Medicine, Chiang Mai University, Chiang Mai, Thailand*, ⁴*Thanyarak Hospital, Chiang Mai, Thailand*, ⁵*Westat, Rockville, MD, United States*, ⁶*Research Institute for Health Sciences, Chiang Mai, Thailand*, ⁷*Neurology, University of California, San Francisco, San Francisco, CA, United States*, ⁸*Psychology, University of Missouri, St. Louis, MO, United States*, ⁹*Huntington Medical Research Institute, Pasadena, CA, United States*

Magnetic resonance imaging (MRI) studies show evidence of brain alteration in Methamphetamine (MA) users. We compare brain structures including gray matter (GM), white matter (WM) and cortical thickness between MA abusers and Healthy control (HC) group, and explore relationship between brain structures and neuropsychological performance (NP) in MA compared with HC. The results demonstrated that MA group revealed poorer cognitive function and reduced volumetrics in critical brain regions that underlie cognitive performance compared to that of the HC group.

1254



Modifications of gray matter volume in migraine patients over four years: a tensor-based morphometry study

Elisabetta Pagani¹, Maria Assunta Rocca^{1,2}, Roberta Messina¹, Bruno Colombo², Giancarlo Comi², Andrea Fallini³, and Massimo Filippi^{1,2}

¹*Neuroimaging Research Unit, San Raffaele Scientific Institute, Vita-Salute San Raffaele University, Milan, Italy*, ²*Department of Neurology, San Raffaele Scientific Institute, Vita-Salute San Raffaele University, Milan, Italy*, ³*Department of Neuroradiology, San Raffaele Scientific Institute, Vita-Salute San Raffaele University, Milan, Italy*

Aim of the study was to explore longitudinal gray matter (GM) changes over a four-year follow up in migraine patients and their association with patients' clinical characteristics and disease activity. Brain dual-echo and 3D T1-weighted scans were acquired from 25 patients with migraine and 25 healthy controls at baseline and after 4 years. At follow up, compared to controls, migraine patients had an increased volume of fronto-parietal regions, whereas they developed atrophy of the right thalamus and occipital areas. The migraine brain changes dynamically over time. Various pathophysiological mechanism might affect different brain regions in migraineurs after 4 years.

Traditional Poster

Neurodegeneration: Alzheimer's

Exhibition Hall

Monday, May 9, 2016: 10:45 - 12:45

1255



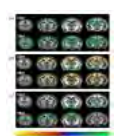
3D Texture Analyses of Quantitative Susceptibility Maps to Differentiate Alzheimer's Disease from Cognitive Normal and Mild Cognitive Impairment

Eo-Jin Hwang¹, Hyug-Gi Kim¹, Chanhee Lee¹, Hak Young Rhee², Chang-Woo Ryu¹, Dal-Mo Yang¹, Tian Liu³, Yi Wang³, and Geon-Ho Jahng¹

¹*Department of Radiology, Kyung Hee University Hospital at Gangdong, Kyung Hee University, Seoul, Korea, Republic of*, ²*Department of Neurology, Kyung Hee University Hospital at Gangdong, Kyung Hee University, Seoul, Korea, Republic of*, ³*Biomedical Engineering and Radiology, Cornell University, New York, NY, United States*

To investigate QSM textures in the subjects with cognitively normal (CN), mild cognitive impairment (MCI) and Alzheimer's disease (AD) and to compare the QSM texture results with those of 3D T1W images, 18 elderly CN, 18 MCI, and 18 AD subjects were scanned both 3D multi-echo gradient-echo and 3D T1-weighted sequences. The 1st and 2nd ordered texture parameters of the QSMs and 3DT1W images were calculated and compared among the three subject groups to differentiate the subject groups. Our results suggest that the demyelination effect could be more dominant than the metal accumulations in AD progression.

1256



Longitudinal DTI detects ApoE isoforms dependent change in white matter

Ling Yun Yeow¹, Xuan Vinh To¹, Xin Hong¹, Boon Seng Wong², and Kai-Hsiang Chuang^{1,2}

¹*Neuro Imaging Group, Singapore Bioimaging Consortium, A*STAR, Singapore, Singapore*, ²*Department of Physiology, National University of Singapore, Singapore, Singapore*

To understand the genetic influence of ApoE isoforms on the brain aging, we conducted longitudinal diffusion tensor imaging (DTI) on transgenic mice expressing human ApoE3 (hApoE3) or hApoE4 gene. Mean FA showed a general trend of hApoE4 » WT > hApoE3 from 12 to 18 months of age. There was age-dependent reduction of FA in all the animals, which was due to increased radial diffusivity. The hApoE4 mice also showed larger increase of parallel diffusivity. These indicate ApoE isoform dependent axonal change with aging.

1257

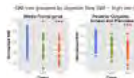


Assessment of metabolism, perfusion and diffusion changes in the hippocampal subfields of MCI and AD using simultaneous PET-MR

Maged Goubran¹, Audrey Peiwan Fan¹, Praveen Gulaka¹, David Douglas¹, Steven Chao², Andrew 5 Graduates of Quon¹, Greg Zaharchuk¹, Minal Vasanawala¹, and Michael Zeineh¹

Hippocampal subfields are selectively affected in AD, however the hippocampus is assessed as a whole in PET studies. In this work we investigate the metabolic, perfusion and diffusion changes within the subfields of patients with MCI and AD using a simultaneous PET-MR scanner. Our preliminary results demonstrate significant reduction in metabolism and perfusion that are appreciated on the subfield level but not when assessing the hippocampus as a whole. This work suggests that subfield assessment is potentially more sensitive to pathological changes in AD than whole hippocampus analysis, and highlights the utility of simultaneous PET-MR as a tool for discovering novel biomarkers in neurodegenerative diseases.

1258



Brain iron accumulation in Alzheimer's disease evaluated using susceptibility-weighted imaging

Amir Fazlollahi^{1,2}, Pierick Bourgeat¹, Ashley I. Bush^{3,4}, Fabrice Meriaudeau², David Ames⁴, Colin L. Masters^{3,4}, Christopher C. Rowe^{4,5}, Victor L. Villemagne^{3,4,5}, and Olivier Salvado¹

¹Australian e-Health Research centre, CSIRO, Brisbane, Australia, ²University of Burgundy, Le Creusot, France, ³Florey Institute of Neuroscience & Mental Health, Melbourne, Australia, ⁴The University of Melbourne, Melbourne, Australia, ⁵Austin Health, Melbourne, Australia

MRI susceptibility weighted imaging (SWI) has shown a promising sensitivity in visualizing iron deposits, while less effort is made to establish a pseudo-quantitative estimate of iron. In this study, an image processing framework was employed to normalize the uncalibrated intensity of SWI with respect to the corresponding value of cerebrospinal fluid. After excluding large detectable veins, the resulting pseudo-quantitative image along with a standard brain atlas, were used to compute regional concentrations of iron in a cohort of Alzheimer's disease. A group-wise analysis was then showed a stepwise increment in SWI-iron along the progression of the disease.

1259



Cerebral Blood Flow Measured by Arterial Spin Labeled MRI Predicts Longitudinal Hippocampal Atrophy in Mild Cognitive Impairment

Long Xie^{1,2}, Sandhitsu R. Das^{1,3}, Arun Pilania^{3,4}, Molly Daffner^{3,4}, Grace E. Stockbower^{3,4}, Sudipto Dolui^{3,5,6}, John A. Detre^{3,5,6}, and David A. Wolk^{3,4}

¹Penn Image Computing and Science Laboratory (PICSL), Department of Radiology, University of Pennsylvania, Philadelphia, PA, United States,

²Department of Bioengineering, University of Pennsylvania, Philadelphia, PA, United States, ³Department of Neurology, University of Pennsylvania, Philadelphia, PA, United States, ⁴Penn Memory Center, University of Pennsylvania, Philadelphia, PA, United States, ⁵Center for Functional Neuroimaging, Department of Radiology, University of Pennsylvania, Philadelphia, PA, United States, ⁶Department of Radiology, University of Pennsylvania, Philadelphia, PA, United States

In this study, we compared regional cerebral blood flow (CBF) measured by arterial spin labeled perfusion MRI (ASL-MRI) with baseline hippocampal volume from structural MRI in predicting likely Alzheimer's disease (AD) progression measured by longitudinal hippocampal atrophy. Stepwise linear regression analyses demonstrated that CBF measurements were significantly associated with longitudinal hippocampal atrophy in entire cohort, as well as just within the MCI patients, while baseline hippocampal volume does not provide complementary information. Our results indicate ASL-MRI could potentially have important utility in identifying candidates for AD related therapeutic intervention studies and clinical trials.

1260



Nested support vector machine applied to structural and diffusion MR features for Alzheimer's disease prediction

Giovanni Giulietti¹, Mara Cercignani², and Marco Bozzali¹

¹Neuroimaging Laboratory, Santa Lucia Foundation, Rome, Italy, ²Clinical Imaging Sciences Centre, Brighton and Sussex Medical School, University of Sussex, Brighton, United Kingdom

The current study is an application of **nested** support vector machine (**SVM**) to distinguish healthy subjects and patients with **Alzheimer's** disease using very few features coming from structural (T1) and diffusion (DWI) MR. After having segmented the T1 images in GM, WM and CSF, mean values of fractional_anisotropy, mean_diffusivity, radial_diffusivity and axial_diffusivity were computed in GM and WM; volume of GM and WM as percentage of total_intracranial_volume were also assessed. Therefore we computed **1023 different SVMs**, one for each possible combination of the 10 features. Surprisingly, the **WM diffusion measures** resulted to be the **most specific of dementia status**.

1261



Quantitative Susceptibility Mapping in Patients with Alzheimer's Disease and Mild Cognitive Impairment

Hyug-Gi Kim¹, Chan-Hee Lee¹, Chang-Woo Ryu², Soonchan Park², Hak Young Rhee³, Kyung Mi Lee⁴, Wook Jin², Dal-Mo Yang², Soo Yeol Lee¹, Tian Liu⁵, Yi Wang⁵, and Geon-Ho Jahng²

¹Biomedical Engineering, Kyung Hee University, Gyeonggi-do, Korea, Republic of, ²Radiology, Kyung Hee University Hospital at Gangdong, Seoul, Korea, Republic of, ³Neurology, Kyung Hee University Hospital at Gangdong, Seoul, Korea, Republic of, ⁴Radiology, Kyung Hee University Hospital, Seoul, Korea, Republic of, ⁵Biomedical Engineering and Radiology, Cornell University, New York, NY, United States

One of the important characteristics of Alzheimer's disease (AD) is the iron accumulations in the brain. To estimate the quantitative susceptibility effects in AD brain, the susceptibility changes were investigated in subjects with 19 cognitive normal (CN), 19 mild cognitive impairment (MCI) and 19 AD. Seven-echo 3D gradient-echo images were obtained to map quantitative susceptibility mapping (QSM) and 3D T1-weighted images using the MPRAGE sequence were also obtained to map gray matter volume (GMV). Both voxel-based and ROI-based analyses were performed to evaluate the group differences. The result showed that QSM can be useful to evaluate the AD brain.



Multilevel classification of Alzheimer's and Mild Cognitive Impairment patients by using Diffusion Tensor Imaging data

Ranganatha Sitaram¹, Josué Luiz Dalboni da Rocha^{2,3}, Ivanei Bramati⁴, Gabriel Coutinho⁴, and Fernanda Tovar Moll⁴

¹*Institute for Medical and Biological Engineering and Department of Psychiatry, Pontificia Universidad Católica de Chile, Santiago, Chile,*

²*Biomedical Engineering, University of Florida, Gainesville, FL, United States, ³University of Florida, Gainesville, FL, United States, ⁴Instituto D'Or de Pesquisa e Ensino, Rio de Janeiro, Brazil, Rio de Janeiro, Brazil*

The proposed novel approach is based on three levels of analyses of DTI data: 1) voxel level analysis of Fractional Anisotropy, 2) connection level based on fiber tracks between brain regions, and 3) network level based connections among multiple brain regions. This novel approach was applied to differentiate between AD, MCI and controls. We achieved accuracy of 93% between AD and controls, 90% between AD and MCI. Main discriminative areas were Hippocampal Cingulum and Parahippocampal Gyrus. The results suggest that our multilevel DTI analysis not only informs difference between brain conditions, but also shows strong potential as diagnostic tool.

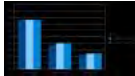


Correlation of 2-year longitudinal structural changes with basal CSF Alzheimer's Disease biomarkers in elderly cognitive healthy subjects

Carles Falcon^{1,2}, Alan Tucholka¹, Juan Domingo Gispert^{1,2}, Gemma Cristina Monte-Rubio³, Lorena Rami^{3,4}, and Jose Luis Molinuevo^{3,4}

¹*BarcelonaBeta Brain Research Center. Pasqual Maragall Foundation, Barcelona, Spain, ²CIBER-BBN, Barcelona, Spain, ³Institut d'Investigacions Biomediques August Pi i Sunyer (IDIBAPS), Barcelona, Spain, ⁴Neurology, Hospital Clinic of Barcelona, Barcelona, Spain*

We report the correlation of two-year gray matter (GM) changes with basal levels of A β 42, p-tau and p-tau/A β 42 in CSF on a sample of 62 cognitively normal subjects (18 A β 42 positive and 26 p-tau positive), aged 60-80. GM volume decrease was correlated with A β 42 in medial and orbital frontal, precuneus, cingulate, medial temporal regions and cerebellum. Correlations with p-tau were located in left hippocampus, parahippocampus and striatal nuclei and with p-tau/A β 42 in ventral and medial temporal areas. We conclude that diverse pathological mechanisms in the preclinical stage could underpin atrophy rates in different regions known to be altered in AD



Impact of image acquisition systems on Alzheimer's disease-related atrophy detection

Pavel Falkovskiy^{1,2,3}, Bénédicte Maréchal^{1,2,3}, Tobias Kober^{1,2,3}, Philippe Maeder¹, Reto Meuli¹, Jean-Philippe Thiran³, and Alexis Roche^{1,2,3}

¹*Department of Radiology, University Hospital (CHUV), Lausanne, Switzerland, ²Advanced Clinical Imaging Technology (HC CMEA SUI DI BM PI), Siemens Healthcare AG, Lausanne, Switzerland, ³LTSS, École Polytechnique Fédérale de Lausanne, Lausanne, Switzerland*

We investigate the potentially confounding effect of using different image acquisition systems (field strength, manufacturers) on automated Alzheimer's disease detection using standardized Alzheimer's Disease Neuroimaging Initiative (ADNI) data. Disease classifiers based on brain volumetric markers computed by FreeSurfer and the MorphoBox prototype were evaluated with and without correcting for variations in acquisition systems. While the correction overall had limited impact on Alzheimer's disease detection, it enabled significant error reduction for the classification of mildly cognitively impaired patients versus both healthy controls and Alzheimer's patients.



Regional CBF and Cognition in Longitudinal ADNI Disease Groups

Sudipto Dolu^{1,2}, Long Xie^{3,4}, David A. Wolk², and John A. Detre^{1,2}

¹*Department of Radiology, University of Pennsylvania, Philadelphia, PA, United States, ²Department of Neurology, University of Pennsylvania, Philadelphia, PA, United States, ³Penn Image Computing and Science Laboratory (PICSL), Department of Radiology, University of Pennsylvania, Philadelphia, PA, United States, ⁴Department of Bioengineering, University of Pennsylvania, Philadelphia, PA, United States*

We evaluated longitudinal changes in regional cerebral blood flow (CBF) for patients at different stages of Alzheimer's disease and correlated CBF with cognition assessed by the clinical dementia rating scale sum of boxes (CDR-SB). Mean CBF in precuneus, posterior cingulate cortex (PCC) and hippocampus were statistically significantly correlated with CDR-SB. However, longitudinal changes in CDR-SB only correlated with CBF change in PCC. There was a statistically significant group difference in baseline PCC-CBF between incipient Alzheimer's patients whose cognitive function deteriorated versus those who didn't, demonstrating that CBF can be used as a predictor of disease progression.



The effect of the medical food Souvenaid on brain phospholipid metabolism in patients with mild Alzheimer's disease: a randomised controlled 31P-MRS study

Anne Rijpma^{1,2}, Marinette van der Graaf^{3,4}, Olga Meulenbroek^{1,2}, Marieke Lansbergen⁵, John Sijben⁵, Marcel Olde Rikkert^{1,2}, and Arend Heerschap³

¹*Geriatric Medicine, Radboud university medical center, Nijmegen, Netherlands, ²Radboud Alzheimer Centre, Donders Institute for Brain, Cognition and Behaviour, Radboud university medical center, Nijmegen, Netherlands, ³Radiology and Nuclear Medicine, Radboud university medical center, Nijmegen, Netherlands, ⁴Paediatrics, Radboud university medical center, Nijmegen, Netherlands, ⁵Nutricia Research, Nutricia Advanced Medical Nutrition, Utrecht, Netherlands*

Loss of neuronal membranes and synaptic integrity are major factors that contribute to the development of cognitive impairment in individuals with Alzheimer's disease (AD). Membrane phospholipid metabolism can be investigated non-invasively using phosphorus Magnetic Resonance Spectroscopy (^{31}P -MRS). Here we report on the results of a double-blind randomised controlled study investigating the effects of the medical food Souvenaid on brain phospholipid metabolism in patients with mild AD. 3D ^{31}P -MRS imaging was performed at baseline and after 4 weeks intervention.



The Influence of Cerebrovascular Disease on Structural Covariance Networks in Prodromal and Early Stages of Alzheimer's Disease

Joanna Su Xian Chong¹, Yng Miin Loke¹, Saima Hilal^{2,3}, Mohammad Kamran Ikram^{3,4}, Xin Xu^{2,3}, Boon Yeow Tan⁵, Narayanaswamy Venketasubramanian⁶, Christopher Li-Hsian Chen^{2,3}, and Juan Zhou^{1,7}

¹Centre for Cognitive Neuroscience, Neuroscience and Behavioural Disorders Programme, Duke-National University of Singapore Graduate Medical School, Singapore, Singapore, ²Department of Pharmacology, National University Health System, Clinical Research Centre, Singapore, Singapore, ³Memory Ageing & Cognition Centre, National University Health System, Singapore, Singapore, ⁴Duke-National University of Singapore Graduate Medical School, Singapore, Singapore, ⁵St. Luke's Hospital, Singapore, Singapore, ⁶Raffles Neuroscience Centre, Raffles Hospital, Singapore, Singapore, ⁷Clinical Imaging Research Centre, The Agency for Science, Technology and Research and National University of Singapore, Singapore, Singapore

Cerebrovascular disease (CVD) frequently co-occurs with Alzheimer's disease (AD), however its effects on the organization of brain networks in AD patients remain unknown. This study aimed to examine the influence of CVD on grey matter (GM) structural covariance (SC) networks in prodromal and early AD patients. Divergent changes in GM volumes and SC of higher-order networks were found between CVD and non-CVD subtypes. Specifically, the default mode network showed changes in non-CVD subtypes but was spared in CVD subtypes. These findings highlight the different pathophysiology underlying AD patients with CVD and those without CVD.



The joint effects of APOE genotype and age on functional network in non-demented old adults

Liang Gong¹, Hao Su¹, Cancan He¹, Qing Ye¹, Feng Bai¹, Chunming Xie¹, and Zhijun Zhang¹

¹Department of Neurology, Affiliated ZhongDa Hospital, School of Medicine, Southeast University, Nanjing, China, People's Republic of

A cross-sectional resting-state functional magnetic resonance imaging study was conducted with 84 aMCI subjects (including 9 APOE ε2, 45 ε3, 28 ε4 carriers) and well-matched 124 cognitively normal (CN) healthy elders (including 35 APOE ε2, 43 ε3, 46 ε4 carriers). The finding revealed that the ε2 carriers and ε4 carriers showed convergent effects on right AFC but divergent effects on left AFC network when CN compared to aMCI patients. Interactive effects of APOE genotypes and age on AFC network further revealed neural basis of ten years earlier on the age of onset in aMCI patients. Further, mediation analysis suggested that connectivity strength mediated the effects of APOE genotypes and age on the cognitive function in aMCI patients.

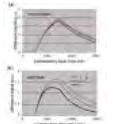


Intrinsic Functional Connectivities of "Where" Visual Network in Patients with Mild Cognitive Impairment

Yanjia Deng¹, Lin Shi^{2,3}, Defeng Wang^{1,4,5}, and ADNI Alzheimer's Disease Neuroimaging Initiative⁶

¹Imaging and Interventional Radiology, The Chinese University of Hong Kong, Hong Kong, China, People's Republic of, ²Department of Medicine and Therapeutics, The Chinese University of Hong Kong, Hong Kong, China, People's Republic of, ³Chow Yuk Ho Technology Centre for Innovative Medicine, The Chinese University of Hong Kong, Hong Kong, China, People's Republic of, ⁴Shenzhen Research Institute, The Chinese University of Hong Kong, Shenzhen, China, People's Republic of, ⁵Research Center for Medical Image Computing, Department of Imaging and Interventional Radiology, The Chinese University of Hong Kong, Hong Kong, China, People's Republic of, ⁶Los Angeles, CA, United States

In order to extend the knowledge on the impaired pattern of "where" visual perception in mild cognitive impairment (MCI) patients, we investigated the connectivity of the "where" visual networks in terms of intrinsic interaction in early and late MCI patients. Resting-state functional MRI data of late MCI, early MCI and matched healthy controls from Alzheimer's Disease Neuroimaging Initiative dataset were analyzed to investigate the alterations of interregional connections of "where" visual networks. Significant increased interregional connectivities in late MCI patients were found, which may extend the current knowledge on the pattern of visual perceptual impairment in MCI patients.

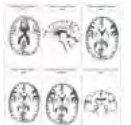


Estimation of Water Exchange across the Blood Brain Barrier using Contrast-enhanced ASL

Helen Beaumont¹, Aimee Pearson², Matthias J van Osch³, and Laura M Parkes¹

¹Centre for Imaging Sciences, University of Manchester, Manchester, United Kingdom, ²Dept of Physics, University of Manchester, Manchester, United Kingdom, ³C.J. Gorter Center for High Field MRI, Dept of Radiology, Leiden University Medical Centre, Leiden, Netherlands

This study investigates the possibility of estimating water exchange across the blood-brain barrier by manipulating the T_1 of blood using a gadolinium-based contrast agent, together with pre- and post-contrast Arterial Spin Labelling measurements. Gadolinium lowers the T_1 of blood, but not of tissue, allowing the proportions of label in intra- and extra-vascular tissue to be estimated. A Look-Locker readout was used to measure the temporal evolution of the ASL signal at four doses of contrast agent. Even with T_1 of approximately 500ms, an ASL subtraction signal was still detected at an inversion time of 2s, indicating that labelled blood water has exchanged with tissue water.



Profiling patterns of white matter injury in normal pressure hydrocephalus pre- and post-intervention using diffusion tensor imaging

Nicole Chwee Har Keong^{1,2}, Alonso Pena³, Stephen J Price⁴, Marek Czosnyka⁴, Zofia Czosnyka⁴, Elise DeVito⁵, Charlotte Housden⁶,

Jonathan H Gillard⁷, Barbara Sahakian⁶, and John D Pickard⁴

¹Neurosurgery, National Neuroscience Institute, Singapore, Singapore, ²Neurosurgery, University of Cambridge, Cambridge, United Kingdom,

³SDA Bocconi School of Management, Milan, Italy, ⁴Neurosurgical Division, Dept of Clinical Neurosciences, University of Cambridge Hospitals NHS Foundation Trust, Cambridge, United Kingdom, ⁵Dept of Psychiatry, Yale University School of Medicine, New Haven, CT, United States,

⁶Department of Psychiatry and MRC/Wellcome Trust Behavioural and Clinical Neuroscience Institute, University of Cambridge, Cambridge, United Kingdom, ⁷Department of Radiology, University of Cambridge, Cambridge, United Kingdom

Normal pressure hydrocephalus (NPH) is a confounding condition of gait disturbance, cognitive decline and urinary incontinence

remediable with surgical intervention. We have used diffusion tensor imaging (DTI) to demonstrate patterns of white matter injury pre- and post-surgical intervention

1272

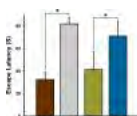


Quantifying the effects of age and the apolipoprotein E $\epsilon 4$ allele on Alzheimer's disease progression
Hao Shu¹, Guangyu Chen¹, Gang Chen¹, B. Douglas Ward¹, Piero G. Antuono², and Shi-Jiang Li¹

¹Department of Biophysics, Medical College of Wisconsin, Milwaukee, WI, United States, ²Department of Neurology, Medical College of Wisconsin, Milwaukee, WI, United States

Aging and the apolipoprotein E (APOE) $\epsilon 4$ allele are two established factors advancing Alzheimer's disease (AD) progression; however, the extent to which these factors effect AD remains unclear. In this study, we employed the event-based probabilistic model to develop an index for characterizing Alzheimer's disease risk event (CARE); we then used the CARE index to quantify the effects of age and the APOE $\epsilon 4$ allele on AD progression. This study demonstrated an aging-related increase in CARE index scores and its exacerbation by the APOE $\epsilon 4$ allele, thus providing a surrogate to quantitatively assess aging and the APOE $\epsilon 4$ allele modulations on AD progression.

1273



Dissecting the Role of Gender in Alzheimer's Disease: A ^1H - $[^{13}\text{C}]$ -NMR Study in APP-PS1 Mice
Anant Bahadur Patel¹, Niharika Rajnala¹, and Kamal Saba¹

¹NMR Microimaging and Spectroscopy, CSIR-Centre for Cellular and Molecular Biology, Hyderabad, India

The population of Alzheimer's disease (AD) is increasing due to increased longevity in human. The dementing condition associated with AD is reported to be more in female than male. In this study, we explored the neurotransmitter metabolism in APP-PS1 female mice, and compared with age matched males, using ^1H - $[^{13}\text{C}]$ -NMR spectroscopy following an administration of $[1,6-^{13}\text{C}_2]$ glucose. The cerebral metabolic rates of glucose oxidation by glutamatergic and GABAergic neurons was found to be reduced in the cerebral cortex, striatum and hippocampus of the transgenic male mice. In contrary, transgenic female mice did not show change in metabolic rates when compared with wild type controls.

1274



Analysis of Functional Connectivity between Hippocampus Subfields and Perirhinal / Parahippocampal in patient with Mild Cognitive Impairment and Alzheimer's Disease
Yafei Wang¹, Yu Sun¹, Lingyi Xu¹, Yue Zhang¹, Jiaming Lu², Bing Liu³, Bing Zhang², and Suiren Wan¹

¹The Laboratory for Medical Electronics, School of Biological Sciences and Medical Engineering, Southeast University, Nanjing, China, People's Republic of, ²Department of Radiology, The affiliated Drum Tower hospital of Nanjing University Medical School, Nanjing, China, People's Republic of, ³National Laboratory of Pattern Recognition, Institute of Automation, Chinese Academy of Science, Beijing, China, People's Republic of

The functional connectivity between hippocampus subfields and perirhinal cortices (PRC)/parahippocampal cortices (PHC) among normal cognition controls (NC), mild cognitive impairment (MCI) and Alzheimer's disease (AD) was investigated in this study. The result shows the significant differences of functional connectivity in 3 pairs of ROIs among NC, AD and MCI. It may reveal that the difference of functional connectivity can be the marker to diagnosis AD and MCI.

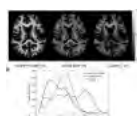
Traditional Poster

Myelin Measurement

Exhibition Hall

Monday, May 9, 2016: 10:45 - 12:45

1275

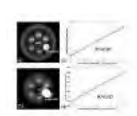


Analyzing Myelin Water Fraction using mRISE
Fang Liu¹, Andrew Alexander², and Alexey Samsonov¹

¹Department of Radiology, University of Wisconsin-Madison, Madison, WI, United States, ²Department of Medical Physics, University of Wisconsin-Madison, Madison, WI, United States

Myelin, a thin layer of sheath-like cell, provides an important role in protecting nerve axon and accelerating neural impulse transmission. Myelin water fraction (MWF) mapping has been recently proposed for assessing myelin content in-vivo. One quantitative MR method called mDESPOT has shown promising results for assessing myelin content. However, this method is lack of consideration of magnetization transfer (MT) effect leading to the complication of interpretation for MWF values. In this study, we proposed a method called mRISE to account for MT effect and investigate the feasibility of assessing myelin content with MT-insensitive MWF as well as additional MT parameters.

1276



Quantification of Myelin by Solid-State MRI of the Lipid Matrix Protons
Cheng Li¹, Alan C. Seifert², Suzanne L. Wehrli³, and Felix W. Wehrli¹

¹Radiology, University of Pennsylvania, Philadelphia, PA, United States, ²Translational and Molecular Imaging Institute, Icahn School of Medicine at Mount Sinai, New York, NY, United States, ³NMR Core Facility, Children's Hospital of Philadelphia, Philadelphia, PA, United States

Myelin is a lamellar liquid crystal consisting of a variety of phospholipids and cholesterol, water and proteins. So far quantitative

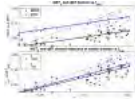
information on myelin density has been obtained primarily indirectly via myelin water quantification or quantitative magnetization transfer. Here, we examined 3D UTE and ZTE methods at 400 MHz demonstrating the feasibility of MRI quantification of reconstituted myelin suspended in D₂O as well as of myelin in lamb spinal cord *in situ*. Results show the magnitude signal amplitude to be linearly correlated with actual myelin content, allowing estimation to be made of myelin fraction in neural tissues.

1277



Quantitative Estimates of Myelin Volume Fraction from T2 and Magnetization Transfer

Kathryn L West^{1,2}, Nathaniel D Kelm^{1,2}, Daniel F Gochberg^{2,3}, Robert P Carson⁴, Kevin C Ess⁴, and Mark D Does^{1,2}



¹Biomedical Engineering, Vanderbilt University, Nashville, TN, United States, ²Vanderbilt University Institute of Imaging Science, Vanderbilt University, Nashville, TN, United States, ³Radiology and Radiological Sciences, Vanderbilt University, Nashville, TN, United States, ⁴Neurology, Vanderbilt University, Nashville, TN, United States

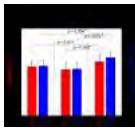
Multiexponential T₂ and quantitative magnetization transfer experiments provide quantitative measures of myelin water fraction (MWF) and bound pool fraction (BPF), respectively. These measures are known to correlate with myelin content in white matter; however discrepancies between the two have been shown. We display that by correcting for all proton pools contributing to MWF and BPF in white matter, we are able to show similar absolute measures of myelin content from MWF and BPF that are nearly equal to each other and close to myelin content measured by quantitative histology.

1278



A Quantitative Evaluation of Normal Appearing White Matter in Multiple Sclerosis: ViSTA MWI and SE MWI.

Joon Yul Choi¹, In Hye Jeong², Se-Hong Oh³, Chang-Hyun Oh^{4,5}, Ho Jin Kim², and Jongho Lee¹



¹Laboratory for Imaging Science and Technology, Department of Electrical and Computer Engineering, Seoul National University, Seoul, Korea, Republic of, ²Department of Neurology, Research Institute and Hospital of National Cancer Center, Goyang, Korea, Republic of, ³Imaging Institute, Cleveland Clinic Foundation, Cleveland, OH, United States, ⁴Department of Electronics and Information Engineering, Korea University, Seoul, Korea, Republic of, ⁵ICT Convergence Technology Team for Health&Safety, Korea University, Seoul, Korea, Republic of

This study investigated the applicability of ViSTA-MWI for the detection of myelin damage in MS. The results show ViSTA-MWI sensitively detects normal appearing white matter damage with better reliability than SE-MWI. Additionally, ViSTA-MWI can discriminate T₁ isointense lesions from T₁ hypointense lesions.

1279



Clinical Feasibility of Myelin Water Fraction (MWF) Imaging Based on 3D Non-selective GRASE Sequence

Dushyant Kumar^{1,2}, Patrick Borchert¹, Jens Fiehler¹, Susanne Siemonsen^{1,2}, and Jan Sedlacik¹

¹Dept. of Diagnostic and Interventional Radiology, Universitätsklinikum Hamburg-Eppendorf, Hamburg, Germany, ²Institute of Neuroimmunology and Multiple Sclerosis, Universitätsklinikum Hamburg-Eppendorf, Hamburg, Germany

Problem: The clinical utility of myelin imaging based on "gold standard" multi echo spin echo (MESE) T2 relaxometry is currently impeded due to requirement of high SNR and need to account for contributions from stimulated pathways. We compare faster GRASE based myelin quantification against those from MESE. Methods: 3D non-selective GRASE and MESE were optimized. Implemented post processing method combines T2-decay model based extended phase graph with spatial regularization framework to improve on noise robustness and accurately account for B1-error. Results & Conclusions: Results demonstrate good consistency between MWF-maps from both sequences, except in left part of frontal brain.

1280



Water content changes in new multiple sclerosis lesions have minimal effect on myelin water fraction

Irene Vavasour¹, Kimberley Chang², Anna Combes³, Sandra Meyers⁴, Shannon Kolind², Alexander Rauscher⁵, David Li¹, Anthony Traboulsee², Alex MacKay^{1,4}, and Cornelia Laule^{1,6}

¹Radiology, University of British Columbia, Vancouver, BC, Canada, ²Medicine, University of British Columbia, Vancouver, BC, Canada,

³Neuroimaging, King's College London, London, United Kingdom, ⁴Physics and Astronomy, University of British Columbia, Vancouver, BC, Canada, ⁵Pediatrics, University of British Columbia, Vancouver, BC, Canada, ⁶Pathology and Laboratory Medicine, University of British Columbia, Vancouver, BC, Canada

Myelin water fraction (MWF) is a useful technique for measuring myelination changes *in vivo*. However, since MWF is the fraction of myelin water over the total water, changes in water content (WC) can influence this measurement. This is particularly relevant in new multiple sclerosis (MS) lesions which may have demyelination but also show significant increases in WC at first appearance that resolve at later times. We compared MWF and myelin water content (MWC=MWF×WC) in new MS lesions. Similar patterns of change were seen with both MWF and MWC indicating that changes in WC had minimal effect on the MWF.

1281



Using T1 and Quantitative Magnetization Transfer to Monitor Tissue Myelin Content in the Lyssolecithin Model of Multiple Sclerosis

Raveena Dhaliwal^{1,2,3}, Daniel J. Korchinski^{1,2,3}, Samuel K. Jensen^{1,2}, V. Wee Yong^{1,2}, and Jeff F. Dunn^{1,2,3}

¹Neuroscience, University of Calgary, Calgary, AB, Canada, ²Hotchkiss Brain Institute, Calgary, AB, Canada, ³Radiology, University of Calgary, Calgary, AB, Canada

Multiple Sclerosis requires treatments that stimulate remyelination and reduce demyelination. Currently, both T1 and the quantitative magnetization transfer parameter bound pool fraction (f) have been found to correlate strongly with myelin content but little is known about the sensitivity of these techniques at different signal to noise ratios. This work demonstrates that T1 is highly sensitive to changes in myelin content but f can miss significant differences in tissue myelin content at a standard signal to noise. MS treatments should be

developed using a multi-modal approach that combines techniques with high sensitivity (T1) and those that have high specificity (f).

1282

Longitudinal Observation of Individual Multiple Sclerosis White Matter Lesions Using Quantitative Myelin Imaging

Hagen H Kitzler¹, Köhler Caroline¹, Wahl Hannes¹, Eisele C Judith², Sean C Deoni³, Brian K Rutt⁴, Tjalf Ziemssen², and Jennifer Linn¹

¹Neuroradiology, Technische Universität Dresden, Dresden, Germany, ²Neurology, Technische Universität Dresden, Dresden, Germany,

³Children's Hospital, Colorado, University of Colorado Medical School, Denver, CO, United States, ⁴Radiology, Stanford University, Stanford, CA, United States

Myelin Imaging is a potential tool to study demyelination and remyelination in inflammatory central nervous system diseases. This work presents a specific approach of tracking the individual myelination in single Multiple Sclerosis lesions and their pattern in Clinically Isolated Syndrome and early MS. Within n = 137 lesions of n = 15 patients we found 25% constant myelin loss, 14% permanent myelin regain, 56% fluctuating myelin content, and, 5% stable myelin reduction. These findings demonstrate an *in vivo* measurable highly dynamic individual lesion myelination status in inflammatory early disease. This method may facilitate to observe damage and reparative mechanism distribution in individual patients.

1283



Direct phase imaging of myelin: a validation study using ultrashort echo time (UTE) sequence and myelin phantoms

Qun He^{1,2}, Vipul Sheth¹, Hongda Shao¹, Jun Chen¹, Graeme Bydder¹, and Jiang Du¹

¹University of California, San Diego, San Diego, CA, United States, ²Ningbo Jansen NMR Technology Co., Ltd., Cixi, Zhejiang, China, People's Republic of

Phase images have been a valuable source of contrast in applications such as venography and for depicting gray-white matter differences with high contrast in high field MR imaging. Phase differences evolve during typical TEs of 10 - 30ms in brain studies. It has been uncertain whether it would be possible to detect signal and obtain phase maps from ultrashort non-water protons in myelin which have typical mean T_{2s} of 0.2 - 0.5 ms. In this study single and bicomponent T_2^* were measured in bovine myelin lipid, brain extract, and myelin basic proton and synthetic myelin and high quality phase maps were produced in each case.

1284



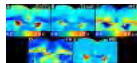
Direct IR-UTE imaging of myelin in healthy volunteers: the effect of T1 variation

Rong Luo¹, Soorena Azam ZAnganeh¹, Hongda Shao¹, Jun Chen¹, Graeme Bydder¹, and Jiang Du¹

¹Radiology, University of California, San Diego, San Diego, CA, United States

MS is a disease that relatively specifically affects myelin which is invisible with conventional sequences. Adiabatic inversion recovery prepared ultrashort echo time (IR-UTE) sequences have been proposed to directly image myelin protons and suppress the long T2 water signal by adiabatic inversion and signal nulling. However, water signal contamination is a major challenge. T1 variation in long T2 white matter, and thus imperfect choice of TI is a potential source of error in direct myelin imaging. We aimed to investigate the T1 variation in long T2 white matter in volunteers, and the effects of this on IR-UTE imaging of myelin.

1285



RAFF4 MRI in detection of demyelinating lesions induced by lysophosphatidyl choline injections in rat

Lauri J Lehto^{1,2}, Alejandra Sierra¹, Aloma Albors¹, Shalom Michaeli², Antti Nurmi³, Laura Tolppanen³, Lynn E Eberly⁴, Silvia Mangia², and Olli Gröhn^{1,2}

¹A. I. Virtanen Institute for Molecular Sciences, University of Eastern Finland, Kuopio, Finland, ²Center for Magnetic Resonance Research, University of Minnesota, Minneapolis, MN, United States, ³Charles River Laboratories, Kuopio, Finland, ⁴Division of Biostatistics, University of Minnesota, Minneapolis, MN, United States

An MRI contrast sensitive to demyelination would be invaluable in assessing a multitude of neurodegenerative diseases. Here, we demonstrate the benefits of a novel rotating frame method entitled Relaxation Along a Fictitious Field in the rotating frame of rank n (RAFFn) in detection of demyelinating lesions induced by lysophosphatidyl choline (LPC) injections in the rat corpus callosum (CC) and dorsal tegmental tract (DTG). RAFFn performed better than magnetization transfer in CC and DTG, and clearly outperformed diffusion tensor imaging in DTG, an area with heterogeneous fiber orientation distribution. Our results demonstrate high potential of RAFFn for imaging demyelinating lesions.

1286

Using diffusion MRI to study demyelination in cortex and deep gray matter in animal model of multiple sclerosis

Tina Pavlin^{1,2}, Vanja Flatberg³, Renate Gruner^{2,4}, Erlend Hodneland^{5,6}, and Stig Wergeland^{7,8}

¹Molecular Imaging Center, Department of Biomedicine, University of Bergen, Bergen, Norway, ²Department of Radiology, Haukeland University Hospital, Bergen, Norway, ³Department of Physics, University of Bergen, Bergen, Norway, ⁴Department of Physics and Technology, University of Bergen, Bergen, Norway, ⁵Christian Michelsen Research, Bergen, Norway, ⁶MedViz Research Cluster, Bergen, Norway, ⁷KG Jebsen Centre for MS-Research, Department of Clinical Medicine, University of Bergen, Bergen, Norway, ⁸The Norwegian Multiple Sclerosis Competence Centre, Department of Neurology, Haukeland University Hospital, Bergen, Norway

We have applied a biophysical model of diffusion to study dendrite density and diffusion in cortex and deep gray matter in an animal model of MS. We have performed DTI on mice brains ex-vivo at baseline, after 3 and 5 weeks of cuprizone exposure, and 4 weeks after termination of exposure. We observed a significant drop in neurite density and an increase in intra-axonal diffusion at 3 and 5 weeks of exposure, and a recovery to baseline values after remyelination. Our study shows the potential of DTI to detect subtle changes in myelin content in gray matter, thereby improving our understanding of the disease.

1287

The reproducibility and statistical power of brain T2 mapping at 7 tesla in naïve rats in vivo
Serguei Liachenko¹

¹National Center for Toxicological Research, US FDA, Jefferson, AR, United States

The baseline behavior of T₂ relaxation at 7 tesla in different parts of the rat brain was studied to provide the foundation for possible biomarker performance evaluation.

1288

High-resolution myelin water imaging using Direct Visualization of Short Transverse Relaxation Time Component (ViSTA) at 7T
Se-Hong Oh¹ and Mark J. Lowe¹

¹Imaging Institute, Cleveland Clinic Foundation, Cleveland, OH, United States

Recently, a new high quality myelin water imaging method, direct visualization of short transverse relaxation time component (ViSTA) has been developed. The ViSTA signal is primarily from short T₂* in the range of myelin water. In this study, we assessed 3D ViSTA sequence for 7T MR imaging which can cover the whole brain. Taking advantage of higher SNR at 7T, ViSTA using 7T MRI provided high-resolution and high-quality myelin water images generating a whole brain volume in clinically reasonable time. And the method successfully detected demyelinated MS lesions.

Traditional Poster

Multiple Sclerosis: Techniques

Exhibition Hall

Monday, May 9, 2016: 10:45 - 12:45

1289

Longitudinal automated detection of white-matter and cortical lesions in relapsing-remitting multiple sclerosis
Mário João Fartaria^{1,2}, Guillaume Bonnier^{1,2}, Tobias Kober^{1,2,3}, Alexis Roche^{1,2,3}, Bénédicte Maréchal^{1,2,3}, David Rotzinger², Myriam Schluep⁴, Renaud Du Pasquier⁴, Jean-Philippe Thiran^{2,3}, Gunnar Krueger^{2,3,5}, Reto Meuli², Meritxell Bach Cuadra^{2,3,6}, and Cristina Granziera^{1,4,7}

¹Advanced Clinical Imaging Technology (HC CMEA SUI DI BM PI), Siemens Healthcare AG, Lausanne, Switzerland, ²Department of Radiology, Centre Hospitalier Universitaire Vaudois (CHUV) and University of Lausanne (UNIL), Lausanne, Switzerland, ³Signal Processing Laboratory (LTS 5), Ecole Polytechnique Fédérale de Lausanne (EPFL), Lausanne, Switzerland, ⁴Neuroimmunology Unit, Neurology, Department of Clinical Neurosciences, Centre Hospitalier Universitaire Vaudois (CHUV) and University of Lausanne (UNIL), Lausanne, Switzerland, ⁵Siemens Medical Solutions USA, Inc., Boston, MA, United States, ⁶Signal Processing Core, Centre d'Imagerie BioMédicale (CIBM), Lausanne, Switzerland, ⁷Martinos Center for Biomedical Imaging, Massachusetts General Hospital and Harvard Medical School, Boston, MA, United States

Magnetic Resonance Imaging(MRI) plays an important role for lesion assessment in early stages of Multiple Sclerosis(MS). This work aims at evaluating the performance of an automated tool for MS lesion detection, segmentation and tracking in longitudinal data, only for use in this research study. The method was tested with images acquired using both a "clinical" and an "advanced" imaging protocol for comparison. The validation was conducted in a cohort of thirty-two early MS patients through a ground truth obtained from manual segmentations by a neurologist and a radiologist. The use of the "advanced protocol" significantly improves lesion detection and classification in longitudinal analyses.

1290

New insight in perivenular lesion formation in multiple sclerosis on weekly susceptibility weighted images
Simon Mure¹, Charles Guttmann², Thomas Grenier¹, Hugues Benoit-Cattin¹, and François Cotton³

¹CREATIS, Villeurbanne cedex, France, ²Center for Neurological Imaging, Brigham and Women's Hospital, Boston, MA, United States, ³CREATIS - HCL, Villeurbanne cedex, France

In this paper, we take advantage of a unique longitudinal MRI dataset acquired at weekly intervals on untreated multiple sclerosis patients. We study the signal dynamics of relapsing-remitting multiple sclerosis lesions on SWI MRI and show, thanks to an unsupervised spatiotemporal clustering algorithm, that specific signal intensity behaviors exist between the veins and the lesions that are synchronous with contrast enhancement on gadolinium-enhanced T1-weighted MRI. Our study shows that vein narrowing depicted on SWI is an early event that appears to precede blood-brain barrier disruption signified by contrast-enhancement.

1291

Lobule-wise quantitative T1 and T2* analysis of cerebellar grey matter in multiple sclerosis patients at 7T MRI
Yohan Boillat¹, Kieran O'Brien^{2,3}, Mário João Fartaria de Oliveira^{4,5}, Guillaume Bonnier^{1,5,6}, Gunnar Krueger^{5,7}, Wietske van der Zwaag^{1,8}, and Cristina Granziera^{1,5,6,9}

¹Ecole Polytechnique Fédérale de Lausanne, Lausanne, Switzerland, ²Siemens Healthcare Pty Ltd, Brisbane, Australia, ³University of Queensland, St-Lucia, Australia, ⁴University of Lausanne, Lausanne, Switzerland, ⁵Advanced Clinical Imaging Technology Group, Siemens, Lausanne, Switzerland, ⁶Centre Hospitalier Universitaire Vaudois, Lausanne, Switzerland, ⁷Healthcare Sector IM&WS S, Siemens Schweiz AG, Lausanne, Switzerland, ⁸Spinoza Centre for Neuroimaging, Amsterdam, Switzerland, ⁹Massachusetts General Hospital and Harvard Medical School, Charlestown, MA, United States

We compared ultra-high field, high resolution quantitative T_1 and T_2^* measurements in the cerebellum of MS patients to that of healthy controls. A correlation between the multiple sclerosis functional scale scores and local T_2^* values was found for several motor and cognitive related lobules. No significant differences between groups were found.

1292

Edema-Correction is Essential for Monitoring Brain Atrophy with BPF
Marcel Warntjes^{1,2}, Anders Tisell^{1,3}, Irene Håkansson⁴, and Peter Lundberg¹

¹Center for Medical Imaging Science and Visualization, Linköping, Sweden, ²SyntheticMR AB, Linköping, Sweden, ³Department of Medical and Health Sciences, Radiation Physics, Linköping, Sweden, ⁴Department of Clinical and Experimental Medicine, Neurology, Linköping, Sweden

The rate of brain atrophy in neuro-degenerative diseases is monitored using the brain parenchymal fraction (BPF, the ratio of brain volume and intracranial volume). The true atrophy, however, may be obscured by the simultaneous brain swelling due to inflammatory processes, disease activity and medication. Measurement of the average relaxation rates and proton density of the brain allows correction for the presence of edematous water. The edema-corrected BPF showed a higher rate of atrophy, 0.495%/year ($p = 0.003$), in comparison to the uncorrected BPF, 0.175%/year ($p = 0.12$), in a group of early-onset Multiple Sclerosis patients.

1293

T_{1p} MRI Demonstrates Increased Contrast-to-Noise-Ratio in MS Lesions Compared to T_2

Jay V Gonyea¹, Richard Watts¹, Angela Applebee², Trevor Andrews^{1,3}, Scott Hipko¹, Joshua P Nickerson¹, Lindsay Thornton⁴, and Christopher G Filippi⁵

¹Radiology-MRI Center for Biomedical Imaging, University of Vermont College of Medicine, Burlington, VT, United States, ²Neurological Sciences, University of Vermont College of Medicine, Burlington, VT, United States, ³Philips Health Tech, Cleveland, OH, United States, ⁴Radiology, University of Florida, Gainesville, FL, United States, ⁵Radiology, North Shore University Hospital-Long Island Jewish, New York, NY, United States

Quantitative MRI measures such as T_2 are limited in their ability of staging MS progression. T_{1p} may be sensitive to low-frequency chemical exchange between proteins and extracellular water. A 3D TSE with whole-brain coverage, spin-lock times of 0, 20, 40, 60, 80, and 100 ms spin-lock times was acquired at 500 Hz. We found that T_{1p} provides better contrast-to-noise-ratio (CNR) than T_2 .

1294

Assessment of whole brain blood flow changes in multiple sclerosis: phase contrast MRI versus ASL

Yulin Ge¹, Olga Marshall¹, Ilya Kister¹, Jean-Christophe Brisset¹, Louise Pape¹, Jacqueline Smith¹, and Robert I Grossman¹

¹Radiology, New York University School of Medicine, New York City, NY, United States

Cerebral blood flow (CBF) is an important characteristic of the brain since it reflects the availability of blood to enable healthy neuronal function. Previous studies in multiple sclerosis (MS) have shown regional hemodynamic changes indicating a state of both increased or decreased perfusion, which may reflect underlying neuroinflammatory activity and impaired vascular perfusion of the disease, respectively. However, it is still unclear how the whole brain blood supply or blood flow changes in MS. This study was to investigate whether global CBF levels are affected in MS compared to controls, while evaluating with two different imaging techniques to confirm the findings.

1295

Focal cerebellar pathology in early relapsing-remitting multiple sclerosis patients: a MP2RAGE study at 3T and 7T MRI

Mário João Fartaria^{1,2}, Guillaume Bonnier^{1,2}, Tobias Kober^{1,2,3}, Kieran O'Brien^{4,5}, Alexis Roche^{1,2,3}, Bénédicte Maréchal^{1,2,3}, Reto Meuli², Jean-Philippe Thiran^{2,3}, Gunnar Krueger⁶, Meritxell Bach Cuadra^{2,3,7}, and Cristina Granziera^{1,7,8,9}

¹Advanced Clinical Imaging Technology (HC CMEA SUI DI BM PI), Siemens Healthcare AG, Lausanne, Switzerland, ²Department of Radiology, Centre Hospitalier Universitaire Vaudois (CHUV) and University of Lausanne (UNIL), Lausanne, Switzerland, ³Signal Processing Laboratory (LTS 5), Ecole Polytechnique Fédérale de Lausanne (EPFL), Lausanne, Switzerland, ⁴Centre for Advanced Imaging, University of Queensland, Brisbane, Queensland, Australia, ⁵Siemens Healthcare Pty Ltd, Brisbane, Queensland, Australia, ⁶Siemens Medical Solutions USA, Inc., Boston, Switzerland, ⁷Signal Processing Core, Centre d'Imagerie BioMédicale (CIBM), Lausanne, Switzerland, ⁸Martinos Center for Biomedical Imaging, Massachusetts General Hospital and Harvard Medical School, Boston, MA, United States, ⁹Neuroimmunology Unit, Neurology, Department of Clinical Neurosciences, Centre Hospitalier Universitaire Vaudois (CHUV) and University of Lausanne (UNIL), Lausanne, Switzerland

In this work, we assessed the sensitivity of MP2RAGE at 7T MRI to detect focal cerebellar pathology, both in grey and white matter. To do this, we compared cerebellar lesion count in 7T and 3T MP2RAGE images in a cohort of MS patients. Lesion detection rate at 7T MRI was higher than the one at 3T, yet the total lesion volume was comparable at different field strengths. Lesion volumes calculated on 7T MP2RAGE images showed higher correlations with clinical scores than the ones at 3T, pointing at a clinical value of 7T MRI for complex regions such as cerebellum.

1296

Phosphorus MR Spectroscopy as a biomarker of improved tissue metabolism after aerobic exercise in Multiple Sclerosis at 7T
Manoj K Sammi¹, Rebecca Spain², Bharti Garg³, Kerry Kuehl³, and William D Rooney¹

¹Advanced Imaging Research Center, Oregon Health & Science University, Portland, OR, United States, ²Department of Neurology, Oregon Health & Science University, Portland, OR, United States, ³Department of Medicine, Oregon Health & Science University, Portland, OR, United States

Moderate exercise has been shown to benefit several aspects of brain health. We investigate the feasibility of aerobic exercise in subjects with Multiple Sclerosis and use of ^{31}P MR spectroscopic imaging as a biomarker.

Exploring Sodium MRI Contrast Beyond Concentration in Multiple Sclerosis Lesions

Robert Stobbe¹, Penny Smyth², Roxane Billey², Leah White², Fabrizio Giuliani², Derek Emery³, and Christian Beaulieu¹¹Biomedical Engineering, University of Alberta, Edmonton, AB, Canada, ²Neurology, University of Alberta, Edmonton, AB, Canada, ³Radiology, University of Alberta, Edmonton, AB, Canada

Two different relaxation-weighted ²³Na sequences were compared to density-weighted ²³Na imaging in the context of multiple sclerosis (MS) and the lesion contrast produced by each sequence was significantly different, thus identifying the presence of substantial ²³Na relaxation change. Given that macromolecular density and structure directly influence the electric field gradients driving orientation of the nuclear electric quadrupole moment and ²³Na relaxation, exploration of ²³Na relaxation change may help in the assessment of MS including axonal loss and demyelination. The use of relaxation-weighted sequences and their relative combination to eliminate sodium concentration dependence is a starting point for ²³Na relaxation exploration.

Traditional Poster

Multiple Sclerosis: Studies

Exhibition Hall

Monday, May 9, 2016: 10:45 - 12:45

1298

MRI detects the effects of demyelination and remyelination on hippocampal structure and function
Harsha Bhattapadhy¹, Jacqueline Chen¹, and Bruce D Trapp¹¹Neurosciences, Cleveland Clinic, Cleveland, OH, United States

Multiple sclerosis (MS) features demyelination of the brain and spinal cord, resulting in impaired and eventual loss of neuronal function. Approximately 65% of MS patients experience cognitive impairment and memory dysfunction. Postmortem analyses reveal hippocampal demyelination and glutamate receptor loss in MS patients, suggesting impaired synaptic function in this brain region critical for memory and learning. Using a mouse model of reversible demyelination, we demonstrate that MRI can detect the loss and restoration of myelin and neuronal function in the hippocampus. Our results suggest that MRI is a powerful pre-clinical tool for testing neuroprotective and reparative therapies targeting the hippocampus.

1299

Cerebellar contribution to motor and cognitive impairment in multiple sclerosis patients: a sub-regional structural MRI analysis
Elisabetta Pagan¹, Maria Assunta Rocca^{1,2}, Alessandro D'Ambrosio^{1,3}, Gianna Carla Riccitelli¹, Bruno Colombo², Mariaemma Rodegher², Andrea Falini⁴, Giancarlo Comi², and Massimo Filippi^{1,2}¹Neuroimaging Research Unit, San Raffaele Scientific Institute, Vita-Salute San Raffaele University, Milan, Italy, ²Department of Neurology, San Raffaele Scientific Institute, Vita-Salute San Raffaele University, Milan, Italy, ³Division of Neurology, Department of Medical, Surgical, Neurological, Metabolic and Aging Sciences, Second University of Naples, Naples, Italy, ⁴Department of Neuroradiology, San Raffaele Scientific Institute, Vita-Salute San Raffaele University, Milan, Italy

Aim of the study was to assess the role of cerebellar global and sub-regional involvement on motor and cognitive impairment in multiple sclerosis (MS) patients. Cerebellar segmentation and lobular parcellation was performed on T1 weighted images from 95 MS patients and 32 healthy controls using SUIT tool. The Nine Hole Peg Test was obtained as a measure of motor performance; patients also underwent cognitive evaluation. Cerebellar posterior-inferior volume accounted for variance in cognitive measures in MS patients, whereas anterior cerebellar volume accounted for variance in motor performance, supporting a critical contribution of regional cerebellar damage to clinical manifestations of MS.

1300

Cross-modal plasticity among sensory networks in neuromyelitis optica spectrum disorders

Paola Valsasina¹, Maria Assunta Rocca¹, Filippo Savoldi¹, Marta Radaelli², Paolo Preziosa¹, Giancarlo Comi², Andrea Falini³, and Massimo Filippi¹¹Neuroimaging Research Unit, San Raffaele Scientific Institute, Vita-Salute San Raffaele University, Milan, Italy, ²Department of Neurology, San Raffaele Scientific Institute, Vita-Salute San Raffaele University, Milan, Italy, ³Department of Neuroradiology, San Raffaele Scientific Institute, Vita-Salute San Raffaele University, Milan, Italy

This study gives a comprehensive description of sensory and motor resting state functional connectivity abnormalities in patients with neuromyelitis optica spectrum disorders (NMOSD) fulfilling the new 2015 diagnostic criteria. Functional connectivity abnormalities found in these patients were compared with isolated optic neuritis and myelitis. Our results suggest different mechanisms of brain reorganization in NMOSD vs isolated optic neuritis and myelitis, with a more evident cross-modal plasticity between sensory systems in NMOSD patients. This result might help to better characterize the different pathophysiological mechanisms occurring in these conditions.

1301

Correlation of transcallosal motor network resting state connectivity with motor performance after 12 months of Fingolimod treatment
Pallab K Bhattacharyya¹, Robert Fox², Jian Lin¹, Ken Sakaie¹, and Mark Lowe¹¹Imaging Institute, Cleveland Clinic, Cleveland, OH, United States, ²Neurological Institute, Cleveland Clinic, Cleveland, OH, United States

Resting state functional connectivity (fcMRI) between left and right primary motor cortices in MS patients on Fingolimod treatment was

studied at baseline (just before the start of the treatment), 6 months and 12 months after start of treatment. Since such fcMRI metric has been previously reported to be reduced, changes in fcMRI over every 6 months interval were correlated with changes in clinical score as measured by 9 hole peg test during the treatment course. A significant difference in the correlation was observed between dominant and non-dominant hand performance in between 6 and 12 months.

1302

Contribution of cortical lesion volume detected with 7T MRI to cortical thinning, thalamic and callosal atrophy in multiple sclerosis
Tobias Granberg^{1,2,3,4}, Russell Ouellette^{1,2}, Constantina Andrada Treaba^{1,2}, Celine Louapre^{1,2}, Sindhuja T Govindarajan^{1,2}, Costanza Gianni^{1,2}, Elena Herranz^{1,2}, Revere P Kinkel⁵, and Caterina Mainiero^{1,2}

¹Athinoula A. Martinos Center for Biomedical Imaging, Department of Radiology, Massachusetts General Hospital, Charlestown, MA, United States, ²Harvard Medical School, Boston, MA, United States, ³Department of Clinical Science, Intervention and Technology, Karolinska Institutet, Stockholm, Sweden, ⁴Department of Radiology, Karolinska University Hospital, Stockholm, Sweden, ⁵Department of Neurosciences, University of California, San Diego, CA, United States

Grey matter pathology contributes to disability in multiple sclerosis (MS), but in vivo sensitivity for cortical lesions is low with conventional MRI. The role of cortical pathology in the dynamic atrophy processes in MS is, therefore, uncertain. Using 7T MRI and longitudinal 3T imaging (mean follow-up 1.9 years), we showed, in a small MS cohort, that cortical lesion volumes at follow-up correlated with cortical thinning in areas known to be predilection sites for cortical demyelination in MS, while thalamic atrophy was more strongly associated with white matter lesions. No effect of cortical lesions was found on corpus callosal atrophy.

1303

Regional analysis of diffusion MRI (DKI/DTI) in patients with multiple sclerosis: Correlation with cognitive function and clinical measures
Phil Lee^{1,2}, Peter Adany¹, Douglas R. Denney³, Abbey J. Hughes³, Sharon G. Lynch⁴, and In-Young Choi^{1,2,4}

¹Hoglund Brain Imaging Center, University of Kansas Medical Center, Kansas City, KS, United States, ²Molecular & Integrative Physiology, University of Kansas Medical Center, Kansas City, KS, United States, ³Psychology, University of Kansas, Lawrence, KS, United States, ⁴Neurology, University of Kansas Medical Center, Kansas City, KS, United States

Diffusion kurtosis imaging (DKI) and diffusion tensor imaging (DTI) techniques were used to evaluate microstructure changes multiple brain regions as well as gray and white matter in patients with multiple sclerosis at various disease stages and types. DKI/DTI parameters in various brain regions were able to distinguish MS subtypes, and to discriminate patients from controls. Microstructure alterations measured by DKI/DTI were region-specific and correlated with cognitive function and clinical status of patients, providing promising metrics in clinical applications to assess disease status and progression.

1304

Investigating Cerebrovascular Reactivity in MS with BOLD, ASL and EEG
Mark J Lowe¹, Wanyong Shin¹, Balu Krishnan², Lael Stone², and Andreas Alexopoulos²

¹Imaging Institute, Cleveland Clinic, Cleveland, OH, United States, ²Neurologic Institute, Cleveland Clinic, Cleveland, OH, United States

Recent reports indicate that cerebrovascular reactivity (CR) may be impaired in multiple sclerosis (MS). Here we report initial studies to use simultaneous measurements of electroencephalography (EEG), regional cerebral blood flow, and BOLD during performance of a motor task. We show that it is possible to produce EEG estimators of a healthy control subject that correlate very highly with BOLD measurements, while the same measurements in an age and gender matched MS patient have a much lower correspondence. Although inconclusive due to the small sample, the methodology shows promise for helping to understand possible CR issues in MS.

1305

Blood brain barrier alterations precede ventriculomegaly in experimental autoimmune encephalomyelitis
Sonia Waiczies¹, Laura Boehmert¹, Jason M. Millward², Stefanie Kox¹, Joao dos Santos Perquito¹, Till Huelnhagen¹, Carmen Infante-Duarte², Andreas Pohlmann¹, and Thoralf Niendorf^{1,3}

¹Berlin Ultrahigh Field Facility (B.U.F.F.), Max Delbrück Center for Molecular Medicine in the Helmholtz Association, Berlin, Germany, ²Institute for Medical Immunology, Charité - Universitätsmedizin Berlin, Berlin, Germany, ³Experimental and Clinical Research Center (ECRC), a joint cooperation between the Charité Medical Faculty and the Max Delbrück Center for Molecular Medicine in the Helmholtz Association, Berlin, Germany

Previously, we observed an enlargement of cerebral ventricles, prior to clinical disease manifestation, in experimental autoimmune encephalomyelitis (EAE). In this study we investigated the kinetics of blood brain barrier (BBB) leakage in relation to changes in ventricle size during EAE progression using pre- and post-contrast T₁-weighted imaging and T₁-mapping. We show that BBB integrity is compromised even earlier than ventriculomegaly, which already occurs prior to the occurrence of neurological symptoms. Furthermore, a partial renormalization and reappearance of BBB disruptions was observed throughout the disease course and these changes appear to occur prior to the normalization and re-expansion of ventricle size.

1306

Investigating the Correlation between Cognitive Fatigue and Brain Iron Deposition in Basal Ganglia in Multiple Sclerosis
Sarah Wood¹, Emilyrose Havrilla^{1,2}, Ekaterina Dobryakova³, Zhiguo Jiang⁴, and Bing Yao^{1,5}

¹Rocco Ortenzio Neuroimaging Center, Kessler Foundation, West Orange, NJ, United States, ²Department of Psychology, Montclair State University, Montclair, NJ, United States, ³Traumatic Brain Injury Laboratory, Kessler Foundation, West Orange, NJ, United States, ⁴Human Performance Engineering Laboratory, Kessler Foundation, West Orange, NJ, United States, ⁵Department of Physical Medicine & Rehabilitation, Rutgers, the State University of New Jersey, Newark, NJ, United States

Basal ganglia play important roles in cognitive fatigue, which is one of the most common symptoms in multiple sclerosis. This study examined the correlation between brain iron concentration measured by MR susceptibility contrast imaging in the basal ganglia and the severity of fatigue in the individuals with multiple sclerosis.

1307

Disruption of functional connectivity of M1 and cerebellum in Multiple sclerosis: a long-range functional dysconnection?

Adnan A.S. Alahmadi^{1,2}, Carmen Tur¹, Matteo Pardini^{1,3}, Peter Zeidman⁴, Rebecca S. Samson¹, Egidio D'Angelo^{5,6}, Ahmed T. Toosy^{1,7}, Karl J. Friston⁴, and Claudia Angela Michela Gandini Wheeler-Kingshott^{1,6}

¹NMR Research Unit, Queen Square MS Centre, Department of Neuroinflammation, UCL Institute of Neurology, London, United Kingdom,

²Department of Diagnostic Radiology, Faculty of Applied Medical Science, KAU, Jeddah, Saudi Arabia, ³Department of Neurosciences,

Ophthalmology and Genetics, University of Genoa, Genoa, Italy, ⁴Wellcome Centre for Imaging Neuroscience, UCL, Institute of Neurology,

London, United Kingdom, ⁵Department of Brain and Behavioral Sciences, University of Pavia, Pavia, Italy, ⁶Brain Connectivity Center, C.Mondino

National Neurological Institute, Pavia, Italy, Pavia, Italy, ⁷NMR Research Unit, Department of Brain Repair and Rehabilitation, Queen Square MS Centre, UCL Institute of Neurology, London, United Kingdom

This study investigated changes in functional and effective connectivity with M1 and anterior cerebellum using psychophysiological interaction (PPI) and resting-state fMRI (rsfMRI), applied to a motor task fMRI dataset in healthy subjects and multiple sclerosis (MS) patients. Results show that M1 in MS patients has reduced long-range connectivity to the contra-lateral hemisphere and the cerebellum and vice versa. Furthermore, MS patients lose visuo-motor integration with parietal areas. This is in contrast to rsfMRI functional connectivity, where connectivity of M1 to areas identified by the PPI network is increased. Results indicate a task-specific disconnection reflecting increased disability, associated also with low frequency maladaptive increased rsfMRI connectivity.

1308

Functional response to a complex visuo-motor task supports local compensatory mechanisms in Multiple Sclerosis

Adnan A.S. Alahmadi^{1,2}, Matteo Pardini^{1,3}, Rosa Cortese¹, Niamh Cawley¹, Rebecca S. Samson¹, Egidio D'Angelo^{4,5}, Karl J. Friston⁶, Ahmed T. Toosy^{1,7}, and Claudia Angela Michela Gandini Wheeler-Kingshott^{1,5}

¹NMR Research Unit, Queen Square MS Centre, Department of Neuroinflammation, UCL Institute of Neurology, London, United Kingdom,

²Department of Diagnostic Radiology, Faculty of Applied Medical Science, KAU, Jeddah, Saudi Arabia, ³Department of Neurosciences,

Ophthalmology and Genetics, University of Genoa, Genoa, Italy, ⁴Department of Brain and Behavioral Sciences, University of Pavia, Pavia, Italy,

⁵Brain Connectivity Center, C.Mondino National Neurological Institute, Pavia, Italy, Pavia, Italy, ⁶Wellcome Centre for Imaging Neuroscience, UCL, Institute of Neurology, London, United Kingdom, ⁷NMR Research Unit, Department of Brain Repair and Rehabilitation, Queen Square MS Centre, UCL Institute of Neurology, London, United Kingdom

We investigated simple and complex (non-linear) relationships between BOLD signals and different applied grip forces in multiple sclerosis (MS) patients and healthy volunteers (HV). Using a power grip event-related paradigm and modelling BOLD responses with a polynomial expansion of force, we show profound and distributed functional network reorganizations in sensorimotor, associative and cerebellar areas, probably indicating compensatory mechanisms in MS.

1309

Patterns of Regional Gray Matter and White Matter Atrophy Progression Contributing to Clinical Deterioration in MS: A 5-Year Tensor-Based Morphometry Study

Elisabetta Pagani¹, Maria Assunta Rocca^{1,2}, Paolo Preziosa¹, Sarlota Mesaros³, Jelena Drulovic³, and Massimo Filippi^{1,2}

¹Neuroimaging Research Unit, San Raffaele Scientific Institute, Vita-Salute San Raffaele University, Milan, Italy, ²Department of Neurology, San Raffaele Scientific Institute, Vita-Salute San Raffaele University, Milan, Italy, ³Clinic of Neurology, Faculty of Medicine, University of Belgrade, Belgrade, Yugoslavia

In this study we investigated the regional patterns of atrophy progression over a five year follow-up in multiple sclerosis (MS) patients and their association with clinical and cognitive deterioration. Clinical (EDSS and phenotype changes), neuropsychological (Rao's battery) and brain MRI assessment were performed at baseline and after 5 years from 66 MS patients. Compared to stable MS patients, those with clinical and cognitive worsening showed a left-lateralized pattern of atrophy. A different vulnerability of the two brain hemispheres to irreversible structural damage may be among the factors contributing to clinical and cognitive worsening in these patients.

1310

Age at disease onset influences gray matter and white matter damage in adult multiple sclerosis patients

Elisabetta Pagani¹, Maria Assunta Rocca^{1,2}, Laura Vacchi¹, Bruno Colombo², Mariaemma Rodegher², Lucia Moiola², Angelo Ghezzi³, Giancarlo Comi², Andrea Falini⁴, and Massimo Filippi^{1,2}

¹Neuroimaging Research Unit, San Raffaele Scientific Institute, Vita-Salute San Raffaele University, Milan, Italy, ²Department of Neurology, San Raffaele Scientific Institute, Vita-Salute San Raffaele University, Milan, Italy, ³Multiple Sclerosis Study Center, Hospital of Gallarate, Gallarate, Italy, ⁴Department of Neuroradiology, San Raffaele Scientific Institute, Vita-Salute San Raffaele University, Milan, Italy

Aim of the study was to explore the extent and distribution of brain gray matter (GM) atrophy and white matter (WM) microstructural abnormalities in adult multiple sclerosis (MS) patients according to their age at disease onset. High-resolution T1-weighted and diffusion tensor MRI scans were acquired from 58 pediatric-onset MS patients, 58 age-matched and 58 disease duration-matched adult-onset MS patients, and 58 healthy controls. The distribution of atrophy and microstructural WM damage were assessed using voxel-wise approaches. Neurodegenerative and inflammatory-demyelinating processes seemed less pronounced in pediatric-onset MS patients. However, with increasing disease duration, an accelerated normal appearing WM damage occurred.

1311

Quantitative T2 and atrophy in multiple sclerosis: A retrospective 7-year study using standard clinical brain images
Md. Nasir Uddin¹, Kelly C. McPhee², Gregg Blevins³, and Alan H. Wilman¹

¹Department of Biomedical Engineering, University of Alberta, Edmonton, AB, Canada, ²Department of Physics, University of Alberta, Edmonton, AB, Canada, ³Division of Neurology, Department of Medicine, University of Alberta, Edmonton, AB, Canada

Proton density and T₂-weighted images are frequently used in clinical MS exams. These two images can be used to obtain accurate T₂ by fitting them with prior knowledge of RF pulse shapes and refocusing flip angles in order to compensate for indirect and stimulated echo contributions. After demonstrating feasibility in healthy controls, we investigate 7-year changes in T₂ in subcortical grey matter in 14 relapsing remitting MS patients and related these with disease severity and brain atrophy.

1312

MRI of Cuprizone Induced Demyelination in Rat Brain

Wendy Oakden¹, Nicholas A Bock², Alia Al-Ebraheem³, Michael J Farquharson³, and Greg J Stanisz^{1,4,5}

¹Physical Sciences, Sunnybrook Research Institute, Toronto, ON, Canada, ²Psychology, Neuroscience and Behavior, McMaster University, Hamilton, ON, Canada, ³Medical Physics and Applied Radiation Sciences, McMaster University, Hamilton, ON, Canada, ⁴Medical Biophysics, University of Toronto, Toronto, ON, Canada, ⁵Neurosurgery and Pediatric Neurosurgery, Medical University of Lublin, Lublin, Poland

The cuprizone mouse model of demyelination is widely used. While initial histological studies in rats reported only spongiform encephalopathy, more recent work has also demonstrated demyelination. In this study we use a high-resolution myelin-contrast optimized MRI protocol to identify regions of altered myelin content in the rat brain. Wistar rats were imaged after 2, 4, and 6 weeks on a cuprizone diet. Luxol fast blue was used to assess demyelination, and X-Ray fluorescence for quantification of transition metals which also affect MRI contrast. This study demonstrates that cuprizone-induced demyelination in the rat brain can be observed *in vivo* using MRI.

1313

In vivo white matter development of Fmr1 knockout mice

Da Shi¹, Jiachen Zhuo¹, Su Xu¹, Mary C. McKenna², and Rao P. Gullapalli¹

¹Diagnostic Radiology, University of Maryland Baltimore, Baltimore, MD, United States, ²Department of Pediatrics, University of Maryland Baltimore, Baltimore, MD, United States

Fragile X syndrome is the most common genetic cause of autism and is modeled with the Fmr1 knockout mouse. To investigate recent report of myelination delay in Fragile X, this study used translational imaging techniques including T₂ mapping and magnetization transfer imaging to determine myelination changes in the developing Fmr1 knockout mouse. Age-related trajectory changes in regional white matter development were observed between the genotypes and may provide insights into the pathophysiology of Fragile X.

1314

Induction of Experimental Autoimmune Encephalomyelitis (EAE) in cynomolgus monkey: a valuable model of auto-immune demyelinating diseases

Julien Flament^{1,2}, Claire-Maëlle Fovet^{1,3}, Lev Stimmer^{1,3}, Philippe Hantraye^{1,2,4}, and Ché Serguera^{1,2}

¹CEA/DSV/IBBM/MIRCen, Fontenay-aux-Roses, France, ²INSERM UMS 27, Fontenay-aux-Roses, France, ³INSERM UMR 1169, Fontenay-aux-Roses, France, ⁴CNRS Université Paris-Saclay UMR 9199, Fontenay-aux-Roses, France

Acquired demyelinating diseases are a major cause of neurological disabilities. If Experimental Autoimmune Encephalomyelitis (EAE) model has been widely used in rodents, it does not recapitulate disease variability observed in humans. We propose for the first time a primate model of EAE without immunomodulatory treatment in *Macaca fascicularis* which exhibited a more developed immune system than rodents. All monkeys developed MRI visible lesions that were significantly correlated to clinical signs onset. Our longitudinal follow up allows a precise monitoring of lesions and may offer the opportunity to better understand biological and physiological processes underlying the pathology of demyelinating diseases.

1315

Spatial and temporal characterization of blood brain barrier permeability with disease progression in the NOD-EAE mouse model using MRI and histology

Mohammed Salman Shazeeb¹, Nellwyn Hagan², Xiaoyou Ying¹, and Andrea Edling²

¹DSAR Bioimaging, Sanofi, Framingham, MA, United States, ²Neuroimmunology, Sanofi, Framingham, MA, United States

Blood brain barrier (BBB) dysregulation is one of the earliest signs of multiple sclerosis (MS) and the mechanism underlying BBB breakdown is not completely understood. The non-obese diabetic experimental allergic encephalomyelitis (NOD-EAE) mouse model of secondary progressive MS offers a preclinical tool to understand BBB breakdown and explore potential therapeutics. MRI is capable of quantifying BBB permeability using gadolinium contrast agent. In this study we quantified the spatial and temporal characterization of BBB permeability in NOD-EAE mice with progressing disease using MRI. These quantifying parameters can potentially be used to test the effect of therapeutic agents on BBB breakdown.

1316

Fluctuations in Ventricle Size during the Progression of Experimental Autoimmune Encephalomyelitis

Laura Boehmert¹, Henning Reimann¹, Stefanie Kox¹, Andreas Pohlmann¹, Thoralf Niendorf^{1,2}, and Sonia Waiczies¹

¹Berlin Ultrahigh Field Facility (B.U.F.F.), Max Delbrück Center for Molecular Medicine in the Helmholtz Association, Berlin, Germany, Berlin, Germany, ²Experimental and Clinical Research Center (ECRC), a joint cooperation between the Charité Medical Faculty and the Max Delbrück

Multiple sclerosis is an autoimmune condition that involves immune cell infiltration through the blood brain barrier, during the initial stages of disease. In the experimental autoimmune encephalomyelitis animal model, we previously observed an increase in ventricle size prior to neurological manifestation. In this study we extended these findings by showing a dynamic fluctuation in ventricle size, with successive re-normalization and re-expansion. Fluctuations in ventricle size commonly ran ahead of clinical relapses and remissions during disease progression. We could identify these findings by following ventricle size for a long period of time (64 days) during the progression of encephalomyelitis.

1317

Whole-Brain Ex-Vivo Imaging of Demyelination in the Cuprizone Mouse with mcDESPOT and DTI

Tobias C Wood¹, Camilla Simmons¹, Joel Torres¹, Flavio Dell' Acqua¹, Anthony Vernon², Samuel A Hurley³, Steve CR Williams¹, and Diana Cash¹

¹Neuroimaging, IoPPN, King's College London, London, United Kingdom, ²Basic and Clinical Neuroscience, IoPPN, King's College London, London, United Kingdom, ³FMRIB Centre, University of Oxford, Oxford, United Kingdom

We demonstrate the feasibility of full-brain high-resolution ex-vivo imaging and analysis of demyelination in the Cuprizone mouse model using multi-component DESPOT and DTI. We found evidence of demyelination in the Cerebellum as well as the Corpus Callosum.

1318

Longitudinal characterization of the Theiler's Murine Encephalomyelitis Virus (TMEV) mouse model using a cryogenic brain coil at 9.4T

Nicola Bertolino¹, Claire M Modica^{1,2}, Michael G Dwyer¹, Paul Polak¹, Trina Ruda¹, Marilena Preda^{1,3}, Jacqueline C Krawiecki^{1,4}, John M Barbieri^{1,5}, Michelle L Sudyn^{1,2}, Danielle M Siebert^{1,6}, Robert Zivadinov^{1,3}, and Ferdinand Schweser^{1,3}

¹Buffalo Neuroimaging Analysis Center, Department of Neurology, Jacobs School of Medicine and Biomedical Sciences, The State University of New York at Buffalo, Buffalo, NY, United States, ²Neuroscience Program, Jacobs School of Medicine and Biomedical Sciences, The State University of New York at Buffalo, Buffalo, NY, United States, ³MRI Molecular and Translational Research Center, Jacobs School of Medicine and Biomedical Sciences, The State University of New York at Buffalo, Buffalo, NY, United States, ⁴Department of Geology, The State University of New York at Buffalo, Buffalo, NY, United States, ⁵Department of Biological Sciences, The State University of New York at Buffalo, Buffalo, NY, United States, ⁶Department of Exercise and Nutritional Sciences, School of Public Health and Health Professions, The State University of New York at Buffalo, Buffalo, NY, United States

Theiler's Murine Encephalomyelitis Virus (TMEV) infection is a mouse model of multiple sclerosis (MS) with a similar disease course to human MS. In susceptible breeds TMEV infections give way to a progressive demyelinating course and a chronic, immune-mediated, demyelinating, neurodegenerative condition that persists for the remainder of the natural life of the animal.

While *post mortem* tissue and motor disability are well-characterized in TMEV, structural and metabolite tissue damage associations are not thoroughly understood. In this work, we studied the TMEV model over 2 months after the infection using advanced MRI with a cryogenic brain coil at 9.4 Tesla.

1319



Lesion Distribution Probability in Japanese Macaque Encephalomyelitis: A Comparison to Human Demyelinating Diseases

Ian Tagge¹, Steven Kohama², Dennis Bourdette³, Randy Woltjer³, Scott Wong², and William Rooney¹

¹Advanced Imaging Research Center, Oregon Health & Science University, Portland, OR, United States, ²Oregon National Primate Research Center, Oregon Health & Science University, Beaverton, OR, United States, ³Neurology, Oregon Health & Science University, Portland, OR, United States

Japanese Macaque Encephalomyelitis bears marked clinical and pathological similarities to multiple sclerosis (MS), acute disseminated encephalomyelitis (ADEM), and neuromyelitis optica. Here, we describe lesion topography typical of JME. This represents an important step in not only understanding this disease, but also in making meaningful comparisons to human demyelinating diseases. Animals most commonly presented with lesions in the cerebellum, followed by the brainstem, internal capsule, and upper cervical spinal cord, most similarly to pediatric MS or ADEM. JME is a novel and exciting non-human primate model of MS-like disease that may help elucidate pathomechanisms of human disease.

1320

Volume differences on quantitative susceptibility map and T2-weighted image of multiple sclerosis lesions at different disease stages and indication for iron activity

Yan Zhang^{1,2}, Dong Zhou², Ajay Gupta², Susan A. Gauthier³, and Yi Wang²

¹Radiology, Tongji hospital, Tongji Medical College, Huazhong University of Science & Technology, Wuhan, China, People's Republic of,

²Radiology, Weill Cornell Medical College, New York, NY, United States, ³Neurology, Weill Cornell Medical College, New York, NY, United States

In this study, we examined different multiple sclerosis (MS) lesion patterns using quantitative susceptibility map (QSM) and compared lesion volumes on T2-weighted (T2w) and QSM images at different lesion stages. The relative lesion QSM/T2w volume increases over 1 year of the lesion onset indicates the participation of iron in chronic active lesions.

1321

Non-invasive Assessments of Biomechanical and Biochemical Properties in Animal and Human Eyes using Multi-modal MRI
Leon C. Ho^{1,2}, Ian A. Sigal^{1,3}, Ning-juan Jan^{1,3}, Chan Hong Moon⁴, Xiaoling Yang¹, Yolandi van der Merwe^{1,3}, Tao Jin⁴, Ed X. Wu², Seong-Gi Kim^{4,5}, Gadi Wollstein^{1,3}, Joel S. Schuman^{1,3}, and Kevin C. Chan^{1,3}

¹UPMC Eye Center, Eye and Ear Institute, Ophthalmology and Visual Science Research Center, Department of Ophthalmology, University of Pittsburgh, Pittsburgh, PA, United States, ²Department of Electrical and Electronic Engineering, The University of Hong Kong, Pokfulam, Hong Kong, ³Department of Bioengineering, Swanson School of Engineering, University of Pittsburgh, Pittsburgh, PA, United States, ⁴Department of Radiology, School of Medicine, University of Pittsburgh, Pittsburgh, PA, United States, ⁵Center for Neuroscience Imaging Research, Institute for Basic Science, Suwon, Korea, Republic of

The microstructural organization and compositions of the corneoscleral shell are central to ocular biomechanics, and are important in diseases such as glaucoma and myopia. In this study, we showed that T2-weighted MRI, diffusion tensor MRI and magnetization transfer MRI can be used to detect and differentiate microstructural and macromolecular changes in freshly prepared ovine eyes under different abnormal conditions including intraocular pressure loading, cross-linking and glycosaminoglycans depletion. We also demonstrated the feasibility of assessing the human sclera with *in vivo* MRI. Multi-modal MRI may be useful for evaluating the biomechanical and pathophysiological mechanisms in the corneoscleral shell non-invasively and quantitatively.

1322

SHINKEI Quant: Simultaneous Acquisition of MR Neurography and T2 Mapping for Quantitative Evaluation of Chronic Inflammatory Demyelinating Polyneuropathy
Masami Yoneyama¹, Osamu Togao², Akio Hiwatashi², Yuriko Ozawa³, Makoto Obara¹, Tomoyuki Okuaki⁴, and Marc Van Cauteren⁴

¹Philips Electronics Japan, Tokyo, Japan, ²Department of Clinical Radiology, Graduate School of Medical Sciences, Kyushu University, Fukuoka, Japan, ³Yasu Clinic, Tokyo, Japan, ⁴Philips Healthcare Asia Pacific, Tokyo, Japan

MR neurography achieves selective depiction of peripheral nerves and detects pathological changes related to neuropathies as a signal abnormality. Recently, we proposed a novel MR neurography sequence (SHINKEI) that provides high-quality MR neurography in the brachial plexus and the lumbosacral plexus. However, SHINKEI could not quantitatively assess the nerve pathology. In this study, we developed a new sequence (SHINKEI-Quant) to simultaneously acquire MR neurography and T₂ mapping by further optimizing the iMSDE preparation. SHINKEI-Quant could simultaneously provide both MR neurography and T₂ maps without prolongation of acquisition time compared with the conventional SHINKEI sequence. This quantitative sequence may be helpful to quantitatively assess the nerve pathology such as chronic inflammatory demyelinating polyneuropathy.

1323

Development of a dedicated solenoidal ring-based RF Coil for MRI of the Larynx
Christoph Leussler¹, Christian Findeklee¹, Peter Mazurkewitz¹, Jürgen Gieseke², and Peter Börnert¹

¹Philips GmbH Innovative Technologies, Hamburg, Germany, ²Philips Deutschland GmbH, Hamburg, Germany

A dedicated solenoidal RF coil for imaging of the larynx was developed for cylindrical MRI systems using a static magnetic field in axial direction. The coil consists of two flexible solenoidal windings entangling the cervix anatomy. Numerical and experimental evaluation demonstrates higher SNR for the region of the larynx compared with conventional neck coil designs.

1324

Non-Gaussian diffusion weighted imaging in the head and neck; how we can improve the clinical diagnostic accuracy beyond ADC
Mami Iima^{1,2}, Akira Yamamoto¹, Shigeru Hirano³, Ichiro Tateya³, Morimasa Kitamura³, and Kaori Togashi¹

¹Department of Diagnostic Imaging and Nuclear Medicine, Graduate School of Medicine, Kyoto University, Kyoto, Japan, ²The Hakubi Center for Advancer Research, Kyoto University, Kyoto, Japan, ³Department of Otolaryngology, Graduate School of Medicine, Kyoto University, Kyoto, Japan

The usefulness of non-Gaussian diffusion parameters for the clinical diagnostic ability in the head and neck was evaluated. 135 (62 malignant/63 benign/10 inflammation) patients were prospectively recruited, and non-Gaussian DWI and IVIM parameters as well as synthetic ADC, which comprises both Gaussian and non-Gaussian effect, were estimated from the DWI datasets with multiple b values. Significant difference in each parameter was observed between malignant and benign lesions. There was a significant difference between inflammation or lymphatic vascular malformation and tumors in K or fIVIM values, providing the potential to improve the DWI diagnostic accuracy by complementing their diagnostic abilities.

1325

Improving Visualization of Superficial Temporal Artery Using Segmented TOF MR Angiography at 7T
Zihao Zhang^{1,2}, Ning Wei^{1,2}, Xiaofeng Deng³, Dehe Weng⁴, Jing An⁴, Yan Zhuo¹, Xiaohong Joe Zhou⁵, and Rong Xue^{1,6}

¹State Key Laboratory of Brain and Cognitive Science, Beijing MR Center for Brain Research, Institute of Biophysics, Chinese Academy of Sciences, Beijing, China, People's Republic of, ²Graduate School, University of Chinese Academy of Sciences, Beijing, China, People's Republic of,

³Department of Neurosurgery, Beijing Tiantan Hospital, Capital Medical University, Beijing, China, People's Republic of, ⁴Siemens Shenzhen Magnetic Resonance Ltd., Shenzhen, China, People's Republic of, ⁵Center for MR Research and Department of Radiology, University of Illinois at Chicago, Chicago, IL, United States, ⁶Beijing Institute for Brain Disorders, Beijing, China, People's Republic of

Time-of-Flight MR Angiography (TOF-MRA) can benefit from better contrast and higher spatial resolution using ultra-high field 7T MRI. In a segmented TOF technique at 7T, the Specific Absorption Rate (SAR) of saturation pulses was reduced to enable the suppression of

venous blood signal. In this study, the TOF technique was successfully used to discriminate between the superficial temporal artery (STA) and vein (STV), and depict blood flow in tiny vessels, facilitating future applications in pre-operative assessment for STA-MCA bypass surgery.

1326

Multiparametric MR neurographic orthopantomogram of the mandibular bone and nerve using ultra-short echo-time imaging, simultaneous multi-slice readout-segmented echo planar imaging and 3D reversed fast imaging with steady state free procession Andrei Manoliu¹, Michael Ho¹, Daniel Nanz¹, Marco Piccirelli², Evelyn Dappa¹, Lukas Filli¹, Andreas Boss¹, Gustav Andreisek¹, and Felix Pierre Kuhn¹

¹*Institute for Diagnostic and Interventional Radiology, University Hospital Zurich, University of Zurich, Zurich, Switzerland*, ²*Department of Neuroradiology, University Hospital Zurich, University of Zurich, Zurich, Switzerland*

We propose a new technique for 'MR neurographic orthopantomograms' using ultra-short echo-time imaging of bone and teeth with morphological and functional neurography. Ten healthy volunteers were scanned at 3.0T. Bone images were acquired using a ultra-short TE sequence. Morphological neurography was performed using dedicated PSIF and SPACE STIR sequences. Functional neurography was accomplished using readout-segmented EPI with simultaneous multi-slice excitation. Image acquisition and post-processing were feasible in all volunteers. All mandibular bones and nerves were assessable and considered normal. Fiber tractography yielded physiological diffusion properties. The presented technique allowed robust assessment of osseous and neuronal structures in a single examination.

1327

One-Second 3-D-Imaging of the Vocal Tract to Measure Dynamic Articulator Modifications

Michael Burdumy^{1,2}, Matthias Echternach², Jan Gerrit Korvink³, Bernhard Richter², Jürgen Hennig¹, and Maxim Zaitsev¹

¹*Medical Physics, University Medical Center Freiburg, Freiburg, Germany*, ²*Institute of Musicians' Medicine, University Medical Center Freiburg, Freiburg, Germany*, ³*Institute of Microstructure Technology, Karlsruhe Institute of Technology, Karlsruhe, Germany*

To accelerate dynamic 3-D imaging of the vocal tract during articulation, a stack-of-stars sequence with golden angle rotation and iterative reconstruction was implemented. Phase correction, peripheral under-sampling, temporal and spatial regularization were applied to reach an acquisition time of 1.3 seconds. The vocal tract modifications of one subject could be successfully analyzed at discrete time steps during phonation of a long note.

1328

The pointwise encoding time reduction with radial acquisition (PETRA) sequence: visualization of intracranial arteries and facial nerve canals

Sachi Okuchi¹, Yasutaka Fushimi¹, Tomohisa Okada^{1,2}, Akira Yamamoto¹, Tsutomu Okada¹, Takuya Hinoda¹, Yutaka Natsuaki³, and Kaori Togashi¹

¹*Diagnostic Imaging and Nuclear Medicine, Graduate School of Medicine, Kyoto University, Kyoto, Japan*, ²*Human Brain Research Center, Kyoto University Graduate School of Medicine, Kyoto, Japan*, ³*Siemens Medical Solutions USA, Inc., Huntington Beach, CA, United States*

The PETRA sequence provided good image quality. We compared the visualization of the intracranial arteries between TOF-MRA and PETRA-MRA, and evaluated the visualization of the facial nerve canal among PETRA and other 3D sequences (MPRAGE and SPACE). PETRA-MRA was less visualized at the peripheral artery, but PETRA-MRA was as well as TOF-MRA at the main trunk. In the visualization of the facial nerve canal, PETRA was better than MPRAGE at all segments and best at labyrinthine. PETRA would be useful for the visualization of intracranial artery and facial nerve canal.

1329

Alterations of resting-state fMRI measurements in individuals with cervical dystonia

Zhihao Li^{1,2}, Cecília N Prudente^{3,4}, Randall Stilla³, Krish Sathian^{5,6}, Hyder A Jinnah⁷, and Xiaoping Hu²

¹*Affective and Social Neuroscience, Shenzhen University, Shenzhen, China*, ²*Biomedical Engineering, Emory University and Georgia Institute of Technology, Atlanta, GA, United States*, ³*Neurology, Emory University, Atlanta, GA, United States*, ⁴*Physical Medicine and Rehabilitation, University of Minnesota, Minneapolis, MN, United States*, ⁵*Neurology, Rehabilitation Medicine, Psychology, Emory University, Atlanta, GA, United States*, ⁶*Rehabilitation R&D Center for Visual & Neurocognitive Rehabilitation, Atlanta VA Medical Center, Decatur, GA, United States*, ⁷*Neurology, Human Genetics and Pediatrics, Emory University, Atlanta, GA, United States*

Cervical dystonia (CD) is a neurological movement disorder where the pathophysiology remains to be characterized. The present rfMRI study explored CD-associated brain alterations of (i) functional connectivity (FC), (ii) fractional amplitude of low frequency fluctuation (fALFF), and (iii) regional homogeneity (ReHo). The results revealed 25 significant regional alterations that confirm and extend existing knowledge. Additionally, using these regional alterations as diagnostic features, a support vector machine classifier identified 8 features that together yielded a maximum classification accuracy of 97%.

1330

Reduced Field-of-View Diffusion Tensor Imaging of the Optic Nerve in Retinitis Pigmentosa at 3T

Yanqiu Zhang¹, Dapeng Shi¹, Xirang Guo², Meiyun Wang¹, and Dandan Zheng³

¹*Radiology, Zhengzhou University People's Hospital (Henan Provincial People's Hospital), Zhengzhou, China*, ²*People's Republic of*

²*Ophthalmology, Zhengzhou University People's Hospital (Henan Provincial People's Hospital), Zhengzhou, China*, ³*GE Healthcare, MR Research China, Beijing, China*, ³*People's Republic of*

DTI can provide *in vivo* information about the pathology of optic nerve (ON) disease, but the ability of DTI to evaluate alterations of ON

in retinitis pigmentosa (RP) has not been explored so far. In this work, we demonstrate that reduced field-of-view DTI is very helpful for the diagnosis of optic neuropathy in patients with RP *in vivo*, which is very critical to connect radiology and ophthalmology together in RP.

1331

PET/MR versus PET/CT in the Initial Staging of Head and Neck Cancer

Tetsuro Sekine^{1,2}, Felipe Barbosa¹, Felix Kuhn¹, Irene A Burger¹, Paul Stolzmann¹, Gaspar Delso³, Edwin ter Voert¹, Miguel Porto¹, Geoffrey Warnock¹, Gerhard Huber¹, Spyros Koliias¹, Gustav Von Schulthess¹, Patrick Veit-Haibach¹, and Martin Huellner¹

¹University Hospital Zurich, Zurich, Switzerland, ²Nippon Medical School, Tokyo, Japan, ³GE Healthcare, Waukesha, WI, United States

Head and neck cancer is supposed to be one field where PET/MR might offer benefits over PET/CT. Our study revealed that whole-body staging with PET/MR yields at least equal diagnostic accuracy as PET/CT in determining the stage of head and neck cancer.

1332

Resectability assessment of head and neck cancer – PET/MR versus PET/CT

Tetsuro Sekine^{1,2}, Felipe Barbosa¹, Gaspar Delso³, Irene A Burger¹, Paul Stolzmann¹, Edwin ter Voert¹, Gerhard Huber¹, Spyros Koliias¹, Gustav Von Schulthess¹, Patrick Veit-Haibach¹, and Martin Huellner¹

¹University Hospital Zurich, Zurich, Switzerland, ²Nippon Medical School, Tokyo, Japan, ³GE Healthcare, Waukesha, WI, United States

Head and neck cancer is supposed to be one field where PET/MR might offer benefits over PET/CT. Our study revealed that there was an insignificant trend towards higher accuracy of PET/MR than PET/CT for the resectability assessment of head and neck cancer.

1333

The impact of shimming on fat suppression in head-and-neck MRI: current practice vs an image based approach

Tim Schakel¹, Jeroen C.W. Siero², Hans Hoogduin², and Marielle Philippens¹

¹Radiotherapy, UMC Utrecht, Utrecht, Netherlands, ²Radiology, UMC Utrecht, Utrecht, Netherlands

In the head-and-neck region, off resonance effects due to magnetic field inhomogeneities can lead to poor fat suppression. In this study we compare the current clinical practice of shimming (volume shim) with the gain of an image based approach. B0 field maps are analyzed using water/fat segmented Dixon images to estimate the fat suppression. Diffusion weighted images are used to verify the estimates for fat suppression. An image based shimming optimization was performed to simulate 1st and 2nd order shim field. Image based shimming is a promising technique to improve subject specific shimming and fat suppression in the head-and-neck region.

1334

Improved MR neurography of the brachial plexus using high permittivity pads

Paul de Heer¹, Jos Oudeman², Aart J Nederveen², and Andrew G Webb¹

¹CJ Gorter Center, Radiology, Leiden University Medical Center, Leiden, Netherlands, ²Radiology, Amsterdam Medical Center, Amsterdam, Netherlands

Imaging the brachial plexus can be challenging due to the large variations in the B0 and transmit B1 fields in the area of the neck and shoulders. These variations can result in poor background tissue and fat suppression as well as reduction in the received signal from the nerves. We wanted to study if the application of high permittivity pads could increase signal/contrast in plexus brachialis imaging. By applying the pads the signal intensity of the nerves increased from 25 to 50 while the background signal stays similar resulting in a greater contrast of the brachial plexus.

1335

Visualization of Auditory Ossicles and Facial Nerve Canal: Comparison between Ultrashort TE MR and CT.

Takao Kumazawa¹, Yasutaka Fushimi¹, Tomohisa Okada^{1,2}, Takuya Hinoda¹, Tsutomu Okada¹, Akira Yamamoto¹, Yutaka Natsuaki³, and Kaori Togashi¹

¹Kyoto University Graduate School of Medicine, Kyoto, Japan, ²Human Brain Research Center, Kyoto University Graduate School of Medicine, Kyoto, Japan, ³Siemens Medical Solutions USA, Inc., Huntington Beach, CA, United States

The visualization of the inner ear and facial nerve canal was compared between PETRA and CT in this study. The total 24 patients who underwent MRI including PETRA and whole brain CT were enrolled, and visualization of auditory ossicles, semicircular canals, and facial nerve canal are evaluated. All of auditory ossicles, semicircular canals, and facial nerve canal were more visible on CT than PETRA, however, facial nerve canal and semicircular canals were commonly recognized, and auditory ossicles were occasionally visualized on PETRA.

1336

Improved banding removal for high resolution bSSFP imaging of the inner ear using SENSE

Eliana NessAiver¹, Dan Zhu¹, Ari Meir Blitz², and Daniel Herzka¹

¹Biomedical Engineering, The Johns Hopkins University School of Medicine, Baltimore, MD, United States, ²Radiology, The Johns Hopkins Hospital, Baltimore, MD, United States

High resolution imaging of the inner ear is a desirable tool for the diagnosis and treatment of inner ear pathologies. In particular, balanced steady state free precession images have a good balance of high SNR, fast imaging times, and novel tissue contrast which

yields satisfactory differentiation of inner ear structures. However, it suffers from banding artifacts in areas of field inhomogeneity. While common clinical practice is to combine two images that are 180° phase cycled from one another, which shifts the bands to different locations in each image, this yields only partial mitigation of the artifact. This study applies parallel imaging techniques to acquire four phase cycled images in a similar timeframe to the original two-image acquisition, in order to produce a combined volume with superior banding removal at little to no extra cost over current clinical practice.

1337

Simultaneous brain and spinal-cord fMRI using slice-based shimming and a reduced FOV
Haisam Islam¹, Christine Law², Sean Mackey³, and Gary Glover⁴

¹Bioengineering, Stanford University, Stanford, CA, United States, ²Stanford University, Stanford, CA, United States, ³Anesthesiology, Perioperative, and Pain Medicine, Stanford University School of Medicine, Stanford, CA, United States, ⁴Radiology, Stanford University, Stanford, CA, United States

Simultaneous functional imaging of the brain and spinal cord would provide valuable understanding of neural information processing. However, this is challenging due to the poor field homogeneity of the spinal cord as well as the typically high spatial resolution desired for it. The higher-order shims available on most scanners are static, and thus cannot switch rapidly between brain and spinal cord acquisitions. Here, we use a dynamic slice-based shim for brain slices and a volume-based shim + reduced FOV acquisition for a neck volume to perform simultaneous functional imaging of both structures of interest.

1338

Diffusion Method to Image Normal Human Optic Nerve
Lazar Fleysher¹, Matilde Inglese^{1,2,3}, Mark J Kupersmith, MD^{2,4}, and Niels Oesingmann⁵

¹Radiology, Icahn School of Medicine at Mount Sinai, New York, NY, United States, ²Neurology, Icahn School of Medicine at Mount Sinai, New York, NY, United States, ³Neuroscience, Icahn School of Medicine at Mount Sinai, New York, NY, United States, ⁴Ophthalmology, Icahn School of Medicine at Mount Sinai, New York, NY, United States, ⁵Siemens Healthcare, USA, New York, NY, United States

In this work we demonstrate an application of a single-shot EPI diffusion sequence with outer-volume suppression to optic nerve imaging. The advantage of this approach is that it is simple and is available on clinical systems. This paves a way to a routine diffusion-encoded clinical examinations of the optic nerve

1339

Relationships between intratumoral heterogeneity parameters using diffusion, perfusion MRI, and FDG PET in head and neck cancer
Su Jin Lee¹, Jin Wook Choi², and Miran Han²

¹Nuclear Medicine, Ajou University School of Medicine, Suwon, Korea, Republic of, ²Radiology, Ajou University School of Medicine, Suwon, Korea, Republic of

MRI and PET can provide tumor biology information noninvasively. ADC from DWI can represent cellularity, DCE-MRI can provide microcirculation, and FDG PET can provide tumor metabolism. Intratumoral heterogeneity is often associated with adverse tumor biology and it can be assessed by these imaging parameters. Tumor heterogeneity on DWI can be simply evaluated by the difference between minimum and maximum ADC value. Metabolism to perfusion ratio can be calculated using DCE-MRI and FDG PET. Texture analysis of PET can be used to evaluate tumor heterogeneity. Thus we investigated the relationships between intraheterogeneity parameters derived from multimodality imaging.

1340

T1 weighted 3D Cube with Dixon water-fat separation for imaging of the orbits
Ken-Pin Hwang¹, Jingfei Ma¹, Ping Hou¹, Ho-Ling Anthony Liu¹, Kang Wang², and T. Linda Chi³

¹Department of Imaging Physics, The University of Texas M.D. Anderson Cancer Center, Houston, TX, United States, ²MR Applications and Workflow, General Electric Healthcare, Waukesha, WI, United States, ³Department of Diagnostic Radiology, The University of Texas M.D. Anderson Cancer Center, Houston, TX, United States

2-point Dixon water-fat separation is implemented in a Cube (3D FSE) sequence. It is compared with IR-FSPGR and Cube with fat saturation for post-contrast T1-weighted high resolution imaging of the orbits. Dixon water-fat separation provided even fat suppression through the imaging volume and maintained the signal efficiency of the other techniques. Optic nerve was well delineated even through areas of high susceptibility, and large vessels were well suppressed relative to nearby structures. We thus demonstrate a promising new technique for evaluating disease in a challenging area with fine structures and high susceptibility.

1341

The value of combining conventional, diffusion-weighted and dynamic contrast-enhanced MR imaging for the diagnosis of parotid gland tumors
Xiaofeng Tao¹, gongxin yang¹, Yingwei Wu², huimin shi¹, pingzhong wang¹, yongming Dai³, wenjing zhu¹, Weiqing gao¹, and qiang yu¹

¹Shanghai Ninth People's Hospital, School of Medicine, Shanghai Jiao Tong University, shanghai, China, People's Republic of, ²Shanghai Ninth People's Hospital, School of Medicine, Shanghai Jiao Tong University, Shanghai, China, People's Republic of, ³PHLIPS healthcare China, shanghai, China, People's Republic of

The aim of this study was to determine the value of combining conventional MR imaging (MRI), diffusion-weighted (DW-MRI) and dynamic contrast enhanced MRI (DCE-MRI) in diagnosing solid neoplasms in the parotid gland. Materials and Methods: A total of 148 subjects (101 with benign and 47 with malignant tumors) were evaluated with conventional MRI, DW-MRI and DCE-MRI prior to surgery and pathologic verification. The items observed with conventional MRI included the shape, capsule and signal intensity of parotid

masses. The apparent diffusion coefficient (ADC) was calculated from DW-MRI that was obtained with a b factor of 0 and 1000 s/mm². A time-intensity curve (TIC) was obtained from DCE-MRI. Results: There were significant differences ($p<0.01$) in the shape, capsule, ADC and TIC between benign and malignant parotid tumors. Irregular neoplasms without capsule, $ADC < 1.12 \times 10^{-3} \text{ mm}^2/\text{s}$, and a plateau enhancement pattern were valuable parameters for predicting malignant neoplasms. A combination of all of these parameters yielded sensitivity, specificity, accuracy, and positive and negative predictive values of 85.1%, 94.1%, 91.2%, and 87.0% and 93.1%, respectively. Conclusion: A combined analysis using conventional MRI, DW-MRI and DCE-MRI is helpful to distinguish benign from malignant tumors in the parotid gland.

1342

Diffusivity of Intraorbital Lymphoma vs. Inflammation: Comparison of Single Shot Turbo Spin Echo and Multishot Echo Planar imaging Techniques

Akio Hiwatashi¹, Osamu Togao¹, Koji Yamashita¹, Kazufumi Kikuchi¹, and Hiroshi Honda¹

¹Clinical Radiology, Kyushu University, Fukuoka, Japan

Diffusion-weighted imaging is useful to characterize orbital lesions. Various techniques were advocated to overcome image degradation in head and neck regions. We compared single shot TSE and multishot EP DWI and concluded that the ADC derived from TSE DWI, not from multishot EP DWI, might help to differentiate orbital lymphoma from inflammation.

1343

Usefulness of solid type stimulator in MR Sialography-Comparison with liquid type stimulator

Kim Sang Min¹ and Kwon Hye Yin¹

¹Pungnap 2-dong, Asan Medical Center, Seoul, Korea, Republic of

A study on alternative to vitamin C juice in sialography MRI.

Traditional Poster

Brain Tumours: Pre-Clinical & Clinical Applications

Exhibition Hall

Monday, May 9, 2016: 10:45 - 12:45

1344

Effect of measured Hematocrit value on Glioma grading using Dynamic contrast enhanced derived MR perfusion parameter

Prativa Sahoo¹, Pradeep Kumar Gupta², Ashish Awasthi³, Chandra Mani Pandey³, Rana Patir⁴, Sandeep Vaishya⁵, and Rakesh Kumar Gupta²

¹Healthcare, Philips India Ltd, Bangalore, India, ²Radiology and Imaging, Fortis Memorial Research Institute, Gurgaon, India, ³Biostatistics, Sanjay Gandhi Post Graduate Institute of Medical Sciences, Lucknow, India, ⁴Neurosurgery, Fortis Memorial Research Institute, Gurgaon, India, ⁵Neurosurgery, Fortis Memorial Research Institute, Lucknow, India

Quantification of DCE-MRI assumes a constant blood hematocrite (Hct) of 45% for adult human population. However Hct varies with disease condition and more with chemotherapy. Correction of the measured signal for blood Hct level is important as blood T1, quantification of contrast agent and arterial input function is dependent on it. Purpose of this study was to investigate the influence of Hct values on glioma grading using DCE-MRI derived perfusion parameters. Study suggest that even though grading of glioma not influenced by Hct values it does affect the kinetic parameters and might be important for monitoring serial assessment of disease progressions.

1345

Can dynamic contrast enhanced MR perfusion metrics accurately discriminate different grades of Gliomas?

Jitender Saini¹, Pradeep Kumar Gupta², Prativa Sahoo³, Rana Patir⁴, Sandeep Vaishya⁵, Arun Kumar Gupta¹, Amey Savarderkar⁶, and Rakesh Kumar Gupta²

¹Neuroimaging & Interventional Radiology, National Institute of Mental Health and Neurosciences, Bangalore, India, ²Radiology and Imaging, Fortis Memorial Research Institute, Gurgaon, India, ³Healthcare, Philips India Ltd, Bangalore, India, ⁴Neurosurgery, Fortis Memorial Research Institute, Gurgaon, India, ⁵Neurosurgery, Fortis Memorial Research Institute, Lucknow, India, ⁶Neurosurgery, National Institute of Mental Health and Neurosciences, Bangalore, India

Dynamic contrast enhanced MRI perfusion is a useful technique for assessment of glioma grading. This technique has been used in the past for discrimination of low from high grade gliomas. This study investigates the ability of DCE perfusion MRI to discriminate Grade II from Grade III and Grade III from Grade IV gliomas. Various DCE pharmacokinetic parameters were also analysed for their ability to distinguish the various grades of gliomas.

1346

Investigation of hypoxia conditions using oxygenation enhance (OE)-MRI measurements in C6 glioma models

Yingwei Wu¹, Yongming Dai², Qi Fan¹, and Xianfeng Tao¹

¹Shanghai Ninth People's Hospital, School of Medicine, Shanghai Jiao Tong University, Shanghai, China, People's Republic of, ²Philips Healthcare, Shanghai, China, People's Republic of

We used oxygenation enhancement (OE)-MRI measurements to investigate hypoxia conditions of gliomas and to evaluate relationship

between histopathology measurements and PSC. Oxygen amplitude maps of C6 glioma models were derived. ROI max and ROI non-max were defined. Time-SI curve from ROI areas was obtained and tissues from ROI areas was evaluated for microvessel density and expression of HIF-1a. We found that microvessel density in ROI non-max area were lower than those in ROI max area and expression of HIF-1a in ROI non-max area were higher than that in ROI max area. PSC had a linear positive correlation with vessel density.

1347

Quantitative DTI-FA Mapping in Prediction of Meningioma fibrous content, Consistency and grade.

Shanker Raja^{1,2}, Wafa AlShawkeer³, Lama Mohammed Almudaimeegh³, Sadeq Al Dandan⁴, and Sharad P George⁵

¹*Radiology, Baylor College of Medicine, Bellaire, TX, United States*, ²*Radiology, KFMC, Riyadh, Saudi Arabia*, ³*King Khalid University Hospital, Riyadh, Saudi Arabia*, ⁴*King Fahad Medical City, Riyadh, Saudi Arabia*, ⁵*Baylor College of Medicine, Houston, TX, United States*

We utilized quantitative FA-maps derived from DTI to evaluate the fibrous content consistency and grade of meningioma. Our results suggest that, quantitative FA mapping is promising in pre-operative prediction of meningioma consistency pre-operatively, but only modestly correlates with histologic grading

1348

Imaging Angiogenesis Genotype of Glioblastoma by Radiomic Features of Multi-modality MRI

Chia-Feng Lu^{1,2,3}, Fei-Ting Hsu⁴, Li-Chun Hsieh⁴, Yu-Chieh Jill Kao^{1,2}, Hua-Shan Liu^{4,5}, Ping-Huei Tsai^{2,4}, Pen-Yuan Liao⁴, and Cheng-Yu Chen^{1,2,4}

¹*Translational Imaging Research Center, College of Medicine, Taipei Medical University, Taipei, Taiwan*, ²*Department of Radiology, School of Medicine, Taipei Medical University, Taipei, Taiwan*, ³*Department of Biomedical Imaging and Radiological Sciences, National Yang-Ming University, Taipei, Taiwan*, ⁴*Department of Medical Imaging, Taipei Medical University Hospital, Taipei, Taiwan*, ⁵*Graduate Institute of Clinical Medicine, Taipei Medical University, Taipei, Taiwan*

The multi-modality and multi-radiomic-feature MRI may provide a more efficient regression model for imaging gene expressions than the conventional radiogenomic approach.

1349

Optimization of glioma biopsy targeting applying T1-DCE MRI parameter maps – A double-blinded prospective study

Vera Catharina Keil¹, Bogdan Pintea², Gerrit H. Gielen³, Matthias Simon², Juergen Gieseke^{1,4}, Hans Heinz Schild¹, and Dariusch Reza Hadizadeh¹

¹*Department of Radiology, Universitätsklinikum Bonn, Bonn, Germany*, ²*Clinic for Neurosurgery and Stereotaxy, Universitätsklinikum Bonn, Bonn, Germany*, ³*Department of Neuropathology, Universitätsklinikum Bonn, Bonn, Germany*, ⁴*Philips Healthcare, Best, Netherlands*

Many centers refrain from implementing semi-quantitative MRI techniques, such as T1w contrast-enhanced MRI (T1-DCE MRI), as a benefit for the patient is questioned. To elucidate if T1-DCE MRI has a benefit, we compared the standard neurosurgical biopsy target selection method (based on T1w contrast-enhanced or FLAIR maps) with a selection based on "hot spots" on K^{trans} maps in a double-blinded, prospective setting with 27 glioma patients. 87 tissue samples were taken (55 K^{trans} -based, 32 standard). K^{trans} -based selection showed a strong tendency to be the more successful targeting method (glioblastoma: n=20/39 vs. n=11/20; p=0.085; WHO III/II: n=12/13 vs. n=6/11; p=0.061).

1350

Cerebrospinal fluid compression in cerebellum on treatment-naïve MRI might be an early indicator of poor survival in Glioblastoma: A preliminary study

Gavin Hanson¹, Prateek Prasanna¹, Jay Patel¹, Anant Madabhushi¹, and Pallavi Tiwari¹

¹*Department of Biomedical Engineering, Case Western Reserve University, Cleveland, OH, United States*

Glioblastoma Multiforme (GBM) is very aggressive form of primary brain tumor, and a key part of GBM pathogenesis is the mass effect of the tumor within the ridge container of the brain vault. Mass effect is strongly associated with mortality in patients with GBM. In this work, we seek to quantify the extent of mass effect throughout the brain volume as manifested on MRI to predict patient survival in GBM patients. We use a MRI-driven tensor based morphometry approach, combined with statistical mapping to allow the identification of regions where the deformation associated with mass effect is correlated with overall survival after diagnosis.

1351

Gadolinium-DTPA-enhanced MR imaging of brain tumors: comparison with T1-Cube and 3D fast spoiled gradient recall acquisition in steady state sequences

Mungunkhuyag Majiguren^{1,2}, Takashi Abe², and Masafumi Harada²

¹*Mongolian National University of Medical Sciences, Ulaanbaatar, Mongolia*, ²*The University of Tokushima, Tokushima, Japan*

We compared the gadolinium enhancement characteristics of a heterogeneous population of brain tumors imaged by T1-Cube and 3D FSPGR at 3T MRI with time-dependent changes. A total of 91 lesions from 52 patients with brain tumors in 3T MRI. Fifty-one of the 91 lesions (56.04%) were depicted with T1-Cube first, and 40 lesions (43.96%), with 3D FSPGR first. 3D FSPGR images would be expected to exhibit greater enhancement than T1-Cube images. However, the overall mean CNR values were higher on T1-Cube images with both order sequences. We suggest the superiority of T1-Cube to 3D FSPGR for the detection of metastatic lesions.

1352

An MRS and PET guided biopsy tool for ultrasound-based intra-operative neuro-navigational systems.

Matthew Grech-Sollars^{1,2}, Babar Vagas³, Gerard Thompson⁴, Tara Barwick^{2,5}, Lesley Honeyfield², Kevin S O'Neill³, and Adam D

¹Division of Brain Sciences, Imperial College London, London, United Kingdom, ²Department of Imaging, Imperial College NHS Healthcare Trust, London, United Kingdom, ³Department of Neurosurgery, Imperial College NHS Healthcare Trust, London, United Kingdom, ⁴Department of Neuroradiology, Salford Royal NHS Foundation Trust, Salford, United Kingdom, ⁵Department of Surgery and Cancer, Imperial College London, London, United Kingdom

Glioma heterogeneity and the limitations of conventional structural MRI to identify aggressive tumour components limits targeting of stereotactic biopsy, and hence tumour characterisation. In vivo MR spectroscopy and PET allow for physiological characterisation of tumour and we here present a method for representing MRS and PET defined regions to biopsy using an ultrasound based neuronavigational system. Our method involves using colour-coded hollow spheres to represent the target biopsy regions, which can be easily identified during the surgery. This approach can be applied to target the most aggressive regions of a tumour and as a tool for imaging biomarker validation.

1353

Translation of 2-hydroxyglutarate MR spectroscopy into clinics

Zhongxu An¹, Sandeep Ganji¹, Vivek Tiwari¹, Edward Pan^{2,3,4}, Bruce Mickey^{2,4,5}, Elizabeth A. Maher^{2,3,5,6}, and Changho Choi^{1,2,7}

¹Advanced Imaging Research Center, University of Texas Southwestern Medical Center, Dallas, TX, United States, ²Harold C. Simmons Cancer Center, University of Texas Southwestern Medical Center, Dallas, TX, United States, ³Department of Neurology and Neurotherapeutics, University of Texas Southwestern Medical Center, Dallas, TX, United States, ⁴Department of Neurological Surgery, University of Texas Southwestern Medical Center, Dallas, TX, United States, ⁵Annette Strauss Center for Neuro-Oncology, University of Texas Southwestern Medical Center, Dallas, TX, United States, ⁶Department of Internal Medicine, University of Texas Southwestern Medical Center, Dallas, TX, United States, ⁷Department of Radiology, University of Texas Southwestern Medical Center, Dallas, TX, United States

2-hydroxyglutarate (2HG) is an important biomarker for IDH-mutated gliomas. Thus in vivo measurement of 2-hydroxyglutarate can provide important information for brain tumor diagnosis and prognosis. Several techniques for *in-vivo* detection of 2HG were reported recently. However, due to limited access to scan parameters in clinical setup, translation of such techniques into clinics is limited. We report the reproducibility of a recently developed clinically-available PRESS-based 1H MRS method, for in vivo 2HG measurement at research and clinical scanners.

1354

Tumor Classification Using Blood Arrival Histogram Obtained by Resting-state fMRI

Tianyi Qian¹, Yinyan Wang^{2,3}, Kun Zhou⁴, Yuanyuan Kang⁴, Shaowu Li^{2,5}, and Tao Jiang^{2,5}

¹MR Collaborations NE Asia, Siemens Healthcare, Beijing, China, People's Republic of, ²Neurosurgery, Tiantan Hospital, Beijing, China, People's Republic of, ³Beijing Neurosurgical Institute, Capital Medical University, Beijing, China, People's Republic of, ⁴Siemens Shenzhen Magnetic Resonance Ltd., APPL, Shenzhen, China, People's Republic of, ⁵Beijing Neurosurgical Institute, Capital Medical University, Beijing, China, People's Republic of

In this study, a new post-processing pipeline of resting-statefMRI (rs-fMRI) was proposed for glioma grading, with the feasibility of extracting the timing information of brain perfusion from BOLD signal. The blood arrival time obtained from rs-fMRI shows unevenly distributed perfusion patterns in tumors. A histogram-based analysis method was employed to analyze the non-uniform distribution that could extract the patterns better than the routine method. The proposed pipeline was able to classify between low- and high-grade gliomas.

1355

Mapping of brain tumor oxygen metabolism in native MRI

Patrick Borchert¹, Lasse Dührsen², Div S. Bolar³, Nils-Ole Schmidt², Jan-Hendrik Buhk¹, Jens Fiehler¹, and Jan Sedlacik¹

¹Neuroradiology, UKE, Hamburg, Germany, ²Neurosurgery, UKE, Hamburg, Germany, ³Martinos Center, MGH, Boston, MA, United States

The QUIXOTIC method was tested in conjunction with ASL to map tumor oxygen metabolism in glioma patients. A higher oxygen extraction fraction was found for low grade gliomas, whereas lower cerebral blood flow was found for high grade gliomas. Both parameters were stable in healthy gray matter. These findings suggest, that the QUIXOTIC method is able to map tumor oxygen metabolism in conjunction with ASL. Furthermore, these findings may suggest, that low grade gliomas may maintain a more aerobic metabolism than high grade gliomas and that the uncontrolled tumor angiogenesis of high grade gliomas may cause hindered tumor perfusion.

1356

Validation of a semi-automatic coregistration of MRI scans in brain tumor patients during treatment follow-up

Jiun-Lin Yan^{1,2,3}, Anouk van der Hoorn^{4,5}, Timothy J Larkin⁶, Natalie R Boonzaier⁶, Tomasz Matys⁵, and Stephen J Price⁶

¹Clinical Neuroscience, University of Cambridge, Cambridge, United Kingdom, ²Neurosurgery, Chang Gung Memorial Hospital, Keelung, Taiwan, ³Department of neurosurgery, Chang Gung University College of Medicine, Taoyuan, Taiwan, ⁴Department of radiology (EB44), University Medical Centre Groningen, Groningen, Netherlands, ⁵Department of radiology, University of Cambridge, Cambridge, United Kingdom, ⁶Brain tumour imaging laboratory, University of Cambridge, Cambridge, United Kingdom

Coregistration of lesional brain MRI between different time points is challenging. We aimed to propose a two staged semi-automatic coregistration methods to overcome the difficulty. Firstly, we calculated the transformation between presurgical tumor and postsurgical resection cavity by using the linear FLIRT co-registration. This creates a transformation matrix used for the progression and pseudoprogression area with optimal correction of variable brain shift. Then we applied this transformation matrix to a non-linear FNIRT transformation to coregister the brain. Validation by using registration target error showed smaller deviation can be achieved by

using this method compared to direct non-linear registration.

1357

Contrast-Enhanced Synthetic MRI for the Detection of Brain Metastases: Comparison Between Synthetic T1-weighted Inversion-recovery Image, Synthetic T1-weighted Image, and Conventional T1-weighted Inversion-recovery Fast Spin-Echo Image.
Misaki Nakazawa^{1,2}, Akiyuki Hagiwara^{2,3}, Masaaki Hori², Christina Andica², Koji Kamagata², Hideo Kawasaki², Nao Takano², Shuji Sato², Nozomi Hamasaki², Kouhei Tsuruta^{1,2}, Sho Murata^{1,2}, Ryo Ueda^{1,2}, Shigeki Aoki², and Atsushi Senoo¹

¹Graduate School of Human Health Sciences, Tokyo Metropolitan University, Tokyo, Japan, ²Department of Radiology, Juntendo University School of Medicine, Tokyo, Japan, ³Graduate School of Medicine, The University of Tokyo, Tokyo, Japan

The purpose of this study was to assess whether contrast-enhanced synthetic MRI is suitable for detecting brain metastases by comparing the lesion-to-white matter contrast, contrast-to-noise ratio, and number of brain metastases detected in synthetic and conventional magnetic resonance images. Synthetic T1IR images had better contrast compared with synthetic T1W or conventional T1IR images. Synthetic T1IR images enabled detection of more metastases than did synthetic T1W and conventional T1IR images even though statistical significance was not detected. Contrast-enhanced synthetic T1IR is useful for detecting brain metastases. Further optimization of contrast weighting is needed to maximize the ability to detect brain metastases. The purpose of this study was to assess whether contrast-enhanced synthetic MRI is suitable for detecting brain metastases by comparing the lesion-to-white matter contrast, contrast-to-noise ratio, and number of brain metastases detected in synthetic and conventional magnetic resonance images. Synthetic T1IR images had better contrast compared with synthetic T1W or conventional T1IR images. Synthetic T1IR images enabled detection of more metastases than did synthetic T1W and conventional T1IR images even though statistical significance was not detected. Contrast-enhanced synthetic T1IR is useful for detecting brain metastases. Further optimization of contrast weighting is needed to maximize the ability to detect brain metastases.

1358

Bayesian Estimation of Microstructural Parameters in Glioma Patients and Comparison with Genetic Analysis
Elias Kellner¹, Marco Reisert¹, Ori Staszewski², Bibek Dhital¹, Valerij G Kiselev¹, Karl Egger³, Horst Urbach³, and Irina Mader³

¹Department of Radiology, Medical Physics, University Medical Center Freiburg, Freiburg, Germany, ²Freiburg, Germany, ³Department of Neuroradiology, University Medical Center Freiburg, Freiburg, Germany

In a recent study, we proposed a method for fast and direct estimation of microstructural tissue parameters such as intra/extraxonal volume fraction and diffusivities based on multishell DWI. In this study, we report the first method application to human gliomas and demonstrate connections of microstructural parameters with genetic markers IDH and 1p19q in a group of 32 patients.

1359

In Vivo Detection of 2-Hydroxyglutarate in Low-Grade Glioma Patients
Elizabeth D Phillips¹, Llewellyn E Jalbert¹, Yan Li¹, Marisa M Lafontaine¹, and Sarah J Nelson¹

¹Radiology and Biomedical Imaging, University of California, San Francisco, San Francisco, CA, United States

While the feasibility of utilizing 2HG as a magnetic resonance biomarker has been established *ex vivo*, several different approaches to obtaining *in vivo* data have been presented. This project aims to assess the concordance of 2HG detection using asymmetric echo PRESS MRSI with IDH1_{R132H} mutation as identified via antibody staining in patients with LGG, and to investigate the relationship of other metabolites detected with this sequence to IDH status. Further research is required before routine clinical implementation of these methods is recommended.

1360

¹H Echo Planar Spectroscopic Imaging of 2-hydroxyglutarate in Gliomas at 7T *in vivo*
Zhongxu An¹, Sandeep Ganji¹, Vivek Tiwari¹, Marco C. Pinho^{1,2}, Edward Pan^{3,4,5}, Bruce E. Mickey^{3,5,6}, Elizabeth A. Maher^{3,4,6,7}, and Changho Choi^{1,2,3}

¹Advanced Imaging Research Center, University of Texas Southwestern Medical Center, Dallas, TX, United States, ²Department of Radiology, University of Texas Southwestern Medical Center, Dallas, TX, United States, ³Harold C. Simmons Cancer Center, University of Texas Southwestern Medical Center, Dallas, TX, United States, ⁴Department of Neurology and Neurotherapeutics, University of Texas Southwestern Medical Center, Dallas, TX, United States, ⁵Department of Neurological Surgery, University of Texas Southwestern Medical Center, Dallas, TX, United States, ⁶Annette Strauss Center for Neuro-Oncology, University of Texas Southwestern Medical Center, Dallas, TX, United States, ⁷Department of Internal Medicine, University of Texas Southwestern Medical Center, Dallas, TX, United States

2-hydroxyglutarate (2HG) is the first imaging biomarker for IDH-mutated gliomas. High-spatial resolution spectroscopic imaging of 2HG is clinically important. We propose a new EPSI read-out scheme to overcome the conventional limitation of EPSI spectral bandwidth at high field. With SNR and linewidth benefit at 7T, we demonstrated the *in vivo* feasibility of this new EPSI method in mapping of 2HG and other important brain metabolites in normal subject and glioma patients at 7T.

1361

Hybrid PET MRI of brain tumours: spatial relationship of tumour volume in FET PET and 3D MRSI
Jörg Mauler¹, Karl-Josef Langen^{1,2}, Andrew A. Maudsley³, Omid Nikoubashman⁴, Christian Filss¹, Gabriele Stoffels¹, and N. Jon Shah^{1,5}

¹Forschungszentrum Jülich, Jülich, Germany, ²Department of Nuclear Medicine, Faculty of Medicine, RWTH Aachen University, Aachen, Germany, ³Miller School of Medicine, University of Miami, Miami, FL, United States, ⁴Department of Neuroradiology, RWTH Aachen University, Aachen, Germany, ⁵Department of Neurology, Faculty of Medicine, JARA, RWTH Aachen University, Aachen, Germany

Gliomas are characterised by an elevated expression of amino acid transporters and cell turnover. The spatial overlap of the

corresponding volumes was analysed in 46 subjects, based on O-(2-[18F]fluoroethyl)-L-tyrosine (FET) uptake, measured with PET and by means of the choline to N-acetyl-aspartate (Cho/NAA) ratio, determined by simultaneously acquired, 3D spatially resolved MR spectroscopic imaging data. The overlap between the respective volumes averaged out to (30±23) % with tumour volumes of (14±15) cm³ and (39±28) cm³ in case of FET uptake and increased Cho/NAA-ratio, respectively. Thus the imaging modalities may represent different metabolic properties of gliomas.

1362

Apparent diffusion coefficient in preoperative grading of gliomas: a comparison between ultra-high and conventional mono-b value diffusion-weighted MR imaging

YuChuan Hu¹, LinFeng Yan¹, ZhiCheng Liu¹, YingZhi Sun¹, DanDan Zheng², TianYong Xu², Wen Wang¹, and GuangBin Cui¹

¹Department of Radiology, Tangdu Hospital, Fourth Military Medical University, Xi'an, China, People's Republic of, ²MR Research China, GE Healthcare China, Beijing, China, People's Republic of

The preoperative grading of gliomas, which is critical for determination of the most appropriate treatment, remains unsatisfactory. As an improved MRI technique, diffusion-weighted imaging (DWI) is considered the most sensitive for early pathological changes and therefore can potentially be useful in evaluating the glioma grades. Recently, apparent diffusion coefficient (ADC) values derived from the high (3000 sec/mm²) b values DWI were reported to improve the diagnostic performance of DWI in differentiating high- from low-grade gliomas⁵. But a mono-exponential model and relatively lower high-b values were used in this study. We used a tri-component model to calculate ultra-high ADC (ADCuH) in our research, aiming to retrospectively compare the efficacy of ultra-high and conventional mono-b value DWI in the glioma grading.

1363

18F-methylcholine PET/CT and magnetic resonance spectroscopy imaging and tissue biomarkers of cell membrane turnover in primary brain gliomas – a pilot study

Matthew Grech-Sollars^{1,2}, Katherine Ordidge^{1,2}, Babar Vaqas³, Lesley Honeyfield², Sameer Khan², Sophie Camp³, David Towey², David Peterson³, Federico Roncaroli⁴, Kevin S O'Neill³, Tara Barwick^{2,5}, and Adam D Waldman^{1,2}

¹Division of Brain Sciences, Imperial College London, London, United Kingdom, ²Department of Imaging, Imperial College NHS Healthcare Trust, London, United Kingdom, ³Department of Neurosurgery, Imperial College NHS Healthcare Trust, London, United Kingdom, ⁴Department of Neuropathology, Imperial College NHS Healthcare Trust, London, United Kingdom, ⁵Department of Surgery and Cancer, Imperial College London, London, United Kingdom

Choline elevation has been reported as a marker of aggressive glioma phenotype in numerous in vivo MRS studies, and more recently 18F-methylcholine-PET has been applied to glioma characterisation. This study examines the relationship between MRS and PET choline measures in defined tumour regions, in order to validate these against tissue biomarkers of choline metabolism and proliferation. Our initial results raise the possibility that imaging markers of choline metabolism are influenced by inflammatory and reactive processes for low grade tumours.

1364

Assessment of Anti-EGFRvIII Chimeric Antigen Receptor (CAR) T cell Therapy for Patients with Glioblastomas using Diffusion, Perfusion and MR Spectroscopy

Sumei Wang¹, Donald M O'Rourke², Sanjeev Chawla¹, Gaurav Verma¹, Gabriela Plesa³, Carl H June³, Marcela V Maus⁴, Steven Brem², Eileen Maloney², Jennifer JD Morrisette⁵, Maria Martinez-Lage⁵, Arati Desai⁶, Ronald L Wolf¹, Harish Poptani^{1,7}, and Suyash Mohan¹

¹Radiology, University of Pennsylvania, Philadelphia, PA, United States, ²Neurosurgery, University of Pennsylvania, Philadelphia, PA, United States, ³Pathology and Laboratory Medicine, Center for Cellular Immunotherapies, University of Pennsylvania, Philadelphia, PA, United States, ⁴Center for Cancer Immunology, Massachusetts General Hospital Cancer Center, Charlestown, MA, United States, ⁵Pathology and Laboratory Medicine, University of Pennsylvania, Philadelphia, PA, United States, ⁶Hematology-Oncology, University of Pennsylvania, Philadelphia, PA, United States, ⁷Cellular and Molecular Physiology, University of Liverpool, Liverpool, United Kingdom

Chimeric Antigen Receptor (CAR) T cell therapy is a novel method of treating tumors. Since EGFRvIII is expressed in some glioblastomas, we evaluated the efficacy of anti-EGFRvIII CART for treating these tumors. Treatment response was assessed via serial MRI scans at 1 and 2 months after CAR-T cell therapy. The rCBVmax and Cho/Cr ratio decreased whereas MD and FA stayed relatively stable for most patients, indicating a positive response that can be assessed by these methods.

1365

Fast Imaging Employing Steady-State Acquisition of Brain Metastasis: from mouse to woman

Donna H Murrell^{1,2}, Keng Yeow Tay³, Eugene Wong^{2,3}, Ann F Chambers^{2,3}, Francisco Perera³, and Paula J Foster^{1,2}

¹Imaging Research Laboratories, Robarts Research Institute, London, ON, Canada, ²Department of Medical Biophysics, Western University, London, ON, Canada, ³London Health Sciences Centre, London, ON, Canada

Brain metastatic burden may be underestimated in the clinic because some tumors are impermeable to Gadolinium (Gd). Preclinical studies by our group demonstrated that fast imaging employing steady-state acquisition (FIESTA) was advantageous for detecting small Gd-impermeable tumors. Here, we show clinical translation of this imaging strategy. We present FIESTA images of human brain metastasis alongside standard clinical MRI and illustrate potential clinical utility of this sequence. Initial data suggests FIESTA can visualize intra-tumor heterogeneity where standard clinical MRI could not. Additional lesions were observed in FIESTA; we hypothesize some may be arachnoid cysts, though metastasis cannot be ruled out.

1366

Distinguishing the Chemical Signature of Different IDH Mutations in Brain Tumor Patients at 7 Tesla

Uzay E Emir¹, Sarah Larkin², Nick de Pennington², Puneet Plaha³, Natalie Voets¹, James McCullagh⁴, Richard Stacey³, Peter Jezzard¹

¹FMRIB Centre, University of Oxford, Oxford, United Kingdom, ²Nuffield Department of Clinical Neurosciences, University of Oxford, Oxford, United Kingdom, ³Department of Neurosurgery, John Radcliffe Hospital, Oxford University Hospitals NHS Trust, Oxford, United Kingdom,

⁴Department of Chemistry, University of Oxford, Oxford, United Kingdom

In this study, we show a proton magnetic resonance spectroscopy (¹H-MRS) acquisition scheme at 7T, enabling discernible 2-HG in the spectra of IDH-mutant patients acquired within 20s and quantify metabolic changes associated with the IDH mutation. Due to the increased sensitivity and specificity of this scheme at 7T, we demonstrate elevated 2-HG and Lactate accumulation in IDH2 R172K (mitochondrial) compared to the IDH1 R132H (cytosolic) mutant tumors in human brains noninvasively.

1367

Developing a Semi-Automatised Tool for Grading Brain Tumours with Susceptibility-Weighted MRI
Maria Duvaldt¹ and Tomas Jonsson¹

¹Dept. of Medical Physics, Karolinska University Hospital, Stockholm, Sweden

In order to make an adequate decision on the further treatment of a glioma cancer patient a tissue sample from the tumour is microscopically analysed and classified on a malignancy scale set by the WHO. In this project a software program with a graphical user interface is developed, where the malignancy grade of a tumour could be found by image analysis of susceptibility-weighted MR images. The parameters examined are the local image variance and intratumoural susceptibility signal and the results show the possibility of distinguishing high grade from low grade astrocytoma by image analysis only.

1368

Non-Gaussian measurements of water diffusion in glioma as a tool for probing tumor heterogeneity and grade.
Fulvio Zaccagna¹, Frank Riemer¹, Mary McLean², Andrew N. Priest³, James T. Grist¹, Joshua Kaggie¹, Sarah Hilborne¹, Tomasz Matys¹, Martin J. Graves¹, Jonathan H. Gillard¹, Stephen J. Price⁴, and Ferdia A. Gallagher¹

¹Department of Radiology, University of Cambridge, Cambridge, United Kingdom, ²Cancer Research UK Cambridge Institute, University of Cambridge, Cambridge, United Kingdom, ³Radiology, Cambridge University Hospitals NHS Foundation Trust, Cambridge, United Kingdom,

⁴Neurosurgery Unit, Department of Clinical Neurosciences, University of Cambridge, Cambridge, United Kingdom

Glioma grade and extent of local infiltration are used to guide surgical tumor management. Heterogeneity imaging is a way of assessing the tumor microenvironment, which may improve diagnosis and therapy planning. Diffusion Kurtosis Imaging (DKI) is a novel promising technique that estimates non-Gaussian water diffusion as a measure of heterogeneity. We investigate the use of DKI in glioma as a tool to improve tumor grading and to estimate infiltration. Our preliminary results show a mean kurtosis of 0.56 ± 0.02 in glioblastoma and 1.14 ± 0.07 in normal-appearing white matter. DKI may thus represent a useful tool for estimation of tumor heterogeneity in glioma.

1369

Impact of semi-automatic delineation of hotspots of contrast enhancing region in predicting the outcome of GBM patients after brain surgery
Adrian Ion-Margineanu^{1,2}, Sofie Van Cauter^{3,4}, Diana M Sima^{1,2}, Frederik Maes^{2,5}, Stefan Sunaert³, Stefaan Van Gool⁶, Uwe Himmelreich⁷, and Sabine Van Huffel^{1,2}

¹ESAT - STADIUS, KU Leuven, Leuven, Belgium, ²Medical IT, iMinds, Leuven, Belgium, ³Department of Radiology, University Hospitals of Leuven, Leuven, Belgium, ⁴ZOL - Ziekenhuis Oost-Limburg, Genk, Belgium, ⁵ESAT - PSI, KU Leuven, Leuven, Belgium, ⁶Department of Pediatric Neuro-Oncology, University Hospitals of Leuven, Leuven, Belgium, ⁷Department of Imaging and Pathology, Biomedical MRI / MoSAIC, Leuven, Belgium

Delineating contrast enhancing (CE) tissue is an integral part of the RANO criteria for therapy response assessment in high-grade gliomas. We propose a semi-automatic delineation of hotspots of CE (HCE) in brain tumour follow-up of 29 glioblastoma multiforme patients after surgery. Based on multi-parametric magnetic resonance data we predict the post-operative evolution of the brain tumour by labelling each patient at each time point as responsive or progressive. The results obtained with our semi-automatic method are better in most of the cases than the results obtained with the original manual delineations. Moreover, our method can efficiently impute missing data.

1370

Automatic normalization of DCE-MRI derived cerebral blood volume (CBV) may improve glioma grading
Prativa Sahoo¹, Indrajit Saha², and Rakesh Kumar Gupta³

¹Healthcare, Philips India Ltd, Bangalore, India, ²Philips Healthcare, Philips India Ltd, Gurgaon, India, ³Radiology and Imaging, Fortis Memorial Research Institute, Gurgaon, India

DCE-MRI derived relative blood volume (rCBV) correlates excellently with grade of glioma. Traditionally rCBV is calculated by dividing CBV value of tumor region with the CBV value from the corresponding contra-lateral region by identifying and placing region of interest (ROI). This technique is tedious and needs user expertise. The main aim of this study was to develop an automatic method to normalize CBV so that the user-induced biasness in glioma grading due to ROI placement can be reduced. Normalized CBV provides a better contrast between tumor and normal region

1371

The Value of CBF Combined With Temporal Information in Grading High-Grade Astrocytomas: A Multi-Inversion-Time Arterial-Spin-Labeling Magnetic Resonance Study
Shuang Yang¹, Tianyi Qian², Jianwei Xiang¹, Yingchao Liu³, Fei Gao¹, Peng Zhao³, Josef Pfeuffer⁴, Guangbin Wang¹, and Bin Zhao¹

This study aimed to demonstrate the feasibility of multi-inversion-time arterial spin labeling (mTI-ASL) for differentiating between WHO III and WHO IV grade astrocytomas, as well as the added value of bolus arrival time (BAT) information in evaluating tumor perfusion. In the first part of this study, we evaluated the reproducibility of mTI-ASL in healthy subjects, and then mTI-ASL was used to evaluate 45 astrocytoma patients. There was no major variation between two consecutive mTI-ASL measurements in healthy volunteers. Furthermore, mTI-ASL provided valuable information for the classification of astrocytomas, while BAT added relevant information for grading by estimating the temporal dynamics of local tumor-mass perfusion.

1372

The effect of prophylactic cranial irradiation on brain diffusion and magnetization transfer
Mary A McLean¹, Nicola L Ainsworth^{1,2}, Anna M Brown¹, Susan V Harden², and John R Griffiths¹

¹CRUK Cambridge Institute, University of Cambridge, Cambridge, United Kingdom, ²Oncology, Addenbrooke's Hospital, Cambridge, United Kingdom

We investigated the effect of prophylactic cranial irradiation (PCI: 25 Gy in 10 fractions) on brain MRI at 3T. Six patients with small cell lung cancer were scanned at 4-month intervals: at diagnosis, following chemotherapy, and following PCI. Paired t-tests before and after PCI in right frontal white matter showed increased ADC and decreased FA and MTR following treatment. However, the parameters did not differ significantly from the scan at diagnosis, and other brain regions showed no significant changes on repeated-measures ANOVA. These observations are consistent with previous reports of more marked changes following higher-dose radiotherapy treatment.

1373

Differentiation of Glioblastoma Multiforme and Primary Cerebral Lymphoma with Diffusion-Weighted MR Imaging
Ching Chung Ko^{1,2}, Yu Chang Lee³, Ming Hong Tai², Tai Yuan Chen¹, Yu Ting Kuo¹, and Jeon Hor Chen^{3,4}

¹Department of Medical Imaging, Chi Mei Medical Center, Tainan, Taiwan, ²Institute of Biomedical Science, National Sun Yat-Sen University, Kaohsiung, Taiwan, ³Department of Radiology, I-Shou University and Eda Hospital, Kaohsiung, Taiwan, ⁴Center for Functional Onco-Imaging, University of California, Irvine, CA, United States

Atypical glioblastoma multiformes (GBMs) with solid enhancing tumor and without visible necrosis may mimic primary cerebral lymphomas (PCLs), and atypical PCLs with visible necrosis may mimic GBMs. This study aimed to differentiate these two brain tumors using qualitative DWI signals and quantitative ADC values acquired in tumoral necrosis, the most enhanced tumor area, and the peritumoral edema. The results showed GBMs tended to have significantly higher ADC in the enhanced tumor area, and lower ADC in the peritumoral edema area than PCLs.

1374

IDH-1 Mutation and Non-Enhancing Component of Glioblastoma

Daniel M Fountain¹, Timothy J Larkin², Natalie R Boonzaier², Jiun-Lin Yan², and Stephen J Price²

¹The Brain Tumour Imaging Laboratory, Division of Neurosurgery, University of Cambridge, Cambridge, United Kingdom, ²Division of Neurosurgery and Wolfson Brain Imaging Centre, The Brain Tumour Imaging Laboratory, Cambridge, United Kingdom

IDH-1 mutated glioblastoma is associated with improved survival, and greater sensitivity to further resection of non-enhancing disease than IDH-1 wild-type. We used structural, diffusion tensor, perfusion and spectroscopic imaging data in a mixed model across the peritumoral region in 54 patients. Applying a mixed model methodology across three levels of data resolution, we demonstrated that IDH-1 mutated tumors demonstrated raised choline and lowered glutamate and glutamine compared to IDH-1 wild-type. The findings provided an AUC of 0.943 when combined with age. We hypothesised this results in greater sensitivity to treatment and reduced excitotoxicity, thus explaining their relatively superior prognosis.

1375

Evaluation of 7T MRI for endoscopic surgical planning and guidance for skull base tumors - preliminary experience
Hadrien A Dyvorne¹, Thomas F Barrett², Bradley N Delman³, Raj K Shrivastava², and Priti Balchandani¹

¹Translational and Molecular Imaging Institute, Icahn school of Medicine at Mount Sinai, New York, NY, United States, ²Neurosurgery, Icahn School of Medicine at Mount Sinai, New York, NY, United States, ³Radiology, Icahn school of Medicine at Mount Sinai, New York, NY, United States

Skull based tumors pose some of the most complex challenges in neurosurgery owing to their proximity to important structures such as optic nerves and arteries. For this reason, surgical planning heavily depends on high quality MR images. In this study we evaluated the performance of 7T imaging against standard scans at 3T and 1.5T for delineating such structures. Furthermore, the high-resolution scans were integrated in the neurosurgical workflow in order to evaluate improvements in surgical time and confidence of surgical decision-making.

1376

Semi-automatic segmentation of medulloblastoma using active contour method
Ka Hei Lok¹, Lin Shi^{2,3}, Queenie Chan⁴, and Defeng Wang^{5,6}

¹Department of Imaging and Interventional Radiology, The Chinese University of Hong Kong, Sha Tin, Hong Kong, ²Department of Medicine and Therapeutics, The Chinese University of Hong Kong, Sha Tin, Hong Kong, ³Chow Yuk Ho Technology Centre for Innovative Medicine, The Chinese University of Hong Kong, Sha Tin, Hong Kong, ⁴Philips Healthcare, Hong Kong, Hong Kong, ⁵Research Center for Medical Image Computing,

Brain tumours are the second commonest form of childhood malignancy while medulloblastoma is the most common brain tumor in children. Accurate Segmentation of medulloblastoma is necessary for maximum tumor surgical removal. We proposed a novel method to segment medulloblastoma by modifying signed pressure function (SPF) function in Gaussians Filtering Regularized Level Set (SBGRLS) method. Quantitative validation is performed in this project. The method is proved to be clinical-oriented which is fast, robust, accurate with minimal user interaction.

1377

Withdrawn - Value of Amide Proton Transfer Imaging in Correlation with Histopathological Grades of Adult Diffuse Gliomas : Comparison and Incremental Value with Dynamic Susceptibility Contrast-Enhanced MRI and Diffusion Weighted Imaging Seung-Koo Lee¹, Yoon Seong Choi², Sung Soo Ahn¹, Ho-Joon Lee¹, and Jinna Kim¹

¹Seoul, Korea, Republic of, ²Radiology, Severance Hospital, Yonsei University College of Medicine, Seoul, Korea, Republic of

We investigated the difference in APT values according to histopathological grades, and compared the diagnostic value of APT with relative cerebral blood volume (rCBV) from dynamic susceptibility contrast-enhanced (DSC) MRI and apparent diffusion coefficient (ADC) from diffusion weighted imaging (DWI) for histopathological grades in adult diffuse gliomas. We optimized APT imaging protocol for clinical setting and found that APT values were increased along with glioma grades, and APT values has incremental values over ADC values for glioma grading. We suggest that APT imaging can be a useful noninvasive imaging biomarker for glioma grading, in combination with ADC.

1378

Time-signal curves analysis of dynamic contrast-enhanced magnetic resonance imaging used in differential diagnosis of pituitary lesions.

shiyun tian¹, Weiwei Wang¹, and yanwei miao¹

¹Radiology Department, the First Affiliated Hospital of Dalian Medical University, Dalian, China, People's Republic of

Pituitary microadenomas are commonly visualized as well-defined lesions that enhance less than the normal pituitary gland, but it is not clear about the enhancement pattern of microadenomas. Our work is to evaluate the TIC type and the five parameters extracted from time-signal curves of DCE-MRI in the normal pituitary gland, microadenoma and the Rathke's cleft cyst.

1379

MR based texture and location analysis of lower grade gliomas combined with genetic mutation information

Manabu Kinoshita¹, Hideyuki Arita², Mio Sakai³, Naoki Kagawa², Yonehiro Kanemura⁴, Yasunori Fujimoto², Katsuyuki Nakanishi³, and Toshiki Yoshimine²

¹Neurosurgery, Osaka Medical Center for Cancer and Cardiovascular Diseases, Osaka, Japan, ²Neurosurgery, Osaka University Graduate School of Medicine, Suita, Japan, ³Radiology, Osaka Medical Center for Cancer and Cardiovascular Diseases, Osaka, Japan, ⁴National Hospital Organization Osaka National Hospital, Osaka, Japan

Extensive genetic analysis of WHO grade 2 and 3 gliomas (lower grade glioma) revealed that they comprise of several disease subtypes with different genetic or molecular backgrounds. The present investigation was conducted to elucidate the differences revealed on MR images including textures and locations of the tumors according to genetic mutation status (IDH and TERT promoter mutation) of lower grade gliomas. T2-entropy, a newly introduced image texture metric revealed that tumor heterogeneity is different depending on genetic status. Furthermore, classic oligodendroglial tumors located at the mid-base frontal lobe while astrocytic tumors occupied much lateral side of the brain.

1380

RADIOMICS of advanced multiparametric MRI in posterior fossa tumors is supreme to the domain wizards! A pilot study

Shanker Raja¹, Sarah Farooq², William Plishker³, Ali Daghiri⁴, Sadeq Wasil Al-Dandan⁵, Abdullah Ali Alrashed⁴, Muhammad Usman Manzoor⁶, and Sharad George⁷

¹Baylor College of Medicine, Bellaire, TX, United States, ²King Fahad Medical City, Riyadh, Saudi Arabia, ³IGI Technologies, College Park, MD, United States, ⁴Medical Imaging, King Fahad Medical City, Riyadh, Saudi Arabia, ⁵Pathology and Laboratory Medicine, King Fahad Medical City, Riyadh, Saudi Arabia, ⁶Radiology, King Fahad Medical City, Riyadh, Saudi Arabia, ⁷Johns Hopkins Aramco Healthcare, Dhahran, Saudi Arabia

We uniquely extracted textural features from multiple sequences of advanced FMRI to preoperatively differentiate posterior fossa tumor histology. Furthermore, as opposed to recently published work (1,3,4) we found that in our series, textural feature subset derived from perfusion images is slightly superior to those of ADC maps. In addition, as expected, the observations from this work concurs that RADIOMICS is definitely on par and probably surpasses domain experts in this endeavour.

1381

Evaluation of vascular permeability in gliomas by using parameter K2 from dynamic susceptibility contrast data-sets and histogram analysis.

Toshiaki Taoka¹, Hisashi Kawai¹, Toshiki Nakane¹, Toshiteru Miyasaka², and Shinji Naganawa¹

¹Radiology, Nagoya University, Nagoya, Japan, ²Radiology, Nara Medical University, Kashihara, Japan

Permeability images can provide additional information to perfusion images in the clinical practice of brain tumors. However, permeability imaging by dynamic contrast enhancement methods requires a long acquisition time. K2 is an index that represents

permeability and can be calculated from the dataset of perfusion images with the dynamic susceptibility contrast method, which requires a short acquisition time. In the current study, we calculated K2 for various grades of gliomas and found that K2 showed a significantly higher 20th percentile value in Grade IV compared to Grade III gliomas, providing useful information for grading of gliomas.

1382

Characterising tumour progression and pseudoprogression on preoperative multimodal MRI imaging
Jiun-Lin Yan^{1,2,3}, Anouk van der Hoorn⁴, Timothy J Larkin⁵, Natalie Rosella Boonzaier⁵, Tomasz Matys⁶, and Stephen J Price⁵

¹Clinical Neuroscience, University of Cambridge, Cambridge, United Kingdom, ²Department of neurosurgery, Chang Gung Memorial Hospital, Keelung, Taiwan, ³Department of neurosurgery, Chang Gung University College of Medicine, Taoyuan, Taiwan, ⁴Department of radiology (EB44), University of Groningen, Groningen, Netherlands, ⁵Brain tumour imaging laboratory, University of Cambridge, Cambridge, United Kingdom, ⁶Department of radiology, University of Cambridge, Cambridge, United Kingdom

Glioblastoma is a highly malignant tumor which recur mostly within 2 cm around the resected contrast enhancement. However, it is difficult to identify tumor invasiveness pre-surgically especially in non-enhanced area. Thus, we aimed to identify possible imaging characteristics preoperatively using multimodal MR techniques in the peritumoral regions that eventually leads to tumor recurrence or progression. Our study showed lower isotropic p, anisotropic q and ADC for progression compared to non-progression regions. In addition, MRS showed a not statistically significant trend of higher choline/NAA, higher choline and lower NAA in these progression area.

1383

Radiogenomic Mapping of Dysregulated Angiogenesis in Glioblastoma.
Kevin, Li-Chun Hsieh¹, Fei-Ting Hsu¹, Chia-Feng Lu¹, and Cheng-Yu Chen¹

¹Translational Imaging Research Center, Taipei Medical University, Taipei, Taiwan

In this TCGA study, we identified several qualitative and quantitative radiomics imaging surrogates in glioblastoma, which can be used to differentiate whether this tumor have dysregulated angiogenesis at the molecular level. These features can also be used to predict disease survival.

1384

Differentiation of glioblastoma multiforme and single brain metastasis by the distribution pattern of intratumoral susceptibility sign derived from susceptibility-weighted imaging
Hyunkoo Kang¹ and Keuntak Roh¹

¹Department of Radiology, Seoul Veterans Hospital, Seoul, Korea, Republic of

Susceptibility-weighted imaging (SWI) is an emerging magnetic resonance imaging (MRI) technique that exploits the susceptibility differences between the tissues. SWI provides the enhancement of small vessels and microhemorrhages and detection of iron in the brain. These characteristics permit SWI to show anatomical and functional heterogeneity of brain tumors by exquisite sensitivity to the blood products and venous vasculature. The aim of this study is to determine whether the distribution pattern of intratumoral susceptibility sign (ITSS) derived from SWI could differentiate glioblastoma multiforme (GBM) and single brain metastasis. We investigated the distribution patterns of ITSS of the tumors and applied an ITSS grading system based on the degree of the ITSS. Then, we compared the grade of the visibility of ITSS in the central portion of tumors (CITSS) and in the tumor capsular area (PITSS) on SWI in consensus. In clinical use, SWI is also useful for differentiating GBMs from metastases.

1385

Differentiating contrast-enhanced glioma from peritumoral edema using the intravascular fraction derived from IVIM MRI - a comparative study with DSC MRI
Yen-Shu Kuo^{1,2}, Han-Min Tseng³, and Wen-Chau Wu⁴

¹Graduate Institute of Biomedical Electronics and Bioinformatics, National Taiwan University, Taipei, Taiwan, ²Radiology, Cathay General Hospital, Taipei, Taiwan, ³Neurology, National Taiwan University Hospital, Taipei, Taiwan, ⁴Graduate Institute of Oncology, National Taiwan University, Taipei, Taiwan

In this study, we performed intravoxel incoherent motion (IVIM) MRI in 25 patients with histologically proven gliomas, and compared the intravascular fraction *f* with the cerebral blood volume derived from dynamic susceptibility-contrast (DSC) MRI (CBV_{DSC}). Results showed that *f* was able to differentiate contrast-enhanced glioma from peritumoral edema by detecting elevated vascularity. Cross-modal comparison indicated that *f* correlated better with contrast-leakage-corrected CBV_{DSC} than uncorrected value.

1386

Normalization of Multi-contrast MRI and Prediction of Tumor Phenotypes
Yong Ik Jeong¹, Charles Cantrell¹, David Mangano¹, Thomas Gallagher¹, Jeffery Raizer¹, Craig Horbinski¹, and Timothy J Carroll¹

¹Northwestern University, Chicago, IL, United States

Genetic profiling of cancers has the potential to identify epigenetic changes that predict response to treatments. In this study, we try to overcome the limitations posed by heterogeneity of tumor phenotypes by using normalized quantitative MRI to predict local gene expression. We report the findings of retrospectively comparing T1, T1 post Gd, T2 and ADC to Verhaak subtypes and pMGMT methylation status in histologically confirmed GBM patients.

1387

Intra- and inter-individual association of FET-PET- and MR-Perfusion-parameters in untreated glioma
Jens Goettler¹, Anne Kluge¹, Mathias Lukas², Stephan Kaczmarz¹, Jens Gempt³, Florian Ringel³, Mona Mustafa², Markus Schwaiger², Claus

¹Department of Neuroradiology, Technische Universität München, Munich, Germany, ²Clinic for Nuclear Medicine, Technische Universität München, Munich, Germany, ³Clinic for Neurosurgery, Technische Universität München, Munich, Germany, ⁴Clinic for Neurology, Technische Universität München, Munich, Germany

¹⁸F-fluoroethyltyrosine (FET) PET and dynamic susceptibility contrast (DSC) perfusion weighted imaging are useful imaging techniques to diagnose glioma and to delineate tumor extension. However it is still unclear whether static and dynamic parameters of FET-PET and DSC are associated with each other. In this study we examined 45 patients with glioma in a hybrid PET-MR 3T scanner assessing FET time-activity-curves and DSC-parameters simultaneously. Static as well as dynamic PET-measures highly correlated with DSC-parameters such as relative cerebral blood volume (rCBV) and relative peak height (rPH). Results point to a complementary role of both modalities pre-therapeutically.

1388

Estimating damage to the blood-brain barrier from radiotherapy treatment
Magne Kleppestø¹, Christopher Larsson¹, and Atle Bjarnerud^{1,2}

¹The Intervention Centre, Oslo University Hospital, Oslo, Norway, ²Department of Physics, University of Oslo, Oslo, Norway

Brain tumors are usually subjected to radiation therapy upon diagnosis. In this work, it is made an attempt at investigating if this therapy might cause injury to the non-cancerous parts of the brain. To this end dynamic contrast-enhanced MRI was used to estimate leakage across the blood-brain barrier. 22 patients were imaged before and after undergoing a treatment schedule, and findings from the two examinations were compared to uncover any change. The data shows no significant variation in either permeability or blood plasma volume.

1389

MR appearance of Primary central nervous system lymphoma: as prognostic factors influencing the response to clinical treatment
jing Liu¹ and shuixing Zhang¹

¹Radiology, Department of Radiology, Guangdong Academy of Medical Sciences/Guangdong General Hospital, Guangzhou, Guangzhou, China, People's Republic of

Currently, the treatment response in primary central nervous system lymphoma (PCNSL) is monitored by serial contrast-enhanced anatomic MR imaging, which often showing characteristic radio-morphological features such as lesion location, strong and homogenous contrast-enhancement, moderate edema and absence of necrosis. The purpose of our study was to investigate the objective response rate (ORR) and identify MR findings as predictors to evaluate the therapeutic response in PCNSL. Our result shows that tumor size, number, location, homogenous enhancement and the planned therapeutic strategy were independent factors correlated with treatment response in patients of PCNSL.

Traditional Poster

Psychiatric Disorders: Major Depression

Exhibition Hall

Monday, May 9, 2016: 10:45 - 12:45

1390

Neural basis of the association between anxiety and depression symptoms in unmedicated major depressive disorder patients
Can-can He¹, Liang Gong¹, Chunming Xie¹, and Yingying Yin¹

¹Department of Neurology, Affiliated ZhongDa Hospital, School of Medicine, Southeast University, Nanjing, China, People's Republic of

In this study, 75 unmedicated MDD patients and 42 cognitively normal(CN) subjects underwent the resting-state functional magnetic resonance imaging (R-fMRI) scan. We found that the MDD patients showed dysfunctional connectivity in wide-spread amygdala functional connectivity(AFC) networks, and these abnormal amygdala connectivity were influenced the trait property in MDD. Further analysis revealed that MDD patients with lower HAMA scores showed milder depressive symptom and greater AFC strength while MDD patients with higher HAMA scores showed more severe depressive symptom and lower AFC strength. Beyond that, the mediation effects of AFC networks on the association between anxiety and depression all reached a significant level in MDD patients.

1391

Corpus callosum morphology and microstructure in late-life depression

Louise Emsell^{1,2}, Christopher Adamson³, Filip Bouckaert¹, Thibo Billiet², Daan Christiaens⁴, Francois-Laurent De Winter¹, Marc Seal³, Pascal Sienaert¹, Stefan Sunaert², and Mathieu Vandenbulcke¹

¹UPC-KU Leuven, Leuven, Belgium, ²Translational MRI, KU Leuven, Leuven, Belgium, ³Developmental Imaging, Murdoch Childrens Research Institute, Melbourne, Australia, ⁴ESAT/PSI, KU Leuven, Leuven, Belgium

Differences in corpus callosum (CC) morphology and microstructure have been implicated in late-life depression (LLD), however it is not clear to what extent microstructural alterations result from partial volume effects arising from macrostructural differences. Here we combined T1 morphological measures (thickness and area) with multiple diffusion MRI measures (fractional anisotropy, radial diffusivity and apparent fibre density (AFD)) to investigate the mid-sagittal CC in 51 patients with LLD and 52 healthy controls. LLD was associated with subtle, independent regional macro- (reduced area) and microstructural (reduced AFD) differences in the corpus callosum, unrelated to depression subtype or illness severity.

1392

7 T MRS Investigation of the Glutamatergic System in Depression

Clark Lemke^{1,2}, Charles Masaki¹, Uzay Emir², Beata Godlewska¹, and Phil Cowen¹

¹Department of Psychiatry, University of Oxford, Oxford, United Kingdom, ²FMRIB, University of Oxford, Oxford, United Kingdom

The glutamatergic system is believed to play a significant role in depression pathology. While many magnetic resonance spectroscopy (MRS) studies of depression have targeted the glutamatergic system, they have all been performed at magnetic field strengths of 4 T or lower – limiting their ability to differentiate between glutamate and glutamine. This study presents the first investigation of the glutamatergic system in depressed subjects at 7 T. Voxels were placed in the occipital cortex, anterior cingulate cortex, and putamen and metabolites were quantified using LCModel. Results indicate a significant decrease in glutamate in the occipital cortex and a significant increase of glutamine in the putamen.

1393

Disrupted reward circuits is associated with cognitive deficits, depression severity, and trait property in unmedicated major depressive disorder

Liang Gong¹, Yingying Yin¹, Cancan He¹, Chunming Xie¹, Yonggui Yuan¹, Zhijun Zhang¹, and Hongxing Zhang²

¹Department of Neurology, Affiliated ZhongDa Hospital, School of Medicine, Southeast University, Nanjing, China, People's Republic of,

²Department of Psychiatry, Henan Provincial Mental Hospital, XingXiang, China, People's Republic of

we employed the resting-state fMRI technique with voxelwise multivariate regression analysis to identify that the disrupted topological organization within reward circuits was significantly associated with cognitive deficits, depression severity, and trait property in major depressive disorder (MDD) patients. Importantly, distinct and common neural pathways underlying cognitive deficit and depression were identified, and implied the independent and synergistic effects of cognitive deficits and depression severity on reward circuits in MDD patients.

1394

Brain grey matter volume alterations in treatment resistant depression -- systematic review and meta-analysis

Xin Xu¹, Jia Liu², and Qiyong Gong²

¹Department of Psychiatry, Huaxi MR Research Center(HMRRC), West China Hospital of Sichuan University, Chengdu, China, People's Republic of,

²Department of Radiology, Huaxi MR Research Center(HMRRC), West China Hospital of Sichuan University, Chengdu, China, People's Republic of

To our knowledge, this is the first study to pool VBM studies for a meta-analysis of grey matter differences among the treatment-sensitive depression (TSD), treatment-resistant depression (TRD) and health control (HC) by using anisotropic effect-size signed differential mapping (AES-SDM). Although both TRD and TSD groups showed abnormal grey matter in frontal and temporal cortex, the exact brain regions were mostly different in both groups except the left inferior frontal gyrus (IFG). Furthermore, grey matter volume reductions in the bilateral cingulate cortex were only observed in the TRD group.

1395

DTI-based connectome analysis of adolescent depression reveals hypoconnectivity of the right caudate

Olga Tymofiyeva¹, Colm G Connolly¹, Tiffany C Ho¹, Matthew D Sacchet², Eva Henje Blom^{1,3}, Kaja Z LeWinn¹, Duan Xu¹, and Tony T Yang¹

¹UCSF, San Francisco, CA, United States, ²Stanford University, Stanford, CA, United States, ³Karolinska Institutet, Stockholm, Sweden

The goal of this study was to perform DTI-based connectome analysis in a cohort of depressed adolescents and matched non-depressed controls. Our findings highlight the role of right caudate connectivity, in particular to frontal gyri, insula, and anterior cingulate, in this population.

1396

Dysfunction of the Cingulo-Opercular Network in First-Episode, Medication-Naive Patients with Major Depressive Disorder

xiaoping wu¹, yanjun gao¹, Pan Lin², Junle Yang¹, Rui Yang³, and Jian Yang⁴

¹Department of Radiology, the Affiliated Xi'an Central Hospital of Xi'an Jiaotong University, Xi'an, China, People's Republic of, ²Key Laboratory of Biomedical Information Engineering of Education Ministry, Institute of Biomedical Engineering, Xi'an Jiaotong University, Xi'an, China, People's Republic of, ³Department of Psychiatry, the Affiliated Xi'an Central Hospital of Xi'an Jiaotong University, Xi'an, China, People's Republic of,

⁴Department of Radiology, the First Affiliated hospital of Xi'an Jiaotong University, Xi'an, China, People's Republic of

Patients with MDD showed abnormalities in the connectivity of the CON. We found abnormal connectivity in MDD patients between the dACC and the bilateral middle frontal gyrus (MFG) and between the middle temporal gyrus (MTG) and precentral gyrus. Moreover, regression analysis showed that depression symptom severity (measured with the Hamilton Depression Rating Scale (HDRS), Hamilton Anxiety Scale (HAMA) and Automatic Thoughts Questionnaire scores (ATQ)) was significantly correlated with the FC values of the CON.

1397

Gray and white matter volume changes and the correlation with depression and anxiety in obese patients revealed by voxel-based morphometry

Jun-Cheng Weng^{1,2}, Chi-Ju Lai¹, Hse-Huang Chao³, Ming-Chou Ho⁴, and Vincent Chin-Hung Chen⁵

¹Department of Medical Imaging and Radiological Sciences, Chung Shan Medical University, Taichung, Taiwan, ²Department of Medical Imaging, Chung Shan Medical University Hospital, Taichung, Taiwan, ³Taiwan Center for Metabolic and Bariatric Surgery, Jen-Ai Hospital, Taichung, Taiwan, ⁴Department of Psychology, Chung Shan Medical University, Taichung, Taiwan, ⁵Department of Psychiatry, Chang Gung Memorial

Obesity is an important health issue in modern society. The prevalence of obesity has been increasing in these years and morbid obesity is related to cardiovascular disease and overall mortality. Past reviews regarded binge eating as a manifestation of dysfunctional reward system and disinhibition. Some authors considered binge eating as a kind of addiction. Recent study demonstrated the more extensive involvement of brain pathways other than reward system. The mechanism of change is not clear. There is scanty of research regarding correlation between change of activation pattern in brain areas in functional MRI, binge eating and psychiatric illness. To gain insight into the correlation of physiological alteration and psychiatric illness and to develop subsequent detectable biomarker are crucial. The goal of our study was to investigate the morphological changes in gray and white matter between obese patients and healthy subjects using voxel-based morphometry (VBM). Our results suggested the changes of the volume in the brain structures may closely linked to the symptom and behavior of obese patients. Apply these novel markers to monitoring and improving cormorbid psychiatric illness will be an essential part of multidiscipline integral care for obese patients.

1398

MR Imaging of Major Depressive Disorder: Effects of Sertraline Treatment

Hung-Wen Kao^{1,2}, Chien-Yuan Eddy Lin^{3,4}, Chu-Chung Huang⁵, Yi-Hui Lin⁶, I-Ling Chung⁷, Yu-Chuan Chang⁸, Guo-Shu Huang¹, and Ching-Po Lin^{2,5,6,9}

¹Department of radiology, Tri-Service General Hospital, National Defense Medical Center, Taipei, Taiwan, ²Department of Biomedical Imaging and Radiological Sciences, National Yang-Ming University, Taipei, Taiwan, ³GE Healthcare, Taipei, Taiwan, ⁴GE Healthcare MR Research China, Beijing, China, People's Republic of, ⁵Institute of Neuroscience, National Yang-Ming University, Taipei, Taiwan, ⁶Institute of Brain Science, National Yang-Ming University, Taipei, Taiwan, ⁷Institute of Biomedical Science, Academia Sinica, Taipei, Taiwan, ⁸Graduate Institute of Biomedical Electronics and Bioinformatics, National Taiwan University, Taipei, Taiwan, ⁹Brain Research Center, National Yang-Ming University, Taipei, Taiwan

We hypothesized that a predictive MR imaging model of sertraline treatment could be established to help treatment planning for patients with Major depressive disorder (MDD). The voxel-based morphometry analysis showed increase volume of the lingual and occipital gyri in patients with MDD as compared with those in healthy controls and the size of the occipital gyrus decreased after 6-week treatment of sertraline. The findings support that patients with MDD might have a functional abnormality of visual areas and antidepressant treatment might shift the abnormal activity in the antidepressant-susceptible brain region to a normal level.

1399

Simultaneous Real-time fMRI and EEG Neurofeedback for Emotion Regulation Training in Depressed Patients

Vadim Zotev¹, Raquel Phillips¹, Masaya Misaki¹, Ahmad Mayeli^{1,2}, and Jerzy Bodurka^{1,3}

¹Laureate Institute for Brain Research, Tulsa, OK, United States, ²Electrical and Computer Engineering, University of Oklahoma, Tulsa, OK, United States, ³College of Engineering, University of Oklahoma, Tulsa, OK, United States

We have performed an exploratory study of emotion self-regulation training in major depressive disorder (MDD) patients using simultaneous real-time fMRI and EEG neurofeedback (rtfMRI-EEG-nf). MDD patients learned to upregulate two fMRI and two EEG target measures, relevant to MDD, using rtfMRI-EEG-nf during a happy emotion induction task. The target measures included fMRI activities of the left amygdala and left rACC, as well as frontal EEG asymmetries in the alpha and high-beta bands. Our results demonstrate that MDD patients can learn to successfully upregulate all four measures simultaneously. These findings may lead to development of more efficient neurotherapies for MDD.

Traditional Poster

Pediatrics

Exhibition Hall

Monday, May 9, 2016: 10:45 - 12:45

1400

Development of a new prototype body holder for MR examination in unanesthetized neonates
Iichiro Osawa¹, Takako Aoki¹, Takashi Ushimi¹, Kaiji Inoue¹, Junji Tanaka¹, and Mamoru Niitsu¹

¹Radiology, Saitama Medical University Hospital, Saitama, Japan

To avoid motion artifacts, neonates often require anesthesia during MRI scans. However, this procedure increases the risk of adverse events such as respiratory depression. We developed a body holding device to minimize motion without anesthesia and examined nine low-birth-weight neonates, comparing MR image quality between unanesthetized and anesthetized conditions. The device is based on a modified spinal immobilizer and is easily handled with a short setup time. We obtained structural images during natural sleep uneventfully, preserving the image quality. In summary, the body holder can reduce the motion of neonates safely and improve image quality.

1401

Adaptive Tissue Cluster Tracking on Quantitative MRI for Fully Automatic Brain Segmentation on Young Children
Marcel Warntjes^{1,2}, Suraj Serai³, James Leach³, and Blaise Jones³

¹Center for Medical Imaging Science and Visualization, Linköping, Sweden, ²SyntheticMR AB, Linköping, Sweden, ³Department of radiology, Cincinnati, OH, United States

Brain tissue properties change rapidly during the first few years of life. This poses a problem for brain segmentation algorithms since

adult tissue definitions for white matter and grey matter do not apply for young children. An automatic tissue cluster tracking algorithm was developed to determine WM and GM cluster positions in a 3-dimensional search-space of quantitative R1 relaxation rate, R2 relaxation rate and proton density. These positions are then used to segment the brain, independent of age.

1402

Distinctive microstructural changes of association white matter tracts during preterm human brain development
Minhui Ouyang¹, Austin Ouyang², Qiaowen Yu², Lina Chalak³, and Hao Huang^{1,4}

¹Department of Radiology, Children's Hospital of Philadelphia, Philadelphia, PA, United States, ²Advanced Imaging Research Center, University of Texas Southwestern Medical Center, Dallas, TX, United States, ³Department of Pediatrics, University of Texas Southwestern Medical Center, Dallas, TX, United States, ⁴Department of Radiology, Perelman School of Medicine, University of Pennsylvania, Philadelphia, PA, United States

Association white matter tracts connecting different cortical regions underlie initial brain circuit formation from mid-fetal to normal time of birth. We examined the microstructure changes of association tracts and compare them to those of commissural, limbic and projection tracts with high resolution diffusion MRI of 10 fetal brains specimens at 20 postmenstrual weeks, 19 in vivo preterm brains at 35 weeks and 17 in vivo brains at 40 weeks. Distinctive microstructural developmental patterns were found in association tract groups compared to other tract groups during 35-40 weeks with DTI-derived metrics (including fractional anisotropy, mean, axial and radial diffusivity measurements).

1403

Measuring Longitudinal Changes in Cerebral Blood Flow and Blood Volume in Neonates with the Intravoxel Incoherent Motion Method
Alex Cerjanic^{1,2}, Ellen Grant³, Borjan Gagoski³, Marie Drottar³, Thea Francel³, Alana Matos³, Clarissa Carruthers³, Jonathan Litt⁴, Ryan Larsen², and Bradley P Sutton^{1,2}

¹Bioengineering, University of Illinois at Urbana-Champaign, Urbana, IL, United States, ²Beckman Institute, University of Illinois at Urbana-Champaign, Urbana, IL, United States, ³Boston Children's Hospital, Boston, MA, United States, ⁴Beth Israel Deaconess, Boston, MA, United States

Diffusion weighted MRI was used on a cohort of 5 neonates to quantify cerebral blood flow and cerebral blood volume through the intravoxel incoherent motion (IVIM) model. Data at two time points, approximately 2 weeks and 14 weeks, were obtained. The obtained pseudodiffusion coefficient and the perfusion fractions were examined across white matter, gray matter, and the basal ganglia for all subjects. A significant longitudinal decrease in the perfusion fraction (-1.12%) was noted in the white matter between 2 and 14 weeks while the static diffusion coefficient of tissue decreased for all tissue classes between those time points.

1404

Quantitative MR relaxometry reveals subcortical T1 differences in very preterm children and adolescents

Ruth L O'Gorman¹, Flavia Wehrle², Tobias C Wood³, Andreas Buchmann⁴, Beatrice Latal⁴, Reto Huber⁴, Sean Deoni⁵, Gareth J Barker³, and Cornelia Hagmann²

¹Center for MR Research, University Children's Hospital, Zurich, Switzerland, ²Neonatology, University Hospital, Zurich, Switzerland, ³Institute of Psychiatry, King's College London, London, United Kingdom, ⁴Developmental Pediatrics, University Children's Hospital, Zurich, Switzerland, ⁵University of Colorado, Denver, CO, United States

Very preterm infants are at an increased risk of neurodevelopmental impairment later in life. This study investigates cerebral microstructural differences in 31 very preterm children and adolescents relative to their term-born peers, using quantitative MR relaxometry. The very preterm group showed significantly increased T1 in the caudate and thalamus and decreased T1 in insula and amygdala/hippocampus, but no significant differences in caudate, thalamus, or total brain volume. These results highlight the vulnerability of basal ganglia, thalamic and cortical structures to neonatal brain injury and underscore the role that quantitative relaxometry may play in evaluating microstructural changes associated with prematurity.

1405

Cortical thinning in young adolescents born preterm with very low birth weight
Tsung-Han Wu¹, Tzu-chao Chuang¹, Ming-Ting Wu^{2,3}, and Pinchen Yang⁴

¹Electrical Engineering, National Sun Yat-Sen University, Kaohsiung, Taiwan, ²School of Medicine, National Yang-Ming University, Taipei, Taiwan, ³Radiology, Kaohsiung Veteran General Hospital, Kaohsiung, Taiwan, ⁴Psychiatry, Kaohsiung Medical University and Kaohsiung Medical University Hospital, Kaohsiung, Taiwan

By using a surface-based method (FreeSurfer), the cortical thickness measurement was performed on young adolescents born preterm with very low birth weight (n = 15, birth weight < 1500 g) and age-matched term born controls (n = 17). The preterms, who present no brain injuries, showed a thicker cortex in parietal, occipital, and temporal regions compared to the controls, suggesting the delay of cortical thinning.

1406

Perfusion and diffusion in the extremely preterm young adult thalamus

Andrew Melbourne¹, Zach Eaton-Rosen¹, Eliza Orasanu¹, Joanne Beckmann², Alexandra Saborowska³, David Atkinson³, Neil Marlow², and Sebastien Ourselin¹

¹Medical Physics and Biomedical Engineering, University College London, London, United Kingdom, ²Institute for Women's Health, University College London, London, United Kingdom, ³University College Hospital, London, United Kingdom

This work investigates the appearance of the thalamus using multiple MR imaging contrasts between a population of extremely-preterm born adolescents and their term-born peers.

1407

Characterizing microstructure and shape of the extremely preterm 19 year-old corpus callosum

Andrew Melbourn¹, Eliza Orasanu¹, Zach Eaton-Rosen¹, Joanne Beckmann², Alexandra Saborowska³, David Atkinson³, Neil Marlow², and Sébastien Ourselin¹

¹*Medical Physics and Biomedical Engineering, University College London, London, United Kingdom*, ²*Institute for Women's Health, University College London, London, United Kingdom*, ³*University College Hospital, London, United Kingdom*

This work investigates the appearance of the corpus callosum using multiple MR imaging contrasts between a population of extremely-preterm born adolescents and their term-born peers.

1408

Deformation-based morphometry identifies brain structural damages in 6 month-old infants with neonatal encephalopathy and predicts their developmental outcome

Hosung Kim¹, Kevin Shapiro², Maria Luisa Mandelli², Hannah Clanley Glass², Dawn Gano², ELIZABETH Rogers³, Donna M Ferriero², Anthony James Barkovich¹, and Duan Xu¹

¹*Radiology & Biomedical Imaging, University of California San Francisco, San Francisco, CA, United States*, ²*Neurology, University of California San Francisco, San Francisco, CA, United States*, ³*Pediatrics, University of California San Francisco, San Francisco, CA, United States*

Neonatal encephalopathy (NE) is a major cause of mortality and permanent neurological disabilities in term infants. Using t1w MRI and DBM, we found that neonatal seizure was related to WM atrophy in multiple locations. Larger birth weight was associated with increased overall GM and WM volumes. A significant association was identified between language ability at 2 years old and increase in GM volume in Wernicke's area. This DBM approach has the potential for predicting early developmental outcome in infants with NE, as the volume of Wernicke's area significantly correlated with the scores of language ability evaluated in early childhood.

1409

Tract-based spatial statistics to assess the effect of histologic chorioamnionitis on white matter development in preterm infants

Devasuda Anblagan^{1,2}, Rozalia Pataky², Margaret J Evans³, Sarah Sparrow², Chinthika Piyasena⁴, Emma J Telford², Scott I Semple^{4,5}, Alastair Graham Wilkinson⁶, Mark E Bastin¹, and James P Boardman^{1,2}

¹*Centre for Clinical Brain Sciences, University of Edinburgh, Edinburgh, United Kingdom*, ²*MRC Centre for Reproductive Health, University of Edinburgh, Edinburgh, United Kingdom*, ³*Department of Pathology, University of Edinburgh, Edinburgh, United Kingdom*, ⁴*Centre for Cardiovascular Sciences, University of Edinburgh, Edinburgh, United Kingdom*, ⁵*Clinical Research Imaging Centre, University of Edinburgh, Edinburgh, United Kingdom*, ⁶*Department of Radiology, Royal Hospital for Sick Children, Edinburgh, United Kingdom*

Chorioamnionitis is associated with preterm birth in around 40% of cases. There are uncertainties about its contribution to diffuse white matter injury associated with preterm birth, and its importance in relation to other injurious exposures experienced by preterm infants. 90 preterm infants, 26 born with histopathological evidence of chorioamnionitis, were scanned at term equivalent age using a whole brain diffusion MRI protocol, and TBSS analysis was run. We found that chorioamnionitis is associated with lower fractional anisotropy, indicative of diffuse white matter injury in preterm infants, and this is independent of known predictors for abnormal brain development after preterm birth.

1410

Synchronous Aberrant Cerebellar and Opercular Development in Fetuses and Neonates with Congenital Heart Disease (CHD)

Alexandra Wong¹, Thomas Chavez², Jodie Votava-Smith², David Miller², Hollie Lai², Sylvia delCastillo², Lisa Paquette³, and Ashok Panigrahy²

¹*New York Medical College, Valhalla, NY, United States*, ²*Los Angeles, CA, United States*, ³*University of Southern California, Los Angeles, CA, United States*

Children with congenital heart disease (CHD) demonstrate problems with multi-domain cognitive control of unknown etiology. Cingulo-opercular and cerebellar brain networks are known to be critical in multi-domain cognitive control including language function. Little is known about the comparative structural growth trajectories of the cerebellum and operculum in CHD patients. To our knowledge, the literature only describes fetal opercular measurements by ultrasound.¹ And, data from the neonatal period is scant, gathered from children suffering from "temporary neurologic dysfunction" or from cadaveric specimens.^{2,3} The fetal cerebellum has been described on MRI mostly in terms of its volume^{4,5} or area⁶ although a few have used linear measurements as the basis of their fetal cerebellar growth illustration.^{7,8,9}

1411

Disrupted Resting State Connectivity in Term Neonates with Complex CHD

Vincent Kyu Lee^{1,2}, Vincent Schmithorst², Shahida Sulaiman¹, Lisa Paquette³, Jodie Votava-Smith³, and Ashok Panigrahy^{1,2}

¹*Radiology, University of Pittsburgh, Pittsburgh, PA, United States*, ²*Radiology, Children's Hospital of Pittsburgh, Pittsburgh, PA, United States*, ³*Cardiology, Children's Hospital of Los Angeles, Los Angeles, CA, United States*

The last trimester of brain development in fetuses with complex congenital heart disease (CHD) is abnormal. In this study, we use ICA analysis on resting BOLD of CHD patients to characterize the neuronal activity and compare it to healthy controls. A total of 117 BOLD images from CHD and healthy neonates were analyzed using Temporal concatenation ICA with MELODIC FSL. Both CHDs and Controls exhibited common RSNs, but CHDs lacked additional RSNs observed in controls. CHD group exhibited ICAs with less complexity than controls, which may be due to global brain dysmaturation with disruption of cortical to subcortical connectivity.

1412

Maternal Obesity Affects Offspring's Brain Resting-State Functional Connectivity

Xuehua Li^{1,2}, Yilu Zhang², Aline Andres¹, R.T. Pivik¹, Charles Glasier², Raghu Ramakrishnaiah², Thomas Badger¹, and XIAWEI OU^{1,2,3}

¹*Arkansas Children's Nutrition Center, Little Rock, AR, United States*, ²*Radiology, University of Arkansas for Medical Sciences, Little Rock, AR, United States*, ³*Arkansas Children's Hospital Research Institute, Little Rock, AR, United States*

Recent studies have reported negative associations between maternal obesity during pregnancy and cognitive/neurodevelopmental outcome of children. It is speculated that neuro-programming differs in offspring of obese and normal weight women. In this study, we evaluated and compared the resting-state functional connectivity in 2-week-old infants born to normal weight or obese mothers, and we observed significant differences in brain connectivity associated with maternal obesity.

1413

Preliminary evaluation of altered brain microstructural in the emotion-cognitive region of children with hemophilia A: a diffusional kurtosis imaging study

Di Hu¹, Ningning Zhang¹, Huiying Kang¹, Xiaolu Tang¹, Yanqiu Lv¹, Kaining Shi², and Yun Peng¹

¹*Beijing Children's hospital, Beijing, China, People's Republic of*, ²*Imaging Systems Clinical Science of Philips Healthcare, Beijing, China, People's Republic of*

Our study is the first to evaluate relationship between emotion disorders and cognitive change in microstructure with hemophilia A, suggesting that the assessment of non-Gaussian directional diffusion using DKI provides more sensitive information about tissue microstructural changes than conventional image method and traditional psychological test.

1414

BRAIN METABOLITE DIFFERENCES IN ONE-YEAR-OLD PRETERM INFANTS WITH INTRAUTERINE GROWTH RESTRICTION: ASSOCIATION WITH STRUCTURAL CHANGES AND NEURODEVELOPMENTAL OUTCOME

Rui Vasco Simoes^{1,2,3}, Emma Muñoz-Moreno⁴, Nuria Bargallo^{5,6}, Magdalena Sanz-Cortes⁷, and Eduard Gratacos^{1,2,3}

¹*Fetal Medicine Research Center, BCNatal (Hospital Clinic and Hospital Sant Joan de Deu), Barcelona, Spain*, ²*Fetal Medicine Research Center, Institut d'Investigacions Biomediques August Pi i Sunyer (IDIBAPS), Barcelona, Spain*, ³*Center for Biomedical Research on Rare Diseases (CIBER-ER), Barcelona, Spain*, ⁴*Experimental MRI 7T Unit, Institut d'Investigacions Biomediques August Pi i Sunyer (IDIBAPS), Barcelona, Spain*, ⁵*Medical Image platform, Institut d'Investigacions Biomediques August Pi i Sunyer (IDIBAPS), Barcelona, Spain*, ⁶*Dept. Radiology, Hospital Clinic, Barcelona, Spain*, ⁷*Dept. Obstetrics and Gynecology, Baylor College of Medicine, Houston, TX, United States*

It is difficult to address the differential effects of Intrauterine growth restriction (IUGR) and prematurity, as they represent two independent problems occurring simultaneously and can both contribute to impaired neurodevelopment. We have studied one-year-old preterm-IUGR infants and preterm and term appropriate for gestational age (AGA) infants, by MRI/MRS at 3T. Preterm-IUGR infants present metabolite profile changes in the frontal lobe, which are associated with brain structural and biophysical alterations, and poorer neurodevelopmental outcome at two years.

1415

Longitudinal metabolite trajectories in the midfrontal gray matter in normally developing South African children

Martha J Holmes¹, Frances C Robertson¹, Francesca Little², Mark F Cotton³, Els Dobbels³, Andre JW van der Kouwe^{4,5}, Barbara Laughton³, and Ernesta M Meintjes¹

¹*MRC/UCT Medical Imaging Research Unit, Department of Human Biology, University of Cape Town, Cape Town, South Africa*, ²*Department of Statistical Sciences, University of Cape Town, Cape Town, South Africa*, ³*Children's Infectious Diseases Clinical Research Unit, Department of Paediatrics & Child Health, Tygerberg Children's Hospital and Faculty of Medicine and Health Sciences, Stellenbosch University, Cape Town, South Africa*, ⁴*A.A. Martinos Centre for Biomedical Imaging, Department of Radiology, Massachusetts General Hospital, Charlestown, MA, United States*, ⁵*Department of Radiology, Harvard Medical School, Boston, MA, United States*

Magnetic resonance spectroscopy (MRS) measures changes in localized brain metabolism that occur alongside structural and functional development. Well-described trajectories of major metabolites with age provide a benchmark of normal brain maturation. In a longitudinal study, we examined the trajectories of NAA, choline and creatine in normally developing South African children at 5, 7 and 9 years. We found age-related increases in NAA and creatine levels, and constant choline levels in the midfrontal gray matter. Since no gender or ethnicity effects were observed, these results are generalizable to a wide pediatric population against which pathology and abnormal development may be compared.

Traditional Poster

Perfusion in Health & Disease

Exhibition Hall

Monday, May 9, 2016: 10:45 - 12:45

1416

Arterial Spin Labeling Measured Choroidal Blood Flow is Reduced in Age-Related Macular Degeneration and Correlates with Severity Level

Weiying Dai^{1,2}, Lauren O'Loughlin¹, Gina Yu³, Li Zhao¹, David Alsop¹, and Jorge Arroyo³

¹*Radiology, Beth Israel Deaconess Medical Center & Harvard Medical School, Boston, MA, United States*, ²*Computer Science, State University of New York at Binghamton, Binghamton, NY, United States*, ³*Ophthalmology, Beth Israel Deaconess Medical Center & Harvard Medical School, Boston, MA, United States*

Age-related macular degeneration (AMD) has been associated with reduced choroidal blood flow. However, current methods do not provide spatial location of reduced choroidal blood flow. Here we explored the feasibility and capability of arterial spin labeling (ASL) magnetic resonance imaging (MRI) in observing reduced choroidal blood flow in AMD patients and the association with their severity levels. Choroidal blood flow was significantly reduced in patients with AMD compared to controls. Most importantly, choroidal blood flow was significantly correlated with the severity levels of AMD. This suggests that ASL may be a useful tool to study the role of choroidal blood flow in the pathogenesis of AMD.

1417

Physiological Fluctuations in the White Matter of Children with Sickle Cell Disease
Jackie Leung¹, Zahra Shirzadi², Bradley MacIntosh^{2,3}, and Andrea Kassner^{1,4}

¹Physiology and Experimental Medicine, The Hospital for Sick Children, Toronto, ON, Canada, ²Medical Biophysics, University of Toronto, Toronto, ON, Canada, ³Sunnybrook Health Sciences Centre, Toronto, ON, Canada, ⁴Medical Imaging, University of Toronto, Toronto, ON, Canada

The pulsatility of the brain has been previously shown to be associated with cerebrovascular dysfunction. Recently, the use resting state BOLD imaging has been proposed to non-invasively assess this pulsatility by calculating the temporal variance in the white matter. This measure is known as physiological fluctuation in the white matter (PF_{wm}). In this study, we compared PF_{wm} acquired in children with sickle cell disease to healthy controls. The results show increased pulsatility in the disease group, providing evidence that this approach has the potential to be a clinically relevant tool in the assessment of cerebrovascular diseases.

1418

Cine Phase-contrast MRI in Pediatric Patients Undergoing Sedation: A Comparative Study With Combined Ketamine-Propofol vs Propofol.

Malek I Makki¹, Philip Buhler², Olivier Baledent³, Christian Kellenberger⁴, Ruth L O'Gorman⁵, Carola Sabandal², Volker Ressel⁵, Markus Weiss², Iainia Scheer⁴, and Achim Schmidt²

¹MRI Research, University Children Hospital, Zurich, Switzerland, ²Anesthesia, University Children Hospital Zurich, Zurich, Switzerland, ³BioFlow Image, Universite de Picardie Jules Verne, Amiens, France, ⁴Radiology, University Children Hospital Zurich, Zurich, Switzerland, ⁵MRI Research, University Children Hospital Zurich, Zurich, Switzerland

The purpose of this investigation was to measure the brain blood flow differences between 2 MRI sedation techniques commonly used in pediatric radiology: propofol-based sedation technique and the combination of ketamine and propofol. We performed retrospectively gated 2D cine phase-contrast MRI in 58 pediatric patients and measured the arterial and jugular blood flows and compared these values between the 2 groups.

1419

Non-Contrast Hybrid Arterial Spin Labeled (NoHASL) Imaging of the Intracranial Arteries

Farah Al-Rawi¹, Elena Trajcevska¹, Dinesh Gooneratne¹, Windell Ang¹, Yuliya Perchyonok^{1,2}, Greg Fitt¹, Andrew Kemp¹, Shivraman Giri³, Davide Piccini⁴, Amy Brodtmann⁵, Helen Dewey⁶, Ioannis Koktzoglou⁷, and Ruth P Lim^{1,2}

¹Radiology, Austin Health, Melbourne, Australia, ²The University of Melbourne, Melbourne, Australia, ³Siemens Healthcare, Chicago, IL, United States, ⁴Siemens Healthcare, Lausanne, Switzerland, ⁵Neurology, Austin Health, Melbourne, Australia, ⁶Neurology, Eastern Health, Melbourne, Australia, ⁷Radiology, NorthShore University HealthSystem, Evanston, IL, United States

A Non-enhanced Hybrid Arterial Spin Labeling MRA (NoHASL) technique for assessment of the intracranial arteries was evaluated. 30 patients with known/suspected cerebral ischemia underwent time of flight MRA (TOF), NoHASL, and contrast enhanced MRA (CE-MRA). 21 arterial segments per patient were assessed by 2 neuroradiologists for image quality and haemodynamically significant stenosis. Overall image quality scores were diagnostic for all three sequences, with NoHASL and CE-MRA performing better for proximal intracranial segments, and TOF MRA performing better for smaller caliber arteries.

1420

Flow-Related Artifacts and Pitfalls in Magnetic Resonance Imaging/Angiography in Neuroradiology
Jae W Song¹

¹Radiology and Biomedical Imaging, Yale University, New Haven, CT, United States

Artifacts related to flow are common and can be a diagnostic pitfall for the interpreting neuroradiologist, if it is not recognized accurately. It is critical for the interpreting neuroradiologist to have a fundamental understanding of the physics that underlie image formation and the types of artifacts that emerge from magnetic resonance imaging and angiography. We present a pictorial essay of commonly encountered flow-related artifacts and pitfalls in magnetic resonance imaging and angiography in neuroradiology and discuss the physics behind the formation of the artifact as well as how to minimize the artifact. Knowledge of these artifacts and pitfalls is essential to arrive at accurate diagnoses.

1421

Preliminary application of arterial spin labeling and intravoxel incoherent motion in crossed cerebellar diaschisis
Hailong Luo¹, Yong Zhang², Xueying Ling¹, Ying Wang¹, and Li Huang¹

¹Medical Imaging Center, the First Affiliated Hospital of Jinan University, Guangzhou, China, People's Republic of, ²GE Healthcare MR Research China, Beijing, China, People's Republic of

In patients with crossed cerebellar diaschisis (CCD), the blood flow and glucose metabolism in the cerebellar was reduced. In this study, arterial spin labeling (ASL) and intravoxel incoherent imaging (IVIM) techniques were used to assess the micro-perfusion change in patients with CCD.

1422

Blood T1 and CBF Quantification in ASL MRI

Hua-Shan Liu^{1,2,3,4}, Abbas F Jawad⁵, Nina Laney⁶, Erum A Hartung⁷, Allison M Port⁸, Ruben C Gur⁹, Stephen Hooper¹⁰, Jerilynn Radcliffe¹¹, Susan L Furth^{6,12}, and John A Detre¹³

¹Department of Neurology, Perelman School of Medicine at the University of Pennsylvania, Philadelphia, PA, United States, ²Graduate Institute of Clinical Medicine, Taipei Medical University, Taipei, Taiwan, ³Department of Medical Imaging, Taipei Medical University Hospital, Taipei, Taiwan,

⁴Translational Imaging Research Center, Taipei Medical University, Taipei, Taiwan, ⁵Department of Pediatrics, Children's Hospital of Philadelphia, Perelman School of Medicine at the University of Pennsylvania, Philadelphia, PA, United States, ⁶Division of Nephrology, Children's Hospital of Philadelphia, Philadelphia, PA, United States, ⁷Division of Nephrology, Department of Pediatrics, Children's Hospital of Philadelphia, Perelman School of Medicine at the University of Pennsylvania, Philadelphia, PA, United States, ⁸Brain Behavior Laboratory, Department of Psychiatry, University of Pennsylvania, Philadelphia, PA, United States, ⁹Department of Psychiatry, University of Pennsylvania, Philadelphia, PA, United States, ¹⁰Department of Allied Health Sciences, University of North Carolina School of Medicine, Chapel Hill, NC, United States, ¹¹Division of Developmental and Behavioral Pediatrics, Department of Pediatrics, Children's Hospital of Philadelphia, Perelman School of Medicine at the University of Pennsylvania, Philadelphia, PA, United States, ¹²Division of Nephrology, Departments of Pediatrics and Epidemiology, Perelman School of Medicine at the University of Pennsylvania, Philadelphia, PA, United States, ¹³Departments of Neurology and Radiology, Perelman School of Medicine at the University of Pennsylvania, Philadelphia, PA, United States

We evaluated three different approaches to blood T1 used to model ASL CBF measurements in a cohort of children with chronic kidney disease and controls. We observed significant changes in blood T1 depending on the approach used, leading to different results for both sex and group differences in CBF. Our results highlight the importance of blood T1 in ASL CBF quantification and suggest that hematocrit-based T1 may be the optimal approach if hematocrit can be measured at the time of the scan, especially for studies in patients with anemia.

1423



Automated extraction of arterial and venous function from time-resolved multiphasic MR angiography

Yoonho Nam¹, Jinhee Jang¹, Song Lee¹, Bumsoo Kim¹, and Myeong Im Ahn¹

¹Department of Radiology, Seoul St. Mary's Hospital, College of Medicine, The Catholic University of Korea, Seoul, Korea, Republic of

Time-resolved multiphasic MR angiography (TRMRA) has been suggested as a useful tool for assessment of anatomical and hemodynamic information of vascular structure. Although TRMRA with contrast agent injection gives huge amount of 4D data, most previous reports have been relied on visual inspection of time series of projection images. Hence, proper processing of acquired 4D data is required to enhance clinical utility of TRMRA. At this point, we propose an automatic extraction algorithm for arterial input function and venous output function in the neck region from 4D TRMRA data.

1424

ASL derived CBF Post Carotid Intervention Predicts Post-Operative Cognitive Impairment

Salil Soman¹, Weiying Dai², Elizabeth Hitchner^{3,4}, Payam Massaband^{5,6}, David Alsop¹, Allyson C Rosen^{7,8}, and Wei Zhou^{3,9}

¹Radiology, Harvard Medical School / BIDMC, Boston, MA, United States, ²Computer Science, State University of New York at Binghamton, Binghamton, NY, United States, ³Vascular Surgery, Stanford University, Stanford, CA, United States, ⁴Veterans Affairs Palo Alto Health Care System, Palo Alto, CA, United States, ⁵Radiology, Stanford University, Stanford, CA, United States, ⁶Radiology, Veterans Affairs Palo Alto Health Care System, Palo Alto, CA, United States, ⁷Psychology, Stanford University, Stanford, CA, United States, ⁸Psychology, Veterans Affairs Palo Alto Health Care System, Palo Alto, CA, United States, ⁹Vascular Surgery, Veterans Affairs Palo Alto Health Care System, Palo Alto, CA, United States

Carotid stenosis significantly increases the risk for stroke. Carotid revascularization surgeries have been shown to reduce this risk, but can also be associated with cognitive impairment that is not clearly linked to cardiovascular risk factors or perioperative complications. We performed baseline, 24 hours and 6 month post-surgery ASL brain CBF imaging, with baseline and 1 month post-operative neuropsychological testing to evaluate if CBF change patterns can predict cognitive impairment post-surgery. We found patterns of CBF change from baseline to 24 hours and 6 months post-surgery that predict decline in verbal learning and memory at 1 month.

1425

DCE derived kinetic perfusion indices predict seizure control in single calcified Neurocysticercosis

Alok Kumar Singh¹, Ravindra Kumar Garg¹, Prativa Sahoo², Hardeep S Malhotra¹, Pradeep Kumar Gupta³, Nuzhat Husain⁴, and Rakesh Kumar Gupta³

¹Department of Neurology, KG Medical University, Lucknow, India, ²Healthcare, Philips India Ltd, Bangalore, India, ³Radiology and Imaging, Fortis Memorial Research Institute, Gurgaon, India, ⁴Pathology, Ram Manohar Lohia Institute of Medical Sciences, Lucknow, India

The purpose of this study was to investigate the utility of DCE derived kinetic parameters and serum MMP-9 in predicting the control of seizures in patients with calcified NCC while these are on AED therapy. We found that during follow up, K_{ep} and K^{trans} values decreased significantly in no recurrence group while increased in recurrence group. The serum MMP-9, a marker of BBB breakdown also supported the DCE derived kinetic metrics. Our results suggest that DCE derived kinetic parameters, might be able to predict the control of seizures in patients with single calcified NCC while these are on AED therapy

1426

Silent Magnetic Resonance Angiography with hybrid Arterial Spin Labeling Techniques

Continuous ASL (cASL) combined with zero TE readout is a promising MRA technique, immune to susceptibility, superb artery selectivity, and being silent. One drawback however, is with cASL along, hollowing artifacts or flow void is likely to appear. In this work, we incorporate and compare different hybrid ASL strategies to eliminate this effect, while keeping the silent nature of zTE MRA.

1427

Altered baseline cerebral blood flow and neurotransmitter levels in episodic and chronic migraine

Lars Michels¹, Franz Riederer^{2,3}, Jeanette Villanueva¹, Andreas Gantenbein⁴, Peter Sandor⁴, Roger Luechinger⁵, Martin Wilson⁶, and Spyros Koliias¹

¹University Hospital Zurich, Zurich, Switzerland, ²Neurological Center Rosenhugel and Karl Landsteiner Institute for Epilepsy Research and Cognitive Neurology, Vienna, Austria, ³University of Zurich, Zurich, Switzerland, ⁴RehaClinic, Bad Zurzach & Baden, Switzerland, ⁵Swiss Federal Institute of Technology, Zurich, Switzerland, ⁶University of Birmingham, Birmingham, United Kingdom

Although it has been described that cerebral blood flow and cortical excitability is altered in migraineurs, it is unknown if these processes may be differentially involved in chronic and episodic forms of the disease. We used arterial spin labeling MRI and magnetic resonance spectroscopy (GABA-editing) to address this problem. We found lower levels of combined glutamate and glutamine in chronic and episodic migraineurs relative to controls. Chronic patients showed hypoperfusion relative to controls and episodic migraineurs. Our results might indicate severe signs of cortical spreading depression in chronic migraineurs. The MRS findings suggest a disturbed excitation-inhibition balance in migraineurs.

Traditional Poster

Neurovascular Disease & Stroke

Exhibition Hall

Monday, May 9, 2016: 10:45 - 12:45

1428

13:45

Disruptions of resting state functional MRI networks in comatose cardiac arrest patients

Ona Wu¹, Brian L. Edlow², Katherine Mott¹, Gaston Cudemus-Deseda³, Ming Ming Ning², Marjorie Villien¹, William A. Copen⁴, James L. Januzzi⁵, Joseph T. Giacino⁶, Eric S. Rosenthal², and David M. Greer⁷

¹Athinoula A Martinos Center for Biomedical Imaging, Department of Radiology, Massachusetts General Hospital, Charlestown, MA, United States, ²Department of Neurology, Massachusetts General Hospital, Boston, MA, United States, ³Department of Anesthesia, Critical Care and Pain Medicine, Massachusetts General Hospital, Boston, MA, United States, ⁴Department of Radiology, Massachusetts General Hospital, Boston, MA, United States, ⁵Department of Cardiology, Massachusetts General Hospital, Boston, MA, United States, ⁶Department of Psychiatry, Spaulding Rehabilitation Hospital, Charlestown, MA, United States, ⁷Department of Neurology, Yale School of Medicine, New Haven, CT, United States

Cardiac arrest patients who were comatose for more than 24 hours were prospectively studied to determine whether changes in the default mode network (DMN) and thalamocortical network (TCN) can be used to predict recovery of arousal. Arousal recovery was defined as either spontaneous eye opening or eye opening in response to stimuli prior to discharge. All patients had significantly altered DMN and TCN networks compared to healthy controls, with patients who failed to demonstrate eye opening having significantly greater disruption. Resting-state functional MRI may play an important role in predicting recovery and patient management decisions in comatose cardiac arrest patients.

1429

13:45

Can Resting-State fMRI Distinguish Healthy Tissues from Perfusion and Diffusion Lesions in Patients with Cerebrovascular Disease?
Thomas Christen¹, Samantha Holdsworth¹, Hesamoddin Jahanian¹, Michael Moseley¹, and Greg Zaharchuk¹

¹Radiology, Stanford University, Stanford, CA, United States

In this work, we acquired whole brain, high-temporal resolution resting-state BOLD fMRI in 10 healthy volunteers, 10 stroke patients, and 8 Moyamoya patients. Using information from co-registered perfusion and diffusion-weighted images, we defined 4 classes of tissue (healthy tissue, chronic perfusion deficit, acute diffusion core, and mismatch) and examined the spontaneous BOLD fluctuation patterns in these different regions. The results suggest that a single, short rs-fMRI sequence contains enough information to distinguish different tissue types in patients with cerebrovascular diseases, obviating the need for gadolinium and potentially dramatically shortening the duration of an acute stroke MR study.

1430

13:45

Early extravasation of the experimental contrast agent GadofluorineM in ischemic stroke predicts infarct severity

Angelika Hoffmann¹, Xavier Helluy¹, Tassilo Dege¹, Reiner Kunze², Hugo Marti², Sabine Heiland¹, Martin Bendszus¹, and Mirko Pham¹

¹Neuroradiology, University of Heidelberg, Heidelberg, Germany, ²Physiology and Pathophysiology, University of Heidelberg, Heidelberg, Germany

Very early post ischemic blood-brain barrier disruption has been difficult to detect *in vivo*. In this study we show that the experimental contrast agent Gadofluorine M visualizes very early blood-brain barrier disruption in a mouse model of ischemic stroke at 9.4T. Contrast agent leakage occurs multifocally along cortical and subcortical microvessels. The degree of leakage predicts final infarct severity and could therefore serve as a new predictive marker in ischemic stroke.

| | | |
|------|-------|--|
| 1431 | 13:45 | <p>An analysis of fast and slow Neurite Orientation Dispersion and Density Index (NODDI) models Kyler K. Hodgson¹, Edward DiBella¹, and Ganesh Adluru¹</p> <p>¹<i>University of Utah, Salt Lake City, UT, United States</i></p> <p>This abstract reports on our analysis of two methods for computing the Neurite Orientation Dispersion and Density Index (NODDI). One method is markedly faster than the other and we demonstrate that the methods are highly similar in both normal and stroke studies. We perform statistical comparisons to draw conclusions regarding the data. Additionally, we report on our findings concerning the tuning of the faster NODDI method to reduce computation time and improve accuracy for specific microstructure maps.</p> |
| 1432 | 13:45 | <p>Quantitative Perfusion, Oxygenation, and CMRO₂ Imaging in Post-Acetazolamide Moyamoya Disease Patients Wendy Ni^{1,2}, Thomas Christen², and Greg Zaharchuk²</p> <p>¹<i>Department of Electrical Engineering, Stanford University, Stanford, CA, United States</i>, ²<i>Department of Radiology, Stanford University, Stanford, CA, United States</i></p> <p>The acetazolamide challenge can be used to assess cerebrovascular reserve and oxygenation in patients with steno-occlusive diseases such Moyamoya, thus enabling evaluation of the quantitative blood oxygen-level dependent (qBOLD) approach of modeling tissue oxygenation. In this study, we mapped post-acetazolamide oxygenation (with transverse relaxation rate R₂'), CBF with arterial spin labeling (ASL), and CBV with dynamic susceptibility contrast (DSC). We found that angiographically abnormal tissues are relatively hypoperfused and hypoxic. Finally, we investigated a qBOLD biophysical model for quantitative tissue oxygenation which suggested no difference in the cerebral metabolic rate of oxygen consumption (CMRO₂) between normal and affected regions.</p> |
| 1433 | 13:45 | <p>Non-parametric acute ischemic stroke penumbra delineation from dynamic DSC-MRI data with convex source separation Sudhanya Chatterjee¹, Dattesh D Shanbhag¹, Uday Patil¹, Venkata Veerendranadh Chebrolu¹, and Rakesh Mullick¹</p> <p>¹<i>GE Global Research, Bangalore, India</i></p> <p>In acute ischemic stroke (AIS), stroke volume is determined by DWI and volume at risk is identified by thresholding deconvolved Tmax map (> 6s). Tmax map is itself influenced by quality of AIF, its location, laterality and deconvolution algorithm. This can potentially impact estimation of "volume at risk". In this work, we describe a CAMNS based source separation method with DSC concentration data to identify perfusion patterns without explicit parametrization of PWI data. We demonstrate that "volume at risk" estimation derived with CWSE may overcome the variability associated with the current methods based on Tmax maps only.</p> |
| 1434 | 13:45 | <p>Zero TE continuous ASL MRA in the characterization of cerebral aneurysm: a feasibility study Song'an Shang¹, Jianxun Qu², Bing Wu², Yingkui Zhang², Xianfu Luo¹, and Jingtao Wu¹</p> <p>¹<i>Department of Radiology, Subei People's Hospital of Jiangsu Province, Yangzhou, China, People's Republic of</i>, ²<i>MR Research China, GE Healthcare, Beijing, China, People's Republic of</i></p> <p>Cerebral aneurysm is a high risk factor for cerebrovascular events. Although DSA is the standard reference, MRA is an alternative and repeatable technique for patients, especially those who are renal dysfunction. Hence, we introduce a novel MRA technique using zero TE and continuous ASL sequence on a clinical 3.0T MR scanner. 10 patients were recruited receiving zTE and TOF MRA acquisitions. Image quality and delineation of aneurysm were compared between two techniques. The results indicated that zTE possesses superiority than TOF, and shows a promise as being a replacement for TOF in imaging of cerebral aneurysm.</p> |
| 1435 | 13:45 | <p>Analysis Methods for Breath-Hold Based Cerebrovascular Reactivity in an Intraoperative Setup Marco Picciarelli¹, Christiaan Hendrik Bas van Niftrik², Oliver Bozinov², Athina Pangalu¹, Antonio Valavanis¹, Luca Regli², and Jorn Fierstra²</p> <p>¹<i>Department of Neuroradiology, University Hospital Zurich, Zurich, Switzerland</i>, ²<i>Department of Neurosurgery, University Hospital Zurich, Zurich, Switzerland</i></p> <p>For the first time during neurosurgery, we determinate intraoperative CVR with Blood Oxygen-Level Dependent (BOLD) fMRI measurements with three cycles of apnea (mimicking BH) in mechanically ventilated neurosurgical patients. BOLD fMRI datasets of five neurovascular patients with unilateral hemispheric hemodynamic impairment were processed with various BH CVR analysis methods. Temporal lag (Phase), percent BOLD signal change (CVR) and explained variance (Coherence) maps were calculated using three different Sine models and two novel "Optimal Signal" model-free methods. Our analysis methods make the intraoperative determination of CVR possible, and increase sensitivity and reproducibility of BH derived BOLD fMRI CVR.</p> |
| 1436 | 13:45 | <p>Co-existing Atherosclerotic Plaques in Intra- and Extra-cranial Arteries and Recurrent Stroke Risk: A 3D MR Vessel Wall Imaging Study Yilan Xu¹, Zechen Zhou², Le He², Donghua Mi³, Rui Li², Chun Yuan^{2,4}, and Xihai Zhao²</p> <p>¹<i>Department of Radiology, Beijing Tsinghua Changgung Hospital, Beijing, China, People's Republic of</i>, ²<i>Center for Biomedical Imaging Research, Department of Biomedical Engineering, Tsinghua University, Beijing, China, People's Republic of</i>, ³<i>Department of Neurology, Beijing Tiantan Hospital, Beijing, China, People's Republic of</i>, ⁴<i>Department of Radiology, University of Washington, Seattle, WA, United States</i></p> |

This study investigated the characteristics of co-existing intra- and extra-cranial atherosclerotic plaques and their relationships with recurrent stroke by using 3D multicontrast vessel wall imaging techniques. We found that 77.6% of stroke patients had co-existing intra- and extra-cranial plaques. The number of co-existing plaques was significantly associated with recurrent stroke before (OR=2.42; 95% CI, 1.04-5.64; p=0.040) and after adjusted for traditional risk factors (OR=3.31; 95% CI, 1.09-10.08; p=0.035). Our findings suggest that the co-existing intra- and extra-cranial plaques are prevalent in stroke patients and the number of co-existing plaques might be an independent indicator for risk of recurrent stroke.

1437

13:45

Intracranial aneurysm wall permeability: a potential risk predictor for rupture
Qi Haikun¹, Peng Liu², and Huijun Chen¹

¹Center for Biomedical Imaging Research, School of Medicine, Tsinghua University, Beijing, China, People's Republic of, ²Department of Neurosurgical, Beijing Neurosurgical Institute and Beijing Tiantan Hospital, Beijing, China, People's Republic of

The rupture risk prediction of unruptured intracranial aneurysm (IA) is very important in clinical practice and increased knowledge of predictors for IA rupture is needed. IA wall permeability has great potential for aneurysm rupture risk prediction, and can be quantified by DCE-MRI. In this study, we measured IA wall permeability using DCE-MRI, and compared it with established clinical/imaging risk metrics. We found IA wall permeability may be independent of aneurysm size and IA wall enhancement providing distinctive information for IA rupture risk prediction.

1438

13:45

Characterizing diffusion heterogeneity changes after acute ischemic stroke
Ona Wu¹, Arne Lauer², Gregoire Boulouis², Lisa Cloonan², Mark Etherton², Abigail S. Cohen², Pedro T. Cougo-Pinto², Katherine Mott¹, William A. Copen³, and Natalia S. Rost²

¹Athinoula A Martinos Center for Biomedical Imaging, Department of Radiology, Massachusetts General Hospital, Charlestown, MA, United States, ²Department of Neurology, Massachusetts General Hospital, Boston, MA, United States, ³Department of Radiology, Massachusetts General Hospital, Boston, MA, United States

Diffusion kurtosis imaging (DKI) has been suggested to be a more sensitive marker for microstructural injury than diffusion tensor imaging (DTI). To investigate this hypothesis, we analyzed DKI data from acute ischemic stroke patients enrolled in a prospective serial MRI study (N=18). Axial diffusivity and axial kurtosis values within the ischemic core were significantly correlated with time-to-MRI. Regional differences in both diffusivity and kurtosis were observed as a function of tissue outcome suggesting DKI may provide complementary information to that obtained from DTI.

1439

13:45

Magnetic Resonance Imaging Detection of Multiple Ischemic Injury Produced by a Mild Transient Cerebral Ischemia Preceded by an Experimental Minor Stroke
Ursula I. Tuor^{1,2}, Min Qiao¹, David Rushforth², and Tadeusz Foniok²

¹Physiology and Pharmacology, University of Calgary, Calgary, AB, Canada, ²Experimental Imaging Centre, University of Calgary, Calgary, AB, Canada

A mild photothrombosis elicited an initial ischemic insult consisting of a small cortical infarct overlying a peri-infarct region of scattered necrosis. One, 2 or 7 days later a relatively short transient middle cerebral artery occlusion was produced. Peri-infarct regions were observed to be susceptible to the second (1 or 2 day later) ischemic event appearing as enhanced T2 increases and increased tissue damage. With one week between insults, there was no T2 increase and less ischemic damage in the peri-infarct region. The results are relevant for improving diagnosis and management of patients with recurrent transient ischemic insults.

1440

13:45

A marker for hyperacute ischemic stroke at ultra-low magnetic field
Mathieu Sarracanie^{1,2,3}, Fanny Herisson⁴, Najat Salameh^{1,2,3}, Cenk Ayata⁴, and Matthew Rosen^{1,2,3}

¹MGH/HST Athinoula A. Martinos Center for Biomedical Imaging, Charlestown, MA, United States, ²Harvard Medical School, Boston, MA, United States, ³Department of Physics, Harvard University, Cambridge, MA, United States, ⁴Department of Radiology, MGH/Neurovascular Research Lab, Boston, MA, United States

Ischemic stroke treatment with a thrombolytic agent given in the hyperacute phase can greatly impact the outcome for stroke patients, however stroke status monitoring with CT and MRI is generally only possible once patients are admitted to a hospital. Here, we demonstrate T_1 contrast at ultra-low magnetic field strength in a rat model of stroke, with subtle changes noticeable as early as t=20min, and more clearly at t=3h and t=24h following stroke onset. We believe that the use of portable, ultra-low field MRI scanners as an early-detection methodology could have great impact on the treatment and monitoring of ischemic stroke.

1441

13:45

Dynamic Changes of Amide Proton Transfer (APT) and Multi-parametric MRI Signals in Transient Focal Ischemia in Rats
Dong-Hoon Lee¹, Xuna Zhao¹, Hye-Young Heo¹, Yi Zhang¹, Shanshan Jiang¹, and Jinyuan Zhou¹

¹Department of Radiology, Johns Hopkins University School of Medicine, Baltimore, MD, United States

APT MRI is a novel imaging technique to provide *in vivo* image contrasts related with the changes of endogenous mobile amide proton concentration and/or tissue pH. In this abstract, based on the quantified APT signals and multi-parametric MR images, we attempted to evaluate signal changes in transient focal ischemia in rat models. Our results clearly showed that the APT imaging can be a useful

technique to predict the ischemia reperfusion status, and to provide the quantitative results more accurately.

| | | |
|--|-------|--|
| 1442 | 13:45 | Quantitative in vivo MRI study of Dahl and Sprague-Dawley rat brains in response to salt loading Kenneth W Fishbein ¹ , Mikayla L Hall ¹ , Mustapha Bouhrara ¹ , Yulia Grigorova ¹ , Jeffrey Long ¹ , Christopher A Morrell ¹ , Edward G Lakatta ¹ , Peter Rapp ¹ , Alexei Y Bagrov ¹ , Richard G Spencer ¹ , and Olga V Fedorova ¹ |
| <p>¹National Institute on Aging, National Institutes of Health, Baltimore, MD, United States</p> | | |
| | | Dahl salt-sensitive rats are a common preclinical model for hypertension. We compared brain morphology and MRI contrast parameters (T_2 , T_2^* , MTR and diffusion) in Dahl and Sprague-Dawley rats on low-salt and high-salt diets. Two of five Dahl rats on a high-salt diet exhibited stroke lesions on T_2 and diffusion-weighted images. Dahl rats had smaller brain and hippocampus volumes and larger percent ventricular volume relative to Sprague-Dawley rats, regardless of diet. Dahl rats on the high-salt diet had thinner cortex, and longer T_2 and shorter T_2^* in whole brain (excluding lesions and ventricles). Dahl rat brains therefore exhibit distinct morphological and contrast features on MRI, some of which are independent of salt loading. |
| <hr/> | | |
| 1443 | 13:45 | High resolution MRI and DTI in a Genetic Mouse Model of Neonatal Hypoxia-Ischemia Injury Cynthia Yang ¹ , Daniele Prociassi ¹ , and Maria L Dizon ^{2,3} |
| <p>¹Radiology, Northwestern University, Chicago, IL, United States, ²Pediatrics, Northwestern University, Chicago, IL, United States, ³Neonatology Division, Prentice Women's Hospital, Chicago, IL, United States</p> | | |
| | | White matter injury in the neonatal brain is characterized by lifelong abnormalities in motor control and plasticity. In vivo assessment of experimental interventions are necessary for the development of novel preventive therapies which are currently lacking. We tested multi direction (64 directions) and multiple b-values (0, 900, 1800 sec/mm ²) DTI as a means to monitor changes and progression of neurological disorders and reorganization following HI injury in a mouse model overexpressing microRNA-21. |
| <hr/> | | |
| 1444 | 13:45 | Relaxation-normalized fast diffusion kurtosis imaging for semi-automatic segmentation of acute stroke lesion Iris Yuwen Zhou ¹ , Yingkun Guo ^{1,2} , Yu Wang ³ , Emiri Mandeville ⁴ , Suk-Tak Chan ¹ , Mark Vangel ¹ , Eng H Lo ⁴ , Xunming Ji ³ , and Phillip Zhe Sun ¹ |
| <p>¹Athinoula A. Martinos Center for Biomedical Imaging, Department of Radiology, Massachusetts General Hospital and Harvard Medical School, Charlestown, MA, United States, ²Department of Radiology, Key Laboratory of Obstetric & Gynecologic and Pediatric Diseases and Birth Defects of Ministry of Education, West China Second University Hospital, Sichuan University, Chengdu, China, People's Republic of, ³Cerebrovascular Diseases Research Institute, Xuanwu Hospital of Capital Medical University, Beijing, China, People's Republic of, ⁴Neuroprotection Research Laboratory, Department of Radiology and Neurology, Massachusetts General Hospital and Harvard Medical School, Charlestown, MA, United States</p> | | |
| | | Kurtosis augments DWI for defining irreversible ischemic injury. However, long acquisition time of conventional DKI limits its use in the acute stroke setting. Moreover, the complexity of cerebral structure/composition makes kurtosis map heterogeneous, limiting the specificity of kurtosis hyperintensity to acute ischemia. With strongest correlation found between mean kurtosis and R1, we proposed the relaxation-normalized fast DKI approach to mitigate the kurtosis heterogeneity in normal brain with substantially reduced scan time. We further demonstrated that this approach enabled semi-automatic lesion segmentation and enhanced stratification of the heterogeneous DWI lesion, aiding the translation of fast DKI to the acute stroke setting. |
| <hr/> | | |
| 1445 | 13:45 | Diffusion and Multi-delay Arterial Spin Labeling Imaging of Cerebral Blood Flow, Cerebrovascular Reserve, and Transit Time in Moyamoya Disease Before and After Acetazolamide Challenge Christian Federau ¹ , Soren Christensen ¹ , Zungho Zun ² , Sun-Won Park ³ , Wendy Ni ¹ , Michael Moseley ¹ , and Greg Zaharchuk ¹ |
| <p>¹Stanford University, Stanford, CA, United States, ²Children's National Medical Center, Washington, DC, United States, ³Seoul National University, Seoul, Korea, Republic of</p> | | |
| | | We assessed the changes in arterial spin labeling cerebral blood flow (CBF) and arterial transit time (ATT), as well as in apparent diffusion coefficient (ADC), before and after acetazolamide challenge in preoperative Moyamoya patients as function of the severity of feeding vessel stenosis. We found a significant increase after acetazolamide challenge in CBF (mL/min/100g) in territories of normal (50.9±19.0 to 66.8±19.3, p<0.0001) and mildly stenosed (52.9±18.8 to 66.2±23.4, p < 0.0001) vessels, but not in severely stenosed/occluded vessels (57.8±31.7 to 58.1±23.4, NS). ATT significantly decreased but no change in ADC was identified after acetazolamide. |
| <hr/> | | |
| 1446 | 13:45 | High lesion-to-wall contrast ratio in intracranial arterial wall imaging using whole-brain IR-SPACE: A potential approach to stroke etiology assessment without the need for MR contrast media Zhaoyang Fan ¹ , Qi Yang ^{1,2} , Shlee Song ³ , Xiuhai Guo ⁴ , Wouter Schievink ⁵ , Xiaoming Bi ⁶ , Gerhard Laub ⁶ , Patrick Lyden ³ , and Debiao Li ^{1,7} |
| <p>¹Biomedical Imaging Research Institute, Cedars-Sinai Medical Center, Los Angeles, CA, United States, ²Radiology, Xuanwu Hospital, Beijing, China, People's Republic of, ³Neurology, Cedars-Sinai Medical Center, Los Angeles, CA, United States, ⁴Neurology, Xuanwu Hospital, Beijing, China, People's Republic of, ⁵Neurosurgery, Cedars-Sinai Medical Center, Los Angeles, CA, United States, ⁶MR R&D, Siemens Healthcare, Los Angeles, CA, United States, ⁷Bioengineering, University of California, Los Angeles, CA, United States</p> | | |
| | | Variable-flip-angle 3D fast spin-echo (SPACE) has emerged as a promising imaging technique to assess intracranial wall abnormalities. |

Gadolinium-based MR contrast medium is usually used to highlight wall lesions which are sometimes unclear on pre-contrast vessel wall images in part due to suboptimal lesion-to-wall contrast. A whole-brain inversion-recovery-prepared SPACE sequence has recently been developed to improve vessel wall delineation by substantially enhanced T1 contrast weighting and cerebrospinal fluid attenuation. To test the hypothesis that the sequence may be used for noncontrast wall evaluation, we evaluated the lesion-to-wall contrast on pre-contrast images from a group of stroke and transient ischemic attack patients.

1447 13:45 Whole-Brain CBF and BAT Template Measured by Multi-TI Arterial Spin-Labeling Technique and Its Application in Cerebellar Infarction
Yelong Shen¹, Bin Zhao¹, Guangbin Wang¹, Shuang Yang¹, Shan Li², Josef Pfeuffer³, and Tianyi Qian⁴

¹Shandong Medical Imaging Research Institute, School of Medicine, Jinan, China, People's Republic of, ²Department of Neurology, Provincial Hospital Affiliated to Shandong University, Jinan, China, People's Republic of, ³Siemens Healthcare, Application Development, Erlangen, Germany, Erlangen, Germany, ⁴Siemens Healthcare, MR Collaborations NE Asia, Beijing, China, People's Republic of

Single-TI ASL usually underestimates the cerebral blood flow in areas with longer blood arrival time, especially in the cerebellum. In this study, we built a template of whole-brain cerebral blood flow and blood arrival time based on multi-inversion time-ASL (mTI-ASL). No significant differences were found when comparing young vs. old groups and female vs. male groups. The application in cerebellar infarction patients demonstrates that mTI-ASL performs better than sTI-ASL especially in areas with longer BAT. The CBF/BAT template created based on normal subjects could be used to better identify perfusion deficits.

Traditional Poster

Spine, MRA & Other Clinical Neuro Applications

Exhibition Hall

Monday, May 9, 2016: 10:45 - 12:45

1448 4D Spiral Flow in MR compatible Spinal Canal Phantom with and without Occlusion
Matthew Lee Dobson¹, Bryan Gootee¹, Michael Kendrick², Robert Bert³, MJ Negahdar¹, and Amir Amini¹

¹Electrical and Computer Engineering, University of Louisville, Louisville, KY, United States, ²VA Medical Center, Louisville, KY, United States, ³Department of Radiology, University of Louisville, Louisville, KY, United States

A 3' clear polycarbonate tube together with a dowel rod extending the entire length of the tube, centered in the middle of the tube, were used to model the spinal canal and the spinal cord. Normal saline solution was used to mimic the Cerebrospinal (CSF) fluid. The dowel rod was centered with winged support structures that were 3D printed from a CAD model. A spinal canal occlude was also 3D printed. 4D flow MR imaging was performed and results indicate that the flow phantom has utility for validation and testing of MR methods for measurement of CSF flow.

1449 A probabilistic framework to learn average shaped tissue templates and its application to spinal cord image segmentation
Claudia Blaiotta¹, Patrick Freund^{1,2}, Armin Curt², Jorge Cardoso³, and John Ashburner¹

¹Wellcome Trust Centre for Neuroimaging, University College London, London, United Kingdom, ²Spinal Cord Injury Center Balgrist, University of Zurich, Zurich, Switzerland, ³Centre for Medical Image Computing, University College London, London, United Kingdom

Magnetic resonance imaging of the spinal cord has a pre-eminent role for understanding the physiopathology of neurological disorders; nevertheless it is confronted with numerous technical challenges, which currently limit its applicability. In this work we focus on the problem of automatically extracting and segmenting the cord, a crucial processing step for neuroimaging studies. We present a novel computational framework that allows delineating structures within the cord, thus providing a reliable and fast alternative to manual segmentation. We test the method on a data set of high-resolution cervical scans and demonstrate the consistency of our results with expert manual annotation.

1450 Diffusional Kurtosis Tractography of Cervical Spinal Cord White Matter with Multi-band EPI Technique
Masaaki Hori^{1,2}, Ryuji Nojiri², Yasuaki Tsurushima², Katsutoshi Murata³, Keiichi Ishigame², Kouhei Kamiya⁴, Yuichi Suzuki⁴, Koji Kamagata¹, and Shigeki Aoki¹

¹Radiology, Juntendo University School of Medicine, Tokyo, Japan, ²Tokyo Medical Clinic, Tokyo, Japan, ³Siemens Japan, Tokyo, Japan, ⁴Radiology, The University of Tokyo, Tokyo, Japan

We investigate the effect of multi-band reduction factor (MBf) on tractography methods, diffusional kurtosis tractography (DKI) -based and diffusion tensor imaging (DTI) -based, and quantitative diffusion metrics in the cervical spinal cord white matter *in vivo*. The numbers of WM tracts increased in DKI tractography, compared with DTI tractography for the same position. Moreover, the numbers of WM tracts decreased in MBf of 3 data, compared with MBf of 2. Unchanged diffusion metrics values were observed on any conditions. DKE-based method seem to be preferable and MBf of 2 is recommended for spinal cord WM tractography.

1451 Quantification and Visualization of CSF flow in the Cervical Spine using 4D Spiral flow MRI
MJ Negahdar¹, Robert Bert², and Amir Amini¹

¹Electrical and Computer Engineering, University of Louisville, Louisville, KY, United States, ²Department of Radiology, University of Louisville,

To determine feasibility of 4D spiral flow in measurement and visualization of CSF flow in the cervical spine, 5 normal volunteers underwent both a 4D spiral flow and a 4D conventional flow. Results indicate that 4D spiral flow achieved highly accurate flow waveforms with a substantial reduction in total scan time.

1452

Regional measures of water diffusion associated with impairment in chronic SCI

Ann S Choe^{1,2,3}, Cristina L Sadowsky^{3,4}, Seth A Smith^{5,6}, Peter C.M. van Zijl^{1,2}, Visar Belegu^{3,7}, and James J Pekar^{1,2}

¹Russell H. Morgan Department of Radiology and Radiological Science, Johns Hopkins University School of Medicine, Baltimore, MD, United States, ²F.M. Kirby Research Center for Functional Brain Imaging, Kennedy Krieger Institute, Baltimore, MD, United States, ³International Center for Spinal Cord Injury, Kennedy Krieger Institute, Baltimore, MD, United States, ⁴Physical Medicine and Rehabilitation, Johns Hopkins University School of Medicine, Baltimore, MD, United States, ⁵Radiology and Radiological Sciences, Vanderbilt University, Nashville, TN, United States, ⁶Vanderbilt University Institute of Imaging Science, Vanderbilt University, Nashville, TN, United States, ⁷Department of Neurology, Johns Hopkins University School of Medicine, Baltimore, MD, United States

Prior studies have shown that DTI allows for noninvasive assessment of the severity of spinal cord injury (SCI). The present study investigated whether subject-specific demarcation of injury (vs. anatomically-driven ROI placement) could enhance the specificity of diffusion measures, specifically, fractional anisotropy (FA). Results showed that FA averaged over the region inferior to the injury epicenter demonstrated significant associations with impairment, suggesting that FA measures in the region are sensitive to Wallerian degeneration in the descending ventrolateral motor columns. We conclude that in chronic SCI, regional analysis of water diffusion using subject-specific injury demarcation may be more specific to impairment.

1453

Quality assessment of a semi-automated spinal disc volume segmentation method

Johanna Kramme¹, Michael Diepers², Matthias Günther^{1,3}, Simone Steinert⁴, and Johannes Gregori¹

¹mediri GmbH, Heidelberg, Germany, ²Kantonsspital Aarau, Aarau, Switzerland, ³Fraunhofer MeVis, Bremen, Germany, ⁴TETEC AG, Reutlingen, Germany

Quality assessment of a semi-automated spinal disc volume segmentation method for use in lumbar herniated disc studies. To demonstrate reliability of an interpolation method which relies on a reduced number of delineated regions of interest (ROI), thereby reducing time and effort by up to 65%.

1454

Assessing neurodegeneration across the spinal axis using high-resolution MRI

Gergely David¹, Eveline Huber¹, Armin Curt¹, Nikolaus Weiskopf^{2,3}, Siawoosh Mohammadi^{3,4}, and Patrick Freund^{1,2,3}

¹Spinal Cord Injury Center, Balgrist, University Hospital Zurich, University of Zurich, Zurich, Switzerland, ²Department of Neurophysics, Max Planck Institute for Human Cognitive and Brain Sciences, Leipzig, Germany, ³Wellcome Trust Centre for Neuroimaging, UCL Institute of Neurology, London, United Kingdom, ⁴Department of Systems Neuroscience, University Medical Center Hamburg-Eppendorf, Hamburg, Germany

Traumatic spinal cord injury (SCI) affects both grey and white matter and may result in atrophy due to anterograde/retrograde degeneration of the motor and sensory tracts. Several studies have investigated the cervical spinal cord in SCI patients, but little is known about the degeneration occurring below the lesion site. In this study, we utilize high-resolution magnetic resonance imaging to demonstrate the feasibility of measuring spinal cord, grey matter and dorsal column area at the cervical and lumbar enlargement. Investigating volumetric differences at both spinal levels allows for a more comprehensive assessment of neurodegeneration in SCI patients.

1455

Improvement of visualization of intracranial blood vessel uniformity on MR angiography using a Silent scan

Yasuhiro Fujiwara¹ and Yoshiyuki Muranaka²

¹Department of Medical Imaging, Faculty of Life Sciences, Kumamoto University, Kumamoto, Japan, ²Radiological Center, Fukui Prefectural Hospital, Fukui, Japan

We evaluated the uniformity of the intracranial vascular signal using a Silent MR angiography (MRA). Experiments with phantoms and healthy subjects revealed that this sequence improved the uniformity of the vascular signal under the condition of complex flow. Silent MRA improved contrast, coefficient of variation, and accuracy for intracranial blood vessels with turbulent flow compared with time-of-flight MRA. The signal intensities obtained by Silent MRA were independent of flow conditions. Although it has limited spatial resolution and requires additional imaging time, this sequence may have the potential to improve the image quality of intracranial blood vessels.

1456

Combining fMRI and probabilistic DTI tractography to improve corticospinal tract visualization in patients with brain tumor

Chen Niu¹, Xin Liu², Pan Lin², Zhigang Min¹, Wenfei Li¹, Liping Guo¹, Maode Wang¹, Qi Li¹, and Ming Zhang¹

¹Department of Medical Imaging, The First Affiliated Hospital of Xi'an Jiaotong University, Xi'an, China, People's Republic of, ²Institute of Biomedical Engineering, Xi'an Jiaotong University, Xi'an, China, People's Republic of

we evaluated a combinatorial approach that used functional activation and anatomical landmark data to define multiple ROIs for CST fiber tracking in patients with a brain tumor. Our results suggest that a combination of fMRI and DTI fiber tracking may provide a more

comprehensive analysis of the CST pathway, which would be beneficial for characterizing spatial relationships between the CST pathway and the tumor. A dual ROI CST fiber tracking approach has the potential to play a critical role in preoperative planning to optimize surgical treatment and improve post-surgical outcome.

1457

Accelerated 3D black blood imaging using quadruple inversion recovery technique

Kohei Yuda¹, Takashige Yoshida¹, Yuki Furukawa¹, Masami Yoneyama², Seishi Takai¹, and Nobuo Kawauchi³

¹*Radiology, Tokyo Metropolitan Police Hospital, Tokyo, Japan*, ²*MR Clinical Scientist, Philips Electronics Japan,Ltd, Tokyo, Japan*, ³*Radiology of division, Tokyo Metropolitan Police Hospital, Tokyo, Japan*

Black blood imaging (BBI) for atherosclerotic plaque compartment usually have evaluated by pre-pulse sequence such as dual inversion recovery(DIR) turbo spin echo (TSE) with cardiac synchronization. This study aimed to evaluate the scan time reduction sequence of zoomed imaging quadruple inversion recovery using VISTA (zQIR-VISTA) in black blood MR imaging of cerebral artery and compare with a conventional VISTA.

Traditional Poster

Neuroimaging Animal Models

Exhibition Hall

Monday, May 9, 2016: 10:45 - 12:45

1458

Diffusion Tensor Imaging sheds light on microstructural brain changes related to the process of vocal learning in juvenile zebra finches. Julie Hamaide¹, Geert De Groot¹, Johan Van Audekerke¹, Marleen Verhoye¹, and Annemie Van der Linden¹

¹*Bio-Imaging Lab, University of Antwerp, Antwerp, Belgium*

Vocal learning in songbirds has until now mainly been studied by invasive methods such as histology and molecular testing. Here we use in vivo Diffusion Tensor Imaging to map the structural development of the zebra finch brain which might help unveil brain areas implicated in the process of song learning and brain areas subject to a downregulation of plasticity characterizing the end of the critical periods which results in song crystallization.

1459

0:15

Comparative Analysis by Magnetic Resonance Imaging of Extracellular Space Diffusion in the Young and Adult Rats

Shuangfeng Yang¹, Hongbin Han^{2,3}, Yan Wang¹, and Yun Peng¹

¹*Imaging Center, Beijing Children's Hospital, Beijing, China, People's Republic of*, ²*Department of Radiology, Peking University Third Hospital, Beijing, China, People's Republic of*, ³*Beijing Key Lab of Magnetic Resonance Imaging Device and Technique, Beijing, China, People's Republic of*

The brain extracellular space is an irregular and tortuous space among neural cells and capillaries. Its normal development is important to maintain electrical signal conduction between cells, material transport and so on, especially in the early stage after birth, during which angiogenesis is not yet complete. ECS may provide the main pathway for metabolites. In the present study, gadolinium-diethylenetriaminepentaacetic acid tracer-based magnetic resonance imaging was employed to realize dynamic imaging and quantitative analysis of the diffusion and clearance of substances in the rat brain in vivo. With this method the differences of diffusion parameters in the young and adult rats can be detected.

1460

0:30

In vivo longitudinal ¹H MRS comparison of hippocampal and cerebellar changes due to Chronic Hepatic Encephalopathy, a rat model study

Veronika Rackayova¹, Olivier Braissant², Corina Berset³, Jocelyn Grosse⁴, Rolf Gruetter^{1,3}, Valérie A. McLin⁵, and Cristina Cudalbu³

¹*Laboratory of Functional and Metabolic Imaging, Center for Biomedical Imaging, Ecole Polytechnique Fédérale de Lausanne (EPFL), Lausanne, Vaud, Switzerland, Lausanne, Switzerland*, ²*Service of Biomedicine, University Hospital of Lausanne, Lausanne, Vaud, Switzerland, Lausanne, Switzerland*, ³*Center for Biomedical Imaging, Ecole Polytechnique Fédérale de Lausanne (EPFL), Lausanne, Vaud, Switzerland, Lausanne, Switzerland*, ⁴*Laboratory of behavioral genetics, Ecole Polytechnique Fédérale de Lausanne (EPFL), Lausanne, Vaud, Switzerland, Lausanne, Switzerland*, ⁵*Swiss Center for Liver Disease in Children, Department of Pediatrics, University Hospitals Geneva, Geneva, Switzerland, Geneva, Switzerland*

Chronic liver disease leads to Hepatic Encephalopathy - spectrum of neuropsychiatric disorders. We investigated potential neurometabolic differences between two key brain regions (hippocampus and cerebellum). Cerebellum shows similar increase of glutamine but lower tNAA, Tau, Cr, Asc and different osmotic response indicating that these regions are influenced unequally.

1461

0:45

In Vivo Imaging of Rapid Structural Brain Plasticity Following Environmental Enrichment in Mice

Jan Scholz¹, Kaitlyn Easson², and Jason P Lerch^{1,3}

¹*Mouse Imaging Centre, Hospital for Sick Children, Toronto, ON, Canada*, ²*Department of Biomedical and Molecular Sciences, Queen's University, Toronto, ON, Canada*, ³*Department of Medical Biophysics, University of Toronto, Toronto, ON, Canada*

The time course of the MRI changes associated with learning and experience is still unclear. Here we show with rapid in vivo imaging that brief periods of environmental enrichment of 24-48 h are associated with volumetric increases in a network of distinct brain areas.

For the first time we show that the size of these changes is directly related to the length of the enrichment. Our results indicate that the volumetric increases might plateau after about 48 h. This suggests that studies of human brain plasticity, which have often imaged after several weeks of training, might have underestimated the speed of these structural changes.

| | | |
|------|------|--|
| 1462 | 1:00 | <p>Neuroanatomical abnormalities in a PAX6 deficient mouse model studied by Voxel Based Morphometry Khan Hekmatyar¹, Anastasia M Bobilev², Kenji K Johnson², and James D Lauderdale²</p> <p>¹<i>Biolimaging Research Center, University of Georgia, Athens, GA, United States</i>, ²<i>Department of Genetics, University of Georgia, Athens, GA, United States</i></p> <p>Heterozygous PAX6 mutations confine not only defects in eye, but also in the brain. Our MRI study reveals the structural abnormalities in the brain of mouse model of Small EyeNeu (PAX6^{Sey Neu/+}) and compare with clinical form of this disease using voxel based morphometry using magnetic resonance imaging.</p> |
| 1463 | 1:15 | <p>3D Map of Perivascular Network in the Rat Brain Magdoom Kulam¹, Alec Brown², Michael A King³, Thomas H Mareci^{2,4,5}, and Malisa Sarntinoranont^{1,5}</p> <p>¹<i>Department of Mechanical & Aerospace Engineering, University of Florida, Gainesville, FL, United States</i>, ²<i>Department of Physics, University of Florida, Gainesville, FL, United States</i>, ³<i>Department of Pharmacology & Therapeutics, University of Florida, Gainesville, FL, United States</i>, ⁴<i>Department of Biochemistry & Molecular Biology, University of Florida, Gainesville, FL, United States</i>, ⁵<i>Department of Biomedical Engineering, University of Florida, Gainesville, FL, United States</i></p> <p>In the absence of lymphatic vessels in the brain, metabolic wastes were known to be cleared out of the brain along perivascular spaces which are annular gaps between blood vessels and the parenchyma. Abnormalities in the perivascular transport have been implicated in neurodegenerative disorders such as Alzheimer's and syringomyelia. In this study, we have obtained a high resolution 3D reconstruction of the perivascular network in the rat brain for the first time. Combining the reconstructed vascular and perivascular networks using the current method with physical models may shed light into mechanisms underlying perivascular transport in normal and pathological states.</p> |
| 1464 | 1:30 | <p>Effects of High-Fat Diet on White Matter Integrity: A Diffusion Tensor Imaging Study in Wistar Rats. Andrzej R. Gaździnski¹, Yu Zhang², Jarosław Orzeł^{3,4}, Bartosz Kossowski⁵, Piotr Bogorodzki⁵, Zuzanna Setkowicz⁶, and Stefan P. Gazdzinski⁷</p> <p>¹<i>Military Institute for Aviation Medicine, Warsaw, Poland</i>, ²<i>University of California San Francisco, San Francisco, CA, United States</i>, ³<i>Faculty of Electronics and Information Technology, Warsaw University of Technology, Warsaw, Poland</i>, ⁴<i>Mossakowski Medical Research Centre Polish Academy of Sciences, Warsaw, Poland</i>, ⁵<i>Warsaw University of Technology, Warsaw, Poland</i>, ⁶<i>Neuroanatomy, Jagiellonian University, Krakow, Poland</i>, ⁷<i>CNS Lab, Military Institute for Aviation Medicine, Warsaw, Poland</i></p> <p>Human DTI studies have demonstrated lower fractional anisotropy and higher mean diffusivity in obese humans. In animal models, high-fat diet is commonly used to induce obesity. However, we observed increase in hippocampal volumes and hippocampal metabolite concentrations in our study of long term effects of high fat diet on brain morphology, function, and behavior in Wistar rats. The results of this DTI study are partially consistent with our previous results. Unchanged or increasing mean diffusivity in certain brain regions likely reflects increased concentration of water. It would lead to lower concentration of metabolites, which is contradictory to our earlier findings.</p> |
| 1465 | 1:45 | <p>In vivo Parametric T₁/R₁ Imaging Correlation with Myelin Density and Microstructure Properties of Rat Corpus Callosum Xiao Wang^{1,2,3}, Xiao-hong Zhu¹, Yi Zhang¹, and Wei Chen¹</p> <p>¹<i>Center for Magnetic Resonance Research, University of Minnesota Medical School, Minneapolis, MN, United States</i>, ²<i>Diagnostic Radiology, University of Minnesota Medical School, Minneapolis, MN, United States</i>, ³<i>Transitional Year Residency Program, Hennepin County Medical Center, Minneapolis, MN, United States</i></p> <p>Corpus callosum (CC) is a prominent white matter commissure of the brain bridging two cerebral hemispheres and communicating between the cortical and subcortical neurons. It is known that the fiber composition and microstructure of CC varies anteriorly to posteriorly (1, 2). Due to different spatial scale, co-register of macro-morphologic MR image with micro-morphologic histology transmission electron microscopy (TEM) of CC is extremely strenuous and challenging yet necessary and important. In the present study, we performed an extensive and near point to point comparison between MR T₁/R₁ imaging <i>in vivo</i> and histological TEM of the entire CC in normal rat. It shows that there is a significantly positive correlation between R₁ and myelin density and negative correlation between R₁ and the axon diameter in normal rat corpus callosum. The overall results indicate that T₁/R₁ images are tightly correlated to myelin density and provide robust assessment of myelin density and axon size <i>in vivo</i>, thus, should provide valuable information of the microstructure properties of the tissue. Moreover, all measures are highly inhomogeneous in CC.</p> |
| 1466 | 2:00 | <p>Longitudinal MRI characterizes the impact of prenatal irradiation on ageing Tine Verreet^{1,2}, Janaki Raman Rangarajan^{3,4,5}, Kristof Govaerts^{5,6}, Frederik Maes^{3,4}, Sarah Baatout¹, Lieve Moons², Mohammed A Benotmane¹, and Uwe Himmelreich^{5,6}</p> <p>¹<i>Radiobiology Unit, Molecular and Cellular Biology, Belgian Nuclear Research Centre, SCK•CEN, Mol, Belgium</i>, ²<i>Laboratory of Neural Circuit Development and Regeneration, University of Leuven (KU Leuven), Leuven, Belgium</i>, ³<i>Electrical Engineering (ESAT-PSI), University of Leuven (KU Leuven), Leuven, Belgium</i>, ⁴<i>Leuven Institute for Neuroscience and Mental Health (LIMN), Leuven, Belgium</i>, ⁵<i>Department of Radiology, University of Leuven (KU Leuven), Leuven, Belgium</i>, ⁶<i>Department of Nuclear Medicine, University of Leuven (KU Leuven), Leuven, Belgium</i></p> <p>¹<i>Radiobiology Unit, Molecular and Cellular Biology, Belgian Nuclear Research Centre, SCK•CEN, Mol, Belgium</i>, ²<i>Laboratory of Neural Circuit Development and Regeneration, University of Leuven (KU Leuven), Leuven, Belgium</i>, ³<i>Electrical Engineering (ESAT-PSI), University of Leuven (KU Leuven), Leuven, Belgium</i></p> |

Leuven), Leuven, Belgium, ⁴Medical IT, iMinds, Leuven, Belgium, ⁵Molecular Small Animal Imaging Center (MoSAIC), Faculty of Medicine, University of Leuven (KU Leuven), Leuven, Belgium, ⁶Biomedical MRI Unit, Department of Imaging and Pathology, Faculty of Medicine, University of Leuven (KU Leuven), Leuven, Belgium

Prenatal exposure to ionising radiation can severely compromise brain development, leading to functional impairment of the brain. Behavioral deficits and/or morphological alterations have been reported, but the consequences of prenatal irradiation at older age remains unexplored. We irradiated pregnant mice with different doses (0.05 to 1.0Gy) at embryonic day 11 and investigated structural sequelae at an old age using *in vivo* longitudinal MRI. Apart from small brain size, we noticed predominant regional changes and increase in brain volume as the mice aged (unlike humans). Hippocampus seems to be affected by exposure to even low-doses and relates to impaired spatio-cognitive performance.

1467 2:15 Gd-enhanced Susceptibility Weighted Imaging in Neonatal Rats
Yu-Chieh Jill Kao^{1,2}, Chia-Feng Lu^{1,2,3}, Hua-Shan Liu^{4,5}, Fei-Ting Hsu⁴, Ping-Huei Tsai^{2,4}, Li-Chun Hsieh⁴, Pen-Yuan Liao⁴, and Cheng-Yu Chen^{2,4}

¹*Translational Research Imaging Center, College of Medicine, Taipei Medical University, Taipei, Taiwan, ²Department of Radiology, School of Medicine, Taipei Medical University, Taipei, Taiwan, ³Department of Biomedical Imaging and Radiological Sciences, National Yang-Ming University, Taipei, Taiwan, ⁴Department of Medical Imaging, Taipei Medical University Hospital, Taipei, Taiwan, ⁵Graduate Institute of Clinical Medicine, Taipei Medical University, Taipei, Taiwan*

Gd-enhanced susceptibility weighted imaging in neonatal rats, which highlights the penetrating vessels in the neonatal brain, may provide a new imaging protocol to investigate pediatric neurological disorders.

1468 2:30 Developing a Rat Model of Brainstem Coma: Initial MRI and MRA Investigations of Basilar Artery Occlusion
Patricia País Roldán¹, Brian Edlow², and Xin Yu¹

¹*Translational Neuroimaging and Neural Control Research Group, High Field Magnetic Resonance Department, Max Planck Institute for Biological Cybernetics, Tübingen, Germany, ²Department of Neurology, Massachusetts General Hospital, Harvard Medical School, Boston, MA, United States*

The ascending reticular activating system (ARAS) of the brainstem mediates arousal, which is an essential component of consciousness. In order to infarct the ARAS and induce an unarousable state in rats, we performed a two-point basilar artery (BA) occlusion. We used high resolution MRI to map the neuroanatomical distribution of the resulting brainstem infarction and MRA to map the penetrating branches of the BA. BA occlusion reproducibly caused medial-ventral brainstem infarction but did not create an unarousable state, suggesting that a larger region of ARAS infarction will be needed to create a rat model of brainstem coma.

1469 5:45 Detection of neuronal activities concerning the retrieval of the conditioned taste aversion with lipopolysaccharide
Chizuko Inui-Yamamoto¹, Fuminori Sugihara¹, Yuki Mori¹, Ting Chen¹, Zhenyu Cheng¹, Yutaka Komai², and Yoshichika Yoshioka¹

¹*Biofunctional Imaging, WPI iFReC, Osaka University, Suita, Japan, ²Single Molecule Imaging, WPI iFReC, Osaka University, Suita, Japan*

It is well known lipopolysaccharides (LPS) is produced by infected bacteria and triggers several acute phase responses after infection. Some reports show that rodents can acquire aversion to the taste stimulus paired with LPS. However, the brain mechanisms in the conditioned taste aversion (CTA) with LPS and in its retrieval remain obscure. To elucidate the brain mechanism in the retrieval of CTA with LPS (LPS-CTA), we tried to visualize the brain activities by using the manganese enhanced MRI (MEMRI). In consequence, we found the activation of DMH in relation with the regulation of body temperature in the retrieval of LPS-CTA cause body.

Traditional Poster

Young Investigator Awards

Exhibition Hall

Monday, May 9, 2016: 14:15 - 16:15

36 10:45 Music-Based Magnetic Resonance Fingerprinting to Improve Patient Comfort During MRI Examinations
Dan Ma¹, Eric Y. Pierre², Yun Jiang², Mark D. Schluchter³, Kawin Setsompop⁴, Vikas Gulani¹, and Mark Griswold¹

¹*Radiology, Case Western Reserve University, Cleveland, OH, United States, ²Biomedical Engineering, Case Western Reserve University, Cleveland, OH, United States, ³Epidemiology & Biostatistics, Case Western Reserve University, Cleveland, OH, United States, ⁴A.A. Martinos Center for Biomedical Imaging, Massachusetts General Hospital, Boston, MA, United States*

An acquisition method named MRF-Music is proposed to mitigate the acoustic noise during MRI scans by producing musical sounds directly from the switching magnetic fields while simultaneously quantifying multiple important tissue properties. MP3 music files were converted to arbitrary encoding gradients, which were then used with varying flip angles and TRs in both 2D and 3D MRF exam to generate T1, T2 and proton density maps. The MRF-Music scans were shown to significantly improve patients' comfort. T1 and T2 measured from phantom and *in vivo* scans were also in good agreement with those from the standard measurements and reported values.

Simultaneous assessment of cardiac metabolism and perfusion using co-polarized [1-13C]pyruvate and 13C-urea
Angus Zoen Lau^{1,2}, Jack Miller^{2,3}, Matthew D Robson¹, and Damian J Tyler^{1,2}

¹*Cardiovascular Medicine, University of Oxford, Oxford, United Kingdom*, ²*Department of Physiology, Anatomy, and Genetics, University of Oxford, Oxford, United Kingdom*, ³*Department of Physics, Clarendon Laboratory, Oxford, United Kingdom*

Assessment of cardiac metabolism and perfusion using hyperpolarized ¹³C substrates enables discrimination between viable, hibernating, and non-viable tissue, but current methods require two separate injections of pre-polarized [1-¹³C]pyruvate and ¹³C-urea, respectively. We propose to use an infusion of co-polarized [1-¹³C]pyruvate/¹³C-urea combined with a flow-sensitized pulse sequence to simultaneously assess both of these parameters in a single injection. Perfusion and metabolic state are modulated using specific interventions, and subsequently detected using the new scan. This probe of both myocardial perfusion and metabolism is anticipated to enable metabolic study of the heart in acute scenarios.

xSPEN: Single-shot magnetic resonance imaging with exceptional resilience to field heterogeneities
Zhiyong Zhang¹, Amir Seginer¹, and Lucio Frydman¹

¹*Chemical Physics, Weizmann Institute of Science, Rehovot, Israel*

Single-shot MRI has been constrained to acquisitions in quality magnets and homogeneous tissues. The present study introduces a methodology that can deliver such images with good SNR, under much poorer field and/or multiple shift conditions. These capabilities are achieved based on new principles whereby images are read using field gradients that are not applied along the direction being encoded. This enables one to accommodate shifts/inhomogeneities into the single-scan image generation protocol, without suffering from miss-registrations, without requiring a priori information for post-acquisition corrections, and without demanding specialized instrumentation. This enables new single-shot investigations that have hitherto escaped from MRI's scope.

Evaluation of Upper Airway Collapsibility Using Simultaneous Multi-Slice Real-Time MRI
Ziyue Wu^{1,2}, Weiyi Chen¹, Michael C.K. Khoo¹, Sally L. Davidson Ward³, and Krishna S. Nayak¹

¹*University of Southern California, Los Angeles, CA, United States*, ²*Alltech Medical Systems, Solon, OH, United States*, ³*Children's Hospital Los Angeles, Los Angeles, CA, United States*

We present a method for simultaneous multi-slice airway collapsibility measurement based on sparse golden-angle radial CAIPIRINHA, with acceleration factor up to 33.3. We present data from patients with obstructive sleep apnea and normal controls. One interesting finding is that a narrower airway site does not always correspond to higher collapsibility. This finding may be of interest to sleep surgeons. Our results also suggest that both compliance and P_{close} were significantly different between healthy controls and OSA patients ($P<0.001$), and both measures can potentially serve as biomarkers.

Interstudy repeatability of self-gated quantitative myocardial perfusion MRI
Devarvat Likhite¹, Promporn Suksaranjit², Ganesh Adluru¹, Nan Hu³, Cindy Weng³, Eugene Kholmovski¹, Chris McGann², Brent Wilson², and Edward DiBella¹

¹*Utah Center for Advanced Imaging Research, Department of Radiology, University of Utah, Salt Lake City, UT, United States*, ²*Division of Cardiovascular Medicine, University of Utah, Salt Lake City, UT, United States*, ³*Department of Internal Medicine, University of Utah, Salt Lake City, UT, United States*

Dynamic contrast enhanced MRI is maturing as a tool in contemporary cardiovascular medicine. A self-gated method that avoids the use of ECG-gating signal has been validated by us for quantitative myocardial perfusion. Our most recent study looks at the inter-study repeatability of this quantitative self-gated method. Our findings show that the multi-slice self-gated (near-systole) approach has a comparable or better repeatability than published ECG-gated single slice studies. The purpose of this abstract is to summarize these findings from our recent work, highlighting the simplicity, ease of use and reliability of the self-gated method for quantitative myocardial perfusion.

Neurovascular uncoupling in resting state fMRI demonstrated in patients with primary brain gliomas
Shruti Agarwal¹, Haris I. Sair¹, Noushin Yahyavi-Firouz-Abadi¹, Raag Airon¹, and Jay J. Pillai¹

¹*Division of Neuroradiology, Russell H. Morgan Department of Radiology and Radiological Science, Johns Hopkins University School of Medicine, Baltimore, MD, United States*

One of the most important potential limitations of presurgical mapping using blood oxygen level dependent functional magnetic resonance imaging (BOLD fMRI) is the phenomenon of neurovascular uncoupling (NVU). NVU can lead to erroneous interpretation of clinical fMRI examinations. The effects of brain tumor-related NVU on task-based BOLD fMRI have been previously published. The purpose of this study is to demonstrate that the problem of brain tumor-related NVU is a significant issue with respect to resting state BOLD fMRI similar to task-based BOLD fMRI, in which signal detectability can be compromised by breakdown of normal neurovascular coupling.

Perfusion & Permeability: Contrast Agent Methods

Exhibition Hall

Monday, May 9, 2016: 16:30 - 18:30

1470

3D CMRO₂ mapping in human brain with direct ¹⁷O-MRI and proton-constrained iterative reconstructions
Dmitry Kurzhunov¹, Robert Borowiak^{1,2}, Marco Reisert¹, Philipp Wagner¹, Axel Krafft^{1,2}, and Michael Bock¹

¹University Medical Center Freiburg, Dept. of Radiology - Medical Physics, Freiburg, Germany, ²German Cancer Research Center (DKFZ), German Cancer Consortium (DKTK), Heidelberg, Germany

This work presents a comparison analysis of different reconstruction techniques for quantification of 3D maps of the cerebral metabolic rate of oxygen consumption (CMRO₂) in human brain. Several ¹⁷O-MR 3D data sets of a healthy volunteer's brain were acquired at a clinical 3 Tesla MR system with inhalation of 70%-enriched ¹⁷O₂ gas. Iterative image reconstruction procedures, e.g. where different co-registered ¹H MR image data sets of high spatial resolution act as edge-preserving constraints, are compared and used to improve the image quality and the precision of CMRO₂ mapping. Anisotropic Diffusion as non-Homogeneous Constraint (ADHOC) is shown to be superior.

1471

Hyperemic Blood-Oxygen Level Dependent MRI of the foot for identifying perfusion defects in those with peripheral arterial disease
Tomoki Fujii¹, Krishna R. Singh², Bill Bordeau³, Joao A. Lima¹, and Bharath Ambale-Venkatesh¹

¹Johns Hopkins University, Baltimore, MD, United States, ²Prairie Vascular Institute, Springfield, IL, United States, ³Zimmer Biomet Biologics, Warsaw, IN, United States

Peripheral artery disease is a major public health concern particularly among the elderly. Although measures such as ankle-brachial index and segmental pressures have been used to characterize disease severity, MRI techniques allow us to assess subclinical vascular function and morphology and may help improve our understanding of vascular adaptations. In a small pilot study, we test whether hyperemia-induced BOLD oxygenation changes are a viable measure of tissue oxygenation in the foot and if they represent the reduced oxygenation seen in PAD.

1472

Contrast Enhanced MRI Reveals Perplexing T2 effect of Aggregate Forming Compounds In the Murine Placenta
Marina Lysenko¹, Noam Ben-Eliezer¹, Inbal E Biton², Joel R Garbow³, and Michal Neeman¹

¹Biological Regulation, Weizmann Institute of Science, Rehovot, Israel, ²Veterinary Resources, Weizmann Institute of Science, Rehovot, Israel, ³Biomedical Magnetic Resonance Laboratory, Mallinckrodt Institute of Radiology, Washington University, St. Louis, MO, United States

The murine placenta is a complex organ, consisting of different cell compartments that greatly influence its blood-flow pattern. Dynamic contrast enhanced (DCE) MRI of murine placental perfusion has been reported previously using both low and high MW contrast media. In this study, we used high-MW, albumin-based macromolecular contrast agent that does not cross the placental barrier, but, instead, forms contrast-based aggregates that accumulate in the maternal vasculature simultaneously with active contrast internalization by trophoblast cells in the labyrinth. To interpret the observed data, we suggest a novel model for describing feto-maternal processing and aggregate formation of labeled albumin in placental DCE-MRI experiments.

1473

Tissue Partial Volume Correction of Perfusion Maps in Dynamic Susceptibility Contrast MRI
André Ahlgren¹, Ronnie Wistam¹, Freddy Ståhlberg^{1,2,3}, and Linda Knutsson¹

¹Department of Medical Radiation Physics, Lund University, Lund, Sweden, ²Department of Diagnostic Radiology, Lund University, Lund, Sweden, ³Lund University Bioimaging Center, Lund University, Lund, Sweden

Partial volume effects (PVE) can significantly affect parameter estimates in perfusion MRI. In contrast to arterial spin labeling (ASL), the impact of PVEs in dynamic susceptibility contrast MRI (DSC-MRI) has not yet been well established. In this work, we assess and compare partial volume correction (PVC) of DSC-MRI and ASL data in 20 healthy subjects. PVC reduced the tissue volume dependence of perfusion estimates in DSC-MRI and ASL. White matter perfusion maps were of higher quality for DSC-MRI. However, for PVC of DSC-MRI we used several assumptions which need further evaluation.

1474

Improved Vascular Transport Function Characterization in DSC-MRI via Deconvolution with Dispersion-Compliant Bases
Marco Pizzolato¹, Rutger Fick¹, Timothé Bouteiller², and Rachid Deriche¹

¹Athena Project-Team, Inria Sophia Antipolis - Méditerranée, Sophia Antipolis, France, ²Olea Medical, La Ciotat, France

Bolus dispersion phenomena affect the residue function computed via deconvolution of DSC-MRI data. Indeed the obtained effective residue function can be expressed as the convolution of the true one with a Vascular Transport Function (VTF) that characterizes the dispersion. The state-of-the-art technique CPI+VTF allows to estimate the actual residue function by assuming a model for the VTF. We propose to perform deconvolution representing the effective residue function with Dispersion-Compliant Bases (DCB) without assumptions on the VTF, and then apply the CPI+VTF on DCB results. We show that DCB improve robustness to noise and allow to better characterize the VTF.

1475

Feasibility and Value of Quantitative Dynamic Contrast Enhancement MR imaging in Evaluation of Orbital Masses in Adults
Liyuan Song¹, Lizhi Xie², and Junfang Xian¹

This work assessed the feasibility of quantitative parameters derived from dynamic contrast enhanced MR imaging (DCE-MRI) and evaluate the value of quantitative dynamic contrast enhanced MR imaging in the diagnosis and differential diagnosis of orbital masses in adults. From the result we can see that it is feasible that quantitative parameters of orbital masses can be derived from DCE-MRI. ROI on the earliest and most enhanced area was optimal for distinguishing benign masses from malignant masses in orbit.

1476

Assessing the repeatability and reproducibility of contrast time courses from a dynamic MRI flow phantom: initial results and experiences

Jacob M. Johnson¹, Leah C. Henze Bancroft², James H. Holmes³, Edward F. Jackson^{1,2}, Frank R. Korosec^{1,2}, Courtney K. Morrison², Roberta M. Strigel¹, Kang Wang³, and Ryan J. Bosca¹

¹Radiology, University of Wisconsin, Madison, WI, United States, ²Medical Physics, University of Wisconsin, Madison, WI, United States, ³GE Healthcare, Madison, WI, United States

The recent development of a multi-modality, commercially available, dynamic flow phantom has provided a means of assessing the repeatability, reproducibility, and fidelity of contrast concentration time courses. In this work, we aimed to develop and evaluate a methodology for assessing the repeatability and reproducibility contrast concentration time courses derived from dynamic contrast-enhanced MR images of this dynamic flow phantom.

1477

Improved Image Quality when estimating Perfusion Parameters using Bayesian Fitting Algorithm

Irene Klærke Mikkelsen¹, Anna Tietze^{1,2}, Lars Ribe¹, Anne Obel³, Mikkel Bo Hansen¹, and Kim Mouridsen¹

¹CFIN, Aarhus University, Aarhus, Denmark, ²Dept. of Neuroradiology, Aarhus University Hospital, Aarhus, Denmark, ³Neuroradiology, Aarhus University Hospital, Aarhus, Denmark

Dynamic Contrast Enhanced Perfusion Imaging (DCE) allows for quantification of the blood-brain barrier integrity in tumor patients. A key post-processing step is to fit a hemodynamic model to DCE data. The fitting procedure can, however, cause spurious voxels and image degradation. We compared the widely used Levenberg-Marquardt fitting algorithm to a Bayesian algorithm. Image quality was assessed in 42 tumor patients. The Bayesian approach provided the highest image quality scores. This was confirmed in simulated data with fewer outliers (spurious voxels) when using the Bayesian approach. The hemodynamic two-compartment model that separates cerebral blood flow and leakage, provides reliable V_e images, when the robust Bayesian fitting algorithm is used.

1478

DCE-MRI at high temporal resolution using undersampled radial FLASH: A phantom study

Jost Michael Kollmeier¹, Volkert Roeloffs¹, and Jens Frahm¹

¹Biomedizinische NMR Forschungs GmbH, Max-Planck-Institut für biophysikalische Chemie, Göttingen, Germany

We present a DCE-MRI experiment using a commercial perfusion flow phantom for quantitative analysis of image series with high spatial and high temporal resolution (107 ms). Both can be obtained by current real-time MRI methods, i.e. radial undersampled radial FLASH and image reconstruction by nonlinear inversion (NLINV). Contrast agent bolus tracking with high CNR and quantitative parameter maps are presented.

1479

Dynamic contrast-enhanced MRI in primary rectal cancer: correlation with histologic prognostic factors

Zhe Han^{1,2}, Juan Chen², Min Chen², Chen Zhang², and Dandan Zheng³

¹Chinese Academy of Medical Science and Peking Union Medical College, Beijing, China, People's Republic of, ²Department of Radiology, Beijing Hospital, Beijing, China, People's Republic of, ³GE Healthcare, MR Research China, Beijing, China, People's Republic of

In this study we compared the association of dynamic contrast-enhanced (DCE)-derived quantitative parameters with the histologic grade, N-stage, epidermal growth factor receptor (EGFR) expression and K-RAS gene mutation of primary rectal cancer. Significant correlations were found between Ktrans values and N-stage, Ktrans values and EGFR expression, Kep values and EGFR expression. DCE-derived quantitative parameters may be a promising imaging biomarker of tumor aggressiveness and prognosis.

1480

Temporal resolution improvement of calibration-free dynamic contrast-enhanced MRI with compressed sensing optimized turbo spin echo: The effects of replacing turbo factor with compressed sensing accelerations

SoHyun Han¹ and Hyungloon Cho¹

¹Biomedical Engineering, Ulsan National Institute Science and Technology, Ulsan, Korea, Republic of

In vivo estimation of Gd-concentration in dynamic contrast enhanced (DCE)-MRI are often compromised from non-negligible T2* effect and limited temporal resolution. In this study, we introduce compressed sensing assisted turbo spin echo (CS-TSE) acquisition to provide accurate Gd-concentration estimation without the need of additional signal calibration, and to achieve a sub-second temporal resolution with extended slice coverage. Phantom verification followed by in vivo arterial input function (AIF) studies validated the faithful concentration estimation of CS-TSE. Robust measurement of first-pass kidney feeding AIF with increased temporal resolution was demonstrated with sub-second temporal resolution.

1481

Gradient optimization using active contour for rapid breast DCE-MRI

Pavan poojar¹, Bikkemane Jayadev Nutandev², Nithin N Vajuvali¹, C.K. Dharmendra Kuman², Ramesh Venkatesan³, and Sairam Geethanath¹

¹Medical Imaging Research Centre, Dayananda Sagar College of Engineering, Bangalore, India, ²Bangalore, India, ³Wipro-GE Healthcare, Bangalore, India

In dynamic scans, the significant values of k-space dependent on the shape of the organ which leads to arbitrary k-space trajectories. Gradient optimization for arbitrary k-space trajectory using active contour is a new acquisition technique that has been applied on six DCE breast data. The arbitrary k-space trajectory was obtained by active contour and gradients are optimized by employing convex optimization based on hardware constraints. Image reconstruction was performed using Fourier transform with density compensation. $\$\$K^{\{trans\}}\$$ and Ve maps were generated for different acceleration factors (1x, 2x, 3x, 4x and 10x) on tumor region to demonstrate utility of the method.

1482

Dictionary based approach for accelerated determination of Pharmacokinetic maps using Partial Least Square regression
Nithin N Vajuvali¹, Shivaprasad Ashok Chikop¹, and Sairam Geethanath¹

¹Medical Imaging Research Centre, Dayananda Sagar Institutions, Bangalore, India

This study is of relevance to MR researchers interested in DCE-MRI. Tofts model is a well-established two compartment model to determine the Pharmacokinetic (PK) maps, which is time consuming due to the presence of iterative curve fitting for each voxel. Current work focuses on the application of Partial Least Square (PLS) regression modelling to determine PK maps. PLS is a statistical method based on PCA and linear regression that provides the relationship between the predictor and response variables. We report 95-98% reduction in time as compared to curve fitting approaches for in silico phantoms and in vivo breast DCE data.

Traditional Poster

Arterial Spin Labeling

Exhibition Hall

Monday, May 9, 2016: 16:30 - 18:30

1483



Reproducibility and Variability of a Look-Locker FAIR ASL Sequence for Quantitative Measurement of Myocardial Blood Flow in Healthy Human Volunteers at 3T

Graeme A Keith¹, Christopher T Rodgers¹, Michael A Chappell², and Matthew D Robson¹

¹Oxford Centre for Clinical Magnetic Resonance Research, University of Oxford, Oxford, United Kingdom, ²Institute of Biomedical Engineering, University of Oxford, Oxford, United Kingdom

A previously presented arterial spin labelling (ASL) method was tested for reproducibility and variability. These measures are important to consider when planning a clinical study. The results presented show that the method has the sensitivity required to detect changes in MBF in pathology and under stress. The variation in individuals is shown to be less than across the sample as a whole. This knowledge will be useful in the planning of future clinical research studies.

1484

T2 Relaxation of Human Blood at 3T Revisited: In Vivo and In Vitro Measurement using TRUST MRI

Adam Bush¹, Jon Detterich², Thomas Coates³, Herbert Meiselman⁴, and John Wood¹

¹Biomedical Engineering/ Cardiology, University of Southern California/ Children's Hospital Los Angeles, Los Angeles, CA, United States,

²Cardiology, Children's Hospital Los Angeles, Los Angeles, CA, United States, ³Hematology, Children's Hospital Los Angeles, Los Angeles, CA, United States, ⁴Physiology and Biophysics, University of Southern California, Keck School of Medicine, Los Angeles, CA, United States

Precise knowledge of the T2 of blood (T2b) is required for spin-echo based blood oxygenation determination methods such as TRUST (T2 Relaxation Under Spin Tagging). In this study we measure the T2b in vivo and vitro using TRUST MRI. After correcting for physiologic variable we found that our model of T2b is statistically significantly different from the models used by other groups. We conclude those model lead to errors in derived parameters including oxygen saturation, oxygen extraction fraction and cerebral metabolic rate.

1485

Reproducibility of abdominal perfusion imaging using velocity selective arterial spin labeling
Marijn van Stralen¹, Esben Thade Petersen^{1,2}, Jeroen Hendrikse¹, and Clemens Bos¹

¹University Medical Center Utrecht, Utrecht, Netherlands, ²Danish Research Center for MR, Hvidovre, Denmark

Abdominal perfusion imaging using contrast media injection is potentially nephrotoxic. Arterial spin labeling (ASL), employing endogenous contrast, was shown using spatially selective labeling strategies. We investigated the reproducibility of velocity selective ASL (VS-ASL), which eliminates delicate label planning and possibly improves perfusion SNR by labeling closer to the target tissue. We show that abdominal VS-ASL is feasible in healthy volunteers and overcome labeling artifacts by pacing and triggering the acquisition with good temporal SNR. However, VS-ASL is sensitive to motion during readout, deteriorating reproducibility. It could benefit from outlier rejection techniques and retrospective motion correction.

1486

Whole brain volumetric perfusion imaging with high spatial resolution using simultaneous multi-slab (SMSB) 3D GRASE pCASL
Yi Wang¹, Xingfeng Shao¹, Steen Moeller², and Danny JJ Wang¹

¹Neurology, UCLA, Los Angeles, CA, United States, ²Center of Magnetic Resonance Research, University of Minnesota, Minneapolis, MN, United States

The temporal SNR of simultaneous multi-slice (SMS) 2D EPI ASL has been shown to be inferior to that of 3D background suppressed GRASE. In this work, we present a novel simultaneous multi-slab (SMSB) 3D GRASE sequence for volumetric pCASL imaging with high spatial resolution. The image quality of SMSB-GRASE was evaluated and compared to a standard 3D GRASE pCASL sequence. Preliminary results demonstrated the feasibility for whole-brain volumetric perfusion imaging at a high spatial resolution, although the drop in RF slice profiles in the overlapped boundary slices still needs to be addressed in future work.

1487

A Perfusion Phantom for Arterial Spin Labeled MRI
Hyo Min Lee^{1,2}, Marta Vidorreta^{3,4}, Yulin Vince Chang³, and John Alan Detre^{3,4}

¹Bioengineering, University of Pennsylvania, Philadelphia, PA, United States, ²Institute for Biomedical Engineering, University and ETH Zürich, Zürich, Switzerland, ³Radiology, University of Pennsylvania, Philadelphia, PA, United States, ⁴Neurology, University of Pennsylvania, Philadelphia, PA, United States

ASL MRI is an appealing biomarker for clinical research and management, but ASL MRI sequences are difficult to calibrate because a reliable phantom for simulating tissue-specific perfusion has yet to be developed. In this work, we describe a prototype perfusion phantom based on 3D printed vessels and mock parenchyma that may allow reliable, ex-vivo assessments of ASL sequences.

1488

Improved Pseudo Continuous Arterial Spin Labeling Efficiency Robustness to Off Resonance and High Velocity
Li Zhao¹ and David C Alsop¹

¹Radiology, Beth Israel Deaconess Medical Center, Boston, MA, United States

Pseudo continuous arterial spin labeling (pCASL) studies can be degraded by magnetic field variations at the labeling plane. We demonstrate through simulations that high velocity efficiency is particularly vulnerable to field offsets. By changing labeling parameters from published recommendations and/or introducing a new RF pulse, the off-resonance sensitivity and peak systolic velocity sensitivity of pCASL can be reduced. Preliminary experimental comparisons of parameters are reported.

1489

3D Arterial Spin Labeling in breast cancer: A case study.
Thorsten Honroth¹, Suzan Vreemann², Marco Vicari¹, Hendrik Laue¹, Ritse Mann², and Matthias Günther^{1,3,4}

¹Fraunhofer MEVIS, Bremen, Germany, ²Radboud University Medical Center, Nijmegen, Netherlands, ³University of Bremen, Bremen, Germany, ⁴mediri GmbH, Heidelberg, Germany

A single-shot 3D arterial spin labeling (ASL) sequence has been developed and optimized for breast cancer imaging. In a case study, its ability to measure the perfusion of a tumor without contrast agents is demonstrated. The resulting ASL perfusion-weighted image of the tumor shows high correspondence with the subtraction image of the contrast-enhanced measurement.

1490

Priors-guided adaptive outlier cleaning for arterial spin labeling perfusion MRI
Ze Wang^{1,2}

¹Hangzhou Normal University, Hangzhou, China, People's Republic of, ²Psychiatry and Radiology, University of Pennsylvania, PHILADELPHIA, PA, United States

ASL CBF signal is derived from the difference between successive labeling and no-labeling images. The low signal-to-noise-ratio and the pairwise subtraction can then result in outliers, which can significantly degrade CBF quantification quality in a typical several minutes scan. A priors-guided adaptive outlier cleaning algorithm was verified in this study. Our results showed that the proposed method improved both CBF quantification quality and CBF measurement stability.

1491

Improving SNR in pulsed arterial spin labeling using multiple inversion modules (MM-PASL)
Jia Guo¹, Richard B. Buxton¹, and Eric C. Wong^{1,2}

¹Radiology, UC San Diego, La Jolla, CA, United States, ²Psychiatry, UC San Diego, La Jolla, CA, United States

The bolus duration in pulsed arterial spin labeling (PASL) is typically short, resulting in low SNR. We propose using multiple inversion pulses to increase the total bolus duration for improved SNR. In this study, a wedge-shaped inversion was combined with a regular slab inversion and a QUIPSS II pulse to lengthen the total bolus duration while keeping the ASL signal quantitative. The preliminary in vivo results showed an SNR improvement of 54% in gray matter, in good agreement with theory, compared to a regular PASL scan. The mean GM CBF values were consistent with PCASL reference scans. This new labeling method should benefit studies using PASL.

A simple and reliable perfusion phantom to measure precise and repeatable arterial spin labeled quantitative perfusion
Joshua S. Greer^{1,2}, Keith Hulsey², Robert E. Lenkinski^{2,3}, and Ananth J. Madhuranthakam^{2,3}

¹*Bioengineering, University of Texas at Dallas, Richardson, TX, United States*, ²*Radiology, UT Southwestern Medical Center, Dallas, TX, United States*, ³*Advanced Imaging Research Center, UT Southwestern Medical Center, Dallas, TX, United States*

Arterial spin labeling (ASL) is a rapidly growing area of interest, primarily because of its ability to provide quantitative perfusion maps non-invasively. But, for the technique to be adopted for clinical use, these quantitative measurements need to be accurate and robust, which will require a quality controlled perfusion phantom to ensure consistency for different magnet strengths and manufacturers. In this study, we demonstrate a simple perfusion flow phantom that can be used to test the precision and repeatability of ASL perfusion measurements.

Considerations of cardiac phase can improve ASL quality in multiple settings
Yang Li^{1,2}, Deng Mao^{1,2}, Zhiqiang Li³, Michael Schär¹, James G. Pipe³, and Hanzhang Lu¹

¹*Russell H. Morgan Department of Radiology and Radiological Science, Johns Hopkins University, Baltimore, MD, United States*, ²*Graduate School of Biomedical Sciences, University of Texas Southwestern Medical Center, Dallas, TX, United States*, ³*Imaging Research, Barrow Neurological Institute, Phoenix, AZ, United States*

Recent studies have identified a cardiac-pulsation induced signal modulation in recommended ASL implementation (pseudocontinuous labeling 1.8s/post-labeling delay 1.8s/background-suppression/3D acquisition). In pCASL with single-shot readout, the ASL signal fluctuation could be reduced by cardiac-triggering scheme. Here is this study, we aim to extend the scope and provide possible solutions to other pCASL settings that suffer from pulsation effect, such as pCASL with 3D segmented readout, perfusion change detecting in CBF manipulations (e.g. hypercapnia), and regular pCASL when cardiac-triggering sequence is not available. We have demonstrated that considerations of cardiac phase can improve ASL data quality in multiple settings.

Assessment of Readout Performance in Arterial Spin Labeling Using Statistical 3D Mapping.
Jalal B. Andre¹, Swati Rane¹, Zhiqiang Li², James G. Pipe², Michael N. Hoff¹, Donna J. Cross¹, and Satoshi Minoshima³

¹*Radiology, University of Washington, Seattle, WA, United States*, ²*Imaging Research, Barrow Neurological Institute, Phoenix, AZ, United States*, ³*Radiology, University of Utah, Salt Lake City, UT, United States*

In this pilot project, we evaluated the effect of various readout schemes on specific ASL imaging metrics assessed by statistical 3D stereotactic surface projection, and applied to a pseudocontinuous labeling scheme that was conserved across all evaluated sequences. We conclude that descriptive statistical 3D mapping can offer insight into the performance of the five differing readout methods.

SAR comparison between CASL and pCASL at high magnetic field (9.4T). Evaluation of the benefit of a separate labeling coil.
Lydiane Hirschler^{1,2}, Jérôme Voiron², Sascha Köhler², Nora Collomb^{1,3}, Emmanuel L. Barbier^{1,3}, and Jan M. Warnking^{1,3}

¹*Université Grenoble Alpes, Grenoble Institute of Neuroscience, Grenoble, France*, ²*Bruker Biospin, Ettlingen, Germany*, ³*Inserm, U836, Grenoble, France*

Arterial Spin Labeling (ASL) is a non-invasive technique to obtain quantitative maps of perfusion. At higher magnetic fields, it benefits from both higher signal-to-noise ratio and longer T₁ but could suffer from higher RF power deposition and thus temperature increase. The latter issue has however not been characterized in animals. In this study, the specific absorption rate (SAR) delivered to a rat was measured in vivo at 9.4T using continuous ASL (CASL) and pseudo-continuous ASL (pCASL) with and without a dedicated labeling coil.

Deformation and resolution issues in partial volume correction of 2D arterial spin labeling data
Jan Petr¹, Henri JMM Mutsaerts², Enrico De Vita^{3,4}, Jens Maus¹, Jörg van den Hoff¹, and Iris Asllani⁵

¹*Institute of Radiopharmaceutical Cancer Research, Helmholtz-Zentrum Dresden-Rossendorf, Dresden, Germany*, ²*Sunnybrook Research Institute, Toronto, ON, Canada*, ³*Lysholm Department of Neuroradiology, National Hospital for Neurology and Neurosurgery, London, United Kingdom*, ⁴*Academic Neuroradiological Unit, Department of Brain Repair and Rehabilitation, UCL Institute of Neurology, London, United Kingdom*, ⁵*Department of Biomedical Engineering, Rochester Institute of Technology, Rochester, NY, United States*

Partial volume (PV) effects are a well-recognized confounder in arterial spin labeling due to its limited spatial resolution. Several algorithms exist to correct for these errors. Nevertheless, PV-correction is rarely used, mainly because the PV maps obtained from segmented T1-weighted images are regarded as not being sufficiently reliable when transformed into ASL space. Here, we show the impact of spatial deformation and resolution in the PV-maps used for PV-correction in the calculation of mean total gray matter (GM) cerebral blood flow (CBF). We also show how the deformations affect the calculation of PV-uncorrected mean GM CBF.

Multiphase pCASL for imaging blood flow in rodent brains
James R Larkin¹, Manon A Simard¹, Alexandre A Khrapitchev¹, Kevin J Ray¹, James A Meakin², Paul Kinchesh¹, Sean Smart¹, Peter Jezzard², Michael A Chappell³, and Nicola R Sibson¹

¹*CRUK and MRC Oxford Institute for Radiation Oncology, Department of Oncology, University of Oxford, Oxford, United Kingdom*, ²*FMRIB Centre, University of Oxford, Oxford, United Kingdom*, ³*Institute of Biomedical Engineering, Department of Engineering, University of Oxford, Oxford, United Kingdom*

Arterial spin labelling perfusion imaging in the rodent brain is easily confounded by off-resonance effects at the tagging plane. These effects are a consequence of the higher field strengths used pre-clinically and the nearby air cavities in the rodent head and neck, something not as problematic in the clinic. By implementing a multiphase pCASL sequence with eight phases spaced at 45° and lying between 0 and 315°, it is possible to obtain data to allow fitting thereby accounting for any off-resonance effects. This process dramatically improves image quality without excessively affecting acquisition time.

1498

Does cardiac triggering improve pCASL signal stability? Isolation of the effect of the last labeled spins by end-of-labeling triggering and extremely long labeling durations
Jasper Verbree¹ and Matthias J.P. van Osch¹

¹*Radiology Department; Leiden Institute for Brain and Cognition; C.J. Gorter Center for High-field MRI, Leiden University Medical Center, Leiden, Netherlands*

In pCASL, the blood tagged at the end-of-labeling period is expected to contribute most to the perfusion signal due to T1 recovery of the labeled spins. The influence on PCASL of cardiac triggering at the end-of-labeling was assessed with simulations and subsequently applied in volunteers. Simulations predict a 9% variation in ASL-signal over the cardiac cycle. In-vivo measurements were unable to show the predicted effect nor a difference in tSNR. Combining with earlier findings concerning cardiac triggering, neither triggering start- or end of labeling triggering improves signal stability, suggesting that cardiac triggering is not beneficial for pCASL.

1499

Neurophysiological effects and dose response curve of tDCS stimulation assessed by pseudo-continuous Arterial Spin Labeling
Mayank V Jog¹, Kay Jann², Lirong Yan², and Danny JJ Wang²

¹*Biomedical Engineering, University of California Los Angeles, Los Angeles, CA, United States*, ²*Neurology, University of California Los Angeles, Los Angeles, CA, United States*

Transcranial Direct Current Stimulation (tDCS) is one of such neuromodulation techniques that applies a small current (1-2mA) using scalp electrodes. Though tDCS has been shown to improve cognition as well as clinical symptoms, the mechanism of action is still unclear.

In this study, we sought to evaluate the neurophysiological effects of tDCS in a typical bilateral motor montage through concurrent Cerebral Blood Flow (CBF) measurements using arterial spin labeling (ASL). We were able to reliably detect increased blood flow under the anode as well as CBF changes in brain-wide networks.

Traditional Poster

Endogenous CEST & MT

Exhibition Hall

Monday, May 9, 2016: 16:30 - 18:30

1500

REGIONAL AND STRUCTURAL CHANGES OF THE SPINAL CORD TISSUE ENCOUNTERED IN AMYOTROPHIC LATERAL SCLEROSIS (ALS): A PRELIMINARY AND PROMISING CHARACTERIZATION USING DTI and ihMT.

Henitsoa Rasoanandrianina^{1,2,3,4}, Aude-Marie Grapperon⁵, Manuel Taso^{1,2,3,4}, Olivier M. Girard^{1,2}, Guillaume Duhamel^{1,2}, Elisabeth Soulier^{1,2}, Lauriane Pini^{1,2}, Audrey Rico⁶, Bertrand Audoin⁶, Maxime Guye^{1,2}, Jean-Philippe Ranjeva^{1,2}, and Virginie Callot^{1,2,3}

¹*CRMBM UMR 7339, Aix-Marseille Université, CNRS, Marseille, France*, ²*CEMEREM, AP-HM, Pôle d'Imagerie Médicale, Hôpital de La Timone, Marseille, France*, ³*Lab-Spine International Associate Laboratory, Marseille/Montréal, France*, ⁴*LBA UMR T 24, Aix-Marseille Université, IFSTTAR, Marseille, France*, ⁵*Service de Neurologie et Maladies neuro-musculaires, AP-HM, Hôpital de La Timone, Marseille, France*, ⁶*Service de Neurologie et Unité NeuroVasculaire, AP-HM, Hôpital de La Timone, Marseille, France*

In this study, regional alteration of the spinal cord (SC) tissue encountered in amyotrophic lateral sclerosis (ALS) were investigated using dedicated SC templates and 3T-multiparametric MRI techniques, in particular diffusion tensor imaging (DTI) and the emerging myelin-specific inhomogeneous magnetization transfer (ihMT) technique. Results collected on 9 patients showed significant alteration of the DTI metrics compared to age-matched controls. They also demonstrated impairment of the MT metrics in the bilateral corticospinal tracts, as well as in the dorsal sensory tracts and the anterior gray matter horns. Combined with reduced ihMT metric variations, this suggests increase of the macromolecular pool, without pronounced demyelination. The structural changes we observed suggest a complex chrono-physiopathology that need to be further investigated.

1501

Mapping the myelin g-ratio: promises and pitfalls

Jennifer SW Campbell¹, Ilana R Leppert¹, Mathieu Boudreau¹, Sridar Narayanan¹, Julien Cohen-Adad^{2,3}, G B Pike^{1,4}, and Nikola Stikov^{2,5}

¹*Montreal Neurological Institute, Montreal, QC, Canada*, ²*Ecole Polytechnique, University of Montreal, Montreal, QC, Canada*, ³*Functional Neuroimaging Unit, University of Montreal, Montreal, QC, Canada*, ⁴*Hotchkiss Brain Institute, University of Calgary, Calgary, AB, Canada*,

⁵*Montreal Heart Institute, Montreal, QC, Canada*

The aggregate myelin g-ratio is a function of the myelin volume fraction (MVF) and the fiber volume fraction (FVF). While this relationship holds in theory, obtaining precise and accurate MRI measures of the MVF and FVF remains a challenge. Most MVF mapping

techniques have been linearly correlated with histology, but the literature suggests that the slope and intercept are acquisition dependent. In this work, we focus on three magnetization transfer (MT) derived MVF metrics (MTR, MT_{sat} and qMT) and explore how improper calibration of the MVF estimates propagates to the aggregate g-ratio. The result of an incorrect MVF calibration is not simply loss in sensitivity to g-ratio changes, but rather g-ratio trends that are statistically significant, incorrect, and highly dependent on the fiber volume fraction changes.

1502

Measurement of the Resonance Frequency of Macromolecular Protons in Brain
Xu Jiang^{1,2}, Peter van Gelderen¹, and Jeff H. Duyn¹

¹AMRI, LFM, NINDS, NIH, Bethesda, MD, United States, ²Physics, University of Maryland, College Park, MD, United States

Studying the spectral asymmetry in Magnetization Transfer (MT) is essential for precise estimation of MT-related parameters from off-resonance MT experiments. Measurement of the delay-dependent water proton saturation following composite MT pulses was used to determine parameters for a 2-pool exchange model. These parameters were further used to calculate saturation levels of macromolecular protons (MPs) following off-resonance MT pulses. The off-resonance frequency for MPs is found to be -2.7 ppm from water for fixed marmoset brain, and -2.56 ppm for human brain. This is consistent with previous studies.

1503

Validation of Provotorov theory of RF saturation to describe inhomogeneous magnetization transfer (ihMT)
Scott D. Swanson¹

¹Department of Radiology, University of Michigan, Ann Arbor, MI, United States

This study shows that Provotorov theory of RF saturation provides an accurate description of inhomogeneous MT (ihMT) in model systems. These results help understand how long proton T1D times lead to large ihMT signals in model systems and in tissues.

1504

Ultrashort Echo Time Magnetization Transfer (UTE-MT) Imaging: Two-Pool vs Three-Pool Modeling
Yajun Ma¹, Graeme Bydder¹, and Jiang Du¹

¹Department of Radiology, UCSD, San Diego, CA, United States

Conventional MT modeling can only be applied to long T₂ tissues since short T₂ tissues such as cortical bone show little or no signal with clinical sequences. Ultrashort echo time magnetization transfer (UTE-MT) imaging is likely to help with this difficulty. In this study we aimed to develop and utilize UTE-MT imaging and compare two-pool with three-pool modeling of bovine cortical bone samples using a clinical 3T scanner.

1505

Estimation of the bound proton pool involved in MT using spin and stimulated echoes
Lukas Pirpamer¹ and Stefan Ropele¹

¹Neurology, Medical University of Graz, Graz, Austria

We here present a proof of concept for a new quantitative MT mapping sequence using spin and stimulated echoes. The approach is based on the fact, that the labeled magnetization of the STEAM signal follows an double-exponential decay due to MT. With the help of a T1 map, a single acquisition with just one mixing time and an integrated spin echo allows to map the fraction of the bound proton pool.

1506

3D Clinical APTw MRI with Improved Contrast Homogeneity
Jochen Keupp¹, Jinyuan Zhou², and Osamu Togao³

¹Philips Research, Hamburg, Germany, ²Department of Radiology, Johns Hopkins University, Baltimore, MD, United States, ³Clinical Radiology, Kyushu University Hospital, Fukuoka, Japan

APTw MRI is an emerging technique for sensitive tissue characterization, in particular in oncology (e.g. tumor grading). Fast-spin-echo(FSE)-Dixon acquisition techniques allow efficient and simultaneous acquisition of APT weighted (APTw) and ΔB_0 information. An improved FSE-Dixon APTw acquisition protocol with intrinsic ΔB_0 correction was implemented on a clinical MRI scanner, using multiple averages with saturation at the amide chemical shift ($\Delta\omega=+3.5$ ppm). Contrast homogeneity was evaluated in a volunteer study and is presented together with initial clinical results on brain tumor patients.

1507

In vivo application of lactate chemical exchange saturation transfer imaging: human exercise study
Catherine DeBrosse¹, Ravi Nanga¹, Puneet Bagga¹, Mohammad Haris², Hari Hariharan¹, and Ravinder Reddy¹

¹Center for Magnetic Resonance and Optical Imaging, University of Pennsylvania, Philadelphia, PA, United States, ²Research Branch, Sidra Medical and Research Center, Doha, Qatar

Metabolic regulation is disrupted in many diseases. As a result, the levels of lactate present in the body are often affected and implicated in disease progression and clinical outcome. To better understand lactate metabolism, an imaging technique with high sensitivity and spatial resolution is required. In this study, a chemical exchange saturation transfer (CEST) magnetic resonance imaging method, based on the exchange between lactate hydroxyl proton and bulk water protons was used to image lactate. As proof-of-principle, LATEST was implemented *in vivo* in exercising human skeletal muscle to image the increased lactate that results from intense

exercise.

1508

Amide Proton Transfer (APT) imaging of brain tumors at 7T: the role of tissue water T1-relaxation properties
Vitaliy Khlebnikov¹, Daniel Polders², Jeroen Hendrikse¹, Pierre A Robe¹, Eduard H Voormolen¹, Peter R Luijten¹, Dennis WJ Klomp¹, and Hans Hoogduin¹

¹*Radiology, University Medical Center Utrecht, Utrecht, Netherlands, ²Philips Healthcare, Best, Netherlands*

The purpose of this study was to provide insight into the effect of water-T1-relaxation (T1w) on Amide Proton Transfer (APT) contrast in tumors. To this end, three different metrics of APT contrast, (mainly novel magnetization transfer ratio (MTRRex), relaxation-compensated MTRRex (AREX) and traditional asymmetry (MTRAsym)) were compared in normal and tumor tissues in a variety of intracranial tumors at 7T. The strong correlation of MTRRex and MTRAsym with T1w and the absence thereof in AREX suggests that much of APT contrast in tumors at 7T originates from the inherent tissue water-T1-relaxation properties.

1509

Monitoring therapeutic response on medullary thyroid carcinoma in chemotherapy by amide proton transfer (APT) imaging in an orthotopic mouse model
Keisuke Ishimatsu¹, Karine Pozo², Shanrong Zhang¹, Koji Sagiyama¹, Osamu Togao¹, James Bibb³, and Masaya Takahashi¹

¹*Advanced Imaging Research Center, University of Texas Southwestern Medical Center, Dallas, TX, United States, ²Department of Psychiatry, University of Texas Southwestern Medical Center, Dallas, TX, United States, ³Department of Psychiatry / Harold C. Simmons Comprehensive Cancer Center / Department of Neurology and Neurotherapeutics, University of Texas Southwestern Medical Center, Dallas, TX, United States*

The objective is to investigate whether amide proton transfer (APT) imaging is useful for evaluation of anticancer treatment responses in chemotherapy. We compared the temporal changes of APT signal with the different treatment strategies using two new drugs, administered individually or in combination, in a mouse model of medullary thyroid carcinoma.

1510

A Study on CrCEST Mapping in Human Brain at 7T MRI
Anup Singh^{1,2}, Mohammad Haris³, Kejia Cai⁴, Hari Hariharan⁵, and Ravinder Reddy⁵

¹*Centre for Biomedical Engineering, Indian Institute of Technology Delhi, New Delhi, India, ²Biomedical Engineering, AIIMS Delhi, New Delhi, India, ³Research Branch, Sidra Medical and Research Center, Doha, Qatar, ⁴Department of Radiology, University of Illinois at Chicago, Chicago, IL, United States, ⁵Department of Radiology, University of Pennsylvania, Philadelphia, PA, United States*

Creatine(Cr) is a significant brain metabolite and its alterations has been reported in various disease conditions. In this study, chemical-exchange-saturation-transfer (CEST) MRI of Creatine(CrCEST) was performed in human brain at 7T MRI scanner. Numerical simulations were also carried out for evaluating contributions from other brain metabolites to CrCEST and a method to reduce this contamination was proposed based upon simulated data observations. Using, conventional CESTasy method, CrCEST has ~50% contribution from Cr. Using proposed subtraction based approach it is feasible to reduce contaminations from other metabolites/molecules and hence making CrCEST more specific to Cr.

1511

Quantitative analysis of the evolution of Multiple Sclerosis (MS) lesion MT and NOE pool concentrations using CEST analysis via MR fingerprinting
Nicolas Geades¹, Amal Samaraweera², William Morley¹, Matthew Cronin³, Nikos Evangelou², Penny Gowland¹, and Olivier Mouglin¹

¹*Sir Peter Mansfield Imaging Centre, University of Nottingham, Nottingham, United Kingdom, ²Division of Clinical Neuroscience, Queen's Medical Centre, University of Nottingham, Nottingham, United Kingdom, ³Brain Imaging and Analysis Centre, Duke University, Durham, NC, United States*

This study presents a method of acquiring quantitative MT and NOE concentration percentages of MS lesions over a period of 30 weeks. MT and NOE mean percentages were compared for WM lesion ROIs and NAWM ROIs, showing a clear drop of both MT and NOE when a lesion appears, followed by a gradual increase in concentrations in the following weeks, indicating remyelination. The fitting results are backed by a parallel repeatability study which shows the repeatability of the method and its noise levels. The results indicate that NOE fitting is very robust against variations in B1 compared to fitting MT.

Traditional Poster

CEST: Agents & Methods

Exhibition Hall

Monday, May 9, 2016: 16:30 - 18:30

1512

Early cancer signs detected by glucoCEST
Francisco Torrealdea¹, Marilena Rega¹, Sebastian Brandner¹, David Thomas¹, and Xavier Golay¹

¹*Brain Repair & Rehabilitation, UCL Institute of Neurology, London, United Kingdom*

In this work, the feasibility of using glucoCEST as a tool for early detection of primary brain tumours is explored. Mice bearing xenograft glioblastoma tumours were scanned longitudinally using a glucoCEST protocol. The results suggest the intriguing possibility that

glucoCEST contrast may be able to detect the presence of cancer at very early stage.

1513

Injectable alginate hydrogel for supporting neural stem cells and imaging of survival using chemical exchange saturation transfer (CEST)
Antje Arnold^{1,2}, Yuguo Li^{1,3}, Guanshu Liu^{1,3}, Peter C.M. van Zijl^{1,3}, Jeff W.M. Bulte^{1,2}, Piotr Walczak^{1,2}, and Kannie WY Chan^{1,3}

¹*Radiology, Johns Hopkins University School of Medicine, Baltimore, MD, United States*, ²*Cellular Imaging Section and Vascular Biology Program, Institute for Cell Engineering, Baltimore, MD, United States*, ³*FM Kirby Research Center, Kennedy Krieger Institute, Baltimore, MD, United States*

Cell therapy is showing promise in treating neurological disorders, but cell survival after transplantation is usually low, which is a major limiting factor for achieving therapeutic efficacy. One of the major hurdles in translating cell therapies to patients is the lack of non-invasive approaches to monitor the cells and their microenvironment after transplantation. We developed an injectable alginate hydrogel that supports cell survival and allows monitoring of cell status using liposomes as the nanosensors after transplantation into the brain. Hydrogel embedded cells survived better as compared to the cells without the hydrogel, and cells transplanted using the nanosensor-labeled hydrogel could be imaged using CEST-MRI.

1514

Chemical exchange-sensitive spin-lock MRI of glucose and deoxyglucose in brain tumors
Tao Jin¹, Bistra Iordanova¹, Ping Wang¹, and Seong-Gi Kim^{2,3}

¹*University of Pittsburgh, Pittsburgh, PA, United States*, ²*Center for Neuroscience Imaging Research, Institute for Basic Science, Suwon, Korea, Republic of*, ³*Department of Biomedical Engineering, Sungkyunkwan University, Suwon, Korea, Republic of*

Glucose uptake and metabolism are important biomarkers for tumor diagnosis and prognosis. Recent studies showed that the glucose uptake and metabolism can be measured by a chemical exchange sensitive spin-lock (CESL) MRI approach with administration of non-labelled glucose or analogs (glucoCESL), providing unique advantage over the widely used position emission tomography technique. In this preliminary study, we evaluated the efficacy of glucoCESL for the study of brain tumor. The sensitivity and spatiotemporal characteristics of CESL signal with administration of D-Glucose, 2-deoxy-D-glucose and L-glucose were compared.

1515

On Resonance VDMP Technique for Improved glucoCEST Detection in Brain Tumors
Xiang Xu^{1,2}, Kannie WY Chan^{1,2}, Huanling Liu^{1,3}, Yuguo Li^{1,2}, Guanshu Liu^{1,2}, Peter C.M. van Zijl^{1,2}, and Jiadi Xu^{1,2}

¹*Department of Radiology and Radiological Science, Johns Hopkins University, Baltimore, MD, United States*, ²*F.M. Kirby Research Center, Kennedy Krieger Institute, Baltimore, MD, United States*, ³*Department of Ultrasound, Guangzhou Panyu Central Hospital, Guangzhou, China, People's Republic of*

An on-resonance variable delay multi-pulse (onVDMP) CEST technique was developed for the detection of fast-exchanging protons. The new method was applied to the detection of glucoCEST signal changes upon venous glucose injection in a mouse tumor model and compared with conventional cw-CEST method. Both methods highlight the tumor and the blood vessels upon glucose injection in mice brain implanted with brain tumors. However compared with cw-CEST, the onVDMP technique increased the tumor contrast to noise ratio by about 50% due to its sensitivity to total fast exchanging protons.

1516

Model-based Extraction of z-spectrum Asymmetry using SYmmetric basis (EASY)
Hoonjae Lee^{1,2} and Jaeseok Park³

¹*Center for Neuroscience Imaging Research (CNIR), Institute for Basic Science (IBS), Suwon, Korea, Republic of*, ²*Department of Brain and Cognitive Engineering, Korea University, Seoul, Korea, Republic of*, ³*Department of Biomedical Engineering, Sungkyunkwan University, Suwon, Korea, Republic of*

CEST MRI is an indirect molecular imaging technique, in which a small molecular signal is amplified by chemical exchange phenomenon. Multiple acquisition of imaging data with varying saturation frequencies, called z-spectrum acquisition, is typically performed, and then subtraction-based MTR asymmetry analysis is employed to investigate the effect of CEST on MRI. However, since the z-spectrum is additionally convoluted by inherent asymmetric MT, NOE, etc, conventional asymmetry analysis is prone to substantial errors. To tackle these problems, in this work we introduce a new, model-based extraction method of the z-spectrum asymmetry using symmetric basis (EASY) to directly characterize the signal sources of the asymmetric z-spectrum.

1517

Rapid 3D spiral CEST
Bing Wu¹, Rui Li², Chien-yuan Lin³, Lin Ma², and Zhenyu Zhou¹

¹*GE healthcare MR Research China, Beijing, China, People's Republic of*, ²*PLA 301 Hospital, Beijing, China, People's Republic of*, ³*GE healthcare MR Research China, Taipei, Taiwan*

There is a growing need for larger spatial coverage and better resolution for CEST (Chemical exchange saturation transfer). In this work, CEST acquisition based on 3D spiral was implemented and tested. Whole brain coverage could be achieved at 8s per spectral point that allows practical application. APT study showed consistent results as previous studies.

1518

Enhanced sensitivity of renal pH measurement with MR-CEST ratiometric imaging of iopamidol in a normal rodent model at 4.7 T
Yin Wu^{1,2}, Iris Yuwen Zhou¹, Takahiro Igarashi¹, Yingkun Guo¹, Lin Li¹, and Phillip Zhe Sun¹

Renal pH was recently quantified with MR-CEST ratiometric imaging of iopamidol at 7 T. However, the two exchangeable proton groups of iopamidol would substantially overlap at lower magnetic field, leading to inaccurate pH quantification. Here, we investigated a Lorentzian-based decoupling algorithm to resolve the two saturation transfer effects for improved ratiometric pH measurement in rodents at 4.7 T. Results exhibits substantially enhanced range and sensitivity of pH measurements. The obtained renal pH maps are consistent with the published results. Therefore, the proposed method provides a novel way for reliable renal pH mapping, which benefits pH quantification at clinical field strengths.

1519

Insight into the Quantitative Metrics of Chemical Exchange Saturation Transfer (CEST) Imaging
Hye-Young Heo^{1,2}, Dong-Hoon Lee¹, Yi Zhang¹, Xuna Zhao¹, Shanshan Jiang¹, and Jinyuan Zhou^{1,2}

¹The Russell H. Morgan Department of Radiology and Radiological Science, Johns Hopkins University School of Medicine, Baltimore, MD, United States, ²F.M. Kirby Research Center for Functional Brain Imaging, Kennedy Krieger Institute, Baltimore, MD, United States

Amide proton transfer (APT) imaging is a novel chemical exchange saturation transfer (CEST)-based MRI modality that can detect various endogenous mobile proteins and peptides in tissue, such as those in the cytoplasm. The APT quantification results depend on the CEST metrics, which is undesirable. In this study, four CEST metrics: (i) CEST ratio (CESTR), (ii) CESTR normalized with the reference value (CESTR^{ref}), (iii) inverse Z-spectrum-based (MTR_{Re}), and (iv) apparent exchange-related relaxation (AREX), were compared using five-pool Bloch equation-based simulations with varied RF saturation powers and magnetic field strength, and in an *in vivo* rat tumor study at 4.7 T.

1520

Fast Whole-Brain Spiral-CEST Encoding with Spectral and Spatial B0 Correction
Sugil Kim^{1,2} and Jaeseok Park³

¹Center for Neuroscience Imaging Research (CNIR), Institute for Basic Science (IBS), Suwon, Korea, Republic of, ²Department of Brain and Cognitive Engineering, Korea University, Seoul, Korea, Republic of, ³Department of Biomedical Engineering, Sungkyunkwan University, Suwon, Korea, Republic of

To develop fast whole-brain spiral-CEST encoding with spectral and spatial correction of magnetic field inhomogeneities

1521

Influence of tissue integrity and external field strength on the exchange-relayed NOE-CEST effect of mobile proteins
Johannes Windschuh¹, Moritz Zaiss¹, Jan-Eric Meissner¹, Steffen Goerke¹, and Peter Bachert¹

¹Division of Medical Physics in Radiology, German Cancer Research Center (DKFZ), Heidelberg, Germany

We investigated the dependencies of the exchange-relayed Nuclear Overhauser Effect (rNOE) observable in Chemical Exchange Saturation Transfer (CEST) experiments on tissue integrity and static magnetic field strength B_0 . By comparison of a homogenized and native sample of white matter tissue of animal brain we could show that the CEST signal of the aliphatic rNOE is independent of tissue structure. The observed increase of all CEST effects on decrease of B_0 probably results from relatively broader saturation bandwidth at lower field strengths. No indication for a rNOE dependency on B_0 differing from that of chemical exchange effects could be found.

1522

Fast Chemical Exchange Saturation Transfer (CEST) Imaging with Variably-accelerated Sensitivity Encoding (vSENSE)
Yi Zhang¹, Hye-Young Heo¹, Dong-Hoon Lee¹, Paul Bottomley¹, and Jinyuan Zhou^{1,2}

¹Division of MR Research, Department of Radiology, Johns Hopkins University, Baltimore, MD, United States, ²F. M. Kirby Research Center for Functional Brain Imaging, Kennedy Krieger Institute, Baltimore, MD, United States

CEST imaging has numerous applications, but its widespread clinical use is hampered by relatively long acquisition times. Here, a novel variably-accelerated sensitivity encoding (vSENSE) method is proposed that provides faster CEST acquisitions than conventional SENSE. The vSENSE approach undersamples k-space variably for images acquired at different saturation frequencies to maximize acquisition speed. vSENSE was validated in a phantom and in 8 patients with brain tumors studied at 3T. The vSENSE method provided a 4-fold acceleration, compared to conventional SENSE which permitted only a 2-fold acceleration, with both compared to a full k-space reconstruction.

1523

Selective Amide- and NOE-CEST- MRI in Prostate at 7T using a Multi-transmit system

Catalina S. Arteaga de Castro¹, Hans J.M. Hoogduin¹, Vitaliy Khlebnikov¹, Peter R. Luijten¹, Dennis W.J. Klomp¹, and Moritz Zaiss²

¹Imaging Division, University Medical Center Utrecht, Utrecht, Netherlands, ²Medical Physics in Radiology, German Cancer Research Center, Heidelberg, Germany

The feasibility of selective NOE- and amide-CEST detection in the prostate at 7T was investigated with a multi-transmit system. Both effects can be acquired simultaneously due to the increased sensitivity and spectral resolution available at 7T. Fitted NOE- and amide-CEST were reproducible within experiments. NOE-CEST was found to be more pronounced than amide-CEST in small and whole prostate ROIs and the peripheral zone showed the lowest amide- and NOE-CEST effects.





Highly-accelerated CEST Measurements in Three Dimensions with Linear Algebraic Modeling

Yi Zhang¹, Hye-Young Heo¹, Dong-Hoon Lee¹, Shanshan Jiang¹, Xuna Zhao¹, Paul Bottomley¹, and Jinyuan Zhou^{1,2}¹Division of MR Research, Department of Radiology, Johns Hopkins University, Baltimore, MD, United States, ²F. M. Kirby Research Center for Functional Brain Imaging, Kennedy Krieger Institute, Baltimore, MD, United States

CEST MRI can provide valuable molecular level information *in vivo*, but its translation to routine clinics is hindered by long imaging times. Regional average CEST measurements often suffice for quantitative evaluation, diagnosis, and treatment assessment, while allowing much shorter scan times. Recently, the spectroscopy with linear algebraic modeling (SLAM) method was adapted for CEST MRI in two dimensions (2D), directly obtaining compartmental-average measurements manifold faster than conventional CEST. Here, the SLAM CEST method is extended from 2D to 3D, and applied to patients with brain tumors with acceleration factors of up to 98-fold.

Model-based direct Extraction of z-spectrum Asymmetry from undersampled k-space using SYmmetric Basis (k-EASY)

Hoonjae Lee^{1,2} and Jaeseok Park³¹Center for Neuroscience Imaging Research (CNIR), Institute for Basic Science (IBS), Suwon, Korea, Republic of, ²Department of Brain and Cognitive Engineering, Korea University, Seoul, Korea, Republic of, ³Department of Biomedical Engineering, Sungkyunkwan University, Suwon, Korea, Republic of

In chemical exchange saturation transfer (CEST) MRI, multiple acquisition of imaging data with varying saturation frequencies is typically performed, which prohibitively prolongs imaging time. Furthermore, conventional, subtraction-based MTR asymmetry analysis is prone to substantial errors, because the z-spectrum is convoluted by CEST as well as inherent asymmetric MT, nuclear Overhauser enhancement (NOE), etc. To tackle these problems, in this work we propose a new, model-based direct Extraction of the z-spectrum Asymmetry from undersampled k-space using SYmmetric basis (k-EASY) that incorporates main field inhomogeneity correction and z-spectrum asymmetry analysis into a framework of compressed sensing.

A CEST signal quantification method for non-steady state

Yi Wang¹, Bing Wu², Yang Fan², and Jia-Hong Gao¹¹School of Physics, Peking University, Beijing, China, People's Republic of, ²MR Research group, GE Healthcare China, Beijing, China, People's Republic of

For quantitative analysis of CEST signal, it is crucial to decrease or eliminate the influence of parameters unrelated to chemical exchange thus emphasizing chemical exchange weight. Recently inverse Z-spectrum method realized analytical calibration but only in situation of steady state. We propose a novel analytical calibration method suitable to non-steady state situation, calculating new indexes which reflect chemical exchange weight better than those commonly used, and verifying its performance in phantom and *in vivo* experiment. This calibration method will be greatly helpful in quantitative CEST data analysis.

Traditional Poster

Contrast Mechanisms: Relaxation Based

Exhibition Hall

Monday, May 9, 2016: 16:30 - 18:30

T2 of cerebrospinal fluid depends on glucose concentration

Alexia Daoust¹, Stephen Dodd¹, Govind Nair¹, Steven Jacobson¹, Daniel Reich¹, and Alan Koretsky¹¹NINDS, NIH, Bethesda, MD, United States

There continues to be interest in using changes in CSF properties to image neurodegenerative diseases. To optimize MRI sequences that enable segmentation of CSF from tissue, we characterized the CSF relaxometric properties at various field strengths *in vivo* and *in vitro*. Our *in vitro* results suggest that *in vivo* T₂ value at high field is incorrect due to residual gradients and that low field is more optimal to quantify CSF relaxivity *in vivo*. We have shown an important difference of *in vitro* CSF T₂ vs saline T₂ that is mostly explained by the relaxivity of glucose.

Temperature dependence of R1, R2* and magnetic susceptibility of ferritin at 7T

Mobeen Ali¹, Penny Gowland¹, and Richard Bowtell¹¹SPMIC, School of Physics and Astronomy, University of Nottingham, Nottingham, United Kingdom

Comparison of post mortem and *in vivo* MR images requires an understanding of the temperature dependence of the NMR parameters that generate relevant image contrast. Here, we therefore evaluated the temperature dependence of the susceptibility and relaxivity of ferritin-doped agar. A phantom containing cylinders doped with different ferritin concentrations was scanned at 7T at temperatures ranging from 5–35°C. R1, R2* and field maps were generated and the variation of each parameter with ferritin concentration was evaluated. The variations of susceptibility, R2* and R1 with ferritin concentration all decreased with increasing temperature with R2* showing the strongest temperature dependence.

1529

Transverse Relaxometry with B1+ Constrained Stimulated Echo Correction
Reza Basiri¹, Marc Lebel², and Paolo Federico³

¹Biomedical Engineering, University of Calgary, Calgary, AB, Canada, ²Alberta Children's Hospital Research Institute, Calgary, AB, Canada, ³Foothills Hospital, Calgary, AB, Canada

Quantitative T_2 mapping provides diagnostic capabilities complementing standard qualitative imaging. However, conventional fitting algorithms to estimate T_2 are prone to bias. In this work, we propose a fitting method that remains applicable to existing datasets while addressing many of the imperfections and shortcomings of current methods. Our proposed method is an extension of stimulated echo correction that highly constrains the estimated transmit field. It was evaluated using simulated and experimental data. We found that variance in the T_2 estimate could be reduced by ~25% in certainly realistic conditions while maintaining full accuracy relative to the current stimulated echo corrected fit. Transverse relaxometry, a quantitative T_2 mapping has shown superior diagnostic capabilities compare with qualitative maps for neurological diseases. However, the conventional fitting Quantitative T_2 mapping provides diagnostic capabilities complementing standard qualitative imaging. However, conventional fitting algorithms to estimate T_2 are prone to bias. In this work, we propose a fitting method that remains applicable to existing datasets while addressing many of the imperfections and shortcomings of current methods. Our proposed method is an extension of stimulated echo correction that highly constrains the estimated transmit field. It was evaluated using simulated and experimental data. We found that variance in the T_2 estimate could be reduced by ~25% in certainly realistic conditions while maintaining full accuracy relative to the current stimulated echo corrected fit.

1530

Simultaneous Multi-Angular Relaxometry of Tissue with Magnetic Resonance Imaging (SMART MRI)
Alexander L Sukstanskii¹, Jie Wen¹, Anne H Cross², and Dmitriy A Yablonskiy¹

¹Mallinckrodt Institute of Radiology, Washington University, Saint Louis, MO, United States, ²Neurology, Washington University, Saint Louis, MO, United States

The cross-relaxation effects between "free" and "bound" water affect the gradient recalled echo (GRE) MRI signal and can bias quantitative measurements of tissue relaxation parameters. Herein we have generalized the classical Ernst equation for the GRE signal dependence on sequence parameters (echo and repetition times, flip angle) by accounting for cross-relaxation effects. The derived equation creates a basis for a new technique - Simultaneous Multi-Angular Relaxometry of Tissue with Magnetic Resonance Imaging (SMART MRI). The technique allows simultaneous quantitative measurements of longitudinal and transverse relaxation rates constants and some essential cross-relaxation parameters without utilizing off-resonance magnetization transfer pulses.

1531

Estimation of the Macro-Molecular Proton R_1 in Human Brain at 3 and 7 T
Peter van Gelderen¹ and Jeff H Duyn¹

¹Advanced MRI, LFMI NINDS, National Institutes of Health, Bethesda, MD, United States

The longitudinal relaxation rate (R_1) of MRI-invisible macro-molecular protons is an important parameter in the generation of MT and T_1 contrast. Despite this, considerable uncertainty exists about its actual value. To address this MT and inversion recovery experiments were jointly analyzed with a 2-pool model of exchange, and estimates were derived for human brain at 3T and 7T.

1532

Temporal Changes in Calculated Values of Longitudinal and Transverse Magnetisation Time Constant Values, T_1 and T_2^* , for Fetal and Adult Simulated Subdural Haematoma
Peter Wright¹, Hannah Webley², Andrew Fry¹, and Elspeth Whitby²

¹MIMP, Sheffield Teaching Hospitals NHS Foundation Trust, Sheffield, United Kingdom, ²Academic Unit of Reproductive and Developmental medicine, University of Sheffield, Sheffield, United Kingdom

Subdural haematoma (SDH) resulting from traumatic brain injury relating to non accidental head injury is unfortunately relatively common in the UK at 36 per 100000 incidence in children < 6 months old. However, adult models are used when aging SDH. This study aimed to compare calculated relaxation time constants, T_2^* and T_1 of fetal and adult blood samples in a simulated SDH for data acquired daily over 28 days. Significant differences between fetal and adult were found in T_2^* and T_1 values for week 1 and weeks 1, 3 and 4 respectively.

1533

3T longitudinal relaxation of human blood with hemoglobin S
Meher Juttukonda¹, Manus Donahue¹, Melissa Gindville², and Lori Jordan²

¹Radiology and Radiological Sciences, Vanderbilt University Medical Center, Nashville, TN, United States, ²Pediatrics, Division of Pediatric Neurology, Vanderbilt University Medical Center, Nashville, TN, United States

Quantitative CBF maps derived from pseudo-continuous ASL (pCASL) may be useful in assessing stroke risk in sickle cell anemia (SCA) patients, but T_1 relaxation of SCA blood must first be characterized. Venous blood samples were collected from SCA patients as well as normal subjects, and an inversion recovery approach was used to quantify the T_1 relaxation times *ex vivo*. For similar hematocrit, oxygenation, and temperature, T_1 relaxation times of SCA blood appear similar to those of normal blood. Therefore, computation of CBF in SCA patients may not be affected by the assumption of normal blood T_1 relaxation.

1534

Fast reconstruction of T2 maps with indirect echo compensation using highly undersampled radial Fast Spin Echo data
Mahesh Bharath Keerthivasan¹, Lindsie Jeffries², Diego Blew³, Jean-Philippe Galons³, Puneet Sharma³, Ali Bilgin^{1,2,3}, Diego R Martin³, and Maria I Altbach³

¹*Electrical and Computer Engineering, University of Arizona, Tucson, AZ, United States*, ²*Biomedical Engineering, University of Arizona, Tucson, AZ, United States*, ³*Medical Imaging, University of Arizona, Tucson, AZ, United States*

There has been increased interest in the quantitative characterization of tissue based on T2. Techniques based on spin-echo (SE) or fast spin-echo (FSE) sequences are time consuming because they require multiple acquisitions for obtaining an adequate number of TE images for accurate T2 mapping. Radial FSE based methods have been introduced for efficient T2 mapping by using TE data from a single k-space data set. In this work, we explore combining the Echo Sharing algorithm for the fast reconstruction of the TE images with SEPG model fitting to compensate for indirect echoes.

1535

Fast Field-Cycling NMR Relaxometry Extended in the Ultra-Low Field Region: Calibration Method and Acquisition of T1-Dispersion Curves that reach 2.3 μ T
Vasileios Zampetoulas¹, Lionel M. Broche¹, and David J. Lurie¹

¹*Aberdeen Biomedical Imaging Centre, School of Medicine & Dentistry, University of Aberdeen, Foresterhill, AB25 2ZD, Aberdeen, United Kingdom, Aberdeen, United Kingdom*

A graph of T_1 versus magnetic field obtained via Fast Field-Cycling (FFC) NMR relaxometry techniques can be developed into a new diagnostic tool thanks to the information about molecular dynamics that it provides. In this work, a novel method that compensates for the environmental fields acting on an FFC relaxometer is analysed, and applied to acquire measurements in the μ T region for the study of much slower molecular motions, that was not previously possible. The results acquired from human cartilage indicate motions occurring in a slow time scale (0.1 to 10 ms), which show promise for clinical studies.

1536

Fast and Accurate T2 Mapping from Multi Spin Echo Data Using Bloch-Simulation-Based Reconstruction: Investigation of intra-subject and inter-scan stability and reproducibility
Veronica Cosi¹, Akio Ernesto Yoshimoto², Timothy Shepherd^{2,3}, KAI Tobias Block^{2,3}, Daniel K Sodickson^{2,3}, and Noam Ben-Eliezer^{2,3}

¹*Department of Specialised, Experimental, and Diagnostic Medicine, University of Bologna, Bologna, Italy*, ²*Bernard and Irene Schwartz Center for Biomedical Imaging, Department of Radiology, New York University School of Medicine, New York, NY, United States*, ³*Center for Advanced Imaging Innovation and Research (CAI2R), New York University School of Medicine, New York, NY, United States*

Accurate quantification of T_2 values *in vivo* poses a long-standing challenge, hampered by the inherent bias of fast multi-SE protocols by stimulated and indirect echoes, non-rectangular slice profile and transmit-field inhomogeneities. This bias, moreover, is dependent on the sequence implementation and parameter-set employed, and thus varies between scanners and vendors. We present full stability and reproducibility tests of a recently developed T_2 mapping technique – the echo-modulation curve (EMC) algorithm – which uses precise Bloch simulations of the pulse-sequence scheme to deliver the true T_2 value of the tissue in a manner that is independent of the parameter-set and scanner being used.

1537

Highly Accelerated T2 Mapping with a Simple Dictionary
Li Zhao¹, Yang Yang², Chuan Huang³, and Craig Meyer²

¹*Radiology, Beth Israel Deaconess Medical Center, Boston, MA, United States*, ²*Biomedical Engineering, University of Virginia, Charlottesville, VA, United States*, ³*Departments of Radiology, Psychiatry, Stony Brook Medicine, Stony Brook, NY, United States*

Parameter mapping can be acquired rapidly by MR fingerprinting. It requires a pseudo random pulse sequence to build an unique dictionary between the evolution of signal and parameters. The problem can be simplified when the dimension of the dictionary is relatively low. Here, we propose a dictionary that accelerates T2 mapping with dictionary and conventional sequence.

1538

Repeatability and sample size estimations for myelin water imaging
Thibo Billiet¹, Stefan Sunaert¹, Bea Van den Bergh¹, Ronald Peeters¹, Mathieu Vandenbulcke¹, and Louise Emsell¹

¹*KU Leuven, Leuven, Belgium*

Currently, only single slice repeatability results for myelin water imaging (MWI) metrics are available. We assessed the within- and between-subject variation of the myelin water fraction (MWF); intra- and extracellular water fraction (IEWF), and intra- and extracellular water geometric mean T2 time (IEW-gmT2) in a whole cerebrum MWI sequence¹. We demonstrated good within- and between subject variability, comparable to previous single-slice results. Future studies may benefit from sample size estimations documented in this work.

1539

Mapping Higher Order Components of the GRE Signal Decay at 7T with Short TE Data through Adaptive Smoothing
Martina F Callaghan¹, Kerrin J Pine¹, Karsten Tabelow², Joerg Polzehl², Nikolaus Weiskopf^{1,3}, and Siawoosh Mohammadi^{1,4}

¹*Wellcome Trust Centre for Neuroimaging, UCL Institute of Neurology, London, United Kingdom*, ²*Weierstrass Institute, Berlin, Germany*, ³*Department of Neurophysics, Max Planck Institute for Human Cognitive and Brain Sciences, Leipzig, Germany*, ⁴*Department of Systems Neuroscience, University Medical Center Hamburg-Eppendorf, Hamburg, Germany*

In vivo histology aims to extract biologically relevant metrics from MRI data. In neuroimaging this includes characterising white matter fibres in terms of orientation, distribution and g-ratio, or determining the cortical myelo- and cyto-architecture. It has been shown, both theoretically and experimentally, that the signal decay in gradient recalled echoes (GRE) exhibits higher order temporal behaviour that is dependent on a variety of intra-voxel microstructural metrics. Here we use adaptive smoothing to generate maps of both the first and second order components of the temporal decay of the GRE signal from short TE data using a time-efficient multi-parameter mapping protocol.

1540

T2* quantitation with chemical shift and multi-echo spiral imaging
Atsushi M Takahashi¹

¹McGovern Institute for Brain Research, Massachusetts Institute of Technology, Cambridge, MA, United States

Quantitation of T_2^* with spiral imaging sequences can be made in two distinct ways: Collecting data at various echo-times results in a measurement of the chemical shift after Fourier transformation along the echo-time dimension. Off resonance is intrinsically corrected by this processing. Alternately, multiple-echo spiral imaging can be used to quantitatively measure T_2^* as long as dephasing from B_0 distortion is small over the duration of the spiral readout. Multiple spiral interleaves are used to reduce the readout time of the spiral. Both methods are demonstrated.

1541

SAFT: Split-Algorithm for Fast T2 Mapping
Tom Hilbert^{1,2,3}, Jean-Philippe Thiran^{2,3}, Reto Meuli², Gunnar Krueger^{2,3,4}, and Tobias Kober^{1,2,3}

¹Advanced Clinical Imaging Technology (HC CMEA SUI DI BM PI), Siemens Healthcare AG, Lausanne, Switzerland, ²Department of Radiology, University Hospital (CHUV), Lausanne, Switzerland, ³LTS5, École Polytechnique Fédérale de Lausanne, Lausanne, Switzerland, ⁴Siemens Medical Solutions USA, Inc., Boston, MA, United States

Numerous iterative reconstruction techniques have been published in the past, facilitating the calculation of quantitative parameter maps based on undersampled k-space data. Model-based approaches, for example, iteratively minimize a cost function that comprises a formulation of the signal behavior. Minimizing this non-linear problem yields the quantitative parameter maps, but is numerically challenging and thus accompanied with reduced robustness and long reconstruction times compared to a direct Fourier transform. Here we suggest a method to split the optimization problem of a model-based T2 mapping into sub-problems which are solved alternately. The splitting results in a more robust reconstruction with less computational cost.

1542

Noise Propagation of Variable Flip Angle T1 mapping with Emphasis on the Precision of RF Transmit Field Mapping
Yoojin Lee^{1,2}, Martina F. Callaghan³, and Zoltan Nagy¹

¹Laboratory for Social and Neural Systems Research, University of Zürich, Zürich, Switzerland, ²Institute for Biomedical Engineering, ETH Zürich, Zürich, Switzerland, ³Wellcome Trust Centre for Neuroimaging, UCL Institute of Neurology, London, United Kingdom

Rational approximation of the SPGR signal provides a simple algebraic expression of T_1 within the VFA framework. For this method, we derive an analytical solution of how the precision in T_1 maps depends on the noise in the B_1^+ map as well as the component SPGR images. We show that the derived equation provides a good prediction of the noise in T_1 measured in-vivo. Further, we show that B_1^+ maps can introduce as much noise into the T_1 maps as the SPGR images for equal input variance.

Traditional Poster

Magnetic Susceptibility

Exhibition Hall

Monday, May 9, 2016: 16:30 - 18:30

1543

The Role of Finite Difference Schemes in Morphology Enabled Dipole Inversion (MEDI) for Quantitative Susceptibility Mapping (QSM)
Youngwook Kee¹, Kofi Mawuli Deh¹, Pascal Spincemaille¹, and Yi Wang¹

¹Weill Cornell Medical College, New York, NY, United States

Since QSM has been recently undergoing clinical trials and the MEDI toolbox plays an important role for this purpose, numerical implementation should be consistent in the sense of continuum limit. In this abstract, we point out a numerically inconsistent finite difference scheme that has been used in the MEDI toolbox and show that by replacing it with a consistent one it drastically improves image quality.

1544

QUASAR: In vivo quantification of magnetic susceptibility in rodents
Ferdinand Schweser^{1,2}, Paul Polak¹, Nicola Bertolino¹, and Robert Zivadinov^{1,2}

¹Buffalo Neuroimaging Analysis Center, Department of Neurology, Jacobs School of Medicine and Biomedical Sciences, The State University of New York at Buffalo, Buffalo, NY, United States, ²MRI Molecular and Translational Research Center, Jacobs School of Medicine and Biomedical Sciences, The State University of New York at Buffalo, Buffalo, NY, United States



Despite increasing exploration of quantitative susceptibility mapping (QSM) in humans and the method's potential to study tissue iron pre-clinically, only few studies have yet applied QSM in alive rodents at ultra-high magnetic field strength. In the present work we hypothesized that the low quality of pre-clinical QSM compared to human QSM is due to the combination of a similar level of non-susceptibility phase contributions with much lower susceptibility variations. Here, we propose a new type of QSM algorithm that accounts for non-susceptibility phase effects and, hence, enables pre-clinical QSM: QUAntitative Susceptibility And Residual mapping (QUASAR).

1545

Effects of fiber orientation and myelin concentration on $R2^*$ ($=1/T2^*$): a fiber orientation and/or myelin concentration corrected $R2^*$ map
Jingu Lee¹, Woojin Jung¹, Yoonho Nam², and Jongho Lee¹

¹*Laboratory for Imaging Science and Technology, Department of Electrical and Computer Engineering, Seoul National University, Seoul, Korea, Republic of*, ²*Department of Radiology, Seoul St. Mary's Hospital, College of Medicine, The Catholic University of Korea, Seoul, Korea, Republic of*

In this work, we measured the effect size of both myelin concentration and fiber orientation in $R2^*$. Additionally, we generated the myelin concentration and/or fiber orientation bias free $R2^*$ maps which may have important applications.

1546

Echo time based influences on quantitative susceptibility mapping

Surabhi Sood¹, Javier Urriola¹, David Reutens¹, Steffen Bollmann¹, Kieran O'Brien², Markus Barth¹, and Viktor Vegh¹

¹*Centre for Advanced Imaging, The University of Queensland, Brisbane, Australia*, ²*Siemens Ltd., Brisbane, Australia*

Quantitative susceptibility mapping is an important magnetic resonance imaging tool which can help define brain structure and composition. Our work aims to explore information contained in the temporal trend by analysing the mapped magnetic susceptibility as a function of echo time from gradient recalled data acquired at 7T. Temporal susceptibility plots were studied in ten brain regions. Parameterisation of image voxel susceptibility compartments has the potential to delineate structural and chemical changes in tissue and formulate biologically meaningful measures. This in turn provides a framework for new imaging biomarker developments in neurodegenerative diseases and disorders affecting the central nervous system.

1547

Application of Laplacian-based Methods to Multi-echo Phase Data for Accurate Susceptibility Mapping
Emma Biondetti¹, David L. Thomas², and Karin Shmueli¹

¹*Department of Medical Physics and Biomedical Engineering, University College London, London, United Kingdom*, ²*Leonard Wolfson Experimental Neurology Centre, UCL Institute of Neurology, University College London, London, United Kingdom*

In Susceptibility Mapping (SM) using multi-echo gradient-echo phase data, unwrapping and/or background-field removal is often performed using Laplacian-based methods. However, SM pipelines in the literature have applied these methods at different stages. Here, using simulated and acquired images, we compared the performance of three pipelines that apply Laplacian-based methods at different stages. We showed that Laplacian-based methods alter the linearity of the phase over time. We demonstrated that only a processing pipeline that takes this into account, i.e. by fitting the multi-echo data over time to correctly estimate a field map before applying Laplacian-based methods, gives accurate susceptibility values.

1548

Quantitative Susceptibility Mapping of the Substantia Nigra in Parkinson's Disease

Xinxin Zhao¹, Hedi An², Tian Liu³, Nan Shen², Binshi Bo⁴, Zhuwei Zhang⁴, Pengfei Weng⁴, Meining Chen⁴, Mengchao Pei⁴, Yi Wang^{3,4}, Dongya Huang², and Jianqi Li⁴

¹*Shanghai Key Laboratory of Magnetic Resonance and Department of Physics, East China Normal University, Shanghai, China, People's Republic of*, ²*Dongfang Hospital Neural Medical Affiliated Tongji University, Shanghai, China, People's Republic of*, ³*Department of Radiology, Weill Medical College of Cornell University, New York, NY, United States*, ⁴*Department of Physics, Shanghai Key Laboratory of Magnetic Resonance and Department of Physics, East China Normal University, Shanghai, China, People's Republic of*

Quantitative susceptibility mapping (QSM) provides excellent contrast of iron-rich deep nuclei to quantify iron in the brains. Clinicians are interested in using QSM to diagnose PD patients. QSM and $R2^*$ values were measured in the whole substantia nigra in patients with PD and healthy controls. The significant difference between PD patients and healthy controls in the substantia nigra was found on QSM but not on $R2^*$ mapping.

1549

Are susceptibility-weighted imaging and quantitative susceptibility mapping suitable to gain additional information on melanoma metastasis of the brain?

Sina Straub¹, Till Schneider^{2,3}, Christian H. Ziener³, Heinz-Peter Schlemmer³, Mark E. Ladd¹, Frederik B. Laun¹, and Martin T. Freitag³

¹*Department of Medical Physics in Radiology, German Cancer Research Center (DKFZ), Heidelberg, Germany*, ²*Department of Neuroradiology, University of Heidelberg, Heidelberg, Germany*, ³*Department of Radiology, German Cancer Research Center (DKFZ), Heidelberg, Germany*

The benefit of susceptibility weighted imaging (SWI) and quantitative susceptibility mapping (QSM) for the detection and quantification of bleeding of brain metastases of malignant melanoma is assessed. QSM shows paramagnetic values for hemorrhagic metastases (0.355 ± 0.097 ppm) and less paramagnetic values (0.239 ± 0.123 ppm) for hemorrhagic metastases that have T1w-native hyperintense signal. Moreover, our findings suggest that T1w-native hyperintense melanoma metastases have relatively diamagnetic susceptibility compared to other structures of the brain.

Susceptibility underestimation in a high susceptibility phantom: dependence on imaging resolution, magnitude contrast and sample orientation

Dong Zhou¹, JingWei Zhang², Pascal Spincemaille¹, and Yi Wang^{1,2}

¹*Radiology Department, Weill Cornell Medical College, New York, NY, United States*, ²*Biomedical Engineering, Cornell University, Ithaca, NY, United States*

The error in digitizing the dipole convolution¹ may become substantial when there is abrupt susceptibility change within a voxel. To evaluate this error, we assessed the accuracy of quantitative susceptibility mapping in a gadolinium balloon phantom with a range of large susceptibility values (0.4 – 3.2 ppm) and imaging resolutions (0.7 – 1.8 mm) at both 1.5T and 3T. Systematic underestimation of the susceptibility values was observed with decreasing imaging resolution. Numerical simulations were performed to match the experimental findings. These show that the underestimation originates directly from the changes in the voxel sensitivity function and that the amount of underestimation is affected not only by imaging resolution, but also magnitude contrast, the use of k-space filters in the image reconstruction, and details of the susceptibility inclusions such as the susceptibility value and geometry.

The use of quantitative susceptibility imaging for the evaluation of acute MS lesion formation

Vanessa Wiggemann^{1,2}, Enedino Hernandez-Torres^{2,3}, Inga C Ibs⁴, Stephanie M Schoerner⁵, Galina Vorobeychik⁶, Luanne Metz⁷, David KB Li^{8,9}, Anthony Traboulsee^{9,10}, and Alexander Rauscher^{2,9,11}

¹*Physics and Astronomy, University of British Columbia, Vancouver, BC, Canada*, ²*Pediatrics, University of British Columbia, Vancouver, BC, Canada*, ³*UBC MRI Research Centre, University of British Columbia, Vancouver, BC, Canada*, ⁴*University of Osnabrueck, Osnabrueck, Germany*, ⁵*Technical University of Dortmund, Dortmund, Germany*, ⁶*Fraser Health MS Clinic, Burnaby, BC, Canada*, ⁷*Clinical Neurosciences, University of Calgary, Calgary, AB, Canada*, ⁸*Radiology, University of British Columbia, Vancouver, BC, Canada*, ⁹*Center for Brain Health, University of British Columbia, Vancouver, BC, Canada*, ¹⁰*Medicine (Neurology), University of British Columbia, Vancouver, BC, Canada*, ¹¹*Child and Family Research Institute, University of British Columbia, Vancouver, BC, Canada*

Using magnetic-susceptibility based MR techniques for the assessment of damage due to multiple sclerosis (MS) has been controversial, in particular in MS lesions where the underlying pathological changes are not yet fully understood. Here, we investigated the changes of the MR frequency and quantitative susceptibility signal during acute MS lesion formation. We observed that both metrics behave similarly, indicating that non-local effects have little contribution to the QSM signal increase and hence dipole inversion might not be required to assess damage during MS lesion formation accurately.

Rapid Quantitative Susceptibility Mapping with Simultaneous Multi-Band Imaging

Nan-Jie Gong¹, Hing-Chiu Chang², Hongjiang Wei¹, Mark Sundman¹, Nan-kuei Chen¹, and Chunlei Liu¹

¹*Brain Imaging and Analysis Center, Duke University, Durham, NC, United States*, ²*Diagnostic Radiology, The University of Hong Kong, Hong Kong, China, People's Republic of*

We demonstrated the feasibility of using the proposed phase correction method for increasing the accuracy of QSM reconstruction from multi-band acquisitions. With multi-band acquisition, we were able to greatly shorten data acquisition time. It is expected that facilitate this method would benefit further clinical application of QSM and QSM based cerebral functional and physiological studies.

Visibility improvement of cerebral blood vessels by High Resolution Quantitative Susceptibility Mapping

Yuya Umemoto¹, Tomohiro Ueno¹, Shin-ichi Urayama², Toshihiko Aso², Hidenao Fukuyama², and Naozo Sugimoto¹

¹*Human Health Sciences, Kyoto University, Kyoto, Japan*, ²*Human Brain Research, Kyoto University, Kyoto, Japan*

In Quantitative Susceptibility Mapping, susceptibility distribution can be obtained by deconvolution of perturbed fields with dipole fields. In our proposed method, High Resolution QSM, we employed densely sampled dipole fields to improve the quality of QSM. To verify the High Resolution QSM, we performed a human study, and acquired QSM input phase data of a healthy human subject. We compared MIP of the High Resolution QSM to that of the tricubically interpolated conventional QSM. In the High Resolution QSM, visibility of several cerebral blood vessels is improved. This means that a susceptibility map with higher spatial resolution is obtained.

Probing the myelin water compartment with saturation recovery, multi-echo GE imaging at 7T

Elena Kleban¹, Benjamin Tendler¹, Penny Gowland¹, and Richard Bowtell¹

¹*The Sir Peter Mansfield Imaging Center, School of Physics and Astronomy, Nottingham, United Kingdom*

The purpose of this work was to investigate the microstructural properties of white matter in the human brain using saturation recovery multi-echo GE imaging at 7T.

Multi gradient-echo data acquired at three different flip-angles from 8 healthy subjects was fitted for corpus callosum to a three-pool model describing the axonal, myelin and external compartments and variation of the relative amplitude of the myelin water signal with flip-angle was used to assess the T_1 values of the different compartments. Results show an increased frequency variation with TE and faster magnitude signal decay at higher flip-angles, consistent with reduced T_1 in the myelin water compartment.

The Effect of Large Slice Thickness and Spacing and Low Coverage on the Accuracy of Susceptibility Mapping

¹*Medical Physics and Biomedical Engineering, University College London, London, United Kingdom*, ²*Centre for Medical Imaging, University College London, London, United Kingdom*

Susceptibility Mapping has emerging clinical applications. To reduce scan time, clinical images are often acquired with large slice spacing/thickness and reduced coverage. The effect of these factors on susceptibility maps has not been investigated. Here, we develop a simple framework to explore the effect of low-resolution and low-coverage in the slice dimension on the accuracy of susceptibility maps. Our experiments with digital phantoms and volunteer images have shown that the error in the estimated susceptibility increases substantially with increasing slice spacing/thickness and decreasing coverage. These results underscore the need for high-resolution, full-coverage acquisitions for accurate susceptibility mapping.

1556

Accelerated Quantitative Susceptibility Mapping at 7T Using 3D Planes-on-a-Paddlewheel (POP) EPI
Daniel Stäb^{1,2}, Steffen Bollmann¹, Christian Langkammer³, Kristian Bredies⁴, and Markus Barth¹

¹*The Centre for Advanced Imaging, The University of Queensland, Brisbane, Australia*, ²*Department of Diagnostic and Interventional Radiology, University of Würzburg, Würzburg, Germany*, ³*Department of Neurology, Medical University of Graz, Graz, Austria*, ⁴*Institute for Mathematics and Scientific Computing, University of Graz, Graz, Austria*

Ultra-high field whole brain susceptibility mapping at an isotropic resolution of 1 mm was performed within 16 seconds using a 3D planes-on-a-paddlewheel (POP) EPI sequence. The non-Cartesian readout scheme is created by rotating a standard EPI readout train around its own phase encoding axis and provides higher flexibility for echo time minimization than conventional 3D EPI. Morphologic images and susceptibility maps obtained were comparable to those acquired with a conventional 4 minute 3D GRE scan.

1557

Quantitative Susceptibility Mapping Using Adaptive Edge-Preserving Filtering: Comparison with COSMOS in Human Brain
Toru Shirai¹, Ryota Sato¹, Yo Taniguchi¹, Takenori Murase², Atsushi Kuratani², Taisei Ueda², Takashi Tsuneki², Yoshitaka Bito², and Hisaaki Ochi¹

¹*Research and Development Group, Hitachi, Ltd., Tokyo, Japan*, ²*Healthcare Company, Hitachi, Ltd., Chiba, Japan*

We have proposed that a QSM reconstruction method combining an iterative least square minimization and adaptive edge-preserving filtering could generate high-quality susceptibility maps. In this study, maps calculated by the proposed method were compared qualitatively and quantitatively with those calculated by COSMOS (a calculation of susceptibility through multiple-orientation sampling) in healthy volunteers. The results from human brain experiments showed good agreement with COSMOS. The proposed QSM reconstruction of single orientation sampling is useful for generating a high-quality susceptibility map of the human brain.

1558

QSM at 3T: Comparison of Acquisition Methodologies

M Louis Lauzon^{1,2,3}, Cheryl Rae McCreary^{1,2,3}, D Adam McLean^{3,4}, Marina Salluzzi^{3,4}, and Richard Frayne^{1,2,3}

¹*Radiology and Clinical Neurosciences, University of Calgary, Calgary, AB, Canada*, ²*Hotchkiss Brain Institute, Calgary, AB, Canada*, ³*Seaman Family MR Research Centre, Calgary, AB, Canada*, ⁴*Calgary Image Processing and Analysis Centre, Calgary, AB, Canada*

We scanned 4 volunteers 3 times each using 8 different QSM variants (unipolar/bipolar readout gradient, accelerated or not, with/without gradient warp-correction), and compared the susceptibility (average and standard deviation) in five deep gray matter tissues using linear mixed effects modeling. Gradient-warp correction was found to decrease the susceptibility estimates by 3-5%, whereas there was no statistical difference in the estimates due to readout polarity or acceleration factor.

1559

Adaptive background phase removal using knowledge-based region detection for quantitative susceptibility mapping
Taichiro Shiodera¹, Takamasa Sugiura¹, Yuko Hara¹, Yasunori Taguchi¹, Tomoyuki Takeguchi¹, Masao Yui², Naotaka Sakashita², Yasutaka Fushimi³, Takuwa Hinoda³, Tomohisa Okada³, Aki Kido³, and Kaori Togashi³

¹*Toshiba Corporation, Kawasaki, Japan*, ²*Toshiba Medical Systems Corporation, Otawara, Japan*, ³*Kyoto University Graduate School of Medicine, Kyoto, Japan*

We propose a background phase removal method for quantitative susceptibility mapping using adaptive kernels depending on brain region. Conventional methods use distance adaptive kernel spherical mean values (SMV) to estimate background phase. However, artifacts occur where kernel sizes are not optimal for certain brain regions. Here, we adapt SMV kernel sizes depending on brain regions which are automatically detected by machine learning methods. The proposed method eliminates tissue phase artifacts near air-tissue interfaces in more central areas such as the sinus. The proposed method also eliminates streak artifacts in susceptibility images.

1560

Effects of concomitant gradients on Quantitative Susceptibility Mapping

Timothy J Colgan^{1,2}, Diego Hernando¹, Samir Sharma¹, Debra E Horng^{1,2}, and Scott B Reeder^{1,2,3,4,5}

¹*Radiology, University of Wisconsin, Madison, WI, United States*, ²*Medical Physics, University of Wisconsin, Madison, WI, United States*,

³*Biomedical Engineering, University of Wisconsin, Madison, WI, United States*, ⁴*Medicine, University of Wisconsin, Madison, WI, United States*,

⁵*Emergency Medicine, University of Wisconsin, Madison, WI, United States*

MR-based Quantitative Susceptibility Mapping (QSM) techniques have multiple potential applications in brain and body imaging. QSM

techniques generally rely on the removal of background field effects to obtain a local B0 map, followed by dipole inversion to estimate the underlying susceptibility distribution. However, concomitant gradients introduce significant unanticipated phase shifts in the acquired data that manifest as errors in the measured B0 field map. Our results demonstrate that CG phase corrections and/or the use of a background field removal algorithm that removes this background field component are necessary for accurate QSM.

1561

QSM: fast selection of optimal regularization weights
Job Gijsbertus Bouwman¹ and Peter R Seevinck¹

¹*Image Sciences Institute, University Medical Center Utrecht, Utrecht, Netherlands*

Quantitative Susceptibility Mapping reconstructions may benefit from L1-regularization and magnitude weighing, however these iterative reconstruction methods are time-consuming. Recently, progression has been made in reducing the reconstruction times with Split Bregman iterations, allowing subject-specific regularization weights. Here a further reduction of the reconstruction time is reported, mostly based on accelerating the automatic selection of the optimal regularization parameter. The overall procedure reduces computational load more than threefold, without accuracy loss. Reduction of reconstruction times, may contribute to realize QSM algorithms which are either clinically feasible, or that may pave the way to include more sophisticated regularization mechanisms.

Traditional Poster

Contrast Mechanisms: Novel Ways of Imaging

Exhibition Hall

Monday, May 9, 2016: 16:30 - 18:30

1562

MR Imaging of Electromagnetic Field Distribution for Treatment Planning in Electrical Stimulation
Woo Chul Jeong¹, Saurav ZK Sajib¹, Nitish Katoh¹, Bup Kyung Choi¹, Hyung Joong Kim¹, Oh In Kwon², and Eung Je Woo¹

¹*Kyung Hee University, Seoul, Korea, Republic of, ²Konkuk University, Seoul, Korea, Republic of*

Electrical stimulations are widely used as therapeutic techniques that are closely related to the electromagnetic fields inside the human body. The electromagnetic field is affected by the injected currents and electrical conductivities of biological tissue, the map of voltage, current density, and magnetic flux density can provide meaningful information for determining the tissue type and current pathways. The signal intensity of current density is proportional to magnetic flux density which can be measured by MREIT. Since the biological tissues show anisotropic characteristic, we introduced a recent DT-MREIT method to better apply it to real situation.

1563

Simultaneous water content, electrical conductivity and susceptibility mapping in meningiomas on a 3T MR-PET scanner
YP Liao¹, A.-M. Oros-Peusquens¹, J. Lindemeyer¹, N. Lechea¹, C. Weiss², G. Stoffels¹, C. Filss¹, K.J. Langen¹, and N.J. Shah^{1,3}

¹*Institute of Neuroscience and Medicine-4, Forschungszentrum Juelich, Juelich, Germany, ²Department of Neurosurgery, University of Cologne, Cologne, Germany, ³Department of Neurology, JARA, Faculty of Medicine, RWTH Aachen University, Aachen, Germany*

The availability of combined MR-PET scanners opens new opportunities for the characterisation of the tumour environments. In this study, MR-based simultaneous water content, electrical conductivity and susceptibility mapping in meningioma patients was implemented based on a multi-echo gradient echo sequence. The information was complemented by characterisation of the tumour with simultaneous FET-PET. This is a powerful combination of parameters which reflect important aspects of tissue physiology and also characterise to a large extent, tumour electromagnetic (EM) properties. This multi-parametric information helps to understand pathological tissue and can be applied to planning nonionizing EM hyperthermia therapy.

1564

Coil Compression for Improved Phase Image Signal-to-Noise Ratio in Electrical Property Tomography
Kathleen M Ropella¹ and Douglas C Noll¹

¹*Biomedical Engineering, University of Michigan, Ann Arbor, MI, United States*

The use of multi-channel receivers is essential for acquiring B_1^+ with sufficient SNR to calculate electrical properties. Combining the individual channel images prior to these calculations typically involves a SENSE-like method or the use of some reference image. In this work we present a modified version of coil compression to provide an automatic and simplified multi-channel array data combination for high SNR phase-based conductivity mapping.

1565

Validation of MR mapping of direct current in a phantom model
Mayank V Jog¹, Robert X. Smith², Kay Jann², Walter Dunn³, Allan Wu², and Danny JJ Wang²

¹*Biomedical Engineering, University of California Los Angeles, Los Angeles, CA, United States, ²Neurology, University of California Los Angeles, Los Angeles, CA, United States, ³Psychiatry, University of California Los Angeles, Los Angeles, CA, United States*

Transcranial Direct Current Stimulation(tDCS) is a neuromodulation technique. Reported to improve clinical conditions as well as cognition, tDCS has potential as a treatment modality since it involves only simple scalp electrodes to drive mA currents. To date, only mathematical modeling has been used to visualize tDCS-applied currents.

In previous work, we used MRI field mapping in a novel paradigm to visualize in-vivo, a component of the magnetic field generated by these currents. The present work completes the picture by validating our current visualization technique via comparison between the measured and simulated current-induced fields in a specially constructed phantom.

1566

Observation of the correlation between Electrical Conductivity and Apparent Diffusion Coefficient values
Sung-Min Gho¹, Jaewook Shin¹, Min-Oh Kim¹, Min Jung Kim², Sooyeon Kim², Jun-Hyeong Kim¹, and Dong-Hyun Kim¹

¹School of Electrical and Electronic Engineering, Yonsei University, Seoul, Korea, Republic of, ²Department of Radiology, Yonsei University College of Medicine, Seoul, Korea, Republic of

Electric conductivity and apparent diffusion coefficient (ADC) give meaningful information to the clinicians and researchers, however, studies related to the relationship of these two phenomena were not substantially proceeded.

In this abstract, we observe the correlation between electrical conductivity and ADC under various situations (i.e. phantom, in vivo brain, and breast tumor case).

1567

MR-based Current Density Imaging during Transcranial Direct Current Stimulation (tDCS)
Saurav ZK Sajib¹, Woo Chul Jeong¹, Nitish Katoh¹, Bup Kyung Choi¹, Hyung Joong Kim¹, Oh In Kwon², and Eung Je Woo¹

¹Kyung Hee University, Seoul, Korea, Republic of, ²Konkuk University, Seoul, Korea, Republic of

Quantitative visualization of induced current density by the electrical stimulation current inside the anisotropic brain region may play an important role to understand the neuro-modulatory effect during transcranial direct current stimulation (tDCS). For ensuring the clinical applications, precise approaches are required to understand the exact responses inside the human body subject to an injected currents. In this study, we reconstruct current density distribution inside the *in vivo* canine brain region by combining the directional information obtained from a DTI-MRI scan and the z-component of the magnetic flux density data using MREIT technique.

1568

QUANTITATIVE 1H MR TISSUE OXIMETRY (QMRO)
Scott C Beeman¹, Joseph JH Ackerman¹, and Joel R Garbow¹

¹Washington University in St. Louis, St. Louis, MO, United States

A direct and non-invasive measure of tissue O₂ would be a major advance. O₂ is paramagnetic and can thus, in principle, be quantified with NMR/MRI. However, such measurements are challenged/masked by two competing effects: (i) magnetization transfer between ¹H spins of tissue water and the solid-like macromolecular matrix (e.g., proteins, cell membranes) and (ii) blood flow, which can bring equilibrium-polarized ¹H spins into the interrogated tissue volume. We describe a strategy for mitigating these confounds and quantify the direct relationship between pO₂ and the MR-measured longitudinal relaxation rate constant, R₁.

1569

Fisher Information Matrix for Optimizing the Acquisition Parameters in Multi-Parametric Mapping Based on Fast Steady-State Sequences
romain valabregue¹ and Ludovic De Rochefort²

¹CENIR, ICM, Inserm U 1127, CNRS UMR 7225, Sorbonne Universités, UPMC Univ Paris 06 UMR S 1127F, Paris, France, ²IR4M (Imagerie par Résonance Magnétique Médicale et Multi-modalités), Univ. Paris-Sud, CNRS, UMR8081, Université Paris-Saclay, Orsay, France

A criterion of A-optimality was used to optimize SSFP sequence acquisition parameters in order to perform multi-parametric mapping of the physical parameters proton density, relaxation rates and apparent diffusion coefficient. A fast calculation of the steady-state was used to estimate the Fisher information matrix from which fitted parameter error was determined from its inverse. Considering a range of possible T1 and T2 values, and relevant ADC, the acquisition parameters were optimized over the four dimensions of TR, prescribed flip angle, RF phase increment and spoiling gradient to achieve the minimum error on the effectively fitted physical parameters. It is demonstrated that choosing targeted T1 and T2 values over a wide range of expected values enables defining acquisition protocols that minimize the error over this range.

1570

dcQSM: Quantitative Susceptibility Mapping by Directly Fitting Complex Images
Zhe Liu¹, Pascal Spincemaille², and Yi Wang^{1,2}

¹Biomedical Engineering, Cornell University, Ithaca, NY, United States, ²Radiology, Weill Cornell Medical College, New York, NY, United States

The quality of Quantitative Susceptibility Mapping (QSM) depends critically on a correct estimation of total magnetic field, which may sometimes be degraded by phase unwrapping failure. We propose to bypass the traditional field estimation and phase unwrapping steps and estimate both background field and local susceptibility distribution directly from complex GRE images, which is referred to as dcQSM. Since no field is explicitly existent in our method, dcQSM eliminates phase unwrapping errors in traditional methods.

1571

Post-mortem reperfusion of the vascular system and examination in MRI: Temperature-dependent characterisation of perfusates and contrast simulations

¹Ludwig Boltzmann Institute for Clinical Forensic Imaging, Graz, Austria, ²Institute of Medical Engineering, Graz University of Technology, Graz, Austria, ³Institute of Legal Medicine, Medical University of Graz, Graz, Austria

MRI evaluation of a post-mortem reperfused cardiovascular system requires a complete filling of vessels, acceptable contrast/image quality and consideration of temperature influences. Assessment of the temperature dependence of viscosity, T1 and T2 of candidate perfusates (n=10) found 3 to be suitable for application in post-mortem MR angiography. Bloch equation simulations were applied to investigate contrast between these liquids and post-mortem myocardium at 1, 8.5, 16 and 23°C. For a FLASH sequence, optimal flip angles were affected by temperature variation and a decrease in contrast (max. 6-12%) was observed when flip angles optimised for one of the other temperatures were applied.

1572

Rapid Simultaneous Detection of Multiple Contrast Agents Using Magnetic Resonance Fingerprinting

Miko H. de Haas^{1,2}, Huihui Ye^{2,3}, Howard H. Chen^{2,4}, Eric M. Gale^{2,4}, Eszter Boros^{2,4}, Peter Caravan^{2,4}, Kawin Setsompop^{2,4}, and David E. Sosnovik^{2,4}

¹Department of Biomedical Engineering, Eindhoven University of Technology, Eindhoven, Netherlands, ²Athinoula A. Martinos Center for Biomedical Imaging, Massachusetts General Hospital, Charlestown, MA, United States, ³Collaborative Innovation Center for Brain Science and the Key Laboratory for Biomedical Engineering of Education Ministry of China, Zhejiang University, Hangzhou, China, People's Republic of,

⁴Department of Radiology, Harvard Medical School - Massachusetts General Hospital, Boston, MA, United States

MR contrast agents are typically imaged using time-consuming sequences, which allows only one parameter of relaxation to be assessed. In this research we used Magnetic Resonance Fingerprinting (MRF) to rapidly assess both T₁ and T₂, and these values were then used to calculate contrast agent concentrations. The primary goal was to quantify two contrast agents residing in a mixed sample. The method showed an accuracy greater than 90% in most cases, indicating its feasibility. In addition, the method was also able to quantify the bound and unbound state of a targeted contrast agent in near real-time.

1573

Black-Blood T2* Mapping with Delay Alternating with Nutation for Tailored Excitation

Shi Su¹, Yanan Ren¹, Caiyun Shi¹, Xiaoyong Zhang^{1,2}, Hairong Zheng¹, Xin Liu¹, and Guoxi Xie¹

¹Lauterbur Research Center for Biomedical Imaging, Shenzhen Institutes of Advanced Technology, Chinese Academy of Sciences, Shenzhen, China, People's Republic of, ²Centers for Biomedical Engineering, College of Information Science and Technology, University of Science and Technology of China, Hefei, China, People's Republic of

T2* mapping provides a means to quantitatively estimate the iron load of tissue, which is closely related to numerous diseases, such as thalassemia, hereditary hemochromatosis and sickle cell disease. However, blood signal would induce artifacts which lead to T2* estimation inaccurate. To address this issue, a novel black-blood T2* mapping technique utilizing Delay Alternating with Nutation for Tailored Excitation (DANTE) preparation module followed by multi-echo gradient echo (GRE) readout (DANTE-GRE) was developed to obtain blood suppressed T2* maps. The proposed method is shown to acquire more accurate T2* maps due to its high SNR and effective blood signal suppression.

Traditional Poster

Renal, Male & Female Pelvis & Fetal

Exhibition Hall

Tuesday, May 10, 2016: 10:00 - 12:00

1574

Detection and Analysis of Renal Cortical and Medullary T2* Heterogeneity with Minkowski Functionals

Sabrina Klix¹, Andreas Pohlmann¹, Jan Hentschel¹, Karen Arakelyan^{1,2}, Mandy Fechner³, Kathleen Cantow², Bert Flemming², Sonia Waiczies¹, Erdmann Seeliger², and Thoralf Niendorf^{1,4}

¹Berlin Ultrahigh Field Facility (B.U.F.F.), Max Delbrück Center for Molecular Medicine, Berlin, Germany, ²Institute of Physiology, Charité Universitätsmedizin, Berlin, Germany, ³Nephrology and Intensive Care Medicine, Campus Virchow-Klinikum and Center for Cardiovascular Research, Charite-Universitätsmedizin Berlin, Berlin, Germany, ⁴Experimental and Clinical Research Center, a joint cooperation between the Charité Medical Faculty and the Max Delbrück Center for Molecular Medicine, Berlin, Germany

Minkowski Functionals (MFs) allow a quantitative analysis of tissue heterogeneity – independent of absolute values, which can be biased by magnetic field strength, B₀ homogeneity, voxel size, etc. Here we applied this technique to characterize renal cortical and medullary T₂* heterogeneity in order to test the feasibility of a differentiation between healthy kidneys, and kidney injuries.

1575

Assessment of Physiological Changes Associated with Renal Fibrosis in a Rat Model

Lei Jiang¹, Paul Territo¹, Brian McCarthy¹, Amanda A. Riley¹, Sourajit Mustafi¹, Yu-Chien Wu¹, Bruce Molitoris², Gary Hutchins¹, and Chen Lin¹

¹Department of Radiology and Imaging Sciences, Indiana University School of Medicine, Indianapolis, IN, United States, ²Department of Medicine, Indiana University School of Medicine, Indianapolis, IN, United States

The objective of this study is to evaluate the capability of quantitative MRI techniques to measure physiological changes associated with

changes in renal function in a rat model. Our investigation suggest that the results of T_2^* mapping, intra-voxel incoherent motion (IVIM), and $T1_p$ imaging are comparable to the published results. These techniques can be used to assess and monitor different aspects of physiological changes in kidney fibrosis.

1576

MRI-based Evaluation of Renal Oxygenation Under the Influence of Carbogen Breathing

Chengyan Wang¹, Rui Zhang², Li Jiang³, Rui Wang⁴, Xiaodong Zhang⁴, He Wang³, Kai Zhao⁴, Lixin Jin³, Jue Zhang^{1,2}, Xiaoying Wang^{1,4}, and Jing Fang^{1,2}

¹Academy for Advanced Interdisciplinary Studies, Peking University, Beijing, China, People's Republic of, ²College of Engineering, Peking University, Beijing, China, People's Republic of, ³Philips Healthcare, Suzhou, China, People's Republic of, ⁴Department of Radiology, Peking University First Hospital, Beijing, China, People's Republic of

Renal oxygenation plays a major role in the evaluation of renal function and has attracted considerable attention in recent years. This study demonstrates the feasibility of using a susceptibility-based MRI technique for measuring renal oxygen extraction fraction (OEF) change under the influence of carbogen (97% O₂, 3% CO₂) breathing. Significant decrease of renal OEF was found during carbogen challenge. Furthermore, the efficacy of this susceptibility-based method was proved by blood pO₂ measurement.

1577

Short-term Evolution of Renal Metabolic Rate of Oxygen (RMRO₂) in an Animal Model of acute intra-renal ischemia Using qBOLD and ASL MRI

Xiaodong Zhang¹, Yue Mi², Jing Wang³, Jingyun Wu¹, Rui Zhang⁴, Yan Sun¹, Xiaoying Wang^{1,4}, Jue Zhang⁴, and Hongyu An⁵

¹Department of Radiology, Peking University First Hospital, Beijing, China, People's Republic of, ²Department of Urology, Peking University First Hospital, Beijing, China, People's Republic of, ³Center for medical device evaluation, China Food and Drug Administration, Beijing, China, People's Republic of, ⁴Academy for Advanced Interdisciplinary Studies, Peking University, Beijing, China, People's Republic of, ⁵Department of Radiology and Biomedical Research Imaging Center, University of North Carolina at Chapel Hill, Chapel Hill, NC, United States

Quantitative measurement of renal oxygen metabolism level is of central importance in understanding and treating renal diseases and renal metabolic rate of oxygen (RMRO₂) can provide a valid criterion for evaluation the renal tissue oxygen metabolism level under both normal and disease states. According to the Fick principle of arteriovenous oxygen difference, the RMRO₂ can be estimated by using a qBOLD and ASL technique. In this study, we will demonstrate the ability to obtain absolute quantitative RMRO₂ noninvasively in normal and unilateral renal artery stenosis rabbits.

1578

Quantitative susceptibility mapping of kidney injury in a model of ischemia reperfusion

Luke Xie¹, Vivian S. Lee², Hongjiang Wei³, Yi Qi⁴, Susan B. Gurley⁵, G. Allan Johnson⁴, and Chunlei Liu³

¹Radiology, University of Utah, Salt Lake City, UT, United States, ²Utah Center for Advanced Imaging Research, Radiology, University of Utah, Salt Lake City, UT, United States, ³Brain Imaging Analysis Center, Radiology, Duke University Medical Center, Durham, NC, United States, ⁴Center for In Vivo Microscopy, Radiology, Duke University Medical Center, Durham, NC, United States, ⁵Medicine-Nephrology, Duke University Medical Center, Durham, NC, United States

BOLD MRI via T_2^* mapping can detect changes in kidney injuries. However, BOLD MRI can be insensitive and the source of signal change is not clear. Quantitative susceptibility mapping (QSM) is very sensitive to molecular composition and can identify sources as paramagnetic, such as deoxygenated hemoglobin. In this study, we applied QSM to characterize the source of signal change and compared it with BOLD T_2^* maps. We used a model of ischemia reperfusion in mouse kidneys and imaged at 1 hr, 1 day, 7 days, and 14 days after injury.

1579

Evaluating Renal Allograft Function at an Early Stage after Transplantation Using Multiparametric MR Imaging

Tao Ren¹, Pan-Li Zuo², Thorsten Feiweier³, Niels Oesingmann⁴, Andre-de Oliveira³, Li-Hua Chen⁵, Cheng-Long Wen⁵, and Wen Shen⁵

¹Radiology, Tianjin Medical University First Center Hospital, Tianjin, China, People's Republic of, ²Beijing, China, People's Republic of, ³Erlangen, Germany, ⁴New York, NY, United States, ⁵Tianjin, China, People's Republic of

We performed intravoxel incoherent motion(IVIM), arterial spin labeling(ASL) and $T1$ mapping MR imaging in 62 renal allograft recipients to determine the diagnostic values of each parameter in renal allograft function evaluation. We found that cortical ADC, ADC_{slow}, ADC_{fast}, PF and RBF were lower for allografts with impaired function than with good function, and $T1$ values were higher for allografts with impaired function than with good function ($P < 0.05$). ADC derived from IVIM and RBF derived from ASL showed a higher diagnostic efficacy to discriminate between allografts with impaired function and allografts with good function.

1580

Magnetic Resonance Diffusion Tensor and q-space imaging in an Animal Model of Chronic Kidney Disease.

Sourajit Mitra Mustafi¹, Paul R. Territo¹, Brian P. McCarthy¹, Amanda A. Riley¹, Jiang Lei¹, Chen Lin¹, Qiuting Wen¹, Bruce A Molitoris², Gary D. Hutchins¹, and Yu-Chien Wu¹

¹Department of Radiology and Imaging Sciences, Indiana University School of Medicine, Indianapolis, IN, United States, ²Department of Medicine, Indiana University School of Medicine, Indianapolis, IN, United States

In this study, we used multi-shell diffusion-weighted imaging in an animal model of Chronic Kidney Disease (CKD). We focus on the functional changes in the kidney using diffusion tensor imaging (DTI) and q-space imaging (QSI). Four Wistar rats received surgical procedure to induce ischemic fibrosis in their left kidney. The multi-shell diffusion-weighted imaging was performed on the acute stage,

day 2 after the surgery. In the acute stage, the renal medulla showed significant decrease in overall diffusivity measured by DTI and increase in tissue restriction measured by q-space imaging.

1581

Assessing fibrotic damage to renal structure and function with T2-weighted and ASL MRI
Christopher Charles Conlin^{1,2}, Yangyang Zhao², Yufeng Huang³, and Jeff Lei Zhang^{1,4}

¹Utah Center for Advanced Imaging Research, University of Utah, Salt Lake City, UT, United States, ²Bioengineering, University of Utah, Salt Lake City, UT, United States, ³Nephrology, University of Utah School of Medicine, Salt Lake City, UT, United States, ⁴Radiology, University of Utah School of Medicine, Salt Lake City, UT, United States

This study examined the suitability of T2 and ASL-measured renal perfusion as biomarkers for fibrotic kidney disease. Renal perfusion was measured in healthy and fibrotic rats using a multi-TI ASL protocol and compared to renal T2 as well as urinary and histological fibrosis markers. Significantly reduced renal perfusion was observed in fibrotic rats, in parallel with increased renal T2, proteinuria, and mesangial matrix in the glomerular tuft. The sensitivity of T2 and perfusion to fibrotic kidney damage suggests that ASL and T2-weighted MRI may provide improved assessment of renal fibrosis and prove useful for the early detection of renal disease.

1582

Combined Intravoxel Incoherent Motion and Diffusion Tensor Imaging for Evaluation Renal Changes in Diabetic Nephropathy
Cheng long Wen¹, Lihua Chen¹, Fan Mao¹, Yu Zhang², and Wen Shen¹

¹Department of Radiology, Tianjin First Center Hospital, Tianjin, China, Tianjin, China, People's Republic of, ²Philips healthcare, Beijing, China., Beijing, China, People's Republic of

The goal of this pilot study was to assess the ADC value in kidney of IVIM and DTI in distinguishing diabetic subjects and healthy controls. In our study, cortical ADC and D of patients with DN were significantly lower than those of healthy controls. The reduction of D values in the cortex and medulla was more obvious than ADC in patients. The results of this study suggested that cortical D and ADC, quantified by kidney IVIM and DTI could be potential imaging biomarkers for DN. IVIM could reflect the renal function more sensitive and accurate in DN patients.

1583

Comparison of Perfusion Indices Derived from Intravoxel Incoherent Motion and Arterial Spin Labeling MRI: Results in Native and Transplanted Kidneys
Tao Ren¹, Pan-Li Zuo², Thorsten Feiweier³, Niels Oesingmann⁴, Andre-de Oliveira³, Li-Hua Chen⁵, Cheng-Long Wen⁵, and Wen Shen⁵

¹Radiology, Tianjin Medical University First Center Hospital, Tianjin, China, People's Republic of, ²Beijing, China, People's Republic of, ³Erlangen, Germany, ⁴New York, NY, United States, ⁵Tianjin, China, People's Republic of

We collected 20 volunteers and 62 renal allograft recipients who underwent intravoxel incoherent motion (IVIM) and arterial spin labeling (ASL) MRI. Comparing cortical perfusion indices, ADCfast and PF derived from IVIM with RBF derived from ASL in native and transplanted kidneys. We found that mean cortical RBF exhibited a significant correlation with PF ($R = 0.50$, $P < 0.05$) in the native kidneys, but both with ADCfast ($R = 0.26$, $P < 0.05$) and PF ($R = 0.32$, $P < 0.05$) in renal allografts. ADCfast and PF are effective indices for monitoring renal perfusion, as well as RBF.

1584

Assessment of Variation induced by Physiological Motion in Multi-Slice Renal Diffusion-Weighted MRI at 3T
Iris FRIEDLI¹, Lindsey Alexandra CROWE¹, Sophie DE SEIGNEUX², and Jean-Paul VALLEE¹

¹Department of Radiology, Geneva University Hospitals, Geneva, Switzerland, ²Department of Nephrology, Geneva University Hospitals, Geneva, Switzerland

Diffusion-Weighted Imaging (DWI) allows the non-invasive assessment of the whole kidney. However, multi-slice DWI remains challenging because of artifacts, such as motion, partly related to the multi-slice acquisition. Despite the use of physiological triggering schemes to limit respiratory artifacts, kidney images can be impacted by the presence of inhomogeneous signal dropout causing slice-to-slice signal variation of signal intensity and Apparent Diffusion Coefficient (ADC). In this study, we highlight the presence of signal dropout in DWI and ADC maps, and present feasibility of a novel motion and signal correction algorithm to provide robust renal DWI.

1585

The effect of hyperbaric oxygen therapy on healthy and diabetic rat kidneys measured with hyperpolarised [1-13C]pyruvate
Thomas Stokholm Nørlinger¹, Per Mose Nielsen¹, Emmeli Mikkelsen¹, Haiyun Qi¹, Kasper Hansen², Peter Kolstrup Agger³, Nikolaj Schmidt², Michael Pedersen², Hans Stødkilde-Jørgensen¹, Frederik Palm⁴, and Christoffer Laustsen¹

¹Department of Clinical Medicine, MR Research Centre, Aarhus, Denmark, ²Department of Clinical Medicine, Comparative Medicine Lab, Aarhus, Denmark, ³Dept. of Cardiothoracic and Vascular Surgery, Aarhus, Denmark, ⁴Department of Medical and Health Sciences, Division of Drug Research, Linköping, Sweden

Hyperbaric oxygen therapy (HBO) is a well-known adjuvant treatment for several medical conditions indicated by the Undersea and Hyperbaric Medical Society. It is generally well tolerated and the kidneys display no adverse side effects after HBO. In diabetes hypoxia has been shown to be an important contributing factor in the development of diabetic nephropathy. In this experiment we investigate whether HBO has a protective effect on the kidney by preventing metabolic derangement as a consequence of hypoxia in the diabetic kidneys.

Monitoring Progressive Kidney Disease in Folic Acid - Induced Nephropathy in Mice by MRI
Inna Linnik¹, Parisa Ranjzad², Adrian S Woolf², and Steve R Williams¹

¹University of Manchester, Centre for Imaging Sciences, Manchester, United Kingdom, ²University of Manchester, Institute of Human Development, Manchester, United Kingdom

To assess progressive kidney disease in a folic acid (FA) induced nephropathy model in mice, kidney T₁ and volume were quantified using MRI. Mice were imaged at 7 T before and at 1, 4 and 6 weeks after FA or vehicle injection. One week after FA, T₁ was significantly higher (P≤0.036) compared to control and correlated with kidney volume (R=0.90). Mice with marked T₁ and volume increases 1 week after FA demonstrated severe fibrosis on histology at week 6. In conclusion, T₁ mapping may provide a marker of the initiation and severity of later chronic kidney disease.

Tumour heterogeneity assessment using histogram analysis of IVIM-based diffusion and perfusion characteristics of cervical cancer
Jose Angelo Udal Perucho¹, Elaine Yuen Phin Lee¹, and Queenie Chan²

¹Department of Diagnostic Radiology, The University of Hong Kong, Hong Kong, Hong Kong, ²Philips Healthcare, Hong Kong, Hong Kong

Histogram analysis of intravoxel incoherent motion (IVIM) diffusion-weighted MRI (DWI) could be a promising quantitative approach in assessing tumour heterogeneity. We retrospectively studied thirty-five treatment-naïve patients with cervical cancer who had IVIM MRI examinations to determine the value of IVIM histogram analysis, as a means of assessing tumour heterogeneity, in relationship with clinical staging. We observed statistically significant differences in most histogram parameters of *f* (perfusion fraction) between patients with early and locally advanced disease but only three histogram parameters of *D* (true diffusion coefficient) were statistically different in patients with early and locally advanced cervical cancer.

Features of Benign Mature Cystic Ovarian Teratomas
Marissa Albert¹, Genevieve Bennett¹, Jonathan Melamed², and Nicole Hindman¹

¹Radiology, NYU School of Medicine, New York, NY, United States, ²Pathology, NYU School of Medicine, New York, NY, United States

Mature cystic teratomas of the ovary are a common ovarian neoplasm, particularly in young patients. The majority of these neoplasms are benign; only a small minority demonstrates malignant potential. Distinguishing benign from malignant tumors is difficult on imaging alone, but has important clinical implications with regards to follow up and surgical excision. This study is the first in the literature to describe the incidence of, and type of, nodular enhancement within benign mature cystic teratomas. Fat containing ovarian lesions with an internal nodule demonstrating peripheral enhancement and internal fat, along with acute angles and lack of extension beyond the cystic wall, can be confidently diagnosed as having a benign nodule and thus compatible with benign mature cystic teratoma.

Feasibility of computed diffusion weighted imaging and optimization of b-value in cervical cancer.
Yusaku Moribata¹, Aki Kido¹, Koji Fujimoto¹, Yuki Himoto¹, Yasuhisa Kurata¹, Fuki Shitano¹, Kayo Kiguchi¹, Ikuo Konishi², and Kaori Togashi¹

¹Department of Diagnostic Imaging and Nuclear Medicine, Graduate School of Medicine, Kyoto University, Kyoto, Japan, ²Department of Gynecology and Obstetrics, Graduate School of Medicine, Kyoto University, Kyoto, Japan

There has been no previous report on the utility of computed DWI with b-values above 1000 s/mm² for the evaluation of cervical cancer. We aimed to evaluate the utility of computed DWI in cervical cancer and investigate the optimal b-value using computed DWI with b-values of 800, 1000, 1300, 1600 and 2000 s/mm². Computed DWI with b-values of 1300 or 1600 s/mm² may be recommended for the clinical evaluation of the extent of cervical cancer.

Assessment of Cervical Cancer using BOLD MR Imaging - R2* Texture analysis
James Brittin¹, Elizabeth Sadowski¹, Kristin Bradley², and Jessica Robbins¹

¹Radiology, University of Wisconsin, Madison, WI, United States, ²Radiation Oncology, University of Wisconsin, Madison, WI, United States

In our study of patients with cervical cancer, after initial treatment, tumors that recurred tended to have a higher heterogeneity on BOLD R2* maps, and tended to have a positive skew in their image histogram. As tumors undergo treatment, the AUC and skewness decreases significantly. Our findings indicate that BOLD MRI texture analysis can be used to assess long-term response to therapy after initial treatment and to follow tumors during treatment. Further studies using BOLD MRI texture analysis in cervical cancer may help elucidate the utility of this technique in the course of treatment of women with cervical cancer.

Ovarian edema and lymphatic obstruction: increased incidence in patients with large fibroid uterus
Alana Amarosa Lewin¹, Genevieve Bennett¹, and Nicole Hindman¹

¹Radiology, New York University School of Medicine, New York, NY, United States

The goal of this investigation was to determine the incidence of findings in asymptomatic patients which were suggestive of outflow obstruction (venous or lymphatic) as evidenced by dilated lymphatics and ovarian engorgement/signs of massive ovarian edema and to correlate these findings with the size of the fibroid uterus as compared to an age matched control population without fibroids. Ovarian edema and/or lymphatic dilatation was noted with increased frequency in asymptomatic patients imaged for fibroid uterus over

asymptomatic female patients without a fibroid uterus imaged for other causes ($p < 0.0001$). Ovarian edema and/or dilated lymphatics in the setting of large fibroid uteri may be due to vascular congestion or lymphatic obstruction. In the absence of pain and symptoms concerning for ovarian torsion, we postulate that these are incidental findings and recommend conservative management as opposed to immediate surgical exploration.

1592

The Quantification of the Iron Contents in the Ovarian Endometrial Cyst; R2 Measurement in Vivo and Vitro
Junko Takahama¹, Hiroshi Kobayashi², Chiharu Yoshimoto², Hiroshi Shigetomi², Masato Uchikoshi³, Takuya Iwabuchi⁴, Nagaaki Marugami¹, and Kimihiko Kichikawa¹

¹*Radiology, Nara Medical University, Kashihara, Japan*, ²*Gynecology, Nara Medical University, Kashihara, Japan*, ³*Siemens AG, Erlangen, Germany*, ⁴*Metallogenics Co., Ltd., Chiba, Japan*

The measurement of R2 values to quantify the iron concentration in vivo and vitro.

1593

Functional Imaging of the Non-Human Primate Placenta With Endogenous BOLD Contrast
Matthias C Schabel^{1,2}, Victoria H.J. Roberts³, Jamie O. Lo³, Antonio E. Frias⁴, and Chris D. Kroenke¹

¹*Advanced Imaging Research Center, Oregon Health & Science University, Portland, OR, United States*, ²*Utah Center for Advanced Imaging Research, University of Utah, Salt Lake City, UT, United States*, ³*Division of Diabetes, Obesity, and Metabolism, Oregon Health & Science University, Portland, OR, United States*, ⁴*Division of Obstetrics and Gynecology, Oregon Health & Science University, Portland, OR, United States*

We describe a non-contrast method for assessing placental perfusion and fetal oxygenation status utilizing quantitative T2* mapping and a novel spatial model, and validate our method using DCE-MRI measurement in pregnant rhesus macaques.

1594

Diffusion-weighted MR imaging using a gamma distribution model for prediction of insignificant prostate cancer
Hiroko Tomita¹, Hiroshi Shinmoto¹, Shigeyoshi Soga¹, Kentaro Yamada¹, Tatsumi Kaji¹, Tomohiko Asano², and Koichi Oshio³

¹*Radiology, National Defense Medical College, Saitama, Japan*, ²*Urology, National Defense Medical College, Saitama, Japan*, ³*Diagnostic Radiology, Keio University, School of Medicine, Tokyo, Japan*

The purpose of this study was to investigate whether the parameters obtained from diffusion-weighted imaging using a gamma model could distinguish a Gleason 6 from a Gleason ≥ 7 disease, and help to improve the prediction of insignificant prostate cancer in active surveillance candidates. Fifty-nine patients who underwent radical prostatectomy were included in this study. ROC analyses for predicting adverse pathologic outcomes in active surveillance candidates showed that the AUC of the parameters of the gamma model were from 0.81 to 0.88. DWI using the gamma model might help to improve the prediction of insignificant prostate cancer in active surveillance candidates.

1595

Magnetic Resonance Spectroscopic Imaging (MRSI) Metabolite Ratio to Predict Malignancy in Patients with Prostate Cancer undergoing MRI-guided prostate biopsy
Juan C. Camacho^{1,2}, Nima Kokabi¹, Peter A. Harri¹, Tracy E. Powell², and Sherif G. Nour^{1,2}

¹*Radiology and Imaging Sciences, Emory University School of Medicine, Atlanta, GA, United States*, ²*Interventional MRI Program, Emory University Hospital, Atlanta, GA, United States*

The study objective is to investigate Magnetic Resonance Spectroscopic Imaging (¹H-MRSI) in prostate lesions and to correlate the values with the results of MRI-guided prostate targeted sampling. A prospective cohort of patients presenting with persistently elevated or rising serum prostate specific antigen (PSA) and at least one lesion suspicious for prostate cancer that underwent MRI guided targeted biopsy was evaluated. Thirty-five consecutive patients were recruited presenting with 179 suspicious lesions. ROC curve analysis demonstrates a poor performance of ¹H-MRSI as a non-invasive imaging biomarker.

1596

Does Intramuscular Glucagon for Prostate MRI Improve Image Quality?
Stephanie T. Chang¹, Shreyas S. Vasanawala¹, and Andreas M. Loening¹

¹*Radiology, Stanford University, Palo Alto, CA, United States*

We retrospectively investigated whether administration of 1 mg of intramuscular (IM) glucagon to decrease bowel peristalsis prior to prostate MRI decreases motion artifact. Two blinded, independent readers reviewed MRI prostate studies of 25 and 26 patients who did and did not receive glucagon, respectively, for motion-related blurring of the prostate, bowel, and lymph nodes on a five-point Likert scale. No significant difference was observed in all categories. Although European Society of Uroradiology (ESUR) and American College of Radiology guidelines recommend using antiperistaltic agents for prostate MRI, our results suggest that IM glucagon may not be necessary.

1597

Detection of Prostate Cancer from Multi-parametric Regional MRI Features
Nelly Tan¹, Nazanin Asvadi¹, Amin Moshkar², Steven Raman², and Fabien Scalzo³

¹*Radiology, UCLA, Los Angeles, CA, United States*, ²*UCLA, Los Angeles, CA, United States*, ³*Neurology, UCLA, Los Angeles, CA, United States*

Our preliminary results suggest that using a trained machine learning algorithm (spectral regression model) to analyze multiparametric is highly accurate for automatically localizing prostate cancer.

1598

To evaluate the damage of renal function in CIAKI rats at 3T: Using ASL and BOLD MRI
Yuhao Dong¹, Wenbo Chen¹, Long Liang¹, Bin Zhang¹, and Shuixing Zhang¹

¹*Radiology, Department of Radiology, Guangdong Academy of Medical Sciences/Guangdong General Hospital, Guangzhou, Guangzhou, China, People's Republic of*

Contrast induced acute kidney injury (CIAKI) is a common complication after the administration of contrast media. The universally acknowledged mechanisms of CIAKI are the ischemia-mediated oxidative stress as well as the arteriolar vasoconstriction resulted from sustained contrast-induced, hypoxia in cortex and medulla. Our study aims to investigate noninvasive arterial spin-labeling (ASL) and blood oxygen level-dependent imaging (BOLD) sequences for measuring renal hemodynamics and oxygenation in different time points and different sites of kidney after contrast media administration. The results showed that ASL combining BOLD can further identify the primary cause of the decrease of renal oxygenation in CIAKI, which provides means for noninvasive monitoring renal function during the first 4 days of CIAKI in clinical routine work.

Traditional Poster

Lung, Hyperpolarised, Mediastinum

Exhibition Hall

Tuesday, May 10, 2016: 10:00 - 12:00

1599

Comparison of bi-exponential and mono-exponential model of diffusion weighted imaging in evaluation of pulmonary nodules or masses: preliminary experience
Xinchun Li¹, Qi Wang¹, Yingjie Mei², Jiaxi Yu¹, Qiao Zou¹, Yingshi Deng¹, and Yudong Yu¹

¹*Department of Radiology, The First Affiliated Hospital of Guangzhou Medical University, Guangzhou, China, People's Republic of, ²Philips Healthcare, Guangzhou, China, People's Republic of*

The differential diagnosis of benign and malignant focal lesions of the lung is a hot and difficult problem in daily chest imaging. The purpose of our study was to evaluate the potential of intravoxel incoherent motion (IVIM)-derived parameters as well as apparent diffusion coefficient (ADC) in differentiating solitary pulmonary lesions. The results demonstrate that IVIM-DWI could be more helpful for distinguishing malignant from benign lesions in lung. D has the best diagnostic efficiency.

1600

MR imaging of saline flooded lung – A feasibility study in a large animal model
Frank Wolfram¹, Thomas Lesser¹, Harald Schubert², Joachim Böttcher³, Jürgen R Reichenbach⁴, and Daniel Güllmar⁴

¹*Department of Thoracic and Vascular Surgery, SRH Wald-Klinikum Gera, Teaching Hospital of Friedrich Schiller University of Jena, Gera, Germany, ²Institute of Laboratory Animal Sciences and Welfare, Jena University Hospital - Friedrich Schiller University Jena, Jena, Germany, ³Institute of Diagnostic and Interventional Radiology, SRH Wald-Klinikum Gera, Teaching Hospital of Friedrich Schiller University of Jena, Gera, Germany, ⁴Medical Physics Group / IDIR, Jena University Hospital - Friedrich Schiller University Jena, Jena, Germany*

MR imaging of ventilated lung is a challenging task. The low proton density with extremely short T2* and local field inhomogeneities on tissue-air interfaces are sub-optimal for MRI. Unilateral lung flooding replaces air content of one lung wing with saline. This experimental method enables sonographic guidance as well as therapeutic ultrasound ablation. The untoward properties of lung might change to ideal conditions with a homogen and high proton density after flooding. The aim of the study was to investigate the feasibility of in-vivo unilateral lung flooding in MR environment and to evaluate the MR imaging capabilities of flooded lung in a large animal model.

1601

Monitoring therapeutic response in anatomy and functions on pulmonary fibrosis by ultra-short echo time (UTE) MRI in an orthotopic mouse model
Masaya Takahashi¹, Keisuke Ishimatsu¹, Shanrong Zhang¹, Hua Lu², and Connie C.W. Hsia²

¹*Advanced Imaging Research Center, University of Texas Southwestern Medical Center, Dallas, TX, United States, ²Pulmonary and Critical Care Medicine, University of Texas Southwestern Medical Center, Dallas, TX, United States*

The purpose of this study was to investigate the ability of in vivo ultra-short echo time (UTE)-MRI for assessment of pulmonary microstructure and functions of ventilation-perfusion in an animal model of pulmonary fibrosis in comparison with high-resolution MRI, physiological global measures and histomorphology.

1602

Optimized four channel phased array coil for mice lung imaging at 11.7 T
Marta Tibiletti¹, Dominik Berthel², Michael Neumaier³, Dorothee Schüler², Detlef Stiller³, and Volker Rasche^{1,4}

¹*Core Facility Small Animal MRI, Ulm University, Ulm, Germany, ²Rapid Biomedical GmbH, Rimpar, Germany, ³Target Discovery Research, In-vivo imaging laboratory, Boehringer Ingelheim Pharma GmbH & Co. KG, Biberach an der Riss, Germany, ⁴Department of Internal Medicine II, Ulm University, Ulm, Germany*

Lung imaging with MRI is challenging, due to the low proton density in the tissue, short T2* values due to multiple air-tissue interfaces, and respiratory and cardiac motion. A major step for providing sufficient signal to noise ratio (SNR) is the availability of dedicated coils optimized for the specific application. In this work, we present a 4-channel mouse phased-array coil optimized for the thoracic anatomy of mice. Depending on the field-of-view an average two- to threefold gain in SNR was observed in direct comparison to a conventional transmitt/receive quadrature coil at 11.7 T.

1603

Three dimensional inversion recovery dual-echo ultrashort echo time imaging with k-space reordering for effective suppression of longer T2 species in lung parenchyma imaging
Neville D Gai¹, Ashkan A Malayeri¹, and David A Bluemke¹

¹*Radiology & Imaging Sciences, NIH, Bethesda, MD, United States*

Effective imaging of short T2 species requires efficient suppression of longer T2 tissues to maximize short T2 contrast and dynamic range. While inversion with segmented k-space acquisition in Cartesian schemes is straightforward, inversion with segmented k-space UTE radial acquisition offers some challenges since the center of k-space is sampled with each acquisition resulting in magnetization modulation related artifacts. Here we perform 3D inversion recovery dual-echo UTE imaging of lung parenchyma using a reordered k-space radial scheme to perform artifact free high contrast imaging of native lung parenchyma.

1604

A new CF-specific MRI-Score: can it predict loss of lung function?
Ilias Tsiflikas¹, Matthias Teufel¹, Sabrina Fleischer¹, Dominik Hartl², Konstantin Nikolaou¹, and Juergen F Schaefer¹

¹*Diagnostic and Interventional Radiology, University Hospital of Tuebingen, Tuebingen, Germany*, ²*Pediatrics I - CF Center, University Hospital of Tuebingen, Tuebingen, Germany*

The study successfully evaluated a new developed CF-specific MRI score. Our results show that the MRI-Score can predict the loss of pulmonary function. Thus, our findings may help that MRI can serve as a novel predictive marker for loss of lung function in CF and thereby help to tailor individualized monitoring and treatment strategies.

1605

Free Breathing Multi-parametric quantitative Assessment of Mesothelioma with MRI
Ravi Teja Seethamraju¹, Noreen Dunham², Donna Oka², Aida Faria², and Ritu Randhawa Gill²

¹*MR R&D, Siemens Healthcare, Boston, MA, United States*, ²*Radiology, Brigham and Women's Hospital, Boston, MA, United States*

We demonstrate that free breathing multi-parametric quantitative assessment of mesothelioma with MRI is feasible. DCE imaging of the thorax with 3D Radial stack of stairs gradient echo (radial VIBE) sequence can be acquired while free breathing and the resulting pharmacokinetic maps are of higher diagnostic value than current standard of 2D or 3D FLASH acquisitions without the need for co-registration. Similarly DWI with readout segmented EPI (RESOLVE) provides similar diagnostic value with a free breathing acquisition. These two biomarkers help improve the evaluation of tumor in mesothelioma patients.

1606

Matrix pencil decomposition of time-resolved proton MRI for robust and improved assessment of lung ventilation and perfusion
Grzegorz Bauman^{1,2} and Oliver Bieri^{1,2}

¹*Radiological Physics, University Hospital of Basel, Basel, Switzerland*, ²*Department of Biomedical Engineering, University of Basel, Basel, Switzerland*

In the contemporary Fourier decomposition lung MRI, time-resolved registered 2D image series are Fourier transformed to identify in a power spectrum the underlying respiratory and cardiac frequencies. Subsequently, the amplitudes corresponding to the respiratory and cardiac motion are extracted voxel-wise to eventually produce ventilation and perfusion images. However, the analysis of truncated oscillatory signals and the peak search in the Fourier spectrum is usually very unstable and inaccurate. Here, we propose to use a robust and fully-automated method of signal analysis using a matrix pencil decomposition in combination with a linear least squares analysis for improved quantitative pulmonary function assessment.

1607

19F Ventilation Imaging of Cystic Fibrosis Patients
Yueh Lee¹, Esther Akinnagbe-Zusterzeel¹, Jennifer Goralski¹, Scott Donaldson¹, Hongyu An², H. Cecil Charles³, and Richard Boucher¹

¹*The University of North Carolina at Chapel Hill, Chapel Hill, NC, United States*, ²*Washington University, St. Louis, MO, United States*, ³*Duke University, Durham, NC, United States*

19F MRI Ventilation imaging of cystic fibrosis patients demonstrates the disease heterogeneity using a straightforward dynamic protocol.

1608

Non-cartesian SENSE reconstruction of 3D UTE Cones for fast MR lung imaging
Konstantinos Zeimpekis^{1,2}, Klaas Pruessmann², Florian Wiesinger³, Patrick Veit-Haibach¹, and Gaspar Delso⁴

¹*Nuclear Medicine, University Hospital Zurich, Zurich, Switzerland*, ²*Information Technology and Electrical Engineering, ETHZ, Zurich, Switzerland*, ³*GE Global Research, Munich, Germany*, ⁴*GE Healthcare, Waukesha, WI, United States*

This study is about a first attempt to use CG-SENSE parallel reconstruction for non-cartesian 3D Ultra-short Echo Time Cones sequence for lung imaging. Primary goal is to test under-sampled data that reduce the scan time effectively to one quarter of the fully sampled acquisition and check if the reconstruction manages to capture lung density signal to be used for accurate PET Attenuation Correction on a PET/MRI since conventional sequences that are currently used do not capture any. We test also the possibility for high resolution lung imaging from the undersampled data reconstructed with CG-SENSE algorithm.

1609

A Segmentation Pipeline for Measuring Pulmonary Ventilation Suitable for Clinical Workflows and Decision-making
Fumin Guo¹, Khadija Sheikh¹, Rachel Eddy¹, Dante PI Capaldi¹, David G McCormack², Aaron Fenster¹, and Grace Parraga¹

¹*Robarts Research Institute, The University of Western Ontario, London, ON, Canada*, ²*Department of Medicine, The University of Western Ontario, London, ON, Canada*

Clinical translation of hyperpolarized ¹²⁹Xe MRI for large-scale and multi-centre applications requires image analysis tools that can provide clinically-acceptable measurements of pulmonary information. Here we proposed a pipeline that consists of ¹H-¹²⁹Xe registration, segmentation and ventilation defects generation for regional and quantitative evaluation of ¹²⁹Xe ventilation. ¹H-¹²⁹Xe registration was performed using a state-of-art registration approach. ¹H MRI segmentation was performed using primal-dual analysis methods and modern convex optimization techniques with incorporation of region information from ¹²⁹Xe MRI. We applied the pipeline across a range of pulmonary abnormalities and this computationally efficient pipeline demonstrated high agreement with reference standard, suggesting its suitability for efficient clinical workflows.

1610

Quantitative Aerosol Deposition in Mechanically-Ventilated Healthy and Asthmatic Rats using UTE-MRI

Hongchen Wang¹, Georges Willoquet¹, Catherine Sebrié¹, Sébastien Judé², Anne Maurin², Rose-Marie Dubuisson¹, Luc Darrasse¹, Geneviève Guillot¹, Ludovic de Rochebort¹, and Xavier Maître¹

¹*Imagerie par Résonance Magnétique Médicale et Multi-Modalités (UMR8081) IR4M, CNRS, Univ. Paris-Sud, Orsay, France*, ²*Centre de Recherches Biologiques, CERB, Baugy, France*

Asthma is the most common chronic respiratory disease treated with inhaled therapy. However, aerosol deposition patterns are complex and imaging methods are needed to improve delivery efficiency. 3D UTE-MRI combined with aerosolized Gd-DOTA had been formerly applied onto spontaneous nose-only-breathing animals. Here, a mechanical administration system was developed to ventilate and nebulize rats. Resulting aerosol distribution and kinetics were compared with free-breathing in healthy and asthmatic animals.

1611

Investigation of the Multiple T2* Compartments in Lung Parenchyma using a 3D Multi-Echo Radial sequence

Aiming Lu¹, Xiangzhi Zhou¹, Mitsue Miyazaki¹, Masao Yui², Masaaki Umeda², and Yoshiharu Ohno^{3,4}

¹*Toshiba Medical Research Inst., Vernon Hills, IL, United States*, ²*Toshiba Medical System Corp, Otawara, Japan*, ³*Advanced Biomedical Imaging Research Center, Kobe University Graduate School of Medicine, Kobe, Japan*, ⁴*Division of Functional and Diagnostic Imaging Research, Department of Radiology, Kobe University Graduate School of Medicine, Kobe, Japan*

T2* mapping with a single-exponential model have been demonstrated to be useful in assessing pulmonary functional loss. However, the model does not fully explain the signal evolution at longer TE. We propose to improve the T2* characterization in the lung parenchyma with a bi-exponential model. Using a 3D multi-echo radial sequence, our results demonstrated that short T2* values and the volume fractions of the two compartments could be obtained on a clinical 3T scanner. In addition to the improved accuracy of the short T2* measurement, the added fraction values could also potentially be used as biomarkers.

1612

T1 relaxation time in lungs of asymptomatic smokers

Daniel Alamidi¹, Simon Kindvall², Penny Hubbard Cristinacce³, Deirdre McGrath³, Simon Young⁴, Josephine Naish³, John Waterton³, Per Wollmer⁵, Sandra Diaz⁵, Marita Olsson⁶, Paul Hockings^{7,8}, Kerstin Lagerstrand¹, Geoffrey Parker^{3,9}, and Lars E Olsson²

¹*Department of Radiation Physics, Institute of Clinical Sciences, Sahlgrenska Academy, University of Gothenburg, Gothenburg, Sweden*

²*Department of Medical Physics, Lund University, Translational Sciences, Malmö, Sweden*, ³*Centre for Imaging Sciences and Biomedical Imaging Institute, Manchester Academic Health Sciences Centre, University of Manchester, Manchester, United Kingdom*, ⁴*AstraZeneca R&D, Alderley Park, United Kingdom*, ⁵*Department of Translational Medicine, Lund University, Malmö, Sweden*, ⁶*AstraZeneca R&D, Mölndal, Sweden*, ⁷*Medtech West, Chalmers University of Technology, Gothenburg, Sweden*, ⁸*Antaros Medical, BioVenture Hub, Mölndal, Sweden*, ⁹*Bioxydyn Ltd, Manchester, United Kingdom*

Tobacco smoking is the primary cause of COPD. MRI may improve the characterization of COPD where T1 of the lungs is a potential biomarker. We investigated whether smoking affects lung T1 in individuals with no known lung disease. Lung T1 measurements were performed in asymptomatic current and never smokers. T1 was shortened with age and an indication of shortened T1 in smokers was observed that most likely reflects early signs of smoking-induced lung pathology. Our results may be of utility to power future prospective studies with larger cohorts and improved regional analysis.

1613

Retrospective reconstruction using recorded cardiac and respiration data of 3D radial acquisition of a human torso

Daniel Güllmar¹, Georg Hille², Martin Krämer¹, Karl-Heinz Herrmann¹, Jürgen R Reichenbach¹, and Jens Haueisen²

¹*Medical Physics Group / IDIR, Jena University Hospital - Friedrich Schiller University Jena, Jena, Germany*, ²*Institute of Biomedical Engineering and Informatics, Faculty of Computer Science and Automation, Technical University Ilmenau, Ilmenau, Germany*

The aim of the study was to acquire 3D radially sampled k-space data of a human torso without breath hold and prospective cardiac triggering. Respiration and cardiac pulsation were continuously recorded simultaneously with MR imaging over a time frame of 1 h. Retrospective data motion triggering was used to reconstruct 8 up to 10 different respiration phases and 12 up to 20 different cardiac cycle phases, resulting in 96 up to 200 different phase combinations. Image quality was evaluated based on SNR, CNR and under sampling artifacts.

1614

Asymmetric line broadening in lung tissue

Lukas Reinhold Buschle¹, Felix Tobias Kurz^{1,2}, Thomas Kampf³, Heinz-Peter Schlemmer¹, and Christian Herbert Ziener¹

¹E010 Radiology, German Cancer Research Center (DKFZ), Heidelberg, Germany, ²Department of Neuroradiology, Heidelberg University Hospital, Heidelberg, Germany, ³Department of Experimental Physics 5, University of Würzburg, Würzburg, Germany

We analyze the local line shape in human lung tissue in dependence of the underlying microscopic tissue parameters such as diffusion coefficient, alveolar size and susceptibility difference. The interplay between susceptibility- and diffusion-mediated effects is discussed in several dephasing regimes. In vivo measurements for human lung tissue show an excellent agreement with simulations of the dephasing process. This allows an improved quantitative diagnosis of early pulmonary fibrosis and emphysema.

1615

Dephasing and diffusion on the alveolar surface

Lukas Reinhold Buschle¹, Felix Tobias Kurz^{1,2}, Thomas Kampf³, Heinz-Peter Schlemmer¹, and Christian Herbert Ziener¹

¹E010 Radiology, German Cancer Research Center (DKFZ), Heidelberg, Germany, ²Department of Neuroradiology, Heidelberg University Hospital, Heidelberg, Germany, ³Department of Experimental Physics 5, University of Würzburg, Würzburg, Germany

In lung tissue, the susceptibility difference between air-filled alveoli and surrounding tissue causes a strong dephasing of spin-bearing particles. The particles experience an averaged magnetic field due to diffusion effects. Thus, the dephasing process slows down. Both diffusion and susceptibility effects are described by the Bloch-Torrey equation that is solved for the local magnetization on the surface of alveoli. The analytical solution of the free induction decay is compared to in vivo measurements in human lung tissue.

1616

Evaluation of three different VIBE Sequences for Pulmonary Lesions Detection in Patients with Lung Cancer

Hong Wang¹, Xing Tang¹, Panli Zuo², Shun Qi¹, and Hong Yin¹

¹Department of Radiology, Department of Radiology, Xijing Hospital, Xi'an, China, People's Republic of, ²Siemens Healthcare, MR Collaborations NE Asia, Beijing, China, People's Republic of

MR imaging is limited by poor evaluation of lung parenchyma due to rapid single decay, low tissue portion density and substantial respiratory motion. In this study, we evaluate three different approaches of VIBE sequences in pulmonary lesions detection, which including a short-TE breath-hold VIBE, DIXON VIBE and a free-breathing Radial VIBE. We found Breath-hold short-TE VIBE and Dixon VIBE sequences have better performance in lesion detection than radial VIBE.

1617

Title: Breath-Hold Peripheral Pulse-Gated Black-Blood T2-Weighted Lung Magnetic Resonance Imaging with the Variable Refocusing Flip Angle Technique

Ryotaro Kamei¹, Yuji Watanabe², Koji Sagiyama¹, Satoshi Kawanami², Atsushi Takemura³, Masami Yoneyama³, and Hiroshi Honda¹

¹Department of Clinical Radiology, Kyushu University Graduate School of Medical Sciences, Fukuoka, Japan, ²Department of Molecular Imaging and Diagnosis, Kyushu University Graduate School of Medical Sciences, Fukuoka, Japan, ³Healthcare, Philips Electronics Japan, Tokyo, Japan

Breath-hold black-blood magnetic resonance imaging of the lung provides promising results in focal lesion screening. Using peripheral pulse gating, we intended to improve the image quality obtained with previously reported methods. Black-blood fat-saturated T2-weighted images were acquired for healthy volunteers at various time points during the pulse cycle. The degree of attenuation of the intraluminal signals was quantified. The longest trigger delay, which corresponds to the systolic phase, provided superior black-blood effects and was considered optimal for signal acquisition. Thus, peripheral pulse gating enabled convenient and effective attenuation of the signals within pulmonary vessels.

1618

Dynamic Contrast-Enhanced Perfusion MR Imaging at 3T System: Influence of Contrast Media Concentration to Capabilities of Pulmonary Perfusion Parameter and Functional Loss Evaluations as Compared with Dynamic Contrast-Enhanced Perfusion Area-Detector CT

Yoshiharu Ohno^{1,2}, Yuji Kishida², Shinichiro Seki², Hisanobu Koyama², Shigeru Ohyu³, Masao Yui³, Takeshi Yoshikawa^{1,2}, Katsusuke Kyotani⁴, and Kazuro Sugimura²

¹Advanced Biomedical Imaging Research Center, Kobe University Graduate School of Medicine, Kobe, Japan, ²Radiology, Kobe University Graduate School of Medicine, Kobe, Japan, ³Toshiba Medical Systems Corporation, Otawara, Japan, ⁴Center for Radiology and Radiation Oncology, Kobe University Hospital, Kobe, Japan

Quantification of perfusion parameter from dynamic CE-perfusion MRI at 3T system may be more difficult than that at 1.5T system, and contrast media concentration may have larger influence to measurement error of perfusion parameter on a 3T system. We hypothesized that a bolus injection protocol with appropriately small contrast media volume can provide accurate pulmonary perfusion parameter on dynamic CE-perfusion MRI at a 3T system. The purpose of this study was to determine the appropriate contrast media volume for quantitative assessment of dynamic CE-pulmonary MRI, when compared with dynamic CE-area-detector CT (ADCT) for

1619

High-resolution 3D ultra-short echo-time imaging of the lung in young children at 3T without sedation
Wingchi Edmund Kwok^{1,2}, Clement Ren³, Gloria Pryhuber⁴, Mitchell Chess¹, and Jason C. Woods⁵

¹Department of Imaging Sciences, University of Rochester, Rochester, NY, United States, ²Rochester Center for Brain Imaging, University of Rochester, Rochester, NY, United States, ³Department of Pediatrics, University of Rochester, Rochester, NY, United States, ⁴Departments of Pediatrics and Environmental Medicine, University of Rochester, Rochester, NY, United States, ⁵Departments of Pediatrics and Radiology, Cincinnati Children's Hospital Medical Center, Cincinnati, OH, United States

Our purpose was to study the feasibility of high-resolution lung ultra-short TE imaging of young children at 3T without sedation and tackle potential challenges. Two subjects aged 7 and 8 with mild cystic fibrosis were recruited. They were supported by a child life specialist and the use of a mock magnet. Siemens work-in-progress UTE and PETRA_D sequences were used for lung imaging. The images depicted the lung parenchyma, airways and vessels, and revealed abnormalities such as bronchial wall thickening. The techniques should be useful for the monitoring of lung development and evaluation of lung diseases in children.

1620

Investigating the Correlation between Alveolar Surface-to-Volume Ratio and Apparent Diffusion Coefficient with Hyperpolarized Xenon-129 MRI
Kai Ruppert^{1,2}, Kun Qing², Talissa A. Altes^{2,3}, and John P. Mugler III²

¹Cincinnati Children's Hospital, Cincinnati, OH, United States, ²University of Virginia, Charlottesville, VA, United States, ³University of Missouri, Columbia, MO, United States

Chemical Shift Saturation Recovery (CSSR) MR Spectroscopy is a method for monitoring the uptake of hyperpolarized xenon-129 (HXe) by lung parenchyma. The purpose of this study was to investigate the correlation between the alveolar surface-to-volume ratio (S/V) as assessed by CSSR spectroscopy and apparent diffusion coefficient measurements in subjects with chronic-obstructive pulmonary disease, healthy smokers and age-matched normals. Only for very short delay times (5 ms or less) a good correlation was established. Surprisingly, the best correlation, and presumably most accurate S/V value, was obtained by using just the red-blood cell peak at the shortest measured delay time of 3ms.

1621

Hyperpolarized Xenon-129 Lung 3D SB-CSI at 1.5 and 3 Tesla

Steven Guan¹, Kun Qing¹, Talissa Altes¹, John Mugler III¹, Borna Mehrad¹, Michael Shim¹, Quan Chen¹, Paul Read¹, James Larner¹, Julian Ruset^{2,3}, Grady Miller¹, James Brookeman¹, William Hersman^{2,3}, and Jaime Mata¹

¹University of Virginia, Charlottesville, VA, United States, ²University of New Hampshire, Durham, NH, United States, ³XeMed, Durham, NH, United States

3D Single-Breath Chemical Shift Imaging (3D SB-CSI) is capable of non-invasively assessing regional lung ventilation and gas uptake/exchange within a single breath-hold, typically less than 13 seconds. From this study, we present preliminary clinical results of 3D SB-CSI from healthy, cystic fibrosis (CF), interstitial lung disease (ILD), and lung cancer (LC) subjects at 1.5T and 3T. Having novel information on regional changes in ventilation and gas uptake/exchange allows for a better understanding of lung physiology, disease progression, and treatment efficacy.

1622

Spatial Fuzzy C-Means thresholding for semi-automated calculation of percentage lung ventilated volume from hyperpolarised gas and ¹H MRI

Paul J.C. Hughes¹, Helen Marshall¹, Felix C. Horn¹, Guilhem J. Collier¹, and Jim M. Wild¹

¹Academic Unit of Radiology, University of Sheffield, Sheffield, United Kingdom

Automating image analysis is key to accelerate quantitative image metric calculation and increase consistency between observers. This work presents a custom-built software to calculate percentage lung ventilated volume (%VV) from hyperpolarised gas and ¹H MRI using spatial fuzzy c-means thresholding. The software developed reduced analysis time and user input resulting in significantly decreased interobserver variability when postprocessing image data.

1623

Differentiating Early Stage and Later Stage Idiopathic Pulmonary Fibrosis using Hyperpolarized ¹²⁹Xe Ventilation MRI
Mu He¹, Scott H. Robertson², Jennifer M. Wang³, Craig Rackley⁴, H. Page McAdams⁵, and Bastiaan Driehuys⁵

¹Electrical and Computer Engineering Department, Duke University, Durham, NC, United States, ²Medical Physics Graduate Program, Duke University, Durham, NC, United States, ³School of Medicine, Duke University, Durham, NC, United States, ⁴Pulmonary, Allergy and Critical Care Medicine, Duke University Medical Center, Durham, NC, United States, ⁵Radiology, Duke University Medical Center, Durham, NC, United States

The use of ¹²⁹Xe MRI to characterize ventilation has received little attention in IPF because these patients exhibit few ventilation defect regions (VDR) compared to those with other obstructive lung diseases. Here, we evaluate other aspects of the ventilation distribution by optimized linear binning. Ventilation distributions were quantified to provide not only VDR, but also low and high-intensity regions (LIR, HIR). We found that HIR was reduced by 3-fold in patients with late versus early stage disease, as measured by GAP IPF stage. Thus, loss of HIR may be a useful marker of disease progression in IPF.

A Dual Loop T/R-Xenon Coil for Homogenous Excitation with Improved Comfort and Size

Wolfgang Loew¹, Robert Thomen¹, Randy Giaquinto¹, Ron Pratt¹, Zackary Cleveland¹, Laura Walkup¹, Charles Dumoulin¹, and Jason Woods¹

¹Imaging Research Center, Cincinnati Children's Hospital Medical Center, Cincinnati, OH, United States

Hyperpolarized gas MRI of lungs requires homogeneous RF excitation and high SNR for proper spin-density mapping with low flip angles. A dual loop T/R ¹²⁹Xe coil was designed and constructed to provide flexibility for a wide range of patient sizes while maintaining high transmit/receive homogeneity for hyperpolarized ¹²⁹Xe imaging and therefore provide high-quality images for identifying and quantifying functional pulmonary deficiencies. Electromagnetic field simulations were used to analyze excitation profiles.

Lobar Ventilation Heterogeneity in Asthma and Cystic Fibrosis Assessed with Hyperpolarized Helium-3 MRI and Computed Tomography

Wei Zha¹, Jeffery N Kammerman¹, David G Mummy², Alfonso Rodriguez¹, Robert V Cadman¹, Scott K Nagle^{1,3,4}, Ronald L Sorkness^{4,5,6}, and Sean B Fain^{1,2,3}

¹Department of Medical Physics, University of Wisconsin-Madison, Madison, WI, United States, ²Department of Biomedical Engineering, University of Wisconsin-Madison, Madison, WI, United States, ³Department of Radiology, University of Wisconsin-Madison, Madison, WI, United States, ⁴Department of Pediatrics, University of Wisconsin-Madison, Madison, WI, United States, ⁵Medicine-Allergy, Pulmonary & Critical Care, University of Wisconsin-Madison, Madison, WI, United States, ⁶Pharmacy, University of Wisconsin-Madison, Madison, WI, United States

Seven cystic fibrosis (CF) and 69 asthma subjects with different severities of disease underwent hyperpolarized helium-3 MRI and multidetector computed tomography (MDCT). Lobar segmentation was performed on proton MRI by referencing corresponding MDCT. The lobar ventilation defect percent (VDP) was measured by adaptive K-means. Pairwise comparison showed that lobar VDP variation patterns were different in CF vs. asthma, although patterns were similar in severe vs. non-severe asthma. Disease-related lobar VDP variation patterns may provide a sensitive indicator for early detection and patterns of progression in obstructive lung disease.

Severity Evaluation in Cystic Fibrosis Using Oxygen-enhanced MRI: Comparison to Hyperpolarized Helium-3 MRI

Wei Zha¹, Stanley J Kruger¹, Robert V Cadman¹, Kevin M Johnson^{1,2}, Andrew D Hahn¹, Scott K Nagle^{1,2,3}, and Sean B Fain^{1,2,4}

¹Department of Medical Physics, University of Wisconsin-Madison, Madison, WI, United States, ²Department of Radiology, University of Wisconsin-Madison, Madison, WI, United States, ³Department of Pediatrics, University of Wisconsin-Madison, Madison, WI, United States, ⁴Department of Biomedical Engineering, University of Wisconsin-Madison, Madison, WI, United States

Oxygen-enhanced MRI using 3D radial ultrashort echo time sequence (OE-MRI) is a promising alternative to evaluate ventilation and defects with wider accessibility and better affordability. Eleven cystic fibrosis (CF) subjects with different severities of disease underwent OE-MRI and HP-MRI. The disease severity ranks on the percent signal enhancement map (PSE) derived from OE-MRI was compared to the whole lung ventilation defect percent (VDP) measured from HP-MRI as a reference standard using Spearman rank correlation. The moderate association between VDP and PSE suggest OE-MRI shows promise for differentiating disease severity in CF.

Can the Forced Oscillation Technique and a Computational Model of Respiratory System Mechanics Explain Asthma Ventilation Defects?

Megan Fennema¹, Sarah Svenningsen¹, Rachel Eddy¹, Del Leary², Geoffrey Maksym³, and Grace Parraga¹

¹Robarts Research Institute, The University of Western Ontario, London, ON, Canada, ²Environmental and Radiological Health Sciences, Colorado State University, Fort Collins, CO, United States, ³School of Biomedical Engineering, Dalhousie University, Halifax, NS, Canada

In patients with asthma, MRI has provided evidence of ventilation-defects and heterogeneity. The etiology of ventilation-heterogeneity is not well-understood, and neither is its relationship with clinically-relevant respiratory-system-impedance measurements. We evaluated the potential relationships between MRI ventilation-defects and respiratory-system-impedance measured *in vivo* using oscillometry and *in silico* using a computational airway-tree-model, in subjects clinically diagnosed with asthma. Both experiments suggested a significant relationship between MRI ventilation-defects and respiratory-system-reactance. *In vivo* experimental data presented here reinforced the validity of our computational airway-tree-model. MRI-derived ventilation-defects in asthmatics can be explained by lung impedance, specifically reactance, measured experimentally and using a computational model.

Quantitative Gas Exchange using Hyperpolarized ¹²⁹Xe MRI in Idiopathic Pulmonary Fibrosis

Ziyi Wang¹, Scott Haile Robertson², Jennifer Wang³, Elianna Ada Bier², Mu He⁴, and Bastiaan Driehuys^{1,2,5}

¹Biomedical Engineering, Duke University, Durham, NC, United States, ²Medical Physics Graduate Program, Duke University, Durham, NC, United States, ³School of Medicine, Duke University, Durham, NC, United States, ⁴Electrical and Computer Engineering, Duke University, Durham, NC, United States, ⁵Radiology, Duke University Medical Center, Durham, NC, United States

Hyperpolarized ¹²⁹Xe MRI exploits solubility and chemical shift to image regional alterations in gas exchange. These properties have been particularly promising for sensitive detection and monitoring of idiopathic pulmonary fibrosis (IPF). Here we seek to refine our analysis of regional gas exchange impairment by mapping the ¹²⁹Xe uptake in blood and barrier tissues relative to gas-phase signal intensity. This work shows that gas exchange impairment is dominated by increased ¹²⁹Xe uptake in barrier tissues.

In situ pH effects within Mycobacterium tuberculosis Infected Mice revealed by UTE-CEST MRI

¹F. M. Kirby Center, Kennedy Krieger Institute, Baltimore, MD, United States, ²Center for Infection and Inflammation Imaging Research, Center for Tuberculosis Research, Johns Hopkins University School of Medicine, Baltimore, MD, United States, ³Russell H. Morgan Department of Radiology and Radiological Science, Johns Hopkins University School of Medicine, Baltimore, MD, United States, ⁴Department of Pediatrics, Johns Hopkins University School of Medicine, Baltimore, MD, United States

A UTE-CEST scheme was developed to acquire CEST spectrum on M. Tuberculosis lesions in mouse lung. The scheme repeats a selective saturation pulse together with an appropriate mixing time; MRI images are acquired using the UTE technique during the mixing times. The UTE readout is able to suppress the respiratory motion artifacts commonly seen in lung MRI. The pattern of the MTRasym spectra in the TB lesion, which is dominated by protein signals, was used to assess lesion pH.

1630

Evaluation of esophageal cancer: comparison of MRI and CT
Wei Wang¹, Wei Li¹, Xueqian Shang¹, and Xiaoying Wang¹

¹Peking University First Hospital, Beijing, China, People's Republic of

The study preliminary compared the ability of non-contrast-enhanced MRI and contrast-enhanced CT in detection, characterization and staging of esophageal cancer. Ten patients' chest CT and MR images were subjectively evaluated. We found that MR was not inferior to CT, and showed superior capacity in detecting early unapparent cancer, delineating the tumor precisely and depicting perfect contrast of surrounding structures. Also MR was relatively safe than contrast-enhanced CT. MR may be a potential useful tool for evaluation esophageal cancer.

1631



Design of a multimodal (¹H MRI/²³Na MRI/CT) anthropomorphic thorax phantom: Initial results at 3 T
Wiebke Neumann¹, Florian Lietzmann¹, Lothar R. Schad¹, and Frank G. Zöllner¹

¹Computer Assisted Clinical Medicine, Medical Faculty Mannheim, Heidelberg University, Mannheim, Germany

Anthropomorphic phantoms are an essential tool for the validation of image registration algorithms of multimodal data and are important for quantification experiments in ¹H and ²³Na MR imaging. A human thorax phantom was developed with insertable lung, liver, rib cage modules and tracking spheres. Evaluation regarding the tissue-mimicking characteristics with ¹H and ²³Na MR and CT imaging shows that the modules possess T₁, T₂ and HU values comparable to those of human tissues. This work presents an MR- and CT-compatible phantom which allows experimental studies for quantitative evaluation of deformable, multimodal image registration algorithms and realistic multi-nuclei MR imaging techniques.

Traditional Poster

Hepatobiliary & Pancreas

Exhibition Hall

Tuesday, May 10, 2016: 10:00 - 12:00

1632

Relationship between transient severe motion of the liver in gadoxetic acid-enhanced arterial phase imaging and changes of arterial oxygen saturation
Akihiko Kanki¹, Tsutomu Tamada¹, Ayumu Kido¹, Kazuya Yasokawa¹, Tomohiro Sato¹, Daigo Tanimoto¹, Minoru Hayashida¹, Akira Yamamoto¹, and Katsuyoshi Ito¹

¹Radiology, Kawasaki Medical school, Kurashiki, Japan

The purpose of our study was to clarify the relationship between transient severe motion in arterial phase imaging (TSMA) and changes in SpO₂ after contrast media administration during gadoxetic acid-enhanced MRI or CT. As the results, the decrease in SpO₂ in arterial phase compared with other phases was less than 1% in both contrast media. The incidence of TSMA was 0% in iodinated contrast media and was 8.2% in gadoxetic acid, respectively. Our study suggests that the cause of TSM in dynamic gadoxetic acid-enhanced MR imaging of the liver may be the ringing artifacts rather than the respiratory-related motion artifacts.

1633

Cholesterol gallstones can be depicted as positive signal using three dimensional ultra-short echo-time at 3T MR scanner
Mamoru Takahashi¹, Yasuo Takehara², Kenji Fujisaki¹, Tomoyuki Okuaki³, Yukiko Fukuma³, Norihiro Tooyama¹, Katsutoshi Ichijo¹, Tomoyasu Amano¹, and Harumi Sakahara⁴

¹Radiology, Seirei Mikatahara General Hospital, Hamamatsu, Japan, ²Hamamatsu University Hospital, Hamamatsu, Japan, ³Philips Electronics Japan, Ltd., Tokyo, Japan, ⁴Hamamatsu University School of Medicine, Hamamatsu, Japan

Using 3D dual echo UTE sequence, all cholesterol gallstones were able to be detected as positive signal in-vitro. Our study may indicate that UTE has an added value of depicting impacted stones or hepatolithiasis as positive signal. In initial clinical experiences, cholesterol gallstones were also successfully visualized as positive signal with UTE.

1634

Non-balanced spin-echo SSFP sequence in the hepatobiliary phase of Gd-EOB-MRI for the differential diagnosis of liver hemangiomas

and metastatic liver tumors

Yukihisa Takayama¹, Akihiro Nishie², Yoshiki Asayama², Kousei Ishigami², Yasuhiro Ushijima², Daisuke Okamoto², Nobuhiro Fujita², Masami Yoneyama³, and Hiroshi Honda²

¹Department of Radiology Informatics and Network, Kyushu University, Graduate School of Medical Sciences, Fukuoka, Japan, ²Department of Clinical Radiology, Kyushu University, Graduate School of Medical Sciences, Fukuoka, Japan, ³Philips Electronics Japan, Tokyo, Japan

A non-balanced spin-echo steady-state free precession (SSFP) sequence is a variant of the gradient echo (GRE) sequence. It provides T2-weighted contrast because it generates the spin echo. It also has high sensitivity to contrast agents' T1-shortening effects. After the optimization of MR parameter settings, the non-balanced spin-echo SSFP sequence in the hepatobiliary phase (HBP) of Gd-EOB-MRI is useful for differential diagnoses of liver hemangiomas and metastatic liver tumors, based on the interpretation of the lesion signal intensity. Here we assessed the diagnostic performance of the non-balanced spin-echo SSFP sequence in the HBP of Gd-EOB-MRI.

1635

Rapid Cartesian versus radial acquisition: comparison of two sequences for hepatobiliary phase MRI at 3 Tesla
Johannes Budjan¹, Philipp Riffel¹, Melissa Ong¹, Stefan O Schoenberg¹, Ulrike I Attenberger¹, and Daniel Hausmann¹

¹Department of Clinical Radiology and Nuclear Medicine, University Medical Center Mannheim, Mannheim, Germany

In patients with breath-holding difficulties, breathing artifacts can result in dramatically reduced image quality during hepatobiliary phase imaging. Rapid Cartesian as well as radial acquisition techniques are approaches to minimize these artifacts. In 21 patients, both techniques were used and compared regarding image quality and lesion conspicuity. For most patients, a high flip angle Cartesian sequence with short breath-hold interval was feasible and resulted in superior overall image quality. Radial techniques proved to be a valuable option for the few patients who were unable to hold even short breath-hold intervals.

1636

Rapid registration of DCE-MRI for improved ROI-based analysis
Yajing Zhang¹, Zhen Jiang², Weiping Liu¹, Feng Huang¹, Ming Yang¹, Allan Jin¹, and Ping Yang¹

¹Philips Healthcare, Suzhou, China, People's Republic of, ²2nd affiliated Hospital of Soochow University, Suzhou, China, People's Republic of

Quantification of dynamic contrast enhanced MRI (DCE-MRI) is often hindered by motion during imaging. Multiple sources of motion require for a non-rigid 3D registration to align dynamic images. This study provided a rapid 3D non-rigid registration tool for DCE liver registration by optimizing the scheme of image matching. The results show that the dynamic images were well aligned in terms of whole liver area and the portal vein area. Meanwhile, the intensity plot demonstrated better representation from the registered images. Computation time of registration was about one minute for the entire scan, making it possible for clinical routine analysis.

1637

Which is more favorable surrogate marker to predict liver fibrosis on Gd-EOB-DTPA enhanced MRI at 1.5T, ADC value on diffusion weighted imaging or quantitative enhancement ratio?
Taiyou Leopoldo Harada¹, Kazuhiro Saito¹, Yoichi Araki¹, Jun Matsubayashi², Toshitaka Nagao², and Koichi Tokuyue¹

¹Radiology, Tokyo Medical University Hospital, Shinjuku-ku, Japan, ²Pathology, Tokyo Medical University Hospital, Shinjuku-ku, Japan

This study is to evaluate which is favorable surrogate marker to predict the liver fibrosis, DWI or quantitative enhancement ratio measured at hepatobiliary phase on Gd-EOB-DTPA enhanced-MRI. Eighty-three patients with 99 lesions were enrolled. ADC was measured at a distance of 5-10 mm from the tumor. Liver-to-muscle ratio (LMR), liver-to-spleen ratio (LSR) and contrast enhancement index (CEI) were calculated. ADC showed no significant difference among fibrosis grades. LMR and CEI showed significant differences between high stage and low stage fibrosis group ($p<0.01$ and $p=0.04$). In conclusion, LMR was best surrogate parameters to distinguish high stage from low stage fibrosis.

1638

Anatomical and Hemodynamic Assessments of Hepatic Vasculatures using 4D-PCA Technique: Initial Experience
Takeshi Yoshikawa¹, Katsusuke Kyotani², Yoshiharu Ohno¹, Shinichiro Seki³, Hisanobu Koyama³, Kouya Nishiyama², and Kazuro Sugimura³

¹Advanced Biomedical Imaging Research Center, Kobe University Graduate School of Medicine, Kobe, Japan, ²Radiology, Kobe University Hospital, Kobe, Japan, ³Radiology, Kobe University Graduate School of Medicine, Kobe, Japan

We introduced new assessment method of liver hemodynamics using 4D-PCA and new flow analytic technique including wall shear stresses. We found 4D-PCA can be clinically used as a non-contrast angiography and our approach enables detailed hemodynamic assessment for each hepatic vessel.

1639

Transient severe motion (TSM) at gadoxetate disodium-enhanced MRI – Comparison of different contrast agent application protocols
Kristina Imeen Ringe¹, Christian von Falck¹, Hans-Juergen Raatschen¹, Frank Wacker¹, and Jan Bernd Hinrichs¹

¹Department of Diagnostic and Interventional Radiology, Hannover Medical School, Hannover, Germany

The purpose of our present study was to evaluate the incidence of TSM at gadoxetate disodium-enhanced MRI using different contrast application protocols, i.e. by variation of contrast injection rate, dose and supplemental nasal oxygen application. In addition to quantitative SNR measurements, motion artifacts and arterial phase image quality were compared. The overall incidence of TSM in our study population was 11.5%, and neither variation of contrast application parameter was able to significantly reduce the occurrence of

these artifacts.

1640

MR angiography of congenital portosystemic shunts in mice
Hongxia Lei^{1,2}, Ana Francisca Soares³, and Rolf Gruetter^{3,4}

¹Animal Imaging and Technology CIBM-AIT, Ecole Polytechnique Fédérale de Lausanne, Lausanne, Switzerland, ²University of Geneva, Geneva, Switzerland, ³Laboratory of functional and metabolic imaging LIFMET, Ecole Polytechnique Fédérale de Lausanne, Lausanne, Switzerland, ⁴University of Lausanne, Lausanne, Switzerland

Abnormal vascular connections within the liver, such as congenital portosystemic shunts occur sporadically in widely used strain of laboratory mice, i.e. the C57BL/6J strain. We showed that with the respiration gating, MR angiography yields vascular structures of mouse liver with excellent quality and thus allowing diagnosing such abnormality non-invasively.

1641

In vivo ³¹P 3D MRSI of the hepatobiliary system with improved coverage due to the 8 channel receive array at 3T enables prospective assessment of phosphatidylcholine in the gallbladder.
Marek Chmelik^{1,2}, Martin Gajdošák^{1,2}, Emina Halilbasic³, Ladislav Valkovič^{1,4}, Wolfgang Bogner¹, Stephan Gruber¹, Michael Trauner³, Siegfried Trattnig^{1,2}, and Martin Kršák^{1,2,5}

¹High Field MR Centre, Department of Biomedical Imaging and Image-guided Therapy, Medical University of Vienna, Vienna, Austria, ²Christian Doppler Laboratory for Clinical Molecular MR Imaging, Vienna, Austria, ³Division of Endocrinology and Metabolism, Department of Internal Medicine III, Medical University of Vienna, Vienna, Austria, ⁴OCMR, RDM Cardiovascular Medicine, University of Oxford, Oxford, United Kingdom

The purpose of this study was to acquire ³¹P-3D-MRSI data with extended coverage of the hepatobiliary system using a 8-channel receive array at 3T. This protocol enables prospective phosphatidylcholine (PtdC) assessment in the gallbladder. As the bile amount in the gallbladder changes according to dietary condition, the protocol was tested pre-/post-meal. After overnight fasting all volunteers had gallbladder filled with the bile visible in both ³¹P-MRSI data as strong PtdC signal at 2ppm and in T₂ weighted images as hyperintense region. A reduced PtdC signal and volume of the gallbladder were visible after digestion of the high fat meal.

1642

Effect of Betaine on Intrahepatic Triglyceride Levels: Reproducibility and Preliminary Results
Adrienne Lee¹, Benjamin Rowland¹, Huijun Liao¹, Ana Maria Grizales², Allison Goldfine², and Alexander Lin¹

¹Center for Clinical Spectroscopy, Brigham and Women's Hospital, Boston, MA, United States, ²Research Division, Joslin Diabetes Center, Boston, MA, United States

Proton magnetic resonance spectroscopy (MRS) is an accurate, noninvasive method used to monitor intrahepatic triglyceride (IHTG) levels in four patients undergoing betaine treatment for nonalcoholic fatty liver disease (NAFLD). Comparison of results in two of the patients with lower IHTG levels at baseline showed a decrease or improvement after betaine supplementation. However, two subjects with baseline elevated levels of IHTG did not show an improvement and in fact showed higher IHTG levels. Reproducibility of primary lipid vs secondary lipid measurements were also obtained and demonstrated high and low reproducibility, respectively.

1643

Application of Gradient Reversal Fat Suppression technology (LIPO) in diffusion-weighted MR imaging of normal pancreas at 3.0T
Jin Shang¹, Qi-yong Guo¹, Bing Yu¹, Yu Shi¹, Kai-ning Shi², and Ying Liu¹

¹Department of Radiology, Shengjing Hospital of China Medical University, Shenyang, China, People's Republic of, ²Imaging Systems Clinical Science, Philips Healthcare, Beijing, China, People's Republic of

At present, traditional fat suppression still brings heavy chemical-shift artifacts in diffusion weighted imaging (DWI) in abdomen 3T magnetic resonance scan. The purpose of this paper is to study the effect of two different DWI sequences for fat suppression on normal pancreas. From the above research, it can be concluded that DWI with LIPO may serve as an more effective method on improving the image quality of pancreas at 3.0T MR.

1644

Multi-Institution Liver Mass Evaluation at 1.5 and 3 T Using Free breathing, Through-time Spiral GRAPPA and Quantitative Perfusion
Shivani Pahwa¹, Hao Liu², Yong Chen³, Sara Dastmalchian¹, Ziang Lu¹, Chaitra Badve⁴, Alice Yu¹, Joshua Batesole⁴, Hamid Chalian⁴, Katherine Wright¹, Shengxiang Rao⁵, Caixia Fu⁶, Ignacio Vallines⁷, Dean Nakamoto⁸, Mark Griswold⁹, Nicole Seiberlich¹⁰, Zeng Mengsu¹¹, and Vikas Gulani¹²

¹Radiology, Case Western Reserve University, Cleveland, OH, United States, ²Zhongshan Hospital, Fudan University, Shanghai, China, People's Republic of, ³Case Western Reserve University, Cleveland, OH, United States, ⁴Radiology, University Hospitals, Cleveland, OH, United States, ⁵Zhongshan Hospital < Fudan University, Shanghai, China, People's Republic of, ⁶Siemens, Shanghai, China, People's Republic of, ⁷Siemens Healthcare, Shanghai, China, People's Republic of, ⁸Radiology, Case Western Reserve University and University Hospitals, Cleveland, OH, United States, ⁹Radiology and Biomedical Engineering, Case Western Reserve University, Cleveland, OH, United States, ¹⁰Biomedical Engineering, Case Western Reserve University, Cleveland, OH, United States, ¹¹Radiology, Zhongshan Hospital, Fudan University, Shanghai, China, People's Republic of, ¹²Radiology, University Hospitals Case Medical Center, Cleveland, OH, United States

Breath holds and lack of a quantitative dimension are the two major challenges in liver MR imaging. Free breathing, perfusion sequences created in academic institutions in the developed world have not been tested in busy and overloaded radiology practices worldwide. We evaluated free-breathing, 3D Through-time Spiral GRAPPA perfusion technique at two different field strengths in the US and China. We found that the perfusion parameters obtained for two most common hepatic lesions ie hepatocellular carcinoma and

metastases were remarkably consistent across sites, though statistically different according to pathology.

1645

Rapid Liver Strain Assessment in a Single Breath-hold using MR Tagging and FastHARP
Nader S. Metwalli^{1,2}, Ronald Ouwerkerk¹, Ahmed M. Gharib¹, and Khaled Z. Abd-Elmoniem¹

¹Biomedical and Metabolic Imaging Branch, National Institute of Diabetes and Digestive and Kidney Diseases, National Institutes of Health, Bethesda, MD, United States, ²Biomedical Engineering Department, Cairo University, Giza, Egypt

Liver fibrosis occurs as a result of long standing chronic liver disease of various etiologies. Reversibility of liver fibrosis has generated considerable attention lately. Early detection of increased liver stiffness would potentially guide towards more effective treatments. Our accelerated acquisition of liver tagging MRI to assess liver mechanics allows larger volumetric coverage and a substantially shorter acquisition time (\approx 80% reduction of total acquisition) than conventional tagging whilst delivering comparable results.

1646

Quantitative Hepatic Lesion Analysis using Dynamic Contrast-Enhanced Magnetic Resonance Imaging
Ramin Jafari¹, Martin R. Prince², Yi Wang², Shalini Chhabra³, Jonathan P. Dyke², and Pascal Spincemaille²

¹Department of Biomedical Engineering, Cornell University, Ithaca, NY, United States, ²Department of Radiology, Weill Cornell Medical College, New York, NY, United States, ³Nuclear Medicine, Weill Cornell Medical College, New York, NY, United States

Tissue Analysis

Traditional Poster

Metabolism & Others

Exhibition Hall

Tuesday, May 10, 2016: 10:00 - 12:00

1647

Predictive equations for abdominal fat depot volumes with MRI as reference in a multi-ethnic cohort of 4.5 year old Asian children
Suresh Anand Sadanathan¹, Navin Michael¹, Mya Thway Tint², Kuan Jin Lee³, Jay Jay Thaung Zaw², Khin Thu Zar Hlaing², Pang Wei Wei², Lynette Pei-Chi Shek⁴, Yap Kok Peng Fabian^{5,6}, Peter D. Gluckman^{1,7}, Keith M. Godfrey⁸, Yap Seng Chong^{1,2}, Melvin Khee-Shing Leow^{9,10}, Yung Seng Lee^{1,4}, Christiani Jeyakumar Henry⁹, Marielle Valerie Fortier¹¹, and S. Sendhil Velan^{1,3}

¹Singapore Institute for Clinical Sciences, A*STAR, Singapore, ²Department of Obstetrics & Gynaecology, Yong Loo Lin School of Medicine, National University of Singapore, Singapore, ³Singapore Biomedicine Consortium, A*STAR, Singapore, ⁴Department of Paediatrics, Yong Loo Lin School of Medicine, National University of Singapore, Singapore, ⁵Department of Paediatric Endocrinology, KK Women's and Children's Hospital, Singapore, ⁶Lee Kong Chian School of Medicine, Nanyang Technological University, Singapore, ⁷Liggins Institute, University of Auckland, Auckland, New Zealand, ⁸MRC Lifecourse Epidemiology Unit & NIHR Southampton Biomedical Research Centre, University of Southampton & University Hospital Southampton NHS Foundation Trust, Southampton, United Kingdom, ⁹Clinical Nutrition Research Centre, Singapore Institute for Clinical Sciences, A*STAR, Singapore, ¹⁰Department of Endocrinology, Tan Tock Seng Hospital, Singapore, ¹¹Department of Diagnostic and Interventional Imaging, KK Women's and Children's Hospital, Singapore

Longitudinal assessment of abdominal fat compartments in children can help delineate some of the early risk factors that can predispose an individual to high abdominal adiposity and insulin resistance. While accurate determination of abdominal fat can be achieved using CT or MRI, it is often not performed in large cohort studies involving young children due to radiation exposure, high costs or poor compliance with scan procedures. The goal of this work is to develop and validate predictive equations for abdominal fat compartments from anthropometric values with MRI-based abdominal fat volumes as reference in multi-ethnic cohort of 4.5 year-old Asian children.

1648

Abdominal Fat-Water Separation in Mice
Amir Moussavi^{1,2}, Susanne Rauh³, Kristin Koetz¹, Stefan Krautwald⁴, and Susann Boretius^{1,2}

¹Funktionelle Bildgebung, Deutsches Primatenzentrum, Göttingen, Germany, ²Molecular Imaging North Competence Center, University Medical Center Schleswig-Holstein, Kiel, Germany, ³Department of Physics, Christian-Albrechts-University, Kiel, Germany, ⁴Department for Nephrology and Hypertension, University Medical Center Schleswig-Holstein, Kiel, Germany

Obesity is currently one of the most relevant health problems and analyzing body-fat-distribution is of great importance in obesity research. Using radial encoded spoiled FLASH, data sets covering the entire abdomen of mice were obtained at 3 different echo times without any gaiting technique. Fat and water signals were separated using the three-point Dixon method and using IDEAL in comparison. Based on this, the visceral and subcutaneous fat compartments were successfully segmented.

1649

Quantification of lipid contents using PRESS and STEAM sequences on magnetic resonance spectroscopy at 9.4 T
Kyu-Ho Song¹, Song-I Lim¹, Chi-Hyeon Yoo¹, and Bo-Young Choe¹

¹Department of Biomedical Engineering, and Research Institute of Biomedical Engineering, The Catholic University of Korea College of Medicine, Seoul, Seoul, Korea, Republic of

The objective of this study is to compare lipid contents using the point-resolved spectroscopy and stimulated echo acquisition mode

1650

Measuring blood perfusion of brown adipose tissue through FAIR imaging
Clemens Diwoky¹, Renate Schreiber¹, and Rudolf Zechner¹

¹*Institute of Molecular Biosciences, University of Graz, Graz, Austria*

Interscapular brown adipose tissue plays an important role in the maintenance of core body temperature of small mammals through a process known as nonshivering thermogenesis. A dense vascular system delivers oxygen for the thermogenesis and is needed for the transport of produced heat from iBAT towards thoracic and abdominal areas. Therefore iBAT blood perfusion is an important parameter for analyzing iBAT activation and function.

The FAIR ASL protocol developed within this study accounts for the high lipid content in the interscapular area as well as the structure of the iBAT vascular system.

iBAT blood perfusion was determined in wildtype mice and the used protocol is justified based on perfusion numbers determined from skeletal muscle.

Traditional Poster

fMRI Connectivity: The Methods

Exhibition Hall

Tuesday, May 10, 2016: 13:30 - 15:30

1651

Directional connectivity in mouse fMRI networks
Md Taufiq Nasseef^{1,2}, Adam Liska^{1,2}, Stefano Panzeri¹, and Alessandro Gozzi¹

¹*Italian Institute of Technology, Center for Neuroscience and Cognitive Systems @UniTn, Rovereto, Italy*, ²*Center for Mind/Brain Sciences, University of Trento, Rovereto, Italy*

Mouse resting-state fMRI (rsfMRI) has revealed the presence of distributed functional connectivity networks including two sets of regions exhibiting neuro-anatomical features reminiscent of the human salience (SN) and default-mode-network (DMN). Here, we applied Granger Causality to investigate the direction of information flow within mouse rsfMRI networks characterized by mono-directional and reciprocal underlying axonal connectivity. We show that multiple intrinsic rsfMRI networks of the mouse brain exhibit robust patterns of directional connectivity towards prefrontal regions, replicating topological features of human rsfMRI networks, and in agreement with higher integrative role subserved by these areas.

1652

A Robust Anesthesia Regime for fMRI in Rodents
Hanbing Lu¹, Julie Brynildsen¹, Li-Ming Hsu¹, Thomas Ross¹, Elliot A Stein¹, and Yihong Yang¹

¹*Neuroimaging Research Branch, National Institute on Drug Abuse, NIH, Baltimore, MD, United States*

In fMRI using animal models, it is of critical importance to develop a robust anesthetic regime that maintains neurovascular coupling, permits longitudinal experiments with minimal invasiveness, and is easy to implement. Recently, using an anesthetic method that combines low doses of dexmedetomidine and low dose of isoflurane, we have successfully identified the default mode network in rat brain, suggesting that this preparation causes minimal suppression of brain network functions. The goal of this study is to systematically characterize and to optimize physiological conditions for fMRI experiments under this anesthetic regime.

1653

Frontal-parietal network functional connectivity characterization in patients with end-stage renal disease by using independent component analysis
Lin Wang¹, Chun-Qiang Lu¹, and Shenghong Ju¹

¹*Department of Radiology, Zhongda hospital, Medical school of Southeast university, Nanjing, China, People's Republic of*

It has been reported that end-stage renal disease (ESRD) patients have cognitive decline in all aspects, especially in attention and executive function, and this is lack of objective noninvasive modalities to monitor the cognition impairment by now. Resting-stage functional MR which can detect the change of brain function as a newly-developing imaging method has been widely used to evaluate the cognitive status in many diseases. Our findings show the aberrant functional connectivity of frontal-parietal network (FPN) in ESRD patients, and supported by the results of neuropsychological tests. FPN functional connectivity may serve as a biomarker to monitor the attention and executive function impairment in patients with ESRD in the future.

1654

Slice-based motion metrics show stronger relationship than volume-based metrics to visual rating of motion artifact
Katherine A Koenig¹, Erik Beall¹, Sally Durgerian², Christine Reece³, Stephen M Rao³, and Mark J Lowe¹

¹*Imaging Sciences, The Cleveland Clinic, Cleveland, OH, United States*, ²*BrainDataDriven LLC, Milwaukee, WI, United States*, ³*Schey Center for*

A motion metric that more closely represents the amount of artifact in the signal could decrease the amount of discarded data and reduce noise in resting state studies. This work compares a sample of 455 resting state scans visually rated for motion corruption to slice-based and volume-based motion metrics. We show that the slice-based metric shows a stronger relationship to visual assessment of motion corruption.

1655

Brain cortical parcellation based on the anisotropy of local spatio-temporal correlation of rs-fMRI at 7T
Afonso Dias¹, Marta Bianciardi², Sandro Daniel Nunes¹, Luís M. Silveira³, Lawrence L. Wald², and Patrícia Figueiredo¹

¹ISR-Lisboa/LARSyS and Department of Bioengineering, Instituto Superior Técnico – Universidade de Lisboa, Lisbon, Portugal, ²Department of Radiology, A.A. Martinos Center for Biomedical Imaging, MGH and Harvard Medical School, Boston, MA, United States, ³INESC-ID, Instituto Superior Técnico – Universidade de Lisboa, Lisbon, Portugal

We propose a new metric of local functional connectivity for the parcellation of the cerebral cortex from resting-state fMRI data. It is based on the hypothesis that the anisotropy of the local spatio-temporal correlation tensor of the BOLD signal is increased in the boundaries between regions of functional segregation within gray matter. We show that the anisotropy of rs-fMRI at 7T can be used to generate cortical parcellations that are partially consistent with the results obtained using the well-established stability map. Further work is needed to investigate the validity and properties of the parcellations based on the proposed metric.

1656

Exploring Resting-State Functional Connectivity Invariants across the Life Span using a Novel Graph Model
Ottavia Dipasquale^{1,2}, Paolo Finotelli³, Isa Costantini¹, Giuseppe Baselli¹, Francesca Baglio², Paolo Dulio³, and Mara Cercignani⁴

¹Department of Electronics, Information and Bioengineering, Politecnico di Milano, Milan, Italy, ²IRCCS, Don Gnocchi Foundation, Milan, Italy,

³Department of Mathematics "F. Brioschi", Politecnico di Milano, Milan, Italy, ⁴Clinical Imaging Sciences Centre, Brighton and Sussex Medical School, Brighton, United Kingdom

In this work we investigated resting-state functional connectivity (FC) changes and invariant properties in 133 healthy people across the life-span (6-79) using a novel graph model that emphasizes centrality of nodes. This model estimates a weight for each node's pair (94 cortical regions) accounting for the node degrees, anatomical distance and FC between them and penalizing the formation of long connections. Preliminary findings in two groups of 25 and 62 year-old subjects highlighted a number of interesting properties and confirmed the important role of the Precuneus and the Cingulate Gyrus, which are characterized by high functional strength and degree.

1657

Assessing the Reliability of Estimated Correlation During the Evaluation of Dynamic Functional Connectivity
Tuo Shi¹, D Rangaprakash¹, and Gopikrishna Deshpande^{1,2,3}

¹AU MRI Research Center, Department of Electrical and Computer Engineering, Auburn University, Auburn, AL, United States, ²Department of Psychology, Auburn University, Auburn, AL, United States, ³Alabama Advanced Imaging Consortium, Auburn University and University of Alabama Birmingham, Auburn, AL, United States

In this work, we propose a novel strategy for selecting the minimum window length required to capture maximum dynamics as well as reliably estimate correlation during dynamic functional connectivity analysis. Using the error in estimated correlation compared to simulated ground-truth correlation as the metric, we compared our method with (i) the fixed window length approach, and (ii) the DCC method. We show that our method can provide minimum window lengths which give more reliable correlation estimates than those obtained from DCC and fixed-window methods. Further, we show that our method can accurately track fast variations in connectivity.

1658

Accuracy and inter-subject reproducibility of default mode networks identified from ASL data
Felipe Barreto^{1,2}, Xufeng Li¹, Amir Moheet³, Anjali Kumar³, Lynn Eberly⁴, Elizabeth Sequist³, Fabrizio Esposito⁵, and Silvia Mangia¹

¹CMRR, Department of Radiology, University of Minnesota, Minneapolis, MN, United States, ²Department of Physics, University of Sao Paulo, Ribeirao Preto, Brazil, ³Department of Medicine, University of Minnesota, Minneapolis, MN, United States, ⁴Division of Biostatistics, University of Minnesota, Minneapolis, MN, United States, ⁵Department of Medicine and Surgery, University of Salerno, Baronissi, Italy

The present study aimed at characterizing the robustness of the default mode network (DMN) extracted at single subject level from ASL datasets with independent component analysis. Three different analyses modes were considered, including the series of perfusion weighted images, the full time series, and the pair-wise average of control/tag images (pseudo-BOLD). Results show that the three analysis modes produce DMNs with similar accuracy at a group level, but the pseudo-BOLD mode resulted in smaller inter-subject variability of the spatial distribution of the single-subject DMNs.

1659

Condition effects on resting-state CBF reproducibility and reliability
Marta Vidorreta^{1,2}, Natalie N Katchmar³, Daniel H Wolf³, and John A Detre^{1,2}

¹Neurology, University of Pennsylvania, Philadelphia, PA, United States, ²Radiology, University of Pennsylvania, Philadelphia, PA, United States,

³Psychiatry, University of Pennsylvania, Philadelphia, PA, United States

Cerebral blood flow (CBF) data were collected with arterial spin labeled (ASL) perfusion MRI in a group of young, healthy subjects over two sessions, scheduled a week apart. CBF and functional connectivity metrics were derived from the CBF time series across four

different resting conditions: 'eyes open', 'eyes closed', 'fixation' (eyes fixated on a cross), and 'PVT' (low-frequency psychomotor vigilance task). Absolute CBF was highly reproducible both within and across sessions. Results suggest that 'fixation' is inferior to the other conditions tested for resting-state ASL reproducibility.

1660

Title: Distinctive relationships between functional and structural connectivity in autism spectrum disorder across different networks—a combined resting-state functional MRI and diffusion spectrum imaging study
Hsiang-Yun Sherry Chien¹, Susan Shur-Fen Gau², and Wen-Yih Isaac Tseng^{1,3}

¹*Institute of Medical Device and Imaging, National Taiwan University College of Medicine, Taipei, Taiwan, Taipei, Taiwan*, ²*Department of Psychiatry, National Taiwan University Hospital and College of Medicine, Taipei, Taiwan, Taipei, Taiwan*, ³*Molecular Imaging Center, National Taiwan University, Taipei, Taiwan, Taipei, Taiwan*

We conducted a data-driven approach to investigate the functional and structural connectivity (FC and SC) within three critical networks in autism spectrum disorder (ASD) and typically developing controls (TD). We found significant weaker SC within the default-mode network, e.g. the cingulum bundles, in ASD compared to TD. Furthermore, we found significant positive correlations between the FC of the right salience network and the SC within the DMN and central executive network (CEN). Given the role of salience network in modulating the switch between the DMN and CEN, our results might imply a distinctive FC-SC relationship across different networks in ASD.

1661

An algorithm for generating uniform random parcellations
Hu Cheng¹, Andrea Koenigsberger¹, Sharlene Newman¹, and Olaf Sporns¹

¹*Psychological and Brain Sciences, Indiana University, Bloomington, IN, United States*

Random parcellations have some advantages over template-based parcellations in network analysis of the brain. An important criterion for assessing the "goodness" of a random parcellation is the parcel size variability. A new algorithm is proposed to create more homogeneous random parcellations than previously reported. The new algorithm takes the actual distance between voxels and local voxel density into account in placing the random seeds. With many random parcellations using our approach, global network properties exhibit normal distribution and the variability across different repetitions of the random parcellation is comparable with inter-subject variability.

1662

Simultaneous PET/MR/EEG to study brain connectivity on different physiological and temporal scales in epilepsy patients
Andre Thielcke¹, Adham Elshahabi², Ilja Bezrukov¹, Suril Gohel³, Mario Amend¹, Holger Schmidt⁴, Matthias Reimold⁵, Holger Lerche², Bharat Biswal³, Bernd J. Pichler¹, Niels Focke², Christian la Fouger⁵, and Hans F. Wehrli¹

¹*Department of Preclinical Imaging and Radiopharmacy, Werner Siemens Imaging Center, Eberhard Karls University of Tuebingen, Tuebingen, Germany*, ²*Neurology & Epileptology and Werner Reichardt Centre for Integrative Neuroscience, Eberhard Karls University of Tuebingen, Tuebingen, Germany*, ³*Department of Biomedical Engineering, New Jersey Institute of Technology, Newark, NJ, United States*, ⁴*Interventional and Diagnostic Radiology, Eberhard Karls University of Tuebingen, Tuebingen, Germany*, ⁵*Nuclear Medicine and Werner Reichardt Centre for Integrative Neuroscience, Eberhard Karls University of Tuebingen, Tuebingen, Germany*

Simultaneous PET/MR/EEG was used in humans to study brain networks in the resting state on slow, medium and fast time scales. We found that the representation of the default mode network (e.g. in terms of correlation between regions) varies between modality and time scale applied. However, for the DMN as well as other networks similarities but also differences between modalities were seen. This work opens the domain for studying brain activity on different physiological (metabolic, hemodynamic and electric) but also on different time scales.

1663

Estimating whole brain connectivity dynamics using spectral clustering
Ivor Cribben¹

¹*Finance and Statistical Analysis, Alberta School of Business, Edmonton, AB, Canada*

A great challenge in neuroscience is the understanding of the dynamic manner in which brain regions interact with one another in both task-based and resting-state brain imaging studies. In this work, we introduce a novel statistical method, called Network Change Point Detection (NCPD), which dynamically clusters brain regions by their functional connectivity. NCPD promises to offer deeper insight into the large-scale characterizations and mechanisms of the brain as it can be used for the dynamic modelling of a very large number of voxels or brain regions. We apply this new method to a resting-state fMRI study.

1664

A voxel by voxel comparison of spatio-temporal correlation tensor derived from the resting-state fMRI and diffusion tensor derived from diffusion weighted images on the human brain using the multiband EPI sequences
Jiancheng Zhuang¹

¹*University of Southern California, Los Angeles, CA, United States*

We test the validity of spatio-temporal correlation tensor method on a set of rfMRI and DTI data which are acquired by multiband EPI sequences and have the same slice and geometry parameters, so we can compare the spatio-temporal correlation tensor and diffusion tensor at a voxel by voxel level in the human brain. We find the spatio-temporal correlation tensor derived from resting-state fMRI does not match with the diffusion tensor calculated from diffusion weighted images in the white matter, which is contradictory to a previous

report of spatio-temporal correlation tensor method.

1665

Investigating the neural substrates of verbal working memory in children with dyslexia: An effective connectivity study
Fu Yu Kwok¹, Beth Ann O'Brien², Kiat Hong Stacey Tay³, and SH Annabel Chen^{1,4}

¹Division of Psychology, Nanyang Technological University, Singapore, Singapore, ²National Institute of Education, Nanyang Technological University, Singapore, Singapore, ³Paediatric Neurology and Developmental Paediatrics, National University Hospital, National University of Singapore, Singapore, Singapore, ⁴Centre for Research And Development Learning, Nanyang Technological University, Singapore, Singapore

Dynamic causal modeling was utilized to examine the effective connectivity during verbal working memory in children with dyslexia and typically developing children. Seven regions of interest—FG, IFG, IOG, IPL, thalamus, inferior cerebellum and superior cerebellum were included into the analyses. Results indicated that the effect of dyslexia led to shift in effective network connectivity. The present study furthered our understanding of the cerebro-cerebellar effective network connectivity in both children with dyslexia and typically developing children. In addition, it provided new insights about the effects of dyslexia on this network.

1666

Data-driven functional sub-division of the sensory-motor network using hierarchical clustering for resting-state fMRI data.
Yanlu Wang¹ and Tie-Qiang Li^{1,2}

¹Clinical Sciences, Intervention and Technology, Karolinska Institute, Stockholm, Sweden, ²Medical Physics, Karolinska University Hospital, Stockholm, Sweden

A data-driven analysis method based on hierarchical clustering was used to analyze the sensory-motor resting-state network from resting-state fMRI data. It was used to analyze the network's functional sub-division, and intra-network functional organization, in different levels of detail. Sub-network for the sensory-motor network as obtained by hierarchical clustering is anatomically and functionally sensible. Further sub-division of the paracentral lobule network hub successfully revealed its functional sub-division in great detail. The intra-network organization of intrinsic functional connectivity derived from spontaneous activity of the brain at rest reflects consistently, the functional and neural anatomic connectivity topography of the resting-state network.

1667

Nonlinear registered seed selection in resting state fMRI
Wanyong Shin¹ and Mark J Lowe¹

¹Radiology, Cleveland Clinic Founcautin, Cleveland, OH, United States

We compared different motor cortex (M1) seed selection methods in a large sample for group resting state (rs-) fMRI analysis. We found that seed selection with non-linear registration improves the statistical power in group analysis

1668

Reproducibility of seed-based rs-fMRI measures at 7 tesla
Katherine A Koenig¹, Sehong Oh¹, Wanyong Shin¹, and Mark J Lowe¹

¹Imaging Sciences, The Cleveland Clinic, Cleveland, OH, United States

This work assesses the reproducibility of seed-based rs-fMRI measures at 7 tesla in a sample of five controls and three patients with multiple sclerosis. We show high reproducibility but with large variation in some subjects.

Traditional Poster

fMRI Connectivity: The Applications

Exhibition Hall

Tuesday, May 10, 2016: 13:30 - 15:30

1669

Investigation of functional baseline neuronal specificity and small-scale network in human primary motor cortex at 7T
Chan Hong Moon¹, Jung-Hwan Kim^{1,2}, and Kyongtae Ty Bae^{1,2}

¹Radiology, University of Pittsburgh, Pittsburgh, PA, United States, ²Bioengineering, University of Pittsburgh, Pittsburgh, PA, United States

Compound signal, BOLD (e.g., de-oxygenation, CBF and CBV) has different neuronal specificity depending on the major source. At high-field such as 7T, stimulus-evoked BOLD (fMRI) is known to be more localized to cortex region mainly due to suppression of short T2* signals in large draining vessels. It is question whether spontaneous-evoked BOLD during resting status (rsfMRI) can be localized to neural response and the correlation with fMRI activation. In this study, we investigated BOLD source during resting status in primary motor cortex using high-resolution 7T, and additionally the advantage of 7T rsfMRI in small-scale brain connectivity.

1670

Dynamic reorganization of intrinsic functional networks in the mouse brain
Joanes Grandjean¹, Maria G. Preti^{2,3}, Thomas AW Bolton², Dimitri Van De Ville², and Markus Rudin⁴

¹ETH and University Zurich, Zurich, Switzerland, ²EPFL, Lausanne, Switzerland, ³University of Geneva, Geneva, Switzerland, ⁴University and ETH Zurich, Zurich, Switzerland

Dynamic functional connectivity was assessed in the mouse brain. High quality resting-state fMRI data were acquired and analysed with sliding window correlations. Re-occurring dynamic functional networks were estimated using dictionary learning from the sliding window correlation matrix. The dynamic functional connectivity analysis reveals rich patterns of interactions, which were absent in the standard static functional connectivity analysis, and may be used to describe specific alterations in mouse models of brain disorders. In particular, the dynamic functional networks present salient features such as between and within module interactions, which complement the static functional connectivity analysis.

1671

Visual Stimulation Altered Human Visual Cortical Functional Connectivity
Jie Huang¹ and David C Zhu²

¹Department of Radiology, Michigan State University, East Lansing, MI, United States, ²Departments of Radiology and Psychology, Michigan State University, East Lansing, MI, United States

Areas across the visual cortex are functionally connected. Certain patterns can induce perceptual illusions/distortions and visual discomfort in most people, headaches in patients with migraine, and seizures in patients with photosensitive epilepsy. This preliminary study investigated visual stimulation effect on human visual cortical functional connectivity (FC). The study found that a 25-min visual stimulation with a stressful pattern significantly enhanced the FC within the visual cortex and altered the FC to V1 in other regions too, with a lasting effect even after the cessation of the stimulation.

1672

Similarity in structural and functional network connectivity evolution over duration of TLE

Victoria L. Morgan¹, Ahmet Cakir², Benjamin N. Conrad¹, Bassel Abou-Khalil³, Adam W. Anderson^{1,4}, Zhaohua Ding¹, and Bennett A. Landman^{1,2}

¹Institute of Imaging Science, Vanderbilt University, Nashville, TN, United States, ²Electrical Engineering and Computer Science, Vanderbilt University, Nashville, TN, United States, ³Neurology, Vanderbilt University, Nashville, TN, United States, ⁴Biomedical Engineering, Vanderbilt University, Nashville, TN, United States

Temporal lobe epilepsy (TLE) is a common and relatively homogeneous form of epilepsy in which seizures originate in the mesial temporal regions including the hippocampus and propagate across the brain. This work represents the first step in characterizing the functional (FC) structural (SC) network connectivity evolution in TLE using MRI. We found consistent decreases in ipsilateral hippocampus and insula FC and SC primarily after 10 years of duration of disease in patients with seizure freedom after surgery. In those with seizure recurrence, there were more severe bilateral hippocampal SC decreases when compared to those with seizure freedom.

1673

Gender related peculiarities of amygdala deactivation during movements
Oleksii Omelchenko¹, Zinayida Rozhkova², and Mykola Makarchuk¹

¹Human and Animal Physiology, Taras Shevchenko National University of Kyiv, Kyiv, Ukraine, ²Medical Clinic BORIS, Kyiv, Ukraine

Men and women might display distinct characteristics of functional organization of neurocognitive brain networks. Considering gender-specific brain functioning under language, emotional and memory tasks execution, we propose fMRI visualization of the brain activated by a movement task for estimation of gender specific motor brain network peculiarities. New evidence for gender related differences in amygdala function was found. Results also give us background for further subdivision of the fMRI normative basis from which we investigate functional brain changes in patients' population.

1674

Longitudinal Study of Motor Recovery After Pontine Infarction with Resting-state fMRI: A Homotopic Connectivity Study
Yi Shan¹, Chaogan Yan², Miao Zhang¹, Dongdong Rong¹, Zhilian Zhao¹, Qingfeng Ma³, Xinian Zuo², Jie Lu⁴, and Kuncheng Li¹

¹Department of Radiology, Xuanwu hospital, Capital Medical University, Beijing, China, People's Republic of, ²Key Laboratory of Behavioral Science and Magnetic Resonance Imaging Research Center, Institute of Psychology, Chinese Academy of Sciences, Beijing, China, People's Republic of, ³Department of Neurology, Xuanwu hospital, Capital Medical University, Beijing, China, People's Republic of, ⁴Department of Nuclear Medicine, Xuanwu hospital, Capital Medical University, Beijing, China, People's Republic of

Impairment of motor function is one of the most severe deficit in ischemic stroke patients. Therefore, evaluations of brain function reorganization during spontaneous motor recovery are extremely valuable. In the present study, we used a voxel-mirrored homotopic connectivity (VMHC) method to investigate the longitudinal functional homotopic changes in patients with pontine infarction during a 180-day-period follow-up. The result shows resting-state fMRI could demonstrate dynamic whole-brain homotopic FC changes in stroke patients which might be helpful to further discuss brain reorganization after stroke. Also, VMHC between cognitive brain areas in acute stage had significant correlation with clinical behavioral performance in chronic period which might be meaningful in predicting motor outcome.

1675

Exploring visual network connectivity in the mouse brain using DCM fMRI
Arun Niranjan¹, Peter Zeidman², Jack A Wells¹, and Mark F Lythgoe¹

¹Centre for Advanced Biomedical Imaging, University College London, London, United Kingdom, ²Institute of Neurology, University College London, London, United Kingdom

Understanding effective (i.e. causal) connectivity in the brain using fMRI with dynamic causal modelling (DCM) has attracted a large amount of interest in recent years. Applications of fMRI to map brain function in the mouse are on the rise, targeting transgenic mouse models of pathology. However, DCM has not yet been applied to mouse brain fMRI, in part due to the difficulties of acquiring high quality data. In this work we demonstrate the use of DCM fMRI to understand effective connectivity in the healthy mouse visual system, showing results consistent with the underlying biology.

1676

Task-related dynamic functional connectivity in fast fMRI

Ashish Kaul Sahib¹, Michael Erb¹, Klaus Scheffler², Thomas Ethofer¹, and Niels Focke³

¹Biomedical magnetic resonance, University of Tuebingen, Tuebingen, Germany, ²Max-Planck-Institute for Biological Cybernetics, Tuebingen, Germany, ³Department of Neurology/Epileptology, University of Tuebingen, Tuebingen, Germany

Recent advances in simultaneous multi-slice imaging have improved the temporal resolution of fMRI. Using a sliding window approach we aimed to capture the dynamic network changes that occur during visual stimulation. We estimated the functional connectivity degree (FCD) at various stimulation lengths and window sizes. We demonstrate that the analysis of dynamic functional connectivity using a sliding window approach is an effective technique to capture whole brain temporal dynamics during a simple block-designed visual experiment (checkerboards). In summary, for the current setup, a window size of 13.s provided an optimum trade-off between temporal smoothness and FCD estimation.

1677

CEEMD-based Multi-Spectrum Brain Networks for Identification of MCI

Li Zheng¹, Long Qian¹, Dandan Zheng², and Jiahong Gao^{3,4}

¹Department of Biomedical Engineering, College of Engineering, Peking University, Beijing, China, People's Republic of, ²GE Healthcare, MR Research China, Beijing, Beijing, China, People's Republic of, ³Beijing City Key Lab for Medical Physics and Engineering, Institute of Heavy Ion Physics, School of Physics, Peking University, Beijing, China, People's Republic of, ⁴Center for MRI Research, Academy for Advanced Interdisciplinary Studies, Peking University, Beijing, China, People's Republic of

The early detection of MCI is of paramount importance for possible delay of the transition from MCI to AD. Recently, several resting-state fMRI based neural imaging studies have been applied for MCI diagnosis by the aid of pattern classification recently. In current study, CEEMD-based high-dimensional pattern classification framework was proposed to identify MCI individuals from subjects who experience normal aging with an accuracy of 93.3 percent, compared to conventional method for brain oscillation separation. In addition, the most discriminant regions selected by our method also reflected the association with MCI, to some degree.

1678

Age related fluctuation energy and variation of dynamic functional connectivity

Yuanyuan Chen¹, Weiwei Wang¹, Xin Zhao¹, Miao Sha¹, Yanan Liu¹, Peng Zhou¹, Hongyan Ni², and Dong Ming¹

¹Tianjin University, Tianjin, China, People's Republic of, ²Tianjin First Central Hospital, Tianjin, China, People's Republic of

To reveal the age related changes of dynamic function connectivity during rest, five networks were extracted from resting stated fMRI data of 36 young people and 32 old people. The sliding window was carefully selected and the FC variation and the fluctuation energy in detailed frequency band were statistically compared. Decreased FCV and slowing fluctuation in inter-networks were mainly found in old group. OCC and CON, OCC and FP were the most consistent inter-networks between this two age related changes. We concluded that FCV and fluctuation energy had provided a new perspective of aging research.

1679

Association between structural and functional inter-subject variability of the motor and visual networks

Maxime Chamberland^{1,2}, Gabriel Girard², Michaël Bernier¹, Michael Paquette², David Fortin³, Maxime Descoteaux², and Kevin Whittingstall^{1,4}

¹Nuclear Medicine and Radiobiology, Université de Sherbrooke, Sherbrooke, QC, Canada, ²Computer science, Université de Sherbrooke, Sherbrooke, QC, Canada, ³Division of Neurosurgery and Neuro-Oncology, Université de Sherbrooke, Sherbrooke, QC, Canada, ⁴Department of Diagnostic Radiology, Université de Sherbrooke, Sherbrooke, QC, Canada

"Your brain is unique" is an unequivocal sentence that has spanned many research topics in the recent years. For example, functional connectivity (FC) based on resting-state fMRI is highly variable from one subject to the next, yet the source of this variability is unclear. Understanding the source of FC variability is important as it is often used in clinical studies. Here, we explore how this might be explained by variability of white-matter structural connectivity (SC) derived from diffusion MRI tractography connectivity matrices. Our results show that, across multiple brain areas, motor and visual networks show the lowest inter-subject variability. This suggests that, at least in these areas, SC might explain a portion of FC variability.

1680

Interhemispheric Functional Connectivity Modulated by Menstrual Cycle

Xinyuan Miao¹, Lin Shi¹, Yan Zhuo², and Yihong Yang³

¹Department of Medicine and Therapeutics, Chinese University of Hong Kong, Hong Kong, Hong Kong, ²Institute of Biophysics, Chinese Academy of Sciences, Beijing, China, People's Republic of, ³National Institute on Drug Abuse, NIH, Baltimore, MD, United States

The functional lateralization of the brain was modulated by the menstrual cycle of women, while the mechanism of which still need to investigate. In this study, we used interhemispheric functional connectivity of the resting-state functional MRI to investigate changes in the symmetrical interhemispheric correlations in women's different menstrual phases. Our results showed that the brainstem and

cerebellum had significantly higher interhemispheric correlations in the early follicular phase than in the mid-luteal phase.

1681

Combining Resting-State fMRI and Perfusion maps for potential Pre-Surgical Planning

Lalit Gupta¹, Prativa Sahoo¹, Pradeep K Gupta², Indrajit Saha³, Rana Patir⁴, Sandeep Vaishya⁴, and Rakesh K Gupta²

¹Philips India Ltd., Bangalore, India, ²Department of Radiology, Fortis Memorial Research Institute, Gurgaon, India, ³Philips India Ltd., Gurgaon, India, ⁴Department of Neurosurgery, Fortis Memorial Research Institute, Gurgaon, India

Mapping of functionally active regions for patients with mass lesions is critical for pre-surgical planning. We have developed an atlas based approach that automatically select seed points from six functional regions (motor and language regions) and computes corresponding functionally connected regions using resting state fMRI data. Functional connectivity maps were super-imposed on MR perfusion maps and structural images. Results were obtained from 22 brain tumor patients. Regions near the tumor with high correlation are seen as active regions that contribute to motor/language activities, combined with perfusion maps may help clinicians for better surgical planning.

1682

Memory and Learning: Visually-evoked Olfactory fMRI Activation Patterns and its Dynamics

Prasanna Karunanayaka¹, Xin Zhang², Michael Tobia¹, Jianli Wang¹, Bin Zhang², Bin Zhu², and Qing Yang¹

¹Radiology, Penn State University, Hershey, PA, United States, ²The affiliated Drum Tower hospital of Nanjing university medical school, Nanjing, China, People's Republic of

Behavioral studies show that human odor perception is highly dynamic, incorporates both spatial and temporal codes, and is easily influenced by information from other sensory systems such as vision. However, the neural representation of odor perception and its dynamic processing by the brain is poorly understood. In this research, using olfactory task fMRI, we attempt to unravel how olfactory-related neural networks interact in both space and time in order to explore how the olfactory and the visual systems integrate information at the central or perceptual levels in the human brain.

1683

Quasi-periodic pattern of fMRI contributes to functional connectivity and explores difference between Major Depressive Disorder and control

Kai Wang¹, Waqas Majeed², Garth Thompson³, Kui Ying⁴, Yan Zhu⁵, and Shella Keilholz⁶

¹Department of Biomedical Engineering, Tsinghua University, Beijing, China, People's Republic of, ²Department of Electrical Engineering, LUMS School of Science and Engineering, Lahore, Pakistan, ³Department of Radiology and Biomedical Imaging, Yale University, New Haven, CT, United States, ⁴Department of Engineering Physics, Tsinghua University, Beijing, China, People's Republic of, ⁵Psychiatry Department, Yu Quan Hospital, Tsinghua University, Beijing, China, People's Republic of, ⁶Department of Biomedical Engineering, Emory University/Georgia Institute of Technology, Atlanta, GA, United States

Quasiperiodic patterns (QPPs) of BOLD fluctuations, first reported in [1,2] are likely contributors to functional connectivity (FC) due to their spatial and temporal structure. FC has been widely used to explore the altered brain organization in patients suffering from psychological disorders like Major Depressive Disorder (MDD). In this project, we examined the contribution of QPPs to FC in both normal subjects and MDD patients. Results showed that QPPs are a major contributor to FC, and that QPP abnormality can be a contributor to or marker of psychiatric or neurological disorders.

1684

Investigation of functional connectivity changes in Alzheimer's disease and amnestic mild cognitive impairment using Degree Centrality

Yong Zhang¹, Naying He², Hua-Wei Lin², Ajit Shankaranarayanan³, Zhenyu Zhou¹, and Fu-Hua Yan²

¹MR Research China, GE Healthcare, Beijing, China, People's Republic of, ²Radiology, Ruijin Hospital, Shanghai Jiaotong University School of Medicine, Shanghai, China, People's Republic of, ³GE Healthcare, Menlo Park, CA, United States

This preliminary study investigated functional connectivity changes in Alzheimer's Disease (AD) and amnestic mild cognitive impairment (MCI) using degree centrality (DC), a novel resting-state fMRI parameter to provide voxel-wise whole brain functional connectivity measurement. Twelve AD patients, twelve MCI patients and fifteen healthy controls were recruited for comparison. As compared to normal controls, AD patients showed the decreased DC in the posterior cingulate cortex while MCI patients showed decreased DC in bilateral cuneus (visual processing) but increased DC in bilateral hippocampus (memory) and right angular gyrus (language). The different patterns of FC changes might provide insight into disease evolution.

1685

Ebola Alters Some, But Not All, Resting-State Intrinsic Functional Connectivity Networks In The Macaque Brain

Eswar Damaraju¹, Margaret Lenz², Jeffrey David Lewine^{1,3}, David Thomasson², Nadia Biassou⁴, Anna Honko², Vince Calhoun¹, and Peter Jahrling²

¹Mind Research Network, Albuquerque, NM, United States, ²Integrated Research Facility/NIAID, Frederick, MD, United States, ³Lovelace Family of Companies, Albuquerque, NM, United States, ⁴NIH Clinical Center, Bethesda, MD, United States

Ebola has the potential to cause both acute and chronic compromise of neurological status. To better understand the relevant neurobiology, a pilot MRI study of infected macaques was performed. Data indicate that Ebola exposure leads to acute disruption of some, but not all, intrinsic connectivity networks, even in the absence of intraparenchymal lesions. These studies represent the first non-invasive functional imaging studies of living, Ebola infected non-human primates.

Aberrant salience network and its functional coupling with default and executive networks in minimal hepatic encephalopathy: a resting-state fMRI study
Hua-Jun Chen¹

¹The First Affiliated Hospital of Nanjing Medical University, Nanjing, China, People's Republic of
Aberrant functional coupling of triple network in MHE

Effect of Brain Tumours on the Default Mode Network
Sukhmanjit Ghuman¹, David Fortin¹, Stephen Cunnane¹, and Kevin Whittingstall¹

¹Centre Hospitalier Universitaire de Sherbrooke (CHUS), Sherbrooke, QC, Canada

The effect of various pathologies on the default mode network (DMN) have been investigated in recent years with some encouraging results. These studies have found that some diseases of the nervous system, such as brain tumours, can have an effect on DMN connectivity. The goal of this novel research was to investigate whether tumours of certain areas of the brain or of certain histological type had disproportionately large effects on the DMN. We believe that DMN connectivity could be developed into a prognostic score in the future which might help clinicians in making key treatment decisions for brain cancer patients.

Training Induced Olfactory Network Changes in Master Sommeliers: Connectivity Analysis Using Granger Causality and Graph-theoretical Approach.
Karthik R Sreenivasan¹, Xiaowei Zhuang¹, Virendra Mishra¹, Zhengshi Yang¹, Gopikrishna Deshpande², Sarah Banks¹, and Dietmar Cordes¹

¹Cleveland Clinic Lou Ruvo Center for Brain Health, Las Vegas, NV, United States, ²AU MRI Research Center, Department of Electrical and Computer Engineering, Auburn University, Auburn, AL, United States

Current study used fMRI to investigate differences in effective connectivity and network topology between a group of trained master sommeliers and untrained control participants during olfactory tasks. Master sommeliers showed stronger connectivity originating from regions involved in higher-level cognitive processes than the controls. There was also increased small-world topology in the sommeliers. These findings provide unique insights into the neuroplasticity in adulthood in the olfactory network which may have added clinical importance in diseases like Alzheimer's and Parkinson's where early neurodegeneration is isolated to regions important in smell.

Structural and Functional Brain Alterations in Uremic restless legs syndrome patients: A Voxel-Based Morphometry and Functional Connectivity Study
DUN DING¹, PENG LI², Ji Xin Liu², Xue Ying Ma², and Ming Zhang²

¹XI'AN JIAO TONG UNIVERSITY, XI'AN, China, People's Republic of, ²XI'AN, China, People's Republic of

To investigate the structure and function changes in the brain in uremic RLS patients using a resting-state function magnetic resonance imaging (fMRI) paradigm, we used A voxel-based morphometry(VBM) method and a seed-based method to find the abnormality in end-stage kidney disease patients. Our results suggest that the characteristics of the connectivity changes may reflect the pathways involved in producing uremic RLS symptoms.

Zinc Nanoparticles Enhance Brain Connectivity in the Canine Olfactory Network: Evidence from an fMRI Study in Fully Unrestrained Conscious Dogs
Bhavitha Ramaiahgari¹, Oleg M Pustovyy², Paul Waggoner³, Ronald J Beyers¹, John Schumacher⁴, Chester Wildey⁵, Edward Morrison², Nouha Salibi^{1,6}, Thomas S Denney^{1,7,8}, Vitaly J Vodyanoy², and Gopikrishna Deshpande^{1,7,8}

¹Dept of Electrical & Computer Engr, AU MRI research center, Auburn University, Auburn, AL, United States, ²Dept. of Anatomy, Physiology & Pharmacology, Auburn University, Auburn, AL, United States, ³Canine Detection Research Institute, Auburn University, Auburn, AL, United States, ⁴Dept. of Clinical Sciences, Auburn University, Auburn, AL, United States, ⁵MRRA Inc, Euless, TX, United States, ⁶MR R&D, Siemens healthcare, Malvern, PA, United States, ⁷Dept. of Psychology, Auburn University, Auburn, AL, United States, ⁸Alabama Advanced Imaging Consortium, Auburn University and University of Alabama Birmingham, Birmingham, AL, United States

There is intense interest in strategies for enhancing olfaction capabilities of dogs for various applications such as bomb detection. Prior fMRI studies showed increased neural activation when zinc nanoparticles were added to the odorants. In this study, we obtained fMRI data from awake and unrestrained dogs when they were exposed to odorants with and without zinc nanoparticles and zinc nanoparticles alone. We observed that zinc nanoparticles up-regulated directional brain connectivity in parts of the canine olfactory network. This provides a mechanistic explanation for previously reported enhancement in the odor detection capability of the dogs in the presence of zinc nanoparticles.

Altered amplitude of low-frequency fluctuations and connectivities in depressed SAPHO syndrome
Jie Lu¹, Yan-ping Duan², Wen-rui Xu¹, Xue-wei Zhang³, Chen Li⁴, and Wei-hong Zhang¹

¹Department of Radiology, Peking Union Medical College Hospital, Beijing, China, People's Republic of, ²Department of Psychology, Peking Union Medical College Hospital, Beijing, China, People's Republic of, ³Department of Interventional radiology, China Meitan General Hospital, Beijing,

To investigate depressed symptoms in SAPHO (Synovitis, acne, pustulosis, hyperostosis, osteitis) syndrome and confirm depression in SAPHO using resting-state functional magnetic resonance imaging (rs-fMRI). We recruited twenty-four SAPHO patients and fifteen age- and gender-matched normal controls (NC). Twelve of the SAPHO patients were diagnosed with depression. Moreover, depressed SAPHO patients (D-SAPHO) were proved to have abnormal amplitude of low frequency fluctuations (ALFF) and functional connectivities (FC) involved in the regional brain changes which showed correlated with the severity of depression. These findings provide crucial information to understand the neural mechanisms of depressed SAPHO and are helpful to diagnose depression in SAPHO.

1692

Cocaine and the synthetic cathinone MDPV reduce small world brain network topology: a rat functional connectivity study
Luis Manuel Colon-Perez¹ and Marcelo Febo¹

¹Psychiatry, University of Florida, Gainesville, FL, United States

Drug abuse has detrimental effects on the brain function, which lead to drug use disorders. In vivo non-invasive biomarkers are needed to determine the neurobiological outcomes of addictive drugs on the brain. Functional MRI and graph theory offer an analytical approach to address brain network changes associated with psychiatric disorders. In the present study we determined the effects of two addictive psychostimulant drugs. Comparison between saline and drug administered shows a reduction in the connectivity at 1 hr but not at 24 hrs. Acute administration of the two psychostimulants studied produce only transient effects lasting at least 1 hr.

1693

Resting-state functional activity and brain network abnormalities in betel nut chewers
Yu-Syuan Chou¹, Ming-Chou Ho², and Jun-Cheng Weng^{1,3}

¹Department of Medical Imaging and Radiological Sciences, Chung Shan Medical University, Taichung, Taiwan, ²Department of Psychology, Chung Shan Medical University, Taichung, Taiwan, ³Department of Medical Imaging, Chung Shan Medical University Hospital, Taichung, Taiwan

Betel nut, also known as areca, is the fourth most commonly used drug worldwide after tobacco, alcohol, and caffeine and also a stimulant and addictive substance. Previously, CM Chen et al. probed into the influence of religious affiliation on heavy betel nut chewing, and studied on the relationship between health risk perception and betel nut chewing. Feng Chen et al. analyzed gray matter abnormalities between betel nut chewers and healthy subjects with voxel-based morphometry (VBM). However, there were few studies mentioned about the functional activity and brain network changes in betel nut chewers using functional magnetic resonance imaging (fMRI). Therefore, our aim was to use resting-state fMRI (rs-fMRI) to investigate the functional differences between betel nut chewers and healthy participants with amplitude of low frequency fluctuations (ALFF) and regional homogeneity (ReHo). The graph theoretical and network-based statistic (NBS) analyses were also used to find the network difference between two groups. Our results revealed different topological organization and poor global integration of the brain network in the betel nut chewers.

1694 Can Cerebral Functional Deficits Be Detected in Patients with Ankylosing Spondylitis? A Cross-sectional Study

Jun Zhao¹, Chuan-Ming Li¹, Xin Wei¹, and Jian Wang¹

¹Radiology, Southwest Hospital, Third Military Medical University, Chongqing, China, People's Republic of

This study aimed to investigate any cerebral function deficits in AS(Ankylosing spondylitis) using functional MRI technology and its possible relationship to clinical and laboratory results. Compared with normal controls, AS patients showed widespread brain fMRI signals. Measurement of functional connectivity strength of the left precuneus and the left middle temporal gyrus may aid in the clinical detection and evaluation

1695

Functional dysconnection between anterior cingulate cortex and thalamus in patients with Kleine-Levin syndrome
Ting-Chih Wang¹, Yao-Chia Shih^{2,3}, Hong-Huei Liu⁴, and Wen-Yih Issac Tseng^{3,5}

¹Department of Electrical Engineering, National Taiwan University, Taipei, Taiwan, ²Institute of Biomedical Engineering, National Taiwan University, Taipei, Taiwan, ³Institute of Medical Device and Imaging, National Taiwan University College of Medicine, Taipei, Taiwan, ⁴Department of Neurology, National Taiwan University Hospital, College of Medicine, National Taiwan University, Taipei, Taiwan, ⁵Molecular Imaging Center, National Taiwan University, Taipei, Taiwan

Kleine-Levin Syndrome is a rare neurological disorder characterized by recurrent episodes of excessive sleepiness and other symptoms listed in the ICSD Diagnostic Criteria for KLS. Its etiology is still unknown nowadays. The most consistent finding in KLS is abnormal thalamic function. Here, we used seed-based analysis to analyze resting state fMRI obtained from 2 patients with KLS. In bilateral thalamic seeding, both patients showed decreased connection between the thalamus and the anterior cingulate cortex. This result could be attributed to alteration of the dorsal pathway in ascending arousal system, and might also explain their attention deficits.

1696

Pinpointing the rat cerebellar and medullary noxious networks with fMRI based fcMRI
Rupeng Li¹, Xiping Liu², Jason Sidabras¹, Christopher Pawela³, Andrzej Jesmanowicz¹, and James Hyde¹

¹Biophysics, Medical College of Wisconsin, Milwaukee, WI, United States, ²Dermatology, Medical College of Wisconsin, Milwaukee, WI, United States, ³Anesthesiology, Medical College of Wisconsin, Milwaukee, WI, United States

Pinpoint acquisition of high resolution, true whole brain scale fcMRI sensorimotor network using seed based analysis. We are able to greatly reduce susceptibility induced artifact in deep brain structures while keeping great SNR and depth sensitivity. fcMRI networks in

cerebellum and modular areas are demonstrated with intermediate reticular nucleus (IRt) observed.

1697

Functional connectivity changes in attention-related networks of childhood leukemia survivors

Charlotte Sleurs¹, Iris Elens², Jurgen Lemiere¹, Thibo Billiet³, Dorothée Vercruyse⁴, Patricia Blijtebier⁵, Marina Danckaerts², Rudi D'Hooghe⁶, Ron Peeters³, Stefan Sunaert³, Anne Uyttebroeck¹, Stefaan Van Gool⁷, and Sabine Deprez³

¹Pediatric Hemato-Oncology, UZ Leuven, Leuven, Belgium, ²Child and Adolescent Psychiatry, UZ Leuven, Leuven, Belgium, ³Radiology, UZ Leuven, Leuven, Belgium, ⁴Gynaecological Oncology, UZ Leuven, Leuven, Belgium, ⁵School Psychology and Child and Adolescent Development, KU Leuven, Leuven, Belgium, ⁶Biological Psychology, KU Leuven, Leuven, Belgium, ⁷Pediatric Hemato-Oncology, University Hospital, Aachen, Germany

Neurocognitive sequelae in childhood leukemia survivors are often related to attentional dysfunction. We investigated whether altered functional brain connectivity might explain neurocognitive sequelae in childhood leukemia survivors. Resting state fMRI was investigated, by using ROI-based connectivity comparisons as well as dual regression analysis at whole-brain level. We demonstrated that the Default Mode Network (DMN) and Inferior Temporal Gyrus, was less functionally connected in childhood leukemia survivors compared to controls. This suggests an altered coherence between activity of the DMN and Fronto-Parietal Network (FPN). Finally, based on this specific connectivity we could predict clearly reduced cognitive flexibility of the patients.

1698

Effects of long-duration isoflurane administration on default mode network of macaque brains

Chun-Xia Li¹ and Xiaodong Zhang^{1,2}

¹Yerkes Imaging Center, Yerkes National Primate Research Center, Emory University, Atlanta, GA, United States, ²Division of Neuropharmacology and Neurologic Diseases, Yerkes National Primate, Atlanta, GA, United States

Long-duration anesthesia administration could cause neurocognitive decline in animals and humans. However, the potential mechanism still remains unclear. In the present study, the functional connectivity of adult rhesus monkeys under maintenance dosage of isoflurane (~1 %) for four hours was examined. The results demonstrate that long-duration isoflurane exposure resulted in decreased functional connectivity in posterior cingulate cortex (PCC) dominant default-mode network (DMN). The MRI findings suggest that the detrimental effects of isoflurane on brain connectivity may be associated with the neurocognitive decline observed in subjects after long-duration administration of isoflurane.

1699

Neurofeedback impact onto the brain networks interaction: fMRI study

Oleksii Omelchenko¹ and Volodymyr Rogozhyn²

¹Human and Animal Physiology, Taras Shevchenko National University of Kyiv, Kyiv, Ukraine, ²Radiology, Medical Clinic BORIS, Kyiv, Ukraine

Concerning the use of audio-visual stimulation (AVS) as a component of neurofeedback therapy for neuropsychiatric disorders we propose to evaluate its effect onto the brain networks interaction. We performed fMRI before and after the AVS. fMRI exams showed considerable increase of the volumes of activation after the AVS and almost complete extinction of the DMN deactivation. RS fMRI showed functional connectivity changes after the AVS (connectivity disruption in visual network, DMN frequency shift). Volume of activation increase and functional connectivity changes could be the marker for prolonged effect of AVS brain stimulation.

1700

Spatial and temporal modulation of brain dynamics in response to task execution

Silvia Tommasin^{1,2}, Daniele Mascali^{1,3}, Tommaso Gili^{1,2}, and Federico Giove^{1,2}

¹Enrico Fermi Centre, Rome, Italy, ²Fondazione Santa Lucia, Roma, Italy, ³Physics, Università La Sapienza, Roma, Italy

Task-related activity influences brain connectivity through a two-level pattern modulation both in attentive networks and in the default mode network. While strengthening the local homogeneity, task execution reduces regional synchronization. It produces correlation patterns with opposite large and small scale properties. Task-related activity influences also the amplitude of the low frequency fluctuations in the same networks. The transition from resting state to steady state task execution, and the way back, causes a persisting slow drift in this quantity.

1701

Multi-node directed cortical network for speech processing revealed by multivariate Granger causality analysis

Yayan Yin¹, Jiahong Gao¹, Bing Wu², Yang Fan², Bingjiang Iyu¹, and Jianqiao Ge¹

¹Peking University, Beijing, China, People's Republic of, ²GE Healthcare, Beijing, China, People's Republic of

For decades, how the information flows among multiple brain regions remains unclear for speech processing, due to the challenge of mapping multi-node directed cortical pathways from brain images. In this work, multivariate Granger causality analysis is employed on functional MR images to reveal the effective connectivity of Chinese language-speech network for the first time. The results showed that left insula and posterior middle temporal gyrus were the strong driver nodes, the left middle frontal gyrus and superior temporal gyrus were the most received nodes in the network. We also found greater interhemispheric connectivity in females compared to males.

1702

Modular Reorganization of Resting-State Brain Network in Patients with Obstructive Sleep Apnea

Bumhee Park¹, Sudhakar Tummala¹, Ruchi Vig¹, Daniel W Kang², Mary A Woo³, and Rajesh Kumar^{1,4,5,6}

¹Anesthesiology, University of California at Los Angeles, Los Angeles, CA, United States, ²Medicine, University of California at Los Angeles, Los

Obstructive sleep apnea (OSA) condition is accompanied by brain tissue injury and functional deficits in regions serving autonomic, neuropsychologic, and cognitive functions. Brain networks are organized into modular systems and assigning vulnerable role for each region in terms of intra- and inter-modular communication provides better understanding for functional deficits in the condition. We examined the modular reorganization of OSA functional networks, and found abnormal intra- and/or inter-modular communication roles in brain regions involved in autonomic, neuropsychologic, and cognitive regulation. The findings suggest that dysfunctions associated with OSA may be related to abnormal information flow, and can be examined with modular reorganization assessment.

1703

Bilateral amygdaloid functional connectivity in chronic alcoholics
Ylin Zhao¹, Jun Chen², and Hui Lin³

¹Radiology, Renmin Hospital of Wuhan University, Wuhan, China, People's Republic of, ²Renmin Hospital of Wuhan University, Wuhan, China, People's Republic of, ³Healthcare, MR Research China, Beijing, China, People's Republic of

FC-MRI is a useful tool for examining functional relationships between the bilateral amygdaloid and whole brain regions. The functional coordination of bilateral amygdala and cerebral cortex was enhanced, and the functional coordination of bilateral amygdala and cerebellum was weakened. Amygdala may be involved in regulating the function of fronto-cerebellar loops. Thus, this method shows promise as a tool for *in vivo* investigations of the functioning of human fronto-cerebellar circuitry. It is our hope that in future studies this technique may provide the opportunity to examine the integrity of networks involving the brain cerebellum in patient groups with chronic alcoholics, a major goal of our research.

1704

Putamen-related regional and network functional deficits in first-episode schizophrenia with auditory verbal hallucinations
Long-Biao Cui¹, Yi-Bin Xi¹, and Hong Yin¹

¹Xijing Hospital, Fourth Military Medical University, Xi'an, China, People's Republic of

Our results suggest an association of abnormal regional function in the putamen and prefrontal cortex and hyperconnectivity between them with AVHs in SZ. The functional interaction of the putamen with DLPFC and Broca's area seems to be crucial for AVHs in SZ. Additionally, the putamen-related regional and network functional deficits may also serve as a potential diagnostic biomarker of AVHs in SZ based on the direct evidence *in vivo* we found. In SZ patients, there is an extensive hypoconnectivity within cortical-striatal-cerebellar networks, which further supports the current thinking about disconnection hypothesis of SZ.

1705

Light isoflurane sedation: an excellent trade-off between anesthesia and awake condition in functional connectivity studies with rats
Jaakko Paasonen¹, Raimo A Salo¹, Artem Shatillo², and Olli Gröhn¹

¹Department of Neurobiology, University of Eastern Finland, Kuopio, Finland, ²Charles River Discovery Services, Kuopio, Finland

Prevention of motion is a prerequisite for preclinical functional connectivity (FC) studies. However, anesthesia alters brain function, and awake protocols may induce stress. Therefore, we investigated the feasibility of using light sedation in FC studies. FC was estimated under 0.1/0.5% isoflurane (subanesthetic doses) with acclimatized rats, and under 1.3% isoflurane (anesthetic dose). Results demonstrate different FC between anesthetic and subanesthetic doses. The physiologic measures suggest, that the 0.5% rats adapted well to imaging, while the 0.1% rats did so insufficiently. Therefore, light isoflurane sedation may provide an excellent combination for FC investigations: minimal stress and motion with normal brain function.

1706

Visual Networks Impairments in Minimal Hepatic Encephalopathy Using Resting-State fMRI
Yun Jiao¹, Xun-Heng Wang², and Tian-Yun Tang¹

¹Jiangsu Key Laboratory of Molecular and Functional Imaging, Department of Radiology, Zhongda Hospital, Medical school of Southeast University, Nanjing, China, People's Republic of, ²College of Life Information Science and Instrument Engineering, Hangzhou Dianzi University, Hangzhou, China, People's Republic of

We applied dual regression to investigated functional connectivity impairments within visual networks for minimal hepatic encephalopathy (MHE) patients' brain. Functional deficits within occipital and lateral visual networks (visual area V2 and V3) were endogenous, and significantly association with neurocognitive impairments. This maybe the reason for the compensatory enhancements within medial visual network (visual area V1) which indicated that patients with MHE had the potential to additionally recruit more neurological resource to process the spatial information from visual areas V2 and V3. Our results demonstrated the possible mechanisms for deficits in visual perception, visuo-spatial orientation, and visuo-constructive abilities in MHE patients

1707

Acupuncture Stimulation changes DMN functional connectivity.

Tomokazu Murase¹, Masahiro Umeda¹, Masaki Fukunaga², Katsuya Maruyama³, Yuko Kawai¹, Yasuharu Watanabe¹, and Toshihiro Higuchi⁴

¹Medical Informatics, Meiji University of Integrative Medicine, Nantan-shi, Japan, ²Cerebral Integration, National Institute for Physiological Sciences, Okazaki-shi, Japan, ³Research&Collaboration, Siemens Japan, Shinagawa-ku, Japan, ⁴Neurosurgery, Meiji University of Integrative Medicine, Nantan-shi, Japan

Clinical studies have shown that acupuncture relieves different kinds of pain. However, the effectiveness of these methods is unclear. We used rs-fMRI and FC analysis to examine the RSN activity before and after acupuncture stimulation. In the result, DMN was changed with or without manual acupuncture. The acupuncture stimulation controls a pain by modifying mechanism of pain transmission.

1708

Intrinsic functional connectivity in patients with presbycusis

Fei Gao¹, Guangbin Wang¹, Bin Zhao¹, Muwei Li², Fuxin Ren¹, and Weibo Chen³

¹Shandong Medical Imaging Research Institute, Shandong University, JINAN, China, People's Republic of, ²College of Electronics and Information Engineering, Sichuan University, Chengdu, China, People's Republic of, ³Philips Healthcare, Shanghai, China, People's Republic of

Presbycusis is the most common sensory deficit in the ageing population. However, little is known about whether the topological properties of brain functional networks is disrupted in patients with presbycusis. Our study demonstrates decreased clustering coefficient, local efficiency and strength in the primary auditory cortex in patients with presbycusis, as compared to age- and gender-matched healthy controls. Our study provides evidence of presbycusis-related disruptions in brain functional networks in patients with presbycusis. It is believed that our findings could be important for exploring functional changes in the central presbycusis.

1709

Altered small world brain function network in patients of lower back pain

Jing Liu¹, Xiufen Liu², zhizheng Zhuo³, Juan Wei⁴, Queenie Chan⁵, and Xiaoying Wang¹

¹Radiology, Peking University First Hospital, Beijing, China, People's Republic of, ²Anesthesiology, Peking University First Hospital, Beijing, China, People's Republic of, ³Philips Healthcare Beijing China, Beijing, China, People's Republic of, ⁴Philips Research China, Shanghai, China, Shanghai, China, People's Republic of, ⁵Philips Healthcare, China, Hongkong, China, People's Republic of

An altered functional network was found in the brain of LP here represents a less optimal network organization in the LP. It has been suggested that the small-world structure reflects an optimal balance between local processing and global integration. And the small-world structure of LP brain networks maybe destroyed due to the chronic LP.

1710

Subregion-specific Resting-State Amygdala Connectivity in Chronic Knee Osteoarthritis Pain: Towards a brain network signature of OA pain

William J Cottam^{1,2,3}, Marianne Drabek^{1,2,3}, Diane Reckziegel^{1,2,3}, and Dorothee P Auer^{1,2,3}

¹Division of Clinical Neuroscience, Radiological Sciences, University of Nottingham, Nottingham, United Kingdom, ²ARUK Pain Centre, University of Nottingham, Nottingham, United Kingdom, ³Sir Peter Mansfield Imaging Centre, University of Nottingham, Nottingham, United Kingdom

Brain network connectivity analysis arguably offers the most sensitive marker to detect dysfunctional brain plasticity underlying the maladaptive nature of chronic pain. Early functional connectivity (fc) studies reveal altered functional connectivity in chronic pain states, but to the best of our knowledge no studies have focussed upon the amygdala. We aimed to investigate whether patients with painful chronic knee OA show altered amygdala connectivity compared to pain-free controls. This study identified increased functional connectivity of specific amygdala subnuclei in chronic OA pain patients compared to healthy subjects.

1711

Time-shift functional connectivity MRI based on specific regional-of-interest for mapping acute ischemic Stroke
xiaokun fang¹, qiang xu², yong zhang³, zhiquang zhang¹, and guangming lu¹

¹Medical Imaging, Jingling Hospital, School of Medicine, Nanjing University, Nanjing, Jiangsu, China, nanjing, China, People's Republic of,

²Medical Imaging, Jingling Hospital, School of Medicine, Nanjing, nanjing, China, People's Republic of, ³MR Research China, GE Healthcare, beijing, China, People's Republic of

To investigate if Time-shift functional connectivity based resting-state fMRI can be used to create maps similar to time-to-maximum of (Tmax) in acute stroke and to determine whether Maps obtained with the SSS seed (superior sagittal sinus) or whole brain as the seed in Time-shift functional connectivity based resting-state fMRI be better in mapping the acute stroke.

1712

Demonstration of brain tumor-induced abnormalities on regional homogeneity (ReHo) resting state fMRI metrics KCC-ReHo & Cohe-ReHo

Shruti Agarwal¹, Noushin Yahyavi-Firouz-Abadi¹, Haris I. Sair¹, Raag Airan¹, and Jay J. Pillai¹

¹Division of Neuroradiology, Russell H. Morgan Department of Radiology and Radiological Science, Johns Hopkins University School of Medicine, Baltimore, MD, United States

Disruption of the normal coupling between neural activity and the consequent microvascular blood flow response (neurovascular uncoupling or NVU) may severely compromise the validity of BOLD fMRI in presurgical planning. The effects of brain tumor-related NVU on resting state BOLD fMRI (rsfMRI) using functional connectivity analysis have been previously published. In this study we evaluated regional homogeneity (ReHo) of rsfMRI data based on Kendall's coefficient of concordance (KCC-ReHo) & Coherence (Cohe-ReHo) and compared the results with the amplitude of low-frequency fluctuation (ALFF) & standard motor tbMRI activation to investigate regional abnormalities due to brain tumor-induced NVU in sensorimotor network.

fMRI Physiology

Exhibition Hall

Tuesday, May 10, 2016: 13:30 - 15:30

1713

Breaking β : Understanding the β -Value in Calibrated Functional MRI
Avery J.L. Berman^{1,2} and Bruce Pike²

¹Montreal Neurological Institute, McGill University, Montreal, QC, Canada, ²Department of Radiology and Hotchkiss Brain Institute, University of Calgary, Calgary, AB, Canada

In calibrated functional MRI (fMRI), the parameter β is used to describe the non-linear dependence of the change in the transverse relaxation rate on the susceptibility offset (Δx) of blood relative to tissue. Estimates of β at high field strengths have generally been assumed or obtained in post-hoc analyses. Using simulations from vessel networks, we present here a detailed description of β 's dependence on vessel radius. We show that the estimate of β is highly dependent on the range of Δx used in the fit. This could have important implications for methods that propose to measure β -values *in vivo* using a contrast agent to alter Δx .

1714



Flow-diffusion constrained estimation of oxygen extraction fraction and tissue oxygen tension by dual calibrated fMRI
Michael Germuska¹, Alberto Merola¹, and Richard G Wise¹

¹CUBRIC, Cardiff University, Cardiff, United Kingdom

An emerging method for quantitative mapping of OEF is by dual calibration of the BOLD signal.^{1,2} However, this method is highly sensitive to measurement noise, resulting in unstable estimates of OEF. An alternative approach is to use flow-diffusion equations to calculate the biophysically supported OEF.³ However, this approach is limited by the need to assume a tissue oxygen tension (PtO₂). We propose a method for combining these two approaches, producing calibrated BOLD estimates of OEF that are constrained by a modelled flow-diffusion relationship of oxygen extraction. The proposed method is shown to produce stable estimates of OEF and PtO₂.

1715

Do human cerebral arteries contain fully oxygenated blood?
Esther AH Warnert¹, Ian D Driver¹, Joseph Whittaker¹, and Kevin Murphy¹

¹Cardiff University Brain Research Imaging Centre, Cardiff University, Cardiff, United Kingdom

When modelling the BOLD response it is often assumed that arterial blood is fully oxygenated, and that therefore contrast is driven solely by changes in venous oxygen saturation. Recent evidence has emerged from rodent studies indicating that precapillary arterioles may have an oxygenation level as low as 78%. Here, we assess arterial oxygenation *in vivo* in humans by using short inversion time ASL in normoxia, as well as hyperoxia. Our results suggest that imaging the BOLD response may not be affected by partially oxygenated arterioles.

1716

Flow Related Changes in Oxygen Extraction Fraction Detected using Streamlined-qBOLD
Alan J Stone¹ and Nicholas P Blockley¹

¹FMRIB, Nuffield Department of Clinical Neurosciences, University of Oxford, Oxford, United Kingdom

In this study we investigate the sensitivity of streamlined-qBOLD for detecting changes in baseline brain oxygenation and therefore its suitability for clinical application to vascular dysfunction and stroke. Baseline brain oxygenation is modulated in a group of normal volunteers using hypocapnia (a reduction in blood CO₂). In this group, streamlined-qBOLD measured significant ($p<0.05$) increases in grey matter R_{2'} and OEF, between normocapnic and hypocapnic conditions. This suggests the technique can provide important metabolic information in cases of vascular dysfunction where flow and brain oxygenation may be impaired.

1717

Detailing the Role of Systemic Blood Pressure in Somatosensory Mouse fMRI
Henning Matthias Reimann¹, Mihail Todiras², Michael Bader², Andreas Pohlmann¹, and Thoralf Niendorf^{1,3}

¹Berlin Ultrahigh Field Facility (B.U.F.F.), Max Delbrueck Center for Molecular Medicine, Berlin, Germany, ²Max Delbrueck Center for Molecular Medicine, Berlin, Germany, ³Experimental and Clinical Research Center, Charite-Universitaetsmedizin, Berlin, Germany

Combining mouse genomics and *functional magnetic resonance imaging* (fMRI) provides a promising tool to unravel the molecular mechanisms of somatosensation and pain. Recent studies suggest a confounding influence of *mean arterial blood pressure* (MABP) on the *blood oxygenation level-dependent* (BOLD) signal for somatosensory stimulation paradigms in mice. MABP alterations induced by transient stimuli can mimic brain activation in small rodents. The abstract provides data, which rely on the monitoring of MABP for mild noxious thermal stimulation in mice. Detailing the role of MABP in mouse fMRI is crucial to ensure the integrity of murine hemodynamic readouts in somatosensation and nociception.

1718

The effect of plasma-dissolved oxygen on the hyperoxic calibrated BOLD signal: a simulation study using the detailed BOLD model
Yuhan Ma¹, Avery Berman¹, and G. Bruce Pike^{1,2}

It has been suggested that during a hyperoxic calibration, the paramagnetic oxygen dissolved in arterial blood plasma can be a confounding factor for the interpretation of the calibrated BOLD signal. In this study, we aimed to predict the relative effect of dissolved oxygen on hyperoxic BOLD signal by expanding the detailed BOLD model with the effect of dissolved oxygen. Our results showed minimal difference in both the relative BOLD signal and the calibration parameter calculated with the effect of dissolved oxygen. Therefore, the influence of the dissolved oxygen in arterial blood plasma on the measured calibrated BOLD signal at 3 T can generally be ignored.

1719

Quantitative Susceptibility Mapping (QSM) based Cerebral Metabolic Rate of Oxygen (CMRO₂) Mapping: Improve Robustness with Preconditioning and Physiological Constraints

Jingwei Zhang^{1,2}, Dong Zhou², Thanh Nguyen², Pascal Spincemaille², Ajay Gupta², and Yi Wang^{1,2}

¹Biomedical Engineering, Cornell University, New York, NY, United States, ²Radiology, Weill Cornell Medical College, New York, NY, United States

This study proposed a new post-processing algorithm with preconditioning and physiological constraints for QSM based CMRO₂ mapping, which eliminated physiologically impossible OEF values and improved the robustness of the technique. Reproducibility of the proposed method was examined. Feasibility of hyperventilation as a more efficient blood flow challenge was also investigated.

1720

High-Resolution CMRO₂ Mapping During a Unilateral Pinch-Force Task

Maria Guidi¹, Christopher J. Steele¹, Laurentius Huber², Leonie Lampe¹, Viola Rjosk¹, Pierre-Louis Bazin¹, and Harald E. Möller¹

¹Max Planck Institute for Human Cognitive and Brain Sciences, Leipzig, Germany, ²NIMH, Bethesda, MD, United States

Motor tasks have been extensively studied with BOLD fMRI. The way the BOLD response scales with task intensity level might come from an increased metabolic activity as well as an increased CBF and CBV. In this study, we aimed at disentangling such contributions combining a gas manipulation session with a pinch-task with simultaneous recording of force values. This way, the Davis model for calibration of fMRI could be applied and the oxygen metabolism changes estimated at every timestep. BOLD signal changes, VASO signal changes, and CMRO₂ changes were shown to weakly scale with the intensity of the pinch-force task.

1721

Is the local functional connectivity anisotropy (LFCA) in white matter caused by neuro-electric activity? An examination of potential confounds for orientation-dependent LFCA in fMRI

Michael J. Tobia¹, David Gallagher¹, Rahul Dewal¹, Sebastien Rupprecht¹, Prasanna Karunanayaka¹, and Qing X. Yang¹

¹Radiology, Penn State Hershey, Hershey, PA, United States

Phantom experiments showed that fluctuating electric current is sufficient to generate local functional connectivity anisotropy (LFCA), and that effects of motion, such as Lorentz forces, cannot explain the alignment of eigenvectors through neighboring voxels or B₀ orientation-dependence. In conclusion, anisotropic correlations of fMRI time series may arise from an alternative non-BOLD contrast mechanism, potentially related to an electric current effect on B₀.

1722

Development of an evaluation system for analgesic drugs targeted to allodynia-specific pain using BOLD fMRI

Naoya Yuzuriha¹, Sosuke Yoshinaga¹, Hiroshi Sato², Sokichi Honda³, Keisuke Tamaki³, Toshihiro Sekizawa³, Akihiko Fujikawa³, and Hiroaki Terasawa¹

¹Department of Structural Biomaging, Faculty of Life Sciences, Kumamoto University, Kumamoto, Japan, ²Bruker Biospin K.K., Yokohama, Japan, ³Drug Discovery Research, Astellas Pharm. Inc., Tsukuba, Japan

The aim of this study is to evaluate the analgesic effect of pregabalin on allodynia-specific pain. fMRI images of fibromyalgia model rats were acquired, before and after pregabalin administration. When treated with saline, the BOLD signal intensities in the S1, IC, and TH were increased upon the laser stimulation by up to 1.7%, 1.3%, and 1.8%, respectively. In contrast, in the pregabalin treated rats, no BOLD responses were detected. It is conceivable that the pain signals were inhibited by pregabalin, and thus the stimulation-induced BOLD responses were not observed. We successfully observed the suppression of allodynia-specific pain responses by pregabalin.

1723

fMRI study of the role of glutamate NMDA receptor in olfactory habituation of olfactory bulb and higher olfactory structures in rats

Fuqiang Zhao¹, Xiaohai Wang², Hatim A Zariwala², Jason M. Uslaner², Andrea K Houghton², Jeffrey L Evelhoch¹, Eric Hostetler¹, and Catherine Diane Gard Hines¹

¹Imaging, Merck Co. & Inc., West Point, PA, United States, ²Neuroscience, Merck Co. & Inc., West Point, PA, United States

fMRI offers an excellent opportunity to study olfactory processing in different olfactory structures. Measurement of the magnitude of odor stimulation-induced activations, and their suppression with agonist/antagonist of different neural receptors can provide important information to understand the mechanism of olfactory habituation. In this study, cerebral blood volume (CBV) fMRI with USPIO was used to measure odorant-induced olfaction in different olfactory structures of rats. The dynamics of habituation in different olfactory structures can be robustly measured by fMRI. MK801 can reverse habituated olfactory responses in all olfactory structures, suggesting that glutamate/NMDA receptor plays a major role in olfactory habituation.

1724

Plastic-adaptive changes after articulatory training in the elderly: An fMRI study
Sachiko Kiyama¹, Atsunobu Suzuki², Shen-Hsing Annabel Chen³, and Toshiharu Nakai¹

¹National Center for Geriatrics and Gerontology, Obu, Japan, ²Nagoya University, Nagoya, Japan, ³Nanyang Technological University, Singapore, Singapore

The present fMRI study explored neural changes in the Japanese elderly after four weeks of articulatory training. We compared real and pseudo words (i.e., the difference in speech plan), and hard and easy consonants to articulate (i.e., the difference in motor plan). Results revealed that their training of pseudo words with easy consonants significantly reduced activity in various regions including language, motor, visual, and cerebellar areas. This finding indicates the neuroplasticity of the adaptive articulation learning ability in the elderly for newly-introduced speech sounds, especially with easy consonants which do not require complex articulatory movements.

1725

Olfactory sensory lateralization in the human brain
Michael J. Tobia¹, Abdou Thiam¹, Prasanna Karunananayaka², and Qing X. Yang¹

¹Radiology, Penn State Hershey, Hershey, PA, United States, ²Radiology, Penn State Hershey, Hershey, PA, United States

The olfactory system is unique from other sensory systems in that it is primarily ipsilateral from the periphery to the central nervous system. Using fMRI and a simple olfactory stimulus detection paradigm, we show a right hemispheric bias for sensory activation stemming from unilateral stimulation to either nostril. This suggests the presence of a contralateral functional organization of the olfactory system.

Traditional Poster

fMRI: Applications

Exhibition Hall

Tuesday, May 10, 2016: 13:30 - 15:30

1726

Both hypnotic and non-hypnotic suggestions dramatically alter clinical and experimental pain report. fMRI indicates stronger hypnotic responses and different mechanisms for clinical versus experimental pain
Stuart Derbyshire^{1,2}, Matthew Whalley³, Stanley Seah⁴, and David Oakley⁵

¹Clinical Imaging Research Centre, National University of Singapore, Singapore, Singapore, ²Psychology, National University of Singapore, Singapore, Singapore, ³Traumatic Stress Service, Berkshire Healthcare NHS Foundation Trust, Reading, United Kingdom, ⁴Psychological Medicine, National University of Singapore, Singapore, Singapore, ⁵Psychology and Language Sciences, University College London, London, United Kingdom

Both hypnotic and non-hypnotic suggestions dramatically alter clinical and experimental pain report. fMRI, however, indicates stronger hypnotic responses and different mechanisms for clinical versus experimental pain. The presence of different mechanisms could only be inferred from the fMRI data and not from the behavioral data.

1727

Mapping "phantom taste" in thermal tasters
Sally Eldeghaidy¹, Martha Skinner², Rebecca Ford², Joanne Hort², and Susan Francis¹

¹Sir Peter Mansfield Imaging Centre, University of Nottingham, Nottingham, United Kingdom, ²Sensory Science Centre, School of Biosciences, University of Nottingham, Nottingham, United Kingdom

Thermal taster status refers to a new taste phenotype in which thermal stimulation of the tongue elicits a "phantom" taste in individuals. The mechanism behind thermal taste is not yet known, but hypothesised to arise from entwined gustatory and trigeminal nerves. Here, we use fMRI to perform the first study to investigate whether cortical areas respond to phantom taste. Subjects underwent fMRI to warming/cooling thermal stimulation. Thermal tasters reported a sweet taste as the taste most prevalent during warming/cooling trials. We show that this "phantom" taste elicits significant activation of primary gustatory cortex including anterior insula and anterior cingulate cortex.

1728

The influence of multi-band acquisition on multiscale entropy derived from resting state BOLD
Charles B Malpas^{1,2}, Tim Silk³, and Marc Seal³

¹Developmental Imaging, Murdoch Children's Research Institute, Melbourne, Australia, ²Department of Medicine, Royal Melbourne Hospital, The University of Melbourne, Melbourne, Australia, ³Murdoch Children's Research Institute, Melbourne, Australia

Multi-scale entropy (MSE) quantifies the complexity of a time-series. Regular, predictable time-series have low MSE, while random time-series have high MSE. In this study, we compared conventional and multi-band acquisitions of resting-state BOLD images to determine their impact on MSE. We found that multi-band acquisitions produced lower MSE compared to non-multi-band acquisition. The effect did not persist when the number of volumes acquired was taken into consideration, suggesting that it is the number of volumes, and not multi-band acquisition per se that influences MSE. The implications for biomarker use are discussed, with particular emphasis on the ageing brain.

Patterns of gray matter alterations in first episode manic adolescents

Li Yao¹, Wenjing Zhang¹, Yuan Xiao¹, Wade Weber², Christina Klein², Rodrigo Patino², Qiyong Gong¹, Melissa DelBello², Su Lui¹, and Caleb Adler²

¹Huaxi MR Research Center, Chengdu, China, People's Republic of, ²Department of Psychiatry and Behavioral Neuroscience, Division of Bipolar Disorders Research, University of Cincinnati College of Medicine, Cincinnati, OH, United States

Gray matter volume and cortical thickness was measured to investigate the anatomical deficit in bipolar patients with severe mania. 60 patients and 29 healthy controls were recruited. Whole brain grey matter volume and cortical thickness measurements were extracted from T1-weighted MRI images and agglomerative hierarchical clustering was performed to subgroup the patients. The grey matter reduction and cortical thinning may underlie affective processing and cognition impairments in patients. In addition, the homogeneous patterns of brain deficits support the manic bipolar patients as a disease with mostly the same pattern of cerebral changes.

Altered structural-functional connectome in unilateral sudden sensorineural hearing loss

Wenliang Fan¹ and Haibo Xu^{1,2}

¹Department of Radiology, Union Hospital, Tongji Medical College, Huazhong University of Science and Technology, Wuhan, China, People's Republic of, ²Department of Radiology, Zhongnan Hospital of Wuhan University, Wuhan, China, People's Republic of

We used graph theoretical network analysis method to explore the alterations of brain structural-functional connectome in two large samples of unilateral sudden sensorineural hearing loss patients within the acute period. While previous neuroimaging studies have uncovered alterations in several specific brain structural and functional networks in patients with USSHL, little is known about the changes in the relationship between structural and functional brain connectome. And how do functional brain networks emerge from structural brain connectivity in USSHL is still unknown.

Feature selection and classification of aMCI subjects using local fMRI activation patterns

Mingwu Jin¹, Xiaowei Zhuang², Tim Curran³, and Dietmar Cordes²

¹University of Texas at Arlington, Arlington, TX, United States, ²Cleveland Clinic Lou Ruvo Center for Brain Health, Las Vegas, NV, United States, ³University of Colorado Boulder, Boulder, CO, United States

Two feature selection methods and four classification methods were applied to fMRI memory activation data obtained from two groups of amnestic MCI (aMCI) subjects and normal control subjects to investigate the classification effectiveness of the memory contrasts and subregions of medial temporal lobe. Least absolute shrinkage and selection operator (LASSO) is more effective than principle component analysis (PCA) for feature selection. The features selected by LASSO can be combined with non-linear classifiers for high classification accuracy. The face-occupation paradigm provides more discriminant power than the paradigms using outdoor pictures or word pairs.

Inter-hemispheric functional dysconnectivity mediates the effect of corpus callosum degeneration on memory impairment in AD and amnestic MCI

Yingwei Qiu¹, Siwei Liu¹, Saima Hilal², Yng Miin Loke¹, Mohammad Kamran Ikram³, Xin Xu², Boon Yeow Tan⁴, Narayanaswamy Venkatasubramanian⁵, Christopher Li-Hsian Chen², and Juan Zhou^{1,6}

¹Multimodal Neuroimaging in Neuropsychiatric Disorders Laboratory, Duke-NUS Graduate Medical School Singapore, Singapore, Singapore, ²Department of Pharmacology, National University Health System, Clinical Research Centre, Singapore, Singapore, ³Memory Aging & Cognition Centre, National University Health System, Singapore, Singapore, ⁴St. Luke's Hospital, Singapore, Singapore, ⁵Raffles Neuroscience Centre, Raffles Hospital, Singapore, Singapore, ⁶Clinical Imaging Research Centre, Technology and Research and National University of Singapore, Singapore, Singapore

The cognitive significance of corpus callosum degeneration and the related functional connectivity changes in AD and amnestic MCI remains largely unknown. Our study attempted to fill this gap of knowledge by examining how selective structural degeneration in CC was associated with memory impairment and whether such relationship was influenced by inter-hemispheric homotopic functional dysconnectivity in AD and amnestic MCI.

Brain Network Segregation and Integration is Altered in Soldiers with Post-traumatic Stress Disorder and Mild Traumatic Brain Injury

D Rangaprakash¹, Gopikrishna Deshpande^{1,2,3}, Jeffrey S Katz^{1,2,3}, Thomas S Denney^{1,2,3}, and Michael N Dretsch^{4,5}

¹AU MRI Research Center, Department of Electrical and Computer Engineering, Auburn University, Auburn, AL, United States, ²Department of Psychology, Auburn University, Auburn, AL, United States, ³Alabama Advanced Imaging Consortium, Auburn University and University of Alabama Birmingham, Birmingham, AL, United States, ⁴U.S. Army Aeromedical Research Laboratory, Fort Rucker, AL, United States, ⁵Human Dimension Division, HQ TRADOC, Fort Eustis, VA, United States

Brain functioning relies on various segregated/specialized neural regions functioning as an integrated-interconnected network. Psychiatric disorders are associated with altered functioning of these brain networks. Using resting-state fMRI, we assessed strength and variability of directional connectivity in brain-networks obtained from U.S. Army Soldiers with PTSD and mTBI. Employing graph-theoretic techniques in a novel framework, we show that PTSD and mTBI are associated with frontal disinhibition of key subcortical and visual regions, which leads to overdrive in parietal association areas, causing increased symptoms. This work is significant given that a mechanistic understanding of underlying network functioning in comorbid PTSD/mTBI has been elusive.

1734

Temporal homogeneity in BOLD time-series: an application to Rolandic epilepsy

Lalit Gupta¹, Jacobus FA Jansen², René MH Besseling², Anton de Louw³, Albert P Aldenkamp³, and Walter H Backes²

¹Philips India Ltd., Bangalore, India, ²Department of Radiology, Maastricht University Medical Center, Maastricht, Netherlands, ³Epilepsy Center Kempenhaeghe, Heeze, Netherlands

We present a novel method that yields a “temporal homogeneity measure” (TeHo), which captures temporal characteristics of the Blood-Oxygen-Level-Dependent (BOLD) time-series in terms of the average decrease in wavelet energy entropy (WEE) as a function of frequency. As an application we have analyzed cerebral abnormalities in the temporal fluctuations of children with Rolandic epilepsy. Results on 22 patients and 22 controls show that the TeHo method is sensitive to detect abnormal BOLD fluctuations in the brains of children with Rolandic epilepsy. These patients showed reduced TeHo, which indicates an altered frequency structure due to the epilepsy.

1735

A Meta-analysis of Neuroimaging Studies of English and Chinese Semantic Processing

HengShuang Liu¹ and SH Annabel Chen^{1,2}

¹Psychology, Nanyang Technological University, Singapore, Singapore, ²Centre for Research And Development in Learning, Nanyang Technological University, Singapore, Singapore

Activation likelihood estimation meta-analyses were adopted to investigate how English and Chinese differ in semantic neural bases. Results reveal that English semantic processing specifically recruited the left visual cortex and left IPL, while the right visual cortex and left MFG were exclusively employed by Chinese semantic processing. This language specialization was reflected in modality effects, as English semantics appeared to be retrieved more acoustically than visually whereas such gradient was diminished in Chinese. Level effects were less differentiated by English and Chinese since language particularities seemed to be cancelled out after within-language comparison between levels. These findings deepened our understanding of how linguistic features, presentation modalities, and levels shape the semantic brain.

1736

BOLD-fMRI signal changes during prolonged heat pain stimulation

Marianne Cleve¹, Alexander Gussew¹, and Jürgen R. Reichenbach¹

¹Medical Physics Group, Institute of Diagnostic and Interventional Radiology, Jena University Hospital - Friedrich Schiller University Jena, Jena, Germany

We performed five BOLD-fMRI measurements in healthy volunteers during prolonged heat pain stimulation to investigate the consistency of brain region specific activation and temporal alterations of brain activation. Left and right insula showed pain related activation in all volunteers and the highest activation values in the left insula at the beginning of the experiment. Compared to the insular regions, ACC and precuneus revealed higher BOLD signal variations during 11 min of noxious stimulation. The findings can be interpreted as region specific habituation effects on pain processing in the human brain.

1737

Therapeutic modulation of somatosensory evoked response in pain-related cortex on chronic lumbago.

CHUZO TANAKA^{1,2}, TOMOKAZU MURASE³, MASAKI FUKUNAGA⁴, MASAHIRO UMEDA⁵, YASUHIRO WATANABE⁵, YUKO KAWAI⁵, SETSUO HAKATA⁶, SHOJI NARUSE⁷, and TOSHIHIRO HIGUCHI⁸

¹NEUROSURGERY, RAKUWA VILLA-IILOS, Kyoto, Japan, ²Meiji University of Integrative Medicine, Kyoto, Japan, ³Meiji University of Integrative Medicine, Kyoto, Japan, ⁴Cerebral Integration, National Institute for Physiological Sciences, Okazaki, Japan, ⁵Medical Informatics, Meiji University of Integrative Medicine, Kyoto, Japan, ⁶Japanese Medical Society of Arthrokinematic Approach, Osaka, Japan, ⁷2nd Okamoto General Hospital, Kyoto, Japan, ⁸Neurosurgery, Meiji University of Integrative Medicine, Kyoto, Japan

To clarify therapeutic modulatory effects on brain activation in pain-related cortex of chronic lumbago using somatosensory stimulation with treatment for pain relief, twenty participants were divided into two groups, S1 activated (S1(+)) and S1 non-activated (S1(-)) group. There were no activated areas in pain-related cortex in S1 (-) group immediately after treatment for pain relief. Immediately after treatment, rs-fMRI of S1(-) group showed a significant signal decrease in contralateral S2 of pain-related network. It was suggested to diminish pain-related network activation by somatosensory stimulation on chronic lumbago immediately after treatment for pain relief.

1738

Concurrent fMRI, [11C]raclopride-PET and deep brain stimulation of the ventral tegmental area

Christin Y. Sander¹, John Arsenault², Bruce R. Rosen¹, Joseph B Mandeville¹, and Wim Vanduffel¹

¹Radiology, Massachusetts General Hospital, Boston, MA, United States, ²Radiology, Massachusetts General Hospital, Charlestown, MA, United States

Deep brain stimulation (DBS) through implantable neurostimulation electrodes that affect dopaminergic control is an important symptomatic therapy in movement disorders, and has been shown to affect reinforcement learning and motivation. In this study, we employ concurrent DBS in the ventral tegmental area during simultaneous PET/fMRI to understand dopaminergic signature of DBS.

1739

Enhancing Creativity and Insight using fMRI Neurofeedback

Wenjing Yan¹, Dustin Scheinost², Alan Snyder³, and Gopikrishna Deshpande^{1,4,5}

¹AU MRI Research Center, Department of Electrical and Computer Engineering, Auburn University, Auburn, AL, United States, ²Department of Diagnostic Radiology, Yale University, New Haven, CT, United States, ³Centre for the Mind, University of Sydney, Sydney, Australia, ⁴Department of Psychology, Auburn University, Auburn, AL, United States, ⁵Alabama Advanced Imaging Consortium, Auburn University and University of Alabama Birmingham, Auburn, AL, United States

Insight problem-solving is not deduced logically and the solution is typically very hard to get (probability of success is approximately 0%) and requires "out of the box" thinking. Using tDCS, Chi et al demonstrated that increasing the excitability of the right anterior temporal lobe (rATL) mitigated cognitive biases and enabled surprisingly large number of people to solve insight problems such as the nine-dot puzzle. Here we test this hypothesis using fMRI-based real-time neurofeedback. We show that 44% of subjects who were able to successfully up-regulate activity in their rATL using neurofeedback, solved the puzzle.

1740

fMRI characterization of pain processing in NaV1.7 Wnt1 KO mice

Giovanna Dilettia Ielacqua¹, Aileen Schroeter¹, David Bühlmann^{1,2}, Felix Schlegel^{1,2}, John N Wood³, and Markus Rudin^{1,4}

¹Institute for Biomedical Engineering, ETH and University of Zurich, Zurich, Switzerland, ²Neuroscience Center Zurich, Zurich, Switzerland,

³Molecular Nociception Group, Wolfson Institute for Biomedical Research, University College London, London, United Kingdom, ⁴Institute of pharmacology and toxicology, University of Zurich, Zurich, Switzerland

Stimulus-evoked fMRI (se-fMRI) measurements in mice have turned out difficult, and so far it is under investigation whether and how se-fMRI applications can yield to reliable and robust readouts. Generally, se-fMRI could be a useful tool to study how the brain processes innocuous and noxious stimuli, i.e. to characterize genetically modified mouse strains, such as mice exhibiting impaired nociception. In this study, NaV1.7-Wnt1 KO mice are characterized with respect to neural processing of different types and strengths of peripheral stimuli and compared to a WT control group. Results of behavioral tests are compared to outcomes of fMRI measurements.

1741

BOLD fMRI investigation of auditory and visual interactions in the inferior colliculus

Patrick P. GAO^{1,2}, Celia M. Dong^{1,2}, Leon C. Ho^{1,2}, Russell W. Chan^{1,2}, Xunda Wang^{1,2}, and Ed X. Wu^{1,2}

¹Laboratory of Biomedical Imaging and Signal Processing, The University of Hong Kong, Hong Kong, China, People's Republic of, ²Department of Electrical and Electronic Engineering, The University of Hong Kong, Hong Kong, China, People's Republic of

Multisensory interaction is crucial for forming an accurate representation of the environment and facilitating behavioral responses. Previous studies of multisensory interaction are focused on the cortex. The midbrain inferior colliculus (IC) is a pivotal station in the auditory pathway. Although evidence suggests that the IC receives non-auditory anatomical and signal input, it remains unclear how other sensory signals interact with auditory processing within the IC. Using BOLD fMRI, this study shows that a strong visual stimulation inhibits IC responses to following noise stimulation. Multisensory interaction therefore occurs much earlier before sensory signals reach the cortex.

1742

Disrupted functional connectivity and structure in the striatum of a mouse model of Huntington's disease

Qiang Li^{1,2}, Gang Li³, Qi Peng³, Dan Wu¹, Hanbing Lu⁴, Yihong Yang⁴, Jiangyang Zhang^{1,5}, and Wenzhen Duan^{3,6,7}

¹Dept. of Radiology, Johns Hopkins University School of Medicine, Baltimore, MD, United States, ²Dept. of Radiology, Tangdu Hospital, Xi'an, China, People's Republic of, ³Dept. of Psychiatry and Behavioral Sciences, Johns Hopkins University School of Medicine, Baltimore, MD, United States, ⁴National Institute on Drug Abuse, Baltimore, MD, United States, ⁵Dept. of Radiology, New York University School of Medicine, New York, NY, United States, ⁶Dept. of Neuroscience, Johns Hopkins University School of Medicine, Baltimore, MD, United States, ⁷Program in Cellular and Molecular Medicine, Johns Hopkins University School of Medicine, Baltimore, MD, United States

Huntington's disease (HD) is an autosomal dominant inherited neurodegenerative disorder, and several MRI modalities have been used to monitor disease progression. To date, little is known regarding the link between altered functional connectivity and structural atrophy and clinical deficits. In this study, we investigated the functional connectivity and structural changes in a mouse model of HD that recapitulate the key neuropathology and phenotype of HD. Our results revealed significant correlations between functional MRI connectivity and structural atrophy, as well as behavioral performance in the mouse model.

Traditional Poster

fMRI: Methods

Exhibition Hall

Tuesday, May 10, 2016: 13:30 - 15:30

1743

Calibration, validation, and sensitivity analysis of a 3D method for the mapping of brain venous oxygenation

Deng Mao^{1,2}, Yang Li¹, Peiying Liu¹, Shin-Lei Peng³, and Hanzhang Lu¹

¹Russell H. Morgan Department of Radiology, Johns Hopkins University, Baltimore, MD, United States, ²Graduate School of Biomedical Sciences, Univ of Texas Southwestern Medical Center, Dallas, TX, United States, ³Department of Biomedical Imaging and Radiological Science, China Medical University, Taichung, Taiwan

The present study aimed to further develop and investigate of a non-invasive, efficient and reproducible technique to map brain venous oxygenation in 3D. We first improved the processing pipeline by subtracting angiogram to remove arterial content and apply thresholds to eliminate poor fitted and low signal voxels. We then calibrated T2* to oxygenation relationship in vitro using the same

technique. In addition, we used hyperoxia challenge to test its sensitivity and combined TRUST MRI method for validation.

1744

High correlation of VasA and vascular reactivity M supports vascular origin of VasA
Samira M Kazan¹, Laurentius Huber², Guillaume Flandin¹, Peter Bandettini², and Nikolaus Weiskopf^{1,3}

¹Wellcome Trust Centre for Neuroimaging, UCL Institute of Neurology, University College London, London, United Kingdom, ²Functional Imaging Methods Laboratory of Brain, National Institute of Mental Health, Washington, DC, United States, ³Department of Neurophysiology, Max Planck Institute for Human Cognition and Brain Sciences, Leipzig, Germany

We recently presented a vascular autocalibration method (VasA) to account for vascularization differences between subjects and hence improve the sensitivity in group studies. Here, we validate the novel calibration method by means of direct comparisons of VasA with the established measure of vascular reactivity, the M-value, obtained during induced hypercapnia. We show strong evidence that VasA is dominated by local vascular reactivity variations similarly to the M-value. We conclude that the VasA calibration method is an adequate tool for application in group studies to help increasing the statistical significance and reflects to a large degree local vascularization.

1745

Enhancement of Event-Related fMRI Studies of the Human Visual System Using Multi-band EPI
R. Allen Waggoner¹, Topi Tanskanen¹, Keiji Tanaka¹, and Kang Cheng^{1,2}

¹Laboratory for Cognitive Brain Mapping, RIKEN - Brain Science Institute, Wako-shi, Japan, ²fMRI Support Unit, RIKEN - Brain Science Institute, Wako-shi, Japan

The potential benefits of multi-band EPI for event-related fMRI studies has received little attention. In this study, we explore the impact of the reduced repetition times permitted by modest levels of slice acceleration on the extent of activation in an event-related study. We also explore the use of this denser sampling to investigate the differences in hemodynamic response to variations in stimuli and differences in the hemodynamic response across brain regions.

1746

Should volumetric, slice-wise or non-linear registration be used for motion correction of fMRI data?
Malte Hoffmann¹ and Stephen J Sawiak^{1,2}

¹Wolfson Brain Imaging Centre, University of Cambridge, Cambridge, United Kingdom, ²Behavioural and Clinical Neuroscience Institute, University of Cambridge, Cambridge, United Kingdom

Motion corruption leads to major artefacts in fMRI which are damaging in studies. Most processing pipelines employ linear registration of the brain volume at each time point. As slices are acquired individually, however, it is possible for each slice to require a different transformation. Here, we compared the efficacy of linear volume registration, independent slice-based registration and volume non-linear registration for retrospective correction of fMRI acquisitions using data from forty non-cooperative patients with substantial motion.

1747

Optimizing SMS-BOLD image reconstruction for resting state analysis and reconstruction time
Ross W. Mair^{1,2}, R. Matthew Hutchison^{1,3}, Stephanie McMains¹, and Steven Cauley²

¹Center for Brain Science, Harvard University, Cambridge, MA, United States, ²A.A. Martinos Center for Biomedical Imaging, Massachusetts General Hospital, Charlestown, MA, United States, ³Department of Psychology, Harvard University, Cambridge, MA, United States

The computational processes required for slice-unaliasing in SMS-BOLD scans are taxing on the scanner reconstruction computers, so data is sometimes observed far from real-time, and reconstruction may lag up to tens of minutes behind the acquisition. A channel compression algorithm has been proposed to counter computational demands of these reconstruction processes. We studied functional networks derived from resting-state scans as a function of slice acceleration, slice-GRAPPA kernel size and channel compression to find an optimal solution for an existing, conventional 3.0 T scanner. Slice-GRAPPA kernel size played little effect in functional network definition and two-fold channel compression was beneficial to reconstruction time without impacting functional network data quality.

1748

Slice-acceleration Related Biases in Multiband-EPI Resting State Functional Connectivity
Zahra Faraji-Dana^{1,2}, Ali Golestani³, Yasha Khatamian³, Simon Graham^{1,2}, and J. Jean Chen^{1,3}

¹Department of Medical Biophysics, University of Toronto, Toronto, ON, Canada, ²Sunnybrook Research Institute, Sunnybrook Health Science Centre, Toronto, ON, Canada, ³Rotman Research Institute, Baycrest Health Science Centre, Toronto, ON, Canada

Resting-state functional connectivity MRI (rs-fcMRI) is most commonly computed as the temporal dependency amongst blood oxygenation Level dependent (BOLD) signal patterns of different brain regions. It has been shown that rs-fMRI can benefit from faster imaging times offered by simultaneous multi-slice (a.k.a. multiband, referred to as "MB") slice-acceleration that enables acquiring "groups" of slices at the same time. However, this slice grouping may incur aliasing artifacts, primarily from motion and physiological fluctuations. These spurious time-dependent signals can adversely affect the rs-fcMRI maps in the simultaneously-acquired slices (i.e., in one slice-group). In this work we investigate two hypotheses 1) the simultaneously sampled physiological noises as well as the residual aliasing introduce a slice-group effect in rs-fcMRI maps; 2) this slice-group effect can be mitigated by physiological noise correction.

Insights in dose dependent effects of isoflurane by analyzing static and dynamic functional connectivity in mice
Qasim Bukhari¹, Aileen Schröter¹, and Markus Rudin^{1,2}

¹Department of Information Technology and Electrical Engineering, Institute of Biomedical Engineering, ETH and University of Zürich, Zürich, Switzerland, ²Institute of Pharmacology and Toxicology, University of Zürich, Zürich, Switzerland

The neurophysiological effects of anesthetics on brain functional networks are not completely understood. In this work we investigated the resting state functional brain networks under different doses of isoflurane in mice. We used static and dynamic functional connectivity (dFC) analysis to get insights in dose dependent effects of isoflurane. The results from dFC analysis show that spatial segregation across brain functional networks is lost with the increasing dose of anesthesia thus it may be indicative of a deep anesthetic state. Static network analysis using dual regression revealed loss of functional connectivity between the bilateral regions, that is also supported with further results showing decrease in functional correlations with increased dose of isoflurane.

Resting-state fMRI as a tool for evaluating level of anesthesia and BOLD fMRI response in anesthetized rats
Jaakko Paasonen¹, Raimo A Salo¹, Joanna K Huttunen¹, and Olli Gröhn¹

¹Department of Neurobiology, University of Eastern Finland, Kuopio, Finland

Anesthesia is a major confounding factor in fMRI studies, because it directly affects brain function. As recent evidence suggests that functional connectivity (FC) changes with anesthetic depth, we investigated whether FC could be used to measure anesthetic depth in preclinical fMRI studies and subsequently predict fMRI responses under five anesthetics. The FC was able to predict the magnitude of fMRI responses under different anesthetics. The FC also changed during 1-h interval with injectable anesthetics. Therefore, we conclude that FC analysis of baseline fMRI data can provide simple way to control one of the key confounding factors in preclinical fMRI studies.

High resolution Macaque MRI at 3T using an 8 channel receive array with shielded birdcage transmit coil
Rou Li¹, Jingqiang Peng², Xiao Chen¹, Xiaoqing Hu¹, Xiaoliang Zhang^{3,4}, Ye Li¹, Xin Liu¹, Hairong Zheng¹, and Zheng Wang²

¹Paul C. Lauterbur Research Center for Biomedical Imaging, Shenzhen Institutes of Advanced Technology, CAS, Shenzhen, China, People's Republic of, ²Institute of Neuroscience, Shanghai Institutes for Biological Sciences, CAS, Shanghai, China, People's Republic of, ³Department of Radiology and Biomedical Imaging, University of California San Francisco, San Francisco, CA, United States, ⁴UCSF/UC Berkeley Joint Graduate Group in Bioengineering, San Francisco, CA, USA, San Francisco, CA, United States

Macaque monkey is a critical model for fMRI to investigate large scale functional network. In this work, an 8 channel loop array with shield birdcage transmit coil is proposed to achieve high resolution homogeneous macaque brain images at 3T MRI. Both phantom and *in-vitro* experiments demonstrate the capability of the proposed design of achieving homogeneous transmit field and high SNR in the whole brain region, which provides the possibility to perform *in-vivo* macaque fMRI experiments to investigate large-scale functional network.

Quantitative vascular imaging with QUTE-CE MRI
Codi Gharagouzloo¹, Ju Qiao², Liam Timms³, Aniket Pandya³, Praveen Kulkarni⁴, Craig Ferris⁵, and Srinivas Sridhar³

¹Bioengineering, Northeastern University, Boston, MA, United States, ²Industrial Engineering, Northeastern University, Boston, MA, United States, ³Physics, Northeastern University, Boston, MA, United States, ⁴Northeastern University, Boston, MA, United States, ⁵Center for Translational Neuroimaging (CTNI), Northeastern University, Boston, MA, United States

We demonstrate a unique type of vascular imaging using ferumoxytol as an iron-oxide nanoparticle contrast agent (CA) and a 3D ultra-short TE (UTE) pulse sequence. The raw UTE signal intensity is shown to be quantitative by comparison to excised blood immediately after imaging with $n=5$ Sprague Dawley rats. In this preliminary study, we calculate the cerebral blood volume (CBV) on a regional basis using a 174-region anatomic atlas that is consistent among animals and is independent of CA concentration.

Optimizing the parameter space for functional-MRI in rodents
Georges Hankov^{1,2}, Basil Künnecke², Markus Rudin^{1,3}, and Markus von Kienlin²

¹Institute for Biomedical Engineering, ETH and University Zurich, Zurich, Switzerland, ²Roche Pharma Research & Early Development, Neuroscience Discovery, Roche Innovation Center Basel, F. Hoffmann-La Roche Pharmaceuticals Ltd, Basel, Switzerland, ³Institute of Pharmacology and Toxicology, University of Zurich, Zurich, Switzerland

In the past years, functional MRI studies in rodents have become increasingly popular. However the parameter space for optimal data acquisition scheme has been poorly explored. In this work, we compare different acquisition methods such as single-shot and segmented Echo Planar Imaging, and PRESTO, to determine which technique offers the best compromise between temporal resolution, geometric distortions, artefacts and signal-to-noise ratio. The results suggest that segmented EPI, using two or three segments, could fulfill the requirements needed for rodent fMRI if ghost artefacts are minimized.

Potential source of MRI signal change during transcranial direct current stimulation
Guoxiang Liu^{1,2}, Takashi Ueguchi^{1,2}, Ikuhiro Kida^{1,2}, Ken-ichi Okada^{1,2}, and Yasushi Kobayashi^{1,2}

¹National Institute of Information and Communications Technology, Suita-shi, Osaka, Japan, ²Osaka University, Suita-shi, Osaka, Japan

In this work, we implemented tDCS experiments on a monkey brain and a phantom at a 7T human MRI scanner to investigate the possibility to measure current flow during tDCS. Our results showed that imaging distortions caused by current in lead wires but not in brain is a possible source of BOLD-like MRI signal changes.

1755

Reproducibility of cerebral sensorimotor activation in functional magnetic resonance imaging in isoflurane-anesthetized rats : A test-retest effect

Won Beom Jung¹, Ji Hoon Cha¹, Geun Ho Im², Sun Young Chae³, and Jung Hee Lee¹

¹Department of Radiology, Samsung Medical Center, Seoul, Korea, Republic of, ²Center for Molecular and cellular imaging, Samsung Biomedical Research Institute, Seoul, Korea, Republic of, ³Samsung Advanced Institute for Health Sciences & Technology, Sungkyunkwan University, Seoul, Korea, Republic of

Blood oxygen level dependent (BOLD)-functional magnetic resonance imaging (fMRI) technique for rats is an emerging field in neuroscience. Inhalation anesthetics are often used for longitudinal fMRI experiments of rodent. Confirming the degree of reproducibility for stimulation induced fMRI response is especially important on longitudinal studies when investigating a time course of functional recovery. In this study, we evaluated the reproducibility or time-dependent changes of fMRI activation in somatosensory cortex in rats under isoflurane anesthesia.

1756

A more sensitive paradigm for direct MR detection of neuronal currents: simulation results
Ileana Hancu¹ and Christopher Hardy¹

¹GE Global Research Center, Niskayuna, NY, United States

Direct detection of neuronal activity through MRI is an active research area. Typical MRI-based approaches for direct detection of neuronal currents use echo-planar imaging, which offers wide spatial coverage at low temporal resolution (>100ms). In this work, we explore a significantly different paradigm, in which we give up wide spatial coverage, gaining the capability of sampling signals at much higher rates. Our simulation results indicate that the ability to compare entire time curves sampled at a high temporal rate leads to an increase in the sensitivity of detecting neuronal currents by a factor of at least 10.

1757

Development of an awake mouse MRI method using soft immobilization for a cryogenic probe system
Etsushi Nakata¹, Shunsuke Kusanagi¹, Kazunari Kimura¹, Rikita Araki², Mitsuhiro Takeda¹, Sosuke Yoshinaga¹, and Hiroaki Terasawa¹

¹Department of Structural Biolimaging, Faculty of Life Sciences, Kumamoto University, Kumamoto, Japan, ²Bruker Biospin K.K., Yokohama, Japan

In animal MRI research, treatments with anesthesia and fixing apparatuses are usually required to suppress MR image blurring due to animal movements. However, the physiological conditions are reportedly affected by anesthesia. At the ISMRM annual meeting in 2013, we reported an easily implemented method for awake mouse brain imaging, which uses softer immobilization with clothes for mice, without surgery and training. Recently, a cryogenic transceive coil system, which greatly enhances the SNR of MR images, was developed and is becoming widely used. We successfully improved our awake MRI method to be applicable to the cryo system, by refining the designed clothes.

Traditional Poster

Image Reconstruction: Post-Cartesian

Exhibition Hall

Tuesday, May 10, 2016: 16:00 - 18:00

1758

Off-Resonance Map Refinement Using Autofocusing for Spiral Water-Fat Imaging
Ashley G Anderson III¹, Dinghui Wang¹, and James G Pipe¹

¹Imaging Research, Barrow Neurological Institute, Phoenix, AZ, United States

Autofocusing was used to estimate residual off-resonance and remove associated blurring in spiral images after initial joint deblurring and water-fat separation with a previously acquired field map.

1759

Joint Water-Fat Separation and Deblurring with Single Spiral In-Out Spin-Echo Imaging
Dinghui Wang¹, Zhiqiang Li¹, Ryan K. Robison¹, and James G. Pipe¹

¹Imaging research, Barrow Neurological Institute, Phoenix, AZ, United States

Spiral in-out readout is an efficient sampling scheme for T2-weighted (T2w) spin-echo (SE) sequences. Two sets of spiral in-out data at different TE are typically acquired so that deblurred water and fat images can be extracted from the spiral-in and the spiral-out data separately, which are then combined together. A method has been recently proposed to reconstruct water and fat images from a single set of spiral in-out data. This work demonstrates the feasibility of using this method as a fast and scan efficient means of fat suppression to reduce the scan time of the spiral T2w SE by a factor of 2.

1760

Spiral Deblurring Using B0 Maps with B0 Drift Correction

Melvyn B Ooi^{1,2}, Dinghui Wang², Ashley G Anderson III², Zhiqiang Li², Nicholas R Zwart², Ryan K Robison², and James G Pipe²

¹Philips Healthcare, Cleveland, OH, United States, ²Imaging Research, Barrow Neurological Institute, Phoenix, AZ, United States

Spiral MRI enables long sampling durations but at the cost of increased sensitivity to B0-field fluctuations. For example, scanner B0-drift will be observed in spiral MRI as a time-varying component of image blurring. A spiral deblurring strategy is presented where a reference B0 map is acquired at the start of the spiral exam; F0 navigators then quickly measure B0 drift over the course of the spiral exam, and are used to calculate B0-drift corrected B0-maps for deblurring of the current scan. F0-navigator accuracy is verified with independent B0-map acquisitions, and improved spiral deblurring is shown for a structural brain scan.

1761

Variable density spiral sampling and reconstruction for spatiotemporally encoded single-shot MRI

Lin Chen¹, Shuhui Cai¹, and Congbo Cai¹

¹Department of Electronic Science, Xiamen University, Xiamen, China, People's Republic of

As an emerging ultrafast imaging method, spatiotemporally encoded single-shot MRI is advantageous because it can resist off-resonance effects while retaining spatial and temporal resolutions comparable to the classical EPI. In this work, a variable density spiral sampling (VDSS) scheme is proposed for SPEN MRI. An optimization algorithm is used to design the sinusoidal readout gradient waveform. A specific gridding algorithm and non-Cartesian super-resolved reconstruction are proposed to retrieve image. Compared to the Cartesian sampling, VDSS can provide images with less artifacts and better spatial resolution.

1762

Single shot spiral imaging at ultra-high field

Maria Engel¹, Lars Kasper¹, Christoph Barmet¹, Klaas Paul Prüssmann¹, and Thomas Schmid¹

¹Institute for Biomedical Engineering, University Zurich and ETH Zurich, Zurich, Switzerland

Fast spiral sequences with concurrent field monitoring, B0 correction and SENSE-reconstruction promise a brave new world for time series MRI.

1763

Use of a radial convolution kernel in the non-uniform Fourier transform

Mark BYDDER¹, Wafaa Zaaraoui¹, and Jean-Philippe Ranjeva¹

¹Aix Marseille Université, MARSEILLE, France

Non-Cartesian reconstructions typically perform a convolution to interpolate irregularly spaced samples onto a regular grid. The number of coefficients in the convolution trades-off accuracy with speed. A radially symmetric convolution kernel provides a favorable trade-off as compared to a separable kernel with the same number of coefficients.

1764

Fast 3D Filtered Back-Projection Reconstruction combined with a New Radial-Acquisition Strategy.

JeongTaek Lee^{1,2}, Jinil Park^{1,2}, and Jang-Yeon Park^{1,2}

¹Center for Neuroscience Imaging Research, Institute for Basic Science, Suwon, Korea, Republic of, ²Department of Biomedical Engineering, Sungkyunkwan University, Suwon, Korea, Republic of

Radial-acquisition imaging is recently gaining more popularity. For RA image reconstruction, both fast Fourier transform via gridding and filtered back-projection are available. Because of the processing time, FFT is dominantly used. If the processing-time issue is resolved, 3D FBP can be promising in the case of FID sampling or echo sampling with mis-centering of k-space. In this study, we propose a strategy that can significantly reduce the reconstruction time of 3D FBP in combination with a new RA scheme. Performance of the proposed method was demonstrated in phantom and human brain imaging at 3T.

1765

GROG Based Sensitivity Map Estimation for Radial Data in MRI

mawish khan¹, Taquwa Aslam¹, and Hammad Omer¹

¹Electrical Engineering, COMSATS Institute of Information Technology, Islamabad, Pakistan

The estimation of receiver coil sensitivity profiles is required for many PMRI algorithms including CG-SENSE. Conventionally, CG-SENSE uses pre-scan method to estimate the sensitivity maps for which a separate scan is required. The novelty in this work is the use of GROG gridding on the central region of the acquired under-sampled cardiac radial data to estimate the receiver coil sensitivities using Eigenvalue method. The results show that GROG based sensitivity map estimation (proposed method) is an effective method without any requirement of a prior scan or body coil image.

1766

Run and Done: Calibrationless Multichannel Continuously Moving Table Whole Body MRI with Immediate Reconstruction

David S Smith¹, Saikat Sengupta¹, Aliya Gifford¹, and E Brian Welch¹

¹Institute of Imaging Science, Vanderbilt University, Nashville, TN, United States

We achieve significantly improved image quality in whole-body continuous moving table MRI without time penalty by using a multichannel, golden angle radial acquisition coupled to a calibrationless reconstruction.

1767

Phase correction in the presence of gradient delays for 3D radial data
Ina Nora Kompan¹ and Matthias Guenther²

¹mediri GmbH, Heidelberg, Germany, ²Fraunhofer Mevis, Bremen, Germany

3D radial acquisitions are prone to gradient delay and phase artifacts, which need to be corrected for. Ideally, the phase can be retrospectively corrected for by assuming the same phase in *k*-space center where all projections meet. However, if data are affected by gradient delays, profiles are shifted at varying angles and might not intersect at all. Here, a simple to apply, novel phase correction method is presented in which the changed trajectory due to gradient delays is incorporated into 3D phase correction. It was shown that artifacts are reduced by 12% compared to only gradient delay corrections.

1768

Accelerating radial MRI using GROG followed by ESPIRiT
Ibtisam Aslam¹, Faisal Najeeb¹, and Hammad Omer¹

¹Electrical Engineering, COMSATS Institute of Information Technology, Islamabad, Pakistan

Accelerated non-Cartesian parallel imaging plays a vital role to reduce data acquisition time in the MR imaging; however the resultant images may contain aliasing artifacts. In this work, the application of ESPIRiT with GROG is proposed to get good reconstruction results from highly under-sampled radial data. The proposed method is tested on 3T short-axis cardiac radial data at different acceleration factors (AF=4, 6 and 9) and compared with pseudo-Cartesian GRAPPA. The results show that the proposed method offers significant improved (e.g. 81% improvement in term of artifact power at AF=4) reconstruction results as compared to conventional pseudo-Cartesian GRAPPA.

1769

K-T ARTS-GROWL: An Efficient Combination of Dynamic Artificial Sparsity and Parallel Imaging Method for DCE MRI Reconstruction
Zhifeng Chen¹, Liyi Kang¹, Allan Jin², Feng Liu³, Ling Xia¹, and Feng Huang²

¹Biomedical Engineering, Zhejiang University, Hangzhou, China, People's Republic of, ²Philips Healthcare (Suzhou) Co. Ltd, Suzhou, China, People's Republic of, ³School of Information Technology and Electrical Engineering, The University of Queensland, Queensland, Australia

Dynamic contrast enhanced (DCE) MRI plays an important role in the detection of liver metastases, characterization of tumors, assessing tumor response and studying diffuse liver disease. It requires a high spatial-temporal resolution. Existing iterative dynamic MRI reconstruction algorithms, such as iGRASP and L+S, realize their functions through iterative schemes. Though the solutions are generally acceptable, yet suffer from significantly high computational cost. This study proposed to use dynamic artificial sparsity and non-Cartesian parallel imaging for high spatiotemporal resolution DCE reconstruction, which results in comparable image quality relative to the above iterative schemes with greatly reduced computational cost.

1770

Simultaneous Multi-slice MRF with Controlled Aliasing Enabled by Temporal Data Sharing
Di Cui¹, Hing-Chiu Chang¹, Hua Guo², Queenie Chan³, and Edward S Hui¹

¹Diagnostic Radiology, The University of Hong Kong, Hong Kong, Hong Kong, ²Department of Biomedical Engineering, Tsinghua University, Beijing, China, People's Republic of, ³Philips Healthcare, Hong Kong, Hong Kong

Magnetic Resonance Fingerprinting (MRF) enables simultaneous quantification of multiple relaxation parameters, which is further accelerated by usage of simultaneous multi-slice (SMS) technique. SENSE based SMS-MRF reconstruction suffers high g-factor penalty due to similar coil sensitivity profiles of collapsed slices. Here we proposed a new method to solve this problem, by data re-grouping from adjacent time points, spatial controlled aliasing is enabled, after dictionary matching, good parameter mapping of 2 slices with nearly the same sensitivity is acquired at half the acquisition time of single-excitation MRF.

1771

Line profile measure as a stopping criterion in CG-SENSE Reconstruction
Taquwa Aslam¹, Mahwish Khan¹, Ali Raza Shahid¹, and Hammad Omer¹

¹Electrical Engineering, COMSATS Institute of information technology, Islamabad, Pakistan

CG SENSE is an iterative algorithm used in PMRI for MR image reconstruction from under-sampled data. One major limitation of CG-SENSE is the appropriate choice of the number of iterations required for good reconstruction results. This paper proposes the use of a correlation measure between the line profiles of the reconstructed images in the current and the previous iteration, as a stopping criterion for the CG-SENSE algorithm. Results of the proposed method are compared with the Bregman distance stopping criterion. The results show that the use of line profile correlation measure acts as an effective stopping criterion in CG-SENSE.

1772

Iterative Progressive Length Conjugate Gradient Reconstruction in MR-PARSE
Charles G Cantrell¹, Parmede Vakil^{1,2}, Donald R Cantrell³, Yong Jeong¹, Sameer A Ansari³, and Timothy J Carroll^{1,3}

¹Biomedical Engineering, Northwestern, Chicago, IL, United States, ²College of Medicine, University of Illinois, Chicago, IL, United States, ³Radiology, Northwestern, Chicago, IL, United States

We have found that performing iterative PLCG dramatically (on average 55% better) improves reconstruction quality of an MR-PARSE acquisition. Moreover, iterative PLCG has shown to be capable of reconstruction in regions with large susceptibility artifact. Consistent frequency measurements allow us to remove static offsets caused by air interfaces near the earholes and sinuses leaving dynamic frequency offsets which transpose linearly to OEF. Furthermore, our approach to prevent local minima solutions, through the use of an iterative PLCG, represents a new approach that may improve upon many other complex reconstruction methods.

1773

Improved identification and clinical utility of pseudo-inverse with constraints (PICO) reconstruction for PROPELLER MRI
Jyh-Miin Lin¹, Andrew J. Patterson², Chung-Wei Lee³, Ya-Fang Chen³, Tilak Das⁴, Daniel Scoffings⁵, Hsiao-Wen Chung⁶, Jonathan H. Gillard¹, and Martin J. Graves²

¹Department of Radiology, University of Cambridge, Cambridge, United Kingdom, ²MRIS unit, Cambridge University Hospitals NHS Foundation Trust, Cambridge, United Kingdom, ³Department of Radiology, National Taiwan University College of Medicine, Taipei, Taiwan, ⁴Addenbrooke's Hospital, Cambridge, United Kingdom, ⁵Department of Radiology, Cambridge University Hospitals NHS Foundation Trust, Cambridge, United Kingdom, ⁶Department of Electrical Engineering, National Taiwan University, Taipei, Taiwan

PROPELLER MRI can reduce motion artifacts. However, the colored noise of PROPELLER could degrade the image quality. Although the iterative Pseudo-Inverse with COnstraints (PICO) has been proposed to improve the image quality metrics, further clinical validation is needed. In this study, two neuroradiologists compared the image quality of PICO with the standard density compensation. Results show that PICO significantly improves the identification of two anatomical structures and the clinical utility.

1774

The Development and Evaluation of the Novel Brain Phantom for the PROPELLER with Motion Correction
Kousaku Saotome¹, Akira Matsushita¹, Koji Matsumoto², Yoshiaki Kato³, Kei Nakai⁴, Yoshiyuki Sankai⁵, and Akira Matsumura⁴

¹Center for Cybernics Research, University of Tsukuba, Tsukuba, Japan, ²Department of Radiology, Chiba University Hospital, Chiba, Japan, ³Medical Technology Department, Kameda General Hospital, Kamogawa, Japan, ⁴Department of Neurosurgery, University of Tsukuba, Tsukuba, Japan, ⁵Faculty of Engineering, Information and Systems, University of Tsukuba, Tsukuba, Japan

Our purpose is to develop the novel brain phantom including low contrast and to verify its potential to emphasize the motion correction effects in PROPELLER. Our proposed phantom set would allow not only to add the ability to low contrast objects but also to provide exact rotations instead of a healthy volunteer. The making process of the phantom consists of making profile curves, transforming to depths of the convexo-concave, printing using 3-D printer, and pouring agarose. This is the novel phantom making process.

Traditional Poster

Reconstruction

Exhibition Hall

Tuesday, May 10, 2016: 16:00 - 18:00

1775

Joint Estimation of Attenuation and Activity Distributions for Clinical non-TOF FDG Head Patient PET/MR Data Employing MR Prior Information
Thorsten Heußer¹, Christopher M Rank¹, Martin T Freitag², Heinz-Peter Schlemmer², Antonia Dimitrakopoulou-Strauss³, Thomas Beyer⁴, and Marc Kachelrieß¹

¹Medical Physics in Radiology, German Cancer Research Center (DKFZ), Heidelberg, Germany, ²Department of Radiology, German Cancer Research Center (DKFZ), Heidelberg, Germany, ³Clinical Cooperation Unit Nuclear Medicine, German Cancer Research Center (DKFZ), Heidelberg, Germany, ⁴Center for Medical Physics and Biomedical Engineering, Medical University Vienna, Vienna, Austria

To improve attenuation correction (AC) and thus PET quantification for PET/MR imaging, we have recently proposed a method to jointly estimate attenuation and activity distributions from the non-TOF PET emission data. Available MR information is used to derive voxel-specific expectations on the attenuation coefficients, favoring the occurrence of pre-selected attenuation values corresponding to air, soft tissue, and bone. We here present first results for clinical non-TOF ¹⁸F-FDG PET/MR data sets of the head region. PET reconstruction was performed using MR-based AC as provided by the vendor, our proposed algorithm, and CT-based AC for comparison.

1776

Robust PET attenuation correction for PET/MR using joint estimation with MR-based priors: application to whole-body clinical TOF PET/MR data
Sangtae Ahn¹, Lishui Cheng¹, Dattesh Shanbhag², and Florian Wiesinger³

¹GE Global Research, Niskayuna, NY, United States, ²GE Global Research, Bangalore, India, ³GE Global Research, Munich, Germany

PET attenuation correction is critical to accurate PET quantitation. For hybrid PET/MR imaging, MR-based attenuation correction (MRAC) has challenges in implants, internal air, bones and lung regions where MR signals are low. To address the challenges and improve robustness and accuracy of MRAC, a joint estimation algorithm with MR-based priors is implemented where prior weights are spatially modulated, providing great flexibility to users. The JE algorithm was applied to whole-body clinical TOF PET/MR data and it was demonstrated that the algorithm can recover the attenuation of implants, abdominal air and lungs in a robust way.

1777

Improved Nyquist ghost removal for single-shot spatiotemporally encoded (SPEN) MRI with joint rank constraint

1778

Exploiting deep convolutional neural network for fast magnetic resonance imaging
Shanshan Wang¹, Zhenghang Su^{1,2}, Leslie Ying³, Xi Peng¹, and Dong Liang¹

¹Shenzhen Institutes of Advanced Technologies, Shenzhen, China, People's Republic of, ²School of Information Technologies, Guangdong University of Technology, Guangzhou, China, People's Republic of, ³Department of Biomedical Engineering and Department of Electrical Engineering, The State University of New York, Buffalo, NY, United States

This paper proposes a deep learning based approach for accelerating MR imaging. With the utilization of a large number of existing high-quality MR images, we train an off-line convolutional neural network (CNN) to identify the mapping relationship between MR images obtained from zero-filled and fully-sampled k-space data. Then the trained CNN is employed to predict an image from undersampled data, which is used as the reference in solving an online constrained imaging problem. Results on in vivo datasets show that the proposed approach is capable of restoring fine details and presents great potential for efficient and effective MR imaging.

1779

Universal iterative denoising of complex-valued volumetric MR image data using supplementary information
Stephan A.R. Kannengiesser¹, Boris Mailhe², Mariappan Nadar², Steffen Huber³, and Berthold Kiefer¹

¹MR Application Predevelopment, Siemens Healthcare, Erlangen, Germany, ²Medical Imaging Technologies, Siemens Healthcare, Princeton, NJ, United States, ³Radiology and Biomedical Imaging, Yale University School of Medicine, New Haven, CT, United States

Spatially varying noise limits acquisition speed and spatial resolution in multi-channel MRI. Conventional single-slice noise-suppressing image filters without additional knowledge about data acquisition, image reconstruction, and noise level, have limited performance and need parameter tuning. In this work, an iterative denoising algorithm is presented which works with standard settings on 3D complex-valued data with supplementary information from the scanner environment.

Initial results from routine clinical imaging are promising: spatially adaptive, as intended, and superior to a commercially available image filter. Non-optimized reconstruction times of up to 15min per volume still need improvement, and further clinical investigations will be performed.

1780

Multi atlas-based attenuation correction for brain FDG-PET imaging using a TOF-PET/MR scanner- comparison with clinical single atlas- and CT-based attenuation correction
Tetsuro Sekine^{1,2}, Ninon Burgos³, Geoffrey Warnock¹, Martin Huellner¹, Alfred Buck¹, Edwin ter Voert¹, M. Jorge Cardoso³, Brian Hutton³, Sebastien Ourselin³, Patrick Veit-Haibach¹, and Gaspar Delso⁴

¹University Hospital Zurich, Zurich, Switzerland, ²Nippon Medical School, Tokyo, Japan, ³University College London, London, United Kingdom, ⁴GE Healthcare, Waukesha, WI, United States

Accurate attenuation correction on PET/MR scanner is challenging. We compared multi-atlas method with clinical single-atlas method. Our study revealed that the error of PET images based on multi-atlas method is reduced from 1.5% to 1.2% compared to the single-atlas method, a 30% improvement.

1781

Uniting Reconstruction Software for Native Use in GPI
Nicholas R. Zwart¹, Ashley G. Anderson III¹, Ryan K. Robison¹, Andrew Li², Mariya Doneva^{2,3}, Frank Ong², Martin Uecker², Michael Lustig², and James G. Pipe¹

¹Imaging Research, Barrow Neurological Institute, Phoenix, AZ, United States, ²Electrical Engineering, University of California, Berkeley, CA, United States, ³Philips Research, Hamburg, Germany

This work proposes the use of the software development platform called GPI (Graphical Programming Interface) as a tool for resourcing other work for integration and comparison. The GPI software structure is designed to facilitate the encapsulation of outside libraries and provides a plug-in model to isolate package dependencies. The library featured in this work is the Berkley Advanced Reconstruction Toolkit (BART) which provides, multi-platform compatible, compressed sensing and parallel imaging algorithms.

1782

Animating Terabytes of Imaging Data from a One-Minute Scan: Interactive Reconstruction of Flexibly Acquired MRI Data
David S Smith¹, Saikat Sengupta¹, Aliya Gifford¹, and E Brian Welch¹

¹Institute of Imaging Science, Vanderbilt University, Nashville, TN, United States

We present a software system called CITRON that can extract, reconstruct, and display images from non-Cartesian MR data at 60 frames per second, allowing the user to vary the reconstruction parameters in real time in order to explore and optimize the reconstructed

images interactively.

1783

Smart Averaging: SNR Improvement by Retrospective Filtering
Rolf Pohmann¹ and Klaus Scheffler^{1,2}

¹*Magnetic Resonance Center, Max Planck Institute for Biological Cybernetics, Tübingen, Germany*, ²*Biomedical Magnetic Resonance, University Tübingen, Tübingen, Germany*

Averaging is a frequently used way to increase the SNR of a measurement. Here we show that spending the additional time for increasing the spatial resolution and applying a retrospective k-space filter can yield a higher SNR gain than conventional averaging. For weighting in two phase encoding directions, this can increase the SNR by up to 25%. For 3D weighting, SNR gain can reach 57%, if the additional acquired k-space points are used to increase the readout duration, and 38% for equal duration for weighted and unweighted acquisition.

1784

Joint Reconstruction of PET and MRI with Attenuation Correction Incorporating TOF Information
Rong Guo¹, Yicheng Chen², Jinsong Ouyang³, Georges El Fakhri³, and Kui Ying¹

¹*Engineering Physics, Tsinghua University, Beijing, China, People's Republic of*, ²*University of California, Berkeley, Berkeley, CA, United States*,

³*Center for Advanced Radiological Sciences, Massachusetts General Hospital, Boston, MA, United States*

Joint reconstruction of PET and MRI is aimed to improve both PET and MR image quality using information from each other's imaging modality. However, the aim cannot be achieved without correcting the attenuation of PET. We proposed a method to correct attenuation during the process of simultaneous PET and MRI images reconstruction. This method integrates PET, MRI and TOF information.

1785

Novel Half Fourier Reconstruction Recovering Signal Loss from Off-resonance
Seul Lee¹ and Gary Glover²

¹*Department of Electrical Engineering, Stanford University, Stanford, CA, United States*, ²*Department of Radiology, Stanford University, Stanford, CA, United States*

Since half k-space reconstruction reduces scan time while keeping spatial resolution, it can be used for T_2^* weighted images such as functional MRI that requires fairly long TE. Functional MRI is sensitive to off-resonance because there exist large susceptibility variations in air-tissue interfaces such as sinuses. Existing half k-space reconstruction is vulnerable to off-resonance since it might lose most of the image energy when there is a large amount of phase shift. In this study, we suggest a new half k-space reconstruction method that is more robust to off-resonance compared to existing reconstruction method.

1786

An FPGA Based Real-Time Data Processing Structure – Application to Real-Time Array Coil Data Compression
Josip Marjanovic¹, Jonas Reber¹, David Otto Brunner¹, Bertram Jakob Wilm^{1,2}, and Klaas Paul Pruessmann¹

¹*Institute for Biomedical Engineering, University and ETH Zurich, Zurich, Switzerland*, ²*Skope Magnetic Resonance Technologies, Zurich, Switzerland*

Data amounts of massive parallel receiver arrays as well as latency requirements of real-time applications such as interventional MRI, navigators etc. prompt for high-speed data preprocessing. First steps in the reconstruction such as noise pre-whitening or channel combinations and compressions can be efficiently performed on FPGAs. Here we present a flexible system and software architecture for such tasks and demonstrate its capability performing real-time coil compression directly in the spectrometer.

1787

A k-space De-Noising Technique for RFI Mitigation and Zipper Artefact Elimination
Yong Liu¹ and Paul R. Harvey²

¹*Philips Research China, Shanghai, China, People's Republic of*, ²*Philips MR, Best, Netherlands*

Extraneous in-band Radio Frequency Interference (RFI) signals can mix with the MR signal of a subject creating artefacts in the image data, usually zipper like artefacts. In order to eliminate/reduce the impact of RFI, this abstract describes a software de-noising method which can be implemented both online and off-line through k-space manipulation.

1788

The Optimal Condition for Maintaining Uniform k-space Coverage after Retrospective Respiratory Gating in 3D Radial-Acquisition Imaging
Jinil Park^{1,2}, Taehoon Shin³, Soon Ho Yoon^{4,5}, Jin Mo Goo^{4,5,6}, and Jang-Yeon Park^{1,2}

¹*Center for Neuroscience Imaging Research, Institute for Basic Science, Suwon, Korea, Republic of*, ²*Department of Biomedical Engineering, Sungkyunkwan University, Suwon, Korea, Republic of*, ³*Diagnostic Radiology and Nuclear Medicine, University of Maryland, Baltimore, MD, United States*, ⁴*Department of Radiology, Seoul National University College of Medicine, Seoul, Korea, Republic of*, ⁵*Institute of Radiation Medicine, Seoul National University Medical Research Center, Seoul, Korea, Republic of*, ⁶*Cancer Research Institute, Seoul National University, Seoul, Korea, Republic of*

Radial-acquisition imaging is suitable for lung imaging because it allows a very short TE and a desirable degree of motion insensitivity. Despite its tolerance to motion artifacts, respiratory motion is still a major reason of causing image artifacts in lung imaging, which motivates the need for the respiratory gating. In retrospective-respiratory gating, it is significant to keep the k -space as uniform as possible after gating. In this study, we explore the optimal condition for obtaining uniform k -space coverage after retrospective gating in consideration of various breathing patterns.

1789 Image Super-resolution Restoration based on Structure Feature in Fourier Domain for MR Images
Lijun Bao¹

¹*Department of Electronic Science, Xiamen University, Xiamen, China, People's Republic of*

In the learning based single image super-resolution restoration, the high frequency information is enhanced by retrieving the high-frequency information from the high resolution training samples. Therefore how to reveal the underlying relations between the HR and the LR patch spaces is the key issue. In this work, we propose to cluster the pre-collected HR example patches to generate subdictionary and select the proper subdictionary for any image patch according to the frequency spectrum feature in Fourier domain, because the Fourier spectrogram can reflect the feature complexity, local directionality and the texture periodicity of the image patch simultaneously.

1790 High-Resolution Susceptibility Weighted Images Derived from fMRI Images using Super-Resolution Reconstruction
Weiran Deng¹, Michael Herbst¹, and V. Andrew Stenger¹

¹*University of Hawaii JABSOM, Honolulu, HI, United States*

A subset of fMRI images is used to reconstruct a structural image at a higher resolution using a Super-Resolution (SR) reconstruction method. The subset of fMRI images are selected such that the translation and rotation between the shots are less than the pixel size and therefore useful for modeling the pixel characteristics. The preliminary results demonstrate the feasibility of reconstructing a structural image with susceptibility contrast from a subset of fMRI images.

1791 Rotation and Translation Estimation from simple 1D MR Navigators
Moosa Zaidi¹, Joseph Cheng¹, Tao Zhang¹, and John Pauly¹

¹*Electrical Engineering, Stanford University, Stanford, CA, United States*

Sensitivity to motion remains a major limitation to the clinical utility of MRI. Self-navigating Cartesian trajectory (Butterfly) can provide coil-by-coil estimates of local linear translation without lengthening scan time or requiring external sensors. We propose to combine translational motion estimates with the geometry of the differing coil sensitivities to estimate global translation and rotation. These estimates can then be used to retrospectively correct for motion. For 2D slices we are successfully able to extract both unknown rotation with known translation and unknown translation and unknown rotation. Extension to 3D is a promising direction for future work.

1792 Selective combination of MRI phase images
Viktor Vegh¹, Kieran O'Brien², David C Reutens¹, Steffen Bollmann¹, and Markus Barth¹

¹*Centre for Advanced Imaging, University of Queensland, Brisbane, Australia, ²Magnetic Resonance, Siemens Healthcare Pty. Ltd., Brisbane, Australia*

Signal phase acquired via gradient recalled echo MRI sequences provides an important source of tissue contrast. The use of phased array coils results in multiple-channel images that have to be combined to form a single image. A robust method of computing phase images has been challenging to develop, primarily due to the distribution of noise in phase images. We propose a new approach of combining phase images by exploiting the inherent noise in signal phase. Our selectively combined signal phase results show an improvement in the quality of the combined phase image in comparison to existing methods.

1793 Partial Fourier fMRI acquisition pipeline for optimal half k-space coverage
Christine Law¹, Gary Glover¹, and Sean Mackey¹

¹*Stanford University, Stanford, CA, United States*

We present a novel idea for quickly detecting the optimal half k -space for use in partial Fourier acquisition. With EPI acquisition, the center of k -space can be offset from the origin by local magnetic field inhomogeneity. This offset can occur in both positive and negative phase encode directions. For partial Fourier acquisition, it is important to sample the portion of k -space containing the center peak. Before data collection using partial Fourier acquisition, a reference scan that collects two time frames (each with different halves of k -space coverage) can be used to determine the proper half of k -space to collect for each slice.

1794 Banding free bSSFP CINE imaging using a multi-frequency reconstruction
Anne Slawig¹, Tobias Wech¹, Johannes Tran-Gia^{1,2}, Henning Neubauer¹, Thorsten Bley¹, and Herbert Köstler¹

Imaging of the beating heart is one of the main challenges in fast MRI. Balanced steady state free precession sequences are fast, yield high signal and have excellent contrast between blood and myocardium. Unfortunately, they are sensitive to field inhomogeneities, which lead to banding artifacts, considerably reducing the image quality. As the steady state tolerates small shifts in frequency it is possible to acquire a frequency-modulated bSSFP. Our study uses such a frequency-modulated approach in combination with a multi-frequency reconstruction to obtain banding free CINE images, with high signal and good contrast.

1795

Combination of Individual Coil QSM at High Field Strength (7T)
Uten Yarach¹, Hendrik Mattern¹, Alessandro Sciarra¹, and Oliver Speck¹

¹Department of Biomedical Magnetic Resonance, Otto-von-Guericke University Magdeburg, Magdeburg, Germany

Phase image reconstruction from multi-channel data at high field strength becomes challenging since a volume body coil that provides the phase offset information is generally not available. Several coil combination techniques are still computation intensive and prone to errors for strongly T2*-weighted data due to the requirement of spatial smoothness of image phases, required phase reference from body coil scan, and also hampered for strongly localized B1 coil sensitivities. These limitations lead to phase image inconsistencies and may cause artifacts in QSMs. We demonstrated here that the coil combination should be considered after performing individual physical and/or virtual coil QSM.

1796

Improving EPI Phase Correction for Breast DWI

Jessica A McKay¹, Steen Moeller², Sudhir Ramanna², Edward J Auerbach², Michael T Nelson², Kamil Ugurbil², Essa Yacoub², and Patrick J Bolan²

¹Department of Biomedical Engineering, University of Minnesota, Minneapolis, MN, United States, ²Department of Radiology, University of Minnesota, Minneapolis, MN, United States

It is important to improve ghost correction in breast DWI using SE-EPI because residual ghosts bias ADC measurements, which reflect malignancy. The standard ghost correction method using a 3-line navigator frequently fails in breast DWI. In this work we implemented several alternative ghost correction strategies. The two best methods outperformed the standard 3-line navigator correction. These techniques applied 1D, linear corrections based on 1) phase maps from separate reference scans and 2) entropy minimization.

1797

Simultaneous Reconstruction of Activity and Attenuation Involving MRI Information as a Prior
Rong Guo¹, Pei Han¹, Yicheng Chen², Jinsong Ouyang³, Georges El Fakhri³, and Kui Ying¹

¹Engineering Physics, Tsinghua University, Beijing, China, People's Republic of, ²UC Berkeley-UCSF Graduate Program in Bioengineering, University of California, Berkeley, Berkeley, CA, United States, ³Center for Advanced Radiological Sciences, Massachusetts General Hospital, Boston, MA, United States

The maximum likelihood activity and attenuation (MLAA) method usually utilizes time-of-flight (TOF) information to solve the problem of attenuation correction. However, the application of TOF brings noise. In this work, we proposed a method, Maximum a Posteriori for simultaneous activity and attenuation reconstruction (MAPAA), which introduces MRI information as prior knowledge into MLAA to reduce noise.

1798

Comparison of strict sparsity and low-rank constraints for accelerated fMRI data reconstruction
Charles Guan¹ and Mark Chiew²

¹Electrical Engineering, Stanford University, Fremont, CA, United States, ²FMRIB Centre, University of Oxford, Oxford, United Kingdom

Functional MRI has been slow to benefit from data acceleration techniques based on non-linear image reconstruction. We present a comparison of two non-linear image reconstruction methods based on sparsity and low-rank models of fMRI data. k-t FOCUSS uses an asymptotic L1 minimization program to solve for a sparse x-f reconstruction. In contrast, k-t FASTER solves for a spatio-temporally low-rank reconstruction using an iterative hard thresholding and matrix shrinkage algorithm, without requiring a pre-specified basis. We applied each algorithm to incoherently sampled fMRI data and demonstrate that the strict rank-constraint method outperforms spectral- and Karhunen-Loeve Transform (KLT)-sparsity across different metrics.

1799

3D Water-Fat Turbo Spin Echo Imaging in the Knee using CS-SENSE
Holger Eggers¹, Christian Stehning¹, Mariya Doneva¹, Elwin de Weerdt², and Peter Börnert^{1,3}

¹Philips Research, Hamburg, Germany, ²Philips Healthcare, Best, Netherlands, ³Department of Radiology, Leiden University Medical Center, Leiden, Netherlands

3D Dixon TSE scans essentially provide the same information as several conventional 2D TSE scans in different orientation, without and with fat suppression. However, their scan time is usually still too long for clinical practice. In this work, the basic feasibility of accelerating a 3D Dixon TSE scan with PD weighting by a combination of compressed sensing and parallel imaging was investigated in knee imaging. Results obtained in half the scan time compared to the use of parallel imaging alone are presented, which indicate that 3D Dixon TSE scans may become as fast as current, conventional 3D TSE scans with fat suppression.

1800

Joint Motion Estimation and Image Reconstruction Using Alternating Minimization
Luonan Wang¹ and Daniel S Weller¹

¹*Electrical and Computer Engineering, University of Virginia, Charlottesville, VA, United States*

This abstract provides a joint motion estimation and image reconstruction method for data acquired using a spiral pulse sequence. It forms a data fitting term with image and motion variables and uses alternating minimization with conjugate gradients to solve the nonlinear optimization problem. This approach will allow MR scanning to be more robust to non-rigid motion while still achieve fast image reconstruction. The new approach will enable MR imaging with children without sedation.

1801

Learning-based Reconstruction using Artificial Neural Network for Higher Acceleration
Kinam Kwon¹, Dongchan Kim¹, Hyunseok Seo¹, Jaejin Cho¹, Byungjai Kim¹, and HyunWook Park¹

¹*KAIST, Daejeon, Korea, Republic of*

A long imaging time has been regarded as a major drawback of MRI, and many techniques have been proposed to overcome this problem. Parallel imaging (PI) and compressed sensing (CS) techniques utilize different sensitivity of multi-channel RF coils and sparsity of signal in a certain domain to remove aliasing artifacts that are generated by subsampling, respectively. In this study, an artificial neural networks (ANN) are applied to MR reconstruction to reduce imaging time, and it is shown that the ANN model has a potential to be comparable to PI and CS.

1802

Reconstruction of Complex Images using Under-sampled Signal at Equal Interval in Phase Scrambling Fourier Transform Imaging
Satoshi ITO¹, Shungo YASAKA¹, and Yoshifumi YAMADA¹

¹*Information and Controls Systems Sciences, Utsunomiya University, Utsunomiya, Japan*

In this paper, we propose a new fast image reconstruction method in which a regularly undersampled signal is used instead of random sampling, as is used in compressed sensing. To diffuse the aliasing artifact caused by under-sampling, we adopt phase-scrambling Fourier transform imaging. The proposed method has an advantage over CS in that the quality of the image does not depend on the selection of the sampling trajectory. Simulation studies and experiments show that the proposed method has almost the same peak signal-to-noise ratio as that of a compressed sensing reconstruction.

1803

Accelerated EPRI Using Partial Fourier Compressed Sensing Reconstruction With POCS Phase Map Estimation and Spherical Sampling
Chia-Chu Chou¹, Taehoon Shin², JiaChen Zhuo², Gadisetti Chandramouli³, Murali Cherukuri³, and Rao Gullapalli²

¹*Electrical Engineering, University of Maryland, College Park, Beltsville, MD, United States*, ²*Diagnostic Radiology and Nuclear Medicine, University of Maryland School of Medicine, Baltimore, MD, United States*, ³*National Cancer Institute, Bethesda, MD, United States*

In Electron Paramagnetic Resonance Imaging (EPRI), each single k-space point is typically acquired per excitation and lengthens the acquisition time. In order to accelerate the imaging process, we raised a new image reconstruction method, Partial Fourier Compressed Sensing (PFCS), to address this problem. With PFCS, the images can be reconstructed from 25% of the k space and hence accelerate the imaging process to less than 1min. We also demonstrated PFCS reconstructed linewidth map were able to monitor the oxygen change in the tumor tissue.

1804

Parameter selection in Total Generalized Variation based reconstruction problems.
Carlos Milovic^{1,2}, Jose Miguel Pinto^{1,2}, Julio Acosta-Cabronero³, Pablo Irarrazaval^{1,2}, and Cristian Tejos^{1,2}

¹*Department of Electrical Engineering, Pontificia Universidad Católica de Chile, Santiago, Chile*, ²*Biomedical Imaging Center, Pontificia Universidad Católica de Chile, Santiago, Chile*, ³*German Center for Neurodegenerative Diseases (DZNE), Magdeburg, Germany*

An strategy for parameter selection in TGV regularized reconstruction problems is presented, with applications to deconvolutions and QSM. This allows fine-tuning of parameters in an efficient way and the use of predictors that are correlated to optimized results in terms of MSRE. This allows users to automatize or accelerate the parameter selection, critical in expensive problems such as QSM and reduce the error in the reconstruction.

1805

SNR and Banding Artifact Reduction Analysis of Phase-Cycled Elliptical Signal Model bSSFP
Steven T. Whitaker¹, Meredith Taylor¹, Haonan Wang¹, and Neal K. Bangerter¹

¹*Electrical Engineering, Brigham Young University, Provo, UT, United States*

Balanced steady-state free precession (bSSFP) provides high signal in short scan times. A new method for combining four or more phase-cycled bSSFP acquisitions was recently proposed that uses an elliptical signal model (ESM) of the bSSFP signal. In this study, we compare the SNR performance and effectiveness at reducing banding artifact of the ESM, complex sum, and sum-of-squares techniques across a range of T1 and T2 values, flip angles, and base SNR levels. Although ESM produces near perfect band removal in high SNR situations, it breaks down for certain tissues and in low SNR situations.

Acquisition

Exhibition Hall

Tuesday, May 10, 2016: 16:00 - 18:00

1806

Echo-planar imaging for a 9.4 Tesla vertical standard bore superconducting magnet using an unshielded gradient coil
Nao Kodama¹ and Katsumi Kose¹

¹*Institute of Applied Physics, University of Tsukuba, Tsukuba, Japan*

Echo planar imaging sequences were developed for a 9.4 Tesla vertical standard bore (~54 mm) superconducting magnet using an unshielded gradient coil. Because EPI requires fast switching of intense magnetic field gradients, eddy currents were induced in the surrounding metallic materials, e.g., the room temperature bore, and this produced serious artifacts on the EPI images. We solved the problem using an unshielded gradient coil set of proper size (39 mm OD, 32 mm ID) and reference scans. The obtained EPI images of a phantom and a plant sample were almost artifact free and demonstrated the promise of our approach.

1807

SERIAL Excitation with Parallel Reception Allows Human Brain Imaging at 9.4 Tesla at Low Power and with Acceptable Image Uniformity across the Full Field of View

Keith R. Thulborn¹, Chao Ma², Ian C. Atkinson¹, Theodore C. Claiborne¹, Steven M. Wright³, and Reiner Umathum⁴

¹*Center for Magnetic Resonance Research, University of Illinois, Chicago, IL, United States*, ²*Beckman Institute, University of Illinois at Urbana-Champaign, Urbana, IL, United States*, ³*Department of Biomedical Engineering, Texas A&M University, College Station, TX, United States*, ⁴*Division of Medical Physics in Radiology, German Cancer Research Center (DKFZ), Heidelberg, Germany*

SERIAL excitation produces uniform image intensity at low power at ultra high field but has not been applied to humans. FLASH sequences modified for sequential single coil excitation while retaining full array receive mode were combined with generalized total variation regularized SENSE reconstruction and 4- and 8- arrayed coils. Images with acceptable uniformity, contrast and resolution over the *in vivo* human brain are demonstrated at 9.4T using low power.

1808

An Optimized Slice Acquisition Order in HASTE Imaging with a Short TR
Wei Liu¹ and Kun Zhou¹

¹*Siemens Shenzhen Magnetic Resonance Ltd, Shenzhen, China, People's Republic of*

In this study, an optimized slice acquisition ordering method was proposed to improve the signal attenuation and contrast alteration caused by the crosstalk and MT effect in multi-slice HASTE imaging using a short TR. It demonstrated that a shorter acquisition time is possible with an optimized slice acquisition order. It allows a shorter TR, whilst maintaining the SNR and contrast similar to the conventional one, which is particularly useful in the abdominal imaging.

1809

Concurrent Excitation and Acquisition in Steady State: T1-Modulation Effects of Frequency Sweep
Ali Caglar Özen¹, Jan Korvink², and Michael Bock¹

¹*Dept. of Radiology - Medical Physics, University Medical Center Freiburg, Freiburg, Germany*, ²*Institute of Microstructure Technology, Karlsruhe Institute of Technology, Karlsruhe, Germany*

Concurrent Excitation and Acquisition (CEA) enables MRI with true zero echo times, and full signal acquisition efficiency. However, frequency sweep along readout gradients results in sequential excitation of spins at different locations, thus a unique TR is experienced by each spin at each radial acquisition spoke. In this work, implications of modulations in transverse magnetization as a function of T1, flip angle and TR were investigated for 2D and 3D radial acquisition schemes with equidistant point trajectory, segmented ordering and golden angle ordering. Resulting changes in point spread function (PSF) of a point source located at the edge of the field of view (FOV) were analyzed and discussed.

1810

Three dimensional T1 and T2* mapping of human lung parenchyma using interleaved saturation recovery and dual echo ultrashort echo time imaging
Neville D Gai¹, Ashkan A Malayeri¹, and David A Bluemke¹

¹*Radiology & Imaging Sciences, NIH, Bethesda, MD, United States*

Lung T1/T2* may be useful in discriminating between normal and pathological tissue particularly in disorders such as fibrosis, edema or emphysema. Quantitative mapping of the lung parenchyma is challenging due to the low proton density, respiratory and cardiac motion and susceptibility effects. Here we describe a technique based on segmented respiratory triggered 3D ultrashort echo time dual-echo radial imaging interleaved with and without a WET saturation pulse to estimate T1 and T2* maps simultaneously in a single scan. The results show that T1/T2* mapping of lung parenchyma can be reliably performed with relatively high resolution in a clinically feasible time.

Potential image artifacts in ultrashort echo-time imaging
Wingchi Edmund Kwok^{1,2}

¹Department of Imaging Sciences, University of Rochester, Rochester, NY, United States, ²Rochester Center for Brain Imaging, Rochester, NY, United States

Ultrashort echo-time imaging has been explored for the study of short T2* tissues. Most ultrashort TE sequences utilize 3D radial center-out k-space sampling. While they are potentially useful for many important applications, they are susceptible to various image artifacts. This abstract describes the appearances, causes and mitigations of some potential artifacts, which include those caused by long readout length, high gradient field, insufficient number of radial projections, off-centered imaging and signal wrap-around. An understanding of these artifacts will help in protocol setting and the identification of related problems. This article should benefit the users of ultrashort TE imaging.

The Harmonized Human Connectome Protocol for Multi-Site Brain MRI Studies

Joshua M Kuperman¹, Nathan S White¹, Hauke Bartsch¹, Matthew Middione², Kun Lu³, Thomas Liu³, Terry Jernigan⁴, Ajit Shankaranarayanan², and Anders M Dale^{1,5}

¹Radiology, University of California, San Diego, La Jolla, CA, United States, ²GE Healthcare, Menlo Park, CA, United States, ³Center for Functional Magnetic Resonance Imaging, University of California, San Diego, La Jolla, CA, United States, ⁴Center for Human Development, University of California, San Diego, La Jolla, CA, United States, ⁵Neurosciences, University of California, San Diego, La Jolla, CA, United States

The benefits of the advanced MRI protocols used in the Human Connectome Project have heretofore only been available on Siemens MRI scanners. We have designed a Connectome-like protocol, called the Harmonized Human Connectome Protocol, which can utilize MRI scanners from additional vendors, specifically GE and Philips. This protocol is particularly relevant for the Adolescent Brain and Cognitive Development Study, which aims to scan over 10,000 children ages 9-10 and follow them longitudinally for ten years. This abstract details the protocol for the GE MR750 scanner and outlines calibration and correction procedures which can be used to further reduce unwanted site/scanner effects.

Retrospective self-gated 3D UTE MRI in the mouse lung

Jinbang Guo^{1,2}, Xuefeng Cao^{1,3}, Zackary I. Cleveland¹, and Jason C. Woods^{1,2}

¹Center for Pulmonary Imaging Research, Cincinnati Children's Hospital Medical Center, Cincinnati, OH, United States, ²Physics, Washington University in St. Louis, St. Louis, MO, United States, ³Department of Physics, University of Cincinnati, Cincinnati, OH, United States

Motion due to respiration is one of the major difficulties in lung imaging of mice, which have a 10-20-fold higher respiratory rate than humans. In this study, we demonstrate that the FID signal amplitude ($k = 0$) as a function of projection number in center-out radial 3D UTE reflects respiratory motion. Retrospective "self"-gating using this FID signal amplitude was applied to extract data for end-expiration and end-inspiration respectively. Quantitative analysis of tidal volumes and lung parenchymal signal match external measurements and physiological expectations.

Highly-efficient free breathing whole heart CINE MRI with self gated 3D CASPR-TIGER trajectory

Muhammad Usman¹, Gastao Cruz¹, and Claudia Prieto¹

¹Division of Imaging Sciences and Biomedical Engineering, King's College London, London, United Kingdom

In this work, we propose to use a novel free-running self-gated 3D CArtesian acquisition with Spiral PROfile ordering and TIny Golden angle step for Eddy Current Reduction, so called CASPR-TIGER. Data is acquired continuously under free breathing (no ECG gating, no pre-pulses interruption) using CASPR-TIGER trajectory and 4D volumes (3D+time) are reconstructed from all available data (100% respiratory scan efficiency) using a soft gating technique combined with temporal total variational (TV) constrained iterative SENSE reconstruction. Feasibility of proposed method is demonstrated in three subjects in a 3-3.6 minutes free breathing acquisition.

4D flow MRI of the cardiovascular system in small animals at 7T with an Ultrashort TE sequence combined with an injection of iron nanoparticle

Aurelien J Trotier¹, Charles R CASTETS¹, William LEFRANCOIS¹, Emeline J RIBOT¹, Eric THIAUDIERE¹, Jean-Michel FRANCONI¹, and Sylvain MIRAU¹

¹RMSB-UMR5536, CNRS - Université de Bordeaux, Bordeaux, France

4D flow MRI on mouse models remains very difficult due to the very small size of vessels and the extremely high cardiac rhythm. To overcome this problem a 3D time-resolved Phase Contrast UTE sequence was combined with an injection of Ultra Small Particles of Iron Oxide to obtain a positive and high signal in blood. The method was exploited to quantify blood flow velocity of the cardiovascular system in mice with a high spatial (200 μ m)³ and temporal resolution (16ms). The total acquisition can be reduced to 25min by limiting the number of acquired projections per cine image.

Motion-correction enabled ultra-high resolution in-vivo imaging of the human brain at 7T
Daniel Gallichan¹

¹CIBM, EPFL, Lausanne, Switzerland

We extended previous work using 3D-FatNavs to enable motion-correction of ultra-high resolution structural acquisitions, including T1-, T2- and T2*-weighted images. Images are of exceptional quality and detail for in-vivo acquisitions.

1817

Quadra-FSE: A Multi-Platform Pulse Sequence for Multispectral qMRI (PD, T1, T2)
Hernan Jara¹, Arnaud Guidon², Jorge A Soto¹, and Osamu Sakai¹

¹*Radiology, Boston University, Boston, MA, United States*, ²*Global MR Applications and Workflow, GE Healthcare, Boston, MA, United States*

Purpose: To describe the quadra fast spin-echo (quadra-FSE) pulse sequence, which is the concatenation of two dual-echo FSE acquisitions differing only in TR and to describe the matching qMRI algorithms for mapping T1, T2, and PD. **Methods:** quadra-FSE was tested at 3T with a multi-compartment agarose phantom and relaxometry was compared to gold standard relaxometry scans using qMRI algorithms developed in house. **Results:** PD, T1, and T2 maps generated with the quadra-FSE scans are accurate and of excellent image quality. **Conclusion:** Concatenation of two DE-FSE scans with different TRs can be used for combined and accurate PD, T1, and T2 mapping.

1818

Optimized Parametric Variable Radius Sampling Scheme for 3D Cartesian k-Space Undersampling Pattern Design
Zechen Zhou¹, Shuo Chen¹, Aiqi Sun¹, Yunduo Li¹, Rui Li¹, and Chun Yuan^{1,2}

¹*Center for Biomedical Imaging Research, Department of Biomedical Engineering, School of Medicine, Tsinghua University, Beijing, China, People's Republic of*, ²*Vascular Imaging Laboratory, Department of Radiology, University of Washington, Seattle, WA, United States*

A parametric variable radius sampling scheme termed Cartesian Under-Sampling with Target Ordering Method (CUSTOM) was introduced for undersampling pattern design to better match the total number of sampling points with the given acceleration factor in 3D Cartesian imaging application. With the same joint parallel imaging and compressed sensing image reconstruction method, parameter optimized CUSTOM has demonstrated its enhanced performance particularly for detail image information restoration in comparison to several undersampling pattern design schemes, as well as its generalization ability in different applications. The prospective experiment validated the feasibility of CUSTOM in clinical settings.

1819

Quiet EPI (QuEPI) for single-shot spin and gradient echo EPI sequences for efficient fetal imaging
Jana Maria Hutter¹, Anthony N Price¹, Lucilio Cordero Grande¹, Emer Judith Hughes¹, Kelly Pegoretti¹, Andreia Oliveira Gaspar¹, Laura McCabe¹, Mary Rutherford¹, and Joseph V Hajnal¹

¹*Centre for the developing brain, King's College London, London, United Kingdom*

Quiet sequences are of particular importance for fetal EPI based imaging, where the necessary protection of the unborn infant can often compromise the efficiency and achievable resolution of the EPI acquisition. This is of particular relevance for connectome type studies, where long functional and diffusion weighted sequences need to be acquired in an efficient and safe way. This abstract presents a quiet SE and GE EPI framework with sinusoidal read-out constant phase and merged crusher strategy, completely flexible and adaptable to the scanner impulse response function leading to a decrease of up to 9dB(A).

1820

Readout Segmentation for Increased Spectral Bandwidth in High Spatial and Spectral Resolution (HiSS) MRI
David Andrew Porter¹ and Marco Vicari¹

¹*Fraunhofer MEVIS, Bremen, Germany*

A novel method of echo-planar spectroscopic imaging is introduced, in which readout segmentation is used to reduce the echo spacing and provide a substantial increase in spectral bandwidth. Results are presented, showing how the technique avoids the aliasing problems that affect conventional applications of high-resolution, spectroscopic imaging at 3T and serves as a robust method for providing spectrally-selective fat and water images. The method is also a promising option for high-bandwidth, spectroscopic imaging studies of metabolites at high field strengths.

1821

Multi-blade Acquisition of Split Turbo Spin Echoes: A Robust and Fast Diffusion Imaging Technique
Kun Zhou¹ and Wei Liu¹

¹*Siemens Shenzhen Magnetic Resonance Ltd., Shenzhen, China, People's Republic of*

A turbo spin echo based sequence for robust and fast diffusion imaging is proposed. It overcomes the non-CPMG problem by split-echo acquisition of turbo spin echo signals. EPI-like readout is used to sample the separated echoes and generate multiple blades for a single k-space. Each blade was corrected for both the inherent phase of separated echoes and off-resonance phase, to avoid the destructive interference. With this technique, the non-CPMG problem can be effectively mitigated at low flip angle refocusing pulses to reduce SAR. Moreover, the off-resonance artifacts can also be reduced especially when high acceleration factor is applied.

1822

A New Approach for Flexible Spatial Encoding Strategy in a Low-Field MRI System
Jiasheng Su¹ and Shaoying Huang¹

For a low-field MRI system, the inverse calculation of the encoding matrix is time consuming and moreover, there is a blurry area at the center of the reconstructed image. To solve this problem, three strategies are proposed. Firstly, QR decomposition is applied to inverse the matrix to eliminate the blurry area. Secondly, the encoding matrix is separated so that the results of the matrix inverse can be reused. Last, the size of encoding matrix is reduced by optimizing sample points. One example is given, the calculation time is reduced, and the imaging quality is improved. The proposed approach increases the imaging capability of a low-field MRI system.

1823

In Vivo Feasibility of Multi-Parametric Mapping Based on Fast Steady-State Sequences

Ludovic de Rochefort¹, Geneviève Guillot¹, Rose-Marie Dubuisson¹, and Romain Valabregue²

¹Imagerie par résonance magnétique médicale et multi-modalités, IR4M, UMR 8081, CNRS-Université Paris-Sud, Université Paris-Saclay, Orsay, France, ²CENIR, ICM, Inserm U 1127, CNRS UMR 7225, Sorbonne Universités, UPMC Univ Paris 06 UMR S 1127F, Paris, France

Fast steady-state sequences combine RF and gradient spoiling to modulate contrasts in MRI. The steady-state depends on many physical and acquisition parameters. Here, in vivo feasibility on brain is shown to map proton density, background phase, flip angle, relaxation rates and apparent diffusion coefficient from such sequences. Multiple volumes were acquired with various optimized prescribed flip angle, spoiling gradients and phase increments, and the complex signal was fitted to the Bloch-Torrey signal model with free diffusion using efficient calculation algorithms. The acquisition of full 3D co-localized multi-parametric maps of relevant MR physical parameters in a realistic scan time is demonstrated.

1824

Dynamic pH quantification from spectrally selective ³¹P MRI in exercising skeletal muscle

Albrecht Ingo Schmid^{1,2}, Martin Meyerspeer^{1,2}, Simon Daniel Robinson^{2,3}, Martin Krssak^{2,3,4}, Michael Wolzt⁵, Ewald Moser^{1,2}, and Ladislav Valkovic^{2,3}

¹Center for Medical Physics and Biomedical Engineering, Medical University of Vienna, Vienna, Austria, ²MR Centre of Excellence, Medical University of Vienna, Vienna, Austria, ³Department of Biomedical Imaging and Image-guided Therapy, Medical University of Vienna, Vienna, Austria, ⁴Department of Internal Medicine 3, Medical University of Vienna, Vienna, Austria, ⁵Department of Clinical Pharmacology, Medical University of Vienna, Vienna, Austria

MR spectroscopy provides valuable information about tissue metabolism but suffers from slow acquisition or poor spatial resolution and coverage. PCr and pH kinetics are the two important quantities derived from ³¹P MR data. MRI has been used to measure PCr in the past, but not pH. Simultaneous fast 3-D gradient-echo images of PCr and Pi were acquired in healthy volunteers at 7T during exercise recovery. pH was calculated from phase images. Results of PCr and pH kinetics are comparable to MRS data. In conclusion, ³¹P MRI is an alternative to ³¹P MRS for fast coverage of multiple ROIs and low SAR.

1825

Accelerated Imaging of the Mouse Body using k-space Segmentation, Cardio-Respiratory Synchronisation and Short, Constant TR: Application to b-SSFP.

Paul Kinchesh¹, Stuart Gilchrist¹, Ana L Gomes¹, Veerle Kersemans¹, John Beech¹, Danny Allen¹, and Sean Smart¹

¹Department of Oncology, University of Oxford, Oxford, United Kingdom

We demonstrate that cardio-respiratory synchronisation can be achieved in conjunction with short TR scans and k-space segmentation to reduce imaging times to below that achievable using standard techniques such as retrospective gating. Our method is generally applicable to other short TR scan modes requiring cardio-respiratory synchronisation. Images of the mouse heart, lung and liver are presented for the b-SSFP scan mode.

1826

Rapid Multi-echo Ultrashort Time Echo Imaging for MR-based Attenuation Correction in PET/MR

Hyungseok Jang^{1,2} and Alan B McMillan¹

¹Department of Radiology, University of Wisconsin, Madison, WI, United States, ²Department of Electrical and Computer Engineering, University of Wisconsin, Madison, WI, United States

Accurate MR-based attenuation correction (MRAC) is necessary to enable quantitative PET imaging in PET/MR. Unfortunately, identification of bone via MR methods is technically challenging due to its short T2*. Thus, ultrashort time echo (UTE) techniques have been proposed. In this study, we explored rapid multi-echo frequency encoded UTE and ramped hybrid encoding (RHE) for UTE-based imaging schemes for MRAC with clinically feasible scan times (<35sec). By using an IDEAL-based signal model for long T2* suppression, multi-echo hybrid encoding UTE imaging performed better than frequency encoded UTE.

1827

Banding-artifact free bSSFP cine imaging using a Geometric Solution approach

André Fischer^{1,2}, Michael N. Hoff³, Piero Ghedin^{1,2,4}, and Anja C.S. Brau²

¹GE Global Research, Garching bei München, Germany, ²Cardiac Center of Excellence, GE Healthcare, Garching bei München, Germany,

³Department of Radiology, University of Washington, Seattle, WA, United States, ⁴GE Healthcare, Waukesha, WI, United States

Banding artifacts in bSSFP sequences pose a challenge in cardiac cine imaging, especially at 3.0T. Recently, a "Geometric Solution" (GS) which is capable of completely removing banding artifacts has been introduced and demonstrated in applications outside the heart. This work investigates the feasibility of extending GS to cardiac cine imaging at 3.0T and explores its potential to enable longer TRs than

have conventionally been feasible with bSSFP, permitting sub-millimeter resolution cine imaging free of banding artifacts.

1828

Myelin Water Fraction with Bipolar Multiecho sequences using k-space shift correction
Hongpyo Lee¹, Yoonho Nam², Min-Oh Kim¹, Dongyeob Han¹, and Dong-Hyun Kim¹

¹*School of Electrical and Electronic Engineering, Yonsei University, Seoul, Korea, Republic of*, ²*Department of Radiology, Seoul St. Mary Hospital, College of Medicine, The Catholic University of Korea, Seoul, Korea, Republic of*

Recently, myelin water fraction was investigated using multi-echo GRE data. Generally, to ensure phase consistency among the echoes, multi-echo acquisitions use unipolar gradients. However, these unipolar gradient multi-echo sequences reduce acquisition efficiency and increase echo spacing. Bipolar gradients would be preferential however, k-space misregistration induced by readout gradient delays and eddy-currents make phase errors, so severe artifacts occur in myelin water imaging. In this abstract, we present a MWI using bipolar gradient multi-echo GRE sequence with k-space shift correction. Compared to unipolar MWI, k-space shift corrected bipolar MWI yields a reduction in ΔTE , which leads to improved SNR and more accurate quantification.

1829

Phase-Encode Ghosting Detection using Multi-Channel Coil Arrays
Tom Hilbert^{1,2,3}, Tobias Kober^{1,2,3}, Jean-Philippe Thiran^{2,3}, Reto Meuli², and Gunnar Krueger^{2,3,4}

¹*Advanced Clinical Imaging Technology (HC CMEA SUI DI BM PI), Siemens Healthcare AG, Lausanne, Switzerland*, ²*Department of Radiology, University Hospital (CHUV), Lausanne, Switzerland*, ³*LTS5, École Polytechnique Fédérale de Lausanne, Lausanne, Switzerland*, ⁴*Siemens Medical Solutions USA, Inc., Boston, MA, United States*

Phase-encode ghosting artifacts frequently occur in magnetic resonance imaging, especially in spin-echo sequence derivatives such as fluid-attenuated inversion recovery. The appearance of these artifacts may cause misinterpretation as tissue pathology, e.g. a lesion. We propose an algorithm to automatically detect these artifacts by analyzing the consistency of the acquired k-space with respect to the assumption of GRAPPA that a k-space sample is a linear sum of its neighboring samples. The performance of the technique is shown in three volunteers. It may help to avoid potential misinterpretation in the future, both for radiological readers and automated post-processing algorithms.

1830

Quantitative Temperature Imaging in Chemically Designed Phantoms
Scott D. Swanson¹, Dariya I. Malyarenko¹, and Thomas L. Chenevert¹

¹*Department of Radiology, University of Michigan, Ann Arbor, MI, United States*

Quantitative temperature mapping

1831

Artifact reduction in 3D radial imaging with out-of-volume saturation pulses
Jacob Macdonald¹, Oliver Wieben^{1,2}, Scott K Nagle², and Kevin M Johnson¹

¹*Medical Physics, University of Wisconsin - Madison, Madison, WI, United States*, ²*Radiology, University of Wisconsin - Madison, Madison, WI, United States*

Streaking artifacts in radial acquisitions from undersampling or data inconsistencies can reduce SNR and make it difficult to discern features in low signal areas. Anatomy that is outside of the imaging volume of interest but within the excitation volume can contribute to these artifacts. We used out-of-volume spatial saturation pulses to suppress these streaking artifacts with minimal scan time penalties. In-vivo acquisitions with spatial saturation showed equal or superior quality in all cases. They should be implemented whenever the additional SAR can be tolerated.

1832

Zigzag-Aligned-Projections in Echo-Planar Imaging
Patrick Alexander Liebig^{1,2}, Robin Martin Heidemann², and David Andrew Porter³

¹*Friedrich-Alexander-Universität Erlangen-Nürnberg, Erlangen, Germany*, ²*Siemens Healthcare GmbH, Erlangen, Germany*, ³*Fraunhofer MEVIS, Bremen, Germany*

A new approach to Echo-Planar Imaging (EPI) is introduced under the name Zigzag-Aligned-Projections (ZAP) that replaces the blipped phase-encoding (PE) gradient with the modulus of the readout (RO). This comes with two significant advantages: the reduction of acoustic noise due to the modified PE gradient and the higher efficiency due to continuous data sampling. ZAP EPI is the only EPI derivative that combines Cartesian GRAPPA using a fixed Kernel size with continuous data sampling. The reduction in acoustic noise was verified experimentally and volunteer images were acquired and processed with two reconstruction techniques.

1833

A Dual Spin-Echo Technique with Hybrid Spiral Readouts for Fast Simultaneous Proton Density- and T2-Weighted Fat-Water Imaging
Zhiqiang Li¹, Dinghui Wang¹, John P Karis², and James G Pipe¹

¹*Imaging Research, Barrow Neurological Institute, Phoenix, AZ, United States*, ²*Neuroradiology, Barrow Neurological Institute, Phoenix, AZ, United States*

Turbo spin-echo (TSE) provides rapid T2-weighted imaging with slightly altered contrast compared to Cartesian spin-echo (SE). A spiral

SE technique has been proposed for fast T2-weighted imaging without degrading the T2 contrast. In this study a dual echo spiral SE with hybrid spiral readouts is developed to simultaneously provide both proton density and T2 contrast without increasing the scan time. Volunteer results from the spiral dual SE technique demonstrate similar contrast to conventional SE, with a scan speed faster than Cartesian mDixon TSE.

1834

Spiral Time of Flight MRA with Dixon Water and Fat Separation
Nicholas R. Zwart¹, Dinghui Wang¹, and James G. Pipe¹

¹*Imaging Research, Barrow Neurological Institute, Phoenix, AZ, United States*

Time of Flight MRA in the head and neck can benefit from Dixon fat signal removal. The spiral trajectory is used to speed up the acquisition allowing 3-echoes to be collected, for Dixon reconstruction, in less time than a conventional single echo ("out-of-phase") cartesian MRA.

1835

Two NSA or not two NSA: does perforator artery detection in white matter benefit from signal averaging?
Lennart Geurts¹, Sander Brinkhof¹, Peter R. Luijten¹, and Jaco J.M. Zwanenburg¹

¹*Radiology, UMCU, Utrecht, Netherlands*

Because cerebral perforating arteries have sub-millimeter diameters and slow blood flow velocities, their blood flow velocity and pulsatility measurements are challenging and limited by noise and partial volume effects. Our previously reported acquisition method used two signal averages (NSA) to increase the signal-to-noise ratio (SNR). We show that decreasing NSA, and thereby reducing scan time by half, has little effect on vessel detection. The NSA=1 coefficients of repeatability (CoR) found in this study are similar to previously published NSA=2 CoR's. Subject motion and small vessel size likely play together to cause a sub-optimal benefit from increased imaging time.

1836

Quantitative analysis of the volume and lipid content of liver and spleen using Dual-echo mDixon sequence and T2WI-STIR sequences in child and adolescent patients with gaucher disease
Xiaojuan TAO¹, Yun PENG¹, Yanqiu LV¹, and Kaining SHI²

¹*Imaging Center of Beijing Children's Hospital Affiliated To Capital Medical University, Beijing, China, People's Republic of, ²Imaging Systems Clinical Science Philips Healthcare, Beijing, China, People's Republic of*

Spleen and liver are common organs involved in Gaucher disease (GD), while few reports have been published on the measurement of volume and lipid content of liver and spleen using MR. This study recruited 42 patients with GD by 1.5T MR. Our results showed that enlargement of spleen was more severe than liver. Spleen has higher lipid content than liver among these patients, while both of them exhibited higher fat fraction than normal value. Our study suggests MRI can be employed to monitor the disease progression and effect of the treatment in children and adolescent patients with GD.

1837

Exploring sodium SSFP MRI in phantoms at 3 Tesla
Rahel Heule^{1,2}, Philipp Madörin^{1,2}, and Oliver Bieri^{1,2}

¹*Division of Radiological Physics, Department of Radiology, University of Basel Hospital, Basel, Switzerland, ²Department of Biomedical Engineering, University of Basel, Basel, Switzerland*

While the steady-state free precession (SSFP) dynamics of spin-1/2 nuclei such as ¹H obey the Bloch equations, a similar mathematical framework for describing and understanding the characteristics of ²³Na SSFP signal behavior is not yet available. In this work, sodium MRI probes were investigated and, in particular, a novel class of phantoms was presented that proved the ability to generate high sodium signal at 3 Tesla without impairment due to the skin effect. By means of balanced SSFP frequency profile measurements, the potential of the novel phantoms to explore ²³Na SSFP was demonstrated.

1838

Artifact reduction of dental implants on high resolution MR imaging
Tim Hilgenfeld¹, Alexander Heil¹, Sebastian Schwindling², David Grodzki³, Mathias Nittka³, Daniel Gareis⁴, Peter Rammelsberg², Martin Bendszus¹, Sabine Heiland¹, and Marcel Prager¹

¹*Division of Neuroradiology, University Heidelberg, Heidelberg, Germany, ²Division of Prosthodontics, University Heidelberg, Heidelberg, Germany, ³Siemens Healthcare GmbH, Erlangen, Germany, ⁴NORAS MRI products GmbH, Höchberg, Germany*

Dental MRI is a new technique which is often impaired by artifacts due to metallic dental implants. Several MRI sequences were developed to reduce susceptibility artifacts (e.g. for orthopaedic implants). Here, we for the first time systematically evaluated MR sequences for artifact reduction in dental implants. Smallest artifact volume was measured for 2D-TSE sequences. Since imaging of dental structures benefit from high resolution and possibility of 3D reconstructions 3D sequences are advantageous. Significant artifact reduction was noted for SPC-WARP measuring only 2.1 times artifact volume of TSE sequence instead of 4.8 times when using standard SPC sequence.

Motion Correction

Exhibition Hall

Tuesday, May 10, 2016: 16:00 - 18:00

1839



Real-time diaphragm navigation using reflected power measurements from a multiple channel transmit RF coil on a human 7T
Aaron T Hess¹, Christopher T Rodgers¹, and Matthew D Robson¹

¹OCMR, University of Oxford, Oxford, United Kingdom

The reflected power of transmit RF coils is influenced by the position of the diaphragm. In this work the diaphragm position is measured in real-time for every RF pulse with a hybrid approach. The set of reflection coefficients are transformed into a diaphragm position using a series of MR diaphragm navigators at the start of the pulse sequence in a learning cycle. We demonstrate high quality respiratory gated data based on gating via this mechanism using standard SAR monitoring hardware with a real-time lag of 23ms and temporal resolution of 4.5ms.

1840

Towards robust c-spine imaging with Cartesian sampling

Guobin Li¹, Zhaopeng Li¹, Chaohong Wang¹, Yang Xin¹, Shuheng Zhang¹, Weijun Zhang¹, Xiaodong Zhou¹, and Weiguo Zhang¹

¹Shanghai United Imaging Healthcare Co., Ltd, Shanghai, China, People's Republic of

C-spine imaging is demanding due to artifacts from CSF flow, patient's swallowing etc., especially in FSE sequence with inversion recovery. By increasing the excitation thickness in FSE sequence, two concomitant saturation bands are realized at both sides of each image slice, which suppress the moving CSF. Furthermore, a snapshot k-space ordering is proposed to further improve the stability of c-spine imaging against irregular flow of CSF and patient's bulk motion.

1841

Rapid and continuous respiratory motion-resolved abdominal MRI using 3D golden-angle spiral projection acquisition

Mootaz Eldib¹, Li Feng², Daniel K Sodickson², Zahi A Fayad¹, and Hadrien A Dyvorne¹

¹Translational and Molecular Imaging Institute, Icahn school of Medicine at Mount Sinai, New York, NY, United States, ²Center for Advanced Imaging Innovation and Research (CAI2R), Bernard and Irene Schwartz Center for Biomedical Imaging, Department of Radiology, New York University School of Medicine, New York, NY, United States

We propose a novel acquisition technique for motion-resolved abdominal imaging. Using a golden angle spiral projection trajectory, we were able to acquire reliable physiologic tracking data while acquiring 3D isotropic resolution images of the entire upper abdomen, resulting in an efficient self-gated sequence. We show that respiratory motion can be fully characterized *in vivo* in a minute-long 1.8 mm isotropic acquisition, which is suitable for applications such as PET/MR motion correction.

1842

A Nonrigid-Motion-Correction Method for Coronary Magnetic Resonance Angiography Using 3D Image-based Navigators

Jieying Luo¹, Nii Okai Addy¹, R. Reeve Ingle¹, Corey A. Baron¹, Joseph Y. Cheng¹, Bob S. Hu^{1,2}, and Dwight G. Nishimura¹

¹Electrical Engineering, Stanford University, Stanford, CA, United States, ²Palo Alto Medical Foundation, Palo Alto, CA, United States

3D image-based navigators (iNAVs) offer the potential to achieve more complete motion correction for coronary magnetic resonance angiography (CMRA). In this work, we develop a method for 3D-iNAV processing to achieve nonrigid motion correction. Both global and localized motion trajectories are extracted from the 3D iNAVs and used to generate candidate motion-corrected images for an autofocus method. Two sets of localized motion trajectories are obtained from deformation fields between 3D iNAVs and reconstructed binned images respectively. Results with this method on whole-heart 3D cones CMRA scans demonstrated improved vessel sharpness as compared to 3D translational motion correction.

1843

Evaluation of motion patterns and their effect on image quality in pediatric populations

Onur Afacan¹, Burak Erem¹, Diona P. Roby¹, Noam Roth², Amir Roth², Sanjay P. Prabhu¹, and Simon K. Warfield¹

¹Radiology, Boston Childrens Hospital and Harvard Medical School, Boston, MA, United States, ²Robin Medical Inc., Baltimore, MD, United States

In this work we report results from a large pediatric study that shows the effect of motion. Motion patterns were measured on 82 children, mean age 13.4 years, in a T1 weighted brain MRI. An expert radiologist graded the images using a 4-point scale ranging from clinically non-diagnostic to no motion artifacts. We used these grades to correlate motion parameters such as maximum motion, mean displacement from a reference point and motion free time. The results will help the motion correction community in better understanding motion patterns in pediatric populations and how it effects image quality.

1844

Prospective Motion Correction in Diffusion Tensor Imaging using Intermediate Pseudo-Trace-Weighted Images

Daniel Christopher Hoinkiss¹, Matthias Guenther¹, and David Andrew Porter¹

¹MR Physics, Fraunhofer MEVIS, Bremen, Germany

Diffusion Tensor Imaging is frequently affected by long-term subject motion. Intermediate pseudo-trace-weighted images enable a real-time image registration with low sensitivity to contrast variation between diffusion-weighted images. These registration results are used

to correct the imaging parameters of the ongoing scan. The algorithm was evaluated on three individual subjects using a dedicated diffusion-weighted imaging sequence. The prospective motion correction was able to reduce the typical long-term motion to a band of approximately ± 0.2 mm for translational and $\pm 0.2^\circ$ for rotational motion, which is far below voxel size, without increasing the total scan time or changing the set of diffusion vectors.

1845

Image Reconstruction System for Compressed Sensing Retrospective Motion Correction for the Application in Clinical Practice
Martin Schwartz^{1,2}, Thomas Küstner^{1,2}, Christian Würslin¹, Petros Martirosian¹, Nina F. Schwenzer³, Fritz Schick¹, Bin Yang², and Holger Schmidt³

¹Section on Experimental Radiology, Department of Radiology, University of Tuebingen, Tuebingen, Germany, ²Institute of Signal Processing and System Theory, University of Stuttgart, Stuttgart, Germany, ³Diagnostic and Interventional Radiology, Department of Radiology, University of Tuebingen, Tuebingen, Germany

Respiratory motion-free images are important in MRI of the human thorax and abdomen. A significant factor is the reconstruction of these images for the application in clinical practice. The objective of the presented work is an integration of an approved motion correction algorithm into the clinical environment to overcome limitations of offline reconstructed images by the utilization of external workstations. Therefore, a reconstruction pipeline based on the open-source framework Gadgetron with new modules for the integration of a motion correction algorithm is demonstrated.

1846

Brain pulsatility across the cardiac cycle revealed by cine 3D integrated-SSFP
Lirong Yan¹, Mayank Jogi¹, Kay Jann¹, Xingfeng Shao¹, and Danny JJ Wang¹

¹Neurology, University of California Los Angeles, Los Angeles, CA, United States

The alternations of brain pulsatility are related to various pathological changes such as traumatic brain injury (TBI) and brain tumor. In the present study, we introduced a new MRI approach to assess the brain's biomechanical features using ECG-gated cine 3D integrated-SSFP, which offers dynamic 3D brain volumes with high spatial resolution. The voxel-wise deformation was derived from jacobian maps over the cardiac cycle. We found that greater deformation in the brain occurs in basal ganglia and brain stem, and then attenuates toward the white matter and brain cortex during the cardiac cycle.

1847

An MR Motion Correction toolbox for registration and evaluation

Thomas Küstner^{1,2}, Verena Neumann², Martin Schwartz^{1,2}, Christian Würslin^{1,3}, Petros Martirosian¹, Sergios Gatidis¹, Nina F. Schwenzer¹, Fritz Schick¹, Bin Yang², and Holger Schmidt¹

¹Department of Radiology, University Hospital Tübingen, Tübingen, Germany, ²Institute of Signal Processing and System Theory, University of Stuttgart, Stuttgart, Germany, ³University of Stanford, Palo Alto, CA, United States

Motion estimation is an important task in MRI. For retrospective motion correction, there is often an image-based registration involved. Hence, the extraction of a reliable and accurate motion model for the underlying application is mainly dependent on the chosen image registration procedure. There are several different image registration methods available, but visualization and evaluation of the derived displacement fields and transformed images often remains an open topic. In the spirit of a reproducible research and for streamlining and simplifying the process, we provide GUIs and evaluation methods to perform and analyze image registration techniques which will be made publicly available.

1848

Autofocusing-based correction of B0 fluctuation-induced ghosting

Alexander Loktyushin^{1,2}, Philipp Ehses¹, Bernhard Schölkopf², and Klaus Scheffler^{1,3}

¹High-field Magnetic Resonance, Max Planck Institute for Biological Cybernetics, Tübingen, Germany, ²Empirical Inference, Max Planck Institute for Intelligent Systems, Tübingen, Germany, ³Biomedical Magnetic Resonance, University of Tübingen, Tübingen, Germany

Long-TE gradient-echo images are prone to ghosting artifacts. Such degradation is primarily due to magnetic field variations caused by breathing or motion. The effect of these fluctuations amounts to different phase offsets in each acquired *k*-space line. A common remedy is to measure the problematic phase offsets using an extra non-phase-encoded scan before or after each imaging readout. In this work, we attempt to estimate the phase offsets directly from the raw image data by optimization-based search of phases that minimize an image distortion measure. This eliminates the need for any sequence modifications and additional scan time.

1849

TArgeted Motion Estimation and Reduction (TAMER): Data Consistency Based Motion Mitigation using a Reduced Model Joint Optimization

Melissa Haskell^{1,2}, Stephen Cauley^{1,3}, and Lawrence Wald^{1,3,4}

¹Athinoula A. Martinos Center for Biomedical Imaging, MGH/HST, Charlestown, MA, United States, ²Graduate Program in Biophysics, Harvard University, Cambridge, MA, United States, ³Harvard Medical School, Boston, MA, United States, ⁴Harvard-MIT Division of Health Sciences and Technology, MIT, Cambridge, MA, United States

We approach the reconstruction of artifact-free images from an object undergoing unknown rigid-body transformations using a joint optimization of the final uncorrupted image and motion parameters. To characterize motion, the joint optimization must estimate 6 additional parameters for each shot in the image acquisition. We demonstrate an efficient method for reconstruction from translation-corrupted *k*-space data by examining iterative improvements to only a small, targeted subset of imaging voxels. The method can be

enhanced by providing incomplete or noisy information from motion sensors or navigator measurements. We discuss generalizing our hybrid greedy and global step non-linear optimization to full rigid-body motion.

1850

A qualitative and quantitative comparison of virtual template based registration methods to control motion in DCE-MRI
Isabella Radl¹, Stephen Keeling², and Rudolf Stollberger^{1,3}

¹*Institute of Medical Engineering, Graz University of Technology, Graz, Austria*, ²*Institute for Mathematics and Scientific Computing, Karl Franzens University of Graz, Graz, Austria*, ³*BioTechMed Graz, Graz, Austria*

Different applications in DCE-MRI suffer from inter-frame misalignment due to physiological motion, which has to be compensated for further analysis of functional parameters. Conventional motion correction methods are usually unable to register images with simultaneous changes of contrast and morphology. Virtual-template based registration overcomes this problem by iteratively generating a motion-less image series with the contrast behaviour of the original DCE data as registration targets. We investigated different methods to generate these virtual-templates and identified Independent Component Analysis as best approach among the investigated techniques. Results were validated on a synthetic kidney phantom and in-vivo myocardial perfusion MRI.

1851

Three dimensional retrospective motion correction using spherical navigator echoes
Patricia M Johnson^{1,2}, Junmin Liu¹, Trevor Wade¹, and Maria Drangova^{1,2}

¹*Robarts Research Institute, London, ON, Canada*, ²*Department of Medical Biophysics, Schulich School of Medicine & Dentistry, London, ON, Canada*

Spherical navigators are k-space navigators that can measure 6-degree of freedom rigid-body motion. Recent developments have reduced processing and baseline acquisition time, making the technique a promising tool for motion correction. This work represents the first time SNAVs have been incorporated into an image sequence and demonstrated for motion correction. SNAVs were incorporated into a gradient echo sequence; this navigated sequence was used to scan 3 volunteers performing directed head motion. The motion-degraded brain images were then retrospectively corrected using the SNAV derived motion parameters. In all cases excellent correction of motion artifacts was observed.

1852

Analysis of Motion and Eddy Currents with 3D Cones Reordering for Whole-Heart Coronary MR Angiography
Mario O. Malavé¹, Nii Okai Addy¹, R. Reeve Ingle¹, Joseph Y. Cheng¹, Corey A. Baron¹, and Dwight G. Nishimura¹

¹*Electrical Engineering, Stanford University, Stanford, CA, United States*

Motion and eddy current artifacts were investigated with simulations, metric measures, and in vivo scans for three different cone acquisition schemes: sequential, multidimensional golden means (MDGM), and phyllotaxis readout orderings. We demonstrate the idea of using the 3D cones phyllotaxis acquisition method for improved motion behavior and low eddy current susceptibility. Also, the sequential ordering method is shown to be more susceptible to motion artifacts while the MDGM introduces eddy current artifacts. When using the phyllotaxis design, the reconstruction demonstrates that a more spread out k-space traversal per heartbeat is more robust to motion and can be obtained without introducing eddy currents.

1853

Robust Self-Gated Free-Breathing 3D Cardiac MRI Using DC Signals and Virtual Coils
Xinwei Shi^{1,2}, Joseph Y Cheng^{1,2}, Michael Lustig³, John M Pauly², and Shreyas S Vasanawala¹

¹*Radiology, Stanford University, Stanford, CA, United States*, ²*Electrical Engineering, Stanford University, Stanford, CA, United States*, ³*Electrical Engineering and Computer Science, UC Berkeley, Berkeley, CA, United States*

In cardiac MRI, self-gating using the DC signal provides a promising alternative to EKG gating. However, the DC signal is often affected by other moving structures in the FOV, such as the liver, which degrades the accuracy of the extracted cardiac triggers. In this work, we demonstrate the use of virtual coils to focus the DC signal on cardiac motion and to provide a robust and generalized self-gating approach for 3D cardiac MRI. In free-breathing 4D-Flow scans of pediatric subjects, the proposed method improved the accuracy of self-gating triggers, and the self-gated images showed comparable quality with EKG gated reference.

1854

Concomitant and seamless saturation bands for suppressing flow artifacts in FSE sequences
Guobin Li¹, Zhaopeng Li¹, Chaohong Wang¹, Yang Xin¹, Weijun Zhang¹, Xiaodong Zhou¹, and Weiguo Zhang¹

¹*Shanghai United Imaging Healthcare Co., Ltd, Shanghai, China*, *People's Republic of*

To reduce pulsatile artifacts of blood flow in FSE imaging, a combined solution is proposed, in which two concomitant saturation bands are achieved at both side of each slice without any extra RF pulses and gradients. Furthermore, through a proper setting of slice acquisition order, flowing blood can be continuously and seamlessly saturated in multi-slice acquisition.

1855

Comparison of respiratory navigator-gating techniques in two-dimensional spoiled gradient-recalled echo sequence
Hirofumi Hata¹, Yusuke Inoue², Ai Nakajima¹, Shotaro Komi¹, Yutaka Abe¹, Keiji Matsunaga², and Hiroki Miyatake¹

¹*Department of Radiology, Kitasato University Hospital, Sagamihara, Japan*, ²*Department of Diagnostic Radiology, Kitasato University School of Medicine, Sagamihara, Japan*

We compared navigator-gating techniques for free-breathing 2D SPGR images of the liver using pencil-beam excitation and self-navigation techniques in 3 T MRI. In pencil-beam navigator, single-check (PB-SC) and double-check (PB-DC) modes were examined. In self-navigator scans, self-navigator signals were acquired in two fashions; before (SN-Pre) or after (SN-Post) the imaging read-out. Visual analysis shows that respiratory waveforms fluctuated in SN-Post. Quantitative and qualitative image evaluations show that PB-DC and SN-Post had better image qualities than the others. Considering scan time was about doubled in SN-Post, PB-DC should be the best for respiratory navigation in 2D SPGR imaging at this stage.

1856

Silent Navigator with Whole Volume Excitation

Yuji Iwadate¹, Atsushi Nozaki¹, Yoshinobu Nunokawa², Shigeo Okuda³, Masahiro Jinzaki³, and Hiroyuki Kabasawa¹

¹*Global MR Applications and Workflow, GE Healthcare Japan, Hino, Tokyo, Japan*, ²*Department of Radiation Technology, Keio University Hospital, Tokyo, Japan*, ³*Department of Diagnostic Radiology, Keio University School of Medicine, Tokyo, Japan*

The conventional pencil-beam navigator suffers from large acoustic noise due to oscillating gradient pulses during RF excitation. We developed a silent navigator technique with whole volume excitation (vNav). The vNav technique reduced acoustic noise to almost the same level as background. In volunteer scan, a waveform of vNav was well correlated with the bellows signal, and motion reduction was demonstrated in 3D-SPGR imaging. The vNav integration into the silent imaging sequence should be examined in the next step.

1857

Auto-Calibrating Wave-CS for Motion-Robust Accelerated MRI

Feiyu Chen¹, Tao Zhang^{1,2}, Joseph Y. Cheng^{1,2}, John M. Pauly¹, and Shreyas S. Vasanawala²

¹*Electrical Engineering, Stanford University, Stanford, CA, United States*, ²*Radiology, Stanford University, Stanford, CA, United States*

In this work, we propose a motion-robust auto-calibrating Wave-CS technique. This technique uses the wave-encoded center k-space and the known point-spread-function (PSF) of wave-encoding to reconstruct a Cartesian central k-space for calibration. The coil sensitivity maps are subsequently estimated with ESPRIT for CS-SENSE reconstruction of under-sampled k-spaces. Results show this approach can reduce the motion artifacts and the aliasing artifacts due to sensitivity variations between the calibration and accelerated wave-encoded acquisitions.

1858

Towards Markerless Optical Tracking for Prospective Motion Correction in Brain Imaging

Julian Maclarens¹, Andre Kyme^{2,3}, Murat Aksoy¹, and Roland Bammer¹

¹*Department of Radiology, Stanford University, Stanford, CA, United States*, ²*Department of Biomedical Engineering, University of California Davis, Davis, CA, United States*, ³*Brain and Mind Centre, University of Sydney, Sydney, Australia*

Prospective motion correction based on optical tracking shows promise for improving image quality in MR brain imaging. To simplify this technique and expedite clinical deployment, it is desirable to avoid attaching markers to the patient's head. Here we demonstrate proof-of-principle markerless tracking using an MR-compatible stereo camera and head coil configuration. We tested the method outside the MR environment using a 6-axis robot, capable of very accurate and repeatable (~20 μ m) motion, to control a head phantom. Close agreement between our pose estimates and the applied motion suggests that accurate markerless tracking of the head is feasible in MRI.

1859

Reduction of Through-Plane Flow Artifacts in Contrast-Enhanced Liver MRI Using Motion-Sensitized Driven-Equilibrium (MSDE):

Comparison of MSDE types

Seiichiro Noda¹, Nobuyuki Toyonari¹, Yukari Horino¹, Masami Yoneyama², and Kazuhiro Katahira¹

¹*Kumamoto Chuo Hospital, Kumamoto, Japan*, ²*Philips Electronics Japan, Tokyo, Japan*

Gadoxetic acid enhanced mDIXON liver MRI has excellent utility for diagnosing hepatocellular carcinoma; however, it often suffers from ghosting flow artifacts from aorta due to increased signal by contrast enhancement. To solve this problem, we attempt to use motion-sensitized driven-equilibrium (MSDE) for reducing through-plane flow artifacts particularly in dynamic contrast-enhanced studies. We showed the effect of MSDE in reducing through-plane flow artifacts particularly in dynamic contrast-enhanced studies. Two types MSDE schemes (MSDE and iMSDE) could significantly decrease flow signals and could therefore reduce flow artifacts sufficiently. In current sequence, iMSDE would be better for clinical studies because of its less sensitivity to field inhomogeneities.

1860

Real Time MRI Motion Correction with Markerless Tracking

Claus Benjaminsen¹, Rasmus Ramsbøl Jensen¹, Paul Wighton², M. Dylan Tisdall², Helle Hjorth Johannessen³, Ian Law³, Andre J. W. van der Kouwe², and Oline Vinter Olesen¹

¹*DTU Compute, Technical University of Denmark, Lyngby, Denmark*, ²*Athinoula A. Martinos Center for Biomedical Imaging, Dept. of Radiology, Massachusetts General Hospital, Boston, MA, United States*, ³*Department of Clinical Physiology, Nuclear Medicine & PET, Rigshospitalet, University of Copenhagen, Copenhagen, Denmark*

Prospective motion correction for MRI neuroimaging has been demonstrated using MR navigators and external tracking systems using markers. The drawbacks of these two motion estimation methods include prolonged scan time plus lack of compatibility with all image acquisitions, and difficulties validating marker attachment resulting in uncertain estimation of the brain motion respectively. We have developed a markerless tracking system, and in this work we demonstrate the use of our system for prospective motion correction, and

show that despite being computationally demanding, markerless tracking can be implemented for real time motion correction.

1861

High-speed, contact-free measurement of the photoplethysmography waveform for MRI triggering
Nicolai Spicher¹, Stefan Maderwald², Mark E. Ladd^{2,3}, and Markus Kukuk¹

¹*University of Applied Sciences and Arts Dortmund, Dortmund, Germany*, ²*Erwin L. Hahn Institute for Magnetic Resonance Imaging, University Duisburg-Essen, Essen, Germany*, ³*Division of Medical Physics in Radiology, German Cancer Research Center, Heidelberg, Germany*

Videos of the human skin exhibit a subtle photoplethysmography signal, which resembles the one measured by pulse oximetry. It was investigated whether the whole photoplethysmography waveform (systolic/diastolic peak, dicrotic notch) can be extracted from two MR-compatible video cameras: A low-speed camera (30 frames-per-second) and a high-speed prototype (250 frames-per-second). We propose a potentially real-time feasible algorithm for signal filtering, which was applied to frames of both cameras. Using pulse oximetry as ground truth, revealed all features of the photoplethysmography waveform. Additionally, performing systolic peak detection showed that the high-speed camera allows for more accurate results in MRI pulse triggering.

1862

A robust motion correction tool for cardiac extracellular volume mapping
Shufang Liu^{1,2,3}, Lin Zhang^{3,4}, Pauline Ferry^{3,4}, Andrei Codreanu⁵, Anne Menini², and Freddy Odille^{3,4}

¹*Institut für Informatik, Technology University of Munich, Munich, Germany*, ²*GE Global Research, Munich, Germany*, ³*Imagerie Adaptative Diagnostique et Interventionnelle, Université de Lorraine, Nancy, France*, ⁴*U947, INSERM, Nancy, France*, ⁵*Centre Hospitalier de Luxembourg, Luxembourg, Luxembourg*

This work present a robust motion correction framework for T1 mapping and ECV mapping. Motion correction within one series and between different series are discussed. Validation is performed on 2 patient data and 6 volunteer data.

1863

Auto-calibrated Iterative SENSE Reconstruction with Rejection of Inconsistent Data
Tim Nielsen¹ and Peter Börnert¹

¹*Philips Research, Hamburg, Germany*

We present a reconstruction method to correct retrospectively for motion artifacts. The method identifies which part of the data set is affected by motion based on redundancy which is typically present in a multi-coil data set. No prior knowledge about coil sensitivity maps is needed. Instead, this information is directly estimated from the data along with the motion corrected image.

1864

PCA-aided improvements on FID-based motion tracking calibrated on resting-state EPI data without intentional motion
Rüdiger Stirnberg¹, Daniel Brenner¹, Willem Huijbers¹, Tobias Kober^{2,3,4}, and Tony Stöcker^{1,5}

¹*German Center for Neurodegenerative Diseases (DZNE), Bonn, Germany*, ²*Advanced Clinical Imaging Technology, Siemens Healthcare, Lausanne, Switzerland*, ³*Department of Radiology, University Hospital Lausanne (CHUV), Lausanne, Switzerland*, ⁴*Department of Electrical Engineering (LTS5), Ecole Polytechnique Fédérale de Lausanne, Lausanne, Switzerland*, ⁵*Department of Physics and Astronomy, University of Bonn, Bonn, Germany*

Accurate and precise head motion tracking has been shown to be feasible using multi-channel free-induction-decay (FID) signals, where positional information is supported by the spatial distribution of the receive coils. Until now, this required subject-specific calibration using simultaneously acquired FID signals and reference motion parameters, e.g. from an external device, while the subject performs controlled motion. In this study, we demonstrate successful calibration of FID navigators using motion parameters extracted from a resting-state fMRI scan without intentional motion. Additionally, extension of the calibration by principal component analysis of the FID data is shown to increase motion prediction accuracy and precision.

1865

Robust prospective motion correction using virtual marker tracking
Niklas Wehkamp¹, Benjamin Richard Knowles¹, Patrick Hücker¹, and Maxim Zaitsev¹

¹*Department of Radiology - Medical Physics, University Medical Center Freiburg, Freiburg, Germany*

Marker fixation remains an unresolved issue in Prospective Motion Correction (PMC) using optical tracking. The most common and simple approach to track motion of the skull is using markers adhered to the face. However, markers applied in this fashion can report erroneous positions due to facial gestures of the subject during the MR examination. The presented approach using multiple markers is a patient friendly solution, offering robust position data for PMC in the presence of facial gestures. The presented approach is a promising solution to stabilize prospective motion tracking and thus to significantly reduce costs for MR imaging facilities.

1866

Single-Shot, Navigator-Based Approach to Retrospective 4D MRI: balanced-SSFP vs. Single-Shot Fast Spin Echo
Daniel V Litwiller¹, Erik Tryggestad², Kieran McGee³, Yuji Iwadate⁴, Lloyd Estkowski⁵, and Ersin Bayram⁶

¹*Global MR Applications & Workflow, GE Healthcare, New York, NY, United States*, ²*Department of Radiation Oncology, Mayo Clinic, Rochester, MN, United States*, ³*Department of Radiology, Mayo Clinic, Rochester, MN, United States*, ⁴*Global MR Applications & Workflow, GE Healthcare, Hino, Tokyo, Japan*, ⁵*Global MR Applications & Workflow, GE Healthcare, Menlo Park, CA, United States*, ⁶*Global MR Applications & Workflow, GE Healthcare, Houston, TX, United States*

One of the motivations for 4D MRI is the need to characterize patient respiratory motion in the context of radiation therapy treatment planning (RTP). Here, we compare two approaches for generating 4D MRI data using dynamic, navigator-based acquisitions with retrospective respiratory compensation, including single-shot balanced-SSFP and single-shot fast spin echo with variable refocusing flip angle (vrfSSFSE). The results presented suggest that both sequences offer a straightforward approach to generating 4D MRI data for MR-guided RTP.

1867

Sub-volume motion detection to speed up image-based navigators and prospective motion correction
Anja Jäger^{1,2}, Thomas Beck², and Andreas Maier¹

¹Pattern Recognition Lab, Department of Computer Science, Friedrich-Alexander- Universität Erlangen-Nürnberg, Erlangen, Germany, ²Siemens Healthcare, MR Application Development, Erlangen, Germany

A method for detection of patient motion based on sub-volumes is presented. Current methods for image-based motion detection are limited because rigid motion parameters can only be detected for full volumes. This limits the potential of navigator acceleration and causes undesirable effects due to respiratory motion in some applications. Our novel approach extends the rigid-body-motion model by detection based on a subset of slices relative to a fully sampled reference volume. It is validated with phantom and in-vivo data and allows for both considerable acceleration of navigator scans and prospective correction of head motion in fMRI applications.

1868

The Effect of MR-based Motion Correction on PET Kinetic Parameters Estimation
Rong Guo¹, Yoann Petibon², Yixin Ma¹, Kui Ying¹, and Jinsong Ouyang²

¹Engineering Physics, Tsinghua University, Beijing, China, People's Republic of, ²Center for Advanced Radiological Sciences, Massachusetts General Hospital, Boston, MA, United States

Bias may be introduced in the estimation of the PET myocardial kinetic parameters by both cardiac and respiratory motion. Simultaneous PET-MR makes it possible to perform MR-based PET motion correction. We have investigated the performance of MR-based motion correction on the estimation of myocardial PET kinetic parametersat

1869

Evaluation of Two Deformable Registration Algorithms for Assessment of Brown Adipose Tissue in Humans
Vanessa Stahl¹, Martin T. Freitag², Armin M. Nagel^{1,3}, Ralf O. Floca⁴, Moritz C. Berger¹, Jan P. Karch⁵, Peter Bachert¹, Mark E. Ladd¹, and Florian Maier¹

¹Medical Physics in Radiology, German Cancer Research Center, Heidelberg, Germany, ²Department of Radiology, German Cancer Research Center, Heidelberg, Germany, ³Department of Diagnostic and Interventional Radiology, University Medical Center Ulm, Ulm, Germany, ⁴Medical and Biological Informatics, German Cancer Research Center, Heidelberg, Germany, ⁵Institute of Physics, Johannes Gutenberg University Mainz, Mainz, Germany

Human brown adipose tissue (BAT) is mostly found in cervical and mediastinal anatomic sites, making MR-imaging challenging because of susceptibility to breathing motion artifacts. Image acquisition under breath-hold requires data registration, especially for long measurement times. Two deformable registration algorithms (Fast Symmetric Forces Demons (FSF), Level Set Motion (LSM)) were evaluated regarding their suitability for compensation of deviations in breath-hold positions. Data processing was based on a volunteer study using distinct anatomical landmarks placed by an experienced radiologist. Landmark positions were evaluated after transformation, showing that FSF is more suitable for registration of thoracic data allowing for human BAT assessment.

1870

Fast and flexible 3D-EPI fat navigators for high-resolution brain imaging at 7 Tesla
Pieter F Buur¹, Wietske van der Zwaag¹, José P Marques², and Daniel Gallichan³

¹Spinoza Centre for Neuroimaging, Amsterdam, Netherlands, ²Donders Institute for Brain, Cognition and Behaviour, Radboud University Nijmegen, Nijmegen, Netherlands, ³Centre d'Imagerie BioMédicale (CIBM), EPFL Lausanne, Lausanne, Switzerland

Motion correction using interleaved fat navigators is a promising approach for high-resolution brain imaging at 7 Tesla. We have implemented a 3D-EPI fat navigator to reduce acquisition time and thereby minimize overhead in sequences with little or no dead time. The efficacy of motion-induced artefact removal using the fat navigators is demonstrated for 0.6 mm isotropic inversion-prepared (MPRAGE) and 0.5 mm isotropic non-prepared 3D TFE (GRE) protocols.

Traditional Poster

Fields, Fields & More Fields

Exhibition Hall

Tuesday, May 10, 2016: 16:00 - 18:00

1871

Correcting Geometric Distortion in B0 Mapping
Paul Chang^{1,2}, Sahar Nassirpour^{1,2}, Ariane Fillmer^{3,4}, and Anke Henning^{1,3}

¹Max Planck Institute for Biological Cybernetics, Tuebingen, Germany, ²IMPRS for Cognitive and Systems Neuroscience, Eberhard Karls University of Tuebingen, Tuebingen, Germany, ³Institute for Biomedical Engineering, UZH and ETH Zurich, Zurich, Switzerland, ⁴Physikalisch-Technische

The task of mapping B_0 fields to characterise shim fields can be challenging since shim fields generate a highly inhomogeneous field that may be difficult to capture. Furthermore this results in geometric distortion of the B_0 map which affects the characterisation of the shim field.

Geometric distortion correction was investigated using a gridded phantom and compared to the effect of using a high bandwidth on the read-out gradient. It was found that using a high bandwidth was more effective in reducing the distortion and that correcting the distortion using a phantom grid was not sufficient.

1872

Quantitative evaluation of mapping of magnetic distortion due to metallic materials

Takahiko Kaneda¹, Kazuya Oshinomi¹, Naoki Ohno², Toshiaki Miyati², and Toru Yamamoto³

¹Graduate School of Health Sciences, Hokkaido University, Sapporo, Japan, ²Division of Health sciences, Graduate School of Medical Sciences, Kanazawa University, Kanazawa, Japan, ³Faculty of Health Sciences, Hokkaido University, Sapporo, Japan

Evidence that the magnetic field distortion of an artificial knee joint and an Elgiloy rod in ppm unit does not change at 0.4-T and 3.0-T MRI was demonstrated. The susceptibility of Elgiloy and Ti alloy rods was derived from the magnetic distortion maps and the value of Ti alloy rod especially agreed with the known susceptibility of its material. The obtained value of the magnetic field distortion is quantitatively reliable.

1873

Estimating B_{1+} of the breast at 7T using a generic distribution

Michael J van Rijssel¹, Josien P W Pluim¹, Peter R Luijten¹, Alexander J Raaijmakers¹, and Dennis W J Klomp¹

¹Center for Image Sciences, UMC Utrecht, Utrecht, Netherlands

Quantitative DCE-MRI requires reliable B_{1+} information. This study presents a simulation-based fast B_{1+} estimation method for DCE breast imaging at 7T. Numerical FDTD simulations were conducted to assess the inter-subject differences in B_{1+} for four volunteers using segmented breast images for the simulation model. Inter-subject differences are shown to be comparable to the accuracy of popular B_{1+} mapping methods, justifying the use of one generic B_{1+} distribution for B_{1+} estimation (coil template). This template was created by averaging the simulated B_{1+} distributions over the four volunteers. We demonstrate the feasibility of this method in three in-vivo cases.

1874

Novel correction method of reception radiofrequency field inhomogeneities for noise corrupted sodium MR images at 3 T using Ensemble Empirical Mode Decomposition

Nadia Karina Paschke¹, Andreas Neubauer¹, and Lothar R Schad¹

¹Computer Assisted Clinical Medicine, Medical Faculty Mannheim, Heidelberg University, Mannheim, Germany

Sodium MRI suffers from low signal-to-noise ratio, which can be compensated by applying surface coils fitting the geometry of interest. Inhomogeneous coil profiles hinder absolute quantification of in vivo tissue sodium concentration, which is crucial for clinical assessment of pathological changes. Adequate corrections of intensity inhomogeneities of reception radiofrequency fields are essential and most standard proton imaging correction methods require manual thresholding. We present a novel and automatic correction approach by postprocessing images with Ensemble Empirical Mode Decomposition without additional scan time. It reduces signal variations by 39%. This is shown in phantoms and in vivo.

1875

Highly accelerated Bloch-Siegert B_{1+} mapping using variational modeling

Andreas Lesch¹, Matthias Schlögl¹, Martin Holler², and Rudolf Stollberger^{1,3}

¹Institute of Medical Engineering, Graz University of Technology, Graz, Austria, ²Institute of Mathematics and Scientific Computing, University of Graz, Graz, Austria, ³BioTechMed Graz, Graz, Austria

In this work we describe a novel method, which is able to reconstruct B_{1+} -maps from highly under-sampled Bloch-Siegert data. This method is based on variational methods and a problem specific regularization approach. We show its capability to achieve successful reconstructions from more than 100times under-sampled 3D-data in the human brain with a mean error below 1%. The results are compared to a fully-sampled reference and a conventional low resolution reconstruction for different under-sampling factors.

1876

Fast Multichannel Transmit Array Calibration Using Coil Locators

Parnian Zarghamravanbakhsh¹, John M Pauly¹, and Greig Scott¹

¹Electrical Engineering, Stanford University, Stanford, CA, United States

Accurate knowledge of magnetic field distribution is necessary for RF shimming and calibration of parallel transmit systems. The incident field distribution depends on relative location of transmit array to sample, also magnitude and phase of coil current (thereby, magnetic field) vary with different sample loading. The RF maps of each coil can be estimated by localizing the transmit array in the image space and circulating RF currents in each coil. In this study, parallel transmit system RF shimming pulses are designed by using transmit coils locator information and coil current measurement without performing experimental B_1 mapping.

Improvement of the Reproducibility of Parallel Transmission at 7T by Breath-Holding During the Calibration Scan
 Taisuke Harada^{1,2}, Kohsuke Kudo¹, Ikuko Uwano³, Fumio Yamashita³, Hiroyuki Kameda^{1,3}, Tsuyoshi Matuda⁴, Makoto Sasaki³, and Hiroki Shirato²

¹Department of Diagnostic and Interventional Radiology, Hokkaido University Hospital, Sapporo, Japan, ²Department of Radiation Medicine, Hokkaido University Graduate School of Medicine, Sapporo, Japan, ³Division of Ultrahigh Field MRI, Institute for Biomedical Sciences, Iwate Medical University, Yahaba, Japan, ⁴MR Applications and Workflow, GE Healthcare, Tokyo, Japan

The aim of our study was to compare the reproducibility of those maps and GRASS images of brain scanned with pTx at 7T between free-breathing (FB) and breath-holding (BH) during the calibration scan. Nine healthy volunteers were scanned by 7T MRI with RF shimming, RF design of pTx, and quadrature transmission (qTx). The reproducibility of B0 and B1+ were better in BH than FB, and the same results was seen in GRASS images. The intensity homogeneity was not different between qTx and RF shimming however was better in RF design than qTx. These results might facilitate the development of pTx.

Magnetic Susceptibility Artefact Correction of Spin-Echo and Gradient-Echo EPI Images
 Gary George McGinley^{1,2}, Atle Bjørnerud^{3,4}, and Øystein Bech Gadmar³

¹Institute for Experimental Medical Research, Oslo University Hospital, Oslo, Norway, ²KG Jebsen Cardiac Research Center and Center for Heart Failure Research, University of Oslo, Oslo, Norway, ³The Intervention Centre, Oslo University Hospital, Oslo, Norway, ⁴Department of Physics, University of Oslo, Oslo, Norway

This study aims to compare the effectiveness of three reverse-gradient method susceptibility artefact correction tools (EPIC, TOPUP, and HySCO) in the correction of spin-echo (SE) and gradient-echo (GE) EPI images of the brain, and to measure the effect of pixel bandwidth, SENSE factor and slice thickness on artefact correction. This was achieved by co-registering the artefacted and corrected images to an anatomical scan and measuring the normalised mutual information (NMI). It was found that EPIC correction resulted in the largest gains in NMI and that more mutual information was recovered at lower pixel bandwidths after EPIC correction.

A robust phase unwrapping method for low-SNR multi-echo MR images based on complex signal modeling
 Taejoon Eo¹

¹Yonsei University, Seoul, Korea, Democratic People's Republic of

We propose a robust phase unwrapping method for low-SNR multi-echo MR images based on complex signal modeling. This method is superior to conventional phase unwrapping methods and provides high-quality unwrapped phase images without any spatial artifacts caused by high noise.

Reference-free Unwarping of Multicoil Single-shot GE-EPI Human brain data at 3T
 Ying Chen¹, Song Chen¹, Hui Liu², and Jianhui Zhong^{1,3}

¹Center for Brain Imaging Science and Technology, Zhejiang University, Hangzhou, China, People's Republic of, ²MR Collaboration Northeast Asia, Siemens Healthcare, Shanghai, China, People's Republic of, ³Collaborative Innovation Center for Diagnosis and Treatment of Infectious Diseases, Zhejiang University, Hangzhou, China, People's Republic of

Single-shot GE-EPI is widely used in fMRI. However, it is susceptible to field inhomogeneity induced geometric distortions, therefore retrospectively unwarping of the single-shot GE-EPI data is important. A commonly used unwarping technique is based on the field map of the image and it would be desirable to acquire the field map at each time point of a dynamic fMRI measurement series. The aim of this abstract is to qualitatively and quantitatively compare the performance of three reference-free unwarping methods on human brain imaging data. Experimental results demonstrate that the field map obtained from measuring the k-space shifts of each voxel can provide more reliable unwarped images.

Traditional Poster

RF Pulses

Exhibition Hall

Tuesday, May 10, 2016: 16:00 - 18:00

Multi-Band Slice-Selective and 2D-Selective RF Excitations with Band-Specific Dephasing Moments for Tailored z-Shimming
 Jürgen Finsterbusch¹

¹Systems Neuroscience, University Medical Center Hamburg-Eppendorf, Hamburg, Germany

T2*-weighted acquisitions used for functional neuroimaging can suffer from through-slice dephasing. Additional, so-called z-shim gradient pulses can be applied in the slice direction to minimize related signal losses. Thereby, a single, slice-specific gradient moment may be sufficient for small target regions like the spinal cord. To combine this z-shimming approach with multi-band acceleration, the individual bands must provide different dephasing moments in the slice direction. This can be realized with appropriate temporal shifts of the individual envelopes as is demonstrated for conventional slice-selective RF excitations and 2D-selective RF excitations for inner-field-of-view imaging.

B1-Insensitive Simultaneous Multi-Slice DWI at 7T using SEAMS PINS
Rebecca Emily Feldman¹, Hadrien A Dyvorne¹, Rafael O'Halloran¹, and Priti Balchandani¹

¹*Translational and Molecular Imaging Institute, Icahn School of Medicine at Mount Sinai, New York, NY, United States*

The higher signal-to-noise-ratio offered at 7T, has been shown to increase the resolution of diffusion MRI as well as the precision and directional certainty of diffusion-based parameters. Two major drawbacks of 7T dMRI include lengthy acquisitions and signal loss due to B₁-inhomogeneity. SMS methods reduce the duration of the acquisition, the refocusing pulses typically used in dMRI are particularly sensitive to B₁ non-uniformities leading to a loss in signal, or even complete signal dropout in parts of the image. We have created a dMRI sequence with SEAMS PINS and an EPI readout that provides immunity to B₁-inhomogeneity.

Optimized amplitude modulated multiband RF pulses
Samy Abo Seada¹, Joseph V Hajnal¹, and Shaikan J Malik¹

¹*Division of Imaging Sciences and Biomedical Engineering, King's College London, London, United Kingdom*

Simultaneous multi-slice imaging can accelerate image acquisition for commonly used diffusion and functional MRI sequences. The design of multiband pulses can be problematic due to their high peak amplitude. Another issue is that the necessary rapid phase and amplitude modulation can be problematic for some current MRI RF systems to reproduce. Phase related issues can be avoided by designing purely amplitude modulated waveforms. We describe how three current multiband pulse design techniques (phase optimisation, time shifting and root-flipping) can be modified to produce purely amplitude modulated pulses and find that the relative peak increase is only about 20-25%.

Spatiotemporally encoded anatomical shape in-plane excitation with reduced profile distortion from field inhomogeneity
Ying Chen¹, Song Chen¹, Zhong Chen², and Jianhui Zhong^{1,3}

¹*Center for Brain Imaging Science and Technology, Zhejiang University, Hangzhou, China, People's Republic of*, ²*Department of Electronic Science, Xiamen University, Xiamen, China, People's Republic of*, ³*Collaborative Innovation Center for Diagnosis and Treatment of Infectious Diseases, Zhejiang University, Hangzhou, China, People's Republic of*

In-plane reduced field-of-view excitation based on two-dimensional radio-frequency pulse (2DRF) has been widely used in many applications. The EPI-style gradient waveform is commonly used in 2DRF implementation. However, at high field, the off-resonance effects during excitation would result in distortions of the profiles obtained. This work is to investigate the feasibility to achieve in-plane selective excitation of anatomically pre-defined regions using SPEN-2DRF pulse under different shim conditions. Experimental results show that the proposed method can produce profiles with significantly improved robustness to distortions at high field than the Fourier-based 2DRF pulse.

Comparison of Root-Flip and Quadratic-Phase RF Pulses for Outer Volume Suppression
Hong Shang¹, Hai Luo², Xia Liu², Gaojie Zhu², and Leping Zha²

¹*Bioengineering, UC Berkeley - UCSF, Berkeley/San Francisco, CA, United States*, ²*AllTech Medical Systems, Chengdu, China, People's Republic of*

Two classes of previously proposed nonlinear phase RF pulses, the quadratic-phase pulse and root-flip optimized pulse, are compared in terms of selectivity, peak B₁ value, pulse energy, and sensitivity to B₁ variations, when applied for spatial outer volume suppression. Root-flip pulses have lower peak B₁ and energy given the same transition width and pulse duration, or sharper transition given the same peak B₁, while quadratic-phase pulses have less sensitivity to B₁ variations that maintains profile shape with B₁ deviations, and thus less prone to residual saturation band magnetization. This work provides insights to pulse designers in regards to nonlinear phase pulse design and application.

B1-Insensitive T2-Preparation Sequence with Outer Volume Suppression and Fat Saturation
David Y. Zeng¹, Jieying Luo¹, Dwight G. Nishimura¹, and Adam B. Kerr¹

¹*Electrical Engineering, Stanford University, Stanford, CA, United States*

A B₁-insensitive T₂-weighted preparation sequence with integrated fat saturation and outer volume suppression for localized cardiac imaging is proposed. The sequence is composed of a BIR-4 90° tip-down pulse, two spectral-spatial adiabatic refocusing pulses and a BIR-4 -90° tip-up pulse. Outer volume suppression is achieved by the spatial selectivity of the first refocusing pulse in x and spatial selectivity of the second refocusing pulse in y. Fat suppression is achieved by spectral selectivity of the refocusing pulses. Numerical simulation and phantom experiments verify the performance of the sequence.

Reduction of RF Pulse Duration using Dephased Transition
Seohee So¹, HyunWook Park¹, Dongchan Kim¹, Hyunseok Seo¹, Jaejin Cho¹, Young Woo Park¹, and Kinam Kwon¹

¹*Electrical Engineering, Korea Advanced Institute of Science and Technology, Daejeon, Korea, Republic of*

Slice profile used for magnetic resonance (MR) imaging has transition region between passband and stopband. Sharper transition performs better slice selection. This abstract proposes method to design short-duration RF pulse without increasing transition region width. Additional phase is merged into a transition region of slice profile. Two RF pulses having different phases are used alternately. The proposed algorithm produces about 30% reduction of RF pulse duration without transition increase.

1888

Minimum-Time VERSE Pulse Correction for Slice Selectivity Improvement in 2D-UTE Imaging

Lucas Soustelle¹, Paulo Loureiro de Sousa¹, Sascha Koehler², Chrystelle Po¹, François Rousseau³, and Jean-Paul Armpach¹

¹Université de Strasbourg, CNRS, ICube, FMTS, Strasbourg, France, ²Bruker BioSpin MRI, Ettlingen, Germany, ³Institut Mines Télécom, Télécom Bretagne, INSERM LaTIM, Brest, France

The Variable-rate Selective Excitation (VERSE) approach allows to achieve very short echo time in 2D-UTE sequences when applied on a selective half-pulse and its paired slice selection gradient. Unfortunately, the latter may suffer from non-linearities and eddy current effects, all the more important on preclinical scanners equipped with strong gradient systems.

An efficient method was implemented on a 7T preclinical scanner to measure the real slice selection gradient profile. A reshaping of the corresponding pulse was made, improving the slice selectivity.

1889

Slice-selective relaxation-matched half-pulses for cortical bone imaging

Ethan M Johnson¹, Kim Butts Pauly², Pejman Ghanouni², and John M Pauly¹

¹Electrical Engineering, Stanford University, Stanford, CA, United States, ²Radiology, Stanford University, Stanford, CA, United States

A method for sensitising 3D UTE sequences to the short-\$T_2\$ range of cortical bone using scaled RF hard pulses has been previously demonstrated for creating CT-like contrast in MR imaging. However whole-volume excitation and encoding is not practical in all contexts. Here, an adaptation for slice-selective half-pulses is presented that enables 2D image encoding for MR-simulated-CT images.

1890

Reduce multislice excitation RF power by ROI optimization method

Yi-Cheng Hsu¹, Ying-Hua Chu¹, and Fa-Hsuan Lin¹

¹Institute of Biomedical Engineering, National Taiwan University, Taipei, Taiwan

A new simultaneous multi-slice excitation method was proposed to reduce RF power delivery by only concerning slice profiles within the imaging object. Compared to MultiPINS, our approach used only 79% of the RF energy to the same result (slice thickness = 3mm, MB factor = 5, 4 bandwidth time product, excitation duration 6380 \$\mu s\$). This excitation method was experimentally demonstrated in spin-echo EPI with blipped CAIPI acquisition.

1891

Low SAR RF-pulse design by joint optimization of RF and gradient shape with physical constraints

Christoph Stefan Aigner^{1,2}, Christian Clason³, Armin Rund⁴, and Rudolf Stollberger^{1,2}

¹Institute of Medical Engineering, Graz University of Technology, Graz, Austria, ²BioTechMed Graz, Graz, Austria, ³Faculty of Mathematics, University of Duisburg-Essen, Essen, Germany, ⁴Institute for Mathematics and Scientific Computing, University of Graz, Graz, Austria

We demonstrate the joint optimization of RF and slice selective gradient shapes with hard constraints such as peak B1 of the pulse and peak slew rate of the gradient via a flexible approach based on optimal control of the full time-dependent Bloch equation and a novel semi-smooth Newton method. The presented approach allows optimization on a fine spatial and temporal grid while enforcing physical and technical limitations on the control variables. The results are validated on a 3T scanner, demonstrating the practical realizability of the presented approach even for short RF pulses.

1892

Reduced peak power in paired excitation and refocusing multiband pulses by quadratic phase modulation in the spatial domain

David G Norris^{1,2} and Jenni Schulz¹

¹Donders Institute for Brain Cognition and Behaviour, Radboud University Nijmegen, Nijmegen, Netherlands, ²Erwin L Hahn Institute, University Duisburg Essen, Essen, Germany

This abstract describes the use of pulses that have a quadratic phase profile in the spatial dimension for simultaneous multi-slice imaging. The quadratic profile reduces the peak voltage needed by an amount dependent on the number of simultaneously excited slices. The pulses have to be used as an excitation-refocusing pair, with the refocusing pulse having half the phase gradient. The echoes from each slice are simultaneously refocused and there are no additional constraints on the pulse duration.

1893

SPINS excitation versus DSC dynamic RF shimming for homogenising high field strength TSE imaging

Ronald Mooiweer¹, Shaikan J Malik², Joseph V Hajnal², Nico van den Berg¹, Peter R Luijten¹, and Hans Hoogduin¹

¹UMC Utrecht, Utrecht, Netherlands, ²Division of Imaging Sciences and Biomedical Engineering, King's College London, London, United Kingdom

In this work the design of SPINS excitation pulses has been expanded for use in TSE sequences and was compared to dynamic RF shimming using DSC in a standard T2w TSE sequence. We have demonstrated homogeneous 90 degree excitation, but in itself this was not sufficient to make TSE images uniform. Manipulating the refocusing pulses (using DSC) remains a necessity.

1894

Slice Profile Effects on non-CPMG SS-FSE Acquisitions
Eric Kenneth Gibbons¹, John Mark Pauly², and Adam Bruce Kerr²

¹Department of Bioengineering, Stanford University, Stanford, CA, United States, ²Department of Electrical Engineering, Stanford University, Stanford, CA, United States

SS-FSE is a robust method for fast image acquisition in areas where there is significant B0 inhomogeneity. Recent efforts have led to expand the capabilities beyond traditional constraints of SS-FSE meeting the CPMG condition. In this work, we examine the effects of various RF pulse types on the stability of the signal using a quadratic phase modulation as well as propose using a novel DIVERSE pulse.

1895

A Shinnar Le-Roux Transform for T1, T2 and Frequency Selective Pulses
Frank Ong¹ and Michael Lustig¹

¹Electrical Engineering and Computer Sciences, University of California, Berkeley, Berkeley, CA, United States

We propose a generalized Shinnar-Le-Roux transform that maps \$\$\$T_1\$\$, \$\$\$T_2\$\$ and frequency selective pulses to multi-dimensional polynomials. We show that the polynomial mapping is one-to-one and hence designing these RF pulses reduces to multi-dimensional polynomial design. We describe a convex approach to the multi-dimensional polynomial design and show preliminary \$\$\$T_2\$\$ and frequency selective pulses.

Traditional Poster

Image Processing & Analysis

Exhibition Hall

Tuesday, May 10, 2016: 16:00 - 18:00

1896

Simultaneous Estimation of Proton Densities and Receiver Coil Sensitivities using Optimized Basis Functions
Dietmar Cordes^{1,2}, Zhengshi Yang¹, Xiaowei Zhuang¹, Karthik Sreenivasan¹, and Le Hanh Hua¹

¹Cleveland Clinic Lou Ruvo Center for Brain Health, Las Vegas, NV, United States, ²Department of Psychology and Neuroscience, University of Colorado, Boulder, CO, United States

In this study, a new algorithm to better model the receiver coil sensitivities with the purpose of obtaining unbiased proton density maps is proposed. Using optimized orthonormal basis functions for the modeling produces an accurate fit of potential inhomogeneities of the signal due to receiver coil bias. The obtained final image of the proton density has low variance, suitable for quantitative diagnostic information of brain tissue. Results are shown for nine MS patients and one control subject.

1897

Multidimensional Diffusion and Relaxation Data Acquisition for Improved Intravoxel Incoherent Motion Analysis
Anna Scherman Rydhög¹, André Ahlgren¹, Freddy Ståhlberg^{1,2,3}, Ronnie Wierstam¹, and Linda Knutsson¹

¹Department of Medical Radiation Physics, Lund University, Lund, Sweden, ²Department of Diagnostic Radiology, Lund University, Lund, Sweden, ³Lund Bioimaging Center, Lund University, Lund, Sweden

Intravoxel Incoherent Motion (IVIM) is a method for quantification of perfusion parameters, such as the perfusion fraction Fb. Unfortunately, CSF partial volume effects are often seen in the estimated blood compartment. This work introduces a novel version of the IVIM model, containing three compartments (tissue, CSF and blood), where multi-TE and multi-TI data are incorporated to yield a direct relaxation estimate. Using this relaxation-compensated model, results were obtained from in vivo measurements in a volunteer. Compared to a non-relaxation-compensated model, the three-compartment model with relaxation-compensated data reduced the CSF contamination.

1898

7TAMlbrainT1w_30 : Whole-brain ultra-high resolution average T1-weighted template at 7 Tesla to improve in vivo depiction of small brain structures
Pierre Besson^{1,2,3}, Arnaud Le Troter^{1,2}, Julien Sein^{1,2}, Gilles Brun^{1,2}, Maxime Guye^{1,2}, and Jean-Philippe Ranjeva^{1,2}

¹Aix-Marseille Université, CNRS, Centre de Résonance Magnétique Biologique et Médicale (CRMBM) UMR 7339, Marseilles, France, ²APHM, Timone Hospital, Pôle d'Imagerie, Centre d'Exploration Métabolique par Résonance Magnétique (CEMEREM), Marseilles, France, ³Siemens Healthcare, St Denis, France

UHF 7T MR scanners offers the possibility to acquire very high resolution in-vivo images, providing a new insight into human brain structural characterization. Nevertheless, in order to obtain highly contrasted and highly spatially resolved atlas, and to compensate for the drop in SNR related to reduction of the voxel size, averaging data among several subjects is needed. We present in this abstract an automatic pipeline that generates a whole brain high-resolution T1-weighted template (called 7TAMlbrainT1w_30) built from MP2RAGE acquisitions obtained in 30 healthy controls at 7T.

Complete partial volume solution for ASL brain perfusion data applied to relapsing-remitting multiple sclerosis patients
 Ruth Oliver^{1,2}, Linda Ly^{1,2}, Chenyu Wang^{1,2}, Heidi Beadnell², Ilaria Boscolo Galazzo^{3,4}, Michael Chappell^{5,6}, Xavier Golay⁷, Enrico De Vita⁷, David Thomas⁷, and Michael Barnett^{1,2}

¹Sydney Neuroimaging Analysis Centre, Sydney, Australia, ²University of Sydney, Sydney, Australia, ³Institute of Nuclear Medicine, University College London, London, United Kingdom, ⁴Department of Neuroradiology, University Hospital Verona, Verona, Italy, ⁵Institute of Biomedical Engineering, University of Oxford, Oxford, United Kingdom, ⁶FMRIB Centre, University of Oxford, Oxford, United Kingdom, ⁷Institute of Neurology, University College London, London, United Kingdom

ASL is a low resolution imaging modality that suffers from the partial volume effect, leading to an underestimation of GM perfusion. This effect has two principle causes; blurring from the point spread function in the slice direction, and inadequate resolution due to the need for large voxels to achieve sufficient SNR. Both may act as confounders for measurement of GM CBF abnormalities. Decreased GM perfusion could reflect neuronal loss or metabolic dysfunction; PV correction allows a decoupling of structure and function. We present the first application of a complete PV correction solution for ASL to a cohort of MS patients.

Anomalous relaxation in the human brain mapped using ultra-high field magnetic resonance imaging and time-fractional Bloch equation
 Shanlin Qin¹, Fawang Liu¹, Ian William Turner^{1,2}, Qiang Yu³, Qianqian Yang¹, and Viktor Vegh³

¹School of Mathematical Sciences, Queensland University of Technology, Brisbane, Australia, ²ARC Centre of Excellence for Mathematical and Statistical Frontiers, Melbourne, Australia, ³Centre for Advanced Imaging, University of Queensland, Brisbane, Australia

MRI models based on integer order calculus lack the ability to accurately map magnitude signal decay in the human brain, likely due to magnetic susceptibility and microstructure variations in tissues. We applied fractional calculus to the Bloch equation with the aim of developing a model capable of matching experimental findings. Solution of the time-fractional Bloch equation resulted in a new five parameter model. We analysed model parameters in nine brain regions using multiple echo gradient recalled echo MRI data from five participants. Time-fractional model parameters may provide new ways of studying microstructure and susceptibility induced changes in the human brain.

Evaluation the cluster-size inference with random field and permutation methods for group-level MRI analysis
 Huanjie Li¹, Lisa D. Nickerson², Yang Fan³, Thomas E. Nichols⁴, and Jia-Hong Gao⁵

¹Department of Biomedical Engineering, Dalian University of Technology, Dalian, China, People's Republic of, ²McLean Imaging Center, McLean Hospital/Harvard Medical School, Belmont, MA, United States, ³GE Healthcare, MR Research China, Beijing, China, People's Republic of, ⁴Department of Statistics and Warwick Manufacturing Group, University of Warwick, Coventry, United Kingdom, ⁵Center for MRI Research, Peking University, Beijing, China, People's Republic of

Threshold-free cluster enhancement (TFCE) outperforms the cluster-size test (CST) based on random field theory and our recent papers provide two voxelation-corrected CST (v-CST and vn-CST) which also show the clear advantage over other CST as well. However, it's not clear which one shows better performance for MRI data analysis. This work provides a very careful, fair and thorough evaluation of the powerful statistical methods, which may be particularly appealing for group-level MRI data analysis.

Arterial segmentation and visual stimulus-induced changes in diameter observed in the human brain
 Alexandre Bizeau^{1,2}, Guillaume Gilbert³, Minh Tung Huynh⁴, Michaël Bernier^{1,2}, Christian Bocti⁵, Maxime Descoteaux^{2,6}, and Kevin Whittingstall^{1,2,4}

¹Department of Radiation Sciences and Biomedical imagery, Université de Sherbrooke, Sherbrooke, QC, Canada, ²Centre d'Imagerie Moléculaire de Sherbrooke (CIMS), Centre de Recherche CHUS, Sherbrooke, QC, Canada, ³MR Clinical Science, Philips Healthcare, Markham, ON, Canada, ⁴Department of Diagnostic Radiology, Université de Sherbrooke, Sherbrooke, QC, Canada, ⁵Department of Medecine, Université de Sherbrooke, Sherbrooke, QC, Canada, ⁶Department of Computer Science, Université de Sherbrooke, Sherbrooke, QC, Canada

When undergoing stimulation, neurons need to be supplied with oxygen and glucose. This demand then induces vasodilation generated by the astrocytes which act on the muscles of the arteries of the human brain. Using time-of-flight magnetic resonance angiography acquisitions, we extracted the apparent diameter of arterial vessels. We then compared diameter with and without visual stimulation and demonstrated that smaller vessels dilate proportionally more than larger ones in the posterior cerebral arteries. Using this method, the investigation of the coupling between neural activity and regional cerebral vasodilation, also called functional hyperemia, is now possible.

An Active Learning platform for automatic MR image quality assessment
 Thomas Küstner^{1,2}, Martin Schwartz^{1,2}, Annika Kaupp², Petros Martirosian¹, Sergios Gatidis¹, Nina F. Schwenzer¹, Fritz Schick¹, Holger Schmidt¹, and Bin Yang²

¹University Hospital Tübingen, Tübingen, Germany, ²Institute of Signal Processing and System Theory, University of Stuttgart, Stuttgart, Germany

Acquired images are usually analyzed by a human observer (HO) according to a certain diagnostic question. Flexible algorithm parametrization and the enormous amount of data created per patient make this task time-demanding and expensive. Furthermore,

definition of objective quality criterion can be very challenging, especially in the context of a missing reference image. In order to support the HO in assessing image quality, we propose a non-reference MR image quality assessment system based on a machine-learning approach with an Active Learning loop to reduce the amount of necessary labeled training data. Labeling is performed via an easy accessible website.

1904

Brain Tissue Clustering Based on Cross-Correlation of Magnetic Resonance Fingerprinting
Mu Lin¹, Xiaozhi Cao¹, Congyu Liao¹, Xu Yan², and Jianhui Zhong¹

¹Center for Brain Imaging Science and Technology, Zhejiang University, Hangzhou, China, People's Republic of, ²MR Collaboration NE Asia, Siemens Healthcare, Hangzhou, China, People's Republic of

Multi-component tissue model with priori T₁ and T₂ have been used to decompose MRF data. We propose that tissue classification can be improved when the selection uses clustering method based on cross-correlation. Our results from phantom and in vivo measurements show that the method successfully separates signal from different tissue types, allows extraction of tissue fractions, and results are more robust with image quality.

1905

Toward a voxel-based analysis (VBA) of quantitative magnetic susceptibility maps (QSM): Strategies for creating brain susceptibility templates
Jannis Hanspach¹, Michael G Dwyer¹, Niels P Bergsland^{1,2}, Xiang Feng³, Jesper Hagemeier¹, Paul Polak¹, Nicola Bertolino¹, Jürgen R Reichenbach^{3,4}, Robert Zivadinov^{1,5}, and Ferdinand Schweser^{1,5}

¹Buffalo Neuroimaging Analysis Center, Department of Neurology, Jacobs School of Medicine and Biomedical Sciences, The State University of New York at Buffalo, Buffalo, NY, United States, ²MR Research Laboratory, IRCCS Don Gnocchi Foundation ONLUS, Milan, Italy, ³Medical Physics Group, Department of Diagnostic and Interventional Radiology, Jena University Hospital - Friedrich Schiller University Jena, Jena, Germany, ⁴Michael Stifel Center for Data-driven and Simulation Science Jena, Friedrich Schiller University Jena, Jena, Germany, ⁵MRI Molecular and Translational Research Center, Jacobs School of Medicine and Biomedical Sciences, The State University of New York at Buffalo, Buffalo, NY, United States

Quantitative susceptibility mapping (QSM) is a recent *in vivo* magnetic resonance imaging (MRI) technique that provides quantitative information about the bulk magnetic susceptibility distribution in tissues, a promising measure for studying brain iron. A voxel-based analysis (VBA) of susceptibility maps would facilitate a better understanding of the intricate anatomical structure (e.g. sub-nuclear regions) of deep gray matter and its relation to diseases and normal aging.

In the present work, we developed and quantitatively assessed six strategies for creating a susceptibility brain template for VBA based on ANTs, representing the first step toward an understanding of sub-nuclear susceptibility changes without the need for *a priori* information.

1906

Automated multi-parametric segmentation of brain veins from GRE acquisition

Serena Monti^{1,2}, Pasquale Borrelli¹, Sirio Cocoza³, Sina Straubb⁴, Mark Ladd⁴, Marco Salvatore¹, Enrico Tedeschi³, and Giuseppe Palma⁵

¹IRCCS SDN, Naples, Italy, ²Department of Electronics, Information and Bioengineering, Politecnico di Milano, Milan, Italy, ³Department of Advanced Biomedical Sciences, University "Federico II", Naples, Italy, ⁴Department of Medical Physics in Radiology, German Cancer Research Center (DKFZ), Heidelberg, Germany, ⁵Institute of Biostructure and Bioimaging, National Research Council, Naples, Italy

A new fully automated algorithm, based on structural, morphological and relaxometric information, is proposed to segment the entire brain deep venous system from MR images. The method is tested on brain datasets at different magnetic fields and its inter-scan reproducibility is also assessed. The proposed segmentation algorithm shows good accuracy and reproducibility, outperforming previous methods and becoming a promising candidate for the characterization of venous tree topology.

1907

Human Head Models from MRI for Head Impact Analysis

Yash Agarwal¹, Philippe Young¹, Ross Cotton¹, Chris Pearce², Siddiq Qidwai³, Amit Bagchi³, and Nithyanand Kota³

¹Simpleware Ltd., Exeter, United Kingdom, ²Atkins, Epsom, United Kingdom, ³U.S. Naval Research Laboratory, Washington, DC, United States

Image-based model generation methods demonstrate the value of creating realistic human head models based on high-resolution MRI data. Head models created by the U.S. Naval Research Laboratory and Simpleware (Exeter, UK) are being used to study head impact and traumatic brain injury; this offers a solution to the problem of limited experimental testing. Results from the modelling methodology and simulation demonstrate a good level of accuracy when compared to experimental benchmarks. The methodology and models have been extended for use in areas such as examining head impact in sports including American football, rugby and cricket.

1908

Improve the Detection of Cartilage Degradation by Dividing the Tissue Unequally – A Comparative Study of Two Methods
Farid Badar¹, Ji Hyun Lee¹, and Yang Xia¹

¹Department of Physics and Center for Biomedical Research, Oakland University, Rochester, MI, United States

The consequences of two different zone-division methods in MRI T2 of articular cartilage were studied, using an animal model of early osteoarthritis (OA). By dividing the cartilage thickness unequally, significant improvement in OA detection can be achieved – both in the deeper cartilage as well as between the contralateral and normal tissue. This improved detection may become important in the clinical

1909

Accurate Synthetic FLAIR Images Using Partial Volume Corrected MR Fingerprinting

Anagha Deshmane¹, Debra McGivney², Chaitra Badve³, Alice Yu⁴, Yun Jiang¹, Dan Ma², and Mark Griswold^{1,2}

¹Biomedical Engineering, Case Western Reserve University, Cleveland, OH, United States, ²Radiology, Case Western Reserve University, Cleveland, OH, United States, ³Radiology, University Hospitals of Cleveland, Cleveland, OH, United States, ⁴School of Medicine, Case Western Reserve University, Cleveland, OH, United States

Synthetic weighted images from quantitative parameter maps suffer from partial volume artifacts which can distort contrast. In this work, Partial Volume MR Fingerprinting is applied to estimate and remove signal due to cerebrospinal fluid (CSF) in the brain, allowing for improved contrast in synthetic FLAIR images generated from MRF relaxation time maps.

1910

Improvement in Glioma Visualization using Subtraction Maps Derived from Contrast-Enhanced T1- and T2-Weighted MR Images

Mohammed Goryawala¹, Bhaswati Roy², Rakesh K Gupta², and Andrew A Maudsley¹

¹Department of Radiology, University of Miami, Miami, FL, United States, ²Department of Radiology, Fortis Memorial Research Institute, Gurgaon, India

Calculated differences between two images of differing T1 or T2 contrasts, or subtraction images, have been presented as a way to improve image contrast for imaging of brain tumors. In this study the performance of subtraction images for differentiation of tumor, edema, and normal appearing white matter (NAWM) is compared to traditionally acquired anatomic MRIs, diffusion tensor imaging (DTI), perfusion weighted imaging (PWI) and MR spectroscopy imaging (MRSI). Results showed a significant increase in contrast for differentiating between enhancing tumor and edematous regions from NAWM using the $\Delta T1$ map and $\Delta T2$ map, respectively, as compared to other parametric maps.

1911

Resource-efficient architecture of FPGA-based 2D FFT processors

Limin Li¹ and Alice M Wyrowicz^{1,2}

¹Center for Basic MR Research, Northshore University Healthsystem, Evanston, IL, United States, ²Department of Biomedical Engineering, Northwestern University, Evanston, IL, United States

The processing rate for real-time multi-slice image reconstruction on an FPGA can be improved significantly by taking advantage of its parallel processing capability. In particular, multiple 2D FFT processors can be embedded into a single FPGA and run simultaneously. In this abstract, we report a new design of a 2D FFT processor with significant reduced usage of hardware resource. Test results show that an important type of resource, DSP48 slice, can be reduced by up to 50% without degrading processing performance, which implies that more 2D FFT cores can be installed into a single FPGA with a given size.

1912

Quantitative image analysis based on Image registration of brain MR and SPECT for dopamine transporter imaging

Takeshi Hara¹, Yuta Takeda¹, Tetsuro Katafuchi², Taiki Nozaki³, Masaki Matsusako³, and Hiroshi Fujita¹

¹Intelligent Image Information, Gifu University Graduate School of Medicine, Gifu, Japan, ²Health Science, Gifu University of Medical Science, Seki, Japan, ³Radiology, St. Luke's International Hospital, Tokyo, Japan

Features in Parkinson's disease (PD) are a degeneration and loss of the dopamine neurons in striatum. ^{123}I -FP-CIT can visualize the distribution by binding to the dopamine neurons. The radioactivated medicine is used for diagnosis of PD and Dementia with Lewy Bodies (DLB). The material can visualize activities in corpus striatum on SPECT images, but the location of the corpus striatum on SPECT images are often lost because of the low uptake. To realize a quantitative image analysis for the SPECT images, image registration technique to determine the region of corpus striatum on SPECT images are required to measure precise uptakes. In this study, we proposed an image fusion technique for SPECT and MR images by intervening CT image taken by SPECT/CT. We employed 30 cases of SPECT/CT and MR cases for the evaluation. 25 of 30 cases were registered correctly with registration errors less than 5mm. These results enable to measure precise uptake on SPECT images based on the segmentation results on MR images.

1913

Incorporation of Nonzero Echo Times in the SPGR and bSSFP Signal Models used in mcDESPOT

Mustapha Bouhrara¹ and Richard G. Spencer¹

¹NIA, NIH, Baltimore, MD, United States

Formulations of the two-component spoiled gradient recalled echo (SPGR) and balanced steady-state free precession (bSSFP) models that incorporate nonzero echo time (TE) effects are presented in the context of mcDESPOT and compared with the conventionally used SPGR and bSSFP models which ignore nonzero TEs. Relative errors in derived parameter estimates from conventional mcDESPOT, omitting TE effects, are assessed using simulations over a wide range of experimental and sample parameters. The neglect of nonzero TE leads to an overestimate of the SPGR and an underestimate of the bSSFP signals. These effects introduce large errors in parameter estimates derived from conventional mcDESPOT.

1914

A noise correction model incorporating weighted neighborhood information for liver R2* mapping

¹School of Automation Engineering, University of Electronic Science and Technology of China, Chengdu, China, People's Republic of, ²School of Biomedical Engineering and Guangdong Provincial Key Laboratory of Medical Image Processing, Southern Medical University, Guangzhou, China, People's Republic of, ³Radiology, University of Wisconsin-Madison, Madison, WI, United States, ⁴School of Mathematical Sciences, University of Electronic Science and Technology of China, Chengdu, China, People's Republic of, ⁵Medical Physics, University of Wisconsin-Madison, Madison, WI, United States, ⁶Biomedical Engineering, University of Wisconsin-Madison, Madison, WI, United States, ⁷Medicine, University of Wisconsin-Madison, Madison, WI, United States, ⁸Emergency Medicine, University of Wisconsin-Madison, Madison, WI, United States

R2* mapping has the potential to provide rapid and accurate quantification of liver iron overload. However, conventional voxelwise liver R2* mapping methods are challenging when using echo images with low signal-noise ratio (SNR). The purpose of this work was to improve liver R2* mapping by a noise correction model incorporating weighted neighborhood information. Simulation and in vivo results demonstrate that the proposed method produces more accurate R2* maps with high spatial resolution compared to two recently proposed R2* mapping methods.

1915

Automatic MR-based Skull Segmentation using Local Shape and Global Topology Priors
Max W.K. Law¹, Calvin M.H. Lee¹, Gladys G. Lo², Jing Yuan¹, Oilei Wong¹, Abby Y. Ding¹, and Siu Ki Yu¹

¹Medical Physics and Research Department, Hong Kong Sanatorium & Hospital, Hong Kong, Hong Kong, ²Department of Diagnostic and Interventional Radiology, Hong Kong Sanatorium & Hospital, Hong Kong, Hong Kong

This abstract proposes a new algorithm that automatically segments the skull from gradient echo based magnetic resonance images to facilitate MR-based radiotherapy planning. The proposed algorithm compared the neighboring voxel intensity to capture local structural information of bone. The structural information was incorporated in a topology template which encapsulated global topology prior of skulls to achieve automatic segmentation. With the sequence-independent structural and topology priors, this method is potentially applicable to other scanning sequences. The segmented skull will be helpful for clinical applications such as cephalometry and MR-based radiotherapy planning to reduce ionizing-radiation received by patients.

1916

Image-based estimation of point spread function in distorted EPI images
Seiji Kumazawa¹, Takashi Yoshiura², Akihiro Kikuchi¹, Go Okuyama¹, Daisuke Shimao¹, and Masataka Kitama¹

¹Hokkaido University of Science, Sapporo, Japan, ²Kagoshima University, Kagoshima, Japan

To correct the distortion in EPI due to field inhomogeneity, the information regarding the signal from adjacent points within each voxel is needed. The PSF approach can provide this information. Our purpose was to develop an image-based-method for estimating the PSF images in the distorted EPI image using T1WI. Our method synthesizes the distorted image to match the measured EPI image through the generation process of EPI image according to a single-shot EPI k-space trajectory and field inhomogeneity. The results demonstrate that the PSF image for each voxel in distorted EPI image can be estimated by proposed method using segmented T1WI instead of additional acquisitions for PSF measurement.

1917

Combining Multi-channel MP2RAGE Images with Minimized Noise
Jing Zhang¹, Bruce Bjornson², and Qing-San Xiang³

¹Applied Science Laboratory, GE Healthcare Canada, Vancouver, BC, Canada, ²Department of Pediatrics, University of British Columbia, Vancouver, BC, Canada, ³Department of Radiology, Department of Physics and Astronomy, University of British Columbia, Vancouver, BC, Canada

Magnetization-prepared rapid gradient echo (MP-RAGE) has been widely used for T₁-weighted imaging. In order to overcome B₁ field inhomogeneity effect, the MP2RAGE sequence was introduced, with two complex images, GRE^{T11} and GRE^{T12}, acquired at two inversion times T₁₁ and T₁₂. The MP2RAGE images are usually calculated from all the coils first and combined later into a final result. We propose an algorithm for multi-channel MP2RAGE image combination with minimized resulting noise.

1918

Improving the Quality of the Multi-b Diffusion Weighted Images Using the Intrinsic Multi-Exponential Pattern
He Wang¹, Kaining Shi¹, Weibo Chen¹, and Guilong Wang¹

¹Philips Healthcare, shanghai, China, People's Republic of

The study developed a methodology to improve the quality of the multi-b DWIs using the intrinsic multi-exponential pattern. It was evaluated on a healthy brain and compared with the mono-exponential model. In addition, its potential value of improving the robustness of IVIM was also evaluated. According to the results, the multi-exponential method can improve the image quality of the multi-b DWIs and may become an effective preprocessing way for the non-monoexponential models.

1919

Multi-Inversion EPI-based imaging of T1 distribution within individual voxels
Ville Rennall¹ and Jonathan R. Polimeni²

¹Department of Neuroscience and Biomedical Engineering, Aalto University School of Science, Espoo, Finland, ²Athinoula A. Martinos Center for Biomedical Imaging, Department of Radiology, Massachusetts General Hospital, Harvard Medical School, Charlestown, MA, United States

T1 mapping using multiple inversion time IR-EPI can provide a large number of different TI values in a short time, which can be utilized to characterize the relaxation time distributions within individual voxels, as an extension to multi-parametric fitting.

1920

Generation of hybrid color images from T1 and T2 acquired simultaneously with MRF
Katherine L. Wright¹, Peter Schmitt², Dan Ma¹, Anagha Deshmane³, Vikas Gulani¹, and Mark Griswold¹

¹*Radiology, Case Western Reserve University, Cleveland, OH, United States*, ²*Siemens Healthcare, Erlangen, Germany*, ³*Biomedical Engineering, Case Western Reserve University, Cleveland, OH, United States*

This work proposes a method for the calculation of a single color image using quantitative T1 and T2 measurements acquired with Magnetic Resonance Fingerprinting. Quantitative MRF parameters are transformed and scaled with the goal of making normal tissues appear in grayscale and tissues with different T1 and T2 values (lesions) appear in color.

1921

High-SNR susceptibility weighted venography (SWV) for multi-echo magnetic resonance (MR) images based on complex signal modeling
Taejoon Eo¹, Dosik Hwang¹, and Jinseong Jang¹

¹*Yonsei University, Seoul, Korea, Democratic People's Republic of*

The multi-echo SWV with the proposed complex signal modeling method can provide high-SNR and multi-contrast phase masks and SWV images. The multiplication number of the phase mask for SWV was increased up to 16 without image degradation even at the long TE of 49.8 ms. More detailed vein structures were visualized with higher- and multiple contrasts than the conventional single-echo GRE SWV.

1922

Estimating Registration Variance Using Deformation Field Perturbations
Jan Scholz¹, Kaitlyn Easson², and Jason P Lerch^{1,3}

¹*Mouse Imaging Centre, Hospital for Sick Children, Toronto, ON, Canada*, ²*Department of Biomedical and Molecular Sciences, Queen's University, Toronto, ON, Canada*, ³*Department of Medical Biophysics, Department of Medical Biophysics, Toronto, ON, Canada*

Most image registration algorithms do not output any information about the variance of the transformation estimates. Here we show that by perturbing input files we can recover this information without modifying the underlying algorithms. We demonstrate that local brain volume estimates can be improved by using the determinant of the average across the distribution of transformations. Our methods will improve morphological analyses, registration-based label alignment, and help find optimal registration parameters.

1923

Graph-based segmentation of signal voids in time series of diffusion-weighted images of musculature in the human lower leg
Martin Schwartz^{1,2}, Günter Steidle¹, Petros Martirosian¹, Bin Yang², and Fritz Schick¹

¹*Section on Experimental Radiology, Department of Radiology, University of Tuebingen, Tuebingen, Germany*, ²*Institute of Signal Processing and System Theory, University of Stuttgart, Stuttgart, Germany*

The segmentation of signal voids, which occur in time-series of single-shot diffusion-weighted images, is important for an accelerated evaluation providing larger studies on this phenomenon. The proposed segmentation is based on a two-stage detection and segmentation approach, which utilizes a graph-based representation with random walker optimization. It was demonstrated that the presented method enables a fast and accurate segmentation of signal voids in time-series of diffusion-weighted images.

1924

Power spectrum detects corpus callosum directionality using T2-weighted MRI in secondary progressive MS patients and controls
Shrushruti Sharma¹ and Yunyan Zhang²

¹*Biomedical Engineering Program, University of Calgary, Calgary, AB, Canada*, ²*Departments of Radiology and Clinical Neurosciences, University of Calgary, Calgary, AB, Canada*

Standard MRI is routinely collected in patient care but is limited in assessing changes in tissue microstructure. We developed a new method to assess tissue directionality using the power spectrum of T2-weighted MRI and validated it using the highly coherent structure, corpus callosum. In controls, power spectrum-derived angles corresponded exactly with the predicted aligning directions of the corpus callosum, and such aligning patterns were interrupted in advanced MS patients with increased variability and angular entropy. Fourier-based power spectrum may provide advanced measures of tissue directionality following myelin and axonal pathology using clinical scans.

1925

The Impact of Polar based initialization and frame time curve selection on Left Ventricle short axis Perfusion MR Segmentation
Doaa Mousa¹, Nourhan Zayed¹, and Inas Yassine^{2,3}

¹*Computer and Systems, Electronic Research Institute, Giza, Egypt*, ²*Systems and Biomedical Engineering, Cairo University, Giza, Egypt*, ³*Medical Informatics and Image processing Lab, Nile University, Giza, Egypt*

Cardiovascular diseases (CVDs) cause 31% of the death rate globally. Automatic accurate segmentation is needed for CVDs early detection. In this paper, we propose a modified workflow to automatically segment the left ventricle (LV) for the short axis cardiac

perfusion MRI (perfusion CMR) images using levelset method. We propose mitigating the initial contour extraction, and modify the technique used to initialize the levelset algorithm in order to improve the accuracy of segmentation results. The system workflow consists of five main modules: preprocessing, localization, initial contour extraction, registration, and segmentation. Our results showed enhancement in the segmentation accuracy by 5%.

1926

Multi-layered Atlas Registrations for Multi-atlas Segmentation of Brain MRI
Han Sang Lee¹ and Junmo Kim¹

¹*School of Electrical Engineering, KAIST, Daejeon, Korea, Republic of*

Multi-atlas segmentation has often suffered from the registration error. We propose a novel method for multi-atlas registration for multi-atlas segmentation inspired by the template generation and deep neural network. We first add an intra-atlas registration layer which performs image-based registration between atlas images to duplicate the atlases. We then add a label-wise registration layer which rectifies the registered images by label-based registration. We present preliminary results of our multi-layered atlas registration on brain MRI segmentation.

1927

The impact of data analysis method, scanner type and scan session on volume measurements of brain structures
Michael Armann^{1,2}, Pavel Falkovskiy^{3,4,5}, Alain Thoeni¹, Tobias Kober^{3,4,5}, Alexis Roche^{3,4,5}, Bénédicte Maréchal^{3,4,5}, Philippe Cattin⁶, Tobias Heye², Oliver Bieri², Till Sprenger⁷, Christoph Stippich², Gunnar Krueger^{4,5,8}, Ernst-Wilhelm Radue¹, and Jens Wuerfel¹

¹*Medical Image Analysis Center (MIAC), Basel, Switzerland*, ²*Department of Radiology, University Hospital of Basel, Basel, Switzerland*, ³*Advanced Clinical Imaging Technology, Siemens Healthcare AG, Lausanne, Switzerland*, ⁴*Department of Radiology, University Hospital (CHUV), Lausanne, Switzerland*, ⁵*École Polytechnique Fédérale de Lausanne, Lausanne, Switzerland*, ⁶*Department of Biomedical Engineering, University of Basel, Basel, Switzerland*, ⁷*Department of Neurology, DKD Helios Klinik, Wiesbaden, Germany*, ⁸*Siemens Medical Solutions USA, Boston, MA, United States*

Performance of FreeSurfer and FSL was compared on T1-weighted 3D MRI data of 22 controls as function of scan session, scanner type and segmentation pipeline. Intra-class correlation coefficients and percentage volume differences were calculated for the segmentation results of both pipelines. Strong agreement was found for whole brain, white matter and cortex. For each pipeline, the impact of experimental factors was assessed by linear mixed effects analysis. We found significant scanner effect on the results of both segmentation pipelines. For subcortical structures, segmentation reliability was higher in FSL than in FreeSurfer, whereas for cortex and WM, FreeSurfer was more stable.

1928

Image Inhomogeneity Correction using Geometric Average of Channels in Sum-of-Squares Multi-channel MR Imaging
Renjie He¹, Yu Ding¹, and Qi Liu¹

¹*United Imaging Healthcare America, Houston, TX, United States*

Geometric average is insensitive to the value variation between components to be averaged, this is used to noticeably reduce the inhomogeneity caused by Sum-of-Squares (SOS) in channel combination in parallel MR imaging.

1929

In-vivo characterization of grey matter microstructure at 3T from the transverse component of the MRI signal
Antoine Lutti¹

¹*LREN, Dept. of Clinical Neurosciences, Centre Hospitalier Universitaire Vaudois, Lausanne, Switzerland*

The characterization of brain microstructure from MRI data requires the development of specific MRI tissue biomarkers and of advanced models linking microscopic tissue properties to MRI signals. We apply the Anderson-Weiss theory, which describes the transverse relaxation of the MRI signal as a function of tissue microstructure, on in-vivo MRI data acquired at 3T. In grey matter, parameter estimates show a strong correlation with histological measures of iron concentration. The time constants provided by the model yield realistic estimates of microscopic compartment size. These results offer a promising perspective for the histological assessment of brain tissue in-vivo using MRI.

1930

Hippocampal subfields segmentation derived from Freesurfer 6.0: a multisite 3T reproducibility study in healthy elderly
Moira Marizzoni¹, Daniele Orlandi¹, Luigi Antelmi², Flavio Nobili³, Mira Didic^{4,5}, David Bartrés-Faz⁶, Ute Fiedler⁷, Peter Schonknecht⁸, Pierre Payoux^{9,10}, Andrea Soricelli^{11,12}, Alberto Beltramello¹³, Lucilla Parnetti¹⁴, Magda Tsolaki¹⁵, Paolo Maria Rossini^{16,17}, Pieter Jelle Visser¹⁸, Regis Bordet¹⁹, Oliver Blin²⁰, Giovanni Battista Frisoni^{1,21}, Jorge Jovicich²², and on behalf of the PharmaCog Consortium¹

¹*LENITEM Laboratory of Epidemiology, Neuroimaging, & Telemedicine — IRCCS San Giovanni di Dio-FBF, Brescia, Italy*, ²*Health Department, Foundation IRCCS Neurological Institute Carlo Besta, Milan, Italy*, ³*Department of Neuroscience, Ophthalmology, Genetics and Mother-Child Health (DINOGLMI), University of Genoa, Genoa, Italy*, ⁴*APHM, CHU Timone, Service de Neurologie et Neuropsychiatrie, Marseille, France*, ⁵*Aix-Marseille Université, INSERM U 1106, Marseille, France*, ⁶*Department of Psychiatry and Clinical Psychobiology, Universitat de Barcelona and IDIBAPS, Barcelona, Spain*, ⁷*LVR-Clinic for Psychiatry and Psychotherapy, Institutes and Clinics of the University Duisburg-Essen, Essen, Germany*, ⁸*Department of Neuroradiology, University Hospital Leipzig, Leipzig, Germany*, ⁹*INSERM, Imagerie cérébrale et handicaps neurologiques, UMR 825, Toulouse, France*, ¹⁰*Université de Toulouse, UPS, Imagerie cérébrale et handicaps neurologiques, UMR 825, CHU Purpan, Place du Dr Baylac, Toulouse, France*, ¹¹*IRCCS SDN, Naples, Italy*, ¹²*University of Naples Parthenope, Naples, Italy*, ¹³*Department of Neuroradiology, General Hospital, Verona, Italy*, ¹⁴*Section of Neurology, Centre for Memory Disturbances, University of Perugia, Perugia, Italy*, ¹⁵*3rd Department of*

Neurology, Aristotle University of Thessaloniki, Thessaloniki, Greece, ¹⁶Dept. Geriatrics, Neuroscience & Orthopaedics, Catholic University, Policlinic Gemelli, Rome, Italy, ¹⁷IRCSS S.Raffaele Pisana, Rome, Italy, ¹⁸Department of Neurology, Alzheimer Centre, VU Medical Centre, Amsterdam, Italy, ¹⁹Department of Pharmacology, EA1046, University of Lille Nord de France, Lille, Italy, ²⁰Pharmacology, Assistance Publique-Hôpitaux de Marseille, Aix-Marseille University-CNRS UMR 7289, Marseille, France, ²¹Memory Clinic and LANVIE - Laboratory of Neuroimaging of Aging, University Hospitals and University of Geneva, Geneva, Switzerland, ²²Center for Mind/Brain Sciences, University of Trento, Rovereto, Italy

In this study we quantify the across-session reproducibility of hippocampus subfields obtained from the recently proposed ex-vivo atlas tool available in Freesurfer version 6.0. We use structural 3T multisite data from 65 healthy elderly participants scanned twice at least a week apart. We show that several subfields like Cornu Ammonis (CA) 1, hippocampal tail, molecular layer and subiculum offer, despite being smaller, comparable reliability errors to the whole hippocampus volume (2%). This suggests that these subfields may be valid and more specific markers to test disease progression in longitudinal studies, like for example Alzheimer's disease.

1931

Identification of Microbleeds on Postmortem Brain of Normal Aging Elderly and Dementia Patients
Shunshan Li¹, Lily Zhou², Mark J Fisher³, Ronald C Kim⁴, Vitaly Vasilevko⁵, David Cribbs⁵, Annlia Hill³, and Min-Ying Su⁶

¹Tu & Yuen Center for Functional Onco-Imaging, Department of Radiological Sciences, university of california, irvine, irvine, CA, United States, ²Sun Yat-Sen Memorial Hospital, Sun Yat-Sen University, Guangzhou, China, People's Republic of, ³Department of Neurology, University of California, Irvine, Irvine, CA, United States, ⁴Department of Pathology, University of California, Irvine, Irvine, CA, United States, ⁵Institute for Memory Impairments and Neurological Disorders, University of California, Irvine, Irvine, CA, United States, ⁶Tu & Yuen Center for Functional Onco-Imaging, Department of Radiological Sciences, University of California, Irvine, Irvine, CA, United States

The postmortem brain MR images include air-bubble artifacts and typical microbleeds(MBs) are less than 200 μ m which make MBs detection very challenging. In this project we developed an optimization MR imaging method to detect possible MBs on postmortem brains of patients with and without dementia, hoping to provide information to guide neuropathological examination to sample the suspicious MBs areas, and improve the chance of identifying true MBs to better understand its role in normal aging and development/progression of dementia, and further develop streamlined automatic MBs detection software.

1932

Dynamic Contrast Enhanced MRI Measurements in Glioma: Comparison Between Two Models
Sameeha Fallatah¹, Rolf Jäger¹, and Xavier Golay¹

¹Brain Repair and Rehabilitation, UCL, Institute of Neurology, London, United Kingdom

Dynamic Contrast Enhanced MRI is used to assess the integrity of the blood brain barrier. A major difficulty for the method to be accepted in the clinics is the variety of pharmacokinetic models used and their strong dependence on the underlying assumptions and/or acquisition parameters. Thus the far simpler methods based on signal intensity curve characteristics are the most commonly used approaches in clinical practice. In this study we compare two different pharmacokinetic models, the extended Tofts model and Lawrence & Lee model in patients with primary brain tumours.

1933

Development and Implementation of a Matlab-based multi-modal 3D visualization, co-registration and quantification platform for assessing brain tumor physiology and metabolism
Gaurav Verma¹, Suyash Mohan¹, Sanjeev Chawla¹, John Y.K. Lee², Sumei Wang¹, Andrew Maudsley³, Steven Brem², and Harish Poptani⁴

¹Department of Neuroradiology, University of Pennsylvania, Philadelphia, PA, United States, ²Department of Neurosurgery, University of Pennsylvania, Philadelphia, PA, United States, ³Department of Radiology, University of Miami, Miami, FL, United States, ⁴Department of Cellular and Molecular Physiology, University of Liverpool, Liverpool, United Kingdom

A 3D visualization, co-registration and quantification platform was developed in Matlab to combine anatomical imaging with physiological and metabolic data from diffusion tensor, perfusion-weighted and echo-planar spectroscopic imaging. This data can be co-registered across modalities and imaging time-points to provide detailed information about the spatial extent of a brain tumor. 3D visualization was applied in datasets from patients undergoing neurosurgery and a separate cohort of patients undergoing long-term Tumor Treating Fields (TTFields) therapy. This visualization platform could have an impact in the planning of neurosurgery and the placement and monitoring of location-sensitive techniques like TTFields.

1934

Non-Contrast-Enhanced Perfusion and Ventilation Assessment of the Human Lung by Means Of Wavelet Decomposition in Proton MRI
David Bondesson^{1,2}, Thomas Gaass^{1,3}, Julien Dinkel^{1,2}, and Berthold Kiefer⁴

¹Josef Lissner Laboratory for Biomedical Imaging, Department of Clinical Radiology, Ludwig-Maximilians-University Hospital Munich, Munich, Germany, ²Comprehensive Pneumology Center, German Center for Lung Research, Munich, Germany, ³Comprehensive Pneumology Center, German Center for Lung Research, Munich, Germany, ⁴Siemens AG Healthcare Sector, Erlangen, Germany

Evaluating regional lung perfusion and ventilation is diagnostically valuable in regards of pulmonary diseases. Standard methods however, expose patients to risks from ionizing radiation and contrast agents. MRI screening is not based on radiation and a new method has previously been presented as a non-contrast-enhanced estimation. This work presents wavelet decomposition as a potential improvement to fourier decomposition for perfusion and ventilation assessment of the human lung in proton MRI.

1935

Regional Brain Tissue Entropy Assessment in Patients with Obstructive Sleep Apnea
Sudhakar Tummala¹, Bumhee Park¹, Ruchi Vig¹, Mary A Woo², Daniel W Kang³, Ronald M Harper^{4,5}, and Rajesh Kumar^{1,5,6,7}

¹Anesthesiology, University of California at Los Angeles, Los Angeles, CA, United States, ²UCLA School of Nursing, Los Angeles, CA, United States, ³Medicine, University of California at Los Angeles, Los Angeles, CA, United States, ⁴Neurobiology, University of California at Los Angeles, Los Angeles, CA, United States, ⁵Brain Research Institute, University of California at Los Angeles, Los Angeles, CA, United States, ⁶Radiological Sciences, University of California at Los Angeles, Los Angeles, CA, United States, ⁷Bioengineering, University of California at Los Angeles, Los Angeles, CA, United States

Obstructive sleep apnea subjects show gray matter volume loss in multiple brain areas, based on voxel-based morphometry procedures, which are less sensitive in detecting subtle chronic/acute gray or white matter changes. We assessed brain injury in recently-diagnosed, treatment naïve OSA subjects by evaluating regional entropy, which measures the extent of homogeneity or randomness in tissue texture, and found significantly decreased regional entropy values in areas regulating autonomic, respiratory, cognitive, and neuropsychologic functions that are deficient in the condition, suggesting predominantly acute tissue pathology in those sites.. The findings suggest that regional entropy can demonstrate acute tissue changes.

1936

Fast simulation of off-resonance artifacts in MRI using FORECAST (Fourier-based Off-REsonanCe Artifact Simulation in the STeady-State)
Frank Zijlstra¹, Job G Bouwman¹, Ieva Braškutė¹, and Peter R Seevinck¹

¹Image Sciences Institute, UMC Utrecht, Utrecht, Netherlands

We present a fast alternative to Bloch simulation for simulation of off-resonance artifacts in steady-state imaging. By assuming a steady-state, the signal equation can be quickly evaluated by using multiple Fast Fourier Transforms. We show an acceleration factor of over 350 for a 2D simulation of a titanium cylinder phantom, while the differences with Bloch simulation were minor. The speed of the proposed method enables 3D simulations at high resolution and may benefit various applications.

1937

Estimation of voxel-wise phase offsets in a phased array coil using multi-echo GRE data
Minju Jo¹, Yoonho Nam², Jeehun Kim¹, Hyeong Geol Shin¹, and Jongho Lee¹

¹Laboratory for Imaging Science and Technology, Department of Electrical and Computer Engineering, Seoul National University, Seoul, Korea, Republic of, ²Department of Radiology, Seoul St. Mary's Hospital, College of Medicine, The Catholic University of Korea, Seoul, Korea, Republic of

In this work, we present a method of estimating the phase offsets in multi-echo GRE data, Multi-Channel Phase Combination using all N echoes (MCPC-N). MCPC-N, which calculates the phase offsets from all echoes, provides more accurate estimation of voxel-wise phase offsets particularly in low SNR.

1938

Characterization of atherosclerotic carotid plaque using MATCH with histopathologic validation: initial clinical experience
Lixin Yang¹, Wei Yu¹, Zhaoyang Fan², and DeBiao Li³

¹Department of Radiology, Beijing AnZhen Hospital, Beijing, China, People's Republic of, ²Biomedical Imaging Research Institute, Cedars-Sinai Medical Center, Los Angeles, CA, United States, ³Biomedical Imaging Research Institute, Cedars-Sinai Medical Center, Department of Bioengineering, University of California, Los Angeles, CA, United States

Purpose: Determine the accuracy of MATCH in the characterization of plaque composition in patients in comparison with the conventional multi-contrast approach, using histopathology as the gold standard.

Methods: Twenty-two patients scheduled for carotid endarterectomy underwent preoperative carotid MRI with MATCH and the conventional protocol, blinded image review for composition identification was performed by 2 radiologists. Carotid histopathological specimens stained with HE and Masson, matched with this two protocol images, Cohen kappa (K) was computed to quantify the agreement in the detection of components among this two protocols and histopathology.

Results: Moderate to good agreement was seen between histopathological specimens and multi-contrast protocol in the detection of plaque components (IH k=0.704, CA k=0.763, LR/NC k=0.844). Similar results were seen between histopathological specimens and MATCH (IH k=0.703CA k=0.740, LR/NC k=0.850).

1939

Optimized 4D flow MRI Processing for Evaluation of Abdominal Blood Flow
Eric James Keller¹, Jeremy Douglas Collins¹, Cynthia K Rigsby², James C Carr¹, Michael Markl^{1,3}, and Susanne Schnell¹

¹Radiology, Northwestern University, Chicago, IL, United States, ²Radiology, Ann & Robert H. Lurie Children's Hospital of Chicago, Chicago, IL, United States, ³Biomedical Engineering, Northwestern University, Evanston, IL, United States

4D flow MRI quantification of abdominal hemodynamics is challenged by a wide range of blood flow velocities and vessel diameters. By adjusting critical pre-processing steps required to analyze 4D flow MRI data, we were able to both recover vessels of interest lost by our previous method and significantly reduce the relative error in flow measurements. We conclude that it is critical to apply background phase error correction prior to any other filters and/or corrections to ensure accurate background offset estimation. Additionally, low venc acquisitions should not be noise corrected to ensure low flow data is not inadvertently deleted.

1940

MRI-SPAMM Based Magnetic Resonance Electrical Impedance Tomography
Kemal Sümser¹, Nashwan Naji^{1,2}, Mehdi Sadighi¹, Hasan Hüseyin Eroğlu^{1,3}, and Murat Eyüboğlu¹

¹Electrical and Electronics Engineering Department, Middle East Technical University, Ankara, Turkey, ²On Leave from Ibb University, Ibb, Yemen,

In magnetic resonance electrical impedance tomography (MREIT) currents are injected to the object during MRI imaging sequence. In this study, we propose a new pulse sequence based on the spatial modulation of magnetization (SPAMM) to be used in MREIT applications. In this pulse sequence, the current is injected during a pre SPAMM module which can be followed by any conventional Magnetic Resonance Imaging pulse sequence for data acquisition. Experimental result in comparison with the simulation result shows that this method is an applicable technique for MREIT data acquisition.

1941

The Influence of Bolus Arrival Time in Pharmacokinetic Analysis of Dynamic Contrast-Enhanced MRI of Breast Masses
Endre Grøvik^{1,2}, Atle Bjørnerud^{1,2}, Tryggve Holck Storås¹, Kjell-Inge Gjesdal³, and Kathinka Dæhli Kurz⁴

¹The Intervention Centre, Oslo University Hospital, Oslo, Norway, ²Department of Physics, University of Oslo, Oslo, Norway, ³Sunnmøre MR klinikk AS, Ålesund, Norway, ⁴Department of Radiology, Stavanger University Hospital, Stavanger, Norway

The purpose was to evaluate the influence of BAT in pharmacokinetic analysis of breast masses, by estimating the kinetic parameters both with and without BAT-delay correction. Thirty-nine verified breast masses were examined using a high temporal resolution EPI sequence. The image-data were analyzed using a two-compartment kinetic model with and without BAT-delay correction. The relationship between the relative parametric error and BAT-delay were investigated. The result indicates that neglecting the delayed BAT leads to an overestimation of K^{trans} , k_{ep} , and, v_e and a underestimation of v_p , and that the delayed BAT needs to be accounted for in the model-based analysis.

Traditional Poster

Elastography

Exhibition Hall

Tuesday, May 10, 2016: 16:00 - 18:00

1942

Liver stiffness in pediatric subjects is lower than in adults, and increases with age: a multifrequency MR elastography study
Emily Etchell¹, Lauriane Jugé^{1,2}, Alice Hatt¹, Ralph Sinkus³, and Lynne E. Bilston^{1,4}

¹Neuroscience Research Australia, Randwick, NSW, Australia, ²School of Medical Sciences, University of New South Wales, Kensington, NSW, Australia, ³BHF Centre of Excellence, Division of Imaging Sciences and Biomedical Engineering, King's College London, London, United Kingdom, ⁴Prince of Wales Clinical School, University of New South Wales, Kensington, NSW, Australia

Magnetic resonance (MR) elastography provides clinical information for chronic hepatic disorders by quantifying an increase in liver stiffness compared to healthy baseline values. Thus far however, baseline stiffness values have only been reported for adults. We aimed to fill this gap by quantifying healthy liver stiffness of children and adolescents. Results showed that pediatric liver stiffness increases with age during normal development, approaching adult values during adolescence. This implies that comparing pediatric liver stiffness measurements to adult baseline values when using MR elastography may miss disease or underestimate disease severity.

1943

MR elastography of intracranial tumors: Initial experience with high-resolution imaging and nonlinear inversion
Curtis L Johnson¹, Emily S Matijevich^{1,2}, Emily D Cullum^{1,2}, Matthew DJ McGarry³, Keith D Paulsen³, Bradley P Sutton^{1,4}, Tracey M Wszalek^{1,2}, and William C Olivero^{1,2}

¹Beckman Institute for Advanced Science and Technology, University of Illinois at Urbana-Champaign, Urbana, IL, United States, ²Carle Neuroscience Institute, Carle Foundation Hospital, Urbana, IL, United States, ³Thayer School of Engineering, Dartmouth College, Hanover, NH, United States, ⁴Department of Bioengineering, University of Illinois at Urbana-Champaign, Urbana, IL, United States

MR elastography has emerged as an important tool for presurgical evaluation of intracranial tumors. Due to the localized nature of the lesion properties of interest, there is a need for high-resolution MRE methods for characterizing tumors. Here we present our initial experience with MRE of intracranial tumors using a protocol based on high-resolution imaging and nonlinear inversion. We found that glial tumors are soft and have a generally low viscosity, while meningeal tumors are stiff and have a very low viscosity.

1944

Cross vendor comparison of gradient recalled echo (GRE) and spin echo-echo planar imaging (SE-EPI) based MR elastography of the liver at 3T.

Suraj D Serai¹, Jonathan R Dillman¹, Hui Wang², and Andrew T Trout¹

¹Radiology, Cincinnati Children's Hospital, Cincinnati, OH, United States, ²Philips Healthcare, Cincinnati, OH, United States

MR elastography (MRE) allows non-invasive evaluation of hepatic stiffness and samples a larger area of the liver than liver biopsy. The high accuracy of MRE for liver fibrosis staging suggests that MRE could potentially replace liver biopsy. MRE has traditionally been performed using a GRE sequence. GRE, however, has SNR limitations at higher field strengths that can result in under-sampling potentially leading to erroneous stiffness values. SE-EPI is an alternative means of performing MRE that has higher SNR, lower susceptibility related signal loss and increased speed. In this work, we compared GRE and SE-EPI MRE across two vendor platforms.

Increasing the Spatial Resolution and Sensitivity of High-Resolution Magnetic Resonance Elastography by Correcting for Subject Motion

and Susceptibility-Induced Image Distortions

Andreas Fehlner¹, Sebastian Hirsch¹, Mykola Kadobianskyi², Patric Birr¹, Eric Barnhill^{1,3}, Martin Weygandt^{2,4}, Johannes Bernarding⁵,

Jürgen Braun⁶, Ingolf Sack¹, and Stefan Hetzer^{2,4}

¹Department of Radiology, Charité - Universitätsmedizin Berlin, Berlin, Germany, ²Berlin Center for Advanced Neuroimaging, Charité - Universitätsmedizin Berlin, Berlin, Germany, ³Clinical Research Imaging Centre, School of Clinical Sciences and Community Health, College of Medicine and Veterinary Medicine, The University of Edinburgh, Edinburgh, United Kingdom, ⁴Bernstein Center for Computational Neuroscience Berlin, Berlin, Germany, ⁵Institut für Biometrie und Medizinische Informatik, Universitätsklinikum Magdeburg, Magdeburg, Germany, ⁶Institute of Medical Informatics, Charité - Universitätsmedizin Berlin, Berlin, Germany

High-resolution Multifrequency MR Elastography (MMRE) is hampered by susceptibility-induced image distortions. We corrected MMRE data of a 3T and 7T MR scanner for motion and EPI distortion artefacts. The correction of subject motion significantly sharpened the images, which was demonstrated by a decrease of the point-spread function. The improvement was highly correlated with the degree of subject motion. Distortion correction enhanced the accuracy of normalization in the MNI152 space as shown by an increase of the correlation between individual and standard tissue probability maps. This method could help increasing the sensitivity of multi-subject studies exploring $|G^*$ e.g. in small subcortical areas.

1946

In vivo multifrequency MR elastography of the human prostate using a surface-based compressed air driver operated in the lower frequency regime

Florian Dittmann¹, Heiko Tzschätzsch¹, Jing Guo¹, Sebastian Hirsch¹, Jürgen Braun², and Ingolf Sack¹

¹Institute of Radiology, Charité, Berlin, Germany, ²Department of Medical Informatics, Charité, Berlin, Germany

We demonstrate the feasibility of in vivo prostate exam utilizing shear waves induced by pressurized-air actuators previously developed for abdominal MRE. High wave amplitudes throughout the prostate were achieved in the lower frequency regime from 30 to 50 Hz. Using a 2D multifrequency wave number inversion algorithm, wave speed maps with sufficiently high resolution are obtained to discriminate between the central zone and peripheral zone despite longer wavelengths pertaining to lower vibration frequencies. The proposed MRE setup promises robust and easy-to-use applications in the clinic without the need of specialized hardware in addition to the abdominal MRE setup.

1947

Reproducibility of low-frequency MR elastography of the human brain

Florian Dittmann¹, Sebastian Hirsch¹, Jing Guo¹, Jürgen Braun², and Ingolf Sack¹

¹Institute of Radiology, Charité, Berlin, Germany, ²Department of Medical Informatics, Charité, Berlin, Germany

Since shear waves at low drive frequencies are nearly unaffected by attenuation, we introduce a brain MRE setup, which is based on remote excitation of intracranial shear waves by a pressurized-air actuator in the regime of 20 Hz. MRE-scans, which were repeated 27 times on three different days for each of six healthy volunteers, show differences between individuals as well as from day-to-day for the same individual. The investigation demonstrates that cerebral low frequency MRE provides a fast and reproducible novel source of mechanical information of brain tissue with less onerous head stimulation as required by conventional MRE.

1948

Quantification of Breast Stiffness using Magnetic Resonance Elastography at 3T: A Reproducibility Study

Prateek Kalra¹, Arunark Kolipaka, PhD¹, Jeffrey R. Hawley, MD¹, and Brian Raterman¹

¹Radiology, Ohio State University Wexner Medical Center, Columbus, OH, United States

Magnetic resonance elastography (MRE) is a non-invasive technique to estimate stiffness of soft tissues and has been applied in the breast. However, none of the earlier studies have extensively tested MRE to induce vibrations in the breast using a soft sternum driver at higher field strength and its repeatability of stiffness measurements. The aim of the study is to estimate breast stiffness using MRE by inducing vibrations using a soft sternum driver in normal volunteers at 3T and to determine the reproducibility of stiffness measurements. Preliminary results show that the MRE-derived stiffness values are reproducible in normal volunteers at 3T and can be further extended to detect breast tumors in patients.

1949

Assessing the viscoelastic properties of abdominal tumour models *in vivo* using MRE

Jin Li¹, Lisa Asher¹, Filipa Lopes², Craig Cummings¹, Alexander Koers^{2,3}, Laura S. Danielson^{2,3}, Louis Chesler^{2,3}, Caroline J. Springer², Jeffrey C. Bamber¹, Ralph Sinkus⁴, Yann Jamin¹, and Simon P. Robinson¹

¹Division of Radiotherapy & Imaging, The Institute of Cancer Research, London, United Kingdom, ²Division of Cancer Therapeutics, The Institute of Cancer Research, London, United Kingdom, ³Division of Clinical Studies, The Institute of Cancer Research, London, United Kingdom, ⁴Division of Imaging Sciences and Biomedical Engineering, King's College London, King's Health Partners, St. Thomas' Hospital, London, United Kingdom

MRE was applied to assess the viscoelastic properties of orthotopic pancreatic ductal adenocarcinoma (PDAC) xenografts, and tumours arising in a transgenic mouse model of *MYCN*-amplified neuroblastoma, within the mouse abdomen. The stromal-rich PDAC tumours were quantified with markedly elevated elasticity (G_d) and viscosity (G_i), whilst the pathologically diverse neuroblastomas exhibit more heterogeneity in their biomechanical properties and were relatively soft. MRE can non-invasively assess the viscoelastic properties of deep-seated tumours arising within the abdomen of mice *in vivo*.

1950

Comparison of breath-hold, respiratory navigated and free-breathing MR Elastography

Ian Gavin Murphy¹, Martin Graves², Scott Reid³, Andrew Patterson², Ilse Gavin Joubert¹, Andrew N Priest², and David J Lomas²

¹*Radiology, Cambridge University Hospitals NHS Foundation Trust, Cambridge, United Kingdom*, ²*Radiology, Cambridge University NHS Foundation Trust, Cambridge, United Kingdom*, ³*GE, Little Chalfont, United Kingdom*

In patients with liver disease, MR elastography (MRE) is a non-invasive method for evaluating fibrosis. MRE is phase-based and sensitive to motion artefact, and is typically performed in end expiration. We found that navigator timed MRE shows no statistical difference to breath-held techniques for stiffness and reproducibility in 6 healthy volunteers, and may prove superior in patients unable to adequately hold their breath

1951

Brain MR elastography with multiband excitation and nonlinear motion-induced phase error correction

Curtis L Johnson¹, Joseph L Holtrop^{1,2}, Aaron T Anderson³, and Bradley P Sutton^{1,2}

¹*Beckman Institute for Advanced Science and Technology, University of Illinois at Urbana-Champaign, Urbana, IL, United States*, ²*Department of Bioengineering, University of Illinois at Urbana-Champaign, Urbana, IL, United States*, ³*Department of Mechanical Science and Engineering, University of Illinois at Urbana-Champaign, Urbana, IL, United States*

We propose a novel sequence for magnetic resonance elastography (MRE) of the brain based on multiband excitation and 3D encoding of the distributed slab with multishot spirals. This sequence allows access to optimal SNR efficiency and reduced distortions from field inhomogeneity, but also parallel imaging acceleration both in-plane and thru-plane without onerous artifacts and g-factor penalties. We also incorporate correction for nonlinear motion-induced phase errors through a k_z -blipped spiral-in 3D navigator. In this abstract we demonstrate the performance of the sequence and its ability to capture whole-brain MRE data at $2 \times 2 \times 2 \text{ mm}^3$ resolution in 3 minutes.

1952

Impact of Field Strength and Image Resolution on MRE Stiffness Estimation

Eric Barnhill¹, Jing Guo², Florian Dittmann², Sebastian Hirsch², Michael Perrins³, Lucy Hiscox³, Tim Herrmann⁴, Johannes Bernarding⁴, Neil Roberts³, Jürgen Braun¹, and Ingolf Sack²

¹*Institute of Medical Informatics, Charité Universitätsmedizin Berlin, Berlin, Germany*, ²*Department of Radiology, Charité Universitätsmedizin Berlin, Berlin, Germany*, ³*Clinical Research Imaging Centre, The University of Edinburgh, Edinburgh, United Kingdom*, ⁴*Institute for Biometrics and Medical Informatics, Otto von Guericke University Magdeburg, Magdeburg, Germany*

We investigated the impact of field strength and image resolution on brain MRE stiffness results. A cohort of 18 healthy volunteer subjects was scanned at 1.5T (2mm isotropic voxels), 3T (2mm) and 7T (1mm), with a fourth set downsampling the 7T to 2mm. Means were 1634 Pa (+/-613) for 1.5T, 1743 Pa (+/-811) for 3T, 1786 (+/-634) Pa for 7T 2mm, and 927 (+/-364) Pa for 7T 1mm. In the paired sign-rank tests, there were no significant effects for field strength. Examination of histograms of example slices suggests that a different distribution of features is being captured at the higher resolution.

1953

Investigation Of The Relationship Between Feature Detail And Stiffness Estimate In Magnetic Resonance Elastography (MRE) Elastograms

Eric Barnhill¹, Florian Dittmann², Sebastian Hirsch², Jing Guo², Jürgen Braun¹, and Ingolf Sack²

¹*Institute of Medical Informatics, Charité Universitätsmedizin Berlin, Berlin, Germany*, ²*Department of Radiology, Charité Universitätsmedizin Berlin, Berlin, Germany*

Magnetic Resonance Elastography (MRE) stiffness estimates show differentiated results by feature scale. Here progressive denoising was applied to study the relation between image sharpness (as measured by Reduced Energy Ratio) and image stiffness estimate (as measured by complex shear modulus magnitude $|G^*|$). Progressive complex-wavelet-based denoising appears to reach stable stiffness estimates in phantom and brain acquisitions. Images of maximum sharpness result in lower overall stiffness estimates than the stable global estimate, suggesting that coarse elasticity estimates do not average fine feature results, but measure a different stiffness scale.

1954

Reducing Time Samples Needed for MR Elastography

Roger Grimm¹, Jun Chen¹, and Richard Ehman¹

¹*Mayo Clinic, Rochester, MN, United States*

A 3D gradient recalled echo sequence has been developed that samples the three shear wave displacement polarization at 3 time points for a total of 9 image samples. A multi-coil recon generates phase difference images and then uses a 3 point discrete Fourier transform to provide the complex displacement fields. The sequence is shown in breast and head applications.

1955

MR Elastography using SS-SE-EPI with reduced FOV: phantom study and preliminary volunteer study for the pancreas

Yohei Itoh¹, Yasuo Takehara², Naoki Ooishi², Masanori Kawade², Tetsuya Wakayama³, Mikio Suga⁴, Takasuke Ushio¹, Yuki Hirai¹, Nobuko Yoshizawa¹, Shuhei Yamashita¹, Hatsuko Nasu¹, and Harumi Sakahara¹

¹*Diagnostic Radiology & Nuclear Medicine, Hamamatsu University school of medicine, Hamamatsu, Shizuoka, Japan*, ²*Department of Radiology, Hamamatsu University Hospital, Hamamatsu, Shizuoka, Japan*, ³*GEHCJ, Hino-shi, Tokyo, Japan*, ⁴*Center for Frontier Medical Engineering, Chiba University, Chiba, Japan*

To achieve the high spatial resolution MR elastography(MRE), it has been reported that combining SS-SE-EPI with a spatially selective

excitation provides an efficient way of reducing FOV. Using this technique, we performed phantom study and pancreatic MRE. We report the result of our study and the point we found when performing the reduced-FOV MRE.

1956

Noise-robust multifrequency wave number inversion for high-resolution MR elastography in the abdomen
Heiko Tzschätzsch¹, Jing Guo¹, Florian Dittmann¹, Sebastian Hirsch¹, Eric Barnhill¹, Jürgen Braun², and Ingolf Sack¹

¹Department of Radiology, Charité - University Medicine Berlin, Berlin, Germany, ²Institute of Medical Informatics, Charité - University Medicine Berlin, Berlin, Germany

Elastography often suffers from limited anatomical resolution due to noise and insufficient elastic deformation. We here introduce noise-robust multifrequency wave number inversion for multifrequency MR elastography. Compound maps of wave speed are obtained, which reveal variations in tissue elasticity in a tomographic fashion, i.e. an unmasked, slice-wise display of anatomical details at pixel-wise resolution. The method is demonstrated using data from the literature including abdominal and pelvic organs such as the liver, spleen, uterus and cervix. Elastic parameters consistent with literature values were obtained even in small regions with low wave amplitudes such as nucleus pulposus and spinal cord.

1957

Development of a novel phantom for routine quality assurance of an MR elastography system
Lumeng Cui^{1,2}, Conrad Yuen³, Ted Lynch⁴, Paul Babyn⁵, Francis M. Bui⁶, and Niranjan Venugopal^{1,5}

¹Department of Medical Physics, Saskatchewan Cancer Agency, Saskatoon, SK, Canada, ²Division of Biomedical Engineering, University of Saskatchewan, Saskatoon, SK, Canada, ³Department of Medical Physics, BC Cancer Agency, Vancouver, BC, Canada, ⁴Non-ionizing Radiation, CIRS Inc., Norfolk, VA, United States, ⁵Department of Medical Imaging, University of Saskatchewan, Saskatoon, SK, Canada, ⁶Department of Electrical & Computer Engineering, University of Saskatchewan, Saskatoon, SK, Canada

Magnetic Resonance Elastography (MRE) is a new imaging technique that combines the acoustic waves and MRI to retrieve elastic properties of tissue. Because MRE is non-invasive, there is great clinical interest for its use in the detection of cancer. In this work, we focus on the design of an MRE phantom to be used in the clinical commissioning of an MRE System. With the aid of newly designed pulse sequences and inversion algorithms we have developed a quality assurance process to validate the efficacy of MRE for applications to many clinical sites (i.e. prostate, cervix, uterus).

1958

Compact and fully automated 3D multifrequency tabletop MR elastography for the measurement of viscoelastic parameters in small tissue samples
Navid Samavati^{1,2}, Clara Körting¹, Toni Drießle³, Stefan Wintzheimer³, Jing Guo¹, Florian Dittmann¹, Ingolf Sack¹, and Jürgen Braun²

¹Department of Radiology, Charité University Medicine, Berlin, Germany, ²Department of Medical Informatics, Charité University Medicine, Berlin, Germany, ³Pure Devices GmbH, Würzburg, Germany

A fully integrated tabletop MR elastography (MRE) system based on a 0.5-T permanent magnet for investigations of small tissue samples is introduced. A 3D spin echo MRE sequence allows control of all MRE parameters including frequency and amplitude of a piezoelectric actuator. The device enables fully automated measurements of maps of viscoelastic parameters in soft tissue samples by 3D multifrequency MRE. Initial results are in good agreement to published data and demonstrate the great potential of the system as a preclinical research unit in histopathological laboratories and operating rooms.

1959

Identification of Myocardial Anisotropic Material Properties using Magnetic Resonance Elastography and the Finite Element Method
Renee Miller¹, Arunark Kolipaka², Vicky Wang³, Martyn Nash³, and Alistair Young¹

¹Anatomy with Radiology, University of Auckland, Auckland, New Zealand, ²Radiology, Biomedical Engineering and Internal Medicine, The Ohio State University Wexner Medical Center, Columbus, OH, United States, ³Auckland Bioengineering Institute, University of Auckland, Auckland, New Zealand

In this study, we examined the determinability of anisotropic stiffness parameters using finite element analysis simulations of harmonic steady-state wave behaviour. Two simulation experiments, of cylindrical phantom and left ventricular geometries, and one phantom experiment using magnetic resonance elastography (MRE) were carried out. The transversely isotropic material properties were determined using a least-squares optimisation algorithm by matching a modelled displacement field to the reference, or MRE, displacement field. The results showed that the parameters were uniquely identifiable even in the presence of noise.

1960

Experimental Validation of High Shear Wave Displacement at Mode Frequencies in MR Elastography
Cemre Ariyurek^{1,2}, Safa Ozdemir^{1,2}, Arif Sanli Ergun³, Yusuf Ziya Ider¹, and Ergin Atalar^{1,2}

¹Department of Electrical and Electronics Engineering, Bilkent University, Ankara, Turkey, ²National Magnetic Resonance Research Center (UMRAM), Ankara, Turkey, ³Department of Electrical and Electronics Engineering, TOBB-University of Economics and Technology, Ankara, Turkey

Experimental validation of modes of shear waves in MR elastography (MRE) is demonstrated. For the first time, frequency response of the actuator is investigated and actuator displacement is measured. Normalizing shear wave displacement to the actuator displacement removes the effect of actuation system and isolates shear wave resonance. It is demonstrated that 10-20 times greater shear wave displacement than applied displacement by the actuator can be observed at resonance. Thus, safety issues in MRE should be reconsidered. Presenting repeatability of determining mode frequency validates feasibility of detecting stiffness changes by observing any shift in mode frequency.

1961

Poroelastic mechanical properties of brain tumors using intrinsic actuation MR elastography
Ligin Solamen¹, Matthew McGarry¹, Elijah Van Houten², Jennifer Hong³, John Weaver^{1,4}, and Keith Paulsen^{1,5}

¹Thayer School of Engineering, Dartmouth College, Hanover, NH, United States, ²Department of Mechanical Engineering, University of Sherbrooke, Sherbrooke, QC, Canada, ³Department of Neurosurgery, Dartmouth-Hitchcock Medical Center, Lebanon, NH, United States, ⁴Department of Radiology, Dartmouth-Hitchcock Medical Center, Lebanon, NH, United States, ⁵Norris Cotton Cancer Center, Dartmouth-Hitchcock Medical Center, Lebanon, NH, United States

Intrinsically actuated poroelastic MR elastography (IA-pMRE) is a technique which estimates tissue mechanical and hydrodynamic properties using measurements of displacement during the cardiac cycle, and does not require external vibration as in traditional MRE. Compared to conventional MRE, which obtains displacements in the range of 25-100Hz, IA-pMRE uses intrinsically generated low frequency (1-2Hz) displacements for elastography reconstruction. IA-pMRE was applied to 7 brain tumor patients and showed a significant difference in both the shear modulus and hydraulic conductivity of brain tissue compared to healthy tissue.

1962

Robust Harmonic Estimation for MR Elastography: Application to Brain
Joshua D. Trzasko¹, Arvin Arani¹, Armando Manduca¹, Kevin J. Glaser¹, Richard L. Ehman¹, Philip A. Araoz¹, and John Huston III¹

¹Mayo Clinic, Rochester, MN, United States

In this work, we adapt the previously-described robust harmonic estimation (RHE) strategy for magnetic resonance elastography (MRE) to brain imaging, and demonstrate that use of this novel signal processing tool improves the accuracy of estimated stiffness information both in a geometrically-accurate phantom and *in vivo*.

Traditional Poster

Diffusion: Clinical Applications

Exhibition Hall

Wednesday, May 11, 2016: 10:00 - 12:00

1963 Prostate Cancer: Correlation of Intravoxel Incoherent Motion MR Parameters with Gleason Score
Dal Mo Yang¹, Hyun Cheol Kim¹, Sang Won Kim¹, and Geon-Ho Jahng¹

¹Radiology, Kyung Hee University Hospital at Gangdong, Seoul, Korea, Republic of

Accurate assessment of prostate cancer aggressiveness is important for deciding treatment strategy. Functional MRI sequences such as DWI and DCE have been shown to provide information about tumor aggressiveness. Patients with high Gleason scores exhibited lower ADC values. In this study, we evaluated the potential of IVIM imaging to predict histologic prognostic parameters by investigating whether various IVIM parameters correlate with the Gleason score. The result indicates D is the best IVIM parameter for discriminating prostate cancers with low GS from prostate cancers with intermediate or high GS.

1964

Application of the inhomogeneous variable flip angle (I-VFA) scheme in hyperpolarized 129Xe DWI
Jianping Zhong^{1,2}, Weiwei Ruan¹, Xianping Sun¹, Chaohui Ye^{1,2}, and Xin Zhou¹

¹State Key Lab Magnet Resonance & Atom & Mol Phys, Wuhan Inst Phys & Math, Chinese Acad Sci, Wuhan, China, People's Republic of, ²School of Physics, Huazhong University of Science and Technology, Wuhan, China, People's Republic of

SNR and resolution are two important parameters for the quantitative assessment of MR images. In k-space, the central part contributes SNR, whereas the edges contribute details. The accuracy of the apparent diffusion coefficient (ADC) calibration was significantly affected by SNR. For hyperpolarized GRE sequences, the homogeneous variable flip angle scheme is sub-optimal and leads to low SNR images. We propose a simple method termed inhomogeneous variable flip angle (I-VFA) to derive ADC of hyperpolarized gases. Higher SNR images and more stable results can be achieved by this simple method.

1965

Is it well-thought-out to scan the preterm neonates at term-equivalent gestational age?
Yanyan Li¹, Chao Jin¹, Xianjun Li^{1,2}, Miaomiao Wang¹, Jie Gao¹, Qinli Sun¹, and Jian Yang¹

¹Department of Radiology, the First Affiliated Hospital of Xi'an Jiaotong University, Xi'an, China, People's Republic of, ²Department of Biomedical Engineering, School of Life Science and Technology, Xi'an Jiaotong University, Xi'an, China, People's Republic of

Considering the extra-environmental associated effects on brain development, it may be unreasonable to scan preterm infants at term-equivalent GA. To clarify this, we aim to explore the effects of postnatal days on neonatal WM maturation by DTI. Results indicate that postnatal days at-scan may be a considerable factor to investigate the WM maturation: during a close to in-uterine period, the absent effects of postnatal days may suggest the reasonability of performing neonatal MR-scans in such period; while as postnatal days increases, observed FA changes may imply the bias of comparing the preterm neonates at term-equivalent GA to term ones.

Exploring the impact of common sequence variations on ADC reliability of lung lesions prior to protocol implementation in multi-centre clinical trials

Marianthi-Vasiliki Papoutsaki¹, Alex Weller¹, Matthew R Orton¹, and Nandita M de Souza¹

¹*Radiotherapy and Imaging, The Institute of Cancer Research, Sutton, London, United Kingdom*

Standardization of diffusion-weighted (DW) protocols in multi-centre clinical trials is challenging. Prior to protocol development, the effect of inter-vendor related sequence variations on the apparent diffusion coefficient (ADC) reliability should be explored. In this study, the reliability of ADC estimates of lung lesions using two optimised DW protocols was assessed by mimicking vendor-related sequence variations. Patients with lung lesions were scanned twice using two DW protocols with different fat suppression techniques, diffusion gradient modes and TEs. These key variations increased the coefficient of variation of the ADC estimates of lung lesions, although absolute values did not differ significantly.

Evaluation of Chemotherapeutic Effects in Patients with Lung Cancer using iShim-integrated Whole-Body Diffusion-Weighted Imaging
Xing Tang¹, Hong Wang², Panli Zuo³, Shun Qi⁴, and Hong Yin⁴

¹*Department of Radiology, Xijing hospital, Xi'an, China, People's Republic of,*

²*Siemens Healthcare, MR Collaborations NE Asia, Beijing, China, People's Republic of,* ³*Department of Radiology, Department of Radiology, Xijing Hospital, Xi'an, China, People's Republic of*

Whole-body diffusion-weighted imaging (WB-

DWI) is now increasingly utilized for evaluation of the patient's response to treatment. The purpose of this study is to evaluate the feasibility of WB-DWI with integrated slice-by-slice shimming (iShim) in patients with lung cancer. We found the SCLC is more sensitive to the chemotherapy than NSCLC using WB DWI.

Diffusion Kurtosis Imaging and Tensor Imaging for Evaluation of Renal Changes in Diabetic Nephropathy: Preliminary study
Fan Mao¹, Lihua Chen¹, Yu Zhang², Tao Ren¹, Chenglong Wen¹, and Wen Shen¹

¹*Tianjin First Center Hospital, Tianjin, China, People's Republic of,* ²*Philips healthcare, Beijing, China, People's Republic of*

Diffusion Tensor Imaging (DTI) as a noninvasive technique can provide valuable information based on the Brownian motion of water. However, the diffusion of water molecules in biological tissue like kidney does not follow a Gaussian distribution. Diffusion Kurtosis Imaging (DKI) can reflect the degree of restriction of hydrogen diffusion movement, and might detect the diffusion changes of kidney diseases more sensitive than DTI. Our study compared diffusion changes of DKI with DTI in kidneys of DN and healthy controls. The result showed DKI can be used for detecting renal changes in diabetes nephropathy with higher sensitivity compared to DTI.

Intravoxel incoherent motion MRI in primary rectal cancer: correlation with histologic prognostic factors
Zhe Han^{1,2}, Juan Chen², Min Chen², Chen Zhang², and Lizhi Xie³

¹*Chinese Academy of Medical Science and Peking Union Medical College, Beijing, China, People's Republic of,* ²*Department of Radiology, Beijing Hospital, Beijing, China, People's Republic of,* ³*GE Healthcare, MR Research China, Beijing, China, People's Republic of*

In this study we compared the association of intravoxel incoherent motion (IVIM) derived parameters with the histologic grade, N-stage, EGFR expression and K-RAS gene mutation of primary rectal cancer. Significant correlations were found between D values and differentiation grade, D* values and N-stage, f values and N-stage. IVIM derived parameters may be a promising imaging biomarker of tumor aggressiveness and prognosis.

Liver metastasis from colorectal cancer; a comparison of reproducibility of ADC between multiple sites and vendors, at 1.5 T and 3 T
Ryan Pathak¹, Neil A Thacker², David M Morris², Philippe Garteiser³, Sabrina Doblas³, Bernard E. Van Beers³, Houshang Amiri⁴, Arend Heerschap⁴, and Alan Jackson¹

¹*The Wolfson Molecular Imaging Centre, University of Manchester, Manchester, United Kingdom,* ²*Centre for Imaging Sciences, University of Manchester, Manchester, United Kingdom,* ³*Laboratory of imaging biomarkers, INSERM, Paris Diderot University, Paris, France,* ⁴*Radboud University Medical Center, Nijmegen, Netherlands*

ADC, calculated from diffusion-weighted MRI, is a potential quantitative imaging biomarker for detection of early treatment response. Imaging in the liver suffers from poor reproducibility, mainly as a result of respiratory motion. In this study we compare reproducibility in a multi-site, multi vendor setting at both 1.5 T and 3 T field strengths, for patients histologically diagnosed with colorectal cancer, who have radiological evidence of liver metastasis.

Differential Diagnosis of Intrahepatic Cholangiocarcinoma and Hepatocellular Carcinoma by Using Diffusion-tensor Imaging
chen lihua¹, liu ailian¹, song qingwei¹, wang heqing¹, sun meiyu¹, li ye¹, chen anliang¹, and xie lizhi²

¹*The Affiliated Hospital of Dalian Medical University, Dalian, China, Dalian, China, People's Republic of,* ²*GE Healthcare, MR Research China, Beijing, China, People's Republic of*

The advent of functional MR imaging has facilitated an increased role for imaging in risk stratification and treatment planning. In this study, DTI and DWI MR measurements were performed to investigate the correlation of the FA and ADC values in ROIs of the

intrahepatic cholangiocarcinoma (ICC) and hepatocellular carcinoma (HCC), and in further the sensitivity, specificity and accuracy of the parameters for the diagnosis. DTI working at present scanning hardware are more capable to detect the pathophysiological changes unattainable compare to conventional MRI techniques.

1972

Evaluation of pathological stage and grade of endometrial carcinoma using sagittal DWI
Shifeng Tian¹, Ailian Liu¹, Ye Li¹, and Jinghong Liu¹

¹*The First Affiliated Hospital of Dalian Medical University, Dalian, China, People's Republic of*

It has been reported that DWI has a high accuracy in the evaluation of the depth of EC, and ADC can predict the pathological grade of EC. The preoperative staging of sag DWI with EC was similar to sag T2WI. ADC value can be used to identify different pathological grades and some different stages of EC, with the increase of the pathological grade the ADC value decreased.

1973

To evaluate renal dysfunction using diffusion weighted magnetic resonance imaging based on intra-voxel incoherent motion (IVIM) and a mono-exponential model – a comparison study
Jiule Ding¹, Jie Chen¹, Zhenxing Jiang¹, Hua Zhou², Jia Di², Wei Xing¹, and Yongming Dai³

¹*Department of Radiology, Third Affiliated Hospital of Suzhou University, Changzhou, China, People's Republic of*, ²*Department of Nephrology, Third Affiliated Hospital of Suzhou University, Changzhou, China, People's Republic of*, ³*Philips Healthcare, Shanghai, China, People's Republic of*

The IVIM model was compared with the mono-exponential model to be used to differentiate sRI from non-sRI in this study. Results indicated that IVIM contributed little to improving the differentiation, therefore the mono-exponential model based ADC, a combination of fast and slow diffusion, might be more suitable as a biomarker image for assessing renal dysfunction.

1974

Estimation of pseudo-diffusion coefficient D* using different settings of low b-values in liver IVIM imaging
Meng-Chieh Liao¹, Cheng-Ping Chien¹, Shih-Han Hung¹, Feng-Mao Chiu², and Hsiao-Wen Chung¹

¹*Graduate Institute of Biomedical Electronics and Bioinformatics, National Taiwan University, Taipei, Taiwan*, ²*Philips Healthcare, Taipei, Taiwan*

The pseudo-diffusion coefficient (D*) in the liver estimated using intravoxel incoherent motion (IVIM) MRI currently suffers from inconsistent values reported in the literature. This study investigated the effect of low b-value settings on the estimation of D*. Data from healthy subjects with sixteen b-values were analyzed, with b-values of 0, 5, 10, and 15s/mm² selectively removed and D* computed using a bi-exponential model. Results show progressive increases in D* estimations, with difference in values by a factor of two, which strongly suggest that the IVIM signals in the low b-value range do not obey single exponential decaying behavior.

1975

Structural Changes of the Superior Longitudinal Fasciculus and Cingulate Gyrus in Post Stroke Depression
Chenfei Ye¹, Heather T Ma¹, Jun Wu², Xuhui Chen², and Changle Zhang¹

¹*Department of Electronic and Information Engineering, Harbin Institution of Technology Shenzhen Graduate School, Shenzhen, China, People's Republic of*, ²*Department of Neurology, Peking University Shenzhen Hospital, Shenzhen, China, People's Republic of*

This study aim to investigate the relationship between depression after onset of stroke and superior longitudinal fasciculus and cingulate gyrus with multi-parameter DTI comparisons. These two brain structures distal to infarct regions were obtained by automatic segmentation and four parameters based on intensity distribution (mean, standard deviation, skewness and kurtosis) were quantitatively measured on each structure. Significant difference in these two structures was found among major depression subjects, mild depression subjects and the normal control. Our results verified that PSD patients latently exhibit neuroanatomical changes in superior longitudinal fasciculus and cingulate gyrus.

1976

High Resolution Cervical Spine DTI in Axial View using Non-triggered Multi-shot Acquisition and SYMPHONY Reconstruction
Xiaodong Ma¹, Zhe Zhang¹, Yuhui Xiong¹, Erpeng Dai¹, Yishi Wang¹, Le He¹, Chun Yuan^{1,2}, and Hua Guo¹

¹*Center for Biomedical Imaging Research, Department of Biomedical Engineering, School of Medicine, Tsinghua University, Beijing, China, People's Republic of*, ²*Vascular Imaging Laboratory, Department of Radiology, University of Washington, Seattle, WA, United States*

In this study, 2D-navigated multi-shot EPI is used to achieve high resolution DTI in the cervical spine without cardiac triggering. A k-space reconstruction method, SYnergistic iMage reconstruction with PHase variatiOn and seNsitivitY (SYMPHONY), is used to correct the ghost artifacts caused by phase variations among different shots. The proposed technique is validated using quantitative analysis in healthy volunteers. Because no cardiac triggering is used, the scan time can be reduced. The improved spatial resolution and scan efficiency are beneficial for the quantitative evaluation of cervical spine in both neuroscience research and clinical diagnosis.

1977

Comparison of different mathematical models for IVIM in healthy human kidneys
Zhongwei Chen¹, Youfan Zhao¹, Zhenhua Zhang¹, Haiwei Miu¹, and Qiong Ye¹

¹*Department of Radiology, The First Affiliated Hospital of Wenzhou Medical University, Wenzhou, China, People's Republic of*

Various mathematical models have been applied in IVIM. Even with the same data, derived results change with the model used. Our

study compared four popular mathematical models of IVIM in healthy human kidneys to explore this technique.

1978

Effects of variations in gestational age and birth anthropometric indicators on diffusion metrics of term neonatal white matter: a cohort study
Chao Jin¹, Yanyan Li¹, Xianjun Li^{1,2}, Miaomiao Wang¹, Jie Gao¹, Qinli Sun¹, and Jian Yang¹

¹Department of Radiology, the First Affiliated Hospital of Xi'an Jiaotong University, Xi'an, China, People's Republic of, ²Department of Biomedical Engineering, School of Life Science and Technology, University of Xi'an Jiaotong, Xi'an, China, People's Republic of

During the life span, brain development would be affected by numerous intra- and inter- factors in a short- or/and long-term period. To reveal typical birth indicators' short-term effects, the effects of gestational age (GA), birth weight, crown-heel length and head circumference on term neonatal white matter were investigated by DTI. Results indicate that term neonates born with higher GA, birth weight and crown-heel length may hint better maturation of brain microstructure; among four birth indicators, GA was the main factor that influenced DTI-metrics. Particularly, longer crown-heel length with leftward superiority in corona radiata may presumably support early motor function.

1979

Assessment of fractional anisotropy of heart using ECG gating and second moment nulling pulse
Tomoya Nakamura¹, Shuhei Shibukawa², Yuma Sainokami², Tomohiko Horie¹, Isao Muro², Terumitsu Hasebe¹, Yutaka Imai², and Tetsuo Ogino³

¹Tokai University Hachioji Hospital, Hachioji, Japan, ²Tokai University Hospital, Isehara, Japan, ³Philips Healthcare Asia Pacific, Shinagawa, Japan

The purpose of this study is to assess the fractional anisotropy (FA) of heart using ECG gating and second moment nulling pulse which is intrinsically insensitive to motion. The FA at motion correction (MC) gradient was significantly higher than at acceleration motion correction (aMC) gradient, therefore, cardiac motion artifact results in an overestimation of FA. In conclusion, the use of second order motion correction gradient enables the quantification of FA at heart and has the potential to contribute to clinical cardiac imaging.

1980

Diffusion MRI of neuro-plasticity following complex motor learning
Maya Faraggi¹, William D Richardson², Derek K Jones³, and Yaniv Assaf^{4,5}

¹Neurobiology, Tel Aviv University, Tel Aviv, Israel, ²Wolfson Institute for Biomedical Research, University College London, London, United Kingdom, ³CUBRIC, Cardiff University, Cardiff, United Kingdom, ⁴Tel Aviv University, Tel Aviv, Israel, ⁵EMRIC, Cardiff University, Cardiff, United Kingdom

Neuroplasticity is the capacity of the nervous system to modify its organization as a result of a dynamic internal or external environment. In this study we aim to use DTI to characterize plasticity dynamics in the mouse brain as a result of a task with two degrees of difficulty. In order to achieve that goal, we assessed motor learning ability using a running wheel with irregularly spaced rungs ("complex wheel"). Diffusion MRI revealed significant micro-structural changes in multiple brain areas expected to be affected by this task including the motor domain, sensory perception regions and white matter tracts .

1981

Fractional diffusion as a probe of microstructural change in a mouse model of Duchenne Muscular Dystrophy
Matt G Hall¹, Paola Porcari², Andrew Blamire², and Chris A Clark¹

¹Institute of Child Health, University College London, London, United Kingdom, ²Newcastle Magnetic Resonance Centre, Newcastle University, Newcastle, United Kingdom

We apply a fractional diffusion model to preclinical data from a mouse model of Duchenne Muscular Dystrophy, and compare to histological measurements of the underlying tissue. We find that the alpha exponent of the model provides contrast which is indicative of the microstructural changes associated with DMD. We observe contrast between the wild type and mdx mouse model.

1982

Optimising Image Quality of Diffusion-Weighted Imaging of the Thyroid at 3.0 Tesla by Using iShim Sequence with iShim on yin-chun liu¹, meng-chao zhang², hong zeng², and lin liu²

¹Ji Lin University sino-Japan hospital, chang chun, China, People's Republic of, ²chang chun, China, People's Republic of

My name is yin-chun liu.I am from Ji Lin University.

1983 Effects of Broad SPAIR Pulse, Continuous Fat Suppression Mode, Flow Compensation on Image Quality and Apparent Diffusion Coeffcient Reproducibility in iShim Diff Weighted Imaging of the Abdomen at 3.0 T
He Sui¹, Mengchao Zhang¹, Hong Zeng¹, and Lin Liu¹

¹Jilin University SINO-JAPAN Hospital, Changchun, China, People's Republic of

To detect the effects of Broad SPAIR Pulse, Continuous Fat Suppression Mode, Flow Compensation on Image Quality and Apparent Diffusion Coeffcient Reproducibilit Weighted Imaging of the Abdomen at 3.0 T

The continuous fat suppression technique and Broad SPAIR Pulse can increase the fat saturation efficiency and decrease the ghost artifacts, when combined with flow y can be further improved without affect ADC values.

High quality of the iShim Diffusion-Weighted Imaging can give a great help of detection of disease.

1984

Age-related changes of white matter diffusion anisotropy measures in old age observed with Double Diffusion Encoding
Marco Lawrenz¹ and Juergen Finsterbusch¹

¹*Systems Neuroscience, University Medical Center Hamburg-Eppendorf, Hamburg, Germany*

With the help of double diffusion encoding experiments with two weighting periods applied successively microscopic tissue parameter can be gained. Rotationally invariant measures of the microscopic diffusion anisotropy such as the MA index may yield additional information complementary to DTI. Recent studies showed that MA can be determined in the living human brain, and normal values and their variation in groups of young and old healthy volunteers have been reported. In this study, the age-correlation of the diffusion anisotropy measures in terms of MA and FA values in a group of old volunteers (> 60 y) is discussed.

1985

Utility of histogram analysis of apparent diffusion coefficient value for distinguishing pituitary atypical adenomas from typical adenomas
Mariko Doai¹, Naoko Tsuchiya¹, Hisao Tonami¹, and Osamu Tachibana²

¹*Radiology, Kanazawa Medical University, Kahoku, Japan*, ²*Neurosurgery, Kanazawa Medical University, Kahoku, Japan*

The purpose of this study is to evaluate the utility of histogram analysis of apparent diffusion coefficient (ADC) value for distinguishing pituitary atypical adenomas from typical adenomas. The ADC maps were reviewed using Ziostation2, and placed a 3D volume-of-interest on the tumor. The entire tumor were computed. Histogram parameters were then compared between atypical adenomas (n=3) and typical adenomas (n=11). Skewness and kurtosis of ADC histogram were significantly lower for atypical adenoma as compared with typical adenoma. ADC histogram analysis on the basis of the entire tumor volume can be useful in distinguishing atypical adenomas from typical adenomas.

1986

DW-MRI for evaluating lesions classified as responding and non-responding on RECIST criteria in patients with relapsed epithelial ovarian and primary peritoneal cancer re-challenged with platinum-based chemotherapy

Jennifer C Wakefield^{1,2}, Jessica M Winfield^{1,2}, Veronica Morgan², Alison MacDonald², Susana Banerjee^{1,2}, Andrew N Priest³, Rebecca A Quest⁴, Susan Freeman³, Andrea G Rockall⁴, and Nandita M deSouza^{1,2}

¹*Division of Radiotherapy and Imaging, Cancer Research UK Cancer Imaging Centre, The Institute of Cancer Research, London, United Kingdom*,

²*The Royal Marsden Hospital, Sutton, United Kingdom*, ³*Department of Radiology, Addenbrooke's Hospital, Cambridge University Hospitals NHS Foundation Trust, Cambridge, United Kingdom*, ⁴*Imaging Department, Imperial College Healthcare NHS Trust, London, United Kingdom*

The utility of Diffusion-weighted MRI (DW-MRI) in defining response by volume reduction or for determining the time-course of apparent diffusion coefficient (ADC) changes indicative of response has not been evaluated in patients with relapsed ovarian or peritoneal cancer. We evaluated post-treatment change in volume and ADC in lesions classified by RECIST criteria as responders and non-responders. We found responding lesions show greater change in volume and equivalent change in ADC to non-responding lesions after one cycle of chemotherapy. In non-responding lesions, the change in these parameters continued at the same rate post-first cycle of chemotherapy, indicating a delayed response.

1987

Hemodynamic-independent fluctuation MRI using self-correction in idiopathic normal pressure hydrocephalus
Naoki Ohno¹, Tosiaki Miyati¹, Marina Takatsuji², Mitsuhiro Mase³, Tomoshi Osawa³, and Yuta Shibamoto⁴

¹*Faculty of Health Sciences, Institute of Medical, Pharmaceutical and Health Sciences, Kanazawa University, Kanazawa, Japan*, ²*Division of Health Sciences, Graduate School of Medical Science, Kanazawa University, Kanazawa, Japan*, ³*Department of Neurosurgery and Restorative Neuroscience, Graduate School of Medical Sciences, Nagoya City University, Nagoya, Japan*, ⁴*Department of Radiology, Nagoya City University, Nagoya, Japan*

Apparent diffusion coefficient (ADC) of the brain significantly changed during the cardiac cycle because of the water-molecule fluctuation. Moreover, this information assists in the diagnosis of idiopathic normal pressure hydrocephalus (iNPH). However, these changes (Δ ADC) are affected by cerebral blood flow. Therefore, we corrected the effect of blood flow by using the diffusion data to evaluate hemodynamic-independent water fluctuation in iNPH. Corrected- Δ ADC was significantly higher in iNPH group compared with control and atrophic ventricular dilatation groups. Hemodynamically independent analysis for water fluctuation MRI makes it possible to obtain more detailed information on biomechanical properties in iNPH.

1988

Diffusion weighted imaging of lymphedema post breast cancer treatment

Ned Charles¹, Elizabeth Dylke¹, David O'Brien¹, Angela Borella², Daniel Moses², Sharon Kilbreath¹, and Roger Bourne¹

¹*University of Sydney, Sydney, Australia*, ²*Spectrum Medical Imaging, Sydney, Australia*

Diffusion weighted imaging was performed in vivo in three patients with forearm lymphedema following lymphadenectomy for breast cancer. The honeycomb-like structure of lymphedema was clearly visible on proton density images. Parameter estimates from fitting monoexponential and kurtosis models to DWI data showed a shift in model parameters corresponding with the areas where lymphedema was present. The parameter shifts suggest an increase in the partial volume of freely diffusing water consistent with

edema, and suggest areas of increased interstitial water not visible in proton density images.

1989

The diagnostic value of Diffusion-weighted imaging in benign breast inflammatory lesions

Lina Zhang¹, Jinli Meng², Jianxun Qu³, Jianguo Chu¹, Ailian Liu¹, Yanwei Miao¹, Qingwei Song¹, Zhijin Lang¹, Jianyun Kang¹, Qiang Wei¹, and Bin Xu¹

¹The 1st affiliated hospital of Dalian Medical University, Da lian, China, People's Republic of, ²Chengban Branch of West China Hospital, Chengdu, China, People's Republic of, ³GE Healthcare, MR Research China, Beijing, Beijing, China, People's Republic of

To evaluate the diagnosis value of conventional MRI and Diffusion-weighted imaging in different subtypes of benign inflammation breast lesions. From the result we can see that morphological features as well as MR manifestations especially ADC findings may be of significant value for diagnosing different benign breast inflammatory lesions.

1990

High-resolution Multi-Station Diffusion imaging using accelerated Multi-Shot Acquisition Mode.

Arnaud Guidon¹, Maggie M Fung², Lloyd Estkowski³, Mei-Lan Chu⁴, Nan-Kuei Chen⁴, and Ersin Bayram⁵

¹Global MR Applications & Workflow, GE Healthcare, Boston, MA, United States, ²Global MR Applications & Workflow, GE Healthcare, New York City, NY, United States, ³Global MR Applications & Workflow, GE Healthcare, Menlo Park, CA, United States, ⁴Brain Imaging and Analysis Center, Duke University Medical Center, Durham, NC, United States, ⁵Global MR Applications & Workflow, GE Healthcare, Houston, TX, United States

This study investigates the feasibility of a multishot acquisition method for high-resolution Whole-Body Diffusion Weighted Imaging (WBDWI) as compared to the standard single-shot EPI. An accelerated Multishot acquisition mode is proposed to reduce the scan time of the high-resolution scan by half.

Traditional Poster

Diffusion: Microstructure

Exhibition Hall

Wednesday, May 11, 2016: 10:00 - 12:00

1991

Reducing acquisition time for axon diameter mapping using global optimization in the spatial-angular-microstructure space

Anna Auria¹, David Romascano¹, Erick J. Canales-Rodriguez², Tim B. Dyrby³, Daniel C. Alexander⁴, Jean-Philippe Thiran^{1,5}, Yves Wiaux⁶, and Alessandro Daducci^{1,5}

¹LTS5, École polytechnique fédérale de Lausanne (EPFL), Lausanne, Switzerland, ²Centro de Investigacion Biomedica en Red de Salud Mental (CIBERSAM), Barcelona, Spain, ³Danish Research Centre for Magnetic Resonance, Copenhagen University Hospital Hvidovre, Hvidovre, Denmark, ⁴Department of Computer Science and Centre for Medical Image Computing, University College London, London, United Kingdom, ⁵University Hospital Center (CHUV) and University of Lausanne (UNIL), Lausanne, Switzerland, ⁶Institute of Sensors, Signals, and Systems, Heriot-Watt University, Edinburgh, United Kingdom

State-of-the-art microstructure imaging methods usually fit biophysical models to the diffusion MRI data on a voxel-by-voxel basis using non-linear procedures that require both long acquisitions and processing time. We recently introduced AMICO, a framework to reformulate these techniques as efficient linear problems and enable faster reconstructions. Here, we propose an extension that enables robust reconstructions from a reduced number of diffusion measurements, thus leading to faster acquisitions, too. Our novel formulation estimates simultaneously the microstructure configuration in all voxels as a global optimization problem, exploiting information from neighboring voxels that cannot be taken into account with existing techniques.

1992

Characterization of Brain White Matter Tissue Structure with Double-Diffusion-Encoded MRI

Yasar Goedecke¹ and Jürgen Finsterbusch¹

¹Systems Neuroscience, University Medical Center Hamburg-Eppendorf, Hamburg, Germany

Double-diffusion-encoding (DDE) or double-wave-vector (DWV) experiments show a signal behavior that is specific for restricted diffusion. Thus, these experiments could provide more direct insight into tissue microstructure than conventional experiments, especially when targeting axon diameters. In this study, a previous DDE-based approach to estimate axon diameters is extended (i) to be applicable without prior knowledge of the fiber orientation, (ii) by considering a more complex tissue composition including spherical cells and an unrestricted compartment to model glial cells and extracellular space, and (iii) using the multiple correlation function framework that provides a more accurate approximation of the MR signal.

1993

Numerical Simulations Comparing Pore Imaging Methods Based on Diffusion-Weighted MR Imaging

Yasar Goedecke¹ and Jürgen Finsterbusch¹

¹Systems Neuroscience, University Medical Center Hamburg-Eppendorf, Hamburg, Germany

In a conventional diffusion-weighted MRI experiment, the signal amplitude depends on the squared magnitude of the Fourier transformation of the pore or cell geometry, i.e. the underlying cell or pore geometry cannot be reconstructed. Several approaches have been proposed that determine the otherwise missing phase information and, thus, can image the pore or cell geometry directly. Here,

the performance of these methods is compared with respect to their applicability in practice, e.g. considering the impact of the noise level, mixtures of pore sizes, orientations, and shapes, and gradient pulse durations and diffusion times achievable on standard MRI systems.

1994

The effect of axon shape and myelination on diffusion signals in a realistic Monte Carlo simulation environment
Michiel Kleinnijenhuis¹, Jeroen Mollink¹, Errin E Johnson², Vitaly L Galinsky³, Lawrence R Frank³, Saad Jbabdi¹, and Karla L Miller¹

¹Oxford Centre for Functional MRI of the Brain, University of Oxford, Oxford, United Kingdom, ²Sir William Dunn School of Pathology, University of Oxford, Oxford, United Kingdom, ³Center for Scientific Computation in Imaging, University of California San Diego, La Jolla, CA, United States

The cylindrical models often used in Monte Carlo diffusion simulations do not resemble the shape of axons very well. In this work, a more realistic substrate derived from electron microscopy data is used to investigate the influence of axon shape and myelination on the diffusion signal. In the DifSim simulation environment, diffusion signals from EM-derived substrates are compared to those from cylindrical substrates matched for volume fraction. Furthermore, the effect of removing the impermeable myelin sheath from the substrate is assessed.

1995

Modelling of diffusion in cultured epithelial cell spheroids
Sisi Liang¹, Madiha Yunus², Eleftheria Panagiotaki³, Byung Kim⁴, Timothy Stait-Gardner⁵, Mikhail Zubkov⁵, Brian Hawkett⁴, William Price⁵, Carl Power⁶, and Roger Bourne²

¹College of Engineering and Science, Victoria University, Melbourne, Australia, ²Discipline of Medical Radiation Sciences, Faculty of Health Sciences, University of Sydney, Sydney, Australia, ³Center for Medical Image Computing, University College London, London, United Kingdom, ⁴Key Centre For Polymer Colloids, University of Sydney, Sydney, Australia, ⁵Nanoscale Organisation and Dynamics Group, School of Science and Health, Western Sydney University, Sydney, Australia, ⁶Mark Wainright Analytical Centre, The university of New South Wales, Sydney, Australia

Cultured epithelial cell spheroids demonstrate many of the physiological properties of glandular epithelia and provide an ideal experimental model for investigation of the distinctive structural properties that may contribute to the reported low water mobility in prostate, breast, and gut epithelia. The structural connections are very similar to those in intact tissue and thus they provide a more realistic model of tissue than previously investigated models based on pelleted yeast or erythrocyte cells. We report an investigation of the correlation between known cell sizes in a spheroid culture and restriction radius estimated by a model of diffusion MRI signals.

1996

Imaging Three Dimensional Temporal Diffusion Spectrum Dispersion Profiles in the Brain
Dan Wu¹, Frances J Northington², and Jiangyang Zhang^{1,3}

¹Radiology, Johns Hopkins University School of Medicine, BALTIMORE, MD, United States, ²Pediatrics, Johns Hopkins University School of Medicine, BALTIMORE, MD, United States, ³Radiology, New York University School of Medicine, New York, NY, United States

The dispersion profile of the temporal diffusion spectrum has been linked to key properties of tissue microstructures, however, its directional variance has not been shown. In this study, we extended the conventional one-dimensional dispersion profile to three-dimensional profile, and characterized its directionality with a tensor representation. The temporal diffusion dispersion (TDD) tensor demonstrated unique contrasts that reflected distinct microstructural organization in the mouse brain, and the high anisotropy from TDD tensors correlated with anisotropic structural arrangements, e.g., in the crossing fiber regions. The TDD contrasts are also sensitive to disrupted microstructures in a neonatal mouse model of hypoxic-ischemic injury.

1997

Spatiotemporal dynamics and patterns of cortical mean kurtosis and fractional anisotropy in the preterm brains
Tina Jeon¹, Aristeidis Sotiras², Minhui Ouyang¹, Min Chen³, Lina Chalak⁴, Christos Davatzikos², and Hao Huang^{1,5}

¹Radiology Research, Children's Hospital of Philadelphia, Philadelphia, PA, United States, ²Center for Biomedical Image Computing and Analytics, University of Pennsylvania, Philadelphia, PA, United States, ³Department of Mathematical Sciences, University of Texas at Dallas, Richardson, TX, United States, ⁴Department of Pediatrics, University of Texas Southwestern Medical Center, Dallas, TX, United States, ⁵Perelman School of Medicine, University of Pennsylvania, Philadelphia, PA, United States

From early 3rd trimester to around birth, the cerebral cortex undergoes dramatic microstructural changes including dendritic arborization that disrupts the radial scaffold, a well-organized columnar organization. Decrease of cortical fractional anisotropy (FA) derived from DTI has been well documented. In this study, we hypothesized that non-Gaussian water diffusion properties (e.g. mean kurtosis or MK) from diffusion kurtosis imaging (DKI) offers unique and complementary information on cortical microstructural changes during this period. The spatiotemporal changes and patterns of cortical FA and MK from 32 to 41 postmenstrual weeks were revealed, demonstrating unique cortical MK maps and clustering patterns during preterm development.

1998

The influence of T2 relaxation in measuring the restricted volume fraction in diffusion MRI
Silvia De Santis¹, Yaniv Assaf², and Derek Jones¹

¹Cardiff University, CUBRIC, Cardiff, United Kingdom, ²Department of Neurobiology, Tel Aviv University, Tel Aviv, Israel

With the increasing popularity of multi-shell diffusion techniques to measure axonal density and diameter, the investigation of the exact origin of the contrast has become a hot topic. Here, we investigate the impact of the echo time in measuring the axonal density and show that the two water compartments are characterised by a different relaxation time T2, making the measures of the volume strongly dependent on the echo time. This suggests caution when comparing data acquired with different setups and introduces a new way of

measuring the differential T2 properties of intra- and extra-axonal water pools.

1999

Diffusion MRI: Disentangling Micro- from Mesostructure and Bayesian Parameter Evaluation
Marco Reisert¹, Elias Kellner¹, Bibek Dhital¹, Jürgen Hennig¹, and Valerij G. Kiselev¹

¹*Department of Radiology, Medical Physics, University Medical Center Freiburg, Freiburg, Germany*

Diffusion-sensitized MRI probes the cellular structure of the human brain, but the primary microstructural information gets lost in averaging over higher-level, mesoscopic tissue organization such as different orientations of neuronal fibers. While such averaging is inevitable due to the limited imaging resolution, we propose a method for disentangling the microscopic cell properties from the effects of mesoscopic structure. The proposed method finds detectable parameters of a given microstructural model and calculates them within seconds, which makes it suitable for a broad range of applications.

2000

Intracellular volume fraction estimation in vivo in single and crossing fibre regions
Sjoerd B Vos^{1,2}, Andrew Melbourne¹, John S Duncan^{2,3}, and Sébastien Ourselin¹

¹*Translational Imaging Group, University College London, London, United Kingdom*, ²*MRI Unit, Epilepsy Society, Chalfont St Peter, United Kingdom*, ³*Department of Clinical and Experimental Epilepsy, UCL Institute of Neurology, London, United Kingdom*

Intracellular volume fraction (ICVF) is a valuable biomarker of neurological disease. As one of two factors in g-ratio estimates it could potentially reveal axonal function from structural MRI measurements. Reliable ICVF estimation is critical for both purposes. With various diffusion models in existence for ICVF estimation, we compared the obtained ICVF values and their reproducibility in voxels with 1, 2, and 3 fibre populations between three diffusion modelling approaches. Absolute ICVF values vary significantly between models as well as between voxels with different fibre complexity.

2001

Modeling diffusion of intracellular metabolites in the mouse brain up to very high b: diffusion in long fibers (almost) accounts for non-monoexponential attenuation
Marco Palombo^{1,2}, Clémence Ligneul^{1,2}, and Julien Valette^{1,2}

¹*CEA/DSV/I2BM/MIRCen, Fontenay-aux-Roses, France*, ²*CNRS Université Paris-Saclay UMR 9199, Fontenay-aux-Roses, France*

We investigate how metabolite diffusion measured up to very high b (60 ms/ μ m²) at relatively short diffusion time (63.2 ms) in the mouse brain can be explained in terms of simple geometries. We model cell fibers as isotropically oriented cylinders of infinite length, and show this can account very well for measured non-monoexponential attenuation. The only exception is NAA, for which the model extracts fiber diameter equal to 0. We show that is theoretically and experimentally compatible with a small fraction of the NAA pool being confined in highly restricted compartments (with short T₂), e.g. a mitochondrial pool.

2002

Evaluation of Diffusion MRI Based Feature Sets for the Classification of Primary Motor and Somatosensory Cortical Areas.
Tara Ganepola^{1,2}, Jiaying Zhang², Hui Zhang², Martin I Sereno³, and Daniel C Alexander²

¹*Department of Cognitive, Perceptual and Brain Sciences, University College London, London, United Kingdom*, ²*Centre for Medical Image Computing, University College London, London, United Kingdom*, ³*Birkbeck-UCL Centre for Neuroimaging, University College London, London, United Kingdom*

In the following work several diffusion based feature vectors (DTI, NODDI, spherical harmonic (SH) invariants and fourth order tensor invariants (T4)) are compared in order to validate their usability in grey matter investigations. It was found that using multi-shell data and non-biophysical models such as SH and T4 achieves the highest classification accuracy between the primary motor and somatosensory cortical areas, and thus is likely to characterise grey matter tissues domains more effectively.

2003

Inferring axon diameter from the apparent cylindrical geocentric diameter in the longitudinal plane
Farshid Sepehrband¹ and Kristi A Clark¹

¹*Laboratory of Neuro Imaging, USC Mark and Mary Stevens Neuroimaging and Informatics Institute, Keck School of Medicine of USC, Los Angeles, CA, United States*

Recent diffusion-weighted imaging techniques have enabled the inference of axon diameter, a valuable neuroanatomical measure^{1,2}. Current techniques fit a cylindrical model of axons to the acquired signal, primarily in the transverse direction. Despite many improvements, sensitivity to small axons is difficult to achieve, primarily due to the scanner's physical limitations. Even with a strong gradient strength system such as the connectome scanner and high SNR, the minimum resolvable axon diameters are greater than 2 μ m, which accounts for only a small proportion of axons in the human brain. Here we utilize Neuman's cylindrical model³, and generalize it to the geocentric direction in the longitudinal plane of axons (Figure 1) to decrease the minimum axon diameter resolvable with a given scanner.

2004

In vivo characterisation of mouse brain glioma using VERDICT MRI and validation with histology

Tom A Roberts¹, Giulia Agliardi¹, Andrada Ianus², Ben Jordan¹, James O Breen-Norris¹, Rajiv Ramasawmy¹, Angela D'Esposito¹, Valerie Taylor¹, Bernard Siew¹, Eleftheria Panagiotaki², Daniel C Alexander², Mark F Lythgoe¹, and Simon Walker-Samuel¹

Vascular Extracellular and Restricted Diffusion for Cytometry in Tumours (VERDICT) is a diffusion MRI technique which uses a 3-compartment model to characterise the vascular (V), extracellular-extravascular (EES) and intracellular (IC) compartments in tumours. VERDICT allows for quantitation of tumour morphology including vascular fraction (fv), intracellular fraction (fic) and cellular radius, hence providing a non-invasive 'biopsy' that can be performed longitudinally. Previously, VERDICT has been applied to subcutaneous mouse tumours¹ and human prostate cancer². For the first time, we apply VERDICT in a mouse model of glioma, examine it in the context of other multi-compartment models and optimise it based on comparison with histological analysis.

2005 Generative statistical models of white matter microstructure for MRI simulations in virtual tissue blocks
Leandro Beltrachini¹ and Alejandro Frangi¹

¹The University of Sheffield, Sheffield, United Kingdom

In silico studies of diffusion MRI are becoming a standard tool for testing the sensitivity of the technique to changes in white matter (WM) structures. To perform such simulations, realistic models of brain tissue microstructure are needed. However, most of the computational results are obtained considering straight and parallel cylinders models, which are known to be too simplistic for representing real-scenario situations. We present a statistical-driven approach for obtaining random models of WM tissue samples based on histomorphometric data available in the literature. We show the versatility of the method for characterising WM voxels representing bundles and disordered structures.

2006 Does Myelin Water Influence DWI?
Kevin D Harkins¹ and Mark D Does^{1,2,3,4}

¹Institute of Image Science, Vanderbilt University, Nashville, TN, United States, ²Biomedical Engineering, Vanderbilt University, Nashville, TN, United States, ³Radiology and Radiological Sciences, Vanderbilt University, Nashville, TN, United States, ⁴Electrical Engineering, Vanderbilt University, Nashville, TN, United States

The presence and movement of myelin water is often neglected from models of DWI signal. This study presents a Monte Carlo simulation illustrating that myelin water diffusion can have a subtle but important impact on measured D_{app} and K_{app} values, and that incorporating myelin water diffusion can influence myelin-content dependent changes in D_{app} and K_{app} .

2007 Characterizing microstructural changes in Multiple Sclerosis lesions using advanced diffusion MRI at 3T and 7T
Silvia De Santis^{1,2}, Matteo Bastiani², Henk Jansma², Amgad Drobly³, Pierre Kolber³, Eberhard Pracht⁴, Tony Stoecker⁴, Frauke Zipp³, and Alard Roebroeck²

¹Cardiff University, CUBRIC, Cardiff, United Kingdom, ²Dept. of Cognitive Neuroscience, Faculty of Psychology & Neuroscience, Maastricht University, Maastricht, Netherlands, ³Department of Neurology and Neuromaging Center, University Medical Center of the Johannes Gutenberg University, Mainz, Germany, ⁴German Center for Neurodegenerative diseases, Bonn, Germany

Aim of this work was to test the ability of conventional (i.e., DTI) and advanced (i.e., CHARMED, stretched exponential) diffusion methods to differentiate between Multiple Sclerosis lesions, normal appearing white matter and healthy controls, at both 3T and 7T. Advanced dMRI at 7T gives the best discriminating power between MS lesions and healthy tissue across WM; DTI is appropriate in areas of low fiber dispersion like the corpus callosum.

2008 Exploring Structural, Diffusive and Thermodynamic Properties of Model Systems with Molecular Dynamics Simulations
Jonathan Phillips¹

¹Institute of Life Science, College of Medicine, Swansea University, Swansea, United Kingdom

This work aims at introducing methods of molecular dynamics (MD) simulation into diffusion MRI modelling. MD allows the study of transport properties (e.g. diffusion), structural properties (e.g. radial distribution functions) and thermodynamic properties (e.g. pressure). Access to all of these properties allows investigation into the links between them. We present the first steps into studying all of these properties (including the diffusion coefficient and kurtosis) in model systems for comparison with MRI data. The system is a binary mixture which includes a diffusing species (the solvent e.g. water) and a larger spatially-fixed species (modelling cellular-sized colloid particles).

2009 Axon diameter distribution influences diffusion-derived axonal density estimation in the human spinal cord: in silico and in vivo evidence
Francesco Grussu¹, Torben Schneider^{1,2}, Ferran Prados^{1,3}, Carmen Tur¹, Sébastien Ourselin³, Hui Zhang⁴, Daniel C. Alexander⁴, and Claudia Angela Michela Gandini Wheeler-Kingshott^{1,5}

¹NMR Research Unit, Queen Square MS Centre, Department of Neuroinflammation, UCL Institute of Neurology, University College London, London, United Kingdom, ²Philips Healthcare, Guildford, Surrey, United Kingdom, ³Translational Imaging Group, Department of Medical Physics and Biomedical Engineering, University College London, London, United Kingdom, ⁴Department of Computer Science and Centre for Medical Image Computing, University College London, London, United Kingdom, ⁵Brain Connectivity Center, C. Mondino National Neurological Institute, Pavia, Italy

Diffusion MRI-derived neurite density is a potential biomarker in neurological conditions. In the brain, neurites are commonly modelled as *sticks* for sufficiently long diffusion times and gradient durations. However, in the spinal cord, large axons are present and typical diffusion times (20-30 ms) may not be sufficiently long to support this model. We investigate via simulations and *in vivo* whether neurite density estimation is affected by the diffusion time in the spinal cord. Short diffusion times lead to bias, while long diffusion times improve accuracy but reduce precision. Therefore, a trade-off accuracy-precision needs to be evaluated depending on the application.

2010

A quantitative measurement of the cell membrane water permeability of expression-controlled AQP4 cells with diffusion weighted MRI
Takayuki Obata¹, Jeff Kershaw², Yasuhiko Tachibana¹, Youichiro Abe³, Sayaka Shibata², Yoko Ikom², Hiroshi Kawaguchi⁴, Ichio Aoki², and Masato Yasui³

¹Applied MRI Research, National Institute of Radiological Sciences, Chiba, Japan, ²Molecular Imaging Center, National Institute of Radiological Sciences, Chiba, Japan, ³Department of Pharmacology, Keio University, Tokyo, Japan, ⁴Human Informatics Research Institute, National Institute of Advanced Industrial Science and Technology (AIST), Tsukuba, Japan

We performed multi-b and multi-diffusion-time DWI on aquaporin-4-expressing and non-expressing cells, and demonstrated a clear difference between the signals from the two cell types. The data was interpreted with a two-compartment model including inter-compartmental exchange. It was also assumed that restricted diffusion of water molecules inside the cells leads to the intracellular diffusion coefficient being inversely proportional to the diffusion-time. Estimates of the water-exchange times with this model were comparable with those measured using an independent optical imaging technique, which suggests that this method might be used to characterize cell-membrane water permeability. As the technique can be applied in routine clinical examination, it has the potential to improve clinical diagnosis.

2011

Acquisition Protocol Optimization for Axon Diameter Mapping at High-Performance Gradient Systems – A Simulation Study
Jonathan I Sperl¹, Ek Tsoon Tan², Miguel Molina Romero^{1,3}, Marion I Menzel¹, Chris J Hardy², Luca Marinelli², and Thomas K.F. Foo²

¹GE Global Research, GARCHING, Germany, ²GE Global Research, NISKAYUNA, NY, United States, ³Institute of Medical Engineering, Technische Universität München, GARCHING, Germany

The measurement of axonal diameter by diffusion MRI techniques has assumed major interest in the research community. While most work has focused on developing and comparing various multi-compartment models, only minor efforts have been undertaken to optimize corresponding acquisition protocols. In this work we perform simulations using a rather simple two-compartment model, but study the effect of various choices of acquisition parameters on the precision and the bias of the fitted parameters. More precisely, we analyze potential sampling strategies in the 2D design space spanned by the two timing parameters (Δ , δ) of the diffusion encoding.

2012

NODDI and AxCaliber diffusion-weighted imaging at ultrahigh field for microstructural imaging of the mouse spinal cord
Ahmad Joman Alghamdi^{1,2}, Hari K Ramachandran³, Ian M Brereton¹, and Nyoman D Kurniawan¹

¹Centre for Advanced Imaging, The University of Queensland, Brisbane, Australia, ²College of Health Sciences, Taif University, Taif, Saudi Arabia, ³Computer Science and Engineering, SRM University, Kattankulathur, India

DTI has been used to measure changes in spinal cord WM, but lacks the specificity in measuring changes in GM and axonal diameter. This study aims to apply NODDI and AxCaliber techniques to measure characteristics of the lumbar spine in C57BL/6 mice, *in-vivo* at 9.4T and *ex-vivo* at 16.4T. The GM orientation distribution index is 3 times that of the WM, and the correlation of ODI to FA is $r=-0.9$, $P<<0.01$ for GM and $r=-0.56$, $P<<0.01$ for WM. AxCaliber analysis determined WM axon diameter populations with an average of 1.55 ± 0.15 mm (*in-vivo*); and 1.37 ± 0.20 mm (*ex-vivo*).

2013

White matter alterations in young adults born extremely preterm: a microstructural point of view.

Zach Eaton-Rosen¹, Andrew Melbourne¹, Joanne Beckmann², Eliza Orasanu¹, Nicola Stevens³, David Atkinson⁴, Neil Marlow², and Sébastien Ourselin¹

¹TIG, UCL, London, United Kingdom, ²UCL EGA Institute for Women's Health, London, United Kingdom, ³UCLH, London, United Kingdom, ⁴CMIC, UCL, London, United Kingdom

We used NODDI and DTI in order to investigate the differences in white matter between young adults born at term, and those born at fewer than 26 weeks completed gestation, using TBSS. The differences in FA were closely mirrored by the differences in orientation dispersion index (ODI) while the intra-axonal volume fraction (Vi) did not show significant differences in the same regions. This suggests that the ODI may be more sensitive to indicators of being born preterm than Vi in the white matter.

2014

Statistical assessment of a model combining IVIM and T2 decay for multi-b-value, multi-echo-time DW-MRI in abdominal organs
Matthew R Orton¹, Neil P Jerome¹, Thorsten Feiweier², Dow-Mu Koh³, Martin O Leach⁴, and David J Collins⁴

¹Radiotherapy and Imaging, Institute of Cancer Research, London, United Kingdom, ²Siemens Healthcare, Erlangen, Germany, ³Department of Radiology, Royal Marsden NHS Foundation Trust, London, United Kingdom, ⁴CRUK Cancer Imaging Centre, Division of Radiotherapy and Imaging, Institute of Cancer Research, London, United Kingdom

The IVIM model is essentially a two-compartment model, and it has previously been noted that the T2 relaxation times in each compartment may not be equal. This work uses the Akaike Information Criterion to compare two combined IVIM-T2 models using data

acquired in various abdominal organs with all combinations of five echo-times and six b-values. The first model has the same T2 in each compartment, the second has different T2s, and we show that the second model has greater statistical support in the liver (but not spleen or kidney), implying that both T2 values can be measured in this organ.

2015

Extensive White Matter Damage in Neuromyelitis Optica Assessed by Neurite Orientation Dispersion and Density Imaging: A Tact-Based Spatial Statistics study

Tomohiro Takamura¹, Shou Murata², Koji Kamagata³, Kouhei Tsuruta², Masaaki Hori³, Michimasa Suzuki³, and Shigeki Aoki³

¹University of Yamanashi, Yamanashi, Japan, ²Tokyo Metropolitan University, Tokyo, Japan, ³Juntendo University, Tokyo, Japan

Recently, patients with neuromyelitis optica (NMO) have shown extensive white matter damage, which could be related not only to Wallerian degeneration resulting from lesions of spinal cord or optic tracts but also to demyelination by using diffusion-tensor (DT) MRI imaging. This study aimed to evaluate the expansion of white matter damage in NMO assessed using neurite orientation dispersion and density imaging (NODDI), as well as its relationship with disease severity by applying Tact Based Spatial Statistics (TBSS).

2016

Comparison of fast and conventional diffusion kurtosis imaging in an anisotropic synthetic phantom

Ganna Blazhenets^{1,2}, Farida Grinberg^{1,3}, Ezequiel Farrher¹, Xiang Gao¹, Mikheil Kelenjeridze⁴, Tamo Xechiashvili⁴, and N. Jon Shah^{1,3}

¹Institute of Neuroscience and Medicine - 4, Forschungszentrum Juelich, Juelich, Germany, ²Institute of Nuclear Physics, University of Cologne, Cologne, Germany, ³Department of Neurology, Faculty of Medicine, JARA, RWTH Aachen University, Aachen, Germany, ⁴Department of Physics, Georgian Technical University, Tbilisi, Georgia

We compare the sensitivity and applicability of two methods for the estimation of mean kurtosis in a multi-sectional, anisotropic diffusion phantom using conventional diffusion kurtosis imaging and a fast protocol for rapid mean kurtosis metric estimation suggested by Hansen et al. (2013). Both methods provide similar image quality and it can be concluded that fast estimation of mean kurtosis is a useful tool that can be used as a fast method for clinical applications. An interesting finding of this work is a stronger dependence of fast computed kurtosis metrics on the orientation of fibres with respect to the static magnetic field than of the conventional method.

2017

Evaluating mean diffusivity and mean kurtosis derived from different diffusion-encoding schemes and signal-to-noise ratio

Chia-Wen Chiang¹, Shih-Yen Lin^{1,2}, Yi-Ping Chao³, Yen-Chung Chang^{4,5}, Teh-Chen Wang⁶, and Li-Wei Kuo¹

¹Institute of Biomedical Engineering and Nanomedicine, National Health Research Institutes, Miaoli, Taiwan, ²Department of Computer Science, National Chiao Tung University, Hsinchu, Taiwan, ³Graduate Institute of Medical Mechatronics, Chang Gung University, Taoyuan, Taiwan, ⁴Department of Medical Imaging, National Taiwan University Hospital, Taipei, Taiwan, ⁵Department of Radiology, National Taiwan University College of Medicine, Taipei, Taiwan, ⁶Department of Radiology, Taipei City Hospital Yang-Ming Branch, Taipei, Taiwan

Diffusion kurtosis imaging (DKI), evaluating the non-Gaussianity of water diffusion, has been demonstrated to be sensitive biomarker in many neurological diseases. However, number of repetition is one of the factors, but people is trying less to investigate it. In this study, normal rats were performed using two different diffusion scheme protocols (15 b-values with six diffusion directions vs. 3 b-values with thirty directions) and with different repetitions. Our results suggesting the protocol with one repetition provides good image quality for DKI analysis in this case.

2018

Maximum b-value dependence of Diffusion kurtosis imaging sensitivity in detecting white matter microstructure

Miao Sha¹, Yuanyuan Chen¹, Xin Zhao¹, Man Sun², Weiwei Wang¹, Hongyan Ni², and Dong Ming¹

¹Tianjin University, Tianjin, China, People's Republic of, ²Tianjin First Center Hospital, Tianjin, China, People's Republic of

Diffusion kurtosis imaging is a powerful technique to measure the non-gaussian diffusion as well as the complicated microstructure. In this paper, we conducted a comparison between different acquisitions with different maximum b-value on normal volunteers. We found that the outcome of diffusion kurtosis imaging was influenced by the maximum b-value in the acquisition. And this influence was highly associated with the microstructure, including both radial profile and angular profile in the structure reconstruction, which indicated the mechanism of non-gaussian under high b-value.

2019

Determination of Microvascular Parameters from Diffusion-Weighted Images

Robert J Loughnan^{1,2}, Damien McHugh^{1,3}, Hamied A Haroon¹, Douglas Garratt², Rishma Vidyasagar^{1,4}, Hojjatollah Azadbakht¹, Penny H Cristinacce¹, Geoff JM Parker^{1,5}, and Laura M Parkes¹

¹Centre for Imaging Sciences, Faculty of Medical and Human Sciences, The University of Manchester, Manchester, United Kingdom, ²School of Physics and Astronomy, The University of Manchester, Manchester, United Kingdom, ³CRUK & EPSRC Cancer Imaging Centre in Cambridge & Manchester, Manchester, United Kingdom, ⁴Melbourne Brain Centre, The Florey Institute of Neuroscience and Mental Health, Melbourne, Australia, ⁵Bioxydyn Limited, Manchester, United Kingdom

Diffusion imaging has been used to probe microstructure and to investigate perfusion via the IVIM model. However, the contribution of microvasculature structure to the diffusion signal has largely been overlooked. Presented here is a novel method for imaging blood velocity and capillary segment length using diffusion-weighted images. We apply a model for extracting perfusion parameters from diffusion-weighted images from 23 people with a range of diffusion times ($\Delta=18, 35$ and 55 ms) and b-values (0-100s/mm²). Mean blood velocity was significantly slower ($P<0.005$) in white matter (0.92 ± 0.03 mm/s) compared to grey matter (0.95 ± 0.04 mm/s). Mean vessel

segment length was significantly shorter ($P<0.0001$) in white matter ($7.97\pm0.13\mu\text{m}$) than in grey matter ($10.35\pm0.20\mu\text{m}$).

2020

Detection of lymphocytes fractions using temporal diffusion spectroscopy
Johannes Riegler¹, Maj Hedehus¹, and Richard A. D. Carano¹

¹*Biomedical Imaging, Genentech, South San Francisco, CA, United States*

Inflammation and T-cell infiltration are important prognostic biomarkers for cancer immunotherapies.¹ Current clinical practice relies on histological assessment of tissue biopsies which is invasive and prone to sampling errors. Temporal diffusion spectroscopy, particularly with short effective diffusion times can estimate cell sizes.^{2,3} Lymphocytes have small diameters compared to typical tumor cells. We therefore tested the ability of temporal diffusion spectroscopy to differentiate between pellets of tumor cells mixed with a varying amount of activated lymphocytes. We observed clearly separable diffusion characteristics for samples containing $> 20\%$ lymphocytes indicating that this approach may have potential to quantify inflammation in highly inflamed tissues.

2021

Estimation of Fiber Packing Correlation Length by Varying Diffusion Gradient Pulse Duration
Hong-Hsi Lee¹, Gregory Lemberskiy¹, Els Fieremans¹, and Dmitry S. Novikov¹

¹*New York University, Center for Biomedical Imaging, New York, NY, United States*

Finite pulse duration Δ of diffusion gradient has typically been a source of bias for quantifying microstructure. Here, we suggest to use the diffusivity dependence on Δ to reveal the correlation length of the fiber packing, an essential μm -level characteristic of microstructure, thereby turning the finite pulse duration to our advantage. We validate our method in a fiber phantom that mimics an axonal packing geometry, and the estimated correlation length matches the fiber radius. Future work will focus on the evaluation of its potential as biomarkers for *in vivo* brain scans, such as axonal density and outer axonal diameters.

2022

Detection of Early Emphysema by Quantifying Lung Terminal Airways with Hyperpolarized ^{129}Xe Diffusion MRI
Weiwei Ruan¹, Jianping Zhong¹, Ke Wang², Yeqing Han¹, and Xin Zhou¹

¹*Wuhan Institute of Physical and Mathematics, Chinese Academy of Sciences, Wuhan, China, People's Republic of*, ²*Department of MRI, zhongnan hospital of wuhan university, Wuhan, China, People's Republic of*

To detect the early emphysema, hyperpolarized xenon diffusion MRI with multi- b values was used to quantify the lung terminal airways in five initial stages of emphysematous rats and five control rats. The D_L (longitudinal diffusion coefficient), r , h , L_M and S/V in the emphysematous group showed significant differences compared to those in the control group ($P<0.05$) and also exhibited a strong linear correlation ($|r|>0.8$) to L_M from histology for all the rats. The results showed multi- b diffusion MRI of hyperpolarized xenon has potential for the diagnosis of emphysema at the early stage.

2023

A Time-Efficient Acquisition Protocol For Multi-Purpose Diffusion-Weighted Microstructural Imaging At 7T
Farshid Sepehrband^{1,2}, Kieran O'Brien^{1,3}, and Markus Barth¹

¹*Centre for Advanced Imaging, University of Queensland, Brisbane, Australia*, ²*Laboratory of Neuro Imaging, USC Mark and Mary Stevens Neuroimaging and Informatics Institute, Keck School of Medicine of USC, Los Angeles, CA, United States*, ³*Siemens Healthcare Pty Ltd, Brisbane, Australia*

Several diffusion-weighted MRI techniques for modeling tissue microstructure have been developed and validated during the past two decades. While offering various neuroanatomical inferences, these techniques differ in their proposed optimal acquisition design, which impede clinicians and researchers to benefit from all potential inference methods, particularly when limited time is available. We examined the performance of the most common diffusion models with respect to acquisition parameters at 7T when limiting the acquisition time to about 10 minutes. The most balanced compromise among all combinations in terms of the robustness of the estimates was a two-shell scheme with b -values of 1,000 and $2,500\text{ s/mm}^2$ with 75 diffusion-encoding gradients, 25 and 50 samples for low and high b -values, respectively.

2024

Extraction of Tissue-Specific ADC Based on Multi-Exponential T2 Analysis
Qiqi Tong¹, Mu Lin¹, Hongjian He¹, Xu Yan², Thorsten Feiweier³, Hui Liu², and Jianhui Zhong¹

¹*Center for Brain Imaging Science and Technology, Department of Biomedical Engineering, Zhejiang University, Hangzhou, China, People's Republic of*, ²*MR Collaboration NE Asia, Siemens Healthcare, Shanghai, China, People's Republic of*, ³*Siemens Healthcare, Erlangen, Germany*

Multi-component diffusion models with each component of its own T_2 value have been studied previously. When the diffusion signal is decomposed into three compartments (short, intermediate and long T_2), the respective ADC values can be obtained. Our results from simulations and *in vivo* measurements show that the model successfully separates signal from different tissue types, allows extraction of tissue-specific ADC, and results are mostly free of partial volume problem. Moreover, an ADC without T_2 effect can also be generated by combining the ADCs of all components.

2025

Single Compartment model estimates of acinar duct measurements from inhaled noble gas MRI: Proof of Concept in alpha-1 antitrypsin deficiency emphysema

Diffusion-weighted MRI provides a way to non-invasively estimate *in vivo* morphometry measurements of the alveolar ducts. Current modelling approaches may not be appropriate for cases of severe tissue destruction where the geometry of the acinar ducts may not be uniform, nor cylindrical. Therefore, in this proof-of-concept evaluation, we used a single-compartment model and multiple b-value diffusion-weighted noble gas pulmonary MRI to generate estimates of acinar duct surface-to-volume ratio and mean-linear-intercept. In cases of very severe emphysema that accompany alpha-one antitrypsin deficiency, this approach well-approximated the severity of lung disease, while the cylindrical model did not.

2026

Use envelope bounding to improve the stability of intravoxel incoherent motion modeling
Cheng-Ping Chien¹, Feng Mao Chiu², and Queenie Chan³

¹*Institute of Biomedical Electronics and Bioinformatics, National Taiwan University, Taipei, Taiwan*, ²*Philips Healthcare, Taipei, Taiwan*, ³*Philips Healthcare, Hong Kong, China, People's Republic of*

Intravoxel incoherent motion (IVIM) model is useful tool to observe the microcirculatory perfusion, but its stability still needs to be improved. We propose the envelope bounding technique to reduce the fluctuated signal at low b-value, and use this new signal profile to fit IVIM model. This improvement gives a more stable outcome with fast diffusion (D*) and perfusion fraction (PF).

2027

Modelling radial and tangential fibres in the neocortex
Luke J. Edwards¹, Siawoosh Mohammadi^{1,2}, Pierre-Louis Bazin³, Michiel Kleinnijenhuis⁴, Kerrin J. Pine¹, Anne-Marie van Cappellen van Walsum⁵, Hui Zhang⁶, and Nikolaus Weiskopf^{1,3}

¹*Wellcome Trust Centre for Neuroimaging, UCL Institute of Neurology, UCL, London, United Kingdom*, ²*Institut für Systemische Neurowissenschaften, Universitätsklinikum Hamburg-Eppendorf, Hamburg, Germany*, ³*Department of Neurophysics, Max Planck Institute for Human Cognitive and Brain Sciences, Leipzig, Germany*, ⁴*FMRIB Centre, University of Oxford, Oxford, United Kingdom*, ⁵*Department of Anatomy, Donders Institute for Brain, Cognition and Behaviour, Radboud University, Nijmegen, Netherlands*, ⁶*Centre for Medical Image Computing, Department of Computer Science, UCL, London, United Kingdom*

The structure of neocortical grey matter is complex due to the crossing intracortical neuronal connections involved in cortical processing. Herein we present a two-step method to capture radial and tangential fibre structure of neocortex from diffusion data: first the radial cortical orientation is extracted voxelwise using surface-based methods, and then a three-compartment diffusion model extracts radial and tangential fibre volume fractions. We demonstrate in a post mortem sample of human V1 tissue that this method captures structure known from histology and comparable diffusion models, implying potential future use as a probe of intracortical neuronal connectivity.

2028

Correlation of diffusion-weighted MRI with cellularity in glandular breast tissue
Narina Norddin^{1,2}, Nyoman Kurniawan³, Gary Cowin³, Carl Power⁴, Geoffrey Watson⁵, Esther Myint⁶, Laurence Gluch⁷, and Roger Bourne¹

¹*University of Sydney, Sydney, Australia*, ²*International Islamic University Malaysia, Pahang, Malaysia*, ³*University of Queensland, Brisbane, Australia*, ⁴*University of New South Wales, Sydney, Australia*, ⁵*Royal Prince Alfred Hospital, Sydney, Australia*, ⁶*Douglass Hanly Moir Pathology, Sydney, Australia*, ⁷*The Strathfield Breast Centre, Sydney, Australia*

Although diffusivity (ADC) changes in tissue are commonly attributed to variations in 'cellularity', direct evidence from breast tissue studies is limited and inconsistent. Here we report a diffusion microimaging and histology investigation of the correlation of mean diffusivity (MD) with cellularity in the glandular component of breast tissue. Diffusion microimaging was performed at 16.4T on fixed normal and cancer tissue samples and matched with post MRI histology. There was a moderate correlation between MD and nuclear count, but only a weak correlation between MD and nuclear area.

2029

Time dependence of diffusion and kurtosis parameters in the rat spinal cord
Sune Nørhøj Jespersen^{1,2}, Brian Hansen¹, Daniel Nunes³, and Noam Shemesh³

¹*CFIN, Aarhus University, Aarhus, Denmark*, ²*Dep. Physics and Astronomy, Aarhus University, Aarhus, Denmark*, ³*Champalimaud Neuroscience Programme, Champalimaud Centre for the Unknown, Lisbon, Portugal*

Non-vanishing diffusion kurtosis and time-dependent diffusion are both hallmarks of nongaussian diffusion in biological tissues. Here we combine measurements of time-dependent DTI parameters and time dependence of mean kurtosis using fast kurtosis imaging in rat spinal cord. We observe substantial time dependence of all parameters in both white and gray matter.

2030

Distinguishing between different microstructural changes using optimised diffusion-weighted acquisitions
Damien J. McHugh^{1,2} and Geoff J.M. Parker^{1,2,3}

¹*Centre for Imaging Sciences, The University of Manchester, Manchester, United Kingdom*, ²*CRUK & EPSRC Cancer Imaging Centre in Cambridge & Manchester, United Kingdom*, ³*Bioxydyn Ltd., Manchester, United Kingdom*

This work investigates the use of optimised diffusion-weighted acquisitions for distinguishing between different microstructural changes relevant to characterising tumour tissue. Optimised protocols are found for a 'baseline' microstructure, and for two distinct changes which would lead to an ADC increase: (1) volume fraction decrease with cell size constant (therefore a decrease in cell density), (2) cell size decrease and coupled volume fraction decrease (therefore a constant cell density). Model fitting simulations are performed with optimised and non-optimised protocols, demonstrating that the improved precision achieved with optimised protocols may be beneficial in terms of distinguishing between these microstructural changes.

2031

Oscillating Gradient Spin Echo Diffusion Tensor MRI of the Brain in Multiple Sclerosis Patients

Christian Beaulieu¹, Corey Baron¹, Penny Smyth², Roxane Bille², Leah White², Fabrizio Giuliani¹, Derek Emery³, and Robert Stobbe¹

¹Biomedical Engineering, University of Alberta, Edmonton, AB, Canada, ²Neurology, University of Alberta, Edmonton, AB, Canada, ³Radiology, University of Alberta, Edmonton, AB, Canada

In diffusion tensor imaging, oscillating gradient spin echo (OGSE) gradient waveforms enable much shorter diffusion times (4 ms) than the typical pulsed gradient spin echo (PGSE, 40 ms) and OGSE was applied here for the first time in multiple sclerosis patients. A different dependence on diffusion time would suggest a change in micro-structural scale within the MS lesions. Compared to normal appearing white matter (NAWM), FLAIR-visible lesions showed reductions of fractional anisotropy (FA) on both PGSE and OGSE. The proportional FA decrease between NAWM and lesions was similar for OGSE and PGSE.

2032

Longitudinal stability of astiction cotton as an anisotropic diffusion phantom

Koji Sakai¹, Toshiaki Nakagawa¹, and Kei Yamada¹

¹Kyoto Prefectural University of Medicine, Kyoto, Japan

To obtain anisotropic diffusion phantom with ease, we evaluated the longitudinal stability of commercially available astiction cotton as an anisotropic diffusion phantom. DTI examinations were performed at 3 T using a whole-body scanner by 20ch head coil for 131 days intermittently (18 times). The DTI analysis was performed and diffusion metrics (ADC and FA) of the phantom were evaluated by comparing standard deviation in one day to the averaged change between two consequence days. The averaged changes of ADC and FA within the experimental term were $0.03 \times 10^{-3} \text{ sec/mm}^2$ and 0.002, respectively. The commercially available astiction cotton showed stability on its diffusivity over four months.

Traditional Poster

Diffusion Analysis & Tractography

Exhibition Hall

Wednesday, May 11, 2016: 10:00 - 12:00

2033

Brain white matter abnormalities in Alzheimer's disease with and without cerebrovascular disease

Fang Ji¹, Ofer Pasternak², Yng Miin Loke¹, Saima Hilal^{3,4}, Mohammad Kamran Ikram¹, Xin Xu^{3,4}, Boon Yeow Tan⁵, Narayanaswamy Venketasubramanian⁶, Christopher Li-Hsian Chen^{3,4}, and Juan Zhou^{1,4}

¹Center for Cognitive Neuroscience, Neuroscience and Behavioral Disorders Program, Duke-National University of Singapore Graduate Medical School, Singapore, Singapore, ²Department of Psychiatry, Brigham and Women's Hospital, Harvard Medical School, USA, Boston, MD, United States, ³Department of Pharmacology, National University Health System, Clinical Research Centre, Singapore, Singapore, ⁴Memory Aging & Cognition Centre, National University Health System, Singapore, Singapore, ⁵St. Luke's Hospital, Singapore, Singapore, ⁶Raffles Neuroscience Centre, Raffles Hospital, Singapore, Singapore

Using a novel free-water method, we examined the white matter tissue deterioration and extracellular water content changes in Alzheimer's disease with and without cerebrovascular disease and vascular dementia. We found that free-water and white matter hyperintensity (WMH) were highly correlated; both might reflect neuroinflammation in dementia. After correcting for increased extracellular water, the degree and extent of white matter integrity decreased in dementia subtypes; nevertheless, the cortical difference between groups remained. Intriguingly, free water compartment (but not WMH volume) was associated with symptom severity. Our findings suggested the potential of free-water method in differential diagnosis and disease progression monitoring.

2034

In vivo exploration of the human brainstem complex pathways at 3 Tesla with track-density imaging: a digital three-dimensional microscope for anatomists

Sophie Sébille¹, Romain Valabregue¹, Anne-Sophie Rolland¹, Chantal François¹, and Eric Bardinet¹

¹Brain and Spine Institute, CNRS UMR 7225 - INSERM U 1127 - UPMC-P6 UMR S 1127, Paris, France

We applied super-resolution TDI, as a tool to gain spatial resolution using post-processing methods, to one healthy individual to highlight the fine details of the anatomical fibers tracts in the brainstem. A 1.25 mm isotropic diffusion data acquired *in vivo* at 3T was used to calculate a 0.2 mm isotropic TDI map. We demonstrated that the super-resolution TDI clearly improved the spatial resolution, as well as the emphasis on different contrast information. These maps can be of help to anatomists to explore the brainstem complex organization by identifying subject-specific tracts.

2035

Optimization of acquisition parameters for diffusion MRI using chemical tracing
Giorgia Grisot^{1,2}, Julia Lehman³, Suzanne N Haber³, and Anastasia Yendiki²

¹Harvard-MIT Health Sciences and Technology, Massachusetts Institute of Technology, Cambridge, MA, United States, ²Athinoula A. Martinos Center for Biomedical Imaging, MGH, Charlestown, MA, United States, ³University of Rochester School of Medicine, Rochester, NY, United States

Determining the optimal diffusion MRI (dMRI) acquisition scheme for reconstructing a brain network of interest with tractography is an open problem, and the lack of ground truth on brain connections makes it challenging to resolve. We use chemical tracing and ex vivo dMRI in macaques to optimize dMRI acquisition with respect to tractography accuracy. We present preliminary results illustrating that 1. There is an upper bound to the angular resolution of dMRI, beyond which tractography accuracy does not improve, and 2. That this finding likely generalizes to in vivo human dMRI.

2036

The best of both worlds: Combining the strengths of TBSS and tract-specific measurements for group-wise comparison of white matter microstructure
Greg D Parker¹, Dafydd LLoyd², and Derek K Jones^{1,3}

¹CUBRIC, School of Psychology, Cardiff University, Cardiff, United Kingdom, ²Ysgol Gyfun Gwyr, Swansea, United Kingdom, ³Neuroscience and Mental Health Research Institute (NMHRI), School of Medicine, Cardiff University, Cardiff, United Kingdom

Tract-specific microstructural measurements are key to many white matter studies. Common tract-specific measurement strategies average measurements along tracts of interest, but are insensitive to localised changes. Alternatively, by searching radially to a co-registered tract skeleton, tract based spatial statistics¹ provides desirable localised comparisons. However, considering one value at each point (the highest value found by radial search), increases susceptibility to outliers, and misses the SNR benefit of averaging multiple estimates within a locale. We propose a hybrid method using tract skeletons to divide streamlines into localised *sections*, comparing averages within each section. Example results in remitted depression are presented.

2037

High-resolution DTI-based cortical connectome reconstructions match incompletely with true axonal projections in rat brain
Michel R.T. Sinke¹, Willem M. Otte^{1,2}, Annette van der Toorn¹, R. Angela Sarabdjitsingh³, Marian Joëls³, and Rick M. Dijkhuizen¹

¹Biomedical MR Imaging and Spectroscopy Group, Center for Image Sciences, University Medical Center Utrecht, Utrecht, Netherlands,

²Department of Pediatric Neurology, Brain Center Rudolf Magnus, University Medical Center Utrecht, Utrecht, Netherlands, ³Department of Translational Neuroscience, Brain Center Rudolf Magnus, University Medical Center Utrecht, Utrecht, Netherlands

The exact relationship between DTI-based tract representations and true axonal projections remains uncertain. We compared the accuracy of tensor-based and constrained spherical deconvolution (CSD)-based tractography, against neuroanatomical tracer data in rat brain. Our study with high spatial and angular resolution postmortem DTI data revealed low tractography accuracy, characterized by significant amount of false positive and false negative streamline connections. Accounting for crossing fibers by CSD did not significantly improve sensitivity and specificity. Because DTI-based tract reconstructions correlate incompletely with true axonal projections in rat brain, even when using an advanced algorithm like CSD, DTI-based connectomics should be interpreted with care.

2038

Model-free Global Tractography
Henrik Skibbe¹, Elias Kellner², Valerij G Kiselev², and Marco Reisert²

¹Faculty of Informatics, Ishii Lab, Kyoto University, Kyoto, Japan, ²Medical Physics, University Medical Center Freiburg, Freiburg, Germany

Tractography based on diffusion-weighted MRI investigates the large scale arrangement of neurite fibers in brain white matter. It is usually assumed that the signal is a convolution of a fiber response function (FRF) with a fiber orientation distribution (FOD). The FOD is the focus of tractography. While in the past the FRF was estimated beforehand and was usually assumed to be fix, more recent approaches estimate the FRF during tractography. This work proposes a novel objective function independent of the FRF, just aiming for FOD reconstruction. The objective is integrated into global tractography showing promising results.

2039

Application of a combined IVIM-DTI model in ECG-triggered imaging of the human kidney
Fabian Hilbert¹, Simon Veldhoen¹, Tobias Wech¹, Henning Neubauer¹, Thorsten Alexander Bley¹, and Herbert Köstler¹

¹Department of Diagnostic and Interventional Radiology, University of Würzburg, Würzburg, Germany

Diffusion tensor imaging (DTI) accounts for anisotropy of diffusion, while the intravoxel incoherent motion (IVIM) model considers a fast moving pseudo-diffusion compartment. In the kidney DTI and IVIM parameters vary significantly depending on the time they are acquired within the cardiac cycle. A combined IVIM-DTI model incorporates anisotropic diffusion and anisotropic pseudo-diffusion parameters. The purpose of this study was to investigate the impact of the cardiac cycle on the combined IVIM-DTI model. While in DTI the fractional anisotropy of the diffusion tensor (FA_D) varies within the cardiac cycle, FA_D does not change in the IVIM-DTI model.

2040

Diffusion-weighted imaging with multiple diffusion time to assess water-exchange between restricted and hindered diffusion components in vivo
Yasuhiko Tachibana^{1,2}, Takayuki Obata^{1,2}, Hiroki Tsuchiya¹, Tokuhiko Omatsu^{1,2}, Riwa Kishimoto^{1,2}, Thorsten Feiweier³, and Hiroshi Tsuji¹

¹Research Center of Charged Particle Therapy, National Institute of Radiological Science, Chiba, Japan, ²Applied MRI Research, National Institute

We performed multi-b and multi-diffusion-time DWI (MbMdt-DWI) on human brain to visualize the mixture of restricted and hindered diffusion components, and also the water exchange between them. The diffusion parameters including the exchange time were calculated. The observed signal patterns clearly indicated the existence of the inter-compartmental water exchange. The calculated exchange time was within the appropriate range assumed from a previous cell-based study *in vitro*. MbMdt-DWI may be useful for assessing micro-diffusion in human brain.

2041

Thinking Outside the Voxel: A Joint Spatial-Angular Basis for Sparse Whole Brain HARDI Reconstruction
Evan Schwab¹, Rene Vidal², and Nicolas Charon³

¹Electrical and Computer Engineering, Johns Hopkins University, Baltimore, MD, United States, ²Biomedical Engineering, Johns Hopkins University, Baltimore, MD, United States, ³Applied Mathematics and Statistics, Johns Hopkins University, Baltimore, MD, United States

Sparse modeling of dMRI signals has become of major interest for advanced protocols such as HARDI which require a large number of q-space measurements. With few exceptions, prior work have developed bases to sparsely represent q-space signals per voxel with additional constraints of spatial regularity. In this work, we propose a single basis to represent an entire HARDI dataset by modeling spatial and angular domains jointly, achieving an unprecedented level of sparsity. With a globally compressed representation we can then redefine HARDI processing, diffusion estimation, feature extraction and segmentation, and drastically reduce acquisition time and data storage.

2042

Assessment of Early Renal Fibrosis Induced in a Murine Model of Streptozotocin Induced Diabetes
Yet Yen Yan¹, Tiffany Hennedige¹, Tong San Koh¹, Lei Zhou², Septian Hartono³, Helmut Rumpel³, Laurent Martarello⁴, James Boon Kheng Khoo¹, Dow-Mu Koh⁵, Kai Hsiang Chuang⁶, Tony Kiat Hon Lim³, Yock Young Dan², and Choon Hua Thng¹

¹National Cancer Centre Singapore, Singapore, Singapore, ²National University Hospital, Singapore, Singapore, ³Singapore General Hospital, Singapore, Singapore, ⁴Roche Translational Medicine Hub, Singapore, Singapore, ⁵Royal Marsden Hospital, London, United Kingdom, ⁶Singapore Biologging Consortium, Singapore, Singapore

Streptozotocin induced diabetes was created in twenty mice while eighteen mice served as control. DTI & IVIM were performed at 0, 12 and 24 weeks after injection of streptozotocin. Histopathological analysis confirmed fibrosis in all diabetic mice. Increase in ADC & tissue diffusivity were found in the diabetes group at week 12, which might reflect an increased tubule volume that outweighed the effects of early fibrosis. FA was significantly reduced in the diabetes group at week 12 and represented tubular damage of renal fibrosis. This study showed the potential of FA as a biomarker of early diabetic nephropathy.

2043

Can Cramer-Rão Lower Bound be used to find optimal b-values for IVIM?
Oscar Gustafsson^{1,2}, Maria Ljungberg^{1,2}, and Göran Starck^{1,2}

¹Department of Radiation Physics, Institute of Clinical Sciences, The Sahlgrenska Academy, University of Gothenburg, Gothenburg, Sweden,
²Department of Medical Physics and Biomedical Engineering, Sahlgrenska University Hospital, Gothenburg, Sweden

Cramer-Rão Lower Bound is commonly used in experiment design optimization. Here we use it to find optimal b-value schemes for IVIM imaging. The optimization was generalized with regard to averaging and the characteristics of the results, given the input and the constraints, were studied. The resulting schemes never included more than the minimum number of four unique b-values, even though multiple sets of tissue parameters were included in the optimization. The optimized b-value schemes were compared to a typical one using simulations.

2044

Abnormal brain white matter skeleton in patients with disorders of consciousness
Huan Wang¹, Youqiu Xie², Ling Weng¹, Qing Ma², Ling Zhao¹, Ronghao Yu², Miao Zhong¹, Xiaoyan Wu¹, and Ruiwang Huang¹

¹Center for the Study of Applied Psychology, Guangdong Key Laboratory of Mental Health and Cognitive Science, School of Psychology, South China Normal University, GuangZhou, China, People's Republic of, ²Coma research group and coma recovery unit, neuroscience institute, guangzhou general hospital of Guangzhou command, GuangZhou, China, People's Republic of

What we did was to use the tract-based spatial statistics (TBSS) approach to examine the changes of diffusion parameters in whole brain white matter of DOC patients relative to healthy controls, and to detect the correlation between the diffusion parameters of white matters and clinical variables.

2045

White matter microstructural deficits in schizophrenia using generalized kurtosis
Arash Nazeri¹, Lipeng Ning², Jon Pipitone¹, David J. Rotenberg¹, Yogesh Rathi², and Aristotle N. Voineskos¹

¹Research Imaging Centre, Centre for Addiction and Mental Health, University of Toronto, Toronto, ON, Canada, ²Brigham and Women's Hospital, Harvard Medical School, Boston, MA, United States

Numerous studies have used diffusion tensor imaging to investigate schizophrenia-related white matter microstructural deficits. Diffusion tensor imaging assumes a Gaussian distribution for the water molecule displacement. However, this assumption may not be valid in the complex biological tissues such as white matter. Using directional radial basis function it is possible to estimate ensemble

average diffusion propagator and generalized kurtosis of water diffusion (a measure of non-Gaussianity). Our results suggest that white matter generalized kurtosis is more sensitive to differences between persons with schizophrenia and healthy controls than diffusion tensor model parameters (particularly in frontotemporal superficial white matter areas).

2046

What is the best method for robust statistical inference on connectomic graph metrics?
Mark Drakesmith^{1,2}, David Linden², Anthony S David³, and Derek K Jones^{1,2}

¹CUBRIC, Cardiff University, Cardiff, United Kingdom, ²Neuroscience and Mental health Research Institute, Cardiff University, Cardiff, United Kingdom, ³Institute of Psychiatry, Psychology and Neuroscience, Kings College London, London, United Kingdom

Connectomic network analyses, while powerful, suffer from high instability, which is problematic for robust statistical inference. The area under the curve (AUC) across thresholds is a common approach, but lacks robustness to this instability. A superior approach is multi-threshold permutation correction (MTPC), but this is computationally expensive. Smoothed AUCs (smAUCs) are less costly and theoretically can achieve the same level of sensitivity as MTPC. smAUC was tested and compared with MTPC in a virtual patient-control comparison. Results show that smAUC sensitivity is not consistently comparable to MTPC and that exhaustive searching across the threshold space is required for robust inference.

2047

Evaluation of IVIM Perfusion Parameters as Biomarkers for Paediatric Brain Tumours
Emma Meeus^{1,2,3}, Jan Novak^{2,3}, Stephanie Withey^{2,3,4}, Lesley MacPherson³, and Andrew Peet^{2,3}

¹Physical Sciences of Imaging in Biomedical Sciences (PSIBS) Doctoral Training Centre, University of Birmingham, Birmingham, United Kingdom, ²Institute of Cancer and Genomic Sciences, University of Birmingham, Birmingham, United Kingdom, ³Department of Oncology, Birmingham Children's Hospital, Birmingham, United Kingdom, ⁴RRPPS, University Hospitals Birmingham NHS Foundation Trust, Birmingham, United Kingdom

This study investigated the bi-exponential IVIM fitting methods and their robustness for applications in the brain. Data simulations relevant to normal brain and tumour were computed to assess the accuracy and precision of the IVIM perfusion parameters. The paediatric patient cohort evaluated the correlation between the IVIM and DSC-MRI derived parameters. The simulation results showed that the perfusion fraction (IVIM-f) was robust enough to provide reliable values using the constrained 1-parameter fit. The robustness was further confirmed with the significant correlation observed between the IVIM-f and DSC-CBV. Therefore, IVIM-f could provide an alternative non-invasive perfusion measure for paediatrics.

2048

Correcting spatial misalignment between fiber bundles segments for along-tract group analysis
Samuel St-Jean¹, Max Viergever¹, Geert Jan Biessels², and Alexander Leemans¹

¹Image Sciences Institute, University Medical Center Utrecht, Utrecht, Netherlands, ²Department of Neurology, Rudolf Magnus Institute of Neuroscience, University Medical Center Utrecht, Utrecht, Netherlands

For diffusion MRI studies relying on statistics computed along fiber trajectories, the extracted values might not be optimally aligned between subjects in the metric space, which could lead to subsequent erroneous statistical analysis. We thus propose a 1D fast Fourier transform based correction algorithm for a fast realignment (< 1 second) directly in the metric space. Our experiments with a) synthetic signals and b) FA values along the uncinate fasciculus from real data show that our fiber-tract realignment algorithm improves the overlap of extracted metrics. This could help researchers uncover relationships of interest which were hidden by residual misalignment at first.

2049

A Theoretical Framework for Sampling and Reconstructing Ensemble Average Propagators in Diffusion MRI
Divya Varadarajan¹ and Justin P Halder²

¹University of Southern California, 90089, CA, United States, ²University of Southern California, Los Angeles, CA, United States

Diffusion MRI can be modeled as sampling the Fourier transform of the Ensemble Average Propagator (EAP). This is potentially advantageous because of extensive theory that has been developed to characterize sampling requirements, accuracy, and stability for Fourier reconstruction. However, previous work has not taken advantage of this characterization. This work presents a novel theoretical framework that precisely describes the relationship between the estimated EAP and the true original EAP. The framework is applicable to arbitrary linear EAP estimation methods, and for example, provides new insights into the design of q-space sampling patterns and the selection of EAP estimation methods.

2050

Phase-correcting Non-local Means Denoising for Diffusion-Weighted Imaging
Sevgi Gokce Kafali^{1,2}, Tolga Çukur^{1,2}, and Emine Ulku Saritas^{1,2}

¹Electrical and Electronics Engineering, Bilkent University, Ankara, Turkey, ²National Magnetic Resonance Research Center (UMRAM), Bilkent University, Ankara, Turkey

Diffusion-weighted imaging (DWI) intrinsically suffers from low SNR due to diffusion-induced signal losses. Multiple acquisitions have to be averaged to attain reasonable SNR level in high-spatial-resolution DWI images. However, subject motion during diffusion-sensitizing gradients creates varying phase offsets between repeated acquisitions, prohibiting a direct complex averaging of the image repetitions. Here, we propose a phase-correcting non-local means denoising filter that combines multiple DWI acquisitions while effectively reducing noise and phase cancellations. Results are demonstrated *in vivo* in the cervical spinal cord at 3T, using a reduced field-of-view DWI with

2051

Rapid Estimation of IVIM Pseudo-Diffusion Fraction with Correction of TE Dependence

Neil Peter Jerome¹, Matthew R Orton¹, Thorsten Feiweier², Dow-Mu Koh³, Martin O Leach¹, and David J Collins¹

¹CRUK Cancer Imaging Centre, Division of Radiotherapy & Imaging, Institute of Cancer Research, London, United Kingdom, ²Siemens Healthcare GmbH, Erlangen, Germany, ³Department of Radiology, Royal Marsden Hospital, London, United Kingdom

The biexponential IVIM model of diffusion does not account for distinct T_2 values for the two components, commonly interpreted as blood and tissue, leading to a TE dependence of the pseudo-diffusion volume fraction parameter f . In this volunteer study, the addition of a small number of DWI scans at different TEs allows for fitting of an extended T_2 -IVIM model, returning TE-independent estimations of liver f ($18.26 \pm 7.3\%$ compared to $27.88 \pm 6.0\%$ from conventional IVIM fitting), and T_2S of 77.6 ± 30.2 and 42.1 ± 6.8 ms for pseudo- and true diffusion compartments, respectively.

2052

Validation of MD map calculation from DWI acquired on a 0.35T MRI scanner in Malawi for acute cerebral malaria

Yuchuan Zhuang¹, Samuel D. Kampondeni^{2,3}, Madalina Tivarus², Michael J. Potchen², Gretchen L. Birbeck⁴, and Jianhui Zhong²

¹Electrical and Computer Engineering, University of Rochester, Rochester, NY, United States, ²Department of Imaging Sciences, University of Rochester Medical Center, Rochester, NY, United States, ³MRI Center, Queen Elizabeth Central Hospital, Blantyre, Malawi, ⁴Department of Neurology, University of Rochester Medical Center, Rochester, NY, United States

Cerebral malaria (CM) is an often fatal disease that still devastates children in Africa. In Malawi, MRIs at 0.35T are obtained on pediatric CM patients, but quantitative analysis remains challenging. This report validates the 0.35T DWI measurements by comparing diffusion scans of normal adult subjects on both 0.35T and 3T MRI scanners. We used ROI analysis, regression analysis and histogram for quantitative validation. Strong consistency between the two data sets indicates that the DWI findings obtained on the 0.35T in Malawi can be used despite its inherent limitations.

2053

Real valued diffusion weighted imaging using decorrelated phase filtering

Tim Sprenger Sprenger^{1,2}, Jonathan I. Sperl², Brice Fernandez³, Axel Haase¹, and Marion Menzel²

¹Technische Universität München, Munich, Germany, ²GE Global Research, Munich, Germany, ³GE Healthcare, Munich, Germany

Due to the intrinsic low signal to noise ratio in diffusion weighted imaging (DWI), magnitude processing often results in an overestimation of the signal's amplitude. This results in low estimation accuracy of diffusion models and reduced contrast because of a superposition of the image signal and the noise floor. We adopt a new phase correction (PC) technique yielding real valued data and maintaining a Gaussian noise distribution. The advantage of PC is shown in a DSI experiment where the Ensemble average propagator is better delineated in the real valued data and delineation improves as the noise floor is lowered.

2054

Non-linear Distortion Correction in Human Optic Nerve Diffusion Imaging

Joo-won Kim^{1,2}, Jesper LR Andersson³, Peng Sun⁴, Sheng-Kwei Song⁴, Robert Naismith⁵, and Junqian Xu^{1,2,6}

¹Department of Radiology, Icahn School of Medicine at Mount Sinai, New York, NY, United States, ²Translational and Molecular Imaging Institute, Icahn School of Medicine at Mount Sinai, New York, NY, United States, ³Oxford Centre for Functional MRI of the Brain, University of Oxford, Oxford, United Kingdom, ⁴Department of Radiology, Washington University, St. Louis, MO, United States, ⁵Department of Neurology, Washington University, St. Louis, MO, United States, ⁶Department of Neuroscience, Icahn School of Medicine at Mount Sinai, New York, NY, United States

A major challenge in optic nerve diffusion MRI is the non-linear optic nerve distortion induced by eye-ball movement. In this work, we developed and evaluated a non-linear registration scheme to improve optic nerve edge alignment over conventional diffusion imaging distortion correction methods. Optic nerve edge plots (both 1D and 2D) were used to evaluate the optic nerve edge alignment for different non-linear registration methods (FSL/fnirt and ANTs) after FSL/topup and FSL/eddy correction of unprocessed diffusion images. Overall, the additional non-linear registration step, regardless of the non-linear registration method used, substantially improved optic nerve edge alignment along all diffusion measurement frames.

2055

Fast implementations of contextual PDE's for HARDI data processing in DIPY

Stephan Meesters¹, Gonzalo Sanguinetti¹, Eleftherios Garyfallidis², Jorg Portegies¹, and Remco Duits¹

¹Department of Mathematics and Computer Science, Eindhoven University of Technology, Eindhoven, Netherlands, ²Computer Science Department, University of Sherbrooke, Sherbrooke, QC, Canada

We present a novel open-source module that implements a contextual PDE framework for processing HARDI data. Its potential in enhancement of ODF/FOD fields is demonstrated where the aim is to enhance the alignment of elongated structures while preserving crossings. The method for contextual enhancement is based on a hypo-elliptic PDE defined in the domain of coupled positions and orientations and can be solved with a shift-twist convolution. The module is available in the DIPY (Diffusion Imaging in Python) software library, which makes it widely available for the neuroimaging community.

2056

Flow-based White Matter Supervoxel Parcellation using Functional Bregman Divergence between Orientation Distribution Functions

Teng Zhang¹, Kai Liu¹, Lin Shi^{2,3}, and Defeng Wang^{4,5}

¹Department of Imaging and Interventional Radiology, The Chinese University of Hong Kong, Hong Kong, Hong Kong, ²Department of Medicine and Therapeutics, The Chinese University of Hong Kong, Hong Kong, Hong Kong, ³Chow Yuk Ho Technology Centre for Innovative Medicine, The Chinese University of Hong Kong, Hong Kong, Hong Kong, ⁴Research Center for Medical Image Computing, Department of Imaging and Interventional Radiology, The Chinese University of Hong Kong, Hong Kong, Hong Kong, ⁵Shenzhen Research Institute, The Chinese University of Hong Kong, Shenzhen, China, People's Republic of

We propose a flow-based supervoxel parcellation method to split white matter into supervoxels with homogeneous diffusion property. In particular, we defined a new similarity metric between orientation distribution functions derived from q-ball imaging according to functional Bregman divergence. The proposed method was applied to high quality data from Human Connectome Project. Our work demonstrated a methodological feasibility to generate supervoxel approach tractography, construction of WM connectivity network, etc.

2057

Generalisability of Image Quality Transfer: Can we approximate in-vivo human brains from dead monkey brains?

Aurobrata Ghosh¹, Viktor Wottschel², Enrico Kaden¹, Jiaying Zhang¹, Hui Zhang¹, Stamatis N. Sotiroopoulos³, Darko Zikic⁴, Tim B. Dyrby⁵, Antonio Crimini⁴, and Daniel C Alexander¹

¹Centre for Medical Image Computing, University College London, London, United Kingdom, ²Institute of Neurology, University College London, London, United Kingdom, ³Oxford Centre for Functional Magnetic Resonance Imaging of the Brain (FMRIB), University of Oxford, Oxford, United Kingdom, ⁴Microsoft Research, Cambridge, United Kingdom, ⁵Danish Research Centre for Magnetic Resonance, Centre for Functional and Diagnostic Imaging and Research, Copenhagen University Hospital Hvidovre, Hvidovre, Denmark

The Image-Quality Transfer (IQT) framework enhances low quality images by transferring information from high quality images acquired on expensive bespoke scanners. Although IQT has major potential in medical imaging, one key question is its dependence on training data. We demonstrate the generalisability of IQT used for super-resolution by showing that reconstruction of in-vivo human images degrades minimally from training on human data from the same study, to data from a different demographic and imaging protocol, to data from fixed monkey brains. Remarkably, a patchwork of fixed monkey brain image-pieces is hardly distinguishable from a reconstruction using pieces of human data.

2058



Anisotropic fractional-motion-based diffusion MRI in the human brain

Yun Liu¹, Yang Fan^{1,2}, and Jia-Hong Gao¹

¹Peking University, Beijing, China, People's Republic of, ²MR Research China, GE Healthcare, Beijing, China, People's Republic of

Several anomalous diffusion models, both empirical and theoretical, were proposed to explain the departure from purely mono-exponential decay of DWI signal in biological tissues. Recently, a fractional motion (FM) based diffusion MRI theory was proposed, which was claimed to be a proper model in the description of diffusion processes in biological systems. However, the tensorial properties of FM related parameters is still unknown. In this work, diffusion magnetic field gradients were applied in several non-linear directions to acquire DWI images. Then, the FM-based parameters were obtained in each diffusion direction and found direction dependent.

2059

Perfusion-free Diffusion Tensor Imaging of Brain Tumors

Zhongwei Zhang¹, Zuhao Li², Yu-Chien Wu³, Dawen Zhao⁴, and Mark E Schweitzer⁵

¹Radiology, UT Southwestern Medical Center, Dallas, TX, United States, ²Radiology, The 1st Affiliated Hospital, Sun Yat-Sen University, Guangzhou, China, People's Republic of, ³Radiology and Imaging Sciences, Indiana University, Indianapolis, IN, United States, ⁴Biomedical Engineering and Cancer Biology, Wake Forest School of Medicine, Winston-Salem, NC, United States, ⁵Radiology, Stony Brook University, Stony Brook, NY, United States

In conventional DTI, the quantitation of various DTI indices was strongly influenced by b-value. In this study, we proposed a new approach that perfusion-free DTI can be fulfilled using IVIM and DTI models.

2060

The value of DTI and DTT in evaluating the protective effect of neuregulin-1 on spinal cord transection models of Sprague-Dawley rats. Tao Gong¹, Guangbin Wang², and Weibo Chen³

¹Shandong University, Jinan, China, People's Republic of, ²Jinan, China, People's Republic of, ³Shanghai, China, People's Republic of

DTI can noninvasive evaluate the injury and prognosis of spinal cord, and NRG-1 has the function of protecting and repairing of injury spinal cord in rats.

2061

Is voxel-based apparent diffusion coefficient reproducible?

Masamitsu Hatakenaka¹, Koichi Onodera¹, Naomi Koyama¹, and Mitsuhiro Nakanishi²

¹Diagnostic Radiology, Sapporo Medical University, Sapporo, Japan, ²Division of Radiology, Sapporo Medical University Hospital, Sapporo, Japan

To evaluate reproducibility of voxel-based ADC, voxel-based ADC of the phantom was measured using clinical 3T MRI system. The direction of motion probing gradient affected the voxel-based ADC significantly in both echo planar imaging and turbo spin echo diffusion-weighted imaging. Also voxel-based ADC differed both between identical positioning examinations and between slightly different positioning examinations. Voxel-based ADC could not be reproduced sufficiently even in a phantom study. It would be

Traditional Poster

Diffusion: Analysis

Exhibition Hall

Wednesday, May 11, 2016: 10:00 - 12:00

2062

Magnetic ROIs enable improved tractography accuracy through oriented prior

Maxime Chamberland^{1,2,3}, Benoit Scherrer³, Sanjay Prabhu³, Joseph Madsen³, David Fortin⁴, Kevin Whittingstall^{2,5}, Maxime Descoteaux¹, and Simon K Warfield³

¹Computer science, Université de Sherbrooke, Sherbrooke, QC, Canada, ²Nuclear Medicine and Radiobiology, Université de Sherbrooke, Sherbrooke, QC, Canada, ³Boston Children's Hospital, Harvard Medical School, Boston, MA, United States, ⁴Division of Neurosurgery and Neuro-Oncology, Université de Sherbrooke, Sherbrooke, QC, Canada, ⁵Department of Diagnostic Radiology, Université de Sherbrooke, Sherbrooke, QC, Canada

Streamline tractography algorithms infer connectivity by following directions which are maximally aligned at every voxel. This rule has even been the definition of the probability of connectivity, with the difference in current and next orientation being defined as uncertainty in connectivity. However, our experiments demonstrate that in regions where multiple fiber pathways interdigitate (e.g. temporal lobe), this heuristic is inadequate and does not necessarily reflect the underlying human brain architecture. Furthermore, we demonstrate that inference of connectivity can be improved by incorporating anatomical knowledge of the expected fiber orientation in regions where this information is known. We applied this heuristic through a new tractography region of interest (ROI) and demonstrate that it provides improved delineation of the expected anatomy.

2063

Effects of cortical regions of interests on tractography and brain connectivity quantification

Tina Jeon¹, Virendra Mishra², and Hao Huang^{1,3}

¹Radiology Research, Children's Hospital of Philadelphia, Philadelphia, PA, United States, ²Lou Ruvo Center for Brain Health, Cleveland Clinic, Las Vegas, NV, United States, ³Perelman School of Medicine, University of Pennsylvania, Philadelphia, PA, United States

Dense white matter (WM) zones just beneath cerebral cortex impede tracking from a cortical region of interest with diffusion MRI data. To address this tracing problem, we can either dilate the parcelated cortex into the adjacent WM to initiate tracing or trace directly from WM interior to these dense WM zones. Here we evaluated with diffusion MRI data from three developmental age groups 1) how much dilation from the segmented cortical gyrus would be sufficient for appropriate WM tracing; and 2) if tracing directly from the WM immediately beneath the dense WM zones will yield the same tractography results.

2064

LOCAL ANALYSIS OF TRACK DENSITY IMAGING FOR THE DETECTION OF WHITE MATTER ALTERATIONS

Rodrigo de Luis-Garcia¹, Angel Luis Guerrero², Miguel Angel Tola-Arribas³, and Santiago Aja-Fernandez¹

¹Universidad de Valladolid, Valladolid, Spain, ²Hospital Clínico Universitario, Valladolid, Spain, ³Hospital Universitario Rio Hortega, Valladolid, Spain

Track-Density Imaging (TDI) can provide super resolution images of the white matter of the brain. As it is based on the results of a whole brain tractography process, it comprises information from different features of the white matter diffusion. We exploit this information by proposing a local analysis approach for TDI, and test it on two different datasets where conventional TBSS analysis using FA did not yield any significant differences. Results revealed the proposed method to be extremely sensitive in the detection of white matter abnormalities, making it a promising tool for white matter group studies.

2065

Minimum number of diffusion encoding directions required to yield a rotationally invariant powder average signal in single and double diffusion encoding

Filip Szczepankiewicz¹, Carl-Fredrik Westin², Freddy Ståhlberg¹, Jimmy Lätt³, and Markus Nilsson⁴

¹Dept. of Medical Radiation Physics, Lund University, Lund, Sweden, ²Dept. of Radiology, Brigham and Women's Hospital, Harvard Medical School, Boston, MA, United States, ³Center for Medical Imaging and Physiology, Skåne University Hospital, Lund, Sweden, ⁴Lund University Bioimaging Center, Lund University, Lund, Sweden

Several analysis techniques of diffusion-weighted data make use of the powder average to yield signal that is invariant to rotation. However, rotational invariance is achieved only at a sufficient directional resolution, which depends on the tissue anisotropy and diffusion encoding strength. In this work we present the minimum number of diffusion directions necessary to yield a rotationally invariant powder average, at arbitrary anisotropy and encoding strength, for single and double diffusion encoding.

2066

Structural connectivity analysis at the voxel level

Jan-Gerd Tenberge¹ and Patrick Schiffner¹

¹University of Münster, Münster, Germany

We present a GPU-accelerated method to compute a structural connectome of the human brain with voxel-level resolution from diffusion weighted images.

2067

On the feasibility of data-driven estimation of Markov random field parameters for IVIM modelling of abdominal DW-MRI: insights into which parameters can be reliably estimated from clinical data
Matthew R Orton¹, Neil P Jerome¹, Mihaela Rata¹, David J Collins¹, Khurum Khan², Nina Tunaru³, David Cunningham², Thorsten Feiweier⁴, Dow-Mu Koh³, and Martin O Leach¹

¹CRUK Cancer Imaging Centre, Division of Radiotherapy and Imaging, Institute of Cancer Research, London, United Kingdom, ²Department of Medical Oncology, Royal Marsden NHS Foundation Trust, London, United Kingdom, ³Department of Radiology, Royal Marsden NHS Foundation Trust, London, United Kingdom, ⁴Siemens Healthcare, Erlangen, Germany

The intravoxel incoherent motion model is of great interest as it gives a more complete characterization of DWI signals. However, estimates of the pseudo-diffusion coefficient D^* are noisy, which can be mitigated using Markov random field (MRF) models. The MRF smoothing weights are usually subjectively chosen; by removing this requirement, we show that while the smoothing weights for the pseudo-diffusion volume fraction and diffusion coefficient can be estimated from the data, smoothing weights for D^* cannot. This suggests that with currently available data, D^* estimates require stabilization by imposing subjective constraints of some kind, such as the MRF used here.

2068

A T1 and DTI fused 3D Corpus Callosum analysis in MCI subjects with high and low cardiovascular risk profile
Yi Lao^{1,2}, Binh Nguyen², Sinchai Tsao², Niharika Gajawelli^{1,2}, Meng Law^{1,3}, Helena Chui^{1,3}, Yalin Wang⁴, and Natasha Lepore^{1,2}

¹Biomedical Engineering, University of Southern California, Los Angeles, CA, United States, ²Radiology, Children's Hospital Los Angeles, Los Angeles, CA, United States, ³Radiology, Keck School of Medicine, University of Southern California, Los Angeles, CA, United States, ⁴School of Computing, Informatics, and Decision Systems Engineering, Arizona State University, Tempe, AZ, United States

Understanding how vascular disease and its risk factors influence Alzheimer's disease (AD) progression may enhance predictive accuracy as well as guide early interventions. Here, we apply a novel T1 and DTI fusion analysis on the 3D corpus callosum (CC) of mild cognitive impairment (MCI) populations with different levels of cardiovascular risk, with the aim of decoupling vascular factors in the prodromal AD stage. Our new fusion method detected significant differences in the anterior CC between MCI subjects with high and low vascular risk profiles. These findings may help to elucidate the interdependent relationship between MCI and vascular risk factors.

2069

Neuroimaging biomarkers for predicting treatment response in schizophrenia based on alteration patterns of the whole brain white matter tracts
Jing-Ying Huang¹, Yu-Jen Chen¹, Chih-Min Liu², Tzung-Jeng Hwang^{2,3}, Yun-Chin Hsu¹, Yu-Chun Lo¹, Hai-Gwo Hwu^{2,3}, and Wen-Yih Isaac Tseng^{1,3,4,5,6}

¹Institute of Medical Device and Imaging, National Taiwan University College of Medicine, Taipei, Taiwan, ²Department of Psychiatry, National Taiwan University Hospital, Taipei, Taiwan, ³Graduate Institute of Brain and Mind Sciences, National Taiwan University College of Medicine, Taipei, Taiwan, ⁴Institute of Biomedical Engineering, National Taiwan University, Taipei, Taiwan, ⁵Department of Medical Imaging, National Taiwan University Hospital, Taipei, Taiwan, ⁶Molecular Imaging Center, National Taiwan University, Taipei, Taiwan

This study aims to identify image biomarkers for schizophrenia patients in order to predict treatment responses on individual subject basis. We develop algorithm that can discriminate remission or non-remission in patients with schizophrenia based on the difference in microstructural integrity of the white matter tracts. The ROC analysis shows that the accuracy of the prediction is 76%.

2070

Individualized prediction of schizophrenia based on patterns of altered tract integrity over the whole brain using diffusion spectrum imaging
Yu-Jen Chen¹, Chih-Ming Liu², Tzung-Jeng Huang², Yun-Chin Hsu¹, Yu-Chun Lo¹, Hai-Gwo Hwu², and Wen-Yih Isaac Tseng^{1,3}

¹National Taiwan University, Institute of Medical Device and Imaging, Taipei, Taiwan, ²National Taiwan University Hospital, Department of Psychiatry, Taipei, Taiwan, ³National Taiwan University, Molecular Imaging Center, Taipei, Taiwan

In this study, we examined the performance of predicting patients with schizophrenia based on the patterns of altered tract integrity over the whole brain. The whole-brain tract information was compared with predefined differences between schizophrenia patients and healthy participants to calculate an index of SLI indicating the similarity to schizophrenia. Our results showed that the prediction performance was high (AUC = 0.86 for males; AUC = 0.77 for females) when we compared the white matter integrities at specific segments on fiber pathways.

2071

De-noising of diffusion-weighted MRI data by averaging of inconsistent input data in wavelet space
Henrik Marschner¹, Cornelius Eichner¹, Alfred Anwander¹, André Pampel¹, and Harald E. Möller¹

¹Max Planck Institute for Human Cognitive and Brain Sciences, Leipzig, Germany

Diffusion Weighted Images datasets with high spatial resolution and strong diffusion weighting are often deteriorated with low SNR. Here, we demonstrate the feasibility of a recently presented repetition-free averaging based de-noising (AWESOME). That technique reduces noise by averaging over a series of N images with varying contrast in wavelet space and regains intensities and object features initially covered by noise. We show that high resolution DWIs are achievable in a quality that almost equals to that obtained from 6fold

complex averaging.

2072

Linear Acceleration of SADD Method for Three Compartments
Ana Karen Loya¹ and Mariano Rivera¹

¹Computer Science, Centro de Investigacion en Matematicas AC, Guanajuato, Mexico

The proposal attempts to model more properly the intra-voxel information from DW-MRI signals in order to obtain tissue diffusion properties in white matter. The method is based on Sparse and Adaptive Diffusion Dictionary (SADD) strategy that dynamically adapts a dictionary of diffusion functions by changing size and orientation of the diffusion tensors. In ISMRM2015, we demonstrated that our accelerated version (LASADD) reduces complexity and computational cost wrt SADD with similar quality results. This work extends the idea of LASADD to three compartments (intracellular, extracellular and cerebrospinal fluid) and presents experimental results depicting the computed properties about the diffusion structure.

2073

Robust assessment of the brain's sheet structure using normalized convolution

Chantal M.W. Tax^{1,2}, Carl-Fredrik Westin², Tom Dela Haije³, Andrea Fuster³, Max A. Viergever¹, Luc Florack³, and Alexander Leemans¹

¹Image Sciences Institute, University Medical Center Utrecht, Utrecht, Netherlands, ²Department of Radiology, Brigham and Women's Hospital, Harvard Medical School, Boston, MA, United States, ³Department of Mathematics and Computer Science, Eindhoven University of Technology, Eindhoven, Netherlands

The theory that brain fiber pathways cross in sheet-like structures has been a topic of debate. This theory is mainly supported by qualitative findings using diffusion MRI tractography, and a comprehensive quantitative analysis is necessary. To this end, an approach was developed to quantify the degree of "sheetness" based on constructing a large amount of loops with tractography. This approach, however, is computationally expensive, cannot cope well with missing peaks, and is only an approximation when the loops are not infinitesimally small. Here we present an alternative, fast, robust, and elegant approach for the computation of the degree of sheetness.

2074

Introducing a structural similarity index and map for quality control in tractography performed using multi-band EPI

Yuichi Suzuki¹, Akira Kunimatsu¹, Kouhei Kamiya¹, Masaki Katsura¹, Harushi Mori¹, Katsuya Maruyama², Thorsten Feiweier³, Kenji Ino¹, Yasushi Watanabe¹, Jiro Sato¹, Keiichi Yano¹, and Kuni Ohtomo¹

¹The Department of Radiology, The University of Tokyo Hospital, Bunkyo-ku, Japan, ²Siemens Japan K.K., Shinagawa-ku, Japan, ³Siemens AG, Erlangen, Germany

We quantitatively evaluated the quality of tractography images captured using the multi-band EPI (MBEPI) compared with those obtained without using MBEPI. We also demonstrated the potential weakness of classic Dice similarity coefficients (DSCs) and introduced a structural similarity (SSIM) index and map as a new method for evaluating the quality of tractography images. A numerical evaluation was enabled by the SSIM index and that the SSIM map was advantageous in that it allows visual confirmation of the structural similarity ratio; in contrast, the DSCs only offered a numerical evaluation.

2075

Single-shot diffusion mapping through overlapping-echo detachment planar imaging technique

Lingceng Ma¹, Congbo Cai¹, Shuhui Cai¹, and Zhong Chen¹

¹Electronic Science Department, Xiamen University, Xiamen, China, People's Republic of

Conventional diffusion MRI tends to be of limited use in real-time imaging, because motion can distort the images from multiple scans. In this study, we propose a new imaging method, single-shot diffusion mapping through overlapping-echo detachment planar (DM-OLED) method, together with corresponding signal separation algorithm, to achieve reliable single-shot diffusion mapping in the order of milliseconds. Numerical simulations were performed to verify the proposed method. The results show that the method is accurate and efficient.

2076

"Noise" in diffusion tractography connectomes is not additive

Michael Paquette¹, Gabriel Girard^{1,2,3}, Maxime Chamberland^{1,2,3}, and Maxime Descoteaux^{1,2}

¹Sherbrooke Connectivity Imaging Lab, Computer Science, Université de Sherbrooke, Sherbrooke, QC, Canada, ²Centre de Recherche CHUS, Université de Sherbrooke, Sherbrooke, QC, Canada, ³Sherbrooke Neuro-Analysis Imaging Lab, Department of Nuclear Medicine and Radiobiology, Université de Sherbrooke, Sherbrooke, QC, Canada

With the increasing popularity of diffusion MRI tractography-based connectomes in the literature, a better analysis of their reproducibility is crucial. Studying connectome differences across a test-retest dataset allows us to investigate their variance. In this work we highlight the non-additive nature of tractography based connectome "noise". This observation holds even when accounting for some of the biggest tractography biases such as seeding density, seeding region, tract volume and fiber length.

2077

Correcting diffusion weighted MR images for signal pile-up and distortions near gas pockets

Laurens D. van Buuren¹, Daniel Polders¹, Maaike T. Milder¹, Floris J. Pos¹, Stijn W. Heijmink¹, Baukelen van Triest¹, and Uulke A. van der Heide¹

Echo-planar imaging is widely used to obtain diffusion images within acceptable time limits. These images suffer from geometric distortions. Additionally, the diffusion signal intensity can be obscured by signal pile-up, when strong variations of the magnetic field occur, for example near gas pockets. We demonstrate in a water phantom that both the signal pile-up and geometric distortions can be corrected by combining the information from EPI images obtained with opposite gradients and a magnetic field map. We applied this method in two patients and show a reduction in signal pile-up and geometric distortions near gas pockets in the rectum.

2078

FRACTAL DIMENSION AS A GLOBAL DESCRIPTOR OF THE WHITE MATTER IN DIFFUSION MRI GROUP STUDIES
Rodrigo de Luis-Garcia¹, Miguel Angel Tola-Arribas², Claudio Delrieux³, and Carlos Alberola-Lopez¹

¹Universidad de Valladolid, Valladolid, Spain, ²Hospital Universitario Rio Hortega, Valladolid, Spain, ³Universidad Nacional del Sur, Bahia Blanca, Argentina

Simple global measures describing the complexity of the white matter architecture can provide useful information when analyzing diffusion MRI data, and can be even capable of finding statistical differences between groups. We propose the use of the fractal dimension of the FA maps for that purpose, and illustrate its potential on a dataset composed of elderly subjects and patients from three different stages of Alzheimer's disease.

2079

Sensitivity of diffusion metrics in complex white matter configurations
Pedro Angel Luque Laguna^{1,2}, Luis Lacerda^{1,2}, Steve C.R. Williams¹, and Flavio Dell'Acqua^{1,2}

¹Neuroimaging, King's College London, LONDON, United Kingdom, ²Natbrainlab, LONDON, United Kingdom

In the context of studies using diffusion MRI, an important criterion to choose between the available diffusion metrics is the sensitivity to detect pathological changes. Sensitivity of diffusion metrics has been shown to vary widely across brain regions although the biological factors behind such variability remain undetermined. In this work we use computational simulations to evaluate the effect that different white matter configurations have on the sensitivity of existing metrics of diffusion and anisotropy. We show that for the same biological change, features of microstructural organisation like the angle of crossing fibres have a significant and characterising effect in the sensitivity of each particular metric.

2080

An assessment of Bayesian IVIM model fitting
Oscar Gustafsson^{1,2}, Mikael Montelius¹, Göran Starck^{1,2}, and Maria Ljungberg^{1,2}

¹Department of Radiation Physics, Institute of Clinical Sciences, The Sahlgrenska Academy, University of Gothenburg, Gothenburg, Sweden,

²Department of Medical Physics and Biomedical Engineering, Sahlgrenska University Hospital, Gothenburg, Sweden

Bayesian model fitting has been proposed as an alternative to the commonly used least squares fitting of the IVIM model. In this work we used Monte Carlo simulations to study the convergence of a Markov Chain Monte Carlo implementation of Bayesian model fitting and compared the resulting model parameters to two least squares model fitting methods. We saw that the convergence of the Bayesian model fitting procedure was affected by noise and compartment sizes. Bayesian model fitting was beneficial for the diffusion coefficient and the perfusion fraction, especially at low SNR

2081

A Fast and Effective Strategy for Artifact Identification and Signal Restoring with HARDI data
Elisa Scaccianoce^{1,2}, Francesca Baglio², Giuseppe Baselli¹, and Flavio Dell'Acqua³

¹Department of Electronics, Informations and Bioengineering, Politecnico di Milano, Milano, Italy, ²RM Lab, Don Carlo Gnocchi Foundation ONLUS, IRCCS S. Maria Nascente, Milano, Milano, Italy, ³NATBRAINLAB, Department of Neuroimaging, Institute of Psychiatry, Psychology and Neuroscience, King's College, London, United Kingdom, London, United Kingdom

HARDI datasets are often prone to different type of artifacts, difficult to detect even by expert users. In this work we propose a fast and effective pipeline for outlier identification and correction of HARDI datasets. Here corrupted data is first identified as outlier and then regenerated using a framework based on signal decomposition using spherical harmonics. This approach was tested on healthy controls and validated with simulated dataset. Our study confirms the efficacy of using SH for artifacts identification and correction.

2082

Novel Strategy for Quantitative Analysis of IVIM Diffusion MRI in Ewing's Sarcoma Family of Tumours
Esha Baidya Kayal¹, Devasenathipathy K², Kedar Khare³, Jayendra Tiru Alampally², Sameer Bakhshi⁴, Raju Sharma², and Amit Mehndiratta^{1,5}

¹Centre for Biomedical Engineering, Indian Institute of Technology Delhi, New Delhi, India, ²Department of Radiology, All India Institute of Medical Sciences, New Delhi, India, ³Department of Physics, Indian Institute of Technology Delhi, New Delhi, India, ⁴BRA IRCH, All India Institute of Medical Sciences, New Delhi, India, ⁵Department of Biomedical Engineering, All India Institute of Medical Sciences, New Delhi, India

Quantitative analysis of IVIM effect reveals both diffusion and perfusion component of tissue. As widely used bi-exponential model is not very reliable, we propose two penalty function: a) Total Variation and b) Huber Penalty function with bi-exponential model for IVIM parametric analysis of soft tissue tumours. Results show better fit to IVIM dataset by our two methods compared to standard BE model and freeware Osirix. IVIM analysis using Total Variation Reduction methodology showed qualitatively and quantitatively better estimation of both perfusion and diffusion component in soft tissue tumours.

2083

Spatial Heterogeneity Mapping of Brain Tumors from 3.0 T Diffusion MR: Quantitative Results Versus Histological Tumour Grade
Lalit Gupta¹, Sundararaman VK¹, and Rakesh K Gupta²

¹Philips India Ltd., Bangalore, India, ²Department of Radiology, Fortis Memorial Research Institute, Gurgaon, India

In a previous study a method based on “texture analysis” of apparent diffusion coefficient maps was proposed for tumor grading, with validation on limited 1.5T data. In this study, we use a modified method and show additional results (46 patients’ data) on 3.0 T data. There was significant difference between high and low grade tumors using heterogeneity measure ($p < 0.05$). 39 out of 46 patients were found to be correctly classified using a threshold in-between mean values of high and low grade tumors. In the other seven patients, the tumors were either very small or had undergone surgical interventions.

2084

The Apparent Range of Spin Movement in Diffusion MRI Data
Tom Dela Haije¹, Andrea Fuster¹, and Luc Florack¹

¹Mathematics and Computer Science, Eindhoven University of Technology, Eindhoven, Netherlands

In this work we investigate the potential of diffusion MRI to measure the maximum range of motion due to diffusion within spatially homogeneous voxels. We show that it is possible to characterize this range even in clinical scanners, and show in data of the human brain how this leads to interesting new ways to extract information from diffusion MRI.

2085 Comparison of Image Quality and Apparent Diffusion Coefficient Reproducibility with Water Excitation Using Binomial Scheme 11, 121, 1331, 14641 in iShim Sequence
Xiaolu Li¹, Mengchao Zhang¹, Hong Zeng¹, and Lin Liu¹

¹Jilin University Sino-Japan Hospital, Chang Chun, China, People's Republic of

Our study is to compare the homogeneity and degree of fat saturation when using water excitation at different binomial scheme (11, 121, 1331, 14641) in iShim (seq) for the clinical image quality.

2086

The Influence of Parallel Imaging in Diffusion Tensor Imaging Using Slice Accelerated Multiband Sequence
Yuanyuan Chen¹, Miao Sha¹, Xin Zhao¹, Xu Yan^{2,3}, Weiwei Wang¹, Xiong Zhang¹, Hongyan Ni³, and Dong Ming¹

¹Tianjin University, Tianjin, China, People's Republic of, ²MR Collaboration NE Asia, Siemens Healthcare, Shanghai, China, People's Republic of, ³Tianjin First Central Hospital, Tianjin, China, People's Republic of

The use of simultaneous multiband radiofrequency (RF) pulses to accelerate volume coverage along the slice direction is becoming increasingly popular. In this work, we attempt to evaluate the impact on parameter calculations of parallel imaging in combination with multiband excitation for DTI applications. The image quality as well as the indexes was compared. This experiment shows that the accelerated multiband sequence are highly reproducible in voxel-based analysis for different parallel imaging factors, with no significant differences ($p < 0.001$). In addition, the parallel imaging factor may have an influence on SNR and distortion of the diffusion images.

2087

A Novel and Cost-effective IVIM MRI Quality Assurance Method
LEI JIANG¹ and CHEN LIN¹

¹Radiology and Imaging Sciences, Indiana University School of Medicine, Indianapolis, IN, United States

Intravoxel incoherent motion (IVIM) MRI measures the combined effect of perfusion in the capillaries and water diffusion in the extracellular extravascular space. However, verification of the accuracy of IVIM is not performed routinely as it requires a flow phantom and a pump with accurate and constant output. Our goal is to develop a practical IVIM quality assurance method based on a simple and compact flow phantom driven by a power injector. We have demonstrated that using a simple phantom and a power injector as standard is feasible and can be easily implemented on many clinical/research scanners

2088

Combining TBSS and atlas-based analysis may reveal white matter abnormalities in Early Tourette Syndrome Children
Yue Liu¹, Jishui Zhang¹, Yue Zhang¹, Hongwei Tian¹, and Yun Peng¹

¹Beijing Children's hospital, Beijing, China, People's Republic of

Tourette syndrome (TS) is a childhood-onset neurobehavioral disorder. The present study investigate the microstructural changes of the white matter involved in children with TS by Diffusion tensor imaging (DTI). This is the first study that used both Tract-Based Spatial Statistics (TBSS) and Atlas-based approach to analyze DTI data of TS children. We found that FA/AD decrease and RD/MD increase in white matter tracts in cortico-striato-thalamo-cortical (CSTC) as well as basal ganglia and thalamus. The positive relation between higher RD, MD and more tics and the negative correlation between higher regional FA values and fewer tics, suggests that these alterations of white matter microstructure represent adaptive reorganization of somatosensory and motor processing in TS.

2089

Brain Structural Connectome using PROPELLER Echo-planar Diffusion Tensor Imaging and Probabilistic Tractography
Ya-Ling Lin^{1,2}, Tsyh-Jyi Hsieh³, and Ming-Chung Chou¹

Diffusion tensor imaging (DTI) was demonstrated to successfully trace three-dimensional trajectory of neuronal fiber tracts in vivo and has been widely utilized in many clinical applications. However, there are two major disadvantages when using conventional single-shot DTI, including the problems of intra-voxel fiber crossings and susceptibility distortions. Therefore, the purpose of this study was to utilize PROPELLER echo-planar DTI technique and probabilistic tractography to construct brain connectivity networks. The results showed that susceptibility distortions significantly deteriorated the results of brain connectivity networks and might erroneously enhance the network difference in clinical applications.

2090

Denoised diffusion spectrum imaging of white matter tracts in the brainstem

Cristina Granziera^{1,2,3,4}, Samuel St-Jean⁵, Alessandro Daducci³, Gunnar Krueger⁶, and Maxime Descoteaux⁷

¹Radiology, A.A. Martinos Center for Biomedical Imaging, Massachusetts General Hospital and Harvard Medical School, Charlestown, MA, United States, ²Neuroimmunology Unit, Neurology, Department of Clinical Neurosciences, Centre Hospitalier Universitaire Vaudois (CHUV) and University of Lausanne (UNIL), Lausanne, Switzerland, ³Signal Processing Laboratory 5 (LTS5), Ecole Polytechnique Fédérale de Lausanne (EPFL), Lausanne, Switzerland, ⁴Advanced Clinical Imaging Technology (HC CMEA SUI DI BM PI), Siemens Healthcare AG, Lausanne, Switzerland, ⁵Image Sciences Institute, University Medical Center Utrecht, Utrecht, Netherlands, ⁶Siemens Medical Solutions USA, Inc., Boston, MA, United States, ⁷Sherbrooke Connectivity Imaging Laboratory (SCIL), University of Sherbrooke, Sherbrooke, Canada

High-angular resolution diffusion (HARDI) MRI, like diffusion spectrum imaging-DSI, provides an accurate tool to investigate the complex white matter structure in the brainstem. However, due to the application of high b-values in the HARDI acquisition, the raw images are SNR limited (SNR<10). In this study, we applied a novel denoising algorithm to low-SNR DSI data. Our results showed that Generalized Anisotropy maps and tractography seeding the periaqueductal grey matter, a small structure in the mesencephalon, match more accurately the underlying anatomy when applying the denoising algorithm.

Traditional Poster

Interventional

Exhibition Hall

Wednesday, May 11, 2016: 13:30 - 15:30

2091



Monitoring temperature changes in the brain during high flow cold air cooling

Åsmund Kjørstad¹, Fabian Temme¹, Jens Fiehler¹, and Jan Sedlack¹

¹Neuroradiology, University Medical Center Hamburg-Eppendorf, Hamburg, Germany

Targeted temperature management is a treatment that seeks to reduce and control the body temperature. We demonstrate a novel localized cooling technique using high flow cold air applied nasally and orally to the airways by monitoring the brain temperature using gradient echo phase imaging at 3T. 2 healthy volunteers were investigated, with one subject being scanned twice and the other once. A significant temperature reduction ($p<0.05$) was seen in the inferior frontal lobe in all three experiments with an average cooling effect of -0.33°C . This demonstrates the feasibility of our proposed high flow cold air system.

2092

Early Assessment of MRgFUS Thalamotomy Using a Diffusion Weighted Steady State MRI Sequence in an In-vivo Porcine Model
Juan Camilo Plata¹, Sam Fielden², Bragi Sveinsson³, Brian Hargreaves⁴, and Craig Meyer²

¹Bioengineering, Stanford University, Las Vegas, NV, United States, ²Biomedical Engineering, University of Virginia, Charlottesville, VA, United States, ³Electrical Engineering, Stanford University, Palo Alto, CA, United States, ⁴Stanford University, Palo Alto, CA, United States

Early detection of thermal lesions generated using MR-guided focused ultrasound systems is critical for treatment feedback. Irreversible changes in the apparent diffusion coefficient (ADC) have been previously shown to be an early indicator for loss of viability in the prostate. Due to poor image quality using standard diffusion weighted imaging strategies inside the focused ultrasound system, radiologists rely on T2-weighted fast spin echoes (FSE) for lesion detection. T2-weighted changes due to lesion formation develop more slowly than ADC changes. We propose using a diffusion-weighted steady state sequence for early detection of thermal lesions inside the focused ultrasound system.

2093

Fast Temperature Estimation from Undersampled k-Space with Fully Sampled Center for Real Time MR Guided Microwave Ablations
Fuyixue Wang¹, Zijing Dong¹, Shuo Chen², Bingyao Chen³, Jiafei Yang³, Xing Wei³, Shi Wang², and Kui Ying²

¹Department of Biomedical Engineering, Tsinghua University, Beijing, China, People's Republic of, ²Key Laboratory of Particle and Radiation Imaging, Ministry of Education, Medical Engineering and Institute, Department of Engineering Physics, Tsinghua University, Beijing, China, People's Republic of, ³Department of Orthopedics, First Affiliated Hospital of PLA General Hospital, Beijing, China, People's Republic of

Real time thermometry is desirable for thermal therapy such as microwave ablation to ensure patient safety. MR temperature imaging using proton resonance frequency (PRF) shift technique can provide temperature maps during the treatment. In this work, we proposed a novel reconstruction framework that estimates temperature changes from undersampled k-space with a few fully sampled k-space points. Simulation studies, phantom heating experiments and human experiments were performed to validate the proposed method. The proposed method can provide temperature images with relatively high accuracy and short reconstruction time at a reduction factor

2094

Temporal Weighted Sliding Window SPIRiT with Golden Angle Radial Sampling for Real Time MR Temperature Imaging
Fuyixue Wang¹, Zijing Dong¹, Haikun Qi², Shi Wang³, Huijun Chen², and Kui Ying³

¹Department of Biomedical Engineering, Tsinghua University, Beijing, China, People's Republic of, ²Center for Biomedical Imaging Research, Department of Biomedical Engineering, School of Medicine, Tsinghua University, Beijing, China, People's Republic of, ³Key Laboratory of Particle and Radiation Imaging, Ministry of Education, Medical Engineering and Institute, Department of Engineering Physics, Tsinghua University, Beijing, China, People's Republic of

Real time MR temperature imaging during thermal therapy is beneficial for monitoring and controlling the treatment in clinical applications. In this work, we explored correlations in the temporal dimension of temperature imaging and proposed a novel method, temporal weighted sliding window SPIRiT using motion-insensitive golden angle radial sampling, to achieve real time temperature imaging. Through simulation studies and phantom heating experiments, we validated the ability of the proposed method to obtain temperature images with relatively high temperature accuracy at a reduction factor of 8.

2095

Spatially-segmented undersampled temperature map reconstruction for transcranial MR-guided focused ultrasound
Pooja Gaur¹, Xue Feng², Samuel Fielden², Craig H Meyer², Beat Werner³, and William A Grissom¹

¹Vanderbilt University, Nashville, TN, United States, ²University of Virginia, Charlottesville, VA, United States, ³University Children's Hospital, Zurich, Switzerland

Accelerated temperature imaging is desirable to improve spatiotemporal coverage during MR-guided focused ultrasound procedures in the brain. Circulating water prevents skull overheating, but also creates signal variations that disrupt correlations between images collected before and during treatment (which are relied on to overcome undersampling artifacts), leading to errors in temperature measurements. We propose a spatially-segmented iterative reconstruction method, which applies the k-space hybrid model to reconstruct temperature changes in the brain and a POCS method to reconstruct the image in the water bath. Separately reconstructing brain and water bath signal results in lower temperature error when undersampling k-space.

2096

3D UTE MR thermometry of frozen tissue: feasibility and accuracy during cryoablation at 3T
Christiaan G. Overduin¹, Jurgen J. Fütterer^{1,2}, and Tom W.J. Scheenen¹

¹Radiology, Radboud University Medical Centre, Nijmegen, Netherlands, ²MIRA Institute for Biomedical Engineering and Technical Medicine, University of Twente, Enschede, Netherlands

Our study assessed the feasibility and accuracy of 3D ultrashort TE (UTE) MR thermometry to dynamically track temperatures across frozen tissue during cryoablation on a clinical MR system at 3T. We demonstrated 3D UTE imaging to achieve measurable MR signal from frozen tissue down to temperatures as low as -40°C within a clinically realistic time-frame (~1min) and with sufficient spatial resolution (1.63mm isotropic). Using a calibration curve, we could derive 3D MR-estimated temperature maps of the frozen tissue, which showed good agreement with matched temperature sensor readings on statistical analysis.

2097

Acceleration of Temperature Mapping with an Ascending Threshold Low Rank Constraint (AscLR)
Fuyixue Wang¹, Zijing Dong¹, Bingyao Chen², Jiafei Yang², Xing Wei², Shi Wang³, and Kui Ying³

¹Department of Biomedical Engineering, Tsinghua University, Beijing, China, People's Republic of, ²Department of Orthopedics, First Affiliated Hospital of PLA General Hospital, Beijing, China, People's Republic of, ³Key Laboratory of Particle and Radiation Imaging, Ministry of Education, Medical Engineering and Institute, Department of Engineering Physics, Tsinghua University, Beijing, China, People's Republic of

Thermal therapies such as microwave ablation require temperature imaging with high temporal resolution to calculate thermal absorption and evaluate the curative effects of the ablation. Thus, acceleration techniques of data acquisition for MR temperature imaging using PRF shift technique are desirable. In this work, we explored the low rank property of k-t space in dynamic MR temperature imaging and proposed a novel fast reconstruction method AscLR with an ascending-threshold low rank constraint. Through simulation studies and microwave heating experiments, we validated the ability of the proposed method to provide relatively accurate temperature estimation at a reduction factor of 8.

2098

Feasibility of Absolute Thermometry of Knee Joint Cartilage using Spin-lattice Relaxation Time
Tomoya Kimura¹, Atsushi Shiina¹, Kenji Takahashi², and Kagayaki Kuroda^{1,3}

¹Course of Electrical and Electronic Engineering, Graduate School of Engineering, Tokai University, Hiratsuka, Japan, ²Department of Orthopaedic Surgery, Nippon Medical School, Tokyo, Japan, ³Center for Frontier Medical Engineering, Chiba University, Chiba, Japan

Temperature dependence of T1 of tissue water in the porcine knee joint cartilage in vitro was examined at 9.4T in comparison with that of the water proton resonance frequency. The absolute value of T1 at each temperature between room temperature and 60°C was reproducible. Hysteresis was negligible during heating and cooling processes. The correlation coefficient with temperature was higher than 0.998, and hence that with water proton chemical shift was also high (≥ 0.996). The temperature coefficient was 1.28%/°C at 30°C for heating and 1.24%/°C for cooling. These results suggested that T1 is a favorable index for thermometry of the knee joint cartilage under thermal therapies.

2099

A Hybrid Model Integrated with Correction of Susceptibility Induced Phase Error in Magnetic Resonance Thermometry
Kexin Deng¹, Yuxin Zhang¹, Yu Wang¹, Bingyao Chen², Xing Wei², Jiafei Yang², Shi Wang³, and Kui Ying³

¹Biomedical Engineering, Tsinghua University, Beijing, China, People's Republic of, ²Department of Orthopedics, First Affiliated Hospital of PLA General Hospital, Beijing, China, People's Republic of, ³Key Laboratory of Particle and Radiation Imaging, Ministry of Education, Department of Engineering Physics, Tsinghua University, Beijing, China, People's Republic of

The temperature dependency of susceptibility, especially for fat, could introduce errors in temperature estimation. To address this problem, a hybrid model integrated with susceptibility change induced phase is proposed to reduce the phase error. Simulation was conducted to validate the proposed model and a water-fat phantom was made and heated to illustrate the effect of susceptibility-induced phase error correction. The proposed model shows more accurate temperature estimation near the water-fat interface both in simulation and phantom heating experiment.

2100

Patient preparation by oral fluid intake for proton resonance frequency shift based MR thermometry in the pancreas
Cyril J Ferrer¹, Lambertus W Bartels¹, Marijn van Stralen¹, Chrit T.W Moonen¹, and Clemens Bos¹

¹University Medical Center Utrecht, Utrecht, Netherlands

Magnetic Resonance Imaging-guided High Intensity Focused Ultrasound has recently been suggested as an alternative treatment modality for pancreatic cancer that is non-invasive, and may be suited for treatment in cases where surgery is not an option. However, using proton resonance frequency shift based thermometry in this area is highly challenging, because of motion and air in the digestive tract near the pancreas. We have shown experimentally that patient preparation by filling the stomach and duodenum with juice can be a pragmatic solution for more precise temperature monitoring during MR-HIFU therapy particularly in the head of the pancreas.

2101

Magnetic Resonance Acoustic Radiation Force Imaging for interventional planning of HIFU therapy in the kidney
Johanna Maria Mijntje van Breugel¹, Martijn de Groot², Charles Mougenot³, Maurice AAJ van den Bosch², Chrit CW Moonen², and Mario AAJ Ries²

¹Radiology, University Medical Center Utrecht, Utrecht, Netherlands, ²University Medical Center Utrecht, Utrecht, Netherlands, ³Toronto, Canada

Hypothesis: MR-ARFI can be deployed in the kidney as an alternative for the thermal test shot at low power.

The employed respiratory gated MR-ARFI sequence in combination with a 450 W excitation tone-burst is sensitive enough to exceed the noise level and to clearly display the focal point of the HIFU beam. Both at 450W and at 1000W the displacement due to the radiation force coincided with the location of the temperature rise due to thermal ablation at equivalent power. Hence, radiation force in combination with a pencil beam navigator to compensate for respiratory motion is a reliable indicator of the location of the thermal lesion and might be an alternative to the low power thermal test shot in highly perfused organs such as the kidney.

2102

MR-Shear Wave Elasticity Imaging (SWEI) with Bipolar Motion-Encoding Gradients
Yuan Zheng¹, Michael Marx¹, Rachelle R. Bitton¹, and Kim Butts Pauly¹

¹Radiology, Stanford University, Stanford, CA, United States

We have demonstrated a method for shear wave elasticity imaging (SWEI). A shear wave was generated by a short focused ultrasound (FUS) pulse, and was tracked by collecting images with different delays (t_{delay}) between the FUS pulse and bipolar motion-encoding gradients (MEG). The time-of-flight (TOF) at each pixel was determined by the zero-crossing of the image phase as a function of t_{delay} . Based on the TOF map, a shear wave velocity map was generated in polar coordinates.

2103

Rapid HIFU refocusing based on MR-ARFI

Charles Mougenot¹, Samuel Pichardo^{2,3}, Steven Engler^{2,4}, Adam Waspe^{5,6}, Elodie Constanciel⁵, and James Drake^{5,6}

¹Philips Healthcare, Toronto, ON, Canada, ²Thunder Bay Regional Research Institute, Thunder Bay, ON, Canada, ³Electrical Engineering, Lakehead University, Thunder Bay, ON, Canada, ⁴Computer Science, Lakehead University, Thunder Bay, ON, Canada, ⁵Hospital for Sick Children, Toronto, ON, Canada, ⁶University of Toronto, Toronto, ON, Canada

Algorithms have been developed that use Magnetic Resonance Acoustic Radiation Force Imaging (MR-ARFI) to maximize the intensity at the focal point of a high intensity focused ultrasound beam in order to compensate for tissue related phase aberrations. A combination of two methods is proposed to achieve refocusing using a clinically acceptable acquisition time at 3T. Compensation of three aberrators inducing a relative intensity of 95%, 67.4% and 25.3% were successfully evaluated in a phantom to retrieve a relative intensity of 101.6%, 91.3% and 93.3% in 10 minutes or 103.9%, 94.3% and 101% in 25 minutes.

2104

High Speed, High Sensitivity MR-ARFI Using a Balanced Steady-State Free Precession Pulse Sequence

We have developed a novel MR-ARFI technique that makes use of transition band balanced steady-state free precession (bSSFP). Due to the strong dependence of image phase on the motion-encoded phase, this technique improves the sensitivity of MR-ARFI measurements over commonly used spoiled sequences. The proposed technique also features high speed, as an ARFI contrast image can be acquired in a few seconds. With its high speed and high sensitivity, the bSSFP-ARFI technique could be useful in confirming/calibrating the HIFU focal spot before thermal ablation treatment.

2105

A Novel method for developing clinical grade active devices dedicated to interventional MRI procedures
Korel Dursun Yildirim¹, Engin Baysoy¹, Zahid Sagiroglu², Çağla Özsoy¹, Ozgur Kocatürk¹, and Şenol Mutlu²

¹*Biomedical Engineering, Boğaziçi University, Institute of Biomedical Engineering, Istanbul, Turkey*, ²*Electrical and Electronics Engineering, Boğaziçi University, Institute of Graduate Studies in Science and Engineering, Istanbul, Turkey*

In this study, A Novel method and system were developed for developing clinical grade active devices dedicated to interventional MRI procedures. Before prototype fabrication, according to desired component dimensions, component values were simulated. With the exact dimensions used in simulations, component prototypes were fabricated via conductive ink as component material. Finally, simulation results and batch top measurements of component values were compared and reliability of simulation results were confirmed.

2106

Real-Time Hemodynamic Monitoring during MR Imaging and Interventional Procedures derived from induced Magnetohydrodynamic Voltages
T. Stan Gregory¹, Ehud Schmidt², John Oshinski³, and Zion Tsz Ho Tse¹

¹*College of Engineering, The University of Georgia, Athens, GA, United States*, ²*Radiology, Brigham and Women's Hospital, Boston, MA, United States*, ³*Radiology, Emory University Hospital, Atlanta, GA, United States*

Magnetic Resonance Imaging (MRI) is increasingly becoming the preferred diagnostic and interventional imaging modality for a variety of diseases. Despite the increasing clinical merit, practical implementation of these procedures in the clinic is oftentimes limited due to the high risk associated with these patient groups and the subsequent need for advanced physiological monitoring for each patient to be cleared for MRI imaging and interventional workflows. The presented method for beat-to-beat SV and continuous aortic flow monitoring within the MRI bore based on Magnetohydrodynamic Voltages (VMHD) induced onto 12-lead Electrocardiograms (ECG), enables MR imaging and MRI-guided interventional procedures for these patients.

2107

Accelerated MR Thermometry in the Presence of Uncertainties

Reza Madankan¹, Wolfgang Stefan¹, Christopher MacLellan¹, Samuel Fahrenholz¹, Drew Mitchell¹, R.J. Stafford¹, John Hazle¹, and David Fuentes¹

¹*Imaging Physics, MD Anderson Cancer Center, Houston, TX, United States*

Compressive sensing and sparse image reconstruction has received significant attention and has demonstrated potential in reduction of acquisition times. However, in many methods, under-sampling strategies are heuristically chosen and empirically validated. This often leads to a relatively larger number of k -space samples than needed for a particular application. The presented work develops a mathematically rigorous and quantitative methodology for k -space under-sampling with respect to model-based reconstruction of MR thermometry. The key idea of the proposed approach is to detect the useful samples of k -space in order to refine the model, and then the refined mathematical model is utilized to reconstruct the image.

2108

Kalman Filtered Bio Heat Transfer Model Based Self-adaptive Hybrid Magnetic Resonance Thermometry
Yuxin Zhang¹, Kexin Deng¹, Shuo Chen², Bingyao Chen³, Xing Wei³, Jiafei Yang³, Shi Wang², and Kui Ying²

¹*Biomedical Engineering, Tsinghua University, Beijing, China, People's Republic of*, ²*Key Laboratory of Particle and Radiation Imaging, Ministry of Education, Department of Engineering Physics, Tsinghua University, Beijing, China, People's Republic of*, ³*Department of Orthopedics, First Affiliated Hospital of PLA General Hospital, Beijing, China, People's Republic of*

The proposed Kalman filtered Bio Heat Transfer Model Based Self-adaptive Hybrid MR Thermometry, abbreviated as KalBHT hybrid algorithm, introduced the BHTE model to synthesize a window on the regularization term of the hybrid algorithm, which leads to a self-adaptive regularization both spatially and temporally with change of temperature. Further, to decrease the sensitivity to accuracy of the BHTE model, Kalman filter is utilized to update the window at each iteration time. Besides, the BHTE model is able to interpolate temperature maps during the acquisition and reconstruction of the next MR image to make real time temperature monitoring possible. To investigate the effect of the proposed model, phantom microwave heating experiment and *in-vivo* experiment with heating simulation were conducted in this study.

2109

Evaluation of the Effect of Trajectory Correction with Radial Sampling on Temperature Imaging
Tongxin Chen¹, Fuyixue Wang¹, Zijing Dong¹, Haikun Qi², Shi Wang³, Huijun Chen², and Kui Ying³

Radial sampling is sensitive to trajectory errors and can cause image distortions. To investigate the effect of trajectory errors on temperature imaging, we first evaluated the use of Trajectory Auto-Corrected Image Reconstruction (TrACR), a method to reconstruct radial images without trajectory errors, for radial temperature imaging. Then, we examined the feasibility of TrACR with only one calibration on dynamic temperature imaging based on the assumption that gradient errors are time-invariant. Through phantom heating experiments, we validated that both of the TrACR and the single-calibration TrACR can correct the errors of normal and golden angle radial sampling and provide improved temperature accuracy.

2110

On-Demand Dynamic Updating of the Temporal Resolution of Interleaved PRFS and T2 Temperature Mapping Methods for MR-HIFU
Steven Engler^{1,2}, Charles Mougenot³, Jochen Keupp⁴, Steffen Weiss⁴, Edwin Heijman⁵, and Samuel Pichardo^{1,6}

¹Thunder Bay Regional Research Institute, Thunder Bay, ON, Canada, ²Lakehead University, Computer Science, Thunder Bay, ON, Canada, ³Philips Healthcare, Toronto, ON, Canada, ⁴Philips Research, Hamburg, Germany, ⁵Philips Research, Eindhoven, Netherlands, ⁶Lakehead University, Electrical Engineering, Thunder Bay, ON, Canada

Temperature changes can be assessed in non-adipose tissue using proton resonance frequency shift MR-thermometry methods based on gradient-echo sequences, and in adipose tissue using apparent T2-mapping MR-thermometry methods based on multi-echo fast spin-echo sequences. It has been previously demonstrated that these sequences can be interleaved to simultaneously monitor temperature in all tissues. In this study we show the feasibility of controlling the sequence duty-cycle of the aforementioned interleaved scanning technique on-demand in order to dynamically change the temporal resolution of the two interleaved scans in response to actual temperature changes and the stage of the hyperthermia application.

2111

Model predictive filtering MR thermometry utilizing ultrasound beam modeling SAR predictions
Henrik Odéen¹, Scott Almquist², Joshua de Bever¹, and Dennis L Parker¹

¹Utah Center for Advanced Imaging Research, Department of Radiology, University of Utah, Salt Lake City, UT, United States, ²School of Computing, University of Utah, Salt Lake City, UT, United States

Thermal model based reconstruction of subsampled MR temperature data for focused ultrasound applications rely on acoustic and thermal parameters that are often analytically determined from a pre-treatment sonication. In this work we combine a thermal model based reconstruction method with ultrasound beam simulations to determine the specific absorption rate in order to avoid potentially damaging the tissue during a pre-treatment sonication. Proof-of-concept experiments are performed in a homogenous gelatin phantom and a gelatin phantom embedded with a plastic skull. The temperature estimations using US modeling show the same accuracy as those using a pre-treatment sonication.

2112

Investigation of temperature dependent changes in signal intensity, T1 and T2* in cortical bone
Henrik Odéen¹, Bradley Bolster², Eun Kee Jeong¹, and Dennis L Parker¹

¹Utah Center for Advanced Imaging Research, Department of Radiology, University of Utah, Salt Lake City, UT, United States, ²Siemens Healthcare, Salt Lake City, UT, United States

Measurements of changes in signal intensity and T1 relaxation time with temperature has been suggested for temperature monitoring in cortical bone during MR guided focused ultrasound treatments. In this study we compare changes in signal intensity, T1, and T2* with temperature using a 3D ultrashort echo time pulse sequence and a 2D gradient recalled echo pulse sequence with short TE. The effects of T1 and T2* change with temperature counteract each other making the change in signal intensity small, and therefore T1 and T2* appears to have the greatest sensitivity to changes in temperature.

2113

Simultaneous PRFS and T1 quantification using bSSFP for Temperature Monitoring
Mingming Wu¹, Matthew Tarasek², Axel Haase³, and Silke Lechner-Greite⁴

¹IMETUM, Technische Universität München, Garching, Germany, ²GE Global Research, Niskayuna, NY, United States, ³Technische Universität München, Garching, Germany, ⁴GE Global Research, Garching, Germany

Inversion Recovery prepared bSSFP sequence is used to quantify T1 and PRFS simultaneously based on a phase sensitive bSSFP readout. This technique allows for temperature mapping in both adipose and aqueous tissues at the same time. The feasibility of this method is shown with means of a cooling down experiment of a heterogeneous phantom. B0 drift correction is performed based on neighboring voxels in the fatty tissue.

2114

MRI-guided robotic arm (MgRA) to target deep brain nuclei in vitro
Yi Chen^{1,2}, Filip Sobczak¹, and Xin Yu^{1,2}

¹Research Group of Translational Neuroimaging and Neural Control, High-Field Magnetic Resonance, Max Planck Institute for Biological Cybernetics, Tuebingen, Germany, ²Graduate School of Neural Information Processing, University of Tuebingen, Tuebingen, Germany

A key challenge of the fiber optic-mediated multi-model fMRI methodologies is locating the fiber tip accurately and precisely to target deep brain nuclei. The requirement of precision is only several hundreds of microns in the animal brains. In this work, a multi degree of freedom robotic arm was developed with the use of step motors. The setup is in compatible with 14.1T MRI scanner. This MRI-guided robotic arm provides visually monitored fiber insertion to reduce the position error significantly in the perfused rat brain.

2115

Fast generation of pseudo-CT in the Head and Neck for MR guided Radiotherapy: Comparison of different UTE readout strategies
Michaela A U Hoesl¹, Peter R Seevinck¹, Matteo Maspero¹, Gert J Meijer², Jan J W Lagendijk¹, Bas W Raaymakers¹, and Cornelis A T van den Berg¹

¹*Center of Image Sciences, University Medical Center Utrecht, Utrecht, Netherlands*, ²*Radiotherapy, University Medical Center Utrecht, Utrecht, Netherlands*

Pseudo-CT (pCT) generation for Head and Neck region based on ultrashort echo time and radial undersampling is investigated in order to reach a clinical acceptable time frame for image acquisition. Two different UTE sequences, a 3D radial "kooshball" and a 3D radial "stack-of-stars" k-space acquisition are compared for image acquisition and pCT result using tissue classification and bulk density assignment. The results suggest that radial undersampling is feasible and thus results in a time frame of clinical relevance of 3 min for image acquisition plus 1 min for post-processing pCT generation.

2116

Iron-based T1 MRI contrast agent for MR-guided drug delivery from temperature sensitive liposomes
Esther Kneepkens¹, Adriana Fernandes², Klaas Nicolay³, and Holger Grüll^{3,4}

¹*Biomedical NMR, Biomedical Engineering, Eindhoven University of Technology, Eindhoven, Netherlands*, ²*Universidade de Lisboa, Lisbon, Portugal*, ³*Eindhoven University of Technology, Eindhoven, Netherlands*, ⁴*Philips Research, Eindhoven, Netherlands*

The aim of this study was to investigate the potential of Fe(III) N-succinyl deferoxamine (Fe-SDFO) as a safe T₁ contrast agent for encapsulation in temperature sensitive liposomes (TSLs) in order to visualize drug release from TSLs when using Magnetic Resonance-guided High Intensity Focused Ultrasound (MR-HIFU). Two TSLs were developed that contained either Fe-SDFO or doxorubicin. Both TSLs showed suitable release and stability characteristics in vitro. An *in vivo* proof-of-concept study was carried out in tumor-bearing rats treated with MR-HIFU. Treated tumors showed an increase in R₁ and future work aims to correlate the R₁ change with tumor drug concentrations.

2117

MR-guided focused ultrasound for antibody delivery in a brain metastasis model
Thiele Kobus^{1,2}, Yongzhi Zhang², Natalia Vykhotseva², and Nathan McDannold²

¹*Radiology and Nuclear Medicine, Radboud University Medical Center, Nijmegen, Netherlands*, ²*Radiology, Brigham and Women's Hospital, Boston, MA, United States*

We studied the treatment effect of HER2-targeting antibodies in combination with MR-guided focused ultrasound (FUS) to disrupt the blood-brain barrier in a breast cancer brain metastasis model. Tumors were implanted in rats and animals either received no treatment, six weekly treatments with antibodies, or six treatments of the antibodies combined with FUS-mediated BBB disruption. MR was used to guide the treatments and monitor tumor volume. 4/10 animals in the FUS+antibody-group responded to the treatment, but none of the other animals did. We could not explain with our results why only some of the FUS+antibody-animals responded and this requires further investigation.

2118

An ultrasound compatible rat RF array for MRI guided high intensity focused ultrasound
Xiao Chen¹, Rou Li¹, Changjun Tie¹, Xiaoqing Hu¹, Xiaoliang Zhang^{2,3}, Chao Zou¹, Xin Liu¹, Hairong Zheng¹, and Ye Li¹

¹*Paul C. Lauterbur Research Center for Biomedical Imaging, Shenzhen Institutes of Advanced Technology, CAS, Shenzhen, China, People's Republic of*, ²*Department of Radiology and Biomedical Imaging, University of California San Francisco, San Francisco, CA, United States*, ³*UCSF/UC Berkeley Joint Graduate Group in Bioengineering, San Francisco, CA, United States*

Due to MRI's unique capability of providing accurate, non-invasive and real-time target localization and temperature monitoring, MRI guided high intensity focused ultrasound (HIFU) has been a critical modality for imaged guided thermal therapy. We propose a 3 channel ultrasound compatible rat array to obtain high resolution and homogeneous rat brain images at 3T for temperature monitoring. Phantom and *in-vivo* imaging experiments in temperature mapping demonstrate the capability of the proposed array to provide homogenous and high SNR images and temperature map in the whole rat brain at 3T, which provides the possibility to perform MRI guided HIFU treatment *in-vivo*.

2119

MR-guided high intensity focused ultrasound mediated hyperthermia for targeted drug delivery to treat pancreatic cancer
Navid Farr¹, Yak-Nam Wang², Samantha D'Andrea³, Frank Starr², Ari Partanen⁴, Kayla Gravelle³, Donghoon Lee⁵, and Joo Ha Hwang^{1,3}

¹*Department of Bioengineering, University of Washington, Seattle, WA, United States*, ²*Applied Physics Laboratory, University of Washington, Seattle, WA, United States*, ³*Department of Medicine, University of Washington, Seattle, WA, United States*, ⁴*Philips Healthcare, Andover, MA, United States*, ⁵*Department of Radiology, University of Washington, Seattle, WA, United States*

Pancreatic cancer has one of the lowest survival rates because current therapies are ineffective. Dense stromal tissue and poor vascular perfusion limits drug penetration and uptake into the tumor. Growing evidence suggests that hyperthermia in combination with temperature sensitive liposomal drug delivery can lead to increased organ perfusion and drug extravasation resulting in high local drug

concentration. We performed MR-guided heating methods that enable accurate and precise spatial and temporal control of heating. Enhanced drug delivery was achieved to treat pancreatic tumors using Magnetic Resonance-guided High Intensity Focused Ultrasound (MR-HIFU) in conjunction with a heat triggered drug delivery system.

2120

An improved tracking technique for real-time MR-guided beam therapies in moving organs
Cornel Zachiu¹, Nicolas Papadakis², Mario Ries¹, Chrit Moonen¹, and Baudouin Denis de Senneville^{1,2}

¹Imaging Division, University Medical Center Utrecht, Utrecht, Netherlands, ²Institut de Mathématiques de Bordeaux, Bordeaux, France

Current methods for real-time MR-guided HIFU and EBRT interventions in moving organs rely on an algorithm that is sensitive to gray-level intensity variations from other sources than motion. In this work, an improved real-time tracking algorithm with increased robustness to such effects is proposed and experimentally compared to the existing methods. Results have shown a notable improvement in the quality of the motion estimates when the proposed method was used, while maintaining real-time capabilities. Our method was shown to be potentially beneficial for MR-guided HIFU and EBRT interventions in the abdomen, where cardiac activity might become problematic for current approaches.

2121

Monitoring tissue damage during MRgHIFU of bone metastases: relating intra-procedural DWI changes to post-procedural appearances
Sharon L Giles¹, Matthew Brown², Jessica M Winfield¹, David J Collins³, Ian Rivens⁴, John Civale⁴, Gail R ter Haar⁴, and Nandita M deSouza¹

¹CRUK Cancer Imaging Centre, The Royal Marsden Hospital NHS Foundation Trust and The Institute of Cancer Research, London, United Kingdom, ²Anaesthetic Department, The Royal Marsden Hospital NHS Foundation Trust, London, United Kingdom, ³CRUK Cancer Imaging Centre, The Institute of Cancer Research, London, United Kingdom, ⁴Therapeutic Ultrasound, The Institute of Cancer Research, London, United Kingdom

This study assessed intraprocedural DWI for detecting extra- and intra-osseous tissue change during MRgHIFU treatment of bone metastases by comparing appearances with post-procedural and Day-30 DWI and T1-W contrast-enhanced image appearances. Change in image appearances for n=9 patients was assessed by 2 observers assigning a consensus score where 0=no, 1=mild, 2=moderate and 3=striking change. Extra-osseous DWI changes were more conspicuous than intra-osseous DWI changes, but were less striking than immediate post-procedural contrast-enhanced changes. However, intra-procedural DWI changes significantly correlated with post-procedural and Day-30 DWI and contrast-enhanced changes, suggesting that intra-procedural DWI can provide an indicator of subsequent extra-osseous tissue damage.

2122

Response of MR Contrast Parameters in Tissues and Tissue Mimicking Phantoms to Histotripsy
Steven P Allen¹, Luis Hernandez-Garcia², Charles A Cain¹, and Timothy L Hall¹

¹Biomedical Engineering, University of Michigan, Ann Arbor, MI, United States, ²fMRI Lab, University of Michigan, Ann Arbor, MI, United States

We estimate the R2 relaxation rate and the apparent diffusion coefficient at 7T in a variety of in vitro tissues and tissue mimicking phantoms after they have been subjected to homogenization by ultrasonic cavitation (histotripsy). The estimated R2 rate of these lesions decreases with increased treatment so long as the lesions are made in materials with high iron content. When lesions are made in brain tissue or phantoms with low iron content, the R2 rate remains unperturbed by homogenization. The apparent diffusion coefficient increases with increasing treatment for all tissues and phantoms.

2123

T2-Mapping as a Predictor for Non-Perfused Volume in MRgFUS Treatments of Desmoid Tumors
Eugene Ozhinsky¹, Matthew D. Bucknor¹, and Viola Rieke¹

¹Radiology and Biomedical Imaging, University of California San Francisco, San Francisco, CA, United States

Desmoid tumors are benign but locally aggressive soft tissue tumors that arise from fibroblast cells. Focused ultrasound has shown promising results in reduction of tumor volume without significant side effects. Post-treatment contrast enhanced MR imaging allows assessment of the non-perfused volume (NPV), the gold standard assessment of the quantity of tumor ablation. However, safety concerns regarding heating of tissue after gadolinium injection prevent further treatment following the NPV assessment. We have shown that T2 mapping can be used to visualize the extent of ablation with focused ultrasound and be used as a predictor of NPV without the need for contrast injections.

2124

Validation of a 4D-MRI motion framework using an MRI-compatible motion phantom
Bjorn Stemkens¹, Rob HN Tijssen¹, Jan JW Lagendijk¹, and Cornelis AT van den Berg¹

¹Department of Radiotherapy, University Medical Center Utrecht, Utrecht, Netherlands

Geometric accuracy is vital for MR-guided radiotherapy. In this study we quantify the geometric fidelity of a retrospectively sorted 4D-MRI and 2D MS cine-MR acquisition, which serve as input for a motion model for dose accumulation mapping and tumor tracking. A linearly moving MRI-compatible motion phantom was used to quantify the positional error in the 4D-MRI and 2D MS acquisitions using a range of user-defined motion trajectories. Geometrical errors were found to be smaller than the voxel or pixel size.

2125

Robust and flexible real-time MRI-guided interventions using coRASOR-mediated passive device tracking
Peter Roland Seevinck¹, Frank Zijlstra¹, Jouke Smink², Sascha Krueger³, Frebus Jan van Slochteren^{4,5}, Steven A.J. Chamuleau⁴, Max A

The Co-RASOR imaging technique for high temporal resolution passive device visualization was implemented in the interventional Suite software package. This facilitates MRI-guided device tracking by combining high temporal resolution color overlays on top of high spatial resolution 3D roadmaps. Titanium needles were accurately depicted in two orthogonal planes with 2.5Hz framerate, facilitating easy freehand needle targeting. The ability to adapt crucial Co-RASOR reconstruction parameters, including the off-resonance value, during the intervention was demonstrated to provide unprecedented flexibility and robustness in device visualization.

Traditional Poster

RF Coils & Arrays

Exhibition Hall

Wednesday, May 11, 2016: 13:30 - 15:30

2126

Design of a forward view antenna for prostate imaging at 7 Tesla

Bart Steensma¹, Dennis Klomp¹, Nico van den Berg¹, Peter Luijten¹, Abe van der Werf², and Alexander Raaijmakers¹

¹University Medical Centre Utrecht, Utrecht, Netherlands, ²Machnet B.V., Maarn, Netherlands

The forward view antenna has been introduced as a novel antenna for ultrahigh field imaging. This study has investigated its potential for prostate imaging where the antenna is placed between the legs, to contribute as an additional element of an existing dipole antenna transceiver array. A significant increase in signal-to-noise ratio is expected because of the generally smaller distance towards the prostate from this side. Numerical simulations and *in vivo* scans show that signal-to-noise ratio in the prostate region increases as a result of adding the forward view antenna to the dipole antenna array.

2127

Multi-Channel Helical-Antenna Inner-Volume RF Coils for Ultra-High-Field MR Scanners

Pranav S. Athalye¹, Milan M. Ilic^{1,2}, Pierre-Francois Van de Moortele³, Andrew J. M. Kiruluta⁴, and Branislav M. Notaros¹

¹Department of Electrical and Computer Engineering, Colorado State University, Fort Collins, CO, United States, ²School of Electrical Engineering, University of Belgrade, Belgrade, Yugoslavia, ³Center for Magnetic Resonance Research, Department of Radiology, University of Minnesota, Minneapolis, MN, United States, ⁴Radiology Department, Massachusetts General Hospital, Harvard Medical School, Boston, MA, United States

RF coil design for human ultra-high-field scanners is an area of intense development, to address difficult challenges including RF excitation spatial heterogeneity and low RF efficiency. We present the development and testing of a novel category of multi-channel RF volume coil structures at both 7T and 10.5T based on a subject-loaded multifilar helical-antenna RF coil. Phantom data show excellent consistency between numerical simulations and experimental results with 4- and 8-channel helical-antenna coil prototypes. This design shows capability for multi-channel RF-transmit technology and parallel imaging. This work may help decide which coil structure should be used for future studies at 10.5T.

2128

A proton-free birdcage coil to enable zero-echo-time MRI without background signal

Markus Weiger¹, David Otto Brunner¹, Thomas Schmid¹, Romain Froidevaux¹, Manuela Barbara Rösler¹, Simon Gross¹, and Klaas Paul Pruessmann¹

¹Institute for Biomedical Engineering, University and ETH Zurich, Zurich, Switzerland

MRI of tissues with very short T2s below 1 ms, such as bone, lung, or myelin is usually performed with 3D radial sequences with ultra-short or even zero TE. However, with these techniques also signals from hardware parts are detected, in particular from the RF coils. Especially the ZTE method is highly sensitive also to materials with extremely short T2 of tens of us. In this work, it is demonstrated how the undesired signal is avoided during coil design and production, presenting for the first time a birdcage coil which is virtually free of proton signal.

2129

Traveling wave MR using an array of regular RF resonators

Xinqiang Yan^{1,2} and Xiaoliang Zhang³

¹Institute of Imaging Science, Vanderbilt University, Nashville, TN, United States, ²Radiology, Vanderbilt University, Nashville, TN, United States, ³Department of Radiology and Biomedical Imaging, University of California San Francisco, San Francisco, CA, United States

In this study, we investigate the feasibility of using regular microstrip resonators as RF array elements for traveling wave parallel imaging. In the proposed microstrip array, electromagnetic decoupling between the array elements is sufficient for the practical use. Additionally, geometric factors and diverse B1 fields from individual array elements can be obtained in a relatively large area in the magnet bore. Furthermore, in non-accelerated imaging applications, this decoupled multi-channel traveling wave method could improve sensitivity of traveling wave MRI, which is currently a main issue for traveling wave MRI.

Slotted-tube-resonator design for whole-body MR imaging at 14T
 Jérémie Daniel Clément¹, Arthur Magill², Hongxia Lei³, Özlem Ipek³, and Rolf Gruetter^{4,5,6}

¹CIBM-LIFMET, Ecole Polytechnique Fédérale de Lausanne, Lausanne, Switzerland, ²Forschungszentrum Jülich, Jülich, Germany, ³CIBM-ALT, Ecole Polytechnique Fédérale de Lausanne, Lausanne, Switzerland, ⁴LIFMET, Ecole Polytechnique Fédérale de Lausanne, Lausanne, Switzerland, ⁵Department of Radiology, University of Geneva, Geneva, Switzerland, ⁶Department of Radiology, University of Lausanne, Lausanne, Switzerland

The purpose of the study was to build a slotted-tube resonator for whole-body MR imaging at 14T. Flip angle maps were computed to assess the transmit field distribution in a phantom. A longitudinal coverage of 8 cm and flip angle homogeneity are observed and spin-echo images were acquired.

An 8Tx/32Rx RF Coil for 7T UHF Body MRI
 Stefan HG Rietsch^{1,2}, Stephan Orzada¹, and Harald H Quick^{1,2}

¹Erwin L. Hahn Institute for MR Imaging, University of Duisburg-Essen, Essen, Germany, ²High Field and Hybrid MR Imaging, University Hospital Essen, Essen, Germany

In order to allow for improved SNR and higher acceleration during image acquisition in the body at 7T, we present a coil with 8Tx/Rx microstrip line elements with meanders and 24Rx loop elements. This coil comprises 8 building blocks each consisting of one Tx/Rx element and 3 overlapping loops which are actively detuned during transmit. With about -19 dB reflection and an average decoupling of more than -30 dB, the SNR can be boosted by about 21% in the abdomen. Evaluation of g-factors as well as in vivo images of healthy volunteers in both abdomen and heart show promising results.

A 7T head coil with 16-channel dual-row transmit and 32-channel receive array for pTx applications and high SNR
 Shajan Gunamony¹, Jens Hoffmann¹, Gregor Adriany², Kamil Ugurbil², and Klaus Scheffler¹

¹Max Planck Institute for Biological Cybernetics, Tuebingen, Germany, ²Center for Magnetic Resonance Research, University of Minnesota, Minneapolis, MN, United States

Transmit elements arranged in multiple rows are beneficial in extending longitudinal coverage and achieve whole brain excitation at ultra-high field strengths. Furthermore, studies have shown that dual-row arrays produce less local SAR. Receive arrays shaped to the contours of the anatomy improves the signal-to-noise ratio (SNR) of the image. In this work, we develop a 2x8 transmit array for spin excitation in combination with a 32-channel high sensitive receive array for human brain imaging at 7T. Critical coil performance parameters like transmit efficiency and SNR were evaluated.

A 7-Tesla Transmit with 32-Channel Receive-Only Array Head Coil for fMRI
 Matthew Finnerty¹, Derick Petrey¹, Paul Taylor¹, Luke Beery¹, Tsinghua Zheng¹, Xiaoyu Yang¹, Hiroyuki Fujita^{1,2,3,4}, Se-Hong Oh⁵, Ken Sakaie⁵, and Mark Lowe⁵

¹Quality Electrodynamics, LLC, Mayfield Village, OH, United States, ²Department of Physics, Case Western Reserve University, Cleveland, OH, United States, ³Department of Radiology, University Hospitals of Cleveland, Cleveland, OH, United States, ⁴School of Information Technology and Electrical Engineering, The University of Queensland, Brisbane, Australia, ⁵Imaging Institute, Cleveland Clinic, Cleveland, OH, United States

While fMRI at 7-Tesla can provide clinically relevant increases in functional sensitivity over 3-Tesla, it also typically uses visual and audio stimulation devices that require additional space accommodations inside the RF coil. In order to accommodate a wider range of stimulus devices than possible with high filling factor designs, a head array coil utilizing a volume transmitter and 32 receive elements for 7-Tesla was constructed inside a versatile mechanical package to support fMRI and other applications.

A Hybrid 8 channel TR Dipole and 8 channel Rx Birdcage Body Coil Array for 7T
 Jan Paska^{1,2}, Martijn Cloos^{1,2}, Gillian Haemer^{1,2,3}, Bei Zhang^{1,2}, and Graham C Wiggins¹

¹Center for Biomedical Imaging, Department of Radiology, NYU School of Medicine, New York, NY, United States, ²Center for Advanced Imaging Innovation and Research (CAI2R), NYU School of Medicine, New York, NY, United States, ³The Sackler Institute of Graduate Biomedical Sciences, NYU School of Medicine, New York, NY, United States

A body array at 7T was optimized in simulation for potential hybrid elements, including dipoles, loops, and birdcage arrays. The optimal coil, consisting of 8 transmit/receive dipoles and an 8ch birdcage receive coil, was built and tested as proof of principle.

Design and construction of a triple-tuned RF probe for ²³Na/³¹P/¹H using traps
 Arthur W. Magill¹, Chang-Hoon Choi¹, Yonghyun Ha¹, and N. Jon Shah^{1,2}

¹Institute of Neuroscience and Medicine - 4, Forschungszentrum Juelich GmbH, Juelich, Germany, ²Department of Neurology, JARA, RWTH Aachen University, Aachen, Germany

Traps may be used to dual-tune an RF probe, either by splitting the resonance of a single tuned circuit, or by blocking coupling at the higher frequency when using a pair of resonant circuits. This work combines both methods to construct a triple-tuned probe consisting of a nested pair of loops. The inner loop incorporates two traps, one to prevent coupling to the outer loop, which is tuned to ¹H, and a second to simultaneously tune the loop to ²³Na and ³¹P. The probe is designed for use at 4T, with resonances at 45MHz (²³Na), 69MHz

2136

Design of quadrature-compensated double-tuned RF surface coil using trap circuits
Chang-Hoon Choi¹, YongHyun Ha¹, Arthur W. Magill¹, and N. Jon Shah^{1,2}

¹*Institute of Neuroscience and Medicine-4, Research Centre Juelich, Juelich, Germany*, ²*Faculty of Medicine, Department of Neurology, JARA, RWTH Aachen University, Aachen, Germany*

A novel double tuned (¹H/²³Na) butterfly/loop surface coil using LCC traps was designed whereby the sodium mode was operated in a quadrature. The performance of this coil was evaluated on a 4T whole-body scanner and compared with a single-tuned butterfly and a loop coil. Images obtained by the quadrature-compensated double-tuned RF coil were more uniform in each slice and the SNRs were slightly higher over the selected ROIs compared to those from the reference coils.

2137

Evaluation of Spiral Extended Monopole Antenna Array with Individual Whields (SEMAS) at 7T
Myung Kyun Woo¹, Chang-Ki Kang², and Zang-Hee Cho³

¹*Electrical and Computer Engineering, Seoul National University, Seoul, Korea, Republic of*, ²*Neuroscience Research Institute, Incheon, Korea, Republic of*, ³*Seoul National University, Seoul, Korea, Republic of*

This abstract is to propose and evaluate the Spiral Extended Monopole antenna Array with individual Shield (SEMAS) coil. This coil was compared with the original Monopole antenna Array (MA) coil and an Spiral Monopole antenna Array coil with no shield (SMA) coil. The SEMAS coil showed larger flip angle than the MA and SMA coils in the inferior areas of the brain and relatively uniform flip angles across the brain.

2138

End-Loaded Dipole Array for 10.5T Head Imaging
Russell Luke Lagore¹, Lance DelaBarre¹, Jinfeng Tian¹, Gregor Adriany¹, Yigitcan Eryaman¹, and J. Thomas Vaughan¹

¹*Center for Magnetic Resonance Research, University of Minnesota, Minneapolis, MN, United States*

The feasibility of human head imaging at 10.5T is demonstrated by the successful acquisition of *in vivo* porcine head images. This is achieved with an 8-element end-loaded dipole array resonant at 10.5T (447MHz). This dipole array is compared in terms of transmit efficiency and signal-to-noise ratio to a high-pass birdcage coil and loop array at 3T, 7T, and 10.5T. All coils share identical dimensions and element count. While both transmit arrays have comparable SNR performance at 7T, the dipole array is inferior in terms of transmit efficiency compared to the loop array and birdcage coil at all field strengths examined.

2139

Transceive surface array of dipole antennas for multi-transmit imaging at 3T
Aidin Ali Haghnejad¹, Shaihan J. Malik², Francesco Padormo², Cornelis A.T. van den Berg¹, Peter R. Luijten¹, Dennis W.J. Klomp¹, Joseph V. Hajnal², and Alexander J.E. Raaijmakers¹

¹*UMC Utrecht, Utrecht, Netherlands*, ²*King's College London, London, United Kingdom*

The birdcage body coil at 3T has some considerable disadvantages. Most of all it has very large power requirements. The use of local transmit arrays severely reduces these power requirements. In this study, we intend to explore the use of dipole antennas as transceive surface array elements at 3T. Three designs are investigated after which a strongly meandering dipole antenna is selected. An array of eight of these element is used for prostate imaging at 3T in a 8ch. multi-transmit MRI system. Using 8x200W input power, 12 μ T is achieved inside the prostate. Relatively homogeneous T2w images have been acquired

2140

A Mixed Dipole and Microstrip Transmit/Receive Array
Xinqiang Yan^{1,2}, John C. Gore^{1,2,3}, and William A. Grissom^{1,2,3}

¹*Institute of Imaging Science, Vanderbilt University, Nashville, TN, United States*, ²*Radiology, Vanderbilt University, Nashville, TN, United States*, ³*Biomedical Engineering, Vanderbilt University, Nashville, TN, United States*

Dipole and microstrip coils produce different and somewhat complementary B1 patterns and hybrid E-field distributions. Based this observation, we developed a 16-channel transmit/receive array for 7T head imaging by interleaving dipole and microstrip elements. Mutual coupling among any elements is <14 dB without including any other decoupling. Compared with 8-channel microstrip-only and dipole-only arrays, the proposed 16-ch dipole+microstrip array has a higher SNR gain and lower g-factor. No decoupling treatment is needed for the mixed dipole and microstrip array, so it can be used as a flexible transceiver array at ultrahigh field.

2141

Design of RF Coils Mixing Elements of Dissimilar Radiation Pattern
Ian RO Connell^{1,2} and Ravi S Menon^{1,2}

¹*Centre for Functional and Metabolic Mapping, Robarts Research Institute, London, ON, Canada*, ²*Department of Medical Biophysics, University of Western Ontario, London, ON, Canada*

At ultra-high field (UHF), multi-channel radio-frequency (RF) arrays have found increasing utility in mitigating wave-like behaviour during transmission (1), while continuing to provide increases in sensitivity to MRI signal with densely filled conformal receive arrays (2). In an

effort to more efficiently excite spin populations, and increase sensitivity to the transverse magnetization during relaxation, work into mixing array elements of dissimilar radiation pattern has been demonstrated to better encapsulate UHF ideal current patterns (3). Application of our method - coupling matrix synthesis - is used to robustly decouple a sample of these array-types.

2142

Cost-Efficient 7ch Rx Shoulder Array for 7T UHF MRI Featuring External Switchbox Detuning
Stefan HG Rietsch^{1,2}, Oliver Kraff¹, Stephan Orzada¹, Andrea Lazik³, and Harald H Quick^{1,2}

¹Erwin L. Hahn Institute for MR Imaging, University of Duisburg-Essen, Essen, Germany, ²High Field and Hybrid MR Imaging, University Hospital Essen, Essen, Germany, ³Department of Diagnostic and Interventional Radiology and Neuroradiology, University Hospital Essen, Essen, Germany

MRI at 7T and above opens the field for high resolution human imaging for example in the shoulder. In order to improve a present setup consisting of an 8ch Tx/Rx shoulder coil using microstrip line elements with meanders, we present an additional low cost 7ch Rx loop coil and utilize a simple approach for detuning of this coil during transmit via a custom built 8ch Tx/Rx switchbox. With the additional 7ch Rx coil a factor of 2 in SNR can be achieved in the center of the humeral head in proton-density weighted images with a spatial resolution of 0.4x0.4x2.5 mm³.

2143

Interchangeable Patient-Specific Receive-Only Carotid Coils for Simultaneous Imaging with Radio Frequency Head Coils at 3 Tesla
Michael J Beck¹, Dennis L Parker¹, Bradley D Bolster, Jr.², Seong-Eun Kim¹, J Scott McNally^{1,3}, Gerald S Treiman^{1,4,5}, and J Rock Hadley¹

¹Utah Center for Advanced Imaging Research, Salt Lake City, UT, United States, ²Siemens Healthcare, Salt Lake City, UT, United States, ³University of Utah Department of Radiology, Salt Lake City, UT, United States, ⁴University of Utah Department of Surgery, Salt Lake City, UT, United States, ⁵Veterans Affairs Department of Surgery (VASLCHCS), Salt Lake City, UT, United States

We developed interchangeable carotid coils that can image simultaneously with clinical head coils. Both 7 and 9 channel carotid coils were built to demonstrate the interchangeability concept. SNR results show that the 7 channel coil has ~4x the SNR and the 9 channel coil has ~3x the SNR of the commercial neck coil at the carotids. The carotid coils image simultaneously with a head coil providing greater coil sensitivity at the carotid bifurcation and extending total coverage from the carotid bifurcation to the circle of Willis.

2144

A Cervical Spine Array Coil with Volume Transmitter at 7 Tesla

Tsinghua Zheng¹, Matthew Finnerty¹, Xiaoyu Yang¹, Matthew Diprimio¹, Luke Beery¹, Paul Taylor¹, Johanna Vannesjo², Stuart Clare², and Hiroyuki Fujita^{1,3,4,5}

¹Quality Electrodynamics, LLC, Mayfield Village, OH, United States, ²FMRIB Centre, Oxford University, Oxford, United Kingdom, ³Physics, Case Western Reserve University, Cleveland, OH, United States, ⁴Radiology, University Hospital of Cleveland, Cleveland, OH, United States, ⁵School of Information and Electrical Engineering, the University of Queensland, Brisbane, Australia

A cervical spine array coil with a volume transmit coil for 7.0 Tesla was constructed and tested. The coil uses one partially shielded birdcage volume transmit coil for generating uniform excitation throughout the cervical spine region and an array of sixteen loop coils for receiving. Initial volunteer imaging demonstrated good coverage and uniformity along cervical spine.

2145

A 6 Channel Transmit-Receive Coil Array for 7T Cervical Spine Imaging
Zidan Yu^{1,2}, Bei Zhang¹, Jerzy Walczyk¹, Gang Chen^{1,2}, and Graham Wiggins¹

¹The Bernard and Irene Schwartz Center for Biomedical Imaging, Department of Radiology, New York University School of Medicine, New York, NY, United States, ²The Sackler Institute of Graduate Biomedical Sciences, New York University School of Medicine, New York, NY, United States

The cervical spine presents a challenging target for 7T RF coils. In this work, we describe a 6 channel transmit-receive cervical spine coil constructed like a cervical collar, wrapping around the back of the neck. In-vivo experiments demonstrate higher transmit efficiency, better B₁⁺ uniformity in the transverse plane and equivalent SNR compared to a RAPID Biomedical cervical spine coil.

2146

Printed Receive Coil Arrays with High SNR

Joseph Corea¹, Balthazar P. Lechene¹, Thomas Grafendorfer², Fraser Robb³, Ana Claudia Arias¹, and Michael Lustig¹

¹UC Berkeley, Berkeley, CA, United States, ²GE Healthcare, Stanford, CA, United States, ³GE Healthcare, Aurora, OH, United States

Extremely thin, lightweight, and flexible receive arrays can be achieved by the use of printed electronics. Coil arrays printed layer-by-layer from solution have shown potential to deliver a comfortable customized fit for many patients. However, relatively low SNR and poor mechanical robustness prevented these devices from performing to their full potential. Here we offer SNR within 3% of a traditionally made coil by using high quality polymeric films as dielectric layers in capacitors, high conductivity inks, and a mechanically robust fabrication processes using fewer printed layers and stronger connections. Using these techniques shoulder and elbow images of a volunteer were obtained.

2147

3D-printed RF Probeheads for Low-cost, High-throughput NMR
R. Adam Horch^{1,2} and John C. Gore^{1,2}

¹Vanderbilt University Institute of Imaging Science, Vanderbilt University, Nashville, TN, United States, ²Department of Radiology & Radiological Sciences, Vanderbilt University, Nashville, TN, United States

3D printing is demonstrated as a new means to fabricate complete RF probeheads for solution-state NMR. Current 3D printing methods yield mm-scale RF coils with integral sample chambers for self-contained NMR probes, and 3D-printed microcoils are imminent given ongoing advances in technology. The unique properties of 3D printing enable facile construction of potentially thousands of coils at low cost, giving way to dense coil arrays for high-throughput NMR and novel coil geometries.

2148

Inverse Design of Dielectric Pads based on Contrast Source Inversion
Wyger Brink¹, Jeroen van Gemert², Rob Remis², and Andrew Webb¹

¹*Radiology, Leiden University Medical Center, Leiden, Netherlands*, ²*Circuits and Systems, Delft University of Technology, Delft, Netherlands*

The design of passive dielectric pads can be an exhaustive procedure with many degrees of freedom to address. In this study we developed a constrained inverse design approach based on the contrast source inversion method. The procedure can yield design guidelines efficiently, enabling automated design of dielectric pads.

2149

Improvement of B1+ Homogeneity along Z-Direction Using Top-Hat Dipole-Antenna pTX Array for Body Imaging at 7 Tesla
Suchit Kumar¹, Joshua Haekyun Park^{2,3}, Young-Seung Jo^{2,4}, Jeong-Hee Kim^{2,3}, Chulhyun Lee², and Chang-Hyun Oh^{1,4,5}

¹*Department of Biomicrosystem Technology, Korea University, Seoul, Korea, Republic of*, ²*Korea Basic Science Institute, Cheongju, Chungcheongbuk-do, Korea, Republic of*, ³*Industrial Technology Institute, Korea University, Sejong City, Korea, Republic of*, ⁴*Department of Electronics and Information Engineering, Korea University, Seoul, Korea, Republic of*, ⁵*ICT Convergence Technology Team for Health&Safety, Korea University, Seoul, Korea, Republic of*

In ultra-high field (UHF), body imaging suffers from B1 inhomogeneity due to shorter wavelength. A range of new RF coil designs has been proposed to overcome this problem. But, B1 inhomogeneity in the coronal plane still exists due to limited coverage. In this work, a novel design of an 8-channel top-hat dipole antenna with parallel transmission is proposed to improve B1+ homogeneity along Z-direction. B1+ field distribution and SAR field were simulated in FDTD solver. Comparison with original dipole antenna array confirms the improved B1+ homogeneity in proposed design.

2150

TMS positioning in MRI using NMR probes
Yi-Cheng Hsu¹, Ying-Hua Chu¹, Pu-Yeh Wu¹, Shang-Yueh Tsai², and Fa-Hsuan Lin¹

¹*Institute of Biomedical Engineering, National Taiwan University, Taipei, Taiwan*, ²*Institute of Applied Physic, National Chengchi University, Taipei, Taiwan*

We propose a method and a system to precisely place the TMS coil inside the MRI using NMR probes. The positioning can be completed in 0.1 s with high translation (0.015 mm) and rotation precision (0.0047°) as well as low bias (~0.8 mm in 50 mm FOV).

2151

Copper plating of conductive silver ink coils for improved SNR performance
J. Rock Hadley¹, Emilee Minalga¹, and Dennis L. Parker¹

¹*Radiology, University of Utah, Salt Lake City, UT, United States*

This work tests how much loop conductivity and SNR is improved with copper plating of the silver ink trace. Coils made with a silver ink base and different amounts of copper plating were compared against solid copper. This work demonstrates that copper plating of silver ink coils is possible and it indicates that significant improvements in coil trace conductivity can be achieved. Consequently, the SNR performance of silver ink coils that have been plated with copper improves over silver ink coils without plating.

2152

13C RF coil combination for cardiac and abdominal human and pig studies
Steffen Ringgaard¹, Rolf F Schulte², James Tropp³, Carsten Kögler⁴, Titus Lanz⁴, Miguel A Navarro⁵, Jan Henrik Ardenkjaer-Larsen^{6,7}, Fraser J Robb⁵, Hans Stødkilde-Jørgensen¹, and Christoffer Laustsen¹

¹*MR Research Centre, Aarhus University, Aarhus, Denmark*, ²*GE Global Research, Munich, Germany*, ³*GE Healthcare, Fremont, CA, United States*, ⁴*Rapid Biomedical, Rimpar, Germany*, ⁵*GE Healthcare, Cleveland, OH, United States*, ⁶*GE Healthcare, Copenhagen, Denmark*, ⁷*DTU, Copenhagen, Denmark*

We have developed and validated a dedicated coil system for human and large animal hyperpolarised 13C measurements. The system consists of an outer two-element transmit coil and an inner 16-element receive coil. It was validated by hyperpolarised experiments in two healthy pigs using a multi-echo spiral CSI sequence. The 13C metabolic images showed good SNR and there was low noise correlation between the receive elements. Hence, the coil system is promising for future human hyperpolarised examinations.

2153

A new monopole intravascular coil with three parasitic elements optimized for MRI 1.5 T
mohammad mohammadzadeh^{1,2} and alireza ghasempour Shirazi¹

¹*ICT, University of applied science and technology, Tehran, Iran*, ²*Shahid Beheshti, Tehran, Iran*

Monopole coil has a thin and flexible structure provides high-resolution MR images from the internal vessels such as aorta and coronary

arteries. However, its SNR homogeneity decreases at higher Tesla MRI systems, leading to increasing the image artifact caused by the wall movement which is not fully compensated using the post processing algorithms. In this study, we introduced a monopole coil with tree parasitic elements and compared its ISNR (Intrinsic SNR) magnitude and distribution homogeneity to a conventional monopole coil with one parasitic element for MRI 1.5 T at 64MHz . We optimized the coil geometry using a fast genetic algorithm written in MATLAB and performed the simulation of the ISNR indices by Involving HFSS and MATLAB inside a saline phantom.

2154

Experimental Implementation of Array-compressed Parallel Transmission at 7T
Zhipeng Cao^{1,2}, Xinqiang Yan^{1,3}, and William A. Grissom^{1,2,3}

¹*Vanderbilt University Institute of Imaging Science, Vanderbilt University, Nashville, TN, United States*, ²*Biomedical Engineering, Vanderbilt University, Nashville, TN, United States*, ³*Radiology, Vanderbilt University, Nashville, TN, United States*

With a constructed 8 channel transmit array and a tunable 2 channel-to-8 coil compression matrix, the array-compressed parallel transmit pulse design is demonstrated on 7T MRI through B1+ mapping and accelerated spiral excitation. Results showed more accurate excitation pattern can be achieved with the compression matrix hardware and compressed parallel transmit pulses than two-channel CP-mode pulses.

2155

Array-compressed parallel transmit pulse design with optimized coil-channel assignments and coil pruning for simultaneous multislice and 3D reduced-field-of-view excitations
Zhipeng Cao^{1,2}, Xinqiang Yan^{1,3}, and William A. Grissom^{1,2,3}

¹*Vanderbilt University Institute of Imaging Science, Vanderbilt University, Nashville, TN, United States*, ²*Biomedical Engineering, Vanderbilt University, Nashville, TN, United States*, ³*Radiology, Vanderbilt University, Nashville, TN, United States*

An improved array-compressed parallel transmit pulse design is proposed and validated to optimally connect transmit arrays with a large number of elements to a few transmit channels. It is further demonstrated to achieve better performance with array-compressed coil designs than conventional designs for multiband RF shimming for human brain imaging and 3D spatially selective excitation for human occipital lobe imaging.

2156

Increasing transmit coil efficiency without local transmit coils: a novel device for locally concentrating B1
Tracy Wynn¹, Olli Friman¹, and Randy Duensing¹

¹*Technology Architecture, Philips/Invivo, Gainesville, FL, United States*

Bore size increases can contribute to decreased efficiency of transmit body coils, but modern protocols often increase the requirements for B1 power. This paper describes a novel solution for concentrating B1 power without the use of a traditional local transmit coil, based on the observation that roughly half of the transmit field from a traditional birdcage coil comes from the end rings. A dual-ring structure, modeled on a birdcage without rungs, was built and shown to enable head imaging with up to a 30% reduction in required RF input power. Uniformity was maintained.

2157

SNR simulations including coupled preamplifier noise
Matthias Malzacher^{1,2}, Markus Vester³, Robert Rehner³, Christopher Stumpf¹, and Patrick Korf¹

¹*Friedrich-Alexander University Erlangen-Nuremberg, Erlangen, Germany*, ²*Computer Assisted Clinical Medicine, University Heidelberg, Medical Faculty Mannheim, Mannheim, Germany*, ³*Siemens Healthcare GmbH, Erlangen, Germany*

Using reciprocity, available SNR from a receive coil array can be calculated by maximizing B₁- at the target voxel for unit input power. However, for strongly coupled or lightly loaded coil elements, the noise figure degradation due to coupled preamplifier noise becomes significant. It is shown here that this effect can be modeled by power loss in a resistive attenuator at each coil port. Thus, it is now possible to simulate any coil configuration, including those where coil coupling cannot be neglected.

2158

New decoupling method for receiver arrays with small coils
Xueming Cao¹, Elmar Fischer¹, Oliver Gruschke², Jan Korvink², Jürgen Hennig¹, and Maxim Zaitsev¹

¹*University Medical Center Freiburg, Freiburg, Germany*, ²*Karlsruhe Institute for Technology, Karlsruhe, Germany*

In receiver coil arrays, the most commonly used decoupling methods are overlap together with low-input-impedance preamplifiers. But very small receiver coils can not be decoupled effectively with these two methods. A new decoupling method, which is helpful for receiver coil arrays with very small coils, is developed here. The coil arrays decoupled with this method have less noise correlation and better performance in highly accelerated imaging in the sample periphery.

2159

Effect of the RF Shield on the Mutual Coupling Between Adjacent and Non-Adjacent Array Elements
Andreas Pfrommer¹, Nikolai I Avdievich¹, and Anke Henning^{1,2}

¹*Max Planck Institute for Biological Cybernetics, Tuebingen, Germany*, ²*Institute for Biomedical Engineering, UZH and ETH Zurich, Zurich, Switzerland*

In this study we investigated the effect of an RF shield on the mutual coupling between adjacent and non-adjacent array elements in a simple model mimicking our previously developed cylindrical eight channel transceiver head array. Both numerical EM simulations and experimental measurements suggest that at 124 MHz and 400 MHz an RF shield can substantially decrease S_{12} for non-adjacent-array elements.

2160

Transmission Line Resonator Segmented with Series Capacitors
Vitaliy Zhurbenko¹, Vincent Boer², and Esben Thade Petersen²

¹*Technical University of Denmark, Kgs. Lyngby, Denmark*, ²*Danish Research Centre for Magnetic Resonance, Centre for Functional and Diagnostic Imaging and Research, Copenhagen University Hospital Hvidovre, Hvidovre, Denmark*

Transmission line resonators are often used as coils in high field MRI. Due to distributed nature of such resonators, coils based on them produce inhomogeneous field. This work investigates application of series capacitors to improve field homogeneity along the resonator. The equations for optimal values of evenly distributed capacitors are presented. The performances of the segmented resonator and a regular transmission line resonator are compared.

2161

Tunable Defected Ground Structure for Decoupling Monopole Antenna Transmit/Receive Arrays in 7T MRI
Xinqiang Yan^{1,2} and William A. Grissom^{1,2,3}

¹*Institute of Imaging Science, Vanderbilt University, Nashville, TN, United States*, ²*Radiology, Vanderbilt University, Nashville, TN, United States*,
³*Biomedical Engineering, Vanderbilt University, Nashville, TN, United States*

Radiative dipole and monopole coil arrays are increasingly used for ultrahigh field MRI, but few decoupling methods have been proposed for radiative arrays. To overcome this problem, we propose a Tunable-Defected-Ground-Structure (TDGS) method to decouple monopole arrays at 7T. This concept was successfully validated by EM simulation, bench test and MR experiments. By using the TDGS method, the cross-talk between two closely-spaced monopoles was reduced from -7 dB to -25 dB. It was also found that the TDGS method had little effect on the original B_1 fields of the individual monopole elements.

2162

Electric-LC resonators decoupling approach for monopole antenna arrays at 7T
Xinqiang Yan¹ and Xiaoliang Zhang²

¹*Key Laboratory of Nuclear Analysis Techniques, Institute of High Energy Physics, Chinese Academy of Sciences, Beijing, China, People's Republic of*, ²*Department of Radiology and Biomedical Imaging, University of California San Francisco, San Francisco, CA, United States*

Induced current elimination (ICE) method could efficiently reduce the element coupling in monopole and dipole arrays, and ultimately improve their SNR and parallel imaging performance. Nevertheless, in current ICE method, the decoupling element has possible effect on the original B_1 field, leading to dark spots at the areas near decoupling elements. To address such effects, we introduce a new structure, electric-LC (ELC) resonator, for decoupling monopole arrays. Based on the simulation and experimental results, ELC resonators could also effectively reduce the coupling of monopoles and meanwhile have less influence on the original B_1 fields of the elements.

2163

RF coil design using circulant and block circulant matrix algebra
Sasidhar Tadanki¹

¹*Electrical and Computer Engineering, Worcester Polytechnic Institute, Worcester, MA, United States*

In this work a simple, efficient method to designing a transmission line volume resonator coil for MR applications is presented. A multiconductor transmission line is represented as a multiport network using its port admittance matrix. Closed form solutions for port resonant mode frequencies are calculated by solving the eigenfunctions of the port admittance matrix using block matrix and circulant block matrix algebra. Detailed analysis and simulated results are presented and compared with standard published results. A dual-tuned surface coil is developed to demonstrate the efficacy of the proposed method.

2164

Analytical theory, circuit and numerical simulations to design a splittable degenerate birdcage for MSK applications.
Riccardo Stara^{1,2,3}, Fabio Morsani², Gianluigi Tiberi^{4,5}, Maria Evelina Fantacci^{2,3}, Massimo Marletta⁶, Virna Zampa⁶, Brian Rutt¹, Alessandra Retico², and Michela Tosetti⁵

¹*Stanford University, Stanford, CA, United States*, ²*Istituto Nazionale di Fisica Nucleare (Pisa), Pisa, Italy*, ³*Dipartimento di Fisica, Universita' di Pisa, Pisa, Italy*, ⁴*IMAGO7, Pisa, Italy*, ⁵*IRCCS Stella maris, Calambrone (Pisa), Italy*, ⁶*Dipartimento di radiologia diagnostica ed interventistica AOU, Pisa, Italy*

The degenerate birdcage is not a common design for ultra-high field transmit array due to the technical difficulties in its construction, such as the interdependence of tuning and degeneracy on the value of capacitors. We present here a combination of an analytical theory, circuit simulations and numerical simulations to be used for an efficient design and construction of the degenerate birdcage at 7T. We demonstrate satisfactory performance in terms of decoupling, B_1^+ homogeneity and B_1^+ efficiency on the workbench and with scanner measurements on phantoms and human volunteers.

2165

Simulation, measurement, and optimization of a microcoil design for MR Microscopy at 9.4 T

MR micro coils provide high SNR images of the mass limited samples. To increase the coil sensitivity and then the image SNR, microcoils geometries are adapted to the sample dimension. However, differences between magnetic susceptibility of the coil conductor and its surrounding materials distorts the B0 magnetic fields homogeneity across the sample. In this study, we measured 2D maps of a solenoid of 1mm diameter and compared them with the simulated results at 9.4 T. Considering the good agreement of the computed and measured maps, effects of the shimming and susceptibility matching processes were assessed in removing the B0 fields inhomogeneities. Simulated results verify that shimming coils are not able to fully cancel the B0 field inhomogeneities but embedding the micro coils in susceptible materials will remove the B0 inhomogeneity completely.

2166

Numerical Comparison of Stacked and Planar Coil Reception Arrays for Prostate MRI at 3 T
Jorge Chacon-Caldera¹, Javier Uranga Solchanga¹, Paulina Kozioł^{1,2}, and Lothar R Schad¹

¹Computer Assisted Medical Medicine, Medical Faculty Mannheim, Heidelberg University, Mannheim, Germany, ²Department of Medical Physics and Biophysics, Faculty of Physics and Applied Computer Science, AGH University of Science and Technology, Krakow, Poland

Prostate MRI is commonly performed using endorectal coils which are invasive. This is done since body planar arrays are not sensitive enough for prostate imaging. Increasing sensitivity of an array for deep structures in the body is not trivial. In this study, we extended the traditional stacked figure-8 and single loop quadrature pair to add more single loop coils and enhanced the sensitivity at the depth of the prostate without increasing the field over a larger lateral area. We compared these arrays to classical planar approaches and found a factor 1.35 increase in maximum localized $|B_1|$ using numerical simulations.

2167

Improvement of B_1^+ Homogeneity and Reduction of Transmit RF Power Using 4-channel Regional RF Shimming in L-spine Imaging at 3T
Yukio Kaneko¹, Kosuke Ito², Masahiro Takizawa², Yoshihisa Soutome^{1,2}, Hideta Habara^{1,2}, Yusuke Seki¹, Tetsuhiko Takahashi², Yoshitaka Bito², and Hisaaki Ochi¹

¹Research and Development Group, Hitachi Ltd., Tokyo, Japan, ²Healthcare Company, Hitachi, Ltd., Chiba, Japan

The B_1^+ inhomogeneity in a human body increases as the strength of a static magnetic field increases. Previous studies showed the effect of the number of RF transmit channels in RF shimming. However, the effect for a partial region of the lumbar spine in a sagittal plane has not yet been investigated. In this study, the effect of the number of RF transmit channels for regional RF shimming in the lumbar spine region was investigated. The results show that 4-channel RF shimming can contribute to improving B_1^+ homogeneity and reducing the transmit RF power more than 2-channel RF shimming.

2168

Optimized MRI RF Body Coil for Integration with In-bore Therapy or Biopsy System
Jiaqi Li¹, Masahiro Fujimoto¹, Amy Sue Meyers¹, Qiong Zhang², and Huaiyu Dong²

¹GE Healthcare, Waukesha, WI, United States, ²GE Healthcare, Beijing, China, People's Republic of

An optimized MRI RF coil for integration with in-bore therapy or biopsy system is discussed. The RF coil is optimally designed into an open Ω shape to allow a much bigger room for therapy or biopsy system. Horizontal rails as well as coil support brackets are integrated with body coil. Such that, the in-bore treatment system can have bigger space and more power. The optimized design also separated HIFU or SWL sub-assembly from high voltage RF parts, which reduces EMI between those two, and safety issue due to liquid leakage from HIFU or SWL sub-assembly is also greatly reduced.

Traditional Poster

MR Engineering Beyond RF Coils

Exhibition Hall

Wednesday, May 11, 2016: 13:30 - 15:30

2169

Frequency-agnostic inexpensive modular FDM receiver design
Edwin Eigenbrodt¹ and Mary Preston McDougall²

¹Texas A&M University, College Station, TX, United States, ²Biomedical Engineering, Texas A&M University, College Station, TX, United States

Here we describe a six channel inexpensive FDM receiver, agnostic to the nuclei of interest or magnetic field strength, implemented straightforwardly using off-the-shelf products, portable, and easily used in conjunction with any system with a single trigger line. The architecture is straightforwardly scalable to 16 channels at a cost of approximately \$1300 per channel. This work describes the receiver architecture and the capabilities are demonstrated by acquiring six channel images from a previously reported mouse array coil, two-channel ¹³C spectra, and comparing the SNR of the receiver to the Varian Inova system.

2170

Scalable, In-Bore Array Receiver Platform for MRI
Jonas Reber¹, Josip Marjanovic¹, David Otto Brunner¹, Andreas Port¹, and Klaas Paul Pruessmann¹

With the number of RF receive channels cable routing and data handling becomes and increasing problem in particular for demanding applications requiring high acquisition duty cycles and bandwidths. To overcome this we present an MR acquisition platform that is capable of acquiring MR signal in-bore and scales its data handling ability with the number of channel. Furthermore the system provides ample, configurable real-time computational power for advanced in-line data processing and low-latency applications.

2171

Frequency Translation for 1H Decoupled Multichannel ¹³C Spectroscopy
Stephen Ogier¹, Mary McDougall^{1,2}, and Steve Wright^{1,2}

¹Electrical and Computer Engineering, Texas A&M University, College Station, TX, United States, ²Biomedical Engineering, Texas A&M University, College Station, TX, United States

Frequency translation is a technique that uses radiofrequency mixers to convert the received signal from one nucleus to another. This technique can be used to adapt ¹H array receivers for use with other nuclei, such as ¹³C. This facilitates the use of arrays with less sensitive nuclei, which will benefit greatly from the SNR enhancement arrays provide.

Frequency translation has been shown to provide a flexible means of adapting receivers for use with other nuclei without signal degradation or corruption.

2172

Explorations of Non-Magnetic Amplifiers for MRI Applications
Sawson Taheri¹, Pascal Stang², John Pauly¹, and Greig C. Scott¹

¹Stanford University, Stanford, CA, United States, ²Mountain View, CA, United States

Broadcast amplifier pallets offer a low-cost solution in creating MR compatible non-magnetic transmit array systems capable of operating in both 1.5T and 3T B_0 fields. We developed a locally deployable PTx array utilizing readily available broadcast amplifier pallets. The conversion of a conventional slow-gated, non-linear FM band (88-108MHz) 1kW pallet to a fast-gated, linear non-magnetic amplifier targeting transmit array deployment in both 1.5T and 3T B_0 fields is demonstrated.

2173

Digital RF Current Sources for safer, adjust-free MRI scanners
Oliver Heid¹, Juergen Heller¹, Xiaoyu Yang², and Hiroyuki Fujita²

¹Corporate Technology, Siemens AG, Erlangen, Germany, ²Quality Electrodynamics, Mayfield Village, OH, United States

We propose direct digital RF switch mode current sources to eliminate image artifacts due to B_1 field amplitude errors without time consuming transmitter calibration and adjustment. In difference to all known linear analog or switch mode RF amplifiers our proposal maintains high efficiency under modulation, and thus provides sufficient average RF power even at low flip angles, e.g. in FLASH sequences. We thus avoid significant, safety critical transmitter oversizing as in conventional MRI scanners.

2174

A Q-switch system for an MRI RF coil operating at 2.5 MHz.
Nicholas R. Payne¹, Lionel M. Broche¹, and David J. Lurie¹

¹Bio-Medical Physics, University of Aberdeen, Aberdeen, United Kingdom

RF coil ringing following an excitation pulse is particularly problematic at low frequency and can prevent the measurement of signals from short-T2 samples or tissues; this issue can be addressed by Q-switching. A Q-switch circuit, designed to operate at 2.5 MHz and reduce the dead-time of an RF coil following an RF pulse, is described. The resulting reduction in coil dead-time allows signal to be detected earlier and RF pulses to be spaced closer together. MOSFETs are used in our design to isolate RF from the DC control system and the circuit can be inductively coupled to any RF coil. The device was found to reduce the duration of coil ringing by a factor of five.

2175

High Powered GaN HEMT devices for Low Powered Q-spoiling at 3T MRI
Jonathan Y Lu¹, Thomas Grafendorfer², Tao Zhang¹, Kamal Aggarwal¹, Fraser Robb³, John M Pauly¹, and Greig C Scott¹

¹Electrical Engineering, Stanford University, Stanford, CA, United States, ²Advanced Coils, GEHC Coils, Stanford, CA, United States, ³GE Healthcare, Aurora, OH, United States

We examine different power depletion mode GaN HEMT devices for use in low power MRI Q-spoiling at 3T. These devices range in their on-resistance and off-capacitance, yielding different blocking impedances. We prototyped FET based Q-spoiling surface coils and compared SNR performances with conventional PIN diode Q-spoiling coils. Our coils enable Q-spoiling when unpowered providing a good safety feature. We tested the robustness of the FET devices in the coils by running fast spin echo sequences at 3T. The SNR performances of our FET based coils are comparable with conventional PIN diode coils without the high current draw.

2176

Analysis of Eddy Currents for High Field RF Coil Design
Yu Li¹, Fangfang Tang¹, Bassem Henin¹, Fabio Freschi^{1,2}, Feng Liu¹, and Stuart Crozier¹

¹School of ITEE, The University of Queensland, Brisbane, Australia, ²Department of Energy, Politecnico di Torino, Torino, Italy

Eddy currents are inevitably induced in the electrically conductive surroundings including the magnet cryostat vessel, RF coil, RF shield and other peripheral metallic structures. This results in image distortion and artefacts. In order to control eddy currents, some studies have also discussed the issue of eddy currents on magnet cryostat vessel and RF shields. In this work, the eddy currents on a 12 channel micro-strip RF array head coil for 7T MRI were analysed and compared with that of a slotted, double-sided copper RF shield. A preliminary approach is proposed to reduce the eddy current effect, without compromising RF performance.

2177

Proton Imaging at 4.7 T Using a Piezoelectric-based Automation System for impedance matching of Monolithic Transmission Line Resonators

Zhoujian Li¹, Sajad Hosseinezadian¹, Geneviève Guillot¹, Georges Willoquet¹, Laurène Jourdain¹, Marie Poirier-Quinot¹, Luc Darrasse¹, and Jean-christophe Ginefri¹

¹*Laboratoire d'Imagerie par Résonance Magnétique Médicale et Multi-Modalités, Université Paris-Sud, Orsay, France*

We have implemented a piezo-motor based automation system for contactless impedance matching of a monolithic Transmission Line Resonator (TLR) operating at 4.7 T. The automation system successfully achieved inductive matching to more than -30dB of the TLR inside the magnet and no artifacts was observed on the image of a rectangular box-shaped water phantom. A second image, acquired in the same condition but in the presence of another piezo-motor fixed on a side of the sample revealed that the close proximity of the piezo-motor to the sample brings B1-field inhomogeneity.

2178

Spherical droplet design and adiabatic excitation for enhanced performance and flip angle control of NMR field probes

Jennifer Nussbaum¹, Simon Gross¹, David O. Brunner¹, Christoph Barmet^{1,2}, Thomas Schmid¹, Benjamin E. Dietrich¹, Markus Weiger¹, and Klaas P. Pruessmann¹

¹*Institute for Biomedical Engineering, University and ETH Zurich, Zurich, Switzerland*, ²*Skope Magnetic Resonance Technologies, Zurich, Switzerland*

To measure the spatiotemporal magnetic field evolution during MR procedures for image reconstruction and real-time field control, best field probe performance is desired. We propose improved field probes with 19F spherical droplet samples formed and positioned with gelled deuterium oxide. It is shown that these spherical samples have an isotropic k-space range and thus de-phase less along the capillary than the common probes. Furthermore, with BIR-4 adiabatic plane rotation pulses the flip angle can be perfectly adjusted, opening a new realm of field monitoring methods.

2179

In vivo Concurrent Excitation and Acquisition MRI with Self-referenced Active Decoupling

Ali Caglar Özen¹, Jan Korvink², Ergin Atalar³, and Michael Bock¹

¹*Dept. of Radiology - Medical Physics, University Medical Center Freiburg, Freiburg, Germany*, ²*Institute of Microstructure Technology, Karlsruhe Institute of Technology, Karlsruhe, Germany*, ³*Electrical and Electronics Engineering, Bilkent University, Ankara, Turkey*

MRI with Concurrent Excitation and Acquisition (CEA) was shown to be feasible by achieving 80 dB analog isolation between transmit and receive coils using an active decoupling method. In this work, active decoupling system was upgraded using pick-up coils for simultaneous recording of the transmit signals. Preliminary results for MRI of a human wrist are represented and discussed.

2180

Wireless Probe Detection For Auxiliary Control Syncing

Jonathan Y Lu¹, Thomas Grafendorfer², Fraser Robb³, John M Pauly¹, and Greig C Scott¹

¹*Dept of Electrical Engineering, Stanford University, Stanford, CA, United States*, ²*Advanced Coils, GEHC Coils, Stanford, CA, United States*, ³*GE Healthcare, Aurora, OH, United States*

We aim to demonstrate methods to wirelessly probe the MRI transmit state without access to the internal MRI hardware itself. We demonstrate two forms of RF pulse detection during a scan with simple magnetic field probes: 1) an electrical link undergoing peak detection and 2) an optical link. We process this signal as an external hardware interrupt into a microcontroller, which can be easily used to bias a coil between receive and transmit mode. Such a setup can be useful in future wireless receive coils.

2181

Monitoring of RF transmit signal in on-coil current-source switch-mode amplification

Natalia Gudino¹, Jacco A de Zwart¹, Qi Duan¹, Peter van Gelderen¹, and Duyu Jeff H¹

¹*Advanced MRI section, LFMI, NINDS, National Institutes of Health, Bethesda, MD, United States*

We demonstrate a new on-coil current-source switch-mode amplifier and communication setup for 7T imaging, which allows monitoring of the RF phase, frequency and amplitude at the amplifier output. This information is made available through a single optical signal per amplifier, making it a practical approach for safety monitoring and fast calibration of on-coil amplifier technology for parallel RF transmission.

2182

Investigation of systematic errors in NMR field probes

Spencer Baird Parent¹, William Bradfield Handler², and Blaine A. Chronik²

¹*Medical Biophysics, Western University, London, ON, Canada*, ²*Physics and Astronomy, Western University, London, ON, Canada*

Using finite elements methods, an investigation of the systematic errors in magnetic field NMR probes is investigated. A NMR field probe is modeled and the field broadening and field offset is investigated as a function of the susceptibility of epoxy. It is shown that susceptibility matching the epoxy drastically reduces field broadening with a minimal effect on field offset. Additionally the effect of air bubbles present in cured epoxy is modeled and the results show that for certain critical regions of the probe the presence of an air bubble can be disadvantageous to the quality of the field probe.

2183

RF field penetrability study of an electrically floating PET insert for simultaneous PET/MRI
Brian J Lee^{1,2}, Ronald D Watkins¹, Chen-Ming Chang^{1,3}, and Craig S Levin^{1,4,5,6}

¹*Radiology, Stanford University, Stanford, CA, United States*, ²*Mechanical Engineering, Stanford University, Stanford, CA, United States*, ³*Applied Physics, Stanford University, Stanford, CA, United States*, ⁴*Physics, Stanford University, Stanford, CA, United States*, ⁵*Electrical Engineering, Stanford University, Stanford, CA, United States*, ⁶*Bioengineering, Stanford University, Stanford, CA, United States*

We have developed a RF-penetrable PET insert for simultaneous PET/MRI and investigated the RF-penetrability with MR experiments and electromagnetic simulations. We have shown that the RF field from the MR body coil penetrates through the inter-module gaps and the ends of the PET insert. We found that ~60% of the RF field transmitted through the ends contributes to the B1 magnitude while the RF field entering through the gaps improves the uniformity provided the ends are also opened. The simulations also show that either shortening the length/height of the modules, or widening the gaps enhances the RF-penetrability by ~16%.

2184

Miniaturized MRI System for Diagnosis of Samples of Low Physical Dimensions using Piezoelectric Receiver and Transmitter
Dhiraj Sinha¹ and Shao Ying Huang¹

¹*Engineering Product Development, Singapore University of Technology and Design, Singapore, Singapore*

An MRI system at small physical dimensions can be developed using a piezoelectric-microcantilever system with the capability of sensing magnetic fields in the range of microtesla to picotesla at room temperature conditions. The RF magnetic field induces voltage in the piezoelectric material which is amplified by the microcantilever which also filters out the signal around its resonant frequency. The cantilever vibration is measured using an optical detection system or by using capacitance to impedance converter. A thick block of piezoelectric material is used as a transmitter in order to replace the transmitting coil.

2185

Clinical-Scale, Stopped-flow ¹²⁹Xe Hyperpolarizer Development

Aaron M. Coffey¹, Panayiotis Nikolaou¹, Kaili Ranta², Iga Muradyan³, Matthew S. Rosen⁴, Samuel Patz³, Michael J. Barlow⁵, Boyd M. Goodson², and Eduard Y. Chekmenev¹

¹*Radiology, Vanderbilt University Institute of Imaging Science, Nashville, TN, United States*, ²*Southern Illinois University, Carbondale, IL, United States*, ³*Brigham & Women's Hospital, Boston, MA, United States*, ⁴*Harvard University, Cambridge, MA, United States*, ⁵*University of Nottingham, Nottingham, United Kingdom*

We report on the development of a first and second generation ¹²⁹Xe hyperpolarizers, capable of producing high (~25-90%) ¹²⁹Xe hyperpolarization at high Xe densities (up to 2000 Torr partial pressure), suitable for clinical and materials MRS/MRI applications.

2186

A hybrid-segmentation atlas method to construct the attenuation correction factor for human pelvic PET/MRI
Hiroshi Kawaguchi^{1,2}, Tadayuki Obata^{2,3}, Hiromi Sano², Eiji Yoshida², Mikio Suga⁴, Yoko Ikoma², Yukari Tanikawa¹, and Taiga Yamaya²

¹*Human Informatics Research Institute, National Institute of Advanced Industrial Science and Technology (AIST), Tsukuba, Japan*, ²*Molecular Imaging Center, National Institute of Radiological Sciences, Chiba, Japan*, ³*Research Center for Charged Ion Therapy, National Institute of Radiological Sciences, Chiba, Japan*, ⁴*Center for Frontier Medical Engineering, Chiba University, Chiba, Japan*

The current attenuation correction method for human pelvic PET/MRI contains several problems such that the attenuation due to bone is not considered and a specific MR imaging, intended for attenuation correction only, is needed. In this study, we proposed a method to generate the distribution of attenuation correction factors with considering the bone attenuation using diagnostic T1-weighted MRI for pelvic PET/MRI scanning. The proposed method is the hybrid of the tissue segmentation based on Gaussian mixture model and the non-linear registration of tissue probability to a subject image. The simulation results showed that attenuation correction using the proposed hybrid method reduced the error on PET image than the conventional method.

2187

Concept of an RF penetrable oval PET insert for MRI system: initial study of the shielding effect

Md Shahadat Hossain Akram¹, Craig S. Levin², Tadayuki Obata¹, Fumihiko Nishikido¹, Eiji Yoshida¹, and Taiga Yamaya¹

¹*Molecular Imaging Center, National Institute of Radiological Sciences, Chiba, Japan*, ²*School of Medicine, Stanford University, Stanford, CA, United States*

A prototype of a novel oval shape PET insert for simultaneous body imaging with the MRI systems has been proposed in this study. The smaller prototype has the minor axis and major axis of 14 cm and 21 cm. 16 copper shielded boxes are positioned on the periphery of the oval frame. The shielding boxes were kept floating to let the RF field penetrate through the gaps in between the 16 modules. To get the required RF field distribution inside the oval PET, the gaps between the shielded modules were varied by doing assumptions following the conformal electric phase angle methods. B1 maps and GRE and SE images were taken and they have a good agreement with the results for without shielding materials. We have found a reduced RF field value with increased noise in the FOV which is mostly

due to shielding materials. The images of GRE and SE have shape distortions due eddy currents.

2188 Extension of the MR field-of-view with HUGE for MR-based attenuation correction in integrated PET/MR
Maike E. Lindemann¹, Jan Ole Blumhagen², and Harald H. Quick^{1,3}

¹*High Field and Hybrid MR Imaging, University Hospital Essen, Essen, Germany*, ²*Siemens Healthcare GmbH, Erlangen, Germany*, ³*Erwin L. Hahn Institute for Magnetic Resonance Imaging, University Duisburg-Essen, Essen, Germany*

In quantitative PET-imaging, it is essential to correct the attenuation of photons in tissue. In combined PET/MR-imaging the attenuation correction (AC) is based on MR-data and subsequent tissue class segmentation. The MR-FOV is limited due to B0-inhomogeneities and gradient nonlinearities. Therefore, the AC-map is truncated and reconstructed PET-data are biased. HUGE (B0-Homogenization using gradient enhancement), which determines an optimal readout gradient to compensate gradient nonlinearities, is evaluated in phantom experiments and applied to MR-imaging of volunteers. The extension of the MR-FOV for MR-based AC showed an improvement of PET-quantification in integrated PET/MR-imaging by reducing the truncated areas of the AC-map.

2189 T1-enhanced segmentation and selection of linear attenuation coefficients for PET/MRI attenuation correction in head/neck applications
Meher Juttukonda¹, Bryant Mersereau¹, Yi Su², Tammie Benzinger², David Lalush¹, and Hongyu An²

¹*Joint Department of Biomedical Engineering, The University of North Carolina at Chapel Hill and North Carolina State University, Chapel Hill, NC, United States*, ²*Mallinckrodt Institute of Radiology, Washington University, St. Louis, MO, United States*

We propose a mapping-based, quantitative T_1 method with patient-specific thresholding for tissue segmentation and assignment of continuous-valued LACs for soft tissues and bone. The proposed method utilizes images from a dual flip angle, dual echo UTE-MR acquisition to segment air, bone, GM, WM, CSF, fat and soft tissue. A conversion from MR relaxation rate R_1 is then utilized to derive continuous-valued LACs to major tissues in the head/neck. The method has been validated in PET data from 23 subjects and has been shown to outperform the vendor UTE method in PET reconstruction accuracy.

2190 Comparison of ECG and Novel Ultrasound Triggering with Spatially Resolved MR-compatible Doppler for Cardio-vascular MRI.
Lindsey Alexandra Crowe¹, Gibran Manasseh¹, Aneta Chmielewski², Thomas de Perrot¹, Hajo Müller³, Rares Salomir¹, and Jean-Paul Vallée¹

¹*Division of Radiology, Faculty of Medicine, Geneva University Hospital, Geneva, Switzerland*, ²*University of Toronto, Hospital for Sick Children, Toronto, ON, Canada*, ³*Division of Cardiology, Geneva University Hospital, Geneva, Switzerland*

A new cardiac MRI triggering method is sought for cases of ECG signal complications due to pathology, or for fetal imaging. We propose feasibility of triggering to carotid ultrasound using an MRI compatible probe using spatially resolved Doppler compared to gold standard ECG. Retrospective processing using Metric Optimized Gating (MOG), is also included for comparison. Imaging modalities were compatible and the positioning of the US probe stable and patient friendly. Phase contrast flow and cine images were successfully obtained in healthy volunteers with ECG, Doppler triggering and MOG. Image quality is highly comparable and accurate functional parameters accessible.

2191 A Combination of Radiomic Features from MRI and Ultrasound Appears to better predict presence of prostate cancer: Validation against whole mount pathology
Mahdi Orooji¹, Mehdi Ailou², Rachel Sparks³, Mirabela Rusu⁴, Nicolas Bloch⁵, Ernest Feleppa⁶, Dean Barratt⁷, Lee Pinsky⁸, and Anant Madabhushi²

¹*Biomedical Engineering, CenteCase Western Reserve University, Cleveland, OH, United States*, ²*Biomedical Engineering, Case Western Reserve University, Cleveland, OH, United States*, ³*Centre for Medical Image Computing, University College of London, London, United Kingdom*, ⁴*Albany, NY, United States*, ⁵*Boston Medical Center, Boston, MA, United States*, ⁶*Lazzi Center for Biomedical Engineering, Riverside Research, New York, NY, United States*, ⁷*University College London, London, United Kingdom*, ⁸*University Hospital Case Medical Center, Cleveland, OH, United States*

To evaluate whether the combination of computer extracted or radiomic image parameters from two complementary modalities, MRI-TRUS can enable better prediction of presence of prostate cancer compared to either modality individually. We considered 12 slides who underwent MRI, TRUS prior to radical prostatectomy. Deformable co-registration methods were used for spatially aligning the pre-operative *in vivo* MRI and ultrasound with the *ex vivo* whole mount radical prostatectomy specimens to establish the ground truth for cancer extent on the imaging. It yielded the best separability between cancer and non-cancer regions with an Area under the operating characteristic curve of 0.88.

2192 An initial experiment of "Flexible PET/MRI" for CNS tumors
Takuya Hinoda¹, Yasutaka Fushimi¹, Tomohisa Okada^{1,2}, Ryusuke Nakamoto¹, Yuji Nakamoto¹, and Kaori Togashi¹

¹*Radiology, Graduate school of Mediine, Kyoto University, Kyoto, Japan*, ²*Human Brain Research Center, Graduate school of Mediine, Kyoto University, Kyoto, Japan*

"Flexible PET (fxPET)", a dual-head mobile DOI-TOF PET system with MR compatibility, is a newly developed device which enable us to examine the positron-emission tomography. In this first trial of the central nervous system (CNS), we tried to confirm the clinical feasibility of the fxPET with a 1.5T MRI scanner. The result of this study showed that fxPET have clinical feasibility in comparison with PET-CT. PET/MRI is an emerging modality. PET/MRI can provide us useful metabolic information to MRI images.

Bo and SAR calculation for a full-ring human head PET system integrated with an 8-element Birdcage coil at 3T
Md Shahadat Hossain Akram¹, Takayuki Obata¹, Mikio Suga², Fumihiko Nishikido¹, Eiji Yoshida¹, and Taiga Yamaya¹

¹National Institute of Radiological Sciences, Chiba, Japan, ²Chiba University, Chiba, Japan

Simultaneous PET/MRI system has attracted much because of its both functional and anatomic imaging capability. In our laboratory, we have developed a human head-size PET/RF-coil integrated modality to be used with existing clinical 3T MRI system (Siemens Magnetom Verio). Eight PET detector modules are integrated with a cylindrical 8-element Birdcage RF coil for simultaneous PET and MRI imaging. In the design each detector has been integrated in between two coil elements. RF interference to PET detector circuits affects PET performance. Also noise generated from PET circuits affects MR image quality. For proper simultaneous operation, PET circuits in each detector-module were installed inside a copper-shielded box. But shielding materials very close to RF coil elements and close to imaging region adversely affects MR imaging quality. In this study we performed B_0 and SAR calculation of our hybrid system. Though there have noticeable changes in the B_0 values, the SAR remains very low.

Realistic Patient-Based E-Phantoms and Simulation of PET-MR Neuroimage Data
Bryant G. Mersereau¹, Meher R. Juttukonda¹, Hongyu An², and David S. Lalush¹

¹Joint Department of Bioengineering, The University of North Carolina at Chapel Hill and North Carolina State University, Chapel Hill, NC, United States, ²Mallinckrodt Institute of Radiology, Washington University in St. Louis, St. Louis, MO, United States

Acquired PET-MR datasets can be problematic to build due to the high logistical and monetary cost associated with recruiting and scanning patients. We propose a new electronic PET phantom (E-phantom) platform to streamline the PET-MR research process. The proposed platform is shown to produce results consistent with acquired PET data reconstructed on manufacturer software and to provide high configurability and flexibility as a simulation tool.

Impact of spatio-temporal resolution on MR-based cardiac motion correction PET-MR
Camila Munoz¹, Christoph Kolbitsch^{1,2}, and Claudia Prieto¹

¹Department of Biomedical Engineering, King's College London, London, United Kingdom, ²Division of Medical Physics and Metrological Information Technologies, Physikalisch-Technische Bundesanstalt, Berlin, Germany

MR-based PET motion correction has been shown to improve image quality in cardiac PET-MR imaging. Here we present a numerical simulation study analysing the impact of temporal and spatial resolution of motion fields on the final image quality of myocardial perfusion PET scans in order to find the most efficient parameters yielding accurate cardiac motion compensation in the shortest possible scan time. Results show that cardiac motion correction is important for accurate assessment of myocardial lesions and that temporal resolution of the motion fields can be strongly optimised without losing diagnostic accuracy, reducing the total exam time in PET-MR imaging.

Removing Gradient Induced Voltages from 12-lead ECGs acquired during DW-EPI and fMRI brain Imaging
Mikayel Dabaghayan¹, Shelley Hua Lei Zhang¹, Zion Tsz Ho Tse², Charles L Dumoulin³, Ronald Watkins⁴, Wei Wang¹, Jay Ward⁵, and Ehud Jeruham Schmidt⁶

¹Radiology, Brigham and Womens Hospital, Boston, MA, United States, ²Engineering, University of Georgia, Athens, GA, United States, ³Radiology, Cincinnati Childrens Hospital Medical Center, Cincinnati, OH, United States, ⁴Radiology, Stanford University, Stanford, CA, United States, ⁵E-Trolz Inc., North Andover, MA, United States, ⁶Radiology, Brigham and Womens Hospital, Newton, MA, United States

We developed a technique to restore the ECG signals distorted by MRI gradient-induced voltages (GIV) acquired during fMRI and DW-EPI brain imaging sequences. Brain EPI sequences produce the largest ECG artifacts, presenting a large challenge to GIV removal. We used a theoretical equation with 19 parameters, which characterized the GIVs at each ECG electrode based on the simultaneously recorded gradient waveforms. A rapid training sequence permitted computing the equation coefficients, followed by real-time gradient-induced voltage removal during imaging. FIR notch filters were subsequently applied to remove some residual spikes. The method succeeded in removing most GIVs, excluding artifacts at the beginning and end of imaging periods, which resulted from amplifier non-linearity.

Real time tracking in the fringe field of a MRI scanner: a solution for more accurate MR guided breast biopsies
Ileana Hancu¹, Robert Darrow¹, Eric Fiveland¹, Elizabeth Morris², Dominic Graziani¹, and Mauricio Castillo-Effen¹

¹GE Global Research Center, Niskayuna, NY, United States, ²Memorial Sloan Kettering Cancer Center, New York City, NY, United States

Many factors contribute to the inaccuracy of MR-guided breast biopsies. Significantly, the lack of real-time visualization of tool advancement towards the biopsy site increases their duration and rate of false negatives. In this work, a novel approach for instrument tracking, relying on the spatial variation of the magnetic field, and using a set of 3 axis accelerometers/gyroscopes/magnetic field sensors, is presented. One dimensional tracking with 1.3mm rms error was demonstrated in the fringe field of a 3T magnet.

STEREO-MC for Connected Spatiotemporal Excitation

Mohan Lal Jayatilake¹, Christoph Juchem², Michael Mullen¹, Gregor Adriany¹, Robin de Graaf², and Michael Garwood¹

A highly uniform magnetic field (B_0) is typically required to generate MR images. In the original STEREO (for STEering REsonance over the Object) method, spatial variations in B_0 are compensated by adjusting pulse amplitudes and frequencies in a temporal manner. Here we present a novel design of a limited set of well-defined multi-coil (MC) arrays that can optimize magnetic field distortions across the object of interest.

2199

Planar-type multi-circular shimming for a 1.0 T permanent magnet
Ryota Yamada¹, Makoto Tsuda¹, Katsumi Kose¹, and Yasuhiko Terada¹

¹Institute of Applied Physics, University of Tsukuba, Tsukuba, Japan

A multi-circular shim coil (MCSC), which consists of a set of localized circular current coils, provides the flexibility to design and produce linear and higher-order magnetic fields that compensate for a given B_0 inhomogeneity both statically and dynamically. However, the concept of the MCSC has currently been realized only for cylindrical base geometries. Here we translated the concept of the MCSC to a biplanar geometry, and a planar-type MCSC was designed and fabricated for an open, 1.0 T permanent magnet system. We concluded that the planar MCSC is a useful device to achieve field homogeneity with reasonable accuracy.

2200

COSI Measure - Open Source Multipurpose Measurement System
Lukas Winter¹, Haopeng Han¹, and Thoralf Niendorf^{1,2,3}

¹Berlin Ultrahigh Field Facility (B.U.F.F.), Max Delbrück Center for Molecular Medicine, Berlin, Germany, ²Experimental and Clinical Research Center (ECRC), a joint cooperation between the Charité Medical Faculty and the Max Delbrück Center for Molecular Medicine, Berlin, Germany, ³MRI.TOOLS GmbH, Berlin, Germany

Cost effective open source imaging (COSI) is a collaborative initiative currently building an affordable low field open source MR scanner with the technical documentation available at www.opensourceimaging.org. As part of this initiative COSI Measure has been developed in order to automatically map the static magnetic field. COSI Measure is an open source multipurpose 3-axis system for ~3000€, which can be equipped with other field mapping probes like electromagnetic field sensors, used for 3D printing / CNC machinery application or other applications, that require programmable submillimeter movement and sensor readouts in space and time.

2201

NiftyWeb: web based platform for image processing on the cloud
Ferran Prados^{1,2}, Manuel Jorge Cardoso¹, Ninon Burgos¹, Claudia Angela Michela Gandini Wheeler-Kingshott^{2,3}, and Sébastien Ourselin¹

¹Translational Imaging Group, Medical Physics and Biomedical Engineering, University College London, London, United Kingdom, ²NMR Research Unit, Queen Square MS Centre, Department of Neuroinflammation, UCL Institute of Neurology, University College London, London, United Kingdom, ³Brain Connectivity Center, C. Mondino National Neurological Institute, Pavia, Italy

This work proposes a new way to publicly distribute image analysis methods and software. This approach is particularly useful when the software code and the datasets cannot be made open source. We leverage the use of Internet and emerging web technologies to develop a system where anyone can upload their image datasets and run any of the proposed algorithms without the need of any specific installation or configuration. This service has been named NiftyWeb (<http://cmictig.cs.ucl.ac.uk/niftyweb>).

2202

About the application of the ICNIRP Guidelines for motion-induced electric fields in MRI
Luca Zilberti¹, Oriano Bottauscio¹, and Mario Chiampi²

¹Istituto Nazionale di Ricerca Metrologica, Torino, Italy, ²Dipartimento Energia, Politecnico di Torino, Torino, Italy

This contribution reports the results of an extended survey, in which the exposure indexes provided by the current Guidelines dealing with motion-induced fields in MRI environments have been computed. The analysis is carried out through numerical simulations, using detailed human models that experience realistic exposure conditions (motion trajectories and MRI scanners). Besides identifying some critical situations (where the exposure indexes may be exceeded), the research puts in evidence some degree of freedom in the evaluation procedure, which might lead to inconsistencies between different assessment approaches.

2203

Semi-automatic multi-feature bone segmentation in the pelvic region using Dixon MRI images acquired in 2 minutes: a preliminary result
Yi Gao^{1,2,3} and Chuan Huang^{4,5}

¹Biomedical Informatics, Stony Brook Medicine, Stony Brook, NY, United States, ²Applied Mathematics and Statistics, Stony Brook Medicine, Stony Brook, NY, United States, ³Computer Sciences, Stony Brook Medicine, Stony Brook, NY, United States, ⁴Radiology, Stony Brook Medicine, Stony Brook, NY, United States, ⁵Psychiatry, Stony Brook Medicine, Stony Brook, NY, United States

In simultaneous PET-MRI, attenuation correction is still a major hurdle due to the high attenuation of the bones and the lack of MR signal in conventional sequences. So far, several approaches have been proposed for bone attenuation correction, including bone segmentation and direct bone imaging. However, almost all available bone segmentation literatures focused on the head, which is arguably one of the easier regions because of its smaller field-of-view (FOV) requirement and the absence of major motion artifacts. Direct bone imaging is another promising approach which is accomplished by using zero-TE imaging, but its application in the body is

challenging due to the larger FOV requirement and current instrumentation limitation such as peak B1. Recent research has demonstrated that PET quantitation can be largely improved even by assigning a fixed bone attenuation value (0.120 cm⁻¹) to all bones. In light of this, we developed a technique that is able to produce good bone segmentation in the pelvic region using a 2-minute 6-echo DIXON MRI acquisition.

2204

100% efficient motion corrected coronary MR angiography using a gradient echo sequence in a 3T PET-MR system
Camila Munoz¹, Radhouene Neji², Peter Weale², Rene Botnar¹, and Claudia Prieto¹

¹Department of Biomedical Engineering, King's College London, London, United Kingdom, ²MR Research Collaborations, Siemens Healthcare, Frimley, United Kingdom

Respiratory motion remains a challenge for coronary MR angiography at 3T. Here we propose an inline 2D translational motion correction scheme using an image-based navigator. Low-resolution navigators are acquired at each heartbeat by spatially encoding the start-up echoes of an ECG-gated gradient echo sequence, allowing for 100% scan efficiency. Results from healthy volunteers show that motion correction improves visualization of the right and left anterior descending coronary arteries. The proposed scheme potentially allows for performing a comprehensive diagnosis of coronary artery disease by acquiring both diagnostic and motion information from MR, that can also be used to correct PET data.

2205

Rapid Eddy Currents Insensitive Field Map Estimation for Accurate B0 Shimming
Hai Luo¹, Bin Wang¹, Gaojie Zhu¹, Wenzhou Wang¹, Xiang Zhou¹, Ziyue Wu¹, and Leping Zha^{1,2}

¹AllTech Medical Systems, Chengdu, China, People's Republic of, ²AllTech Medical Systems, Cleveland, OH, United States

3D dual echo gradient echo sequence is commonly used to obtain the field map for B0 shimming. The maps contain the true B0 fields mixed with eddy currents induced magnetic field changes averaged over the echo time difference, which compromise the shimming accuracy. A calibration sequence with alternating gradient polarities is proposed to measure the eddy currents term. Quadratic surface fitting is then applied to produce smooth eddy currents calibration maps over the full imaging volume containing only the first and second order components. The actual rapid in-vivo shimming sequence runs later, using the calibration maps to remove the eddy currents influences during the post-processing, with partial Fourier acquisition on phase encoding and slice encoding directions to reduce the scan time. The fast method provides means of eddy currents insensitive shimming, as well as reduced sensitivity to motion.

2206

Feasibility of Non-invasive Proton-Density Fat Fraction Evaluation using a Single-sided MR device
Vanessa L. Landes¹, Eamon K. Doyle^{1,2}, Pablo J. Prado³, John C. Wood^{1,2}, and Krishna S. Nayak⁴

¹Biomedical Engineering, University of Southern California, Los Angeles, CA, United States, ²Cardiology, Children's Hospital Los Angeles, Los Angeles, CA, United States, ³One Resonance, LLC, San Diego, CA, United States, ⁴Electrical Engineering, University of Southern California, Los Angeles, CA, United States

We investigate the use of a magnet with flat field isosurfaces over 4 cm for assessment of proton density fat fraction (PDFF). We experimentally demonstrate a correlation between PDFF and apparent T2 in phantoms. Apparent T2 measurement variability is low enough to produce invertible curves of T2 vs. PDFF in intervals of 2% PDFF for a 0 – 17% PDFF range at 0°C and intervals of 4% PDFF for a 0 – 12% PDFF range at 23°C in milk and cream mixtures. The long-term goal is to use this device for in-vivo clinical applications, such as measurement of intra-hepatic and intra-muscular fat.

2207

Ultra-Low-Field Spin Manipulation for Precise Flip-Angle and T\$\$\$-Determination
Kilian Wolfgang¹, Frank Seifert¹, Silvia Knappe-Grüneberg¹, Jens Voigt¹, Eva Al-Dabbagh¹, and Isaac Fan¹

¹Physikalisch-Technische Bundesanstalt (PTB), Braunschweig and Berlin, Germany

Two distinct methods for precise flip angle determination for hyperpolarized rare gas samples are presented and were performed in ultra low magnetic field environment (\$\$ \approx \mu \$\$T). The repetitive coherent excitation method is rather fast and allows for preserving most of the initial polarization whereas the incoherent excitation method is time consuming but determines the relaxation parameters \$\$ T_1 \$\$ and \$\$ T_2^* \$\$ inherently.

2208

Optimization of a switching circuit for a matrix gradient coil
Stefan Kroboth¹, Kelvin J. Layton¹, Feng Jia¹, Sebastian Littin¹, Huijun Yu¹, Jürgen Hennig¹, and Maxim Zaitsev¹

¹Medical Physics, University Medical Center Freiburg, Freiburg, Germany

A matrix gradient coil consisting of 84 small coil elements was designed and constructed at our institution. Driving each coil element with an individual amplifier is impractical due to the high current requirements. To resolve this limitation, groups of coil elements can be connected in series and driven by a limited number of amplifiers. Such grouping configurations are obtained for one or several target fields. In the latter case, the configurations need to be switched with a switching circuit. We propose an algorithm to minimize the number of necessary switches to reduce the complexity and cost of this circuit.

MR Safety

Exhibition Hall

Wednesday, May 11, 2016: 13:30 - 15:30

2209

Magnetically Induced Force Measurements per ASTM F2052 of Active Implantable Medical Device Lead Materials
Michael Childers¹, Roya Hashemi Rad¹, Richard Williamson¹, and Shiloh Sison¹

¹St. Jude Medical, Sylmar, CA, United States

This abstract presents magnetically induced force measurements per ASTM F2052 of materials commonly used in implantable leads. Implantable leads which are constructed solely from tested materials which pass the magnetically induced force testing acceptance criteria (i.e. gravity force), may not require magnetically induced force testing per ASTM F2052 for MR conditionality with 3 T MR scanners.

2210



Detailing the MR Safety of Intraocular Tantalum Markers Used for Treatment Planning of Proton Beam Therapy of Uveal Melanoma: A 7.0T Study

Eva Oberacker¹, Katharina Paul¹, Lukas Winter¹, Celal Oezerdem¹, Antje Els¹, Andreas Pohlmann¹, Laura Boehmert¹, Stefanie Kox¹, Min-Chi Ku¹, Till Huelnhagen¹, Oliver Stachs², Jens Heufelder^{3,4}, Andreas Weber^{3,4}, and Thoralf Niendorf^{1,5}

¹Berlin Ultrahigh Field Facility (B.U.F.F.), Max Delbrück Center for Molecular Medicine in the Helmholtz Association, Berlin, Germany,

²Department of Ophthalmology, University of Rostock, Rostock, Germany, ³Department of Ophthalmology, Charité University Medicine, Berlin, Germany, ⁴BerlinProtonen, Helmholtz Zentrum Berlin, Berlin, Germany, ⁵Experimental and Clinical Research Center (ECRC), a joint cooperation between the Charité Medical Faculty and the Max Delbrück Center for Molecular Medicine in the Helmholtz Association, Berlin, Germany

This work examines the MR safety of intraocular tantalum markers used in proton beam therapy of uveal melanoma. RF power deposition induced heating was studied using electromagnetic field and temperature simulations. Magnetic force acting on the marker was investigated and image artifacts were assessed. Minor local increase of RF power deposition was observed for SAR_{0.075g} but not detectable for SAR_{1g}. Measurements showed no detectable magnetic attraction of the implant. FSE based imaging showed only small artifacts barely exceeding the thickness of the sclera. Our studies indicate that intraocular tantalum markers do not constitute a per se contraindication for 7.0T MRI.

2211



SAR/B1+ calibration workflow for safe, high duty-cycle parallel transmission imaging at ultra-high field
Filiz Yetisir¹, Bastien Guerin², Lawrence Wald^{2,3}, and Elfar Adalsteinsson^{1,3}

¹Electrical Engineering and Computer Science, Massachusetts Institute of Technology, Cambridge, MA, United States, ²Dept. of Radiology, Martinos Center for Biomedical Imaging, Charlestown, MA, United States, ³Harvard-MIT Division of Health Sciences Technology, Institute of Medical Engineering and Science, Cambridge, MA, United States

In this work, we propose a pTx safety workflow that will enable high duty cycle imaging at high field systems. Several SAR and B₁⁺ calibration steps are suggested for a complete analysis including modeling the TX array, testing it over time and different loads and finding a safety margin to account for RF system imperfections. Good qualitative agreement was achieved between the simulated and measured B₁⁺ maps for the TX array. 11% and 6° standard deviation was observed in the magnitude and the relative phase maps over time. A maximum difference of 16% was observed between offline and online calculated local SAR values due to RF system imperfections.

2212

Direct optical measurement of the RF electrical field for MRI
Isabelle Saniour¹, Anne-Laure Perrier², Gwenaël Gaborit^{2,3}, Jean Dahdah³, Lionel Duvillaret³, and Olivier Beuf¹

¹CREATIS, Université de Lyon ; CNRS UMR5220 ; Inserm U1044 ; INSA-Lyon ; Université Claude Bernard Lyon 1, Villeurbanne, France, ²IMEP-LAHC, UMR 5130 ; Université de Savoie, Le Bourget-du-Lac, France, ³Kapteos, Sainte-Hélène du Lac, France

In MRI, a real time monitoring of the magnitude of the electric field prevents the patient from safety hazards due to heating phenomenon. A sub-cm electro-optical probe was used to localize and measure the E-field in 4.7-T MRI. This probe is formed from an electro-optic crystal that changes its refractive indexes according to the applied E-field. The results show that the probe is non-perturbative regarding the E-field and does not affect the quality of MR images. Six clear E-field concentrations were localized at proximal and distal sides of the transceiver coil. Their magnitudes vary between 10000V/m and 20000V/m.

2213

On Peripheral Nerve Stimulation of a Compact, Asymmetric Head-Only Gradient Coil: Head Orientation Dependence
Seung-Kyun Lee¹, Kishore V. Mogatadakala², Dominic Graziani¹, Jean-Baptiste Mathieu², Thomas K.-F. Foo¹, and Matt A. Bernstein³

¹GE Global Research, Niskayuna, NY, United States, ²GE Healthcare, Florence, SC, United States, ³Mayo Clinic, Rochester, MN, United States

Head orientation dependence of the peripheral nerve stimulation (PNS) thresholds and the induced electric fields of a high-performance, asymmetric head-only gradient coil were studied experimentally and by numerical simulation. In the experiment, the gradient field direction was fixed and the subject head was rotated in the transverse plane. The subject-reported PNS thresholds nearly doubled when the head's anterior-posterior direction was parallel to the gradient compared to when the head was approximately perpendicular to the gradient. Human-body-model simulation suggested that the orientation dependence may be primarily due to locally concentrated electric fields in the corrugated regions of the face.

2214

Positioning to decrease hot spots caused by an intramedullary rod implanted in a forearm
Yu Kikuchi¹, Minghui Tang¹, and Toru Yamamoto²

¹Graduate School of Health Sciences, Hokkaido university, sapporo, Japan, ²Faculty of Health Sciences, Hokkaido university, sapporo, Japan

RF heating causes most of incidents during MRI examinations. There still are patients who were implanted metallic products before the advent of MRI and MR compatibility of most such products is unknown. It was reported that an MRI examination of a patient implanted an intramedullary rod in his forearm was aborted due to a heating claim from the patient. In this study, we confirm RF heating of such patient by using an electromagnetic analysis software dedicated for MRI, and shows that positioning of an implanted arm can decrease SAR sufficiently enough to take MRI examinations.

2215

Assessment of Radio Frequency Induced Heating On or Near Implants during MRI – some open issues
Mikhail Kozlov^{1,2} and Gregor Schaefers^{1,3}

¹MR:comp GmbH, Gelsenkirchen, Germany, ²Max Planck Institute for Human Cognitive and Brain Sciences, Leipzig, Germany, ³Magnetic Resonance Institute for Safety, Technology and Research GmbH, Gelsenkirchen, Germany

We evaluated locations of maximum temperature rise ($\max(\Delta T)$) and the dependence of $\max(\Delta T)$ on RF-induced power deposition (P_{total}) for some generic implants. ΔT spatial and temporal variations were investigated. To fulfill ASTM F2182-11a setup requirements, the temperature probe should be placed with submillimetre precision at location that cannot be predicted by a full wave electromagnetic simulation alone. It is a challenge to validate with small uncertainty P_{total} calculated using EM simulation by only measuring SAR or VLD value at some points in space, if the field probe sensor size is larger than one tenth of the wire diameter.

2216

Reduction of the E field at the tip of implanted wires generated by pTx coils using RF current measurements
Gerd Weidemann¹, Frank Seifert¹, and Bernd Ittermann¹

¹Physikalisch-Technische Bundesanstalt (PTB), Braunschweig and Berlin, Germany

The possibility to reduce implant heating is an added value option of parallel transmission. An orthogonal-projection method (OPM) is presented to reduce the E fields at the tip of wire type implants by using voltage vectors orthogonal to the vector inducing the worst case RF current at the protruding end of the implant. Experiments confirm that the minimization of RF current at the protruding end leads to a distinct reduction of the electric field at the tip of the wire. Low-hazard steering conditions for n -element pTx coils can be determined in real time during an MR investigation from the measurement of only n complex valued RF currents at the protruding end of the implant.

2217

Visualization and Localization of Implanted Devices with Parallel Transmit Array Using Reversed RF Polarization
Parnian Zarghamravanbakhsh¹, John M Pauly¹, and Greig Scott¹

¹Electrical Engineering, Stanford University, Stanford, CA, United States

The radiofrequency (RF) transmit field can induce current in implanted devices; therefore, it is essential to detect and minimize coupling to stimulator leads and guide-wire structures. Reverse polarization has been proposed as low-RF-power method to safely detect current in the implanted devices using birdcage coil. The purpose of this study is to demonstrate feasibility of combining knowledge of coil current and location with reverse polarization method using parallel transmit array to detect and localize implanted wires.

2218

Heating of lead electrodes disconnected from sacral stimulator during routine lumbar MRI at 3T with receive-only coil
Pallab K Bhattacharyya¹, Howard Goldman², Mark J Lowe¹, Adrienne Quirouet², and Stephen E Jones¹

¹Imaging Institute, Cleveland Clinic, Cleveland, OH, United States, ²Glickman Urological Institute, Cleveland Clinic, Cleveland, OH, United States

RF heating testing during lumbar scans of Medtronic Interstim II (Model 3058) implantable pulse generator (IPG) connected to Medtronic Quadipolar Nerve Stimulator Lead (Model 3889) at 3T whole body Siemens TIM Trio scanner with receive-only cervical-lumbar-thoracic coil was performed. Temperatures of the electrodes were measured by using fiber optic sensors with fluoroptic monitoring with the IPG and lead placed inside an ASTM gel phantom. No electrode heating was observed when the lead was connected with the IPG in any of the scans, while considerable heating was observed when the IPG was disconnected and taken out of the phantom.

2219

Comparing RF heating simulations and experimental results in pTx coils: an evaluation of three simulation methods
Hongbae Jeong¹, Peter Jezzard¹, and Aaron Hess²

¹FMRIB Centre, University of Oxford, Oxford, United Kingdom, ²Department of Cardiovascular Medicine, University of Oxford, Oxford, United Kingdom

In this study, we conducted thermal simulations using EM simulation software and compared these to proton resonance frequency (PRF) thermometry using an ultra-high-field MR phantom. RF heating was measured in the magnet environment using a PRF-based 3D GRE on a 8-channel pTx coil. Three types of simulation method were assessed and compared with experimental data. Amongst the three simulation methods the realistic capacitance simulation was closest to the experimental measurement. In conclusion, PRF RF

2220

Statistical Equivalence Test Protocol for RF Performance of AIMD Systems
Li-Yin Lee¹, Shiloh Sison², Shi Feng³, Kishore Kondabatni⁴, and Richard Williamson⁵

¹BioStatistics, St. Jude Medical, Sylmar, CA, United States, ²Electrical Engineering, St. Jude Medical, Sunnyvale, CA, United States, ³Electrical Engineering, St. Jude Medical, Sylmar, CA, United States, ⁴St. Jude Medical, Sylmar, CA, United States, ⁵Program Management, St. Jude Medical, Sylmar, CA, United States

Test methods for MRI safety and RF safety of AIMD systems has been defined through ISO/TS 10974 are cumbersome to perform on every device and lead combination. A clear method for determination that two likely equivalent systems has not been described. The Concordance Correlation Coefficient has been described for this purpose in assay comparison. This paper evaluates the CCC method for RF equivalence in presence of measurement uncertainty, and confirms that the CCC method is simple and robust for this purpose.

2221

Modelling the RF safety of tattoo pigment ink for subjects undergoing 7 Tesla MRI
Hongbae Jeong¹, Aaron Hess², and Peter Jezzard¹

¹FMRIB Centre, University of Oxford, Oxford, United Kingdom, ²Department of Cardiovascular Medicine, University of Oxford, Oxford, United Kingdom

Despite many reports of skin burns in the region of tattoos, there are few safety studies concerning RF heating caused by tattoos. Manufacturers of tattoo ink are numerous and use a range of dye ingredients, making it difficult to assess the electromagnetic properties of each ink pigment. An anchor-shaped tattoo was modelled 1mm under the skin layer in the region of the cervical spine to predict a possible skin burn generated by RF coil. A simulation model of RF heating in tattoo pigment is proposed, which shows that certain tattoo pigments may lead to severe skin burns when performing high field MRI.

2222

Heterogeneous gelatin-based head phantom for evaluating DBS heating
Clare McElcheran¹, Benson Yang², Fred Tam², Laleh Golenstani-Rad³, and Simon Graham²

¹University of Toronto, Toronto, ON, Canada, ²Sunnybrook Health Sciences Centre, Toronto, ON, Canada, ³Massachusetts General Hospital, Charlestown, MA, United States

A method to create a heterogeneous head phantom with long implanted wires to improve the evaluation of tissue heating surrounding deep brain stimulation (DBS) leads is presented. The phantom consists of three different oil-in-gelatin dispersions with electrical properties that mimic grey matter, white matter and cerebral spinal fluid (CSF) as well as a human skull. 3D printing technology was used to create gelatin moulds and an acrylic casing. A CT scan of the human skull was obtained to create a mesh-based digital representation. Thus, the physical phantom has an associated mesh-based digital model which can be used in electromagnetic simulation.

2223

Potentially hazardous materials left behind after an MRI installation
Ken E Sakaie¹, Wanyong Shin¹, and Lowe J Mark¹

¹Imaging Institute, The Cleveland Clinic, Cleveland, OH, United States

We share our experience discovering and removing metallic objects left behind after a routine MRI hardware upgrade. The results suggest that vigilance is necessary despite the routine nature of such an upgrade.

2224

Increased Signal Intensity of brain structures on unenhanced T1-weighted images following 35 or more GBCA administrations
Yang Zhang^{1,2}, Yan Cao¹, George Shih¹, Elizabeth Hecht³, and Martin R Prince^{1,4}

¹Radiology, Weill Cornell Medical Center, New York, NY, United States, ²Radiology, Qilu Hospital, Shandong University, Jinan, China, People's Republic of, ³Columbia University, New York, NY, United States, ⁴Radiology, Columbia University, New York, NY, United States

In 16 patients with 35 or more linear GBCA administrations increased T1 signal on unenhanced images was observed in dentate nucleus (100%), globus pallidus (100%), cerebral peduncles (100%), substantia nigra (88%), red nucleus (88%), colliculi (81%), posterior thalamus (75%), superior cerebellar peduncle (56%), internal capsule (50%), head of caudate nucleus (31%), body of caudate nucleus (25%), whole thalamus (25%), pons (13%), anterior commissure (13%), posterior brain stem (6%), pituitary gland (6%), mammillary body (6%) and putamen (6%). The source of T1 signal increase is unknown but may relate to GBCA administration. No clinical significance was identified.

2225

Power deposition into a metallic hip prosthesis exposed to switched gradient fields
Luca Zilberti¹, Oriano Bottauscio¹, Mario Chiampi², Jeffrey Hand³, Hector Sanchez Lopez⁴, Rüdiger Brühl⁵, and Stuart Crozier⁶

¹Istituto Nazionale di Ricerca Metrologica, Torino, Italy, ²Dipartimento Energia, Politecnico di Torino, Torino, Italy, ³Division of Imaging Sciences and Biomedical Engineering, King's College London, London, United Kingdom, ⁴Department of Engineering, Universitas Dian Nuswantoro, Semarang, Indonesia, ⁵Physikalisch-Technische Bundesanstalt, Berlin, Germany, ⁶School of Information Technology and Electrical Engineering, University of Queensland, St. Lucia, Australia

Concern has been recently raised about the possible heating of massive metallic implants, in particular hip prostheses, due to the gradient fields used in MRI. Thus, this contribution discusses the computation of the power density deposited by the magnetic field into the implant, which represents the first step to estimate the thermal heating. The analysis is based on numerical simulations, performed through a computational formulation applied to an anatomical model of the body. The results provide evidence of the role of the three gradient coil axes and of the different harmonic components of the signals in this power deposition process.

2226

Testing of a compact ultrasound scanner for use inside clinical interventional MRI suite

Chi Ma¹, Zaiyang Long¹, Diana M Lanners¹, Donald J Tradup¹, Joel P Felmlee¹, David A Woodrum¹, Nicholas J Hangiandreou¹, and Krzysztof R Gorny¹

¹Department of Radiology, Mayo Clinic, Rochester, MN, United States

The suitability of a compact Samsung ultrasound (US) system for real-time imaging guidance of treatment device positioning inside 1.5T interventional magnetic resonance imaging (iMRI) suite was assessed. The US system was tested in a proposed site-specific configuration. Magnetic displacement forces exerted by the static magnetic field on each of the US system components were estimated at the proposed locations. Image quality of both MRI and US systems with the US system set to different operating modes were evaluated. Results demonstrate that this particular US system is suitable for use in the site-specific configuration at our 1.5T iMRI suite.

2227

An Evaluation of Radio Frequency Induced Power Deposition of Coaxial Leads with an Implant Model

Mikhail Kozlov^{1,2} and Gregor Schaefers^{1,3}

¹MR:comp GmbH, Gelsenkirchen, Germany, ²Max Planck Institute for Human Cognitive and Brain Sciences, Leipzig, Germany, ³Magnetic Resonance Institute for Safety, Technology and Research GmbH, Gelsenkirchen, Germany

We performed 3-D electromagnetic simulations of coaxial leads and numerically obtained the lead models to evaluate power deposition and the voltage induced at the lead proximal end with the lead models. No correlation between peak volume loss density and deposited powers at the tip and the ring was observed. In some cases deposited power at the ring exceeded deposited power at the tip. However further extensive simulations of induced heating behavior should be done before final conclusions regarding coax lead design preferences are made.

2228

Influence of electrical properties of lead insulation on radio frequency induced heating during MRI

Mikhail Kozlov^{1,2} and Gregor Schaefers^{1,3}

¹MR:comp GmbH, Gelsenkirchen, Germany, ²Max Planck Institute for Human Cognitive and Brain Sciences, Leipzig, Germany, ³Magnetic Resonance Institute for Safety, Technology and Research GmbH, Gelsenkirchen, Germany

We evaluated the dependence of RF-induced power deposited at a hot spot (p) on insulating electrical properties for insulated stainless steel wires of 1.5 mm in diameter with insulation thickness of 0.5 mm. Lead transfer functions (TF) were obtained by 3-D electromagnetic simulations. TF and p depended significantly on electrical properties of insulation. Increased insulator conductivity resulted in decreased p . For all insulated wires investigated non-uniform RF excitation resulted in higher power deposition than uniform RF excitation.

2229

Design and simulation of a nested 4 channel 1H and 3 channel ¹³C coil for glycogen NMR experiments in the calf muscle at 7 T
Sigrun Goluch^{1,2,3}, Roberta Krieg^{1,2,3}, Elmar Laistler^{2,3}, Martin Gajdošík^{4,5}, and Martin Kršák^{1,4,5}

¹Division of Endocrinology and Metabolism, Department of Internal Medicine III, Medical University of Vienna, Vienna, Austria, ²MR Center of Excellence, Medical University of Vienna, Vienna, Austria, ³Center for Medical Physics and Biomedical Engineering, Medical University of Vienna, Vienna, Austria, ⁴High-Field MR Center, Department of Biomedical Imaging and Image-Guided Therapy, Medical University of Vienna, Vienna, Austria, ⁵Christian Doppler Laboratory for Clinical Molecular MR Imaging, Medical University of Vienna, Vienna, Austria

Due to the inherently low sensitivity of carbon-13 NMR, ¹³C spectroscopic experiments at 7T require specifically optimized double tuned local RF transceive arrays for high SNR, exhibiting sufficient electrical isolation between the arrays to enable 1H decoupling and high SAR efficiency as to not invoke SAR limits during proton decoupling. In this work we present the simulation and optimization of a 7 channel nested ¹H/¹³C RF transceive coil array for ¹³C metabolic studies in the human calf muscle at 7 T.

2230

Assessment of RF induced heating of intracranial Micro-depth electrodes during MRI

Anastasia Papadaki^{1,2}, David Carmichael³, Andrew McEvoy^{4,5}, Anna Miserocchi^{4,5}, Tarek Yousry^{1,2}, Beate Diehl^{4,6}, Louis Lemieux⁴, and John S Thornton^{1,2}

¹Lysholm Department of Neuroradiology, National Hospital for Neurology and Neurosurgery, UCLH, London, United Kingdom, ²Department of Brain Repair and Rehabilitation, UCL Institute of Neurology, London, United Kingdom, ³Imaging and Biophysics Unit, UCL Institute of Child Health, London, United Kingdom, ⁴Department of Clinical and Experimental Epilepsy, UCL Institute of Neurology, London, United Kingdom, ⁵Department of Neurosurgery, National Hospital for Neurology and Neurosurgery, London, United Kingdom, ⁶Department of Neurophysiology, National Hospital for Neurology and Neurosurgery, London, United Kingdom

In this study we assessed temperature changes (ΔT) during MRI in the vicinity of microwires EEG electrodes in a phantom. Measurements were performed at 1.5T during a high SAR TSE sequence for two different depth electrode arrangements with and

without microwires. Although we observed a small temperature rise due to the presence of microwires the maximum temperature change ΔT did not exceed 1°C at 1.5T.

2231

SAR and patient orientation for 3 T 2-channel parallel transmit pelvis imaging
Mariya Lazebnik¹

¹*GE Healthcare, Waukesha, WI, United States*

This work investigates the impact of patient orientation on SAR for 3 Tesla two-channel parallel transmit (pTx) pelvis imaging. SAR simulations were performed on two human body models in a supine position in a 70 cm-diameter 3 T body coil in a pelvis landmark, in both "head first" and "feet first" patient entry orientations. Whole body SAR, peak spatial SAR, and SAR ratio (= peak SAR / whole body SAR) were computed for quadrature and pTx excitations. Patient position and orientation can cause peak SAR and SAR ratio to vary significantly and must be considered when evaluating pTx excitation.

2232

Subject-specific SAR prediction in adults and children at 7.0T

Gianluigi Tiberi^{1,2}, Mauro Costagli^{1,2}, Laura Biagi², Alessio De Ciantis³, Nunzia Fontana⁴, Riccardo Stara^{5,6}, Mark R Symms⁷, Mirco Cosottini⁸, Renzo Guerrini³, and Michela Tosetti^{1,2}

¹*Imago7, Pisa, Italy*, ²*IRCCS Stella Maris Foundation, Pisa, Italy*, ³*Meyer Children's Hospital, Firenze, Italy*, ⁴*Dipartimento di Ingegneria dell'Informazione, Pisa, Italy*, ⁵*National Institute of Nuclear Physics (INFN), Pisa, Italy*, ⁶*Stanford University, Stanford, CA, United States*, ⁷*General Electric ASL Scientist (EMEA), Pisa, Italy*, ⁸*Department of Translational Research and New Surgical and Medical Technologies, Pisa, Italy*

In this study we propose a procedure which allows the prediction of global and local subject-specific SAR exposure for commonly used 7.0T sequences. Prerequisites for such prediction are: sequences' SAR exposure simulated on the generic anatomic models; subject-specific measured B_1^+ maps. Validation has been provided through phantom experiment. We observed that: SILENT and FLAIR can be safely used in all subjects, both adults and children; FLAIR is more SAR demanding than SILENT; predicted SAR exposure does not show a significant variation with subject weight.

2233

Safety of MR Imaging of Patients with Cardiac Implanted Devices

El-Sayed H. Ibrahim¹, Laura Horwood¹, Jadranka Stojanovska¹, Luba Frank¹, Anil Attili¹, Hakan Oral¹, and Frank Bogun¹

¹*University of Michigan, Ann Arbor, MI, United States*

This study examines whether MRI is safe in patients with cardiac implantable electronic device (CIED) excluded from published protocols, e.g. patients with abandoned leads or pacemaker dependency. A total of 162 MRI scans were obtained in 142 consecutive patients with CIED's. Cardiac scans were performed in 94 patients and spinal/brain scans were performed in 47 patients. Only one patient developed ventricular tachycardia during a spine scan and was removed from the scanner for device reactivation without consequences. No other adverse events were noted. The devices interrogated parameters essentially remained the same immediately, 1-week after, and 3-months after the scans.

2234

The Potential for Eddy Current Induced Peripheral Nerve Stimulation from an Active Implanted Device Canister

Xin Chen¹, Jonathan Edmonson², and Michael Steckner¹

¹*Toshiba Medical Research Institute USA, Inc., Mayfield Village, OH, United States*, ²*Medtronic CRHF, Mounds View, MN, United States*

We used numerical simulations to investigate the potential for increased PNS likelihood with implanted device. Modeling of a gradient coil loaded with a human subject with a metallic implanted canister showed that the electric field around the device can increase by up to 3 fold, suggesting increased PNS likelihood.

2235

Prospective Observational Post-marketing Study on the Safety of Gadoterate Meglumine - Final Results in the pediatric cohort of over 1,600 children

Yun Peng¹

¹*Beijing Children's Hospital, Beijing, China, People's Republic of*

An observational post-marketing study was conducted in 10 countries to prospectively collect safety data in adults and children who were scheduled to undergo routine Magnetic Resonance Imaging (MRI) with administration of gadoterate meglumine (Dotarem®). The incidence of Nephrogenic Systemic Fibrosis (NSF) in routine practice was assessed through specific follow-up of patients with moderate to severe renal impairment. Final results in a large pediatric sub-population of over 1,600 children showed a very good safety profile of gadoterate meglumine with only one adverse event reported in a child and no suspicion of NSF reported.

2236

Scanner-specific verification of Transmit RF Body Coil B_1 -field to inform clinical triage of patients with implanted devices
Chi Ma¹, Krzysztof R Gorny¹, Christopher P Favazza¹, Robert E Watson¹, and Heidi A Edmonson¹

¹*Radiology, Mayo Clinic, Rochester, MN, United States*

Exclusion of scanning with transmit RF body coil may prohibit access to life-saving diagnoses for patients with MR-conditional

implantable devices. Manufacturer provided plots of RF B1-field indicate that RF energy over the implant may be significantly reduced if the implant is kept outside of the 50-55cm long transmit RF body coil. Scanner-specific B1-field measurements and RF-induced heating measurements confirm reduction in heating as conductive material moves away from scanner isocenter. B1-field measurements lateral to the central scanner axis demonstrate local peaks in the B1-field that would not be identified from the IEC-required manufacturer plots.

2237

Magnetic Displacement Force and Safety of Coronary Artery Stents at 7 Tesla.
Christian Hamilton-Craig^{1,2}, Jess Cameron¹, Gregory Brown¹, and Graham Galloway^{1,3}

¹Centre for Advanced Imaging, University of Queensland, Brisbane, Australia, ²Richard Slaughter Centre of Excellence in CVMRI, The Prince Charles Hospital, Brisbane, Australia, ³Translational Research Institute, Brisbane, Australia

Currently, there are minimal data regarding the magnetically induced displacement force of coronary artery stents, in 7.0 T MR. We tested a range of commonly implanted coronary artery stents for maximal displacement force at 7T. CoCr stents appear to have safe deflection properties at 7T. However 316L-SS and PtCr stents exhibit increased magnetically induced displacement forces, and may be not be considered conditionally safe at 7.0T

2238

Electrocorticography grids might cause excessive heating during MR imaging
Emad Ahmadi¹, Reza Atefi¹, Emad Eskandar², Alexandra J. Golby³, Michael H. Lev¹, Rajiv Gupta¹, and Giorgio Bonmassar¹

¹Radiology, Massachusetts General Hospital, Boston, MA, United States, ²Neurosurgery, Massachusetts General Hospital, Boston, MA, United States, ³Neurosurgery, Brigham and Women's Hospital, Boston, MA, United States

Electrocorticography grids are routinely implanted over the cortex for pre-surgical planning in epilepsy surgery. We propose that MR imaging at 3T might cause heating injury in patients with implanted electrocorticography grids.

2239

Sugar free tissue-mimicking MRI phantoms for improved signal-to-noise ratio
Carlotta Ianniello^{1,2}, Ryan Brown¹, Martijn Cloos³, Qi Duan⁴, Jerzy Walczyk³, Graham Wiggins³, Daniel K Sodickson^{2,3}, and Riccardo Lattanzi^{2,3}

¹Radiology, Center for Advanced Imaging Innovation and Research (CAI2R) and Center for Biomedical Imaging, Department of Radiology, New York University School of Medicine, New York, NY, United States, ²The Sackler Institute of Graduate Biomedical Science, New York University School of Medicine, New York, NY, United States, ³Center for Advanced Imaging Innovation and Research (CAI2R) and Center for Biomedical Imaging, Department of Radiology, New York University School of Medicine, New York, NY, United States, ⁴Laboratory of Functional and Molecular Imaging, NINDS, National Institutes of Health, Bethesda, MD, United States

We investigated Polyvinylpyrrolidone (PVP) as an alternative to sugar to control relative permittivity in tissue-mimicking MR phantoms. We constructed a two-compartment phantom filled with water solutions of PVP and NaCl, the latter used to control conductivity. A lower amount of PVP than sugar is required, allowing low permittivity materials to be realized. While signal decreases rapidly in sugar-based phantoms, PVP materials have long T_2^*/T_2 , making PVP-based phantoms suitable for the validation of MR-based electrical properties mapping techniques that rely on high SNR of signal and B_1^+ maps. PVP solutions are relatively inexpensive, easy to mix and do not require preservatives.

2240

Experimental evaluation of heating and SAR reduction with a dielectric insert at 3T
Christopher Sica¹, Sebastian Rupprecht¹, and Qing X Yang¹

¹Radiology, Penn State College of Medicine, Hershey, PA, United States

Prior work has suggested that a dielectric insert can reduce the SAR in the brain at 3T. These previous results were obtained via electromagnetic simulations. Here, we present an experimental evaluation of SAR reduction in a phantom with a dielectric insert.

Traditional Poster

MSK

Exhibition Hall

Wednesday, May 11, 2016: 16:00 - 18:00

2241

Multi-parametric assessment of thigh muscles in patients with limb girdle muscular dystrophies (LGMD): preliminary results.
Alberto De Luca^{1,2}, Maria Grazia D'Angelo³, Denis Peruzzo², Fabio Triulzi⁴, Alessandra Bertoldo¹, and Filippo Arrigoni²

¹Department of Information Engineering, University of Padova, Padova, Italy, ²Neuroimaging Lab, Scientific Institute IRCCS Eugenio Medea, Bosisio Parini (LC), Italy, ³Functional Rehabilitation Unit, Neuromuscular Disorders, Scientific Institute IRCCS Eugenio Medea, Bosisio Parini (LC), Italy, ⁴Department of Neuroradiology, Scientific Institute IRCCS Ca Granda Foundation - Ospedale Maggiore Policlinico, Milan, Italy

Limb girdle muscular dystrophies (LGMD) are a heterogeneous family of disorders characterized by the substitution of muscles with fat and fibrotic tissue. In this work we show the initial results of our acquisition protocol, that included DW-MRI, T_2 mapping and DIXON imaging, on two subtypes of LGMD (type 2A and 2B). Statistical tests and Pearson's correlation were performed on parametric maps at

single muscle level. Preliminary results show that multi-parametric MRI is promising in the characterization of LGMD subtypes on the thigh. Considered MRI techniques show different sensibilities to damages induced by muscular dystrophies and can be considered complimentary.

2242

Multiparametric voxel-based analysis of standardized uptake values and apparent diffusion coefficients in soft-tissue tumors with a positron emission tomography-magnetic resonance system: Application for evaluation of treatment effect
Koji Sagiyama¹, Yuji Watanabe², Ryotaro Kamei¹, Sungtak Hong³, Satoshi Kawanami², Yoshihiro Matsumoto⁴, and Hiroshi Honda¹

¹Department of Clinical Radiology, Graduate School of Medical Sciences, Kyushu University, Fukuoka, Japan, ²Department of Molecular Imaging and Diagnosis, Graduate School of Medical Sciences, Kyushu University, Fukuoka, Japan, ³Healthcare, Philips Electronics Japan, Fukuoka, Japan, ⁴Department of Orthopaedic Surgery, Graduate School of Medical Sciences, Kyushu University, Fukuoka, Japan

A combination of single measurements would be necessary to improve the efficacy of evaluating the treatment effect in heterogeneous soft-tissue tumors. This study aimed to investigate the feasibility of direct voxel-by-voxel comparison of SUVs and ADCs with the PET/MR system in the evaluation of the treatment effect in soft-tissue tumors. The ADCs and SUVs were recorded on a voxel-by-voxel basis for all slices. The scatter plots clearly demonstrated significant difference between pre- and post-treatment. Multiparametric voxel-based analysis of SUVs and ADCs could be a promising tool for evaluating the treatment effect in soft-tissue tumors.

2243

Predicting re-tear after repair of full-thickness rotator cuff tear: 2-Point Dixon MR quantification of fatty muscle degeneration – Initial experience with 1-year follow-up
Taiki Nozaki¹, Atsushi Tasaki², Saya Horiuchi¹, Junko Ochi¹, Jay Starkey¹, Takeshi Hara³, Yukihisa Saida¹, Yasuyuki Kurihara¹, and Hiroshi Yoshioka⁴

¹Radiology, St.Luke's International Hospital, Tokyo, Japan, ²Orthopaedic Surgery, St.Luke's International Hospital, Tokyo, Japan, ³Intelligent Image Information, Gifu University, Gifu, Japan, ⁴Radiological Sciences, University of California, Irvine, Orange, CA, United States

Rotator cuff tear is a common cause of shoulder pain and disability. Minimally-invasive arthroscopic rotator cuff repair is increasingly popular for treatment of full-thickness rotator cuff tear. However, operative outcomes are far from perfect. Postoperative re-tears are associated with greater fatty degeneration. The purpose of this study was to quantify the pre- and post-operative muscular fatty degeneration using a 2-Point Dixon sequence in patients with rotator cuff tears treated by arthroscopic rotator cuff repair. Further, we aim to assess the relationship of preoperative fat fraction values within rotator cuff muscles between patients who experience re-tear and those who do not.

2244

In vivo 1H MRS using 3 Tesla to investigate the metabolic profiles of joint fluids in different types of knee diseases
Geon-Ho Jahng¹, Wook Jin¹, Dong-Cheol Woo², Chanhee Lee¹, Chang-Woo Ryu¹, and Dal-Mo Yang¹

¹Department of Radiology, Kyung Hee University Hospital at Gangdong, Kyung Hee University, Seoul, Korea, Republic of, ²Biomedical Research Center, Asan Institute for Life Sciences, Asan Medical Center, Seoul, Korea, Republic of

To assess the ability of proton MR spectroscopy to identify the apparent heterogeneous characteristics of metabolic spectra in effusion regions in human knees using a high-field MRI system, 84 patients with effusion lesions underwent proton MRS with PRESS single-voxel MRS using a clinical 3.0 Tesla MRI system. Nonparametric statistical comparisons were performed to investigate any differences in metabolites among the degenerative osteoarthritis, traumatic diseases, infectious and an inflammatory disease groups. There were no significant differences among the three groups for the CH3 ($p=0.9019$), CH2 ($p=0.6406$), and CH=CH lipids ($p=0.5467$) and water ($p=0.2853$).

2245

Reliability of MR quantification of rotator cuff muscle fatty degeneration using a 2-point Dixon technique in comparison with the qualitative modified-Goutallier classification
Saya Horiuchi¹, Taiki Nozaki¹, Atsushi Tasaki², Akira Yamakawa², Yasuhito Kaneko³, Takeshi Hara⁴, Yasuyuki Kurihara¹, and Hiroshi Yoshioka³

¹Radiology, St Luke's International Hospital, Tokyo, Japan, ²Orthopedics, St Luke's International Hospital, Tokyo, Japan, ³Radiological Sciences, University of California, Irvine, Orange, CA, United States, ⁴Department of Intelligent Image Information, Gifu University, Gifu, Japan

The assessment of presurgical rotator cuff muscle fatty degeneration is a main determinant of management in patients with rotator cuff tears. The modified-Goutallier classification has been widely accepted as a qualitative method for evaluation of fatty degeneration in current practice. However, reproducibility is insufficient because it is shown to be highly observer-dependent. The objective of this study was to quantify fatty degeneration of the supraspinatus muscle by using 2-point Dixon technique, and to evaluate the inter- and intra-observer reliability of quantitative analysis of fatty degeneration in comparison with the qualitative modified-Goutallier classification.

2246

T2 and T1rho values of grade 1 early degenerative cartilage in the distal femur using angle/layer dependent approach
Yasuhito Kaneko^{1,2}, Taiki Nozaki^{1,3}, Hon Yu^{1,4}, Kayleigh Kaneshiro¹, Ran Schwarzkopf⁵, and Hiroshi Yoshioka¹

¹Radiological Sciences, University of California, Irvine, Orange, CA, United States, ²Orthopaedic Surgery, Saitama City Hospital, Saitama, Japan, ³Radiology, St. Luke's International Hospital, Tokyo, Japan, ⁴John Tu and Thomas Yuen Center for Functional Onco-Imaging, University of California, Irvine, Orange, CA, United States, ⁵Orthopaedic Surgery, University of California, Irvine, Orange, CA, United States

We assessed patterns of T2 and T1rho value change with Outerbridge grade 1 lesions in OA patients compared to healthy control

cartilage utilizing angle and layer dependent approach. T1rho values were more sensitive than T2 values to detect early cartilage degeneration with higher values in OA cartilage than in healthy control. However, T2 and T1rho values in grade 1 cartilage degeneration with signal heterogeneity can be lower compared to those in healthy cartilage.

2247

Morphological, Compositional, and Fiber Architectural Changes in from Unilateral Limb Suspension Induced Acute Atrophy Model in the Medial Gastrocnemius Muscle.

Shantanu Sinha¹, Vadim Malis², Robert Csapo¹, Jiang Du¹, and Usha Sinha³

¹*Radiology, University of California at San Diego, San Diego, CA, United States*, ²*Physics, University of California at San Diego, San Diego, CA, United States*, ³*Physics, San Diego State University, San Diego, CA, United States*

Acute muscle atrophy is characterized by a loss of muscle mass and muscle force. Changes are likely to occur in muscle composition, microenvironment, and fiber architecture which could impact muscle function. This study focuses on the changes in these parameters using MR based fat and connective tissue quantification and DTI in a model of acute atrophy induced by Unilateral limb suspension (ULLS). The % changes in fat and connective tissue were minimal while significant decreases were found in fiber diameter (decrease) and in the pennation angle. These changes could be primarily responsible for muscle force loss in acute atrophy.

2248

Usefulness of thin-slice 3D MR imaging using 3D FSE sequence with variable flip-angle refocusing RF pulses for assessing the popliteomeniscal fascicles of the lateral meniscus in knee MR imaging at 3T

Masayuki Odashima¹, Tsutomu Inaoka¹, Hideyasu Kudo¹, Tomoya Nakatsuka¹, Rumiko Ishikawa¹, Shusuke Kasuya¹, Noriko Kitamura¹, Hiroyuki Nakazawa¹, Koichi Nakagawa², and Hitoshi Terada¹

¹*Radiology, Toho University Sakura Medical Center, Sakura, Japan*, ²*Orthopedic Surgery, Toho University Sakura Medical Center, Sakura, Japan*

Thin-slice 3D MR imaging of the knee joint using 3D FSE sequence with variable flip-angle refocusing RF pulses may improve the visualization of the three popliteomeniscal fascicles of the lateral meniscus in comparison with conventional 2D MR imaging of the knee joint.

2249

Quantitative knee cartilage T2 mapping with in situ mechanical loading using prospective motion correction
Thomas Lange¹, Benjamin R. Knowles¹, Michael Herbst^{1,2}, Kaywan Izadpanah³, and Maxim Zaitsev¹

¹*Department of Radiology, University Medical Center Freiburg, Freiburg, Germany*, ²*John A. Burns School of Medicine, University of Hawaii, Honolulu, HI, United States*, ³*Department of Orthopedic and Trauma Surgery, University Medical Center Freiburg, Freiburg, Germany*

Robust T2 mapping of knee cartilage with in situ mechanical loading using prospective motion correction is demonstrated for the patellofemoral and tibiofemoral knee compartments. T2 maps are reconstructed from multiple spin-echo data acquired with slice position updates before every excitation. While T2 maps of the tibiofemoral joint do not show significant changes in response to loading, maps of the patellofemoral joint show a substantial load-induced T2 reduction in the superficial cartilage layers. In particular, the T2 of tangential fibers at the cartilage surface appears to undergo a strong reduction due to a load-induced increase of tissue anisotropy.

2250



CSF-Free Imaging of the Lumbar Plexus using Sub-Millimeter Resolutions with 3D TSE

Barbara Cervantes¹, Houchun Harry Hu², Amber Pokorney², Dominik Weidlich¹, Hendrik Kooijman³, Ernst Rummel¹, Axel Haase⁴, Jan S Kirschke⁵, and Dimitrios C Karampinos¹

¹*Diagnostic and Interventional Radiology, Technische Universität München, Munich, Germany*, ²*Radiology, Phoenix Children's Hospital, Phoenix, AZ, United States*, ³*Philips Healthcare, Hamburg, Germany*, ⁴*Zentralinstitut für Medizintechnik, Garching, Germany*, ⁵*Neuroradiology, Technische Universität München, Munich, Germany*

High-resolution MRI with 3D turbo spin echo (TSE) is arising as an accurate, non-invasive method for detecting disease and injury in the nerves of the lumbar plexus. Imaging of the lumbar plexus with 3D TSE frequently faces signal contamination of the cerebrospinal fluid (CSF) within the spine. Increasing spatial resolution in 3D TSE can affect flowing signal. The present study describes numerically the effects of the imaging gradients in 3D TSE on flowing CSF and demonstrates *in vivo* that CSF can be completely suppressed without modifications to refocusing angle modulation when sub-millimeter voxel sizes are used with 3D TSE.

2251

An assessment of the repeatability and sensitivity of T2 mapping in low-grade cartilage lesions at 3 and 7 Tesla

Vladimir Juras^{1,2}, Laurent Didier³, Vladimir Mlynarik¹, Pavol Szomolanyi¹, Stefan Zbyn¹, Nicole Getzmann³, Joerg Goldhahn³, Stefan Marlovits⁴, and Siegfried Trattnig^{1,5}

¹*Department of Biomedical Imaging and Image-Guided Therapy, High Field MR Centre, Medical University of Vienna, Vienna, Austria*

²*Department of Imaging Methods, Institute for Measurement Science, Bratislava, Slovakia*, ³*Novartis Institutes for Biomedical Research, Basel, Switzerland*, ⁴*Department of Traumatology, Medical University of Vienna, Vienna, Austria*, ⁵*Christian Doppler Laboratory for Clinical Molecular MR Imaging, Vienna, Austria*

An assessment of the reliability of T2 mapping was achieved with a 3D-TESS sequence in patients with cartilage lesions ICRS Grade I-II. Since low-grade cartilage lesions are not usually accompanied by collagen matrix remodeling, we tested the sensitivity of T2 to detect these lesions at 3 and 7T. It seems that the reproducibility of 3T T2 mapping is higher than that of 7T; however, the sensitivity of T2 mapping for the detection of low-grade cartilage lesions was greater at the ultra-high field. T2 mapping could be used in the future as a

good alternative to cartilage biopsies in future clinical trials on new therapies aimed at cartilage regeneration.

2252

Non-Contrast, Flow-Independent, Relaxation-Enhanced Subclavian MR Angiography Using Inversion Recovery and T2 Prepared 3D Gradient-Echo DIXON Sequence
Masami Yoneyama¹, Nobuyuki Toyonari², Seiichiro Noda², Yukari Horino², Kazuhiro Katahira², and Marc Van Cauteren³

¹Philips Electronics Japan, Tokyo, Japan, ²Kumamoto Chuo Hospital, Kumamoto, Japan, ³Philips Healthcare Asia Pacific, Tokyo, Japan

This study showed a novel non-contrast MR angiography sequence based on gradient echo DIXON sequence with flow-independent relaxation-enhanced method (Relaxation-Enhanced Angiography without Contrast and Triggering: REACT) for evaluating thoracic outlet syndrome. This could provide high-quality MRA with robust fat suppression entire the subclavian area with/without arm abduction.

2253

Toward a 7T MRI protocol for the evaluation of early osteoarthritis in knee cartilage

Daniel J. Park¹, Neal K. Bangerter^{2,3}, Antony J. R. Palmer¹, Haonan Wang², Bragi Sveinsson⁴, Brian Hargreaves⁴, and Siôn Glyn-Jones¹

¹Nuffield Department of Orthopaedics, Rheumatology, and Musculoskeletal Sciences, University of Oxford, Oxford, United Kingdom,

²Department of Electrical and Computer Engineering, Brigham Young University, Provo, UT, United States, ³Department of Radiology, University of Utah, Salt Lake City, UT, United States, ⁴Radiology, Stanford University, Stanford, CA, United States

Osteoarthritis, a disease that is a burden to society and individuals, has 3 major stages of progression in cartilage: (1) glycosaminoglycan loss; (2) collagen matrix degeneration; and (3) fissures and volume and thickness loss. A protocol is proposed to measure the progression of each of these stages of OA at 7 Tesla in about 30 minutes: (1) T1p to measure glycosaminoglycan changes; (2) modified DESS measurements of T2 and ADC to measure collagen matrix integrity; and (3) high resolution phase cycled bSSFP images to measure changes in morphology.

2254

3D Longitudinal MRI studies on novel tissue-engineered bone constructs in living rats : Volume & Perfusion assessments

Neha KOONJOO^{1,2}, Clément Tournier³, Aurélien Trotier^{1,2}, Didier Wecker⁴, William Lefrançois^{1,2}, Didier Letourneau⁵, Joëlle Amédée Vilamitjana³, Sylvain Miraux^{1,2}, and Emeline J Ribot^{1,2}

¹CNRS-UMR 5536, Centre de Résonance Magnétique des Systèmes Biologiques, Bordeaux, France, ²Metropolitan, ³University of Bordeaux, Bordeaux, France, ⁴U1026, Bioingénierie Tissulaire (BioTis), Bordeaux, France, ⁵Bruker Biospin MRI GMBH, Ettlingen, Germany,

INSERM U 1148, Cardiovascular Bio-engineering Laboratory, Paris, France, ⁵Metropolitan

In tissue engineering, correct bone regeneration in large bone defects is a major issue. MRI has revealed its high potential to assess continuous tracking of three differently conditioned bone constructs implanted in the rats' femoral condyles. These constructs aimed at evaluating cumulative effects of hydroxyapatite and/or fucoidan in osteogenesis and vascularization. A water-selective bSSFP sequence with fat suppression and banding artifacts correction was implemented for volumetric measurements. 3D Dynamic-contrast enhanced MRI was applied and pixel-wise analysis resulted in fairly good constructs perfusion evaluation. 3D images spotted distinct volume changes and promising area under curve evolution.

2255

Quantifying bone marrow inflammatory edema in psoriatic arthritis using pixel-based morphometry

Ioanna Chronaiou^{1,2}, Ruth Stoklund Thomsen³, Else-Marie Huuse-Røneid^{2,3}, and Beate Sitter¹

¹Department of Radiography, Sør-Trøndelag University College, Trondheim, Norway, ²Department of Circulation and Medical Imaging, Norwegian University of Science and Technology, Trondheim, Norway, ³St Olav's University Hospital, Trondheim, Norway

Psoriatic arthritis (PsA) is a highly heterogeneous inflammatory disease that manifests with inflammation in sacroiliac (SI) joints and spine among other symptoms. PsA patients (N=12) underwent magnetic resonance (MR) imaging examinations to assess the extent of SI joint inflammation. A pixel-based morphometric method for accurate quantification of bone marrow inflammatory edema was compared to SPARCC assessment in MR images of psoriatic arthritis patients with low or very low inflammatory activity. A significant correlation was found, suggesting pixel-based morphometry as a reliable and sensitive quantitative method for measuring inflammation in bone marrow.

2256

Statistical Comparison of Commonly Used Kinetic Models for Dynamic Contrast Enhanced Magnetic Resonance Imaging of Rheumatoid Arthritis in the Wrist

Sameer Khanna^{1,2}, Nicolas Pannetier¹, Jing Liu¹, and Xiaojuan Li¹

¹Radiology, University of California, San Francisco, San Francisco, CA, United States, ²University of California, Berkeley, Berkeley, CA, United States

There has been a lack of statistical analysis to determine which kinetic model is best suited for analysis of the wrist. This study aims to rectify this by comparing the most commonly used models: Modified Tofts (MT), Two Compartment Uptake (2CU), and Two Compartment Exchange (2CX). Goodness of fit is analyzed by reduced chi squared, while statistical significance between models is determined by wilcoxon signed-rank.

2257

Reduced Field of View Multi-Spectral Imaging through Coupled Coil and Frequency Bin Encoding

Andrew S. Nencka¹, Shiv S. Kaushik¹, and Kevin M. Koch¹

Advanced methods for imaging around metallic implants yield most benefit in the neighborhood around the implant. However, due to the extent of the anatomy in the region of the implant, large field of view acquisitions are often required. In this work, it is shown that a low-resolution acquisition can be used to inform a subsequent reduced field of view acquisition. Significant reductions in the imaged field of view are possible due to the combination of both spatially varying coil sensitivity profiles along with spatially varying resonance frequency bins. Artifact free regions in the neighborhood of the implant are possible with extreme field of view reductions because of the rapid spatial variability of the imaged resonance frequency bins.

2258

Cortical bone quality as a biomarker for diabetes risk in post-menopausal Chinese-Singaporean women: a preliminary study
Francesca A. A. Leek¹, Anna Therese Sjoholm¹, Christiani Jeyakumar Henry², Xiaodi Su³, Marlena C. Kruger⁴, and John J. Totman¹

¹*A*STAR-NUS Clinical Imaging Research Centre, Singapore, Singapore*, ²*A*STAR Clinical Nutrition Research Centre, Singapore, Singapore*, ³*A*STAR Institute of Materials Research and Engineering, Singapore, Singapore*, ⁴*School of Food and Nutrition, College of Health, Massey University, Palmerston North, New Zealand*

The feasibility of utilising proximal femur cortical bone quality as a biomarker for diabetes risk in post-menopausal Chinese-Singaporean women was investigated. Non-dominant proximal femurs were imaged with quantitative CT (QCT) and MR for the assessment of volumetric bone mineral density (vBMD) and cortical bone porosity. A significant ($p<0.01$; $n=8$) positive correlation between MRI vBMD and QCT vBMD for the region of maximum cortical thickness was shown. Whether MRI vBMD is associated with fracture risk and if it is sensitive to changes due to dietary or drug intervention needs to be investigated to fully assess the clinical potential of this method.

2259

Assessment of trabecular bone quality of the proximal femur in vivo: A Preliminary Study
Maria Kalimeri¹, Christiani Jeyakumar Henry², Xiao Di Su³, Marlena C. Kruger⁴, and John J. Totman¹

¹*A*STAR-NUS Clinical Imaging Research Centre, Singapore, Singapore*, ²*Clinical Nutrition Research Centre, Singapore, Singapore*, ³*Institute of Materials Research and Engineering, Singapore, Singapore*, ⁴*School of Food and Nutrition, College of Health, Massey University, Palmerston North, New Zealand*

Osteoporosis is a skeletal disorder that affects predominantly postmenopausal women. The screening method for osteoporosis is Dual X-ray Absorptiometry (DXA), which has several limitations, including the inability to differentiate between trabecular and cortical bone. 3D imaging modalities can give information about each bone component, which contribute to bone strength in different ways. MRI is an attractive alternative due to lack of ionising radiation. In this abstract, we present a method for bone density assessment of trabecular bone in the proximal femur using MRI. Strong correlations with both DXA and Quantitative Computed Tomography (QCT) measurements of similar regions were observed.

2260

T2-weighted Multispectral Imaging for Postoperative Imaging of Patients with Lumbar Spinal Fusion
Daehyun Yoon¹, Kathryn Stevens¹, and Brian Hargreaves¹

¹*Radiology, Stanford University, Palo Alto, CA, United States*

T2-weighted MRI is essential to detect neural compression in the lumbar spine after spinal fusion surgery in patients with recurrent radicular symptoms. Unfortunately, off-resonance artifacts induced from lumbar fusion devices make the conventional T2-weighted MR images extremely challenging or impossible to interpret. We present a modified version of MAVRIC-SL, an MR sequence designed to correct for metal-induced artifacts, to allow T2 contrast, significantly improving diagnostic capabilities in the postoperative lumbar spine.

2261

Evaluation of Chronic Inflammatory Demyelinating Polyneuropathy: New Simultaneous T2 mapping and neurography method with 3D Nerve-Sheath Signal Increased with Inked Rest-Tissue Rapid Acquisition of Relaxation Enhancement Imaging (SHINKEI Quant)
Akio Hiwatashi¹, Osamu Togao¹, Koji Yamashita¹, Kazufumi Kikuchi¹, Masami Yoneyama², and Hiroshi Honda¹

¹*Clinical Radiology, Kyushu University, Fukuoka, Japan*, ²*Philips Electronics Japan, Tokyo, Japan*

MR neurography (MRN) is a useful technique with which to evaluate abnormal conditions of the peripheral nerves such as chronic inflammatory demyelinating polyradiculoneuropathy (CIDP). We have developed a new simultaneous T2 mapping and MRN method called SHINKEI Quant. Patients with CIDP could be distinguished from normal subjects in size and T2 value of the peripheral nerves with SHINKEI Quant.

2262

Vertebral Bone Marrow Fat Quantification and its Relationship with Bone Mineral Density: Using Multi-Echo MRS and Multi-Echo Dixon
Na Chai¹, Panli Zuo², Stephan Kannengiesser³, Andre De Oliveira³, Shun Qi¹, and Hong Yin¹

¹*Department of Radiology, Xijing Hospital, Xi'an, China*, ²*Siemens Healthcare, MR Collaborations NE Asia, Beijing, China*, ³*People's Republic of, Application Predevelopment, Siemens Healthcare, Erlangen, Germany*

Using the multi-echo ¹H-MRS and multi-echo Dixon VIBE, we measured the proton density fat fraction (PDFF) using MR imaging in the bone marrow of L2-L4 vertebra, and compared with the bone mineral density (BMD) measured using computed tomography (CT). The results showed a significant correlation between PDFF measured using the two methods, and also PDFF with BMD.

Calcific Longus Colli Tendinitis: Emphasis on MRI Appearance with Variations in Anatomical Correlation
Tamami Shirakawa¹, Kazutoshi Inamura², Yasuhisa Tanaka³, Takeshi Hoshikawa³, Megumi Kuchiiki¹, and Atsuko Oda¹

¹*Radiology, Tohoku Central Hospital, Yamagata, Japan*, ²*Otolaryngology, Tohoku Central Hospital, Yamagata, Japan*, ³*Orthopaedic Surgery, Tohoku Central Hospital, Yamagata, Japan*

Calcific longus colli tendinitis is an inflammatory lesion in the prevertebral space. When prevertebral effusion is observed on MRI, awareness of the prevertebral muscle swelling with signal change and the associated mass effect would suggest that the main site of the lesion is the prevertebral space, not the retropharyngeal space and may thus prevent both misdiagnosis as a retropharyngeal abscess and unnecessary treatment. The variability in the level of calcification and prevertebral effusion is highlighted in the present study in order to assist in the establishment of the correct radiological diagnosis.



Combined Spiroergometry and ³¹P MRS in human calf muscle during high intense exercise
Kevin Tschiesche¹, Alexander Gussew¹, Christian Hein², and Jürgen Rainer Reichenbach¹

¹*Medical Physics Group, Institute of Diagnostic and Interventional Radiology, Jena University Hospital - Friedrich Schiller University Jena, Jena, Germany*, ²*Ganshorn Medizin Electronic GmbH, Niederlauer, Germany*

The aim of this work was the implementation of combined spirometric and ³¹P MRS measurements. We adapted a commercial gas exchange system by extending the gas sampling line from 3 m to 5 m to perform acquisitions of pulmonary ventilation in a MR scanner. Calibration measurements showed changes in an appropriate range in the delay- and response time.



Observation of in vivo lactate metabolism in skeletal muscle using hyperpolarized ¹³C MRS
JAE MO PARK¹, Sonal Josan¹, Dirk Mayer², Ralph E Hurd³, Youngran Chung⁴, David Bendahan⁵, Daniel M Spielman¹, and Thomas Jue⁴

¹*Radiology, Stanford University, Stanford, CA, United States*, ²*Diagnostic Radiology and Nuclear Medicine, University of Maryland, Baltimore, MD, United States*, ³*Applied Sciences Laboratory, GE Healthcare, Menlo Park, CA, United States*, ⁴*Biochemistry and Molecular Medicine, University of California - Davis, Davis, CA, United States*, ⁵*Centre de Resonance Magnétique Biologique et Médicale, Aix-Marseille University, Marseille, France*

The present study reports the use of hyperpolarized [¹-¹³C]lactate and [²-¹³C]pyruvate to measure the rapid pyruvate and lactate kinetics in rat skeletal muscle. The results provide support for a critical underpinning of both the glycogen shunt model and the intracellular lactate shuttle hypothesis, and cautions against an overly simplistic view of glycolytic end products as merely hypoxia biomarkers.

Quantitative magnetization transfer MRI of in-situ and ex-situ meniscus
Mikaël Simard¹, Emily J. McWalter², Garry E. Gold², and Ives R. Levesque^{1,3}

¹*Medical Physics, McGill University, Montreal, QC, Canada*, ²*Radiology, Stanford University, Stanford, CA, United States*, ³*Research Institute of the McGill University Health Centre, Montreal, QC, Canada*

Quantitative magnetization transfer (QMT) probes macromolecular content in tissue and may be a useful tool in the early detection of meniscal degeneration. QMT mapping of the meniscus was performed in 3 cadaver knee specimens in situ, and repeated ex situ following dissection and immersion in perflubron. After extraction, a decrease in the restricted pool fraction f was noted, while T1obs and T1f increased. A trend towards lower values of the exchange rate kf was noted after excision. T2 and T2r were relatively constant. The variation in QMT parameters may be caused by the diffusion of perflubron into the ex situ samples.

Ultrashort echo time magnetization transfer (UTE-MT) imaging and modeling – magic angle independent biomarkers of tissue properties
Yajun Ma¹, Hongda Shao¹, Michael Carl², Eric Chang¹, and Jiang Du¹

¹*Department of Radiology, UCSD, San Diego, CA, United States*, ²*Global MR Application & Workflow, General Electric, San Diego, CA, United States*

Magnetic resonance imaging biomarkers such as T₂ and T_{1rho} have been widely used in the evaluation of osteoarthritis (OA). The principal confounding factor for T₂ and T_{1rho} measures is the magic angle effect, which may result in a several fold increase in T₂ and T_{1rho} values when the fibers are oriented near 55° (the magic angle) relative to the B₀ field. This often far exceeds the changes produced by OA, and may make definitive interpretation of elevated T_{1rho} and T₂ values difficult or impossible. Magic angle independent MR biomarkers are highly desirable for more accurate assessment of OA. In this study we report the use of two-dimensional ultrashort echo time magnetization transfer (UTE-MT) imaging and modeling for magic angle independent assessment of the tissue properties.

NEW MR PARAMETERS TO ASSESS AND MONITOR TENDON XANTHOMAS

James F Griffith¹, Teresa M Hu², David KW Yeung¹, D F Wang¹, Fan Xiao¹, and Brian Tomlinson²

¹*Imaging and Interventional Radiology, The Chinese University of Hong Kong, Hong Kong SAR, Hong Kong*, ²*Medicine, The Chinese University of Hong Kong, Hong Kong SAR, Hong Kong*

Achilles tendon xanthoma is a key clinical indicator of familial hypercholesterolaemia (FH) and associated cardiovascular disease. Treatment that reduces the size of tendon xanthoma also benefits the arterial manifestations of FH. Ultrasound and MRI are often used to detect and monitor treatment response of tendon xanthomas using parameters such as tendon thickness, width and cross-sectional

area. However, MR-based parameters derived from the DIXON technique to determine tendon volume and intratendinous percentage fat fraction may be more sensitive than traditional US and conventional MRI.

2269

Magnetic resonance imaging evaluation of acetabular morphology and long-term prognosis in developmental dysplasia of the hip in childhood
Mingming Lu¹, Peng Peng¹, Yu Zhang², and Fei Yuan¹

¹Affiliated Hospital of Logistics University of Chinese People's Armed Police Forces, Tianjin, China, People's Republic of, ²Philips Healthcare, Beijing, China, People's Republic of

This study aimed to investigate the efficacy of MRI for evaluating morphology and long-term prognosis of acetabulum in pediatric patients with DDH. The bony acetabular index (BAI), cartilaginous acetabular index (CAI), acetabular anteversion index of bone (BAAV) and cartilage (CAAV) were measured and cartilaginous index (CI=(BAI-CAI) / BAI) was computed. There was obvious differences with statistical significance in the CI between non-reduced group and reduced group ($t=2.315$, $P=0.24$), and age was also negatively correlated with the CI ($r = -0.345$, $P = 0.01$). The CI can preliminarily predict the long-term prognosis of DDH after reduction.

2270

Use of Adding T2 Mapping Sequence to a Routine MR Imaging Protocol to Evaluate of the Articular Cartilage Changes of the Knee and Ankle Joint with Hemophilia in Children
Ningning Zhang¹, Yanqiu Lv¹, Kaining Shi², Di Hu¹, Huiying Kang¹, Yue Liu¹, Runhui Wu³, and Yun Peng¹

¹Imaging Center, Beijing Children's Hospital, Capital Medical University, Beijing, China, People's Republic of, ²Imaging System Clinical Science, Philips Healthcare, Beijing, China, People's Republic of, ³Hematology Center, Beijing Children's Hospital, Capital Medical University, Beijing, China, People's Republic of

T2 mapping sequences can help detect changes in the water and collagen content. This sequence have been used extensively in osteoarthritis research studies to detect disease and treatment related changes in articular cartilage(1-3). However, little is known about the early cartilage changes in hemophilia patients, and once established, arthropathy follows a progressive and non-reversible process despite the use of factor concentrates.

2271

DTI can monitor changes in articular cartilage after a mechanically induced injury
Uran Ferizi¹, Ignacio Rossi², Oran Kennedy², Thorsten Kirsch², Jenny Bencardino¹, and Jose Raya¹

¹Department of Radiology, New York University School of Medicine, New York, NY, United States, ²Orthopaedic Surgery, New York University School of Medicine, New York, NY, United States

The development of novel treatment strategies that would prevent joint replacement surgery at young age, as a result of PTOA, is critical. Hours after non-contact rupture of the anterior cruciate ligament, high concentrations of PG and type II collagen fragments are found in the synovial fluid. DTI has emerged as an imaging biomarker that can assess both PG content and collagen architecture with greater accuracy than T2 or Na imaging. The current interpretation of DTI measurements is that changes in the level of proteoglycans (PG) affect the mean diffusivity (MD) index from the DTI, while the collagen structure affects the fractional anisotropy (FA). This study examines the feasibility of DTI, by using biomechanics for simulating a controlled cartilage damage. We find that DTI metrics are sensitive to the early changes in the cartilage as a result of injury. Specifically, the correlations of the mean diffusivity (MD) are statistically significant, but those of fractional anisotropy (FA) are not. The additional validation with histology, as well as a clinical scanning environment make these results important in the translation of DTI to clinical practice.

2272

A new method for accurate detection of cartilage lesions in femoroacetabular impingement using quantitative T₂ mapping: preliminary validation against arthroscopic findings at 3 T
Noam Ben-Eliezer^{1,2}, Akio Ernesto Yoshimoto², KAI Tobias Block^{1,2}, Roy Davidovitch³, Thomas Youm³, Robert Meislin³, Michael Recht^{1,2}, Daniel K Sodickson^{1,2}, and Riccardo Lattanzi^{1,2}

¹Center for Advanced Imaging Innovation and Research (CAI2R), New York University School of Medicine, New York, NY, United States, ²Bernard and Irene Schwartz Center for Biomedical Imaging, Department of Radiology, New York University School of Medicine, New York, NY, United States, ³Department of Orthopedic Surgery, New York University Hospital for Joint Diseases, New York, NY, United States

Early diagnosis of cartilage defects is critical for the success of corrective surgical procedures in patients with femoroacetabular impingement (FAI). T₂ is a biomarker for early biochemical degeneration of cartilage, but in vivo T₂ mapping is challenging while commonly used techniques based on exponential fit of multi spin-echo protocols are inaccurate. We used a Bloch simulation based T₂ mapping technique – the EMC algorithm – to retrospectively quantify reliable T₂ values in the hip cartilage of FAI patients. We then defined a normalized T₂-index using an internal reference and showed that it allows detection of surgically confirmed cartilage lesions with 95% accuracy.

2273

Elevated adiabatic $\text{$_{1}T_{-1}\rho$}$ and $\text{$_{2}T_{-2}\rho$}$ in articular cartilage are associated with symptoms and structural changes in early osteoarthritis
Victor Casula^{1,2}, Mikko J. Nissi^{3,4}, Jana Podlipská^{1,5}, Marianne Haapea^{6,7}, Simo Saarakkala^{1,2,7}, Ali Guermazi⁸, Eveliina Lammentausta^{2,7}, and Miika T. Nieminen^{1,2,7}

¹Research Unit of Medical Imaging, Physics and Technology, University of Oulu, Oulu, Finland, ²Medical Research Center, University of Oulu and Oulu University Hospital, Oulu, Finland, ³Department of Applied Physics, University of Eastern Finland, Kuopio, Finland, ⁴Diagnostic Imaging

Adiabatic $\text{$_T\{1\rho\}$}$, adiabatic $\text{$_T\{2\rho\}$}$ and $\text{$_T\{2\}$}$ of articular cartilage (AC) were compared between patients with pre- or early radiographic knee osteoarthritis (OA) (KL=1,2) and volunteers. Further comparisons were performed after classifying the subjects according to different signs of OA, including symptoms and functional impairment assessed by the Western Ontario and McMaster Universities questionnaire (WOMAC) and presence of structural changes assessed by MRI OA Knee Score (MOAKS). Increased adiabatic $\text{$_T\{1\rho\}$}$ and $\text{$_T\{2\rho\}$}$ were significantly associated with clinical signs of OA. The findings suggest that novel rotating frame of reference techniques have considerable potential for *in vivo* OA research and clinical use.

2274

ZTE Imaging of Joints: Unmasking the Bone

Ryan Breighner¹, Sonja Eagle¹, Gaspar Delso², Hollis G. Potter¹, and Matthew F. Koff¹

¹Department of Radiology and Imaging - MRI, Hospital for Special Surgery, New York, NY, United States, ²General Electric Healthcare, Zurich, Switzerland

Standard magnetic resonance imaging protocols fail to generate sufficient positive contrast for the direct imaging of bone. This study demonstrates the use of zero echo time (ZTE) imaging of the appendicular skeleton. Knee, shoulder, ankle, and wrist joints were imaged and scan parameters were varied between subjects to optimize acquisition of joints of interest. ZTE images permitted the visualization of fine tendinous structures in addition to bone. ZTE may prove useful when concurrent imaging of tendon and bone is required or when bone imaging is necessary but radiation dose is undesirable, due to patient age or anatomy.

2275

Study of Hemodynamics in Human Calf Muscle during Low-Intensity Exercise Using Single-Subject Independent Component Analysis

Zhijun Li¹, Prasanna Karunanayaka¹, Matthew Muller², Christopher Sica¹, Jian-Li Wang¹, Lawrence Sinoway², and Qing X. Yang^{1,3}

¹Center for NMR Research, Department of Radiology, College of Medicine, The Pennsylvania State University, Hershey, PA, United States, ²Heart and Vascular Institute, College of Medicine, The Pennsylvania State University, Hershey, PA, United States, ³Department of Neurosurgery, College of Medicine, The Pennsylvania State University, Hershey, PA, United States

Unlike in human brain imaging, normalization to a common template during exercising is a difficult proposition in muscle-imaging studies. Still, motion artifact has been an issue for dynamic analysis of exercise paradigm. We used individual Independent Component Analysis (ICA) to identify the "motion component" during exercise (rhythmic plantar-flexion) and anatomical and temporal features of BOLD signal. We simultaneously identified the lower leg muscle groups and their common hemodynamic behaviors under a low-level exercise paradigm and revealed an intriguing hemodynamic respond characteristic with a prominent transient increase and followed by a negative BOLD signal sustained to the end of exercise.

2276

The Effect of Physical Activity on ³¹P-MRS Bioenergetic Measurements and Assessment of Muscle Quality in the Baltimore Longitudinal Study of Aging

Ariel C. Zane¹, Donnie Cameron¹, Seongjin Choi¹, David A. Reiter², Kenneth W. Fishbein², Christopher M. Bergeron¹, Eleanor Simonsick¹, Richard G. Spencer², and Luigi Ferrucci³

¹Translational Gerontology Branch, NIH/National Institute on Aging, Baltimore, MD, United States, ²Laboratory of Clinical Investigation, NIH/National Institute on Aging, Baltimore, MD, United States, ³Intramural Research Program, NIH/National Institute on Aging, Baltimore, MD, United States

We examined the effect of high intensity physical activity on the post-exercise PCr recovery rate (k_{PCr}), testing whether the decline in muscle quality may be attributed to an age-related decline in muscle mitochondrial capacity. In-vivo ³¹P MRS measurements were obtained before, during, and after a rapid knee-extension exercise. The cross-sectional results in the BLSA show that both age and frequency of physical activity are significant predictors of k_{PCr} . However, neither is significantly correlated with a strength-based assessment of muscle quality.

2277

Classification of signal voids in time-series of diffusion-weighted images of the lower leg by simultaneous MRI and EMG measurements: Initial findings

Martin Schwartz^{1,2}, Günter Steidle¹, Petros Martirosian¹, Ander Ramos-Murguialday³, Bin Yang², and Fritz Schick¹

¹Section on Experimental Radiology, Department of Radiology, University of Tuebingen, Tuebingen, Germany, ²Institute of Signal Processing and System Theory, University of Stuttgart, Stuttgart, Germany, ³Institute for Medical Psychology and Behavioural Neurobiology, University of Tuebingen, Tuebingen, Germany

Diffusion-weighted images of the lower leg have shown to be impaired by signal voids in different muscle groups with unknown underlying physiological processes. For more detailed insight into this topic, simultaneous surface electromyography measurements of the electrical activity of muscles during the MR scan were recorded. A classification of the appeared signal voids in the diffusion-weighted images based on initial findings in the EMG measurements is demonstrated.

2278

Noninvasive Evaluation of Foot Oxygen Extraction Fraction with Multi-shot Asymmetric Spin Echo Method

Fei Gao¹, Chengyan Wang², Rui Zhang¹, Xiaodong Zhang³, Kai Zhao³, Jue Zhang^{1,2}, Xiaoying Wang^{2,3}, and Jing Fang^{1,2}

In this study, a multi-shot ASE sequence with 32 varied echo shifts was implemented to acquire the source images for foot muscle OEF quantification. Three healthy volunteers (mean age 23 ± 1 years, range 22-24) were recruited to undergo the imaging of the foot using a 3.0-T whole-body scanner. The OEF and R2' maps indicate the feasibility of the proposed multi-shot ASE sequence in quantifying foot muscle OEF. These results hold promise for some clinical uses, for example, to study vascular function in peripheral artery disease.

2279

Comparison of Single-shot ASE and Multi-shot ASE Sequence for Measurement of Lower Extremity Muscle Oxygenation
CY Wang¹, L Jiang², R Zhang³, XD Zhang⁴, H Wang², K Zhao⁴, LX Jin², J Zhang^{1,3}, XY Wang^{1,4}, and J Fang^{1,3}

¹Academy for Advanced Interdisciplinary Studies, Peking University, Beijing, China, People's Republic of, ²Philips Healthcare, Suzhou, China, People's Republic of, ³College of Engineering, Peking University, Beijing, China, People's Republic of, ⁴Department of Radiology, Peking University First Hospital, Beijing, China, People's Republic of

Recently, MRI based methods for measuring muscle oxygen extraction fraction (OEF) have been reported. Asymmetric spin-echo (ASE) sequence combining with a susceptibility model is the most widely used approach. However, conventional ASE sequence uses single-shot (SS) EPI for data acquisition, which suffers from the problem of severe susceptibility artifacts and distortion due to the relatively long echo train length (ETL). One solution is to employ multi-shot (MS) EPI instead of SS EPI for data acquisition. With the use of MS-ASE technique, much higher spatial resolution could be achieved for lower extremity muscle imaging.

2280

A simplified method to determine tissue-water T2 from CPMG image data in fat infiltrated skeletal muscle: application in the forearm in Duchenne muscular dystrophy

Nick Zafeiropoulos¹, Valeria Ricotti², Matthew Evans^{1,3}, Jasper Morrow³, Paul Matthews⁴, Robert Janiczek⁵, Tarek Yousry^{1,3}, Christopher Sinclair^{1,3}, Francesco Muntoni², and John Thornton^{1,3}

¹Neuroradiological Academic Unit, UCL Institute of Neurology, London, United Kingdom, ²Dubowitz Neuromuscular Centre, UCL Institute of Child Health, London, United Kingdom, ³MRC Centre for Neuromuscular Diseases, London, United Kingdom, ⁴Imperial College London, London, United Kingdom, ⁵GlaxoSmithKline, London, United Kingdom

A simplified CPMG signal decay model was used to determine muscle-water T2 (T2m) in fat-infiltrated skeletal muscle, using a predetermined mono-exponential approximation to the fat decay component. This approach enabled the stable estimation of T2m in the forearm muscles of non-ambulant Duchenne muscular dystrophy patients and healthy controls from a multi-echo CPMG acquisition with only 12 echo-times. Values obtained were in good agreement with previous reports, and largely independent of muscle fat content.

2281

Quantification of Cartilage Loss of Knee Joints using Automated Segmentation in Patients with Osteoarthritis and Meniscus Tears: a primary study

Wen-Jing Hou¹, Pan-Li Zuo², Esther Meyer³, Jun Zhao¹, and Wei Chen¹

¹Radiology, Southwest Hospital, Third Military Medical University, Chongqing, China, People's Republic of, ²Siemens Healthcare, MR Collaboration NE Asia, Beijing, China, People's Republic of, ³Siemens Healthcare, Erlangen, Germany

Quantitative cartilage morphometry on MR images is a valuable tool to reveal changes of cartilage in pathological knees. In this study, we used an automated cartilage segmentation software to quantifying the cartilage loss in osteoarthritis patients, meniscus tears patients and compared with the control healthy subjects. The aim of this study was to examine whether there is dominant cartilage which has the most loss in cartilage volume in osteoarthritis and meniscus tears. The outcome is that using the precise quantification of cartilage change in percentage is valuable to specify the most venerable cartilage in pathological knees.

2282

Increased heterogeneity in T2-relaxation times in the dystrophic soleus muscle

Constantinos Anastasopoulos^{1,2}, Melissa Hooijmans¹, Jedrek Burakiewicz¹, Andrew G. Webb¹, Janbernd Kirschner², Jan J.G.M. Verschuur³, Erik H. Niks³, and Hermien E. Kan¹

¹Gorter Center, Leiden University Medical Center, Leiden, Netherlands, ²Pediatric Neurology and Muscle Disorders, University Clinic Freiburg, Freiburg, Germany, ³Department of Neurology, Leiden University Medical Center, Leiden, Netherlands

The interpretation of muscle T2 relaxation times in muscular dystrophies is complicated by the disease progression, as both inflammation and increased fat content result in a longer T2. We measured water-T2 in two muscles of the lower leg using a tri-exponential fitting of the T2 decay in patients with DMD and healthy controls. We found a significantly higher T2-heterogeneity in the soleus muscle of patients, with no significant difference between the two groups in average T2 values. T2-heterogeneity should be taken into consideration when using the water T2 of the diseased muscle as an outcome measure for therapeutic interventions.

2283

Reliability of fat content measurement of lumbar vertebrae marrow and lumbar paraspinal muscle using 3D DIXON Fat Fraction Quantification

Yong Zhang¹, Aihong Yu¹, Yu Zhang², Chao Wang³, Yangyang Duan Mu¹, Chenxin Zhang¹, Zhuang Zhou⁴, Wei Zhao¹, Ling Wang¹, and Xiaoguang Cheng¹

¹radiology, Beijing Jishuitan hospital, Beijing, China, People's Republic of, ²radiology, Philips Healthcare, Beijing, China, Beijing, China, People's Republic of, ³Beijing Institute of Traumatology and Orthopedics, Beijing, China, People's Republic of, ⁴Orthopedics, The Third Hospital of Hebei

This study aimed to evaluate the reliability of fat content measurement of lumbar vertebrae marrow and lumbar paraspinal muscle using an multi-echo 3D DIXON method. A total of 31 volunteers (15 males and 16 females) were included in this study and underwent liver mDIXON-quant MR imaging by an radiologist and this examinations were repeated by another radiologist within 2 weeks. The radiologists measured fat content of L3, psoas (PS), erector spinae (ES), and multifidus (MF) muscles on the central L3 axial MR images on ISP V7 workstation and after 2 weeks they repeated the same measurements. Our results showed mean fat content of L3, PS, ES, MF was 38.19%, 3.52%, 3.48%, 3.53% for males and 32.11%, 3.40%, 7.06%, 7.14% for females. The repeatability and reproducibility of measurement of fat content, T2* and R2* of L3, PS, ES, MF was high (the intra-observer ICC and inter-observer ICC all >0.9). Fat content measurement of lumbar vertebrae marrow and lumbar paraspinal muscle using mDIXON-quant imaging has high reliability and be potentially used in clinical practice.

2284

Investigating Regional Variations of Acetyl Carnitine In Thigh and Calf Muscles In Vivo using PRESS Localized Long TE-based MR Spectroscopy

Rajakumar Nagarajan¹, Zohaib Iqbal¹, Manoj K Sarma¹, S. Sendhil Velan², and M.Albert Thomas¹

¹*Radiological Sciences, University of California Los Angeles, Los Angeles, CA, United States*, ²*Laboratory of Molecular Imaging, Singapore Bioimaging Consortium, Singapore, Singapore*

Skeletal muscle plays a major role in the development of insulin resistance (IR) and progression to type 2 diabetes. A recent work has used long TE (350ms) based PRESS localized spectrum in the vastus lateralis region of thigh muscle without any exercise to investigate acetylcarnitine, a compound formed when acetyl-Coenzyme A exceeds use by the tricarboxylic cycle in the mitochondria. This work focused on examining regional variations of acetylcarnitine in the thigh and calf muscles using the long TE MRS. Our preliminary results show the unequivocal presence of acetylcarnitine in lean, young healthy thigh muscle regions and decreased level in one diabetic type 2 patient.

2285

Quantitative Off-Resonance-Based Metallosis Assessment Near Total Hip Replacements: Correlating an Imaging Biomarker with Histology

Kevin M Koch¹, Matthew F Koff², Parina Shah², S S Kaushik¹, Andrew Nencka¹, and Hollis G Potter²

¹*Radiology, Medical College of Wisconsin, Milwaukee, WI, United States*, ²*Magnetic Resonance Imaging, Hospital for Special Surgery, New York, NY, United States*

The failure of hip arthroplasty may be attributed to metallic or polyethylene debris generated from implant components. The metallic components, and their associated debris are composed of cobalt-chromium alloys, which have a strong paramagnetic magnetic susceptibility relative to biological materials. Previously, we demonstrated a mechanism to utilize MRI data to qualitatively highlight cobalt-chromium debris deposits *in vivo*. In the current study, we extend this work to provide a quantifiable regional metallosis metric. In addition, this regional quantitative metric is shown to statistically correlate with local histology metallosis scores in subjects undergoing total hip revision surgery.

2286

Slab Thickness Calibration for Selective 3D-MSI

Kevin M Koch¹ and S S Kaushik¹

¹*Radiology, Medical College of Wisconsin, Milwaukee, WI, United States*

Slab selection is a crucial component of 3D-MSI metal artifact reduction sequences, due to the need to reduce phase-encoded fields of view for body imaging applications in the hip, spine, and shoulder. However, existing commercial 3D-MSI sequences are prone to signal loss at the edges of prescribed slabs. Here, we explain the source of this signal loss and demonstrate a calibration algorithm that can be used to reduce this slab-boundary signal loss in 3D-MSI. The presented methods are demonstrated on a calibrated 3D-MSI total hip replacement dataset acquired at 1.5T.

2287

Diffusion Tensor Imaging for Peripheral Nerves in the Upper Extremities using Realtime B0 Correction & Image based Distortion Correction: A feasibility study

Maggie Mei Kei Fung¹, Ek Tsoon Tan², David Soon Yiew Sia³, and Darryl Sneag³

¹*MR Apps & Workflow, GE Healthcare, New York, NY, United States*, ²*MR, GE Global Research Center, Niskayuna, NY, United States*, ³*MRI Research Lab, Hospital of Special Surgery, New York, NY, United States*

Diffusion tensor imaging (DTI) can potentially be helpful in visualizing peripheral nerves and assessing nerve damages. However, upper extremity DTIs (wrist, elbows & arm) are susceptible to distortion and fat suppression failure, especially in arms-down position where the area of interest is far from iso-center and can have more B0 inhomogeneity. In this study, we aim to investigate whether a combination of B0 correction methods can help reduce fat suppression failure, improve spatial misalignment and thus improve nerve tracking. We observed consistent fat suppression improvement at the wrist, but no significant improvement in spatial accuracy.

2288

Development of an Automated Shape and Textural Software Model of the Paediatric Knee for Estimation of Skeletal Age.

Caron Parsons^{1,2}, Charles Hutchinson^{1,2}, Emma Helm², Alexander Kenneth Clarke³, Asfand Baig Mirza³, Qiang Zhang⁴, and Abhir Bhalerao⁴

There are multiple methods available for skeletal age determination in the paediatric endocrine population. Only two methods, using left hand and wrist x-rays are in frequent clinical use, however Greulich & Pyle is based on data collated between 1931 and 1942 and Tanner Whitehouse uses data from as far back as 1949. We present the initial results of an automated software model of shape and textural analysis of the physes of the knee.

2289

3D Printed Phantom for Optimization of Trabecular Bone Structure Imaging
Cem M Deniz^{1,2}, Greg Chang³, and Ryan Brown¹

¹Department of Radiology, Center for Advanced Imaging Innovation and Research (CAI2R) and Bernard and Irene Schwartz Center for Biomedical Imaging, New York University School of Medicine, New York, NY, United States, ²The Sackler Institute of Graduate Biomedical Sciences, New York University School of Medicine, New York, NY, United States, ³Department of Radiology, Center for Musculoskeletal Care, New York University Langone Medical Center, New York, NY, United States

Phantoms have been used in MRI for sequence optimization and scanner calibrations. Recent developments in 3D printing technology have provided tools to manufacture application specific phantoms in a fast and reliable way. In this work, we used 3D printing technology to build a resolution phantom for optimization of trabecular bone structure imaging. We used rods with different thickness, orientation and spacing for capturing the range of possible trabecular bone structures. Developed phantom was used to investigate the effect of slice thickness on trabecular bone structure imaging.

2290

High resolution 3D steady-state imaging for peripheral nerves at 7T
Daehyun Yoon¹, Sandip Biswal¹, Brian Rutt¹, Amelie Lutz¹, and Brian Hargreaves¹

¹Radiology, Stanford University, Palo Alto, CA, United States

For the past few decades, MRI has been increasingly used for identifying peripheral nerve injury, causing chronic and neuropathic pain. Unfortunately, a substantial number of MRI examinations fails to find the causative nerve damage, possibly because it is too subtle or small. Recent developments of PET-MRI demonstrated improved detection capability of the nerve damage, but the precise anatomic characterization of the detected lesion still remains challenging. We introduce high-resolution 3D steady-state imaging sequences at 7T that enable examination of microstructures of peripheral nerves in extremities. We believe our methods have great potential for improving diagnosis of various pain syndromes.

2291

Diagnostic performance of susceptibility-weighted magnetic resonance imaging (SWMRI) for the assessment of subacromial spur formation causing subacromial impingement syndrome (SAIS)
Dominik Nörenberg^{1,2}, Marco Armbruster¹, Yi-Na Bender², Thula Walter², Gerd Diederichs², Bernd Hamm², Ben Ockert³, and Marcus R. Makowski^{2,4}

¹Department of Clinical Radiology, Munich University Hospitals Campus Großhadern, Germany, Munich, Germany, ²Department of Radiology, Charité, Berlin, Germany, Berlin, Germany, ³Department of Trauma and Orthopedic Surgery, Shoulder and Elbow Service, Munich University Hospitals Campus Großhadern, German, Munich, Germany, ⁴King's College London, Division of Imaging Sciences and Biomedical Engineering, London, United Kingdom, London, United Kingdom

Shoulder pain is regarded as the second most common musculoskeletal disorder in the general population. 44 % of shoulder pain syndromes are related to subacromial shoulder impingement (SAIS) due to rotator cuff tear (RCT) and glenohumeral joint arthritis. Especially subacromial spur formation is associated with SAIS and RCT. Our study demonstrates that SWMRI allows for a reliable detection and precise 3D-localization of subacromial spur formation under the coracoacromial arch in patients with SAIS and provides superior evaluation of diamagnetic spur formation compared to standard shoulder MRI using conventional radiography as a reference.

2292

Metal implant imaging using highly undersampled phase-cycled 3D bSSFP
Damien Nguyen^{1,2}, Tom Hilbert^{3,4,5}, Jean-Philippe Thiran^{5,6}, Tobias Kober^{3,4,5}, and Oliver Bieri^{1,2}

¹Radiological Physics, Dep. of Radiology, University of Basel Hospital, Basel, Switzerland, ²Department of Biomedical Engineering, University of Basel, Basel, Switzerland, ³Advanced Clinical Imaging Technology (HC CMEA SUI DI BM PI), Siemens Healthcare AG, Lausanne, Switzerland, ⁴Department of Radiology, University Hospital (CHUV), Lausanne, Switzerland, ⁵LTSS, École Polytechnique Fédérale de Lausanne, Lausanne, Switzerland, ⁶Department of Radiology, University Hospital Lausanne (CHUV), Lausanne, Switzerland

In this study, we explore the possibility of using a highly undersampled 3D phase-cycled balanced Steady-State Free-Precession (bSSFP) sequence (trueCISS) to image metal implants in the body and compare it to the Slice Encoding for Metal Artifact Correction (SEMAC) method. We show that the trueCISS approach not only offers qualitatively good morphological images, but also delivers quantitative maps that could potentially improve the overall diagnostic quality and efficiency within a clinically reasonable time.

2293

Diagnosis of Chronic Hip Pain After Total Hip Arthroplasty Using SEMAC-VAT MR Imaging
Yimin Ma¹, Panli Zuo², Mathias Nittka³, and Xiaoguang Cheng⁴

¹Department of radiology, Department of radiology, Jishuitan Hospital, Beijing, China, Beijing, China, China, People's Republic of, ²Siemens

With the rapid development of medicine technology, total hip arthroplasty (THA) is now widely used in the treatment of endstage hip osteoarthritis, severe hip fracture, hip bone tumor, and so forth. THA can relieve hip pain and improve the activity of the joints, while it still brings some unexpected complications, such as periprosthetic bone resorption, periprosthetic fractures, and metallic implants dislocation. Since then, distortion-free MRI near metal, like SEMAC-VAT MR, has shown its great clinical potential in diagnosing patients treated with THA.

2294

The changes in vertebra subchondral bone and cartilage endplate perfusion of degenerated intervertebral disks : a quantitative DCE-MRI study

Jiao WANG¹, Yun fei ZHA¹, Dong XING¹, Lei HU¹, Chang sheng LIU¹, Hui LIN², and Yuan LIN¹

¹Department of Radiology, Renmin Hospital of Wuhan University, Wuhan 430060, China, Wu han, China, People's Republic of, ²GE Healthcare China, Shanghai 200000, China, Shang hai, China, People's Republic of

To explore the relationship between the vertebra subchondral bone (VSB), the cartilage endplate (CEP) perfusion with intervertebral disc degeneration (IVDD). 18 individuals underwent lumbar conventional and DCE-MRI. The cranial and caudal VSB and CEP perfusion parameters (K^{trans} , K_{ep} , V_e) were measured. The VSB perfusion parameters K_{ep} of Pfirrmann I and II, Pfirrmann I and IV, Pfirrmann III and IV, the cranial CEP K_{ep} of Pfirrmann III and II showed significant difference. In the early progress of IVDD, its metabolism increase compensatory, clinical research should put more emphasis on early onset stage of IVDD such as in Pfirrmann II.

2295

Mitochondrial function as measured by ³¹P Magnetic Resonance Spectroscopy between lean Chinese and Asian-Indian males

Ivan P.W. Teng¹, Jamie X.M. Ho¹, Trina Kok¹, Philip Lee², Melvin K.S. Leow³, Hong Chang Tan⁴, Chin Meng Khoo⁵, George K Radda⁶, and Mary C Stephenson^{1,5}

¹Clinical Imaging Research Centre, A*STAR-NUS, Singapore, Singapore, ²SBIC, A*STAR, Singapore, Singapore, ³SICS, A*STAR, Singapore, Singapore, ⁴Department of Endocrinology, SGH, Singapore, Singapore, ⁵Department of Medicine, NUS, Singapore, Singapore, ⁶Biomedical Research Council, A*STAR, Singapore, Singapore

Previous studies have indicated differences in insulin sensitivity between lean Indian and Chinese men. In this study we used ³¹P MRS and a dorsiflexion task to assess muscle mitochondrial function, thought to be associated with insulin sensitivity, via PCR recovery rates. No inter-ethnic group differences were observed in measured blood parameters (HbA1c, fasting blood glucose level and M-value) between groups. However, positive correlations were observed between tPCR and both HbA1c and fasting blood glucose levels suggesting poorer mitochondrial function. No correlation was observed with M-value. Larger sampling sizes are necessary for these correlations and group differences to reach statistically-significant conclusions.

2296

Quantification of Magnetization Transfer parameters in across different muscle groups

Chun Kit Wong¹, Jamie X. M. Ho¹, and Mary Stephenson^{1,2}

¹A*STAR-NUS Clinical Imaging Research Centre, Singapore, Singapore, ²Department of Medicine, National University of Singapore, Singapore, Singapore

Quantitative magnetization transfer (qMT) parameters can potentially be used as biomarker of diseases. In this study, qMT parameters' nominal value are determined for selected muscle groups in healthy human subjects' forearm, mid-thigh, and calf. Nominal values of qMT parameters are determined by taking the mean value across the subjects for each muscle group. From the results, strong correlations of qMT parameters between certain muscle groups within the same individual subjects are observed, suggesting that the qMT parameters' variation is biological in origin.

2297

Articular Cartilage Assessment Using T1p Mapping in Early Osteoarthritis Patients with Knee joint Pain

Jin Qu¹, Xinwei Lei¹, Ying ZHAN¹, Huixia Li¹, and Yu Zhang²

¹Tianjin First Center Hospital, Tianjin, China, People's Republic of, ²Philips Healthcare, Beijin, China, People's Republic of

The purpose of this study was to evaluate articular cartilage degeneration in healthy subjects and patients with knee joint-pain as the only clinical manifestation using T1p measurements and to examine the interrelationship between cartilage abnormalities. Quantitative assessment of cartilage was performed using T1p mapping technique in 5 healthy volunteers and 17 knee joint-pain patients. T1p values were significantly elevated among patients with knee joint-pain compared to normal controls. Proteoglycan reduced in patients with knee joint-pain as the only clinical manifestation. Comparing to routine MR, T1p mapping could be more useful for these patients

2298 Bone marrow perfusion study on different BMD groups in elderly female

Chaoyang Zhang¹, Hu Xianghui², Heather T. Ma², Li Liang², and Chenfei Ye²

¹Harbin Institute of Technology Shenzhen Graduate School, Shenzhen, China, People's Republic of, ²Shenzhen, China, People's Republic of

This study utilized dynamic contrast enhanced (DCE) MRI and blood oxygen level dependent (BOLD) MRI as imaging method, using half quantitative analysis of two kir

Qualitative and Quantitative Diagnosis of Meniscal Tears Using SWI Compared with T2mapping at 3-Tesla MRI
Jun Zhao¹, Wei Chen¹, Jian Wang¹, Shuai Li², and Wen-Jing Hou¹

¹*Radiology, Southwest Hospital, Third Military Medical University, Chongqing, China, People's Republic of, ²MR Collaborations NE Asia, Siemens Healthcare, Beijing, China, People's Republic of*

In the past reports, invariably irregularity and high-signal-intensity changes of the free edge of meniscus may lead to a false-positive MR imaging, in addition, MR imaging of the knee invariably missed small meniscal tears, tears and abnormalities of the meniscal free edge, and at times large, unstable tears, result in false-negative. In recent decades, new MR image of water-tissues and collagen-rich tissues, including cartilage, menisci and tendon, has undergone significant progress, which are biological MR image techniques for the characterization tissues .This study was to compare the diagnostic performance of SWI (Susceptibility Weighted Imaging) in the evaluation of meniscal tears at 3T MR with those of a T2 Mapping sequence, using phase value and T2 value as the quantitative parameters. The phase value was a good predictor to diagnose meniscal tears.

Magnetization transfer MRI Evaluation of Autologous Chondrocyte Membrane Transplantation in The Knee Joint
Yi-Bin Xi¹, Fan Guo¹, Chun-Li Zhang¹, Hu Xu¹, Long-Biao Cui¹, Chen Li¹, Ping Tian¹, Wei-Guo Li², and Hong Yin¹

¹*Xijing Hospital, Fourth Military Medical University, Xi'an, China, People's Republic of, ²Bioengineering, University of Illinois at Chicago, Chicago, IL, United States*

Magnetization transfer MRI Evaluation of Autologous Chondrocyte Membrane Transplantation in The Knee Joint

Structural and Biomechanical Properties of Hypertrophic Articular Cartilage Using Microscopic Magnetic Resonance Imaging
David J Kahn¹, Daniel Mittelstaedt¹, and Yang Xia¹

¹*Physics and Center for Biomedical Research, Oakland University, Rochester, MI, United States*

High-resolution T2 imaging of AC is able to quantitatively measure depth-dependent features of articular cartilage (AC). When the cartilage articular surface (AS) is oriented normal (0°) to the external magnetic field, healthy AC takes on a laminar appearance that indicates the superficial zone (SZ), transitional zone (TZ), and radial zone (RZ), where collagen fibers are oriented parallel, random, and perpendicular to the AS [1]. When the AS is oriented at the magic angle (55°), the nuclear dipolar interaction is minimized and the tissue appears homogeneous. Compression of AC has effects that change many zonal properties [2,3], and hypertrophy may alter the biomechanical function and depth-dependent collagen ultra-structure of AC.

quantitative UTE imaging of the Achilles tendon enthesis of PsA patients and healthy volunteers

Bimin Chen^{1,2}, Hongda Shao¹, Michael Carl³, Arthur Kavanaugh⁴, Graeme M Bydder¹, and Jiang Du¹

¹*Radiology Department, UCSD, San Diego, CA, United States, ²Radiology Department, The first affiliated hospital of Jinan University, Guangzhou, China, People's Republic of, ³GE of Rheumatology, Allergy, and Immunology, UCSD, San Diego, CA, United States*

Achilles tendon enthesitis is the source of the the heel pain of PsA patients. The current measures based on pressure being placed on various entheses during physic specific. Also it's very time consuming and poorly reproducible. MR imaging with ultrashort echo time (UTE) sequences provides a good option for assessing entheses, \

Assessment of Tibial Nerve and Common Peroneal Nerve in Diabetic by Diffusion Tensor Imaging: a Feasibility Study
Chao Wu¹, Bin Zhao¹, Guangbin Wang¹, Shanshan Wang¹, and Hongjing Bao¹

¹*Shandong Medical Imaging Research Institute, Shandong university, Jinan, China, People's Republic of*

This study aimed to measure the FA and ADC values by quantitative DTI at the tibial nerve and common peroneal nerve and determine whether DTI can be used in the DPN. 25 healthy volunteers and 13 patients with DPN were underwent MR examinations at 3T including DTI of knee. The FA values of both tibial nerve and common peroneal nerve in DPN patients were significantly lower than those in healthy volunteers. The ADC values in DPN patients were higher than those in healthy groups. DTI may thus be a reliable method to added diagnostic value in patients with DPN.

Molecular Imaging & Contrast Agents

Fluorescence-based Quantification of Gadolinium-bound Liposomes using Carbostyryl 124-sensitized DTPA
Lindsay Kathleen Hill^{1,2}, Stewart Russell^{3,4}, Dung Minh Hoang¹, and Youssef Zaim Wadghiri¹

¹*Radiology, NYU School of Medicine, New York, NY, United States, ²Biomedical Engineering, SUNY Downstate Medical Center, Brooklyn, NY, United States, ³Thayer School of Engineering, Dartmouth College, Hanover, NH, United States, ⁴Department of Mechanical Engineering, The City College of New York, New York, NY, United States*

Advancement in the field of Gadolinium-bound contrast agent discovery is reliant on the development and characterization of novel constructs made in-house. However, the assessment of physicochemical properties and *in vivo* pharmacokinetics, requiring highly sensitive measurements, is often impeded by the lack of analytical techniques that are simultaneously sensitive, affordable, and accessible. Here we demonstrate that Carbostyryl 124-sensitized DTPA can be incorporated into a lipid-based microparticle, allowing for rapid quantification of Gadolinium concentration with nanomolar sensitivity using a readily available fluorescence plate reader. This sensitive and convenient technique could rapidly propel the characterization of novel MR contrast agents.

2305

Nanocrystal Loaded Polymeric Microparticles for Multimodal Imaging

Nutte Teraphongphom¹, Peter Chhour², John Eisenbrey³, Pratap Chandra Naha², Walter Witschey², Borirak Opasanont⁴, Lauren Jablonowski¹, David Peter Cormode², and Margaret Wheatley¹

¹Biomedical Engineering, Drexel University, Philadelphia, PA, United States, ²Radiology, University of Pennsylvania, Philadelphia, PA, United States, ³Radiology, Thomas Jefferson University, Philadelphia, PA, United States, ⁴Chemical and Biological Engineering, Drexel University, Philadelphia, PA, United States

To create multimodal contrast agents, we hypothesized that the shell of polymeric microparticles could accommodate additional payloads. We therefore modified microparticles by encapsulating nanoparticles including quantum dots, magnetic iron oxide nanoparticles, or gold nanoparticles to create bi-modality platforms in a manner that minimally compromised the performance for each individual imaging technique (ultrasound, fluorescence imaging, computed tomography and MRI).

2306

Development of facile protocols for stable nanoparticle formulations of ¹⁹F MR molecular imaging probes

Eric A Tanifum^{1,2}, Chandresh Patel¹, Robia Pautler², and Ananth Annapragada^{1,2}

¹Texas Children's Hospital, Houston, TX, United States, ²Baylor College of Medicine, Houston, TX, United States

Perfluorocarbons and perfluoropolymers are currently the major molecules of choice in ¹⁹F MRI contrast agents. These molecules generally have magnetically diverse ¹⁹F atoms and are very hydrophobic. The latter characteristic greatly hinders easy access to stable formulations for broad usage and the former generates chemical shift artifacts which result in blurred images. We have synthesized several hydrophilic organofluorine molecules all bearing magnetically equivalent ¹⁹F atoms and demonstrated that they are amenable to facile liposome nanoparticle formulation protocols. The resulting particles are highly stable and present a great potential for diverse applications as ¹⁹F MRI molecular imaging probes.

2307

A Ratiometric Bioresponsive MRI Contrast Agent for Rapid Monitoring of Biological Processes

Tanja Savić¹, Serhat Gündüz², Rolf Pohmann³, Nikos Logothetis⁴, Klaus Scheffler³, and Goran Angelovski¹

¹Research group "MR Neuroimaging agents", Max Planck Institute for Biological Cybernetics, Tübingen, Germany, ²Research Group "MR Neuroimaging agents", Max Planck Institute for Biological Cybernetics, Tübingen, Germany, ³High-Field Magnetic Resonance, Max Planck Institute for Biological Cybernetics, Tübingen, Germany, ⁴Physiology of Cognitive Processes, Max Planck Institute for Biological Cybernetics, Tübingen, Germany

A number of bioresponsive MRI contrast agents have been developed, with the aim of producing the maximal signal difference for a given biological event. This paper introduces an approach which substantially improves the detection of physiological events with fast kinetics. A nanosized, calcium-sensitive dendrimeric probe was developed and characterized by means of a balanced steady-state free precession imaging protocol. Results show an almost four times greater contrast gain per unit of time as compared to conventional T1-weighted imaging with small sized contrast agents. Consequently, this ratiometric methodology has a profound significance for future studies of biological dynamic processes by means of MRI.

2308

A Targeted Host-Guest MRI Contrast Agent for Breast Cancer Molecular Imaging

Zhuxian Zhou^{1,2}, Zheng Han¹, and Zheng-Rong Lu¹

¹Biomedical Engineering, Case Western Reserve University, Cleveland, OH, United States, ²Chemical and Biological Engineering, Zhejiang University, Hangzhou, China, People's Republic of

To produce MRI detectable signal enhancement for the biomarker on cancer cell surface, we developed a targeted host-guest nanosized contrast agent cRGD-POSS-βCD-(DOTA-Gd)-Cy5. The nanosized host-guest systems are preferable for facile synthesis of customized and functionalized imaging agent. Here, a cyclic peptide cRGD targeting to cancer cell $\alpha_v\beta_3$ -integrin, a macrocyclic Gd(III) chelate and Cy5 fluorescent probes were loaded on the nanosized carrier by host-guest interaction. cRGD-POSS-βCD-(DOTA-Gd)-Cy5 can provide strong contrast enhancement to delineate malignant tumors during molecular MR and fluorescent imaging in a mouse 4T1 breast cancer model.

2309

Biodegradable glycoged-based nanoprobe as a multimodal tumor-targeting contrast agent

Andrea Galisova¹, Daniel Jirak¹, Marketa Jiratova¹, Martin Hraby², Maria Rabyk², Aneta Pospisilova², and Milan Hajek¹

¹MR Unit, Institute for Clinical and Experimental Medicine, Prague, Czech Republic, ²Academy of Sciences, Institute of Macromolecular Chemistry, Prague, Czech Republic

An effective cancer diagnostic and therapeutic contrast agent with suitable properties including high specificity and safety is in high demand. In this study, accumulation of a biocompatible and biodegradable glycogen-based nanoprobe (GG-Gd-DOTA-Dy) was tested

and compared to a commercially available contrast agent (gadoterate meglumine). Relaxivity and MR imaging of the probe was performed on the phantoms. The uptake of the agents was measured on the tumor-bearing rats at several time points after the contrast agent administration by MRI and fluorescence imaging. We found out that the novel probe is superior to a commercially available contrast agent regarding the relaxivity and accumulation in the tumor tissue.

2310

In-vivo quantification of focal vessel wall changes following vascular injury in a murine model of atherosclerosis
Begona Lavin Plaza¹, Alkystis Phinikaridou¹, Marcelo Andia², Silvia Lorrio Gonzalez¹, and Rene Botnar¹

¹*Imaging Sciences and Biomedical Engineering, King's College London, London, United Kingdom*, ²*Pontificia Universidad Católica de Chile, Santiago de Chile, Chile*

Despite the beneficial effect of percutaneous transluminal coronary angioplasty and stent implantation, negative vascular remodeling remains as one of the most important complications of interventional cardiology. These procedures may damage the vessel wall, particularly the endothelium, leading to a dysfunctional state characterized by impaired vasodilation, increased leukocyte adhesion and permeability that constitute the initial steps of atherosclerosis. The arterial tree can be divided in either "athero-susceptible" areas, e.g. arterial branches and curvatures, where blood flow is turbulent and shear stress is multidirectional or "athero-resistant" areas, e.g. abdominal aorta, where blood flow is laminar and shear stress is low. In this study, we investigated (1) whether an "atherosclerotic-resistant" segment of the vascular tree, like the aorta, can be switched into an "atherosclerotic-susceptible" area following endothelial injury and (2) whether such a switch in vessel wall remodeling is associated with changes in vascular permeability that can be assessed in-vivo using the albumin binding MR contrast agent, gadofosveset.

2311

Vascular-targeted Magnetic Nanoparticles for Image-guided Cancer Therapy
Sudath Hapuarachchige¹, Robert Ivkov², and Dmitri Artemov¹

¹*Department of Radiology and Radiological Science, Johns Hopkins University School of Medicine, Baltimore, MD, United States*, ²*Department of Radiation Oncology and Molecular Radiation Sciences, Johns Hopkins University School of Medicine, Baltimore, MD, United States*

Bionized nanoferrites are magnetic nanoparticles, which can be used as contrast agents and therapeutic platforms for alternating magnetic field (AMF) induced hyperthermia. One important application is enhancing of vascular permeability in tumors for delivery of nanodrugs. We studied BNF nanoparticles specifically targeted to the tumor vasculature via VEGF receptors ligands. Targeted BNF particles were visualized by intravital multiphoton and MR imaging, and increased accumulation of targeted BNF was detected in breast cancer models.

2312

BBN-assembled Gadolinium oxide nanoprobe for targeted bimodal imaging in vitro and in vivo
Danting Cui¹, Xiaodan Lu¹, Chenggong Yan¹, Xiang Liu¹, Yingjie Mei², Meirong Hou¹, Yikai Xu¹, and Ruiying Liu³

¹*Department of Medical Imaging Center, Nanfang Hospital, Southern Medical University, Guangzhou, China, People's Republic of*, ²*Philips Healthcare, Guangzhou, China, People's Republic of*, ³*School of Pharmaceutical Sciences, Southern Medical University, Guangzhou, China, People's Republic of*

Bombesin (BBN) is a peptide exhibiting high affinity for the gastrin-releasing peptide receptor (GRPr). To develop a BBN-assembled nanoprobe based on Gd2O3 was efficient for earlier tumor detection. Gd2O3 was conjugated with 5(6)-carboxyfluorescein and bombesin for MR/optical bimodal imaging of GRPr positive tumor. Gd2O3-FI-PEG NPs without bombesin-modified NPs were tested as non-targeted control. MRI and optical imaging in vitro and vivo confirmed BBN-assembled Gd2O3 nanoprobe exhibited better binding affinity to GRPr positive tumor than the control group. The nanoprobe may provide opportunities to further biomedical application.

2313

Combining Multi-therapy in Singlet Vehicle
Yuqi Yang¹, Shizhen Chen¹, Sha Li¹, Lianhua Liu¹, and Xin Zhou¹

¹*Wuhan Institute of Physics and Mathematics, Chinese Academy of Sciences, Wuhan, China, People's Republic of*

Two types of water-insoluble texphyrins (TP), anticancer drug Gd-TP and photosensitizer Lu-TP, were synthesized and loaded onto RGD-functionalized graphene quantum dots (GQDs) via π-π stacking. The obtained complex could be used as a MRI-fluorescent imaging multi-model probe for cancer therapy. Compared with conventional photodynamic therapy (PDT), our method demonstrated better therapy efficiency for deeper tissue, because a laser with longer wavelength was applied to active the photosensitizer Lu-TP. Furthermore, reactive oxygen species resulted from the reaction between redox active drug Gd-TP and cellular reducing metabolites and photothermal effect from GQDs led cancer cells more impressionable to PDT from Lu-TP.

2314

Short-lived mesenchymal stem cells accelerate healing of acid skin burns – an MRI cell tracking study using iron oxide, fluorine and bioluminescence imaging
Ghulam Muhammad^{1,2}, Jiadi Xu³, Jeff W.M. Bulte¹, Anna Jablonska¹, Piotr Walczak^{1,4}, and Miroslaw Janowski⁵

¹*The Russell H. Morgan Department of Radiology and Radiological Science, Johns Hopkins University, Baltimore, MD, United States*, ²*Stem Cell Laboratory, University of the Punjab, Lahore, Pakistan*, ³*F.M. Kirby Research Center, Kennedy Krieger Institute, Baltimore, MD, United States*, ⁴*Department of Radiology, University of Warmia and Mazury, Olsztyn, Poland*, ⁵*Johns Hopkins University, Baltimore, MD, United States*

Incidence of acid burns due to accidents and attacks is on the rise and mesenchymal stem cell transplantation is a promising therapeutic strategy. Cell tracking makes treatment more precise. We have compared two MRI tracking strategies: SPIO nanoparticles-

based ¹H MRI and ¹⁹F nanoemulsion "hot-spot" MRI. Bioluminescence imaging was used as a reference standard for monitoring cell survival. Susceptibility artifacts due to skin injury compromised the interpretation of ¹H imaging, while ¹⁹F MRI was capable of providing information on cell location and survival. The SPIO nanoparticles and fluorine nanoemulsion had no detrimental effect on the therapeutic activity and survival of MSCs.

2315

Absolute Quantification of Stem Cell Transplant in MRI
Muhammad Jamal Afridi¹, Arun Ross², and Erik M Shapiro³

¹Department of Radiology, Department of Computer Science, Michigan State University, East Lansing, MI, United States, ²Department of Computer Science, Michigan State University, East Lansing, MI, United States, ³Department of Radiology, Michigan State University, East Lansing, MI, United States

We describe an image analysis strategy for quantifying the location and number of transplanted stem cells from MRI images. MRI-based single cell detection facilitates the use of machine learning algorithms for spot detection. Using convolutional neural networks, automatic and intelligent cell enumeration was first developed on *in vitro* agarose samples containing a known number of labeled cell mimics. Then, the validated image analysis approach was used to quantify stem cell transplants in rodent brains. An accuracy of 99.8% was achieved on *in vitro* samples and 94.6% on *in vivo* examples.

2316

Automatic *in vivo* detection of transplanted cells in MRI using transfer learning paradigm
Muhammad Jamal Afridi¹, Arun Ross², Steven Hoffman², and Erik M Shapiro³

¹Department of Radiology and Department of Computer Science, Michigan State University, East Lansing, MI, United States, ²Department of Computer Science, Michigan State University, East Lansing, MI, United States, ³Department of Radiology, Michigan State University, East Lansing, MI, United States

Despite advances in machine learning and computer-vision, many MRI studies rely on tedious manual procedures for quantifying imaging features, i.e. cell numbers, contrast area etc. Development of intelligent, automatic tools for quantifying imaging data requires large scale data for their training and tuning, which in the clinical arena is challenging to obtain. Here, we present an approach that obviates the need for large scale data collection to develop an intelligent and automatic tool for single cell detection in MRI. Our strategy achieves 91.3% accuracy for *in vivo* cell detection in MRI despite using only 40% of the data for training.

2317

Cell tracking with fluorine-19 MRI and zirconium-89 PET - a multi-modal approach

Kai D. Ludwig¹, Benjamin L. Cox^{1,2,3}, Myriam N. Bouchlaka^{4,5}, Stephen A. Graves¹, Justin J. Jeffery⁵, R. Jerry Nickles¹, Bryan P. Bednarz^{1,6}, Christian M. Capitini^{4,5}, and Sean B. Fain^{1,6,7}

¹Medical Physics, University of Wisconsin-Madison, Madison, WI, United States, ²Morgridge Institute for Research, Madison, WI, United States, ³Laboratory for Optical and Computational Instrumentation, University of Wisconsin-Madison, Madison, WI, United States, ⁴Pediatrics, University of Wisconsin-Madison, Madison, WI, United States, ⁵Carbone Cancer Center, University of Wisconsin-Madison, Madison, WI, United States, ⁶Radiology, University of Wisconsin-Madison, Madison, WI, United States, ⁷Biomedical Engineering, University of Wisconsin-Madison, Madison, WI, United States

Methods for non-invasive cell tracking may greatly enhance the ability to assess efficacy of cellular-based therapies. A dual-labeled (⁸⁹Zr and ¹⁹F) cell labeling approach could inform and potentially improve *in vivo* cell tracking sensitivity and clinical adoption. Here, we show longitudinal detection of localized cell injections with ¹⁹F MRI and the ability to quantify the number of cells within a voxel. Additionally, ⁸⁹Zr cell tracking results shows a high sensitivity for intravenous delivery of cells with longitudinal signal detection. Future work aims to combine both cell tracking approaches utilizing the dual-modality imaging platform on a PET/MRI system.

2318

Interaction of Manganese and Iron in R1 mapping in a Low Concentration Setting
Chien-Lin Yeh¹, Carlos J. Perez-Torres¹, and Ulrike Dydak^{1,2}

¹School of Health Sciences, Purdue University, West Lafayette, IN, United States, ²Radiology and Imaging Sciences, Indiana University School of Medicine, Indianapolis, IN, United States

Being able to use MRI to estimate brain Mn accumulation is of high interest in occupational Mn exposure settings. As a first step towards absolute quantification of brain Mn concentration in exposed humans using MRI, the interaction between Mn and Fe and their combined effect to R1 need to be explored. Our results suggest that a model only assuming independent linear contributions of Mn and Fe already explains the R1 data well. However introducing a cross term of Mn and Fe in the equation improves the fits, suggesting a Mn-Fe interaction.

2319

Glutamate-sensitive CEST and MEMRI as novel biomarkers for studying ALS pathophysiology
Amit Kumar Srivastava^{1,2}, Jiadi Xu³, Peter C.M. van Zijl^{2,3}, Nicholas J Maragakis⁴, and Jeff W.M. Bulte^{1,2,3}

¹Cellular Imaging Section, Institute for Cell Engineering, Johns Hopkins University, Baltimore, MD, United States, ²Russel H. Morgan Department of Radiology and Radiological Science, Johns Hopkins University, Baltimore, MD, United States, ³F.M. Kirby Research Center for Functional Brain Imaging, Kennedy Krieger Institute, Baltimore, MD, United States, ⁴Neurology, Johns Hopkins University, Baltimore, MD, United States

Amyotrophic lateral sclerosis (ALS) is characterized by selective loss of motor neurons. ALS treatment is very difficult because disease manifestation and diagnosis often happen much later than when ALS pathology occurs in the patient. In this study, we developed two

non-invasive MRI biomarkers for the early detection of disease pathology and its progression thereafter. A newly developed Glutamate-sensitive CEST showed higher signal intensity in the spinal cord level of ALS at pre-symptomatic stage, an indicator of initiation of ALS pathology. Manganese-enhanced MRI showed higher T1-weighted signal in the ALS spinal cord at post-symptomatic stage suggesting activation of astrocytes.

2320

Longitudinal MEMRI Characterization of a Novel Mouse Medulloblastoma Model

Harikrishna Rallapalli¹, Eugenia Rafaela Volkova¹, I-Li Tan², Alexandre Wojcinski², Alexandra L Joyner², and Daniel H Turnbull¹

¹*Skirball Institute and Radiology, New York University School of Medicine, New York, NY, United States*, ²*Developmental Biology, Sloan Kettering Institute, New York, NY, United States*

In this work, we describe a powerful longitudinal Manganese-enhanced magnetic resonance imaging (MEMRI) strategy to characterize a novel mouse medulloblastoma model. An activated Smoothened mutation was engineered to induce proliferative growth in the cerebellum. Lesions were monitored using MEMRI up to postnatal day P100, and 3D tumors were segmented for quantitative volumetric analysis. Qualitative analysis has shown a ~50% chance of regression overall (n=21), and preliminary quantitation has suggested a combined progression/regression growth model. With this model, we aim to guide diagnostic decisions from early timepoints and quantify therapeutic efficacy.

2321

Mn cell uptake mechanisms in organotypic rat hippocampal slice cultures

Alexia Daoust¹, Stephen Dodd¹, and Alan Koretsky¹

¹*NINDS, LFMN, NIH, Bethesda, MD, United States*

MEMRI can be used for different applications such as tracing neuronal connections or functional imaging. However, Mn cellular uptake is still unclear. We studied this mechanism by the use of MEMRI in a hippocampal organotypic slice culture. After added Mn to the medium for 2h, we obtained an optimal MR contrast that was affected by Ca channel manipulation. Mn cellular uptake was also affected by the presence of other metals that use divalent metal transporters (DMT-1). Our results suggest a strong capacity of our technique to study the cellular mechanisms related to MEMRI.

2322

Distributed T2 relaxation model for polydisperse nanoparticle systems

Bashar Issa¹

¹*Physics, UAE University, Al-Ain, United Arab Emirates*

Theories describing $1/T_2$ enhancement due to the presence of superparamagnetic particles agree well with experimental and Monte Carlo (MC) simulation data under the condition that the particles are monodisperse both in size and magnetization. We present a $1/T_2$ distributed model that takes into account the particle size and magnetization distributions. We average the individual $1/T_2$ components exhibited by each group of particle with a uniform particle size. MC simulations of the model successfully predict $1/T_2$ within the MAR regime confirming the implicit assumption that the spins are able to sample all the particles' radii and magnetizations within the echo time.

2323

Quantifying exchange in host-guest systems for hyperpolarized xenon

Sergey Korchak¹, Wolfgang Kilian¹, Leif Schröder², and Lorenz Mitschang¹

¹*Physikalisch-Technische Bundesanstalt (PTB), Braunschweig and Berlin, Germany*, ²*Leibniz-Institut für Molekulare Pharmakologie (FMP), Berlin, Germany*

The reversible binding of xenon to host structures is fundamental to the development of novel contrast agents employing hyperpolarized xenon and chemical exchange saturation transfer (HyperCEST) for molecular imaging. The rates for entering and leaving the host depend on atomic details and affect the obtainable contrast rendering them pivotal for the selection of hosts and optimization of imaging methods. However, different exchange processes may apply whose contributions are difficult to assign. Exchange spectroscopy experiments are proposed which enable straightforward disentanglement of the exchange kinetics and quantification of individual contributions. The approaches are exemplified for the cryptophane-xenon host-guest system.

2324

CEST Nuclear Overhauser Enhancement imaging of protein misfolding in mice at different stages of prion disease

Eleni Demetriou¹, Mohamed Tachroud¹, Marilena Rega², Francisco Torrealdea¹, Karin Shmueli³, Mark Farrow⁴, and Xavier Golay¹

¹*Brain Repair and Rehabilitation, Institute of Neurology, London, United Kingdom*, ²*Institute of Neurology, London, United Kingdom*, ³*Medical Physics and Biomedical Engineering, University College of London, London, United Kingdom*, ⁴*MRC prion unit, Institute of Neurology, London, United Kingdom*

Prion diseases are fatal neurodegenerative disorders which are caused by abnormal conformational changes of cellular prion protein. Chemical Exchange Saturation Transfer (CEST) imaging of NOE effects has been proposed as a new imaging mechanism to monitor protein folding by MRI. In this study, prion-infected mice were imaged at three stages of prion disease (asymptomatic, early-stage and late-stage) to investigate whether prion propagation could be detected in their brains. We concluded that NOE values at different stages of prion disease provide additional evidence of prion protein misfolding occurring in the brains of diseased mice.

2325

SUV-quantification in physiological lung tissue in an integrated PET/MR-System: Impact of lung density and bone tissue.
Ferdinand Seith¹, Holger Schmidt¹, Sergios Gatidis¹, Ilja Bezrukov², Christina Schraml¹, Christina Pfannenberg¹, Christian la Fougère³, Konstanin Nikolaou¹, and Nina Schwenzer¹

¹*Radiology, Universitätsklinikum Tübingen, Tübingen, Germany*, ²*Max-Planck-Institut, Tübingen, Germany*, ³*Nuclear Medicine, Universitätsklinikum Tübingen, Tübingen, Germany*

Attenuation correction (AC) plays a key role in the quantification of tracer uptake in positron emission tomography (PET), expressed as standardized uptake value (SUV). The segmentation method is the standard approach for AC in whole-body PET/magnetic resonance imaging (MRI) that has been implemented into the software of most vendors. However, this method is neglecting bone and applies only one single patient-independent attenuation coefficient for the whole lung. Our study could demonstrate that both, differences lung density and surrounding bone tissue can have significant influence on SUV measurement of physiological lung tissue, mostly affecting the posterior regions.

2326

IN VIVO 19F MRI QUANTIFICATION USING B1+/B1-CORRECTION

Ina Vernikouskaya^{1,2}, Alexander Pochert³, Mika Lindén³, and Volker Rasche^{1,2}

¹*Internal Medicine II, University Hospital of Ulm, Ulm, Germany*, ²*Small Animal MRI, University of Ulm, Ulm, Germany*, ³*Inorganic Chemistry II, University of Ulm, Ulm, Germany*

Quantification of ¹H MR contrast agents (CA) is limited by the only indirect visualization of the changes of the relaxation properties of the surrounding tissue. Using alternative nuclei such as fluorine (¹⁹F) as CA enables direct and quantifiable readout of local CA aggregations, since the ¹⁹F signal linearly correlates with its local concentration. However non-uniformity of the transmit/receive radiofrequency fields impact the resulting absolute signal, leading to wrong quantification results. Application of an easy-to-use time-efficient B_1^+/B_1^- -mapping technique for correction of the ¹⁹F signal *in vivo* is presented in this work.

2327

Temporally flexible artifact suppression high field SSFP images using Golden Angle incremented linear combination Steady-state Free Precession (LCSSFP) in DESPOT1/2 images

H. Douglas Morris¹ and J. Andrew Derbyshire²

¹*NIH Mouse Imaging Facility, National Institutes of Health, Bethesda, MD, United States*, ²*Functional MRI Facility, National Institutes of Health, Bethesda, MD, United States*

Rapid imaging of endogenously labeled neuroprogenitor cells in the rat brain is shown using high-field MRI and efficient Steady-State Free Precession sequences. A RF-phase cycle progression based on the Golden Angle is used to produce Linear Combination SSFP (LCSSFP) images without banding artifacts. The method yields high resolution images with few global distortions suitable for cell tracking and calculating relaxation images.

Traditional Poster

Hyperpolarised C-13 & Other Nuclei

Exhibition Hall

Wednesday, May 11, 2016: 16:00 - 18:00

2328

Development of Calibrationless Parallel Imaging Methods for Clinical Hyperpolarized Carbon-13 MRI Studies

Yesu Feng¹, Jeremy Gordon¹, Peter Shin¹, Cornelius von Morze¹, Michael Lustig², Peder E.Z. Larson¹, Michael A. Ohliger¹, Lucas Carvajal¹, James Tropp³, John M Pauly⁴, and Daniel B. Vigneron¹

¹*Radiology and Biomedical Imaging, UCSF, San Francisco, CA, United States*, ²*EECS, UC Berkeley, Berkeley, CA, United States*, ³*GE Healthcare, Fremont, CA, United States*, ⁴*Electrical Engineering, Stanford, Stanford, CA, United States*

Hyperpolarized (HP) ¹³C imaging requires fast data acquisition due to the fast T1 relaxation. Parallel imaging methods are well suited for acceleration of data acquisition, yet conventional parallel imaging schemes require explicit calibration of coil sensitivity which presents significant challenge to HP ¹³C imaging. In this study, a calibrationless parallel imaging method was tested and applied to HP ¹³C MRI. A 2-fold acceleration was achieved when this technique was applied together with a 2D EPI readout. This strategy is being extended for 3D HP ¹³C EPI for improved volumetric coverage and better temporal resolution for future clinical studies.

2329

Using a Low Rank plus Sparse Reconstruction Approach to Accelerate 3D Dynamic bSSFP Hyperpolarized Carbon-13 MR Imaging
Eugene Milshteyn¹, Cornelius von Morze¹, Galen D Reed², Hong Shang¹, Peter J Shin¹, Peder EZ Larson¹, and Daniel B Vigneron¹

¹*Radiology and Biomedical Imaging, UCSF, San Francisco, CA, United States*, ²*HeartVista, Menlo Park, CA, United States*

Hyperpolarized ¹³C MR can provide unique imaging assessments of metabolism and perfusion in various disease conditions *in vivo*. High spatiotemporal resolution is needed to best characterize these processes. This project used a low rank plus sparse reconstruction with the bSSFP acquisition to achieve high isotropic resolution dynamic 3D imaging with multiple hyperpolarized substrates.

2330

Direct arterial injection of hyperpolarized compounds into tumor tissue enables rapid detection of metabolism with minimal dilution
Steven Reynolds¹, Stephen Metcalf², Rebecca Collins³, Edward Cochrane³, Simon Jones³, Martyn Paley¹, and Gillian Tozer²

¹Academic unit of radiology, University of Sheffield, Sheffield, United Kingdom, ²Department of Oncology and Metabolism, University of Sheffield, Sheffield, United Kingdom, ³Department of Chemistry, University of Sheffield, Sheffield, United Kingdom

Hyperpolarizing drug candidates could allow insights into their mode of action and metabolic fate. However, administering drug molecules at high concentrations can lead to adverse effects in animals. We have developed a method for directly administering substrates to tumor tissue by infusion through a single supplying artery, thus maximizing tumor drug delivery and minimizing T1 relaxation and systemic toxicity. The net signal gain for arterially injected ¹³C-pyruvate was x54, compared with the systemically administered venous route. Hyperpolarized custom ¹³C-labeled CA1 was arterially administered and its parent peak observed, *in vivo*, at its expected chemical shift (58ppm).

2331

Characterisation of adipose tissue-derived mesenchymal stem cell using hyperpolarized MRS
Anja Bille Bohn¹, Nathalie Nielsen², Christoffer Laustsen², Hans Stødkilde-Jørgensen², and Lotte Bonde Bertelsen²

¹The department of Clinical Immunology, Aarhus University Hospital, Aarhus, Denmark, ²MR Research Centre, Aarhus University, Aarhus University Hospital, Aarhus, Denmark

Synopsis: Studies of metabolism in stem cells have revealed a shift in the balance between glycolysis, mitochondrial oxidative phosphorylation and oxidative stress during the maturation of stem cells. In the stem cells, pyruvate from glycolysis will mainly be metabolized to lactate as a result of an uncoupling of the citric acid cycle and the oxidative phosphorylation pathway, thus the application of a novel metabolic cell culture tool could add valuable information to the studies of stem cell characterisation during development. In the present study we use hyperpolarised [1-¹³C] pyruvate to characterise mesenchymal stem cells harvested from adipose tissue.

2332

The formulation of hyperpolarized ¹³C pyruvate solutions influences the labeling of myocardial metabolites *in vivo*
Hikari A. I. Yoshihara¹, Jessica A. M. Bastiaansen², Corinne Berthonneche³, Arnaud Comment¹, and Juerg Schwitter⁴

¹Institute of Physics of Biological Systems, Swiss Federal Institute of Technology (EPFL), Lausanne, Switzerland, ²Department of Radiology, University Hospital Lausanne (CHUV) and University of Lausanne (UNIL), Lausanne, Switzerland, ³Cardiovascular Assessment Facility, University Hospital Lausanne (CHUV), Lausanne, Switzerland, ⁴Division of Cardiology and Cardiac MR Center, University Hospital Lausanne (CHUV), Lausanne, Switzerland

In developing an intact rat model for myocardial ischemia using hyperpolarized ¹³C pyruvate, different compound formulations were evaluated. Infusion of 4-hydroxy-TEMPO-polarized sodium [1-¹³C]pyruvate was compared to an equivalent dose of buffered trityl radical-polarized [1-¹³C]pyruvic acid. Whereas higher levels of polarization and MRS signal were obtained with trityl radical, the metabolite signals normalized to total signal were lower. In particular, [1-¹³C]lactate signal relative to total signal was markedly higher using TEMPO-polarized pyruvate. [¹³C]bicarbonate and [1-¹³C]alanine signals were affected to a lesser degree. This study demonstrates the composition of the infused hyperpolarized pyruvate solution can significantly affect its metabolism *in vivo*.

2333

Rapid decarboxylation of hyperpolarized [13C]ketobutyrate in mouse liver *in vivo*
Cornelius von Morze¹, Irene Marco-Rius¹, Celine Baligand¹, Robert Bok¹, John Kurhanewicz¹, Daniel Vigneron¹, and Michael Abram Ohliger^{1,2}

¹Radiology and Biomedical Imaging, University of California San Francisco, San Francisco, CA, United States, ²UCSF Liver Center, San Francisco, CA, United States

We investigate the rapid metabolic conversion of hyperpolarized (HP) [1-¹³C]α-ketobutyrate, a molecular analog of pyruvate, in mouse liver *in vivo* as compared to [1-¹³C]pyruvate. Previously, it has been noted that in liver, there is relatively less conversion of [1-¹³C]α-ketobutyrate to its reduction product, [1-¹³C]hydroxybutyrate when compared to the conversion of [1-¹³C]pyruvate to [1-¹³C]lactate. This difference in conversion likely represents a different LDH activity in liver1. In this study, we examine the decarboxylation of ketobutyrate into bicarbonate, which we have found to be unexpectedly elevated when compared to pyruvate, presumably also via PDH and/or a related enzyme.

2334

Intraperitoneal substrate administration for ¹³C metabolic imaging in a mouse model of abdominal metastasis
Justin Y.C. Lau^{1,2}, Aws Abdul-Wahid³, Albert P. Chen⁴, Jean Gariépy^{1,3}, and Charles H. Cunningham^{1,2}

¹Medical Biophysics, University of Toronto, Toronto, ON, Canada, ²Physical Sciences, Sunnybrook Research Institute, Toronto, ON, Canada, ³Biological Sciences, Sunnybrook Research Institute, Toronto, ON, Canada, ⁴GE Healthcare, Toronto, ON, Canada

Conventionally, hyperpolarized ¹³C substrates are administered via intravenous injection. In this abstract, a novel route of hyperpolarized substrate delivery via intraperitoneal injection is demonstrated for observing metabolism in a mouse model of abdominal metastasis. 2D CSI revealed lactate signal in tumour-bearing mice, but only pyruvate signal in a control mouse. An extended time window of dynamic metabolic imaging may be possible with intraperitoneal administration due to the longer *in vivo* pyruvate T₁ of 54 s as measured by dynamic 3D EPI. Intraperitoneal administration of hyperpolarized ¹³C substrates is a promising complementary technique well suited for observing poorly vascularized metastatic nodules.

2335

In vivo Assessment of Metabolic Derangements in Renal Ischemia-Reperfusion Injury using Carbon-13 HP-MRI
Mehrdad Pourfathi^{1,2}, David D. Aufhauser³, Douglas R. Murken³, Zhonglin Wang³, Stephen J. Kadlec¹, Heather Gatens¹, Ali Naji³, Matthew H. Levine^{3,4}, and Rahim R. Rizi¹

¹*Radiology, University of Pennsylvania, Philadelphia, PA, United States*, ²*Electrical and Systems Engineering, University of Pennsylvania, Philadelphia, PA, United States*, ³*Department of Surgery, Division of Transplant Surgery, University of Pennsylvania, Perelman School of Medicine, Philadelphia, PA, United States*, ⁴*Department of Surgery, Children's Hospital of Philadelphia, Philadelphia, PA, United States*

Renal ischemia reperfusion injury (IRI) and its manifestation of acute kidney injury (AKI) is a significant source of morbidity in diverse medical and surgical scenarios, for which there is no current therapeutic modality. AKI contributes significantly to hospital stay, morbidity, and mortality. Despite the extensive metabolic derangements that accompany renal IRI, there is an absence of clinically useful markers to predict the clinical course following AKI in an expedient manner. Here, we demonstrate the feasibility of using hyperpolarized carbon-13 MRI to image metabolic activity in the mice recovering from renal IRI.

2336

[¹³C]-tert-butanol-2-β-D-galactose: A potential new hyperpolarized imaging agent for in vivo imaging of senescent cells
Keshav Datta^{1,2}, Shie-Chau Liu¹, Stephen R Lynch³, Zixin Chen¹, Ralph Hurd⁴, Jianghong Rao¹, and Daniel Mark Spielman^{1,2}

¹*Dept. of Radiology, Stanford University, Stanford, CA, United States*, ²*Dept. of Electrical Engineering, Stanford University, Stanford, CA, United States*, ³*Dept. of Chemistry, Stanford University, Stanford, CA, United States*, ⁴*Applied Sciences Lab, GE Healthcare, Menlo Park, CA, United States*

We evaluated the potential for the use of [¹³C]-tert-butanol-bGal as hyperpolarizable agent for in vivo imaging of senescent cells. The chemical shift between [¹³C]-tert-butanol-bGal and bGal-cleaved [¹³C]-tert-butanol was found to be 7.4ppm, more than adequate for in vivo detection. [¹³C]-tert-butanol-bGal was also found to polarize well (~30%) with [¹³C]-tert-butanol-bGal and [¹³C]-tert-butanol yielding T₁ relaxation times of 22s and 34s respectively, very promising for in vivo studies.

2337

Concentration-dependent hepatic metabolism in vivo using a near physiological dose range of hyperpolarized [¹⁻¹³C]pyruvate
Emine Can¹, Jessica A. M. Bastiaansen^{2,3}, Hikari A. I. Yoshihara^{4,5}, Rolf Gruetter^{3,5,6}, and Arnaud Comment¹

¹*Institute of Physics of Biological Systems, École Polytechnique Fédérale de Lausanne (EPFL), Lausanne, Switzerland*, ²*Department of Radiology, University Hospital Lausanne (CHUV), Lausanne, Switzerland*, ³*Department of Radiology, University of Lausanne (UNIL), Lausanne, Switzerland*, ⁴*Institute of Physics of Biological Systems, EPFL, Lausanne, Switzerland*, ⁵*Laboratory for Functional and Metabolic Imaging, EPFL, Lausanne, Switzerland*, ⁶*Department of Radiology, University of Geneva, Geneva, Switzerland*

Hyperpolarized ¹³C-labeled pyruvate provides assessment of real-time liver mitochondrial enzymatic activities directly by labeling TCA cycle intermediates. However the technique is limited by the requirement of supraphysiological concentrations due to the low basal concentrations of metabolic intermediates. In this study we showed the feasibility of detecting liver metabolism *in vivo* with HP ¹³C pyruvate administered at plasma concentrations of at most 7-fold of the basal levels. Different metabolic response to the concentration change shows that the adaptation to supraphysiological levels can obscure feeding state-depending metabolic differences in liver.

2338

Pool size effects in experiments with hyperpolarized [¹³C]ketobutyrate
Cornelius von Morze¹, Peder E Larson¹, Michael A Ohliger¹, Ralph E Hurd², John Kurhanewicz¹, and Daniel B Vigneron¹

¹*Department of Radiology and Biomedical Imaging, University of California, San Francisco, San Francisco, CA, United States*, ²*GE Healthcare, Menlo Park, CA, United States*

The purpose of this abstract was to investigate pool size effects in experiments with hyperpolarized [¹³C]α-ketobutyrate (αKB), a molecular analog of pyruvate which also has substantial activity with LDH. In contrast to pyruvate, formation of the reduction product [¹³C]α-hydroxybutyrate (αHB) necessarily reflects net metabolic flux as opposed to label exchange. We observed little change when co-injecting αHB but a large increase in the αHB-to-αKB ratio when co-injecting lactate. This suggests that the observed conversion of αKB to αHB only reflects net metabolic flux even in the presence of a large pool of reduction product.

2339

Feasibility of sensing small molecule thiols using hyperpolarized [¹³C]cyanate
Cornelius von Morze¹, Chloe Najac¹, Robert R Flavell¹, David E Korenchan¹, Pavithra Viswanath¹, Lucas Carvajal¹, John Kurhanewicz¹, Sabrina M Ronen¹, Daniel B Vigneron¹, and David M Wilson¹

¹*Department of Radiology and Biomedical Imaging, University of California, San Francisco, San Francisco, CA, United States*

The purpose of this study was to show basic feasibility of non-invasively detecting small molecule thiols using hyperpolarized [¹³C]cyanate. We detected rapid formation of the expected hyperpolarized S-[¹³C]carbamyl thiol adduct after adding cysteine to liquid hyperpolarized [¹³C]cyanate samples. This work demonstrates a new non-enzymatic approach for detecting small molecule thiols such as reduced glutathione, which could be very useful for research on oxidative stress.

2340

¹³C dynamic nuclear polarization NMR for quantification of metabolic flux of endothelial progenitor cells
Nathalie Nielsen¹, Christoffer Laustsen¹, Hans Stødkilde-Jørgensen¹, and Lotte Bonde Bertelsen¹

¹*MR Research Centre, Department of Clinical Medicine, Aarhus University Hospital, Aarhus University, Aarhus, Denmark*

This study aims to quantify the metabolic flux in EPCs in order to characterize the metabolic changes occurring during in-vitro culturing utilized for cell expansion, 3D scaffolds and suspension. [$1-^{13}\text{C}$] hyperpolarized pyruvate is injected to a NMR compatible bioreactor system and the conversion is detected and measured as the lactate/pyruvate ratio. Activation assays and qPCR is performed to support the results. The lactate/pyruvate (6 ± 1.07 fold) and LDH activity is increased in cell suspension culturing. Together with an elevated PDH expression in suspension cultures our conclusion is that adherent cells metabolically compensate in the suspension culture due to the environmental conditions.

2341

Optimizing flip angles for metabolic rate estimation in hyperpolarized carbon-13 MRI
John Maidens¹, Jeremy W. Gordon², Murat Arcak¹, and Peder E. Z. Larson²

¹*Electrical Engineering & Computer Sciences, University of California, Berkeley, Berkeley, CA, United States*, ²*Radiology & Biomedical Imaging, University of California, San Francisco, San Francisco, CA, United States*

Hyperpolarized carbon-13 MRI experiments typically aim to distinguish between healthy and diseased tissues based on the rate at which they metabolize an injected substrate. Existing approaches to determine flip angle sequences for kinetic measurements have used metrics such as signal variation and signal-to-noise ratio, but are not optimized to provide the most reliable metabolic rate estimates. Here we present a flip angle sequence that maximizes the Fisher information about the metabolic rate. We demonstrate through numerical simulation that flip angle sequences optimized using the Fisher information lead to lower variance in metabolic rate estimates than existing sequences. We then validate this optimized sequence *in vivo* with experiments in a prostate cancer mouse model.

2342

Dual-Echo EPI Sequence for Integrated Distortion Correction in 3D Time-Resolved Hyperpolarized ^{13}C MRI
Benjamin J. Geraghty^{1,2}, Albert P. Chen³, and Charles H. Cunningham^{1,2}

¹*Physical Sciences, Sunnybrook Research Institute, Toronto, ON, Canada*, ²*Dept. of Medical Biophysics, University of Toronto, Toronto, ON, Canada*, ³*GE Healthcare, Toronto, ON, Canada*

A novel dual echo EPI sequence is proposed for providing a built-in correction for off-resonance in time resolved, volumetric hyperpolarized ^{13}C metabolic mapping with [$1-^{13}\text{C}$]pyruvate. The phase evolution between two echoes was used to correct EPI distortion and improve spatial registration with the underlying anatomy. A correction term obtained from a fully phase encoded dual echo EPI proton reference scan was required to account for odd/even echo asymmetry in the ^{13}C phase maps. Proof-of-concept dual echo EPI *in vivo* rat data was acquired on a clinical 3T MR scanner and corrected images are presented.

2343

Optimization and application of bipolar gradient for flow-suppressed hyperpolarized ^{13}C CSI in mouse liver at 9.4T
Hansol Lee¹, Joonsung Lee², Eunhae Joe¹, Seungwook Yang¹, Jae Eun Song¹, Young-suk Choi³, Eunkyung Wang³, Ho-Taek Song³, and Dong-Hyun Kim¹

¹*Department of Electrical & Electronic Engineering, Yonsei university, Seoul, Korea, Republic of*, ²*Center for Neuroscience Imaging Research, Institute for Basic Science, Sungkyunkwan University, Suwon, Korea, Republic of*, ³*Department of Radiology, Yonsei University College of Medicine, Seoul, Korea, Republic of*

In hyperpolarized ^{13}C MRI, high signal intensity of vasculature can cause errors in quantification of metabolites or conversion rate constants. The bipolar gradient was used to suppress vascular signal for accurate quantification. However, the velocity of vessel can vary depending on anesthetic level and pulsation. Furthermore, additional T_2^* relaxation signal loss can be induced by delayed data acquisition in ultra-high field (9.4T) due to short T_2^* . In this study, the bipolar gradient was optimized to minimize additional signal loss and mitigate variable velocity, then the optimized bipolar gradient was implemented for hyperpolarized ^{13}C CSI and applied to mouse liver experiment.

2344

Mis-Estimation and Bias of Hyperpolarized ADC Measurements Due to Slice Profile Effects
Jeremy W Gordon¹, Eugene Milshteyn¹, Irene Marco-Rius¹, Michael Ohliger¹, Daniel B Vigneron¹, and Peder EZ Larson¹

¹*Radiology & Biomedical Imaging, University of California - San Francisco, San Francisco, CA, United States*

Hyperpolarized diffusion weighted imaging has the potential to noninvasively assess transporter expression and probe specific metabolite microenvironments. However, the imperfect RF excitation profile and the transient, non-recoverable hyperpolarization lead to non-uniform depletion of M_2 . After multiple RF pulses, this results in excess signal at later excitations, potentially biasing ADC estimation. Scaling the slice-select gradient can correct for this deviation, minimizing bias and providing more precise ADC measurements of hyperpolarized substrates.

2345

Design and test of a double-nuclear RF coil array for 1H MRI and ^{13}C MRS at 7T
Omar Rutledge¹, Tiffany Kwak¹, Peng Cao¹, and Xiaoliang Zhang¹

¹*Radiology and Biomedical Imaging, University of California, San Francisco, San Francisco, CA, United States*

RF coil operation at 7T is fraught with technical challenges, making expansion of 7T into clinical imaging difficult. In this work, a microstrip transmission line and a wire loop coil were combined to form a double-nuclear RF coil array for proton magnetic resonance imaging and carbon magnetic resonance spectroscopy at the ultrahigh magnetic field strength of 7T. Network analysis revealed a high Q-factor and excellent decoupling between the coils. Proton images and carbon spectra were acquired with high sensitivity. The

2346

Feasibility of probing lactate metabolism and neuroprotection in a mouse model of stroke using hyperpolarized ^{13}C -lactate
Mor Mishkovsky¹, Lara Buscemi², Ximena Castillo², Mario Lepore³, Arnaud Comment⁴, Lorenz Hirt², and Jean-Noël Hyacinthe^{5,6}

¹*Laboratory of Functional and Metabolic Imaging, Ecole Polytechnique Fédérale de Lausanne (EPFL), Lausanne, Switzerland*, ²*Department of Clinical Neurosciences, Centre Hospitalier Universitaire Vaudois, Lausanne, Switzerland*, ³*Centre d'Imagerie Biomédicale (CIBM), Ecole Polytechnique Fédérale de Lausanne (EPFL), Lausanne, Switzerland*, ⁴*Institute of Physics of Biological Systems, Ecole Polytechnique Fédérale de Lausanne (EPFL), Lausanne, Switzerland*, ⁵*School of Health Sciences - Geneva, University of Applied Sciences and Arts Western Switzerland, Geneva, Switzerland*, ⁶*Image Guided Intervention Laboratory, University of Geneva, Geneva, Switzerland*

Stroke is a major public health challenge in the context of the current demographic changes. Among a wide range of applications, hyperpolarized magnetic resonance enables *in vivo* real-time measurement of biochemical transformations of hyperpolarized ^{13}C -labeled precursors, including lactate, a known neuroprotectant in stroke at the preclinical level. This study shows the feasibility of measuring lactate metabolism *in vivo* in a mouse model of stroke (MCAO) following intravenous injection of hyperpolarized L-[1- ^{13}C]lactate. Calculated pyruvate-to-lactate ratio shows an increased labeling of the pyruvate pool in MCAO when compared to sham. This feasibility study suggests new perspectives to understand lactate biodistribution and its neuroprotective effect in stroke.

2347

Robust, Quantitative Methods Applied to Clinical Hyperpolarized C-13 MR of Prostate Cancer Patients

Peder Eric Zufall Larson¹, Jeremy Gordon¹, John Maidens², Murat Arcak², Hsin-Yu Chen¹, Galen Reed¹, Ilwoo Park¹, Rahul Aggarwal³, Robert Bok¹, Sarah J Nelson¹, John Kurhanewicz¹, and Daniel B Vigneron¹

¹*Radiology and Biomedical Imaging, University of California - San Francisco, San Francisco, CA, United States*, ²*Electrical Engineering & Computer Sciences, University of California - Berkeley, Berkeley, CA, United States*, ³*Medicine, University of California - San Francisco, San Francisco, CA, United States*

Clinical evaluation of metabolic MRI using hyperpolarized C-13 agents has begun in earnest at multiple sites with the availability of the SpinLab commercial polarizer. For this technology to succeed, robust imaging and analysis methods for quantification of metabolic activity are required. We have developed and are applying efficient dynamic imaging methods, robust kinetic models, and specialized calibration schemes to enable accurate and reproducible quantification in clinical hyperpolarized MR studies.

2348

A Molecular Imaging Approach to Mercury Sensing Based on Hyperpolarized ^{129}Xe Molecular Clamp Probe

Qianni Guo¹, Qingbin Zeng¹, Weiping Jiang¹, Xiaoxiao Zhang¹, Qing Luo¹, and Xin Zhou¹

¹*Wuhan Institute of Physics and Mathematics, Chinese Academy of Sciences, Wuhan, China, People's Republic of*

Mercury contamination is widespread and arises from a variety of natural sources. We propose the use of hyperpolarized ^{129}Xe nuclear magnetic resonance (NMR) spectroscopy for the sensitive detection of Hg^{2+} ions in aqueous solution. We develop a biosensor whose molecular structure is like a clamp. When interact with Hg^{2+} in aqueous solution, the molecular structure of the biosensor could be changed as a clamp from "open" to "closed". This molecular structure change causes the distance between the two cryptophane cages of the biosensor become closer, and the electron cloud of them overlapped. As a result, comparing with normal downfield chemical shifts of the reported xenon biosensors for metallic ions, the Xe caged in the cryptophane moiety shows a upfield chemical shift change from 66.5 ppm to 66.1 ppm. Images were obtained using a CSI method previously used for clinical MRI.

2349

Investigating Spectral Selectivity of the bSSFP Sequence for High Resolution 3D Dynamic Hyperpolarized ^{13}C MRI at 3T Using C2-Pyruvate and Urea

Eugene Milshteyn¹, Cornelius von Morze¹, Hong Shang¹, Galen D Reed², and Daniel B Vigneron¹

¹*Radiology and Biomedical Imaging, UCSF, San Francisco, CA, United States*, ²*HeartVista, Menlo Park, CA, United States*

Hyperpolarized ^{13}C MR imaging can provide simultaneous assessments of metabolism and perfusion to study disease processes. High resolution dynamic imaging is needed to fully understand these processes, but is challenging, especially on clinically relevant systems. This project investigated new methods for spectral selectivity with SNR-efficient bSSFP sequences to provide improved high resolution 3D dynamic *in vivo* HP ^{13}C MR imaging at 3T.

2350

Toward Spectroscopically Selective Imaging of Hyperpolarized Pyruvate and its Metabolites Using Binomial Pulses In Balanced Steady-State Free Precession

Gopal Varma¹, Patricia Coutinho de Souza¹, Leo Tsai¹, Rupal Bhatt², and Aaron Grant¹

¹*Radiology, Beth Israel Deaconess Medical Center and Harvard Medical School, Boston, MA, United States*, ²*Medicine, Beth Israel Deaconess Medical Center and Harvard Medical School, Boston, MA, United States*

Balanced steady-state free-precession (bSSFP) offers high sensitivity and good temporal resolution, and makes efficient use of hyperpolarized magnetization. Several strategies for spectroscopically selective imaging with bSSFP have been proposed [1-5]. Here we investigate the use of simple binomial excitation pulses to selectively null the signals from either pyruvate or lactate, the two dominant metabolites in tumors, thereby obtaining images that are dominated by either lactate or pyruvate, respectively. The method is robust to off-resonance effects, and can be used to augment existing spectroscopic bSSFP techniques.

MRSI

Exhibition Hall

Wednesday, May 11, 2016: 16:00 - 18:00

2351

Rosette Spectroscopic Imaging (RSI) of human brain at 7T

Claudiu Schirda¹, Tiejun Zhao², Hoby Hetherington¹, Victor Yushmanov¹, and Jullie Pan¹¹*Radiology, University of Pittsburgh School of Medicine, Pittsburgh, PA, United States, ²Siemens Medical Solutions, Pittsburgh, PA, United States*

Rosette Spectroscopic Imaging (RSI) has been shown to provide similar or superior encoding speed and sensitivity to echo-planar (EPSI) and spiral spectroscopic imaging (SSI), while using much lower peak gradient and slew rates. Fully encoded k-t space 3D acquisitions with 0.4ml voxel size in 7.2mins (20x20x12, spectral width SW=1923Hz --6.47ppm, Gmax=7.1mT/m and Smax=86mT/m/ms), and 2D acquisitions as short as 36s (1cc) to a 9.5min dual-echo TE=17/34ms J-refocused with 0.16ml voxel (4mm in-plane, 48x48, SW=2778Hz -9.35ppm, Gmax=5.1mT/m and Smax=18mT/m/ms) were collected at 7Tesla in phantoms, controls and patients with epilepsy and tumors.

2352

Concentrically circular echo planar spectroscopic imaging at 3T and 7T with partial temporal interleaving

Neil Wilson¹, Hari Hariharan¹, M. Albert Thomas², and Ravinder Reddy¹¹*Radiology, University of Pennsylvania, Philadelphia, PA, United States, ²Radiology, University of California, Los Angeles, CA, United States*

We use concentric circular echo planar k-space readout to spectroscopic sampling at high field. At high field, higher bandwidths are required which are difficult to achieve using echo planar techniques due to gradient limitations. Often temporal interleaving is employed to mitigate this. Circular k-space sampling is unique among the echo planar trajectories in that different rings can be sampled at different rates, requiring only partial temporal interleaving.

2353

Rapid, High-Resolution 3D 1H-MRSI of the Brain based on FID Acquisitions

Mohammed Azeem Sheikh¹, Fan Lam², Chao Ma², Bryan Clifford³, and Zhi-Pei Liang³¹*Physics, University of Illinois at Urbana-Champaign, Urbana, IL, United States, ²Beckman Institute, University of Illinois at Urbana-Champaign, Urbana, IL, United States, ³Electrical and Computer Engineering, University of Illinois at Urbana-Champaign, Urbana, IL, United States*

In 1H-MRSI, data is typically acquired with spin echo sequences with relatively long acquisition delay, often motivated by the need for water, lipid, and baseline suppression. Here, we present a new method to obtain high-resolution 1H-MRSI data with an FID-based acquisition that has a very short acquisition delay, enabled by a new scheme for nuisance signal removal. The new acquisition method enables short repetition time and rapid acquisition of spectroscopic data. Experimental results demonstrate *in vivo* 3D 1H-MRSI of the brain with isotropic 3 mm resolution in 15 minutes.

2354

A comparison of lipid suppression by double inversion recovery, L1- and L2-regularisation for high resolution MRSI in the brain at 7 T

Gilbert Hangel¹, Bernhard Strasser¹, Michal Povážan¹, Martin Gajdošík¹, Stephan Gruber¹, Marek Chmelík¹, Siegfried Trattnig^{1,2}, and Wolfgang Bogner¹¹*MRCE, Department of Biomedical Imaging and Image-guided Therapy, Medical University of Vienna, Vienna, Austria, ²Christian Doppler Laboratory for Clinical Molecular MR Imaging, Vienna, Austria*

Reliable lipid suppression is essential for robust quantification of parallel imaging accelerated high- resolution MRSI. This work compared the performance of non-selective lipid suppression using double inversion recovery (DIR) with the application of L1- and L2-regularisation during data processing for single-slice MRSI with a 64×64 matrix and a GRAPPA-acceleration of nine in five volunteers. While DIR featured the best lipid suppression, it increased the measurement time and reduced metabolite SNR. L1 and L2 did not have these downsides, but twice as much lipid signal remained, with L1 increasing the data pre-processing time before spectral quantification by a factor of six.

2355

Crusher coil lipid suppression for volumetric 1H echo-planar spectroscopic imaging of the human brain at 7 Tesla

Karim Snoussi^{1,2}, Joseph S. Gillen^{1,2}, Michael Schär^{1,2}, Vincent O. Boer³, Richard A.E. Edden^{1,2}, and Peter B. Barker^{1,2}¹*Russell H. Morgan Department of Radiology and Radiological Science, Johns Hopkins University School of Medicine, Baltimore, MD, United States, ²Kennedy Krieger Institute, Baltimore, MD, United States, ³Department of Radiology, University Medical Center Utrecht, Utrecht, Netherlands*

Suppression of extra cranial lipid signals is a significant challenge for MR spectroscopy at high field. This study describes the use of a crusher coil in a volumetric proton echo-planar spectroscopic imaging (EPSI) sequence for 7T. It is shown *in vivo* that the application of the crusher coil improves the spin-echo 7T EPSI sequence and allows to record high quality spectroscopic imaging data with extended 3D coverage and low RF power deposition.

Achieving High Spatiotemporal Resolution for 1H-MRSI of the Brain
 Fan Lam¹, Chao Ma¹, Qiegen Liu¹, Bryan Clifford^{1,2}, and Zhi-Pei Liang^{1,2}

¹Beckman Institute, University of Illinois at Urbana-Champaign, Urbana, IL, United States, ²Department of Electrical and Computer Engineering, University of Illinois at Urbana-Champaign, Urbana, IL, United States

We present a novel strategy to achieve high spatiotemporal resolution for 1H-MRSI of the brain. The proposed acquisition scheme is characterized by: (a) the use of EPSI-based rapid spatiotemporal encoding with an extended k-space coverage; (b) sparse sampling of (k,t)-space; (c) time-interleaved k-space undersampling, and (d) acquisition and use of navigator signals for determining subspace structures. This special acquisition is enabled by a subspace-based data processing and reconstruction method that can effectively remove nuisance signals and obtain high-quality reconstructions from sparse and noisy data. Experimental data have been acquired to demonstrate the potential of the proposed method in producing time-resolved spatiotemporal distributions.

Measurement reproducibility of the spiral encoding GABA-edited MEGA-LASER 3D-MRSI in the brain at 3T
 Petra Hnilicová¹, Michal Považan², Bernhard Strasser², Ovidiu C Andronescu³, Dušan Dobrota¹, Siegfried Trattnig², and Wolfgang Bogner²

¹Department of Medical Biochemistry, Jessenius Faculty of Medicine in Martin, Comenius University in Bratislava, Martin, Slovakia, ²Department of Biomedical Imaging and Image-guided Therapy, MR Center of Excellence, Medical University of Vienna, Vienna, Austria, ³Department of Radiology, Martinos Center for Biomedical Imaging, Harvard Medical School, Boston, MA, United States

In vivo assessment of neurotransmitter levels can improve the understanding of several pathological processes. For non-invasive GABA* and Glx mapping *in vivo* within one scan, we applied a spiral-encoded GABA-edited MEGA-LASER 3D-MRSI sequence with real time corrections, achieving the ~3 cc nominal resolution in ~20 minutes. Via test-retest assessment in 14 healthy volunteers (7 men/7 women) we confirmed the measurement reproducibility and inter- and intra-subject variability of GABA* and Glx ratios and thus validated that our method may be used in (pre)clinical studies of neurotransmitters alterations in the brain at 3T.

Comparison of high-resolution FID-MRSI in the brain between 3 and 7 Tesla
 Eva Heckova¹, Stephan Gruber¹, Bernhard Strasser¹, Michal Považan¹, Gilbert Hangel¹, Siegfried Trattnig^{1,2}, and Wolfgang Bogner¹

¹High Field MR Center, Department of Biomedical Imaging and Image-guided Therapy, Medical University of Vienna, Vienna, Austria, ²Christian Doppler Laboratory for Clinical Molecular MR Imaging, Vienna, Austria

Magnetic resonance spectroscopic imaging (MRSI) allows to measure different metabolites in the brain. SNR and spectral resolution increases at higher magnetic fields. We compared FID-MRSI with ultra short acquisition delay (1.5 ms) and a very high spatial resolution in the same group of healthy subjects at 3T and 7T. We found 1.87-fold increased SNR and decreased CRLBs at 7T in comparison with 3T. The higher spectral resolution at 7T allows to distinguish between NAA and NAAG and reliable detect other metabolites like Glx or Tau. Accelerating the acquisition techniques leads to lower SNR, however not to substantially decreased quantification precision.

Fast and efficient free induction decay MRSI at 9.4 T: assessment of neuronal activation-related changes in the human brain biochemistry
 Grzegorz L. Chadzynski^{1,2}, Jonas Bause², G. Shajan², Rolf Pohmann², Klaus Scheffler^{1,2}, and Philipp Ehses^{1,2}

¹Biomedical Magnetic Resonance, Eberhard-Karls University of Tübingen, Tübingen, Germany, ²High-field Magnetic Resonance Center, Max Planck Institute for Biological Cybernetics, Tübingen, Germany

The aim was to design a MRSI-FID sequence for ultra-high field applications with high acquisition speed and sampling efficiency. The sequence allows acquisition of a 32x32 voxel matrix within approximately 2 min, down to 30 sec using parallel imaging. We have examined the suitability of this approach for assessing biochemical changes in the human visual cortex during a visual stimulus. Obtained results were in accordance with other functional MRS studies and indicate that the developed sequence is suitable for rapid monitoring of stimulus evoked changes in human brain biochemistry at a very high spatial resolution.

Quantitative Comparison of SNR between High and Low Resolution of 3D Chemical Shift Imaging (CSI)
 Byeong-Yeul Lee¹, Xiao-Hong Zhu¹, and Wei Chen¹

¹Center for Magnetic Resonance Research, Radiology, University of Minnesota, Minneapolis, MN, United States

Spatial averaging of multiple high-resolution CSI (hrCSI) voxels is commonly employed to gain SNR and improve quantification of metabolites. Using *in vivo* 17-oxygen 3D CSI, we compared SNR between spatial averaging of multiple hrCSI voxels and a single voxel acquired with low-resolution CSI (lrCSI) with matched sample volume and position. SNR from voxel averaging was much lower than that of lrCSI caused mainly by the increased noise level by spectral summation. This study clearly demonstrates that the acquisition of high-resolution data with spatial averaging faces a large trade-off of SNR. Therefore, it should be taken consideration carefully for the choice of an appropriate voxel size of high-resolution CSI for *in vivo* study of neurological or metabolic diseases.

Removal of Nuisance Signal from Sparsely Sampled 1H-MRSI Data Using Physics-based Spectral Bases
 Qiang Ning^{1,2}, Chao Ma², Fan Lam², Bryan Clifford^{1,2}, and Zhi-Pei Liang^{1,2}

¹Electrical and Computer Engineering, University of Illinois, Urbana-Champaign, Urbana, IL, United States, ²Beckman Institute for Advanced

A novel nuisance removal method is proposed for ^1H -MRSI. The method uses spectral bases generated for water and subcutaneous lipids using quantum simulation, and can perform nuisance signal removal directly from (k,t)-space data. Consequently, the proposed method is able to handle sparsely sampled MRSI data, which provides a desirable flexibility for designing accelerated ^1H -MRSI data acquisition schemes. Experimental results demonstrate that the proposed method is capable of removing nuisance signals from ^1H -MRSI data acquired from the brain without water and lipid suppression pulses.

2362

Neurochemical Changes in Thalamus and Midbrain of Patients with Obstructive Sleep Apnea Syndrome using Accelerated Echo Planar J-resolved Spectroscopic Imaging

Manoj Kumar Sarma¹, Paul Michael Macey², Rajakumar Nagarajan¹, Ravi Aysola³, and M. Albert Thomas¹

¹*Radiological Sciences, UCLA School of Medicine, Los Angeles, Los Angeles, CA, United States*, ²*School of Nursing, UCLA School of Medicine, Los Angeles, Los Angeles, CA, United States*, ³*Division of Pulmonary and Critical Care Medicine, UCLA School of Medicine, Los Angeles, Los Angeles, CA, United States*

Obstructive sleep apnea syndrome (OSAS), which have many comorbidities including hypertension and other cardiovascular diseases, leads to autonomic, cognitive, and affective abnormalities. The thalamus, and midbrain are key structures that serve such functions through critical relays in nuclei but the status of this region is unclear OSAS. Here, we examined neurochemical changes in the thalamus and midbrain of OSAS patients to better understand the nature of tissue changes using compressed sensing based 4D echo-planar J-resolved spectroscopic imaging (EP-JRESI) and prior knowledge fitting (ProFit) algorithm for metabolite quantification. We observed significantly increased mI/Cr in midbrain and bilateral thalamus. Significantly increased Glx/Cr, Glu/Cr was found in right thalamus and midbrain, and decreased tNAA/Cr, NAA/Cr in left thalamus and midbrain respectively. Thalamus showed significantly reduced tCho/Cr bilaterally. We also found significantly decreased GPC/Cr, increased Gln/Cr, Asc/Cr in right thalamus and increased Asc/Cr in midbrain. The findings will help to explain structural brain changes in OSAS. Most of these metabolites can be manipulated through pharmacological approaches, and could serve as a biomarker of any possible intervention.

2363

Prior Knowledge Fitting (ProFit) of Non-uniformly Sampled 5D Echo Planar Spectroscopic Imaging Data : Effect of Acceleration on Concentrations and Cramer Rao Lower Bounds

Zohaib Iqbal¹ and M. Albert Thomas¹

¹*Radiological Sciences, University of California - Los Angeles, Los Angeles, CA, United States*

The five dimensional echo planar spectroscopic imaging (5D EP-JRESI) sequence uses an echo planar readout, non-uniform sampling (NUS), and compressed sensing reconstruction to obtain two dimensional spectra from three spatial dimensions. However, the effects of NUS and reconstruction on quantitation results and fit quality parameters, such as the Cramer Rao Lower Bound (CRLB), are unknown. This study uses the new Prior knowledge Fitting (ProFit) algorithm to fit the 5D EP-JRESI results acquired using retrospective as well as prospective NUS. Comparison to the full data demonstrates that the 5D EP-JRESI method can sample 8-times faster while retaining accurate metabolite ratios and CRLB values.

2364

Ultrashort TE 3D spectroscopic imaging for high SNR imaging and bi-exponential signal decay characterization of sodium Jetse S. van Gorp¹, Paul W. de Bruin², and Peter R. Seevinck¹

¹*Image Sciences Institute, University Medical Center Utrecht, Utrecht, Netherlands*, ²*Radiology, Leiden University Medical Center, Leiden, Netherlands*

Sodium relaxation behavior has been related to structural and cellular integrity, which is of interest for early disease detection. However, the short T_2^* values, bi-exponential relaxation behavior and low sensitivity makes accurate signal characterization challenging. In this work a 3D-UTE-FID-SI sequence was developed to measure the sodium decay curve with a 32kHz temporal resolution and sub-ms TE to characterize the bi-exponential signal decay characteristics of sodium *in vitro* and *in vivo*.

Traditional Poster

MRS Methods

Exhibition Hall

Wednesday, May 11, 2016: 16:00 - 18:00

2365

Accounting for GABA editing efficiency and macromolecule co-editing to allow inter-vendor comparisons of GABA+ measurements Ashley D Harris^{1,2,3,4,5}, Nicolaas AJ Puts^{1,5}, Laura Rowland⁶, S. Andrea Wijtenburg⁶, Mark Mikkelsen⁷, Peter B Barker^{1,5}, C. John Evans⁷, and Richard AE Edden^{1,5}

¹*FM Kirby Center for Functional Brain Imaging, Kennedy Krieger Institute, Baltimore, MD, United States*, ²*CAIR Program, Alberta Children's Hospital Research Institute, University of Calgary, Calgary, AB, Canada*, ³*Radiology, University of Calgary, Calgary, AB, Canada*, ⁴*Hotchkiss Brain*

Differences in GABA+ MEGA PRESS acquisitions between vendors are quantified in terms of the editing efficiency of GABA and the fractional co-editing of macromolecules. Accounting for these two parameters results in moderate agreement among the different vendors considered.

2366

Towards a neurochemical profile of the amygdala using SPECIAL at 3 tesla
Florian Schubert¹, Ralf Mekle¹, Simone Kühn², Jürgen Gallinat³, and Bernd Ittermann¹

¹Physikalisch-Technische Bundesanstalt (PTB), Braunschweig and Berlin, Germany, ²MPI for Human Development, Berlin, Germany, ³Universitätsklinikum Hamburg-Eppendorf, Hamburg, Germany

Since disturbed amygdala function is linked to psychiatric conditions insight into its biochemistry, particularly the neurotransmitters, is required. We combined the SPECIAL MRS sequence with FAST(EST)MAP implementation, corrections for frequency drift, relaxation, CSF volume, and a basis set including a measured macromolecule spectrum for quantification of metabolites in the amygdala in 20 volunteers at 3T. Beyond quantification of the three main metabolites plus myo-inositol with excellent precision, for the first time glutamate was determined reliably and separately from glutamine. Using a basis set without macromolecules introduced a systematic overestimation of concentrations. Glutamine and glutathione was quantifiable only in a subset of spectra.

2367

Estimation of *in vivo* γ -aminobutyric acid (GABA) levels in the neonatal brain
Moyoko Tomiyasu^{1,2}, Noriko Aida³, Jun Shibasaki⁴, Katsutoshi Murata⁵, Keith Heberlein⁶, Mark A. Brown⁷, Eiji Shimizu², Hiroshi Tsuji¹, and Takayuki Obata¹

¹National Institute of Radiological Sciences, Chiba, Japan, ²Chiba University, Chiba, Japan, ³Department of Radiology, Kanagawa Children's Medical Center, Yokohama, Japan, ⁴Kanagawa Children's Medical Center, Yokohama, Japan, ⁵Siemens, Tokyo, Japan, ⁶Biomedical Imaging Technology Center, Burlington, MA, United States, ⁷University of Colorado, Cary, NC, United States

We examined *in vivo* brain γ -aminobutyric acid (GABA) levels of neonates and compared them with those of children. In this study, 32 normal neonates and 12 normal children (controls) had their brain GABA levels measured using clinical 3T edited-MRS. The neonates exhibited significantly lower GABA+ levels than the children in both the basal ganglia and cerebellum, which is consistent with previous *in vitro* data. While significantly higher GABA+/Cr levels were detected in the neonatal cerebellum, care should be taken when comparing GABA+/Cr levels between different ages. This is the first report about the *in vivo* brain GABA levels of neonates.

2368

Assessment of Lipid Changes in Obese Calf Using Multi-Echo Echo-planar Correlated Spectroscopic Imaging
Rajakumar Nagarajan¹, Raissa Souza¹, Edward Xu¹, Manoj K Sarma¹, S. Sendhil Velan², Cathy C Lee³, Theodore Hahn³, Catherine Carpenter⁴, Vay-Liang Go⁵, and M. Albert Thomas¹

¹Radiological Sciences, University of California Los Angeles, Los Angeles, CA, United States, ²Laboratory of Molecular Imaging, Singapore Bioimaging Consortium, Singapore, Singapore, ³Geriatrics, VA Greater Los Angeles Healthcare System, Los Angeles, CA, United States, ⁴UCLA Schools of Nursing, Medicine, and Public Health, Los Angeles, CA, United States, ⁵UCLA Department of Medicine, Los Angeles, CA, United States

Obesity is a serious public health problem associated with high rates of morbidity and mortality. One-dimensional MR spectroscopy suffers from overlapping spectral resonances which can complicate metabolite identification and quantitation. Two-dimensional spectroscopic techniques have been demonstrated in calf muscle to reduce the problem of spectral overlap. In this study, we used the four dimensional (4D) multi-echo echo planar correlated spectroscopic imaging (ME-EPCOSI) technique to quantify the lipids and metabolites in soleus, tibialis anterior and gastrocnemius calf muscles of obese and normal healthy subjects. The 4D ME-EPCOSI acquired data enabled less ambiguous quantitation of metabolites, unsaturated and saturated fatty acids in different calf muscle regions using IMCL ratios and unsaturation indices.

2369

Simultaneous modeling of spectra and apparent diffusion coefficients.
Victor Adalid Lopez¹, André Doering¹, Sreenath Pruthviraj Kyathanahally¹, Christine S. Bolliger¹, and Roland Kreis¹

¹Depts. Radiology and Clinical Research, University Bern, Bern, Switzerland

Diffusion weighted spectroscopy can provide information on the diffusion of metabolites and the microstructure of brain tissue. A method for simultaneous fitting of spectra related by mono-exponential diffusion weighting is introduced, which is similar to simultaneous fitting of a 2DJ or inversion recovery data set. As shown for simulated white matter data, the method improves both, accuracy and precision of ADC estimation for all metabolites. It is also illustrated with diffusion data obtained from human gray matter at 3T.

2370

Novel Triple-refocusing ^1H MRS at 3T for detection of GABA in human brain *in vivo*
Zhongxu An¹, Sandeep Ganji¹, Vivek Tiwari¹, and Changho Choi¹

¹Advanced Imaging Research Center, University of Texas Southwestern Medical Center, Dallas, TX, United States

Reliable detection of GABA is important for research studies in neuro-psychiatric diseases. *In vivo* ¹H GABA resonances extensively overlap with the neighboring resonances of glutamate and glutamine. We present an optimized single-shot triple-focusing 1H MRS method which fully resolved GABA 2.29-ppm signal at 3T.

2371

Prospective frequency correction for TE-averaged semi-LASER
Chu-Yu Lee¹, In-Young Choi^{1,2,3}, Peter Adany¹, and Phil Lee^{1,3}

¹Hoglund Brain Imaging Center, University of Kansas Medical Center, Kansas city, KS, United States, ²Department of Neurology, University of Kansas Medical Center, Kansas City, KS, United States, ³Department of Molecular & Integrative Physiology, University of Kansas Medical Center, Kansas City, KS, United States

Frequency drifts during MRS acquisition results in broad and distorted spectral lineshapes, a reduced SNR and quantification errors. The consequence of frequency drifts is particularly significant in spectral-editing sequences, because spectral editing critically relies on narrow-band frequency selective pulses or accurate spectral alignments among scans for subtraction/addition of spectra. Frequency drift can occur due to subject's movement and/or MR system instability. Even in advanced MR systems with self-shielded gradients, significant frequency drifts occur due to eddy current-induced heating and cooling of passive shim materials, particularly after MR scans with heavy gradient duty cycles. The effects of frequency drifts can be mitigated through prospective and retrospective frequency corrections. Currently, most spectral-editing methods use post-processing approaches to correct the effects of frequency drifts retrospectively. In this study, we have developed a prospective frequency correction method and implemented it in a semi-LASER based TE-averaged sequence for glutamate detection.

2372

Automatic Multi-layer Classification System of Brain Tumor Based on Multi-modality MRI and Clinical Information
Yafei Wang¹, Yue Zhang¹, Lingyi Xu¹, Yu Sun¹, Lei Xiang², Meiping Ye², Suiren Wan¹, Bing Zhang², and Bin Zhu²

¹The Laboratory for Medical Electronics, School of Biological Sciences and Medical Engineering, Southeast University, Nanjing, China, People's Republic of, ²Department of Radiology, The Affiliated Drum Tower Hospital of Nanjing University Medical School, Nanjing, China, People's Republic of

Classification or grading of brain tumor alone would not be enough for clinical use, therefore we designed a comprehensive multi-layer system combining the two functions together. Firstly, we designed it as a three-layer system according to clinic workflow. Then, we extracted new features from multi-modality MRI and patients' clinical information, which were easily ignored or difficult found by eyes. And then we implemented SVM and Tumor Model to classify tumor type and tumor grade. This study proposed a novel multi-layer system for clinic use by reducing the diagnosis uncertainty.

2373

Reproducibility and gender-related effects on macromolecule suppressed GABA and Glx metabolites
Muhammad Gulamabbas Saleh¹, A Alhamud¹, Jamie Near², Frances Robertson¹, André J.W. van der Kouwe³, and Ernesta M Meintjes¹

¹Human Biology, MRC/UCT Medical Imaging Research Unit, University of Cape Town, Cape Town, South Africa, ²Douglas Mental Health University Institute and Department of Psychiatry, McGill University, Montreal, QC, Canada, ³Athinoula A. Martinos Center for Biomedical Imaging, Massachusetts General Hospital, Charlestown, MA, United States

Several studies have characterized short and long term reproducibility of Glx and GABA+, but not macromolecule (MM) suppressed GABA. Further, gender-related differences have been observed in GABA+, but these may, in part, be due to inter-individual variations of MM. Motion and magnetic field inhomogeneity can hamper the consistent application of frequency-selective pulses at 1.7ppm necessary for effective GABA editing. We demonstrate that the shim and motion-navigated MEGA-SPECIAL sequence produces well-edited GABA and Glx spectra. LCModel quantification yields the best reproducibility. Observed gender-related differences in GABA highlight the need for gender-matching in studies investigating differences in GABA concentrations.

2374

1H-MRS of Human Liver at 3 T: Relaxation Times and Metabolite Concentrations
Jan Weis¹, Fredrik Rosqvist², Joel Kullberg¹, Ulf Risérius², and Håkan Ahlström¹

¹Department of Radiology, Uppsala University, Uppsala, Sweden, ²Department of Public Health and Caring Sciences, Uppsala University, Uppsala, Sweden

Proton MR spectroscopy of healthy human liver was performed at 3 T MR scanner. The purpose of this study was to estimate glycogen (Glycg), choline-containing compounds (CCC), water, and lipid (-CH₂)_n relaxation times T₁, T₂, and absolute concentration of Glycg, CCC, and fat. Experiments were performed using multiple breath-hold technique. Spectra were processed by LCModel. T₁ and T₂ values were obtained by mono-exponential fitting spectral intensities versus repetition or echo times. Quantification of liver Glycg, CCC and lipids is important for understanding changes in lipid and glucose metabolism due to metabolic disorders.

2375

Gradient-heavy sequences degrade the quality of subsequent spectroscopy acquisitions
Benjamin C Rowland¹, Fatah Adan¹, Huijun Liao¹, and Alexander P Lin¹

¹Centre for Clinical Spectroscopy, Brigham and Women's Hospital, Boston, MA, United States

B0 frequency drift is a well-known phenomenon which can have a significant impact on MR spectroscopy, affecting both peak resolution and metabolite quantification. B0 drift is particularly associated with gradient-heavy EPI sequences like DTI. In a study of 53 subjects receiving DTI and MRS, the mean FWHM more than doubled as a result of frequency drift and metabolite concentrations were often

2376

Elucidation of the downfield spectrum of human brain at 7T using multiple inversion recovery delays and echo times
Nicole D Fichtner^{1,2}, Anke Henning^{2,3}, Niklaus Zoelch², Chris Boesch¹, and Roland Kreis¹

¹Depts. Radiology and Clinical Research, University of Bern, Bern, Switzerland, ²Institute for Biomedical Engineering, UZH and ETH Zurich, Zurich, Switzerland, ³Max Planck Institute for Biological Cybernetics, Tuebingen, Germany

Characterization of the full ¹H spectrum may allow for better monitoring of pathologies and metabolism in humans. The downfield part (5-10ppm) is currently less well characterized than upfield; this work aims to benefit from higher field strength in order to quantify T₁ and T₂ in the downfield spectrum in human grey matter at 7T. We fitted downfield spectra to a heuristic model and obtained relaxation times for twelve peaks of interest. The T₁'s are higher than those at 3T downfield; peaks with lower T₁'s may include macromolecules. The T₂'s are mostly shorter than those reported for upfield peaks at 7T.

2377

Tissue correction strategy impacts GABA quantification: a study in healthy aging

Ashley D Harris^{1,2,3,4}, Eric Porges⁵, Adam J Woods^{5,6}, Damon G Lamb^{5,7}, Ronald A Cohen⁵, John B Williamson^{5,8}, Nicolaas AJ Puts^{3,4}, and Richard AE Edden^{3,4}

¹Radiology, University of Calgary, Calgary, AB, Canada, ²CAIR Program, Hotchkiss Brain Institute and Alberta Children's Hospital Research Institute, Calgary, AB, Canada, ³Russell H Morgan Department of Radiology and Radiological Science, The Johns Hopkins University, Baltimore, MD, United States, ⁴FM Kirby Center for Functional Brain Imaging, Kennedy Krieger Institute, Baltimore, MD, United States, ⁵Center for Cognitive Aging and Memory (CAM), McKnight Brain Institute, Department of Aging and Geriatric Research, University of Florida, Gainesville, FL, United States, ⁶Department of Neuroscience, University of Florida, Gainesville, FL, United States, ⁷Brain Rehabilitation and Research Center, Malcom Randall Veterans Affairs Medical Center, Gainesville, FL, United States, ⁸Brain Rehabilitation and Research Center, Brain Rehabilitation and Research Center, Gainesville, FL, United States

There are various strategies for tissue correction for MRS. Here, using data from a healthy aging cohort, we show that the selection of tissue correction method can change the conclusions that are drawn from data.

2378

Towards low power EPR Imaging using Frank poly-phase pulse sequence

Nallathamby Devasahayam¹, Randall H. Pursley², Thomas J. Pohida², Shingo Matsumoto³, Keita Saito⁴, Sankaran Subramanian⁵, and Murali C. Krishna⁴

¹Radiation Biology Branch, National Cancer Institute, Bethesda, MD, United States, ²Center for Information Technology, Bethesda, MD, United States, ³Graduate School of Information Science and Technology, Sapporo, Japan, ⁴National Cancer Institute, Bethesda, MD, United States, ⁵Indian Institute of Technology Madras, Chennai, India

Electron Paramagnetic Resonance (EPR) imaging is suited well for small animal physiological imaging with its unique capability of generating *in vivo* quantitative oxygen maps. The main bottleneck in scaling up pulsed EPR imaging to human anatomy is that the required RF power of US federal food and drug administration (FDA), specific absorption rate (SAR) limits. In Frank Sequence we are using power levels on the order of 250 microwatts in a crossed coil resonator with ~35 dB isolation. Using a 256 pulse polyphase Frank Sequence, it was possible to obtain images with good SNR.

2379

Hitchhikers guide to voxel segmentation for partial volume correction of *in-vivo* magnetic resonance spectroscopy

Scott Quadrelli^{1,2}, Carolyn Mountford³, and Saadallah Ramadan²

¹Queensland University of Technology, Brisbane, Australia, ²The University of Newcastle, Newcastle, Australia, ³The Translational Research Institute, Brisbane, Australia

Whilst many studies have detailed the impact of partial volume effects on proton magnetic resonance spectroscopy quantification, there is a paucity of literature explaining how voxel segmentation can be achieved using freely available neuroimaging packages. Here we aim to demonstrate a practical guide to magnetic resonance spectroscopy (MRS) voxel segmentation, partial volume correction and detail how to extract other MR metrics (such as DTI, fMRI) from a MRS voxel.

2380

Enhancement of signal intensity using a wireless coil for FT-EPR oximetry study

Ayano Enomoto¹, Gadisetty V. R. Chandramouli², Alan P Koretsky³, Chunqi Qian⁴, Murali K Cherukuri¹, and Nallathamby Devasahayam¹

¹Radiation Biology Branch, National Cancer Institute, Bethesda, MD, United States, ²GenEpria Consulting Inc., Columbia, MD, United States, ³National Institute of Neurological Disorders and Stroke, National Institutes of Health, Bethesda, MD, United States, ⁴Department of Radiology, Michigan State University, East Lansing, MI, United States

Sensitivity enhancement is required to detect the weak signals with Fourier transform Electron Paramagnetic Resonance (FT-EPR). In the proposed method, a small amount of sample was placed at a distance less than half the diameter of the receiving surface coil. The signal was enhanced by a wirelessly pumped coil. Presently, we used the TCNQ for our studies to study signal enhancement. Here, we achieved 7-fold of improvement in signal intensity in compared with conventional FT-EPR acquisition. We will show the results of *in vivo* oximetry using oxygen sensing solids LiPc and LiNc in *in vivo* applications to measure tissue oxygenation.

Assessment of serine quantification reproducibility using advanced ^1H -MRS in the human brain at 3T
Homa Javadzadeh^{1,2} and Jean Théberge^{1,2,3}

¹Department of Medical Biophysics, University of Western Ontario, London, ON, Canada, ²Imaging Division, Lawson Health Research Institute, London, ON, Canada, ³Diagnostic Imaging Department, St. Joseph's Health Care, London, ON, Canada

D-serine supplements alleviate some of the most debilitating features of schizophrenia believed to be associated with glutamatergic abnormalities. Assessment of endogenous serine is impossible using standard proton Magnetic Resonance Spectroscopy (^1H -MRS). This work employs a novel ^1H -MRS sequence called DANTE-PRESS (D-PRESS) and presents test-retest reliability study for serine levels acquired at 3T in phantoms and initial data in two human subjects. We conclude that reproducibility and precision of serine measurements on a 3.0T scanner is sufficient to assess endogenous levels *in vivo* and is a valuable tool to examine abnormalities in schizophrenia and monitor supplementation.

Large Improvements of RF field Transmission Efficiency and Detection Sensitivity for Ultrahigh-field *In vivo* ^{31}P MRS using Emerging Technology of Ultrahigh Dielectric Constant Material
Byeong-Yeul Lee¹, Xiao-Hong Zhu¹, Sebastian Rupprecht², Michael T. Lanagan³, Qing X. Yang^{2,4}, and Wei Chen¹

¹Center for Magnetic Resonance Research, Radiology, University of Minnesota, Minneapolis, MN, United States, ²Center for NMR Research, Radiology, The Pennsylvania State College of Medicine, Hershey, PA, United States, ³Engineering Science and Mechanics, The Pennsylvania State College of Engineering, University Park, PA, United States, ⁴Neurosurgery, The Pennsylvania State College of Medicine, Hershey, PA, United States

Compared to ^1H MRS, X-nuclei MRS for human application faces two challenges: higher requirement of RF power (thus, higher SAR) for achieving the same RF pulse flip angle due to a relatively lower gyromagnetic ratio, and still limited SNR even at high/ultrahigh field. In this report, we demonstrate that up to 200% SNR gain was achieved with ultra high dielectric constant (uHDC) materials incorporated into the RF volume coil for ^{31}P MRS at 7T. Concomitantly, the RF power optimized for acquiring the spectra was significantly reduced by 200%. Our data demonstrated that incorporating uHDC with RF coil can significantly boost SNR and reduce RF transmission power X-nuclei MRS applications on top of using high field strength magnet that has approached to its technologic limits.

9.4 Tesla ^1H -MRS of Glutamate and GABA in a 3.6 cubic-mm volume using an optimized UTE-STEAM sequence
Nicola Bertolino¹, Paul Polak¹, Marilena Preda^{1,2}, Robert Zivadinov^{1,2}, and Ferdinand Schweser^{1,2}

¹Buffalo Neuroimaging Analysis Center, Department of Neurology, Jacobs School of Medicine and Biomedical Sciences, The State University of New York at Buffalo, Buffalo, NY, United States, ²MRI Molecular and Translational Research Center, Jacobs School of Medicine and Biomedical Sciences, The State University of New York at Buffalo, Buffalo, NY, United States

In-vivo ^1H -MR spectroscopy is a non-invasive technique able to detect metabolites providing important information from investigated tissue. GABA and Glutamate are two metabolites altered in many neurological diseases, although challenging to quantify *in vivo* because of a number of technical issues: voxel localization, low concentration, short T2, overlapping peaks and spin-spin coupling. In this work we developed an optimized parameter set for an ultra-short TE STEAM.

Effects of Storage Conditions on Transverse Relaxation in Bovine Articular Cartilage
Kyle W. Sexton¹, Hasan Celik¹, Kenneth W. Fishbein¹, and Richard G. Spencer¹

¹National Institute on Aging, National Institutes of Health, Baltimore, MD, United States

Quantification of cartilage matrix components with nuclear magnetic resonance has potential applications to the early diagnosis of osteoarthritis. Ex-vivo cartilage samples are often used to observe the MR parameters of healthy and degraded cartilage. To ensure the accuracy of MR parameters, the storage of the explants is extremely important. DPBS is often used to immerse cartilage tissue specimens during imaging, with the assumption that it prevents dehydration. In this study it was found that storing BAC tissue explants in DPBS can rapidly and significantly increase the observed T2 values. An alternative storage medium to maintain T2 stability is Fluorinert.

Frequency correction based on interleaved water acquisition improves spectral quality in MM-suppressed GABA measurements *in vivo*
Nicolaas AJ Puts^{1,2}, Kimberly L Chan¹, Ashley D Harris^{1,2,3,4}, Peter B Barker^{1,2}, and Richard AE Edden^{1,2}

¹Radiology and Radiological Science, Johns Hopkins University, Baltimore, MD, United States, ²F.M. Kirby Center for Functional Brain Imaging, Kennedy Krieger Institute, Baltimore, MD, United States, ³Alberta Children's Hospital Research Institute, University of Calgary, Calgary, AB, Canada, ⁴Radiology, University of Calgary, Calgary, AB, Canada

MM-suppressed GABA measurements use symmetric editing of both MM and GABA signals. Frequency drift, either by gradient induced heating/cooling, or motion, significantly affects the editing efficiency of GABA and MM. To stabilize the center frequency, we interleaved the unsuppressed water acquisition throughout the scan and used it to correct the frequency, in eight healthy participants, and compared this to a condition without frequency correction. Frequency correction improves spectral quality of MM-suppressed GABA editing *in vivo*.

Single volume localization without RF refocusing for dynamic hyperpolarized ^{13}C MR spectroscopy
Albert P Chen¹, Ralph E Hurd², Angus Z Lau³, and Charles H Cunningham^{4,5}

A method for single volume dynamic hyperpolarized ¹³C MRS acquisition is proposed. Using a slice selective pulse-acquire pulse sequence with 2D spiral readout this technique enables 3D localization of the MRS data. By confining the readout trajectory to each dwell time, the raw data sampled during the trajectory are averaged by the digital filter, thus the output data represent only the center voxel and no k-space data sorting and reconstruction are required. This sequence can be used practically the same way as a standard pulse-acquire acquisition for HP¹³C experiments, but the spectrum will be localized to a 3D volume.

2387

Metabolic ratios can increase or decrease sample size requirements and statistical significance in magnetic resonance spectroscopy
Sarah E. Hoch¹, Ivan I. Kirov², and Assaf Tal³

¹Radiology, Sheba Medical Center, Ramat-Gan, Israel, ²Radiology, New York University Langone Medical Center, New York, NY, United States, ³Chemical Physics, Weizmann Institute of Science, Rehovot, Israel

Metabolite ratios are often used to simplify metabolic quantification. It is often implicitly assumed that they are also statistically favorable when both numerator and denominator metabolites change in opposing manners. Herein, we show that even for such cases, both sample size requirements and statistical significance depend non-trivially on taking the ratio. We conclude that care must be taken when deciding between ratios and absolute quantification during study design.

2388

Improved semi-LASER sequence with short echo time for ultra-high field using selective GOIA refocusing pulses

Michal Považan^{1,2}, Lukas Hingerl¹, Bernhard Strasser¹, Gilbert Hangel¹, Eva Heckova¹, Stephan Gruber¹, Siegfried Trattnig^{1,2}, and Wolfgang Bogner¹

¹High Field MR Center, Department of Biomedical Imaging and Image-guided Therapy, Medical University Vienna, Vienna, Austria, ²Christian Doppler Laboratory for Clinical Molecular MR Imaging, Vienna, Austria

MR spectroscopy (MRS) profits from ultra-high field (UHF) with higher SNR and enhanced spectral resolution. However, the higher demand on bandwidth of RF pulses together with power limitations complicate the utilization of localization sequences such as PRESS or STEAM. A semi-LASER sequence appears to be a suitable candidate for UHF MRS if properly optimized. We aimed to implement selective GOIA refocusing pulses and optimize the gradient scheme to yield shortest echo time possible on a volume coil. Our semi-LASER sequence outperformed the conventional sequences in terms of SNR and chemical shift displacement artifact and proved to be applicable at UHF.

2389

Assessment of intracellular lipids of non-adipose pancreatic cells

Jan Weis¹, Lina Carlblom¹, Lars Johansson¹, Olle Korsgren², and Håkan Ahlström¹

¹Department of Radiology, Uppsala University, Uppsala, Sweden, ²Department of Immunology, Genetics and Pathology, Uppsala University, Uppsala, Sweden

A 1.5 T clinical scanner was used for proton MR spectroscopy (¹H-MRS) of human pancreas allografts. The main purpose was to estimate intracellular lipid content in non-adipose pancreatic cells. The secondary aim was to quantify total fat and choline-containing compounds. Spectrum processing was performed in the time domain using MRUI software package. It was demonstrated that ¹H-MRS is an effective method for non-invasive estimation of intracellular lipid content in non-adipose pancreatic cells. This knowledge could be helpful in studies of various aspects of β-cell function (insulin production).

2390

Assessment and retrospective correction of rotation-induced signal attenuation in diffusion-weighted spectroscopy

Michael Dacko¹, Benjamin Knowles¹, Patrick Hücker¹, Maxim Zaitsev¹, and Thomas Lange¹

¹Medical Physics, University Medical Center Freiburg, Freiburg, Germany

Diffusion-weighted spectroscopy of the brain is a highly motion-sensitive MR method as a consequence of the large voxel size and low metabolite diffusion coefficients. In this work, we correct for voxel displacement during DWS experiments with prospective motion correction and investigate the signal attenuation due to rotation-induced intra-voxel dephasing. Phantom experiments with 'synthetic' rotations confirmed the theoretically predicted signal attenuation. High correlation between rotational motion and attenuation of the residual water peak was observed in vivo. Retrospective rejection criteria based on the recorded motion tracking data and on the residual water peak amplitude are compared.

2391

Fast automatic voxel positioning with non-rigid registrations for improved between-subject consistency in MRS

Young Woo Park¹, Dinesh K. Deelchand², James M. Joers², Brian J. Soher³, Peter B. Barker⁴, HyunWook Park¹, Gülin Öz², and Christophe Lenglet²

¹School of Electrical Engineering, Korea Advanced Institute of Science and Technology, Daejeon, Korea, Republic of, ²Department of Radiology, Center for Magnetic Resonance Research, University of Minnesota Medical School, Minneapolis, MN, United States, ³Department of Radiology, Duke University Medical Center, Durham, NC, United States, ⁴Department of Radiology, Johns Hopkins University School of Medicine, Baltimore, MD, United States

During the typical acquisition of single-voxel Magnetic Resonance Spectroscopy (MRS) the corresponding voxel-of-interest (VOI) must be selected manually, which induces some degree of variability. To address this, several automated VOI positioning methods, using rigid registration and aimed at follow-up scans of the same subject, have been proposed. This approach can be generalized to cross-subject scans, but with additional considerations for the anatomical variability. We hypothesized that non-rigid registration methods will minimize inter-subject variability in the tissue content of the VOI. Here, we present an analysis of registration strategies aimed at a reliable cross-subject automatic VOI positioning for MRS data acquisition.

2392

MM-suppressed GABA measurements are highly susceptible to B0 field instability

Richard Anthony Edward Edden^{1,2}, Ashley D. Harris^{1,2,3,4}, Nicolaas Puts^{1,2}, Kimberly L. Chan^{1,2,5}, Michael Schar¹, and Peter B. Barker^{1,2}

¹Russell H. Morgan Department of Radiology and Radiological Science, The Johns Hopkins University, Baltimore, MD, United States, ²F.M. Kirby Center for Functional Brain Imaging, Kennedy Krieger Institute, Baltimore, MD, United States, ³Department of Radiology, University of Calgary, Calgary, AB, Canada, ⁴Hotchkiss Brain Institute and Alberta Children's Hospital Research Institute, Calgary, AB, Canada, ⁵Department of Biomedical Engineering, The Johns Hopkins University, Baltimore, MD, United States

J-difference-edited measurements of GABA are usually contaminated up to 50% by macromolecular (MM) signal. It is possible to suppress this signal using a symmetrical editing motif, which relies upon partially inverting the MM signals to an equal degree in the two halves of the edited experiment. In the event of B₀ field offset, the symmetry breaks down and either positive or negative MM signal rapidly contaminates the measured GABA signal. Here, we investigate this issue using simulations and in vivo experiments.

2393

HERMES: Hadamard Encoding and Reconstruction of MEGA-Edited Spectroscopy

Kimberly L Chan^{1,2,3}, Nicolaas AJ Puts^{2,3}, Peter B Barker^{2,3}, and Richard AE Edden^{2,3}

¹Biomedical Engineering, Johns Hopkins School of Medicine, Baltimore, MD, United States, ²Radiology and Radiological Science, Johns Hopkins School of Medicine, Baltimore, MD, United States, ³F.M. Kirby Center for Functional Brain Imaging, Kennedy Krieger Institute, Baltimore, MD, United States

Hadamard Encoding and Reconstruction of MEGA-Edited Spectroscopy, HERMES, is a novel method of the simultaneous, separable detection of overlapping metabolite signals. Classic J-difference editing involves the acquisition of two subspectra, with editing pulses applied to the target molecule (ON) or not (OFF). HERMES edits multiple metabolites simultaneously by acquiring all combinations of OFF/ON for each (i.e. four experiments to edit two metabolites) and uses a Hadamard-like addition-subtraction reconstruction to generate separate edited spectra for each target metabolite. In this abstract, we describe the method and demonstrate its application to NAA/NAAG editing, using simulations, and phantom and in vivo experiments.

2394

Resolving Choline from Taurine in In-Vivo Magnetic Resonance Spectra at 9.4 T

Marissa E. Fisher¹, Brennen J. Dobberthien¹, Anthony G. Tessier^{1,2}, and Atiyah Yahya^{1,2}

¹Department of Oncology, University of Alberta, Edmonton, AB, Canada, ²Department of Medical Physics, Cross Cancer Institute, Edmonton, AB, Canada

The Cho peak at 3.2 ppm contains significant signal contamination from the taurine (Tau) resonance in rat and mouse brain spectra, even at the high field strength of 9.4 T. The purpose of this work is to optimise TE₁ and TE₂ (echo times) of a Point RESolved Spectroscopy (PRESS) sequence to minimize Tau signal in the Cho spectral region at 9.4 T by exploiting the J-coupling evolution of the Tau protons. The determined optimal {TE₁, TE₂} combination was found to be {25 ms, 50 ms}. The efficacy of the timings was verified on rat brain *in vivo*.

2395

Diffusion weighted MR spectroscopy without water suppression allows to use water as inherent reference signal to correct for motion-related signal drop

André Döring¹, Victor Adalid Lopez¹, Vaclav Brandejsky¹, Roland Kreis¹, and Chris Boesch¹

¹Depts. Radiology and Clinical Research, University Bern, Bern, Switzerland

A non-water suppressed diffusion-weighting MR spectroscopy sequence based on metabolite-cycling and STEAM is presented and tested in-vitro and in-vivo. The water peak as an inherent reference facilitates a post processing correction of the signal drop induced in individual acquisitions by cardiac and other motion. The correction leads to improved spectral resolution on one hand, but more importantly also to more accurate fitting of ADC values that are found to be smaller than without correction and most likely closer to the true values - and hence better suited for physiological interpretation.

2396

Sustained GABA reduction induced by anodal Transcranial Direct Current Stimulation (tDCS) in motor cortex: A Proton Magnetic Resonance Spectroscopy Study

Harshal Jayeshkumar Patel¹, Sandro Romanzetti^{2,3}, Antonello Pellicano¹, Kathrin Reetz^{2,3}, and Ferdinand Binkofski^{1,4}

¹Division of Clinical Cognitive Sciences, Department of Neurology, RWTH Aachen University Hospital, Aachen, Germany, ²Department of Neurology, RWTH Aachen University Hospital, Aachen, Germany, ³Jülich Aachen Research Alliance (JARA) — Translational Brain Medicine, Aachen and Jülich, Germany, ⁴Research Center Jülich GmbH, Institute of Neuroscience and Medicine, Jülich, Germany



Transcranial direct current stimulation (tDCS) modulates cortical excitability. In this study we investigated long term effects of anodal

stimulation on inhibitory neurotransmitter concentration using proton magnetic resonance spectroscopy (MRS). Our results indicates that excitatory tDCS cause locally reduction in GABA and it remains in decreased state over a period of 60 minutes presumably due to the decrease of activity of glutamic acid decarboxylase(GAD)67.

2397

In Vivo Detection of Omega-3 Fatty Acids at 7 T with MEGA-sLASER

Lukas Hingerl¹, Martin Gajdošík¹, Michal Považan¹, Bernhard Strasser¹, Gilbert Hangel¹, Martin Kršák¹, Siegfried Trattnig^{1,2}, and Wolfgang Bogner¹

¹High Field MR Centre, Department of Biomedical Imaging and Image-guided Therapy, Medical University of Vienna, Vienna, Austria, ²Christian Doppler Laboratory for Clinical Molecular MR Imaging, Medical University of Vienna, Vienna, Austria

We present a method for detecting omega-3 fatty acids (FA) at 7 T by 1H-MR spectroscopy (MRS) using a MEGA-sLASER editing sequence with 12 kHz AFP GOIA-WURST(16,4) pulses for localization. sLASER localization offers reduced sensitivity to B_1 inhomogeneities, lowers pulse power requirements compared to PRESS or STEAM and the localization pulses substantially reduce the 4-compartment effect. The spectra of in vivo measurements at the echo times TE=332 ms, 465.4 ms and 1130 ms show the omega-3 signal very well.

2398

Cerebral Acetate Transport and Utilization in the Rat Brain in vivo using ^1H MRS: Consequences of a revised acetate volume of distribution value

Masoumeh Dehghani M.¹, Bernard Lanz¹, Nicolas Kunz², Pascal mieville³, and Rolf Gruetter^{1,2,4,5}

¹Laboratoire d'imagerie fonctionnelle et métabolique(LIFMET), École Polytechnique Fédérale de Lausanne (EPFL), Lausanne, Switzerland, ²Centre d'imagerie Biomedicale(CIBM), École Polytechnique Fédérale de Lausanne (EPFL), Lausanne, Switzerland, ³Institute of Chemical Sciences and Engineering, École Polytechnique Fédérale de Lausanne (EPFL), Lausanne, Switzerland, ⁴Department of Radiology, University of Lausanne, Lausanne, Switzerland, ⁵Department of Radiology, University of Geneva, Geneva, Switzerland

Metabolic modeling of metabolite ^{13}C turnover curves in brain with ^{13}C -labeled acetate infused as tracer substrate requires prior knowledge of the transport and uptake kinetics of Ace. The aim of this study was to determine the kinetics of transport and utilization for acetate uptake in the rat brain using specific distribution volume of Ace(V_d) in the rat brain. The dependency of estimated CMR_{ace} to distribution volume of Ace in the rat brain highlights the importance about a refined determination of V_d for Ace in brain metabolic studies.

2399

Interleaved measurements of BOLD response and energy metabolism in exercising human calf muscle

Adrianus J. Bakermans¹, Chang Ho Wessel², Paul F.C. Groot¹, Erik S.G. Stroes², and Aart J. Nederveen¹

¹Department of Radiology, Academic Medical Center, Amsterdam, Netherlands, ²Department of Vascular Medicine, Academic Medical Center, Amsterdam, Netherlands

Typically, dynamic MR studies of exercising skeletal muscle are limited to measurements of only one parameter. Obtaining multiple parameters simultaneously during a single experiment would provide more insight into (patho-)physiology. Here, we report on interleaved acquisitions of quantitative T_2^* maps for assessments of the BOLD response, and ^{31}P -MR spectra for measuring phosphocreatine recovery kinetics during an exercise-recovery protocol in healthy subjects and peripheral artery disease (PAD) patients. We demonstrate that with such interleaved acquisitions, it is feasible to dynamically assess both tissue oxygenation as well as muscle energy metabolism in the human calf muscle during a single exercise session.

2400

Artificial intelligence for high-resolution nuclear MRS under inhomogeneous magnetic fields

Qiu Wenqi¹, Wei Zhiliang¹, Ye Qimiao¹, Chen Youhe², Lin Yulan¹, and Chen Zhong¹

¹Department of Electronic Engineering, Xiamen University, Xiamen, China, People's Republic of, ²Department of Mechanical and Electrical Engineering, Xiamen University, Xiamen, China, People's Republic of

High-resolution multi-dimensional nuclear magnetic resonance (NMR) spectroscopy serves as an irreplaceable and versatile tool in various chemical investigations. In this study, a method based on the concept of partial homogeneity is developed to offer two-dimensional (2D) high-resolution NMR spectra under inhomogeneous fields. Oscillating gradients are exerted to encode the high-resolution information, and a field-inhomogeneity correction algorithm based on pattern recognition is designed to recover high-resolution spectra. The proposed method improves performances of 2D NMR spectroscopy under inhomogeneous fields without increasing the experimental duration or significant loss in sensitivity, and thus may open important perspectives for studies of inhomogeneous chemical systems.

2401

2D Relaxometry and Diffusivity of Human Knee Synovial Fluid after ACL-injuries Studied Using HR-MAS NMR

Kaipin Xu¹, Subramaniam Sukumar¹, John Kurhanewicz¹, and Xiaojuan Li¹

¹Radiology, University of California, San Francisco, San Francisco, CA, United States

To better understand the pathological progression of osteoarthritis (OA), techniques based on high resolution magic angle spinning (HR-MAS) NMR spectroscopy are developed for the study of relaxation times (T_1 , T_2 , and $T_{1\text{p}}$) and diffusion coefficient (D) of human knee synovial fluids (SF) harvested from 1 OA and 8 anterior cruciate ligament (ACL) injured patients.

2402

Towards fast and highly localized spectroscopy using miniaturized coils in a 14.1T animal scanner
Marlon Arturo Pérez Rodas^{1,2}, Jörn Engelmann¹, Hellmut Merkle¹, Rolf Pohmann¹, and Klaus Scheffler^{1,3}

¹*Ultra High-field Magnetic Resonance Center, Max Planck Institute for Biological Cybernetics, Tübingen, Germany*, ²*Graduate Training Centre of Neuroscience, IMPRS for Cognitive and Systems Neuroscience, University of Tübingen, Tübingen, Germany*, ³*Department for Biomedical Magnetic Resonance, University of Tübingen, Tübingen, Germany*

The distinction of functional activity between cortical layers in the brain by MRI or MRS requires high spatial and temporal resolution. High spatial resolution can be achieved by increasing the gradient strength or by using the intrinsic volume selectivity of miniature coils, even in conventional animal scanner. In the present work, initial results for highly-localized spectroscopy within seconds are presented, for a phantom metabolite solution and cell cultures in a 14.1T animal scanner using a 2mm-diameter circular coil. The larger signals from the major metabolites in ~1.5µL were detected in 24sec on the phantom solution with an acceptable SNR.

2403

DRESS localized FAST technique at 7T uncovers the relation between mitochondrial capacity and ATP synthase flux in exercising gastrocnemius medialis muscle
Marjeta Tušek Jelenc^{1,2}, Marek Chmelík^{1,2}, Barbara Ukropcová^{3,4}, Wolfgang Bogner^{1,2}, Siegfried Trattnig^{1,2}, Jozef Ukopec⁴, Martin Kršák^{1,2,5}, and Ladislav Valkovič^{1,2,6,7}

¹*High Field MR Centre, Department of Biomedical Imaging and Image-guided Therapy, Medical University of Vienna, Vienna, Austria*, ²*Christian Doppler Laboratory for Clinical Molecular MR Imaging, Vienna, Austria*, ³*Institute of pathophysiology, Faculty of Medicine, Comenius University, Bratislava, Slovakia*, ⁴*Obesity section, Diabetes and Metabolic Disease Laboratory, Institute of Experimental Endocrinology, Slovak Academy of Sciences, Bratislava, Slovakia*, ⁵*Division of Endocrinology and Metabolism, Department of Internal Medicine III, Medical University of Vienna, Vienna, Austria*, ⁶*Department of Imaging Methods, Institute of Measurement Science, Slovak Academy of Sciences, Bratislava, Slovakia*, ⁷*University of Oxford Centre for Clinical Magnetic Resonance Research, University of Oxford, John Radcliffe Hospital, Oxford, United Kingdom*

The aim of the study was to investigate the relation between the maximum oxidative flux (Q_{max}), a valid measure of muscular mitochondrial capacity and ATP synthase flux (F_{ATP}) measured in exercising gastrocnemius medialis muscle in healthy young and elderly subjects. Furthermore, we explored the possibility of direct measurement of both, Q_{max} and F_{ATP_ex} in a single experiment. The dynamic experiment consisted of the acquisition of baseline data during two minutes of rest, six minutes of aerobic plantar flexion exercise (during which a 3.5 minutes long FAST measurement was performed), and six minutes of recovery. Our data showed significant correlation between ATP synthase flux in exercising muscle and maximal oxidative flux.

Traditional Poster

Metabolic Profiling

Exhibition Hall

Wednesday, May 11, 2016: 16:00 - 18:00

2404 Metabolomic characterization of ovarian tumors by ex vivo magnetic resonance spectroscopy
Feng-Hua Ma¹, Jin-Wei Qiang², Guo-Fu Zhang¹, Ya-Min Rao³, Hai-Min Li⁴, and Song-Qi Cai⁴

¹*Department of Radiology, Obstetrics & Gynecology Hospital, Shanghai Medical College, Fudan University, Shanghai, China, People's Republic of China*, ²*Department of Radiology, Jinshan Hospital, Shanghai Medical College, Fudan University, Shanghai, China, People's Republic of China*, ³*Department of Radiology, Obstetrics & Gynecology Hospital, Shanghai Medical College, Fudan University, Shanghai, China, People's Republic of China*, ⁴*Department of Radiology, Jinshan Hospital, Shanghai Medical College, Fudan University, Shanghai, China, People's Republic of China*

Coherent results obtained by *ex vivo* and *in vivo* measurements allow the translation of biomarker findings from studies of tissue specimens (*ex vivo*) to those of patients (*in vivo*), and therefore it is important to establish how well correlated these metabolic profiles are. Such correlation has been evaluated for brain tumors, prostate cancer and cervical cancer, but without comparison of ovarian tumors. In this study we try to investigate the relationship between the Cho/Cr from *in vivo* MRS and the Cho/TSP of *ex vivo* MRS from tissue samples and the potential to bridge molecular and imaging diagnostics.

2405

Neurochemical profiles of the rat forepaw cortex during electrical and laser light stimulations measured with proton MR spectroscopy
Nathalie Just¹, Lydia Wachsmuth¹, Florian Schmid¹, and Cornelius Faber¹

¹*Translational Imaging Centre, University of Münster, Münster, Germany*

Optogenetics is a more and more recognized technique for investigating neuronal populations in the rodent brain. Combined to fMRI (OfMRI), more understanding could be achieved. However, the effects of powerful light on the tissue remain poorly understood. Here, experiments were conducted to investigate the effects of blue laser light on the metabolism of the primary somatosensory cortex.

2406

AAV serotype 9 vector transducing the human alpha-L-iduronidase gene normalizes hippocampal and cerebellar neurochemical profiles in a mouse model of mucopolysaccharidosis type I
Ivan Tkac¹, Igor Nestrasil², R Scott McIvor³, Kelley Kitto⁴, Carolyn A Fairbanks⁴, Karen Kozarsky⁵, Walter C Low⁶, Chester B Whitley², and Lalitha Belur³

¹*Center for Magnetic Resonance Research, University of Minnesota, Minneapolis, MN, United States*, ²*Dept. of Pediatrics, University of Minnesota, Minneapolis, MN, United States*, ³*Department of Biochemistry, University of Minnesota, Minneapolis, MN, United States*, ⁴*Department of Cell Biology and Molecular Medicine, University of Minnesota, Minneapolis, MN, United States*, ⁵*Department of Biochemistry, Molecular Biology and Cell Biology, Northwestern University, Evanston, IL, United States*, ⁶*Department of Biochemistry, Molecular Biology and Cell Biology, Northwestern University, Evanston, IL, United States*

Minneapolis, MN, United States, ³Dept. of Genetics and Cell Biology, University of Minnesota, Minneapolis, MN, United States, ⁴Dept. of Pharmaceutics, University of Minnesota, Minneapolis, MN, United States, ⁵REGENXBIO Inc., Rockville, MD, United States, ⁶Dept. of Surgery, University of Minnesota, Minneapolis, MN, United States

Mucopolysaccharidosis type I (MPS I) is a lysosomal storage disease caused by the deficiency in α -L-iduronidase (IDUA) enzyme which results in lysosomal accumulation of glycosaminoglycans. The purpose of this study was to assess the ability of the adeno-associated virus (AAV) - mediated IDUA gene therapy to prevent the pathological neurochemical changes associated with the MPS I disease. The efficacy of the gene therapy was assessed by *in vivo* ¹H MRS at 9.4T using knockout mice deficient for IDUA, a well-established murine model of MPS I.

2407

Region-specific Neurochemical profile differences in juvenile rat model for ADHD and control strain: a 1H MRS study @ 11.7T
Alireza Abaei¹, Francesca Rizzo², Dinesh K Deelchand³, Anne Subgang¹, Johannes T. Schneider⁴, Andrea G. Ludolph⁵, and Volker Rasche^{1,6}

¹Medical Faculty, Core Facility Small Animal MRI, Ulm University, Ulm, Germany, ²Institute of Anatomy and Cell Biology, University of Ulm, Ulm, Germany, ³University of Minnesota, Minneapolis, MN, United States, ⁴Bruker BioSpin MRI GmbH, Ettlingen, Germany, ⁵Department of Child and Adolescent Psychiatry, University of Ulm, Ulm, Germany, ⁶Department of Internal Medicine II, University Hospital Ulm, Ulm, Germany

Assessment and reliable quantification of brain metabolites is of great interest for diagnosis and monitoring of neurodegenerative psychiatric disorders. Challenging in this context is the required spectral fidelity demanding a combination of rapid data acquisition, optimal frequency and phase correction, and excellent shimming of the volume of interest. In this contribution, an optimized STEAM sequence was combined with image-based shimming and single-shot frequency and phase correction. The method was applied to assessment of the difference between the metabolic profile of spontaneous hypertensive rats and Wistar-Kyoto rats. Statistically significant differences could be quantified in the striatum and the prefrontal cortex.

2408

Biochemical Characteristics in Amyotrophic Lateral Sclerosis Detected by 7T MR Spectroscopy

Nazem Atassi^{1,2}, Maosheng Xu^{3,4}, Christina Triantafyllou⁵, Boris Keil^{2,6}, Christopher Long⁷, Robert Lawson^{1,2}, Paul Cernasov^{1,2}, Elena Ratti^{1,2}, Paganoni Sabrina^{1,2}, Nouha Salibi⁸, Ravi Seethamraju⁹, Bruce Rosen^{2,3}, Merit Cudkowicz^{1,2}, and Eva-Maria Ratai^{2,3}

¹Neurology, Massachusetts General Hospital, Boston, MA, United States, ²A. A. Martinos Center for Biomedical Imaging, Charlestown, MA, United States, ³Radiology, Massachusetts General Hospital, Boston, MA, United States, ⁴Radiology, First Affiliated Hospital of Zhejiang Chinese Medical University, Hangzhou, China, People's Republic of, ⁵Siemens Healthcare, Erlangen, Germany, ⁶Massachusetts General Hospital, Boston, MA, United States, ⁷MIT Sloan Neuroeconomics Lab, Cambridge, MA, United States, ⁸Siemens Healthcare, Auburn, AL, United States, ⁹Siemens Healthcare, Charlestown, MA, United States

The purpose of this study was to quantify brain metabolites in Amyotrophic Lateral Sclerosis (ALS) patients using 7-Tesla MR spectroscopy and investigate how these metabolites correlate with clinical outcomes. Patients with ALS had significantly decreased N-acetylaspartate (NAA), glutamate (Glu) and GABA in the left motor cortex consistent with neuronal injury or loss. NAA/Cr and glutathione/Cr correlated with the revised ALS Functional Rating Scale. Increased pathological reflexes, a clinical marker of upper motor neuron degeneration correlated positively with myo-Inositol/Cr and choline/Cr, and negatively with NAA/Cr. 7T MRS can provide effective biomarkers in ALS patients which correlate well with clinical outcomes.

2409

Investigation of Glucose-phosphates in Skeletal Muscle Biopsies by 1H HR-MAS NMR: Comparison between Active and Sedentary Subjects

Gaëlle Diserens¹, Martina Vermathen², Nicholas T. Broskey³, Chris Boesch¹, Francesca Amati^{1,3}, and Peter Vermathen¹

¹Depts Clinical Research and Radiology, University of Bern, Bern, Switzerland, ²Dept. Chemistry & Biochemistry, University of Bern, Bern, Switzerland, ³Dept. of Physiology, University of Lausanne, Lausanne, Switzerland

The aim of this ¹H HR-MAS NMR study was to investigate biopsies of skeletal muscles comparing athletes, sedentary slim and sedentary obese subjects. ¹H HR-MAS allows the direct assessment of glucose-phosphates contained in skeletal muscle biopsies, as was also previously shown. The current study is the first example for a potential application, demonstrating differences in glucose-phosphates between muscle tissues from athletes and sedentary subjects. The results suggest that quantitative assessment by ¹H HR-MAS NMR of Glc-1P and Glc-6P being key players in energy metabolism may prove important for metabolic studies in biopsies.

2410

Intratumoral Agreement of HR-MAS MR spectroscopic profiles in the Metabolic Characterization of Breast Cancer

Vivian Youngjean Park¹, Dahye Yoon², Ja Seung Koo¹, Eun-Kyung Kim³, Seung Il Kim⁴, Ji Soo Choi¹, Suhkmann Kim⁵, and Min Jung Kim¹

¹Yonsei University College of Medicine, Seoul, Korea, Republic of, ²Department of Chemistry and Chemistry Institute for Functional Materials, Pusan National University, Busan, Korea, Republic of, ³Radiology, Yonsei University College of Medicine, Seoul, Korea, Republic of, ⁴Surgery, Yonsei University College of Medicine, Seoul, Korea, Republic of, ⁵Pusan National University, Busan, Korea, Republic of

We investigated whether intratumoral location and biospecimen type affect the metabolic characterization of breast cancer assessed by HR-MAS MR spectroscopy. This prospective study included 87 tumor tissue samples in 31 patients with invasive breast cancer, obtained from the center and periphery of surgical specimens and preoperatively by CNB. Specimens were assessed with HR-MAS MR spectroscopy. Overall, intratumoral location and biospecimen type had limited influence on the metabolic characterization of breast cancer assessed by HR-MAS MR spectroscopy. However, some metabolites are differentially expressed and caution is recommended in clinical decision-making based solely on metabolite concentrations, especially PC and PE.



Proton MR Metabolic Profiling in combination with serum procalcitonin levels as rapid indicators for differentiation of Urosepsis
Suruchi Singh¹, Tanushri Chatterji², Manodeep Sen², Ishwar Ram³, and Raja Roy¹

¹Centre of Biomedical Research, Lucknow, India, ²Department of Microbiology, Dr Ram Manohar Lohia Institute of Medical Sciences, Lucknow, India, ³Department of Urology, Dr Ram Manohar Lohia Institute of Medical Sciences, Lucknow, India

This study is a new approach for the diagnosis of Urosepsis using Proton MR spectroscopy along with serum procalcitonin levels. The study insights, NMR based metabolic profiling for differentiation of Urosepsis, a medical emergency which requires immediate patient care. The analysis takes less than one hour for disease identification, thus enabling quick and efficient patient management. The Principal Component Analysis (PCA) displayed that glucose and lactate in serum were the major confounders in differentiating Urosepsis cases from Healthy controls. The training set of Partial least square Discriminant analysis (PLS-DA) provided precise prediction of the test set in serum samples.

Chemosensory analysis of medicinal plants by NMR phytometabolomics
Rama Jayasundar¹ and Somenath Ghatak¹

¹NMR, All India Institute of Medical Sciences, New Delhi, India

There is increasing interest in systems approach in healthcare, from clinical medicine, diet and nutrition, pharmacology to plant-based drug development. The potential of NMR to study medicinal plants as a whole to evaluate system parameters such as organoleptic properties have been explored in detail in this study. Since taste is a chemosensory effect, NMR has been used for this analysis of medicinal plants along with Electronic tongue based chemometrics for objective measurement of taste. The results indicate an active role for NMR in chemosensory research.

Magnetic resonance spectroscopy (MRS) of post-traumatic epileptogenesis
Amna Yasmin¹, Olli Gröhn¹, Asla Pitkänen¹, and Riikka Immonen¹

¹Department of Neurobiology, A.I. Virtanen Institute University of Eastern Finland, Kuopio, Finland

Traumatic brain injury (TBI) is the main cause of mortality and morbidity worldwide. Up to 53 % of TBI patients with penetrating head injuries develop epilepsy in later part of life. Unavailability of biomarkers for epileptogenesis is a major unmet clinical need, and is the greatest obstacle on the way of developing treatment in patients at risk, e.g., after TBI. Objective of this study is to determine metabolic profile in perilesional cortical area in clinically relevant TBI rat model and correlate MRS findings with EEG and histological outcomes in search for biomarkers. Results: Six out of 13 parameters showed changes at some follow point. Findings of long TBI follow up will help to investigate cellular and molecular mechanisms underlying post-traumatic epileptogenesis and identify reliable biomarkers that could serve as therapeutic targets for the development of new antiepileptogenic and antiseizure compound.

Cervicovaginal fluid acetate, a marker for preterm birth in symptomatic pregnant women
Emmanuel Amabebe¹, Steven Reynolds², Victoria Stern¹, Jennifer Parker³, Graham Stafford³, Martyn Paley², and Dilly Anumba¹

¹Academic unit of Reproductive and Developmental Medicine, University of Sheffield, Sheffield, United Kingdom, ²Academic unit of Radiology, University of Sheffield, Sheffield, United Kingdom, ³School of Dentistry, University of Sheffield, Sheffield, United Kingdom

We characterized the metabolite profile of cervicovaginal fluid (CVF) of a cohort of pregnant women presenting with symptoms of preterm labor by both ¹H Magnetic Resonance spectroscopy and spectrophotometric acetate enzyme assay. Acetate normalized integral ($P=0.002$) and spectrophotometry ($P=0.006$) were significantly higher in the women who delivered preterm compared to their term counterparts. Both methods were predictive of PTB <37 weeks (acetate integral: AUC=0.75, spectrophotometry: AUC=0.74). Elevated CVF acetate in women with symptoms of preterm labor appears predictive of preterm delivery. In these women, a clinical assay of acetate in CVF may prove of clinical utility for predicting PTB.

Proton MR Metabolic Profiling in Bodyfluids for differentiation of Meningitis in adults
Tanushri Chatterji¹, Dr. Suruchi Singh², Dr. Manodeep Sen¹, Dr. Ajai Singh³, Prof. Raja Roy², and Dr. J.K Srivastava⁴

¹Microbiology, Dr. Ram Manohar Lohia Institute of Medical Sciences, Lucknow, India, ²Centre of Bio-Medical Research, Lucknow, India,

³Neurology, Dr. Ram Manohar Lohia Institute of Medical Sciences, Lucknow, India, ⁴Amity Institute of Biotechnology, Amity University, Lucknow, India

This study explored diagnostic utility based on the analysis of CSF, serum and urine for differential diagnosis of bacterial (BM) and tubercular meningitis (TBM) in adults using ¹H NMR metabolic profiling. This may render rapid diagnosis of meningitis resulting to the decline of mortality by appropriate and timely treatment regimen. The Discriminant Functional Analysis (DFA) identified acetate, alanine, malonate and choline containing compounds as significant metabolites among case and control. The Orthogonal Signal Correction Principal Component Analysis (OSC-PCA) of significant metabolites clearly differentiated case vs control group in serum and urine samples, while a clear classification could not be obtained for CSF samples.

High Resolution ¹H NMR-based Metabolomics study of Serum in Parkinson's disease
Pawan Kumar¹, Sadhana Kumari¹, Senthil S Kumaran¹, Shefali Chaudhary¹, Vinay Goyal², Madhuri Behari², S N Dwivedi³, Achal

¹Department of NMR and MRI Facility, All India Institute of Medical Sciences, New Delhi, India, ²Department of Neurology, All India Institute of Medical Sciences, New Delhi, India, ³Department of Biostatistics, All India Institute of Medical Sciences, New Delhi, India

We used ¹H NMR technique to investigate the serum samples of 6 patients with Parkinson's disease (PD) and 6 healthy controls (HC) using 700 MHz NMR spectrometer and the data were processed using the Agilent software, Vnmrj2.3A. PLS-DA multivariate analysis was performed to explore biochemical dissimilarities between PD patients and HC using MetaboAnalyst (3.0) software. We observed significantly elevated levels of lactate, glutamate and methyl guanidine PD patients in comparison with HC on t-test, suggesting protein metabolism impairment, mitochondrial dysfunction and oxidative stress in PD patients.

2417

A Proton Magnetic Resonance Study to Investigate Dietary Influences on Blood Plasma of patients with Celiac Disease
Uma Sharma¹, Deepti Upadhyay¹, Govind Makharla², Prasenjit Das³, Siddharth Datta Gupta³, and Naranamangalam R Jagannathan¹

¹Department of NMR and MRI Facility, All India Institute of Medical Sciences, New Delhi, India, ²Department of Gastroenterology and human Nutrition, All India Institute of Medical Sciences, New Delhi, India, ³Department of Pathology, All India Institute of Medical Sciences, New Delhi, India

The present study demonstrated dietary induced variations on the metabolic profile of blood plasma of CeD patients. Increased valine was seen in CeD non-vegetarians compared to CeD vegetarians. Both CeD vegetarians and non-vegetarians showed increased concentrations of gluconeogenic amino acids like alanine and glycine compared to healthy subjects. Increased pyruvate and creatine in CeD vegetarians compared to healthy vegetarians indicates impaired energy supply. Decreased creatinine in CeD vegetarians and non-vegetarians compared to healthy subjects is due to protein malabsorption in CeD. The study illustrates the nutritional status of CeD patients and healthy subjects on the basis of their dietary intake.

2418

NMR-based Metabolomic Study of Serum in Diabetic Retinopathy
Virendra Kumar¹, Tanmoy Bagui², Rashmi Mukherjee², Vertika Rai², Pawan Kumar¹, and Chandan Chakraborty²

¹Department of NMR, All India Institute of Medical Sciences, New Delhi, India, ²School of Medical Science & Technology, Indian Institute of Technology Kharagpur, Kharagpur, India

Diabetic retinopathy (DR), is a major cause of blindness, caused by prolonged diabetes. However, this morbidity is largely preventable and treatable. The progression of DR from prolonged diabetes involves complex metabolic de-regulations. ¹H NMR-based metabolomics of serum have potential to study dysregulation in metabolites of DR patients. Results of the PCA and PLS-DA analysis revealed metabolic differences in DR patients compared to healthy subjects. Using such a study, we may observe the severity of disease based on metabolic fingerprints and it may serve as a platform for screening of molecular targets for a more efficient therapeutic intervention.

2419

Acute Spinal Cord Injury (ASCI) Metabolomics Through 1H-NMR Spectroscopy: Metabolic alterations with time & treatment
Alka Singh¹, Suruchi Singh², Saloni Raj¹, Ravindra Kumar Garg³, Abbas Ali Mahdi⁴, Raja Roy², and Rajeshwar Nath Srivastava¹

¹Orthopaedic Surgery, King George's Medical University, Lucknow, India, ²Centre of Biomedical Research, Lucknow, India, ³Neurology, King George's Medical University, Lucknow, India, ⁴Biochemistry, King George's Medical University, Lucknow, India

It mainly focuses on finding significant metabolites in serum using 1H NMR based spectroscopic methods and to study the variation of concentration of these metabolites during the recovery of the patient ongoing treatment after surgery. Significant metabolites, namely, lactate, glycine, acetone and succinate were identified using statistical methods (ANOVA along with Mann-Whitney U test) and are found to be elevated during the time of injury. The levels gradually decrease as the patient recovers in an average period of six months. This is a prospective case-control preliminary study on recovery of the patient during acute spinal cord injury.

2420

Pathological glutamatergic neurotransmission in Gilles de la Tourette Syndrome

Ahmad Seif Kanaan^{1,2}, Sarah Gerasch², Isabel Garcia-Garcia¹, Leonie Lampe¹, André Pampel¹, Alfred Anwander¹, Jamie Near³, Kirsten Müller-Vahl², and Harald E. Möller¹

¹Max Planck Institute for Human Cognitive and Brain Sciences, Leipzig, Germany, ²Department of Psychiatry, Hannover Medical School, Hannover, Germany, ³Douglas Mental Health University Institute and Department of Psychiatry, McGill University, Montreal, QC, Canada

We hypothesized that glutamatergic signalling is related to pathophysiology of Gilles de la Tourette syndrome (GTS) and investigated glutamatergic metabolism within cortico-striatal regions using 1H-MRS at baseline and during treatment. Absolute metabolite concentrations were calculated with the consideration of voxel compartmentation following frequency and phase drift correction in the time domain. GTS patients exhibited reductions in striatal and thalamic [Glx], which were normalized with treatment and were correlated with clinical severity parameters. Our results implicate glutamatergic metabolism in GTS pathophysiology and indicate a possibly dysfunctional astrocytic-neuronal coupling system, which would have profound effects on the dopaminergic modulation of cortico-striatal input.

2421

7T MRS AND 18F AV45 PET NEURONAL MARKERS IN ELDERLY HIV+ SUBJECTS: EFFECTS OF SEROSTATUS AND COGNITIVE IMPAIRMENT
Mona A Mohamed¹, Peter B Barker¹, Richard L Skolasky², Heidi Vornbrock Roosa³, Yun Zhou¹, Weiguo Ye¹, Noble George¹, James Brasic¹, Dean F Wong¹, and Ned Sacktor³

In this study, 7T MRS and 18F AV45 PET were used to measure brain metabolites and amyloid burden in Elderly HIV subjects. These reliable biomarkers can be used in assessing the relation between normal aging, HIV and the degree of HIV Associated Neurocognitive Disorders (HAND).

Traditional Poster

DWI & MRS in Cancer

Exhibition Hall

Thursday, May 12, 2016: 10:30 - 12:30

2422

Noise-corrected exponential DWI using multi-acquisition MRI facilitates quantitative evaluation of whole-body skeletal tumour burden in patients with metastatic prostate cancer.

Matthew David Blackledge¹, Nina Tunariu^{1,2}, Zaki Ahmed², Julie Hughes², Raquel Perez-Lopez^{1,2}, Dow Mu Koh^{1,2}, David J Collins^{1,2}, and Martin O Leach^{1,2}

¹*CRUK Cancer Imaging Center, Division of Radiotherapy and Imaging, Institute of Cancer Research, London, United Kingdom*, ²*MRI, Royal Marsden Hospital, London, United Kingdom*

We evaluate the potential utility of storing all imaging acquisitions from whole-body diffusion-weighted MRI (WBDWI) studies. This provides the possibility of using weighted least-squares fitting to obtain maps of ADC uncertainty, invaluable to clinicians wishing to report confidence in ADC estimates. Furthermore, we describe for the first time a novel post-processing technique that combines ADC and ADC uncertainty information into a single computed image: noise-corrected exponential WBDWI. We demonstrate that this technique provides excellent contrast between bone metastases and background healthy tissue, but does not suffer from the same T2 shine-through and/or coil sensitivity artefact present in conventional DW-images.

2423

Proton MRS monitoring of Atkins-based dietary therapy in patients with glioma

Peter B Barker^{1,2}, Subechhya Pradhan¹, Yanqin Lin^{1,3}, Karisa C Schreck⁴, Doris D.M. Lin¹, Jaishri Blakeley^{4,5}, and Roy E Strowd^{5,6}

¹*Radiology, Johns Hopkins Univ School of Medicine, Baltimore, MD, United States*, ²*F.M. Kirby Research Center for Functional Brain Imaging, Kennedy Krieger Institute, Baltimore, MD, United States*, ³*Department of Electronic Science, Xiamen University, Xiamen, China, People's Republic of*, ⁴*Neurology, Johns Hopkins Univ School of Medicine, Baltimore, MD, United States*, ⁵*Oncology, Johns Hopkins Univ School of Medicine, Baltimore, MD, United States*, ⁶*Department of Neurology and Internal Medicine, Wake Forest School of Medicine, Winston Salem, NC, United States*

5 patients with high grade glioma were enrolled in an 8-week dietary therapy program based on the modified Atkin's diet. Tumor and contralateral brain metabolism was monitored before and after therapy using proton MRS. Significant reductions in contralateral NAA were observed post treatment, as well as increases in acetone in both lesion and contralateral brain. MRS may be useful for monitoring the efficacy of dietary therapy in patients with malignant glioma.

2424

MR spectroscopy for 2HG detection in mIDH gliomas: Comparison of sensitivity improvement using different refocusing RF pulses with and without outer volume suppression

Sunita B Thakur^{1,2}, Ralph Noeske³, Robert Young⁴, Justin Cross⁵, and Ingo Mellinghoff⁶

¹*Medical Physics, Memorial Sloan Kettering Cancer Center, New York, NY, United States*, ²*Radiology, Memorial Sloan Kettering Cancer Center, New York, NY, United States*, ³*Berlin, Germany*, ⁴*Radiology, New York, NY, United States*, ⁵*Memorial Sloan Kettering Cancer Center, New York, NY, United States*, ⁶*New York, NY, United States*

Isocitrate dehydrogenase IDH mutations in gliomas have ability to produce R-2-hydroxyglutarate (2HG). Directly measuring 2HG using non-invasive MR spectroscopy is an attractive strategy to accurately predict IDH mutation status and provide useful diagnostic and prognostic information. Quantification of 2HG metabolite may have potential advantages to evaluate treatment response in IDH1/2 targeted inhibitor trials. Here we report the optimization of subecho times on GE 3T scanners using phantoms to detect 2HG with the maximum sensitivity. We also evaluated the effect of different refocusing pulses on 2HG sensitivity with and without outer volume suppression (OVS) pulses. Part of these results were also verified with in-vivo data.

2425

Imaging response to 90-yttrium radioembolization with volumetric ADC DWI in patients with metastatic liver cancer

Russell Rockne¹, Syed Rahmanuddin^{1,2}, John J. Park², and Jinha M. Park²

¹*Dept. of Information Sciences/ Mathematical Oncology, Beckman Research Institute City of Hope, Duarte, CA, United States*, ²*Radiology, Helford Clinical Research Hospital | Beckman Research Institute, Duarte, CA, United States*

The purpose of this study is to evaluate changes in tumor volume and mean ADC before and after 90-yttrium (Y90) radioembolization for patients with metastatic liver cancer. Eighteen patients were identified in a retrospective study. Volumetric analysis of lesions before and after therapy showed a consistent increase in ADC ($p < 0.001$), suggesting a decrease in cellularity. Changes in tumor volume measured on post-gadolinium (PG) T1 MRI were not statistically significant. Additional MRIs following Y90 treatment should be analyzed with clinical outcomes to determine whether early changes in ADC following therapy may serve as an early indicator of response.

2426

Distortion-Free bSSFP-based Diffusion MRI: Preliminary Experience using an MRI-Guided Radiotherapy System
Yu Gao^{1,2}, Yingli Yang³, Novena Rangwala¹, and Peng Hu^{1,2}

¹*Radiological Sciences, University of California, Los Angeles, Los Angeles, CA, United States*, ²*Physics and Biology in Medicine, University of California, Los Angeles, Los Angeles, CA, United States*, ³*Radiation Oncology, University of California, Los Angeles, Los Angeles, CA, United States*

DWI is a promising imaging biomarker for tumor response evaluation, and the purpose of this work is to develop a distortion-free DW sequence that is reliable for adaptive treatment planning. ADC accuracy of our proposed diffusion-prepared segmented bSSFP-based sequence against the standard spin-echo single-shot echo-planar-imaging was quantitatively validated on a diffusion phantom. Geometric reliability was confirmed on both phantom and in-vivo experiments. Preliminary patient study on a MRI-Guided radiotherapy system showed high geometric accuracy and promising tumor detection capability. All these demonstrate the feasibility of using the DW-SSFP sequence for longitudinal tumor response evaluation and treatment planning.

2427

Application of High B-Value High-Resolution Diffusion-Weighted Imaging in Differentiating Malignant from Benign Thyroid Nodules
Qingjun Wang¹, Yong Guo¹, Jing Zhang¹, Minghua Huang¹, Qinglei Shi², and Tianyi Qian²

¹*Radiology, Chinese Navy General Hospital, Beijing, China, People's Republic of*, ²*Scientific Marketing, Siemens Healthcare, Beijing, China, People's Republic of*

In this study, we evaluated the advantages of using high b-value high-resolution diffusion-weighted MR imaging (DWI) to differentiate between malignant and benign thyroid nodules. This prospective study included 28 consecutive patients with thyroid nodules (14 malignant nodules in 10 patients and 24 benign nodules in 20 patients). Three b-values including b-values of 0, 800 and 2000 sec/mm² and a Readout Segmentation Of Long Variable Echo-trains (RESOLVE) imaging technique were used in the high b-value high-resolution DWI. The results showed that the high b-value high-resolution DWI can further increase the diagnostic accuracy for thyroid nodules with the best sensitivity, specificity and area under receiver operating characteristic curve (AUC) than low b-value or single high b-value.

2428

Comparison of Capability for Postoperative Recurrence Evaluation in Non-Small Cell Lung Cancer among Whole-Body MRI with and without DWI, MR/PET, PET/CT and Conventional Radiological Examinations

Yoshiharu Ohno^{1,2}, Yuji Kishida², Shinichiro Seki², Hisanobu Koyama², Kota Aoyagi³, Hitoshi Yamagata³, Takeshi Yoshikawa^{1,2}, Masao Yui³, Yoshimori Kassai³, Katsusuke Kyotani⁴, and Kazuro Sugimura²

¹*Advanced Biomedical Imaging Research Center, Kobe University Graduate School of Medicine, Kobe, Japan*, ²*Radiology, Kobe University Graduate School of Medicine, Kobe, Japan*, ³*Toshiba Medical Systems Corporation, Otawara, Japan*, ⁴*Center for Radiology and Radiation Oncology, Kobe University Hospital, Kobe, Japan*

Recurrence assessment is very important for management of postoperative non-small cell lung cancer (NSCLC) patients. We hypothesized that whole-body PET/MRI and MRI with DWI have a potential for improving recurrence assessment as compared with whole-body PET/CT and conventional radiological examinations in NSCLC patients. The purpose of this study was to directly compare the diagnostic performance for postoperative lung cancer recurrence assessment among whole-body PET/MRI, MRI with and without DWI, PET/CT and conventional radiological examination in NSCLC patients.

2429

Heterogeneity of IDH+ glioma metabolism evaluated by CSI

Benjamin C Rowland¹, Min Zhou¹, Huijun Liao¹, Nils Arvold², Raymond Y Huang³, and Alexander P Lin¹

¹*Centre for Clinical Spectroscopy, Brigham and Women's Hospital, Boston, MA, United States*, ²*Radiation Oncology, Brigham and Women's Hospital, Boston, MA, United States*, ³*Radiology, Brigham and Women's Hospital, Boston, MA, United States*

MR spectroscopy is a powerful technique for understanding tumour metabolism. Chemical shift imaging allows spatial variations in spectra to be observed at the cost of signal to noise and acquisition time. In this abstract we examine the heterogeneity of metabolite concentrations in both tumour and healthy tissue, in particular the onco-metabolite 2-hydroxyglutarate, to ascertain if the benefits of CSI outweigh the penalties.

2430

Prediction of Medulloblastoma survival using the Water Proton Resonance Frequency

Ben Babourina-Brooks¹, Sarah Kohe¹, Andrew Peet¹, and Nigel Davies²

¹*University of Birmingham, Birmingham, United Kingdom*, ²*University Hospitals Birmingham, Birmingham, United Kingdom*

The rate of improvement in survival, among children with brain tumours, has decreased in recent years and novel prognostic markers that may contribute to treatment stratification and improved outcomes are required. Medulloblastoma tumours have a high rate of mortality due to their aggressive nature, however some do not. MRS can measure absolute water proton resonance frequency (PRF), which is sensitive to temperature and other features of the tumour microenvironment. This could be utilized as a potential prognosis marker, however has not been explored. This study assessed the water PRF as a predictor of survival in a medulloblastoma patients, using MRS at diagnosis.

2431

In-vitro 1H-MRS of living human melanoma cells at 9.4T

Katarzyna Pierzchala¹, Nicolas Kunz¹, and Rolf Gruetter¹

There is increasing need of a more human cell model to recapitulate the *in-vivo* cell-cell interactions, presenting physiological relevance. Magnetic resonance spectroscopy (MRS) has the potential to diagnose many tumors and to characterize their metastatic potential. In this study we present the metabolic profile of highly metastatic human melanoma cells line WM793. We demonstrate the feasibility of characterizing *in-vitro* living melanoma cells by 1H-MRS with a total number of 9 metabolites quantified, covering energy markers (Glc, Lac, Ace), amino acids (Glu, Ala) and anti-oxidant (Tau, Asc) and cell membrane precursor (Cho).

2432

Characterisation of disease heterogeneity in malignant pleural mesothelioma using mixture modelling of ADC and R2

Lin Cheng¹, Matthew D. Blackledge¹, David J. Collins¹, Nina Tunariu^{1,2}, Neil P. Jerome¹, Matthew R. Orton¹, Veronica A. Morgan³, Martion O. Leach¹, and Dow-Mu Koh^{1,2}

¹Division of Radiotherapy and Imaging, Cancer Research UK Cancer Imaging Centre, Institute of Cancer Research, London, United Kingdom,

²Radiology, Royal Marsden Hospital, London, United Kingdom, ³Clinical MRI Unit, Royal Marsden Hospital, London, United Kingdom

Disease heterogeneity in patients with malignant pleural mesothelioma (MPM) makes it challenging to characterise solid disease and assess response following treatment. Computed Diffusion-Weighted MRI (cDWI) provides improved contrast between disease and background tissues, and facilitates total disease segmentation. A mixture modelling of ADC and R2 with semi-automatic segmentation on the cDWI is proposed to assess disease heterogeneity in MPM, with demonstration of its utility on a paired pre/post-treatment dataset. The mixture modelling methodology successfully characterised disease heterogeneity for two MPM patients, and can provide additional quantitative functional disease response characterisation compared with using only a single parameter.

2433

Apparent diffusion coefficient ratio as a potential inter-institutional marker for histological grade of bladder cancer

Soichiro Yoshida¹, Fumitaka Koga², Hiroshi Tanaka³, Hiroshi Fukushima², Yasukazu Nakanishi², Minato Yokoyama¹, Junichiro Ishioka¹, Kazutaka Saito¹, Yasuhisa Fujii¹, and Kazunori Kihara¹

¹Urology, Tokyo Medical and Dental University Graduate School, Tokyo, Japan, ²Urology, Tokyo Metropolitan Cancer and Infectious diseases Center Komagome Hospital, Tokyo, Japan, ³Radiology, Ochanomizu Surugadai Clinic, Tokyo, Japan

We evaluated standardized apparent diffusion coefficient value (ADC ratio) by taking the ratio of the ADC of the cancer tissue (T-ADC) to that of the gluteus maximus (G-ADC) can be a biomarker for predicting histological grade under two different imaging conditions. Two independent bladder cancer cohorts including 107 and 47 patients were evaluated. There was a significant difference in T-ADC between the cohorts, but no significant difference in the ADC ratio was observed. The ADC ratio significantly correlated with grade, as was the T-ADC. The ADC ratio might serve as an inter-institutional biomarker for predicting histological grade of bladder cancer.

Traditional Poster

Tumour Response to Therapy

Exhibition Hall

Thursday, May 12, 2016: 10:30 - 12:30

2434

GluCEST MRI: A Biomarker for Glutamine Metabolism in Cancer

Rong Zhou¹, Puneet Bagga¹, Kavindra Nath¹, David Mankoff¹, Hari Hariharan¹, and Ravinder Reddy¹

¹Radiology, University of Pennsylvania, Philadelphia, PA, United States

We presented the very first evaluation of glutamate chemical exchange saturation transfer (GluCEST) MRI to detect pharmacodynamic effect of small molecule drugs that target cancer glutaminolysis pathway. Conversion of glutamine to glutamate is a rate limiting step along this pathway. Inhibition of this conversion leads to reduction of cellular glutamate concentration that can be detected by GluCEST *in vivo* and confirmed by ex vivo high resolution 1H MRS of tumor homogenates.

2435

Use of iron contrast agents to detect brain tumor treatment response based on stimulating the innate immune system

Yang Runze^{1,2}, Susobhan Sarkar², Daniel J Korchinski¹, Ying Wu¹, V Wee Yong^{2,3}, and Jeff F. Dunn^{1,2}

¹Radiology, University of Calgary, Calgary, AB, Canada, ²Clinical Neuroscience, University of Calgary, Calgary, AB, Canada, ³Oncology, University of Calgary, Calgary, AB, Canada

Glioblastoma Multiforme (GBM) is the most aggressive brain cancer with an abysmal prognosis. It has been shown that monocytes can be activated to suppress GBM stem cells using Amphotericin B (Amp B). We propose that monocytes can be labeled using intravenous injection of ultra-small iron oxide nanoparticles (USPIO), which will allow us to detect a rapid treatment response. We showed that Amp B treated animals significantly decreased T2* compared to vehicles, showing the presence of USPIO within the tumor. This shows that USPIO can be an effective tool to monitor cancer therapies that stimulate innate immunity.

2436

Diffusion weighted magnetic resonance imaging as an early predictor of survival in patients with liver-dominant metastatic colorectal cancer following 90-Yttrium-microsphere radioembolization

Frederic Carsten Schmeel¹, Birgit Simon¹, Julian Alexander Luetkens¹, Frank Träber¹, Leonard Christopher Schmeel¹, Hans Heinz Schild¹,

Imaging-based response assessment to local interventional therapies is essential for further therapy decisions in patients with advanced malignancies. Therefore, we investigated whether early post-therapeutic changes in diffusion-weighted MRI using quantifications of the apparent diffusion coefficient (ADC) could predict the outcome of patients with liver-dominant metastatic colorectal cancer after radioembolization with 90-Yttrium microspheres (RE). Uni- and multivariate survival analyses were performed comparing various variables with potential impact on overall survival. Our results reveal that an increase in the post-therapeutic minimal ADC remained the strongest and only independent predictor of overall survival shortly after radioembolization.

2437

Quality Assurance Methodology for Multicenter Clinical Trials using MRI – Experiences from the NCI National Clinical Trial Network (NCTN) Imaging and Radiation Oncology Core (IROC) Service

Preethi Subramanian¹, Jun Zhang², Shivangi Vora², Marc Gollub³, Deborah Schrag⁴, Xiangyu Yang⁵, Lawrence Schwartz⁶, and Michael V Knopp⁷

¹Radiology, The Ohio State University, Columbus, OH, United States, ²Radiology, The Ohio State University, Columbus, OH, United States,

³Radiology, Memorial Sloan Kettering Cancer Center, New York, NY, United States, ⁴Dana Farber Cancer Institute, Boston, MA, United States, ⁵The Ohio State University, Columbus, OH, United States, ⁶Radiology, Columbia University, New York, NY, United States, ⁷Radiology - Wright Center of Innovation, The Ohio State University, Columbus, OH, United States

Quality Assurance Methodology for Multicenter Clinical Trials using MRI

2438

Early detection of photoimmunotherapy-induced tumor cell death with hyperpolarized [1,4-13C2]fumarate

Shun Kishimoto¹, Jeeva Munasinghe², Marcelino Bernardo¹, Hellmut Merkle³, Keita Saito¹, James B Mitchell¹, Jan Henrik Ardenkjær-Larsen⁴, Peter L Choyke¹, and Murali Cherukuri¹

¹NCI, Bethesda, MD, United States, ²NINDS, Bethesda, MD, United States, ³LFMI, Bethesda, MD, United States, ⁴GE Health Care, Brondby, Denmark

Photoimmunotherapy (PIT) is a novel therapy for cancer treatment. PIT combines a targeted antibody with the photon absorber, IR700, which, after exposure to near infrared (NIR) light induces highly selective tumor necrosis with almost no side effects to normal adjacent tissue. PIT is now in Phase I clinical trials in head and neck cancers. Although NIR PIT can be highly effective, the size of the lesion does not immediately change and it may take several weeks for the tumor to completely respond anatomically. Thus, detecting early therapeutic response in the absence of anatomic change is of interest. Here, we demonstrate the effects of NIR PIT on 13C magnetic resonance spectroscopy (MRS) in an animal model (EGFR positive A431 tumor) using 13C labeled hyperpolarized (HP) pyruvate and fumarate. Interestingly, the lactate-to-pyruvate ratio was almost unchanged, while the malate-to-fumarate ratio showed a significant difference in PIT treated tumors. This is explained by the difference of the bio distribution of these tracers. Hyperpolarized 13C labeled fumarate MRS is a promising method for detecting early PIT mediated cell necrosis.

2439

Characterization of HPV positive oropharyngeal tumors using intravoxel incoherent motion DW-MRI before and during radiation therapy

Ramesh Paudyal¹, Praveen Venigalla², Jingao Li^{2,3}, Nadeem Riaz², Jung Oh Hun¹, David Aramburu Nuñez¹, Vaois Haztglo⁴, Yonggang Lu⁵, Joseph O Deasy¹, Nancy Lee², and Amita Shukla-Dave¹

¹Medical Physics, Memorial Sloan Kettering Cancer Center, New York, NY, United States, ²Radiation Oncology, Memorial Sloan Kettering Cancer Center, New York, NY, United States, ³Radiation Oncology, Jiangxi Cancer Hospital, Nanchang, China, People's Republic of, ⁴Radiology, Memorial Sloan Kettering Cancer, New York, NY, United States, ⁵Radiation Oncology, Washington University, St Louis, MO, United States

This study aims to characterize human papillomavirus (HPV) positive (+) oropharyngeal cancer (OPC) using intravoxel incoherent motion (IVIM) DW-MRI performed before and during chemo-radiation therapy. A consensus clustering algorithm based on the hierarchical clustering and Pearson correlation distance was performed using the weekly IVIM DW-MRI metrics of D, f and D*, total tumor volume and delivered radiation dose. It demonstrated the presence of two HPV+ clusters. A trend towards significant increase in D during the pre- and intra-treatment (week 3) IVIM DW-MR data suggested that patients in cluster 2 may benefit with use of less aggressive therapy.

2440

Treatment response assessment of malignant cancer cells to alpha-lipoic acid and a 213Bi-anti-EGFR-MAb with hyperpolarized [1-13C]-pyruvate

Benedikt Feuerecker¹, Christian Hundhammer¹, Christof Seidl², Alfred Morgenstern³, Frank Bruchertseifer³, Reingard Senekowitsch-Schmidtke¹, and Markus Schwaiger¹

¹Department of Nuclear Medicine, Technische Universität München, Munich, Germany, ²Department of Obstetrics and Gynaecology, Technische Universität München, Munich, Germany, ³European Commission Joint Research Centre Institute for Transuranium Elements, Karlsruhe, Germany

In the light of up regulation of glycolysis in tumors of the Warburg type, hyperpolarized ¹³C-labeled metabolic tracers offer new possibilities to probe fast metabolic pathways in real-time. As such, we assessed therapy response of malignant cancer cells to alpha-lipoic acid and a ²¹³Bi-anti-EGFR-MAb with hyperpolarized [1-¹³C]-pyruvate. Our results point to the fact that treatment of LN18 glioblastoma cells with LPA resulted in decreased proliferation/viability and reduced lactate export. Beyond, we demonstrated that NMR of hyperpolarized [1-¹³C]-pyruvate proved to be adequate for monitoring the response of bladder carcinoma cells to treatment with a ²¹³Bi-anti-EGFR-MAb as indicated by elevated pyruvate turnover.

2441

Quantification of transverse relaxation time changes in rectal tissue during fixation at ultra-high field MRI
Quincy van Houtum¹, Dennis D.W.J. Klomp¹, and Marielle M.E.P. Philippens¹

¹Imaging, UMC Utrecht, Utrecht, Netherlands

In this study we investigate the transverse relaxation effects at 7T during the fixation process in rectal specimens as a preparation for 7T MRI validation of rectal tumor regression with pathology. T2 and T2* were measured every 2 hours during fixation process in six different pig recta. Images allowed mapping of relaxation time at high spatial resolution. The circular muscle showed a decrease of 25% in T2* whilst other tissues remained constant over time for both parameters. A T2* decrease of 25% is seen in the circular muscle of the rectal wall was noticed whilst other tissue-regions remained constant. High resolution and SNR allowed for anatomical delineation and measuring the change of transverse relaxation times.

2442

MRI biomarkers for pancreatic ductal adenocarcinoma
Navid Farr¹, Paolo Provenzano², Joshua Park³, Sunil Hingorani², and Donghoon Lee³

¹Department of Bioengineering, University of Washington, Seattle, WA, United States, ²Fred Hutchinson Cancer Research Center, Seattle, WA, United States, ³Department of Radiology, University of Washington, Seattle, WA, United States

Pancreatic cancer is a devastating disease with poor prognosis. Pancreatic tumor therapy has been ineffective in part because pancreatic tumors have a dense stroma inhibiting penetration of chemotherapeutic drugs into the tumor. We performed multi-parametric MRI at high resolution to noninvasively assess tumor progression and responses to effective treatment. We used T1 and T2 relaxation, diffusion, magnetization transfer effects along with 3 dimensional volume measurements to characterize the tumors. MR measurements were then compared with histopathological results.

2443

Can Diffusion Weighted MRI Assess Early Response of Lymphadenopathy to Induction Chemotherapy in Nasopharyngeal Cancer: A Heterogeneity Analysis Approach
Manijeh Beigi¹, Anahita Fathi Kazerooni¹, Mojtaba Safari¹, Marzieh Alamolhoda², Ahmad Ameri³, Shiva Moghdam⁴, Mohsen Shojaee Moghdam⁵, and Hamidreza Saligheh Rad¹

¹Medical Physics and Biomedical Engineering, School of Medicine, Quantitative MR Imaging and Spectroscopy Group, Research Center for Cellular and Molecular Imaging, Institute for Advanced Medical Imaging, Tehran, Iran, ²Statistics, Shiraz University of Medical Science, Shiraz, Iran, ³Oncology, Shahid Beheshti University of Medical Science, Tehran, Iran, ⁴Oncology, Tehran, Iran, ⁵Payambaran Imaging Center, Tehran, Iran

Induction chemotherapy is an effective way to control subclinical metastasis in locally-advanced nasopharyngeal cancer patients. Diffusion-weighted MRI is a noninvasive imaging technique allowing some degree of tissue characterization by showing and quantifying molecular diffusion. Histogram analysis on ADC map could be carried out to reveal physiological alterations early after IC. For this purpose, several quantitative metrics from ADC-map were explored to obtain the most accurate feature(s) as potential predictive biomarker for early response of the lymphnode to IC. If the outcome can be predicted at an early stage of the treatment, the patient could be spared from unnecessary treatment toxicity.

2444

Multiparameter MRI Response Assessment in a Phase I Trial of Hypofractionated Stereotactic Irradiation with Pembrolizumab and Bevacizumab in Patients with Recurrent High Grade Gliomas
Olya Stringfield¹, John Arrington², Solmaz Sahebjam³, and Natarajan Raghunand¹

¹Cancer Imaging & Metabolism, Moffitt Cancer Center, Tampa, FL, United States, ²Radiology, Moffitt Cancer Center, Tampa, FL, United States, ³Neuro-Oncology, Moffitt Cancer Center, Tampa, FL, United States

In this ongoing phase 1 study, we are investigating combined pembrolizumab and bevacizumab therapy with hypofractionated radiotherapy in recurrent glioma. The objective of this work is to develop a non-invasive response assessment measure using multiparameter MRI (mpMRI) scans acquired as part of clinical care which may precede volumetric changes in response to therapy.

2445

Integrated Positron Emission Tomography/ Magnetic Resonance Imaging in the Treatment of Cervical Cancer: Preliminary Results
Sharmili Roy¹, Dennis Lai-Hong Cheong¹, Mary C. Stephenson¹, Trina Kok¹, Evelyn Laurens¹, Joshua D. Schaefferkoetter¹, John James Totman¹, Vicky Koh², Johann Tang², Joseph Ng², Jeffrey Low², and Bok Ai Choo²

¹A*Star-NUS Clinical Imaging Research Centre, Singapore, Singapore, ²National University Health System, Singapore, Singapore

Response assessment after radical radiation therapy (RT) is typically performed months post treatment completion due to confounding acute RT effects. This study presents feasibility and early results on the ability of PET/MRI in visualizing early tumor changes in the cervix even during RT. This could potentially provide actionable information for treatment modifications prior to the completion of standard of care.

2446

Prostate Cancer: DCE-MRI parameter changes during radiotherapy
Lucy Elizabeth Kershaw^{1,2}, Andrew McPartlin^{2,3}, Ben Taylor⁴, Ananya Choudhury^{2,3}, and Marcel van Herk²

¹CMPE, The Christie NHSFT, Manchester, United Kingdom, ²Manchester Academic Health Sciences Centre, The University of Manchester,

In this pilot work, our aim was to measure plasma flow (F_p) and permeability-surface area product (PS) through the course of RT in prostate tumour and normal tissue to determine whether significant changes could be detected early in treatment. We detected significant increases in F_p and PS during radiotherapy in this small patient group.

2447

The feasibility of performing intravoxel incoherent motion MRI for esophageal cancer and an initial comparison with dynamic contrast-enhanced MRI

Sophie E. Heethuis¹, Lucas Goense^{1,2}, Peter S.N. van Rossum^{1,2}, Irene M. Lips¹, Richard van Hillegersberg², Jelle P. Ruurda², Marco van Vulpen¹, Gert J. Meijer¹, Jan J.W. Lagendijk¹, and Astrid L.H.M.W. van Lier¹

¹Department of Radiotherapy, UMC Utrecht, Utrecht, Netherlands, ²Department of Surgery, UMC Utrecht, Utrecht, Netherlands

The aim of this study was to investigate whether intravoxel incoherent motion (IVIM) MRI could be a non-invasive alternative for dynamic contrast-enhanced (DCE) MRI for response prediction in patients with esophageal cancer. The feasibility of IVIM was researched, followed by a first comparison with DCE-MRI. It was found that non-rigid registration improved the fitting of the IVIM parameters significantly. Comparison of IVIM and DCE-MRI suggested an inverse relation between perfusion fraction and area-under-the-concentration curve (AUC).

2448

Restriction Spectrum Imaging based tumor cellularity performs better than ADC in patients newly diagnosed with Glioblastoma Multiforme

AnithaPriya Krishnan¹, Carrie R. McDonald¹, Nikdokht Farid², Anders M. Dale^{1,3}, and Nathan S. White^{1,3}

¹MMIL, Radiology, University of San Diego, La Jolla, CA, United States, ²Division of Neuroradiology, University of San Diego, La Jolla, CA, United States, ³Center for Translational Imaging and Precision Medicine, University of San Diego, La Jolla, CA, United States

Contrast enhancing (CE) volumes are unreliable in the pseudo-progression window post radiotherapy and ADC based estimate of tumor cellularity is significantly affected by edema. Here, we provide preliminary evidence that Restriction Spectrum Imaging (RSI) based tumor cellularity performs better than ADC, supplements structural volumes and is significantly predictive of overall survival (OS). The study also highlights the need for higher b values as the association of ADC (in CE) with outcomes was observed only when high b values were used for ADC estimation and with b=1500s/mm², ADC in edema ROI was not independent of edema volume ($r=0.7$)

2449

High resolution imaging of ex-vivo humane pancreas specimen at high field MRI

Quincy van Houtum¹, Marielle M.E.P. Philippens¹, Maarten M.S. van Leeuwen², Frank F.J. Wessels², and Dennis D.W.J. Klomp¹

¹Imaging, UMC Utrecht, Utrecht, Netherlands, ²Radiology, UMC Utrecht, Utrecht, Netherlands

The aim of this study is to demonstrate high resolution MR imaging of ex vivo pancreas-specimen while maintaining the in vivo shape and orientation. A pancreaticoduodenal specimen was positioned inside a 3T MRI while maintaining in vivo shape and orientation using substitutes for anatomical features. A 3D TSE sequence with a spatial resolution of 0.45x0.45x2mm, was used for acquisition. Images showed contrast between multiple anatomical structures, allowed for discrimination between tumor and healthy tissue and showed an underestimation of tumor size on CT. Image quality holds promise for improved guidance during PA and registration with in vivo MRI.

2450

Hormonal effect on time-dependent diffusion of the breast fibroglandular tissue

Sungheon Gene Kim^{1,2}, Eric Sigmund^{1,2}, Melanie Moccaldi^{1,2}, Thorsten Feiweier³, and Linda Moy^{1,2}

¹Center for Advanced Imaging Innovation and Research, Radiology, New York University School of Medicine, New York, NY, United States,

²Bernard and Irene Schwartz Center for Biomedical Imaging, Radiology, New York University School of Medicine, New York, NY, United States,

³Siemens Healthcare GmbH, Erlangen, Germany

This study is to investigate the potential of the surface-to-volume ratio obtained from multiple diffusion times to measure mammary duct microstructural changes induced by hormonal variation. Seven premenopausal women were scanned twice using a stimulated-echo diffusion sequence; one in the follicular phase of the menstrual cycle and again in the luteal phase. In 6 out of 7 subjects, the surface-to-volume ratio measured with 69 and 173 ms was significantly reduced in the luteal phase compared to the follicular phase. The length scales obtained in our study are consistent with the duct diameters reported in previous ex-vivo studies.

Traditional Poster

Clinical MRI of Solid Tumour

Exhibition Hall

Thursday, May 12, 2016: 10:30 - 12:30

2451

Quantitative Evaluation of the Effect of Bone on Pelvic Lesion Uptake for MR-based Attenuation Correction on an Integrated Time-of-Flight PET/MRI System

Andrew Leynes¹, Jaewon Yang¹, Dattesh Shanbhag², Sandeep Kaushik², Florian Wiesinger³, Youngho Seo¹, Thomas Hope¹, and Peder Larson¹

The current clinical standard for extracranial MR-based attenuation correction (MRAC) on hybrid PET/MRI systems is the use of a Dixon-type sequence to generate a continuous-value fat-water map. The exclusion of bone in Dixon MRAC contributes a clinically significant amount of underestimation in bone lesion uptake. Bone information from a zero echo-time (ZTE) MRI pulse sequence is combined with the Dixon MRAC to produce a hybrid ZTE-Dixon MRAC. The work demonstrates, using PET/MRI patient data, that the Dixon MRAC (neglecting bone) is underestimating bone lesion uptake by a clinically significant amount (>10%) when compared to the hybrid MRAC (including bone).

2452

Multivariate assessment of brain glioma using hybrid IVIM and DK MRI
Ya-Fang Chen¹, Hsiang-Kuang Liang², and Wen-Chau Wu^{3,4}

¹Medical Imaging, National Taiwan University Hospital, Taipei, Taiwan, ²Radiation Oncology, National Taiwan University Hospital, Taipei, Taiwan, ³Graduate Institute of Oncology, National Taiwan University, Taipei, Taiwan, ⁴Clinical Medicine, National Taiwan University, Taipei, Taiwan

In the present study, we investigated the feasibility of hybrid intravoxel incoherent motion and diffusion kurtosis MR imaging in assessing brain gliomas. Our data showed that combined intravascular fraction (a surrogate measure of cerebral blood volume), diffusion coefficient (a measure of diffusivity), and diffusion kurtosis coefficient (a measure of diffusion heterogeneity) may better demarcate brain gliomas through exploration of multiple pathophysiological aspects.

2453

Comparison of HCC Tumor-Size measured in MRI and Histopathology – Does the Sequence matter?
Marco Armbruster¹, Dominik Nörenberg¹, Katharina Hoffmann², Joachim Andrassy², and Harald Kramer¹

¹Department of Clinical Radiology, Ludwig-Maximilian-University Munich, Munich, Germany, ²Department of Visceral Surgery, Ludwig-Maximilian-University Munich, Munich, Germany

Size measurements of hepatocellular carcinoma lesions play an important role in treatment algorithms of this disease, however little is known about which MRI sequence has the highest accuracy. This study shows, that there is a significant variance in size assessment of different MRI sequences and phases, while the hepatobiliary-phase seems to be best correlated to histopathologic measurements as the standard of reference and delineates HCC lesions most sharply.

2454

Fractional Enhancement metric improves SNR and visualisation of quantitative two-point contrast-enhanced MRI in retroperitoneal sarcoma
Matthew David Blackledge¹, Christina Messiou^{1,2}, Jessica M Winfield^{1,2}, Dow Mu Koh^{1,2}, David J Collins^{1,2}, and Martin O Leach^{1,2}

¹CRUK Cancer Imaging Center, Division of Radiotherapy and Imaging, Institute of Cancer Research, London, United Kingdom, ²MRI, Royal Marsden Hospital, London, United Kingdom

We compare two enhancement fraction parameters that may be used for quantification of two-point contrast-enhanced MRI studies: The relative enhancement and the fractional enhancement. Using computer simulations we show that fractional enhancement is better behaved in the presence of imaging noise, resulting in better SNR for this parameter over a range of intrinsic longitudinal tissue relaxivities and contrast medium concentrations. Further, in a cohort of 25 patients with retroperitoneal sarcoma, fractional enhancement significantly outperformed the relative enhancement in terms of visual assessment of contrast-to-noise, signal-to-noise, tumour detection, imaging artefacts and within tumour contrast.

2455

Assessing Myeloma Focal Lesion Conspicuity on Dixon Images
Timothy James Pengilley Bray¹, Saurabh Singh¹, Arash Latifoltojar¹, Kannan Rajesparan¹, Farzana Rahman¹, Alan Bainbridge², Shonit Punwani¹, and Margaret A Hall-Craggs¹

¹Centre for Medical Imaging, University College London, London, United Kingdom, ²Medical Physics, University College London, London, United Kingdom

Dixon imaging is becoming more widely used in multiple myeloma (MM) and can provide both functional and anatomical information. We observed that myeloma lesions seemed more conspicuous on fat only (FO) images than on conventional in-phase T1, and therefore hypothesised that lesion detection rates would be higher on FO images. In this research, we show that reader sensitivity, positive predictive value and confidence are indeed higher on FO images. This may be because myeloma lesions cause a proportionately greater change in fat content than in water content. We suggest that Dixon imaging should be used in preference to T1 imaging alone when performing WB-MRI.

2456

Proton Magnetic Resonance Spectroscopy (1-H MRS) of Sputum and Exhaled Breath Condensate: A Non-invasive Tool for Lung Cancer Screening
Naseer Ahmed¹, Tedros Bezabeh^{2,3}, Renelle Myers⁴, Omkar B Ijare³, Shantanu Banerji¹, Reem Alomran¹, Zoann Nugent¹, and Zoheir Bshouty⁴

¹CancerCare Manitoba, Winnipeg, MB, Canada, ²Chemistry, University of Guam, Mangilao, Guam, ³Chemistry, University of Winnipeg, Winnipeg,

We undertook this study to determine if ¹H Magnetic Resonance Spectroscopy (MRS) can provide an alternate tool for the screening of lung cancer. Metabolic profiles of sputum and exhaled breath condensate (EBC) samples were obtained from 15 patients (cancer, n=8 and control, n=7) using a Bruker Avance 400 MHz NMR spectrometer. Methanol was detected at a significantly lower concentration in the EBC samples ($p<0.05$). Absence of glucose and lower concentration of glycoprotein ($p<0.05$) were observed in the sputum samples of the cancer patients. MRS may serve as a screening tool for lung cancer in high-risk patients but this requires validation in a larger study.

2457

Quantifying Pathologies and Improving Tractography in Brain Tumor Using Diffusion Basis Spectrum Imaging
Peng Sun¹, Kim J. Griffin¹, Hung-Wen Kao^{2,3}, Chien-Yuan Eddy Lin^{4,5}, Ching-Po Lin^{3,6}, and Sheng-Kwei Song¹

¹Radiology, Washington University in St. Louis, St. Louis, MO, United States, ²Department of Radiology, Tri-Service General Hospital, National Defense Medical Center, Taipei, Taiwan, ³Biomedical Imaging and Radiological Sciences, National Yang-Ming University, Taipei, Taiwan, ⁴GE Healthcare, Taipei, Taiwan, ⁵GE Healthcare MR Research China, Beijing, China, People's Republic of, ⁶Institute of Neuroscience, National Yang-Ming University, Taipei, Taiwan

Patients with brain tumors usually exhibit heterogeneous tissue features. Our results suggest DBSI-derived indices can quantify each individual feature. In addition, DBSI-derived tractography can visualize white matter tracts through confounding tumor and peritumoral edema.

2458

Software development for evaluating hepatic heterogeneity and its application in hepatocellular carcinoma
Tae-Hoon Kim¹, Chang-Won Jeong¹, Jong-Hyun Ryu¹, Hong-Young Jun¹, Dong-Woon Heo¹, Sung-Chan Kang¹, and Kwon-Ha Yoon^{1,2}

¹Imaging science-based research center, Wonkwang University School of Medicine, Iksan, Korea, Republic of, ²Radiology, Wonkwang University Hospital, Wonkwang University School of Medicine, Iksan, Korea, Republic of

In this paper, we developed the quantification software for evaluating the voxel-based cellular heterogeneity of gadoxetic acid-enhanced magnetic resonance imaging (MRI) in the liver. Our software is clinically applied to accurately quantify and interpret the alterations of liver functions in patients with hepatocellular carcinoma.

2459

Statistical Clustering of Parametric Maps from Quantitative Dynamic Contrast Enhanced MRI and an Associated Decision Tree Model for Non-Invasive Tumor Grading of Solid Clear Cell Renal Cell Carcinoma
Yin Xi¹, Qing Yuan¹, Yue Zhang¹, Ananth Madhuranthakam^{1,2}, Jeffrey Cadeddu³, Vitaly Margulis³, James Brugarolas^{4,5}, Payal Kapur^{3,6}, and Ivan Pedrosa^{1,2}

¹Radiology, UTSouthwestern Medical Center, Dallas, TX, United States, ²Advanced Imaging Research Center, UTSouthwestern Medical Center, Dallas, TX, United States, ³Urology, UTSouthwestern Medical Center, Dallas, TX, United States, ⁴Internal Medicine, UTSouthwestern Medical Center, Dallas, TX, United States, ⁵Developmental Biology, UTSouthwestern Medical Center, Dallas, TX, United States, ⁶Pathology, UTSouthwestern Medical Center, Dallas, TX, United States

We propose a method that provides a simplified visual representation of tumor vascular heterogeneity in clear cell renal cell carcinoma (ccRCC) based on the combination of multiple parametric maps from quantitative dynamic contrast-enhanced (DCE) MRI analysis. Using this approach we observed an association between the tumor grade and vascular heterogeneity, especially in medium size tumors. A decision tree model was developed to predict high grade and low grade histology in solid ccRCCs, which may help in management decisions by providing additional information about the tumor biology beyond tumor size.

2460

Validation of Interstitial Volume Fraction Quantification Performed with Dynamic Contrast-Enhanced Magnetic Resonance Imaging in Skeletal Swine Muscle
Stefan Hindel¹, Anika Söhner¹, Marc Maaß², and Lutz Lüdemann¹

¹University Hospital Essen, Essen, Germany, ²Wesel Protestant Hospital, Wesel, Germany

We assessed the accuracy of interstitial volume fraction v(e) measurements in low-perfused tissue performed using dynamic contrast-enhanced magnetic resonance imaging (DCE-MRI) with a gadolinium-based contrast agent. A 3D gradient echo sequence with k-space-sharing was used to determine v(e) in muscle tissue of twelve pigs. The evaluation was performed with the simple and extended Tofts model and the 2-compartment exchange model using different acquisition durations (ADs). The v(e) values determined by MRI were compared with the histologic analysis of muscle tissue sections. There was good agreement between histology and DCE-MRI modeling but also a strong dependence on AD with the Tofts models.

2461

Quantification of Blood Volume Fraction Using Dynamic Contrast-Enhanced Magnetic Resonance Imaging in Skeletal Swine Muscle
Stefan Hindel¹, Anika Söhner¹, Marc Maaß², and Lutz Lüdemann¹

¹University Hospital Essen, Essen, Germany, ²Wesel Protestant Hospital, Wesel, Germany

We estimated the blood volume fraction in low perfused tissue using dynamic contrast-enhanced magnetic resonance imaging (DCE-MRI). The blood volume fraction v(b) was measured in hind leg muscle of pigs weighing approx. 60 kg. MRI was performed using a 3D gradient echo sequence with k-space-sharing and either a gadolinium-based (gadoterate meglumine) or an intravascular contrast agent (gadofosveset trisodium). Comparison of the different DCE-MRI methods with histology revealed good agreement between histological

2462

A simplified spin and gradient echo (SAGE) DSC-MRI approach for the simultaneous assessment of brain tumor perfusion, permeability, and cellularity
Ashley M Stokes¹, Jack T Skinner², and C. Chad Quarles¹

¹*Department of Imaging Research, Barrow Neurological Institute, Phoenix, AZ, United States*, ²*National Comprehensive Cancer Network, Philadelphia, PA, United States*

Dynamic susceptibility contrast (DSC-MRI) MRI is routinely used for brain tumor imaging and has shown promise as an early biomarker for treatment response. Conventional DSC-MRI is susceptible to contrast agent leakage effects, reducing the reliability of the resulting blood volume maps. The use of a simplified spin and gradient echo (SAGE) sequence, combined with robust processing strategies for correction of leakage effects, could facilitate more rapid clinical translation and adoption of DSC-MRI for brain tumor imaging. Taken together, the simplified SAGE approach and subsequence leakage correction provides a clinically feasible strategy for the simultaneous assessment tumor perfusion, permeability and cellularity.

2463

Robust and Efficient Pharmacokinetic Parameter Estimation: Application to Prostate DCE-MRI

Soudabeh Kargar¹, Eric G Stinson², Eric A Borisch², Adam T Froemming², Akira G Kawashima³, Lance A Mynderse⁴, Joshua D Trzasko², and Stephen J Riederer²

¹*Biomedical Engineering and Physiology, Mayo Graduate School, Rochester, MN, United States*, ²*Radiology, Mayo Clinic, Rochester, MN, United States*, ³*Radiology, Mayo Clinic, Scottsdale, AZ, United States*, ⁴*Urology, Mayo Clinic, Rochester, MN, United States*

The use of MRI for planning targeted biopsy and evaluation of recurrence is becoming more common; in particular, Dynamic Contrast-Enhanced MRI (DCE-MRI) as part of multi-parametric MRI, is used for assessment of tumor angiogenesis and monitoring the effectiveness of therapy. We are interested in accurate estimation of K_{trans} and K_{ep} as an indication of change in perfusion patterns in benign and malignant tissue. We developed a robust and efficient numerical optimization technique to find the (nonlinear) least squares estimates of K_{trans} and K_{ep} from 3D DCE-MRI. The perfusion maps generated with this technique match the Levenberg Marquardt method and DynaCAD.

2464

The Influence of Pre-load Contrast Agent Dosing Schemes on DSC-MRI Data

Natenael B. Semmineh¹, Kelly Gardner¹, Jerrold L. Boxerman², and C. Chad Quarles¹

¹*Imaging Research, Barrow Neurological Institute, Phoenix, AZ, United States*, ²*Diagnostic Imaging, Rhode Island Hospital, Providence, RI, United States*

Brain tumor DSC-MRI studies can be confounded by T_1 and T_2^* effects that occur when the contrast agent extravasates. Traditionally a combination of CA pre-loading and leakage correction techniques are used to minimize T_1 leakage effects, but currently there is no consensus on the most robust dosing scheme. Using simulations we demonstrate that pre-load dosing schemes significantly alter blood volume estimates. This computational approach is being utilized to identify a CA dosing scheme that minimizes total CA dose and yields robust CBV measures across a range of physical, physiological and pulse sequence parameters.

2465

Non-uniform noise correction in dynamic contrast-enhanced MR images reveals superiority of the two compartmental exchange model over the extended Tofts and the adiabatic approximation to the tissue homogeneity models in glioma patients
Georgios Krokos¹, Neil Thacker¹, Ibrahim Djoukhadar¹, David Morris¹, Alan Jackson¹, and Marie-Claude Asselin¹

¹*Medical and Human Sciences, University of Manchester, Manchester, United Kingdom*

Variability in the underlying assumptions and mathematical formulations of the commonly used models for pharmacokinetic analysis of dynamic contrast-enhanced (DCE) MRI data make model selection not straightforward[1]. The variable noise in DCE-MR images affects the precision of parameters such that correcting the chi-square for the non-uniform noise is required for model comparison[2]. After noise correction, the two-compartmental exchange model fitted the data better, particularly in grade IV glioma, compared to the extended Tofts and adiabatic approximation to the tissue homogeneity models. Lengthening the acquisition duration not only provided more precise parameter estimates but also reduced the mathematical correlations between parameters.

2466

Cerebral blood flow measurements correlate well in paediatric brain tumour patients using ASL- and DSC-MRI
Jan Novak^{1,2}, Stephanie Withey^{1,2}, Lesley MacPherson³, and Andrew Peet^{1,2}

¹*Institute of Cancer and Genomic Sciences, University of Birmingham, Birmingham, United Kingdom*, ²*Oncology, Birmingham Children's Hospital, Birmingham, United Kingdom*, ³*Radiology, Birmingham Children's Hospital, Birmingham, United Kingdom*

Low grade paediatric brain tumours are increasingly being targeted by anti-vasculature therapies. It is therefore of particular interest to assess perfusion in these pathologies. We assessed paediatric tumour perfusion using both arterial spin labelling (ASL) and dynamic susceptibility contrast (DSC) on a 3T Philips Achieva scanner. Blood flow maps were produced for both techniques where good qualitative agreement was found illustrated by strong, significant pixel-by-pixel correlations. We found that tumour blood flow measured by ASL and DSC significantly correlated ($p = 0.714$, $P = 0.047$) suggesting ASL can be used instead of DSC for this measurement.

2467

Automated segmentation of soft tissue sarcoma into distinct pathological regions using diffusion and T2 relaxation
Shu Xing¹, Carolyn R. Freeman², Sungmi Jung³, and Ives R. Levesque^{4,5}

¹Physics, McGill, Montreal, QC, Canada, ²Radiation Oncology, McGill University Health Center, Montreal, Canada, ³Pathology, McGill University Health Center, Montreal, Canada, ⁴Medical Physics Unit, McGill University, Montreal, QC, Canada, ⁵Research Institute, McGill University Health Center, Montreal, QC, Canada

In this work, we propose a novel method to automatically distinguish various pathological tissue types within tumors, in particular soft tissue sarcoma. Pathological tissue signatures within the tumor, including high cellularity, high T₂ content, or necrosis, can be interpreted from the combination of T₂-weighted images, DW-MRI (b=500-1000 s/mm²) and ADC maps. We propose an automated approach that compares the ADC, the T₂, and a quantified surrogate for the high-b-value DW-MRI image, between the tumor and a reference tissue, to segment the tumor. Delineating tumor sub-regions is useful in assessing the overall tumor environment and may inform sub-region-targeted radiation dose-painting.

2468

Proton-Density Fat Fraction measurement: A Viable Quantitative Biomarker for Differentiating Adrenal Adenomas from Nonadenomas
Xiaoyan Meng¹, Xiao Chen¹, Yaqi Shen¹, Zhen Li¹, Xuemei Hu¹, Hui Lin², and Daoyu Hu¹

¹radiology, Tongji hospital, Tongji medical college, Huazhong university of science and technology, Wuhan, Hubei province, China, People's Republic of, ²GE Healthcare, Wuhan, Hubei, China, People's Republic of

The aim of our study was to compare the accuracy of PDFF measurements and conventional IP/OP images for quantifying the fat content of adrenal gland nodules and for distinguishing adenomas from nonadenomas. Our results showed that PDFF imaging provided almost accuracy compared with IP/OP imaging. PDFF could be a simpler diagnostic tool for discriminating adenomas from nonadenomas, with a high sensitivity and a relatively high specificity, thus avoiding complicated data calculations. This technique is potentially a helpful and a widely applicable method for diagnosing adrenal gland nodules in clinical studies.

2469

Three-time point method of dynamic contrast-enhanced MRI in discrimination of ACTH-producing and non-functional pituitary adenomas based on whole-tumor quantification
Miaomiao Wang¹, Chao Jin¹, Jianxin Guo¹, Lihong Chen¹, Tingting Qu¹, Hui Hao¹, and Jian Yang¹

¹Department of Radiology, the First Affiliated Hospital of Xi'an Jiaotong University, Xi'an, China, People's Republic of

Quantitative characterizations of functional vascularity of ACTH-producing and non-functioning pituitary adenomas are critical to identify their differences in clinics. From this, a semi-quantitative method, i.e. three-time point method of DCE-MRI was proposed to detail the dynamic enhanced features and thus distinguish them. The results indicate that based on the enhancement time-signal curve, the volume percentage of the two groups are different in the washout-type curve. Particularly, in wash-out phase of the curve, the descending slope of ACTH-producing is greater than that in non-functioning pituitary adenoma.

2470

Amide proton transfer (APT) Imaging in Head and Neck Cancer: preliminary results

Benjamin King Hong Law¹, Ann D King¹, Kunwar S Bhatia¹, Anil T Ahuja¹, Brigitte B Ma², David Ka-Wai Yeung², Yi-Xiang Wang¹, and Jing Yuan³

¹Department of Imaging and Interventional Radiology, The Chinese University of Hong Kong, Shatin, Hong Kong, ²Department of Clinical Oncology, The Chinese University of Hong Kong, Shatin, Hong Kong, ³Medical Physics and Research Department, Hong Kong Sanatorium & Hospital, Happy Valley, Hong Kong

Amide proton transfer (APT) imaging is a promising functional MRI technique that investigates the chemical exchange processes between free water and mobile amide protons in cancers. It is sensitive to small variations in these amide protons but the potential value of APT imaging in head and neck cancer is unknown. We have shown APT imaging of head and neck cancer is feasible, although the success rate varies with tumour site. No difference was found between the APT parameters of undifferentiated nasopharyngeal carcinoma and head and neck squamous cell carcinoma in this small preliminary study, but larger studies are needed.

Traditional Poster

Breast Cancer

Exhibition Hall

Thursday, May 12, 2016: 10:30 - 12:30

2471

Co-registration of pre-biopsy and biopsy MRIs to facilitate lesion localization for MR-guided breast biopsies
Mirabela Rusu¹, Elizabeth A. Morris², Elizabeth J. Sutton², and Ileana Hancu¹

¹GE Global Research, Schenectady, NY, United States, ²Memorial Sloan Kettering Cancer Center, New York, NY, United States

Lesion identification in MR-guided biopsy exams can be hampered by many factors, including large deformations and limited tissue perfusion due to breast compression. Multiple post-contrast scans, image subtraction and maximum intensity projection map generation may be needed to relocate the lesion. This preliminary study suggests that non-rigid registration between the (uncompressed breast) pre-biopsy series and the (compressed breast) biopsy series may facilitate fast and accurate lesion

2472

The test-retest reliability of fat-water ratio MRI derived breast density measurements and automated breast segmentation
Jie Ding¹, Patricia A Thompson², Marilyn T Marron³, Maria Altbach^{3,4}, Denise Roe^{3,5}, Jean-Philippe Galons⁴, Cynthia A Thomson³, Fang Wang⁶, Alison Stopeck⁷, and Chuan Huang^{1,8,9}

¹Biomedical Engineering, Stony Brook University, Stony Brook, NY, United States, ²Pathology, Stony Brook Medicine, Stony Brook, NY, United States, ³Cancer Center, University of Arizona, Tucson, AZ, United States, ⁴Medical Imaging, University of Arizona, Tucson, AZ, United States, ⁵Epidemiology and Biostatistics, University of Arizona, Tucson, AZ, United States, ⁶Stony Brook Medicine, Stony Brook, NY, United States, ⁷Hematology and Oncology, Stony Brook Medicine, Stony Brook, NY, United States, ⁸Radiology, Stony Brook Medicine, Stony Brook, NY, United States, ⁹Psychiatry, Stony Brook Medicine, Stony Brook, NY, United States

It has been shown that breast density (BD) value derived from fat-water-ratio MRI (FWR-MRI) strongly correlates with standard digital mammogram derived BD. The fact that no ionizing radiation is associated with FWR-MRI makes it a lower-risk modality for long term BD monitoring and clinical trials. However, data regarding the individual and group level variability and reliability of this method needs to be established. Conventional approaches for FWR-MRI derived BD rely on manually drawn regions-of-interest. These processes are cumbersome and prone to measurement bias, which may limit the application of FWR-MRI derived BD. Automated breast segmentation has been proposed to resolve this problem and limited results to date are promising. Additional data including an evaluation of BD reliability from manual versus automated measurements is still needed. In this study, we evaluate the test-retest reliability of the FWR-MRI derived BD and the quality of data using manual versus automated breast segmentation. Our results demonstrate the high reliability of the FWR-MRI derived BD measure, Fra80, with a typical error of less than 0.02 for both automated and manual breast segmentation. Moreover, our automated breast segmentation protocol yields more reliable Fra80 BD measures compared to the labor-intensive manual segmentation method.

2473

Dependence of Breast Pharmacokinetic Parameters on pre-contrast T1 and flip angle
Subashini Srinivasan¹, Bruce L Daniel¹, and Brian A Hargreaves¹

¹Radiology, Stanford University, Stanford, CA, United States

Pharmacokinetic (PK) models have been used to estimate physiological parameters such as permeability and dispersion of the contrast agent and is estimated using the acquired signal, pre-contrast T10, and the acquisition flip angle. In this work, we have determined the dependence of the dispersion models' and Tofts models' PK parameters on T10 and B1 maps, as well as the errors introduced by using constant T10 and B1 values in 11 biopsy-proven tumors. Our results show that PK parameters such as kep of Tofts model and kappa of mLDRW dispersion model are less dependent on T10 and B1 and could potentially be used with higher accuracy and precision even when T10 and B1 maps are not acquired.

2474

Estimation of breast tumour tissue diffusion parameters from histological images and Monte-Carlo simulations
David Naves Sousa¹, Filipa Borlinhas¹, and Hugo Alexandre Ferreira¹

¹Institute of Biophysics and Biomedical Engineering, Faculdade de Ciências da Universidade de Lisboa, Lisboa, Portugal

Diffusion-Weighted Imaging is a MRI technique that is able to distinguish between benign and malignant breast tumours via the Apparent Diffusion Coefficient (ADC). Nevertheless, this parameter provides very limited information regarding tissue microstructure. Here, is presented an approach to estimate the intracellular (Di) and extracellular (De) diffusion coefficients, and cell membrane permeability of tumour tissues which makes use of known ADC values, histological images and Monte-Carlo simulations of diffusion processes. Results show that distinct combinations of (Di, De, P) correlate with tumour type, and that a decreased De was observed in malignant tumours in agreement with known extracellular matrix changes.

2475

Magnetic resonance lymphangiography in breast cancer related lymphoedema shows differences between affected and unaffected arms
Marco Borri¹, Maria A. Schmidt¹, Julie C. Hughes¹, Erica D. Scurr¹, Kristiana D. Gordon^{2,3}, Peter S. Mortimer^{2,3}, Dow-Mu Koh¹, and Martin O. Leach¹

¹CR-UK Cancer Imaging Centre, The Royal Marsden NHS Foundation Trust and The Institute of Cancer Research, London, United Kingdom, ²Cardiac and Vascular Sciences, St. George's, University of London, London, United Kingdom, ³Skin Unit, The Royal Marsden NHS Foundation Trust, London, United Kingdom

The pathophysiology of breast cancer related lymphoedema (BCRL) is not well understood, one of the main limiting factors being a lack of information on lymphatic collecting vessels. We have recently proposed a novel contrast-enhanced magnetic resonance lymphangiography protocol which allows the identification of lymphatics via the use of associated contrast uptake curves. In this work we have quantified differences between affected and unaffected arms in a cohort of patients with unilateral BCRL. Our analysis did not detect significant differences in vessel counts between the two sides within different sections of the forearm. However, there was a statistically significant difference in vessel diameter between the two arms; lymphatics within the affected arms presented with a larger diameter.

2476

Reproducibility of quantitative magnetization transfer imaging of the healthy breast at 3T
Lori R. Arlinghaus¹, Richard D. Dortch^{1,2}, Jennifer G. Whisenant², Hakmook Kang³, and Thomas E. Yankeelov^{1,2}

Magnetization transfer (MT) imaging is sensitive to changes in the macromolecular content of tissue and is, therefore, gaining increased attention as a noninvasive approach to probe the complex tumor environment in cancer. The ratio of macromolecular protons to the protons in the free water pool, or pool size ratio (PSR), can be quantified with quantitative MT (qMT) imaging and may be useful for detection of changes in macromolecular content early in the course of treatment. In this study, we explore the repeatability of PSR measurements in healthy breast fibroglandular tissue at 3T to serve as a benchmark for future longitudinal studies of breast cancer treatment.

2477

Amide CEST at 7T: A possible biomarker for response to neoadjuvant chemotherapy in breast cancer
Erwin Krikken¹, Moritz Zaiss², Vitaliy Khlebnikov¹, Hanneke W.M. van Laarhoven³, Dennis W.J. Klomp¹, and Jannie P. Wijnen¹

¹Radiology, University Medical Center Utrecht, Utrecht, Netherlands, ²Deutsches Krebsforschungszentrum, Heidelberg, Germany, ³Medical Oncology, Academic Medical Center Amsterdam, Amsterdam, Netherlands

Neoadjuvant chemotherapy has an important role in the treatment of breast cancer and the need for early detection of treatment response is high. As a non-invasive method able to predict treatment response is lacking, we investigated the feasibility of using amide CEST MRI at 7T as a biomarker. Six patients were included after informed consent was given. The ATP signal was robust and repeatedly detectable in the same patient. Significant differences were seen in amide signal before and after the first cycle of chemotherapy.

2478

A compact and easy to handle set-up for high quality MR Elastography of the breast.

Jurgen H Runge¹, Jules L Nelissen^{2,3}, Larry de Graaf², Barbara Molenkamp⁴, Suzan van der Meij⁴, Klaas Nicolay², Gustav J Strijkers³, Jaap Stoker¹, Anneloes E Bohte¹, Aart J Nederveen¹, Ondrej Holub⁵, and Ralph Sinkus⁵

¹Radiology, Academic Medical Center, Amsterdam, Netherlands, ²Biomedical NMR, Eindhoven University of Technology, Eindhoven, Netherlands, ³Preclinical and Translational MRI, Academic Medical Center, Amsterdam, Netherlands, ⁴Surgery, Academic Medical Center, Amsterdam, Netherlands, ⁵Biomedical Engineering, King's College London, London, United Kingdom

Distinction between benign and malignant breast lesions remains difficult with conventional (dynamic) contrast-enhanced MRI. MR Elastography (MRE) can distinguish benign and malignant tissues based on their viscoelastic properties but breast MRE has not found widespread use in daily clinical practice, because of the complex equipment required and cumbersome data acquisition. Here we present a compact, easy to handle breast MRE set-up that allows the acquisition of high quality, artefact-free MRE data. This set-up was designed, built and tested at two different institutions in volunteers and a patient.

2479

Dual-Parametric MR Imaging with Read-Out Segmented Diffusion-Weighted and High Temporal Resolution Dynamic Contrast-Enhanced Imaging Improves the Differentiation of Malignant and Benign Breast Lesions

Bin Wu^{1,2}, Yanqiong Chen², Hui Liu³, Xu Yan³, Caixia Fu⁴, Dan Wang¹, Jian Mao², Dominik Nickel⁵, Berthold Kiefer⁵, Yajia Gu², and Weijun Peng²

¹Radiology, Shanghai Proton and Heavy Ion Center, Fudan University Cancer Center, Shanghai, China, People's Republic of, ²Radiology, Fudan University Shanghai Cancer Center, Shanghai, China, People's Republic of, ³NEA MR Collaboration, Siemens Ltd, Shanghai, China, People's Republic of, ⁴Siemens Shenzhen Magnetic Resonance Ltd, Shenzhen, China, People's Republic of, ⁵Siemens Healthcare GmbH, Erlangen, Germany, Forchheim, Germany

We investigated the clinical value of a dual-parameter classification method in differentiating benign and malignant breast lesions using readout-segmented diffusion-weighted imaging (RS-DWI) and quantitative dynamic contrast-enhanced magnetic resonance imaging (DCE-MRI), and found they correlated with histological results.

2480

Proton Density Water Fraction as a Measurement of Breast Fibroglandular Tissue Volume and Concentration
Roberta M Strigle^{1,2,3}, Leah Henze Bancroft², Diego Hernando¹, and Scott B Reeder^{1,2,3,4,5,6}

¹Radiology, University of Wisconsin, Madison, WI, United States, ²Medical Physics, University of Wisconsin, Madison, WI, United States, ³Carbone Cancer Center, University of Wisconsin, Madison, WI, United States, ⁴Biomedical Engineering, University of Wisconsin, Madison, WI, United States, ⁵Emergency Medicine, University of Wisconsin, Madison, WI, United States, ⁶Medicine, University of Wisconsin, Madison, WI, United States

Elevated breast density confers an increased risk for breast cancer. Accurate and precise measurement of the amount of fibroglandular breast tissue has potential to serve as a quantitative imaging biomarker of risk for the development of breast cancer. In this work we introduce novel, confounder corrected chemical-shift encoded (CSE)-MRI techniques to measure the proton density water fraction (PDWF). Estimation of PDWF with CSE-MRI addresses potential confounders that negatively impact accuracy, precision, and reproducibility, enabling protocol independent quantification of the volume and concentration of fibroglandular tissue in the breast.

2481

Utility of semi-quantitative analysis of initial enhancement using TWIST-VIBE in the diagnosis of breast lesions
Mariko Goto¹, Koji Sakai¹, Kayu Takezawa¹, Hiroshi Imai², Elisabeth Weiland³, and Kei Yamada¹

¹Radiology, Kyoto Prefectural University of Medicine, Kyoto, Japan, ²Siemens Japan K.K., Tokyo, Japan, ³Siemens Healthcare GmbH, Erlangen, Germany

The prototype TWIST-VIBE sequence improves the temporal resolution of breast MRI while preserving spatial resolution. High-temporal resolution TWIST-VIBE was performed during the initial enhancement phase and high-spatial resolution routine DCE MRI in a single session, and whether the additional information of initial enhancement analysis using TWIST-VIBE improved the diagnostic accuracy of breast MRI was evaluated. The combination of BI-RADS and new parameters of initial enhancement (MS and TTE) calculated from TWIST-VIBE has the potential to increase the specificity of breast MRI and may be useful as additional information to determine the need for biopsy.

2482

Application of Histogram Analysis of Pharmacokinetic Parameters in Dynamic Contrast-Enhanced MR Imaging of Breast lesions with CAIPIRINHA-Dixon-TWIST-VIBE Technique
Yiqi Hu¹, Tao Ai¹, and Liming Xia¹

¹Tongji Hospital, department of radiology, Wuhan, China, People's Republic of

The overlap of pharmacokinetic parameters values exists between benign and malignant lesions. Most previous studies chose mean pharmacokinetic parameters when elevating the state of breast lesions perfusion. However, tumors are heterogeneous that are marked by microenvironmental factors and thus manifests as radiologic heterogeneity. The mean pharmacokinetic parameter values may overlook the subtle but important difference between breast lesions. Thus, the aim of our study is to investigate the feasibility of histogram analysis of pharmacokinetic parameters including Ktrans, kep, ve in breast DCE-MRI imaging and determine which metric of each pharmacokinetic parameter may best help differentiate benign from malignant lesions.

2483

Influence of fat suppression to evaluate T1 values in breast cancer: assessing the reliability of pharmacokinetic parameters
Kayu Takezawa¹, Mariko Goto¹, Koji Sakai¹, Hiroyasu Ikeno¹, Katsuhiko Nakatsukasa², Hiroshi Imai³, and Kei Yamada¹

¹Radiology, Kyoto Prefectural University of Medicine, Kyoto, Japan, ²Breast Surgery, Kyoto Prefectural University of Medicine, Kyoto, Japan, ³Siemens Japan K.K, Tokyo, Japan

The influence of fat suppression on T1 values and pharmacokinetic parameters in breast cancer were evaluated using a prototype Dixon-TWIST-VIBE technique. We measured T1 values of breast cancers on both fat suppression and not-fat suppression data sets and we calculated K^{trans} values using same ROI that employed on T1 value measurements. Our result suggests that the fat suppression might influence T1 values in breast cancer, and reliability of K^{trans} seemed inappropriate as an absolute value. On the other hand, the assessment of intra-patient K^{trans} change might be feasible.

2484

Rapid T1 and T2 Measurements of Breast Tissue at 3T using Multi-TR, Multi-TE Spectroscopy
Leah C Henze Bancroft¹, Roberta M Strigel^{1,2,3}, Gavin Hamilton⁴, Scott B Reeder^{1,2,5,6,7}, and Diego Hernando²

¹Medical Physics, University of Wisconsin-Madison, Madison, WI, United States, ²Radiology, University of Wisconsin-Madison, Madison, WI, United States, ³University of Wisconsin Carbone Cancer Center, University of Wisconsin-Madison, Madison, WI, United States, ⁴Radiology, University of California, San Diego, San Diego, CA, United States, ⁵Medicine, University of Wisconsin-Madison, Madison, WI, United States, ⁶Biomedical Engineering, University of Wisconsin-Madison, Madison, WI, United States, ⁷Emergency Medicine, University of Wisconsin-Madison, Madison, WI, United States

The highly heterogeneous distribution of fat and fibroglandular tissue in the breast makes obtaining accurate measures of T1 and T2 relaxation times difficult. Here, a rapid, multi echo, multi TR spectroscopy sequence is used to measure the T1 and T2 relaxation times of fat and fibroglandular tissue in the breast at 3T. Partial voluming effects are accounted for through accurate measurement of the proton density fat fraction.

2485

3D MRI Breast Density Change in Women with Hormonal Positive Breast Cancer Following Adjuvant Hormonal Therapy
Yoon Jung Choi¹, Jeon-Hor Chen^{2,3}, Shunshan Li², Po-Han Chen⁴, Pei-Yu Liu⁴, Inyoung Youn¹, and Min-Ying Su²

¹Department of Radiology, Kangbuk Samsung Hospital, Seoul, Korea, Republic of, ²Center for Functional Onco-Imaging, Department of Radiological Sciences, University of California Irvine, Irvine, CA, United States, ³Department of Radiology, Eda Hospital and I-Shou University, Kaohsiung, Taiwan, ⁴Department of Medical Imaging, China Medical University, Taichung, Taiwan

Hormonal regimens may affect breast tissue with the change of breast volume or composition. This study was to apply a well-established breast and fibroglandular tissue segmentation method to analyze the density changes in patients receiving adjuvant hormonal therapy. The results showed that pre-menopausal women had a higher density reduction, presumably due to their more abundant fibroglandular tissues that can be decreased, but a high variation was observed. The density reduction assessed by 3D MRI may be used as a surrogate marker to correlate with metabolic genotyping, and further used in combination to better predict patient's prognosis.

2486

Does the Initial Enhancement Ratio (IER) Predict which Malignancies are Biologically Significant on a Pre-operative Breast MRI?
Neeti R Bagadiya¹, Laura Heacock¹, Yiming Gao¹, Meghan Jardon¹, Samantha Heller¹, and Linda Moy¹

¹Radiology, New York University, New York, NY, United States

Breast MRI allows preoperative identification of patients who may have extensive disease at presentation and allows for appropriate surgical planning and treatment. Despite the high sensitivity of MRI, the role of preoperative surgical staging of breast cancer patients is controversial. There is concern that the high false positive rates of breast MRI lead to additional biopsy procedures and surgeries [1,2].

Abbreviated breast MRI (AB-MR), defined as the first post-contrast scan, has been proposed as an exam that may have a higher specificity compared to conventional breast MRI [3,4]. Two recent studies show that AB-MR has a high PPV for and may preferentially selects for biologically significant tumors, thereby reducing overdiagnosis and overtreatment. The concept of a biologically significant breast cancer has not been defined. We hypothesized that since invasive carcinomas usually demonstrate fast initial uptake of contrast, a threshold of enhancement as determined by initial enhancement ratio (IER) may be associated with the identification of biologically significant breast cancers [5]. We evaluated a cohort of women with known cancer who underwent MRI guided needle localization (MRNL) for a finding that was suspicious for additional disease. We examined whether there was an association with the IER and the likelihood that it would be detected on AB-MR exam. Using Dynacad software we retrospectively reviewed the IER of MRI detected synchronous cancers that underwent MRNL. We found there is a significant correlation between invasive cancers and IER that can aid in the detection of biologically significant synchronous cancers on MRI.

Traditional Poster

Prostate Cancer

Exhibition Hall

Thursday, May 12, 2016: 10:30 - 12:30

2487

MR measurements of luminal water in prostate gland

Shirin Sabouri¹, Ladan Fazli^{2,3}, Silvia Chang^{4,5}, Richard Savdie³, Edward Jones⁶, Larry Goldenberg^{2,3}, and Piotr Kozlowski^{2,3,4,7}

¹*Physics and Astronomy, University of British Columbia, Vancouver, BC, Canada*, ²*Vancouver Prostate Centre, Vancouver, BC, Canada*, ³*Urologic Sciences, University of British Columbia, Vancouver, BC, Canada*, ⁴*Radiology, University of British Columbia, Vancouver, BC, Canada*, ⁵*Vancouver General Hospital, Vancouver, BC, Canada*, ⁶*Pathology, Vancouver General Hospital, Vancouver, BC, Canada*, ⁷*UBC MRI Research Center, Vancouver, BC, Canada*

Measurement of relative amount of lumen in prostatic tissue can provide useful information for diagnosing of many prostatic diseases. Using multi-exponential T₂ mapping, the fractional volume of the luminal space, or so called luminal water fraction (LWF), in the prostatic tissue can be determined. In order to use the LWF as a proportional representative of the true percentage of lumen, it is important to investigate the correlation between the two parameters. We have acquired and analyzed MR images of 10 subjects, and found a significant correlation between the LWF and the percentages of lumen in tissue.

2488

Textural analysis of multiparametric MRI detects transition zone prostate cancer

Harbir Singh Sidhu¹, Salvatore Benigno¹, Balaji Ganeshan², Nikos Dikaios¹, Edward William Johnston¹, Clare Allen³, Alex Kirkham³, Ashley M Groves², Hashim Uddin Ahmed⁴, Mark Emberton⁴, Stuart A Taylor¹, Steve Halligan¹, and Shonit Punwani¹

¹*Centre for Medical Imaging, University College London, London, United Kingdom*, ²*Institute of Nuclear Medicine, University College London, London, United Kingdom*, ³*Radiology, University College London Hospital, London, United Kingdom*, ⁴*Research Department of Urology, University College London, London, United Kingdom*

Transition zone (TZ) prostatic tumors are more difficult for radiologists to detect on multiparametric MRI compared with peripheral zone tumors and are systematically undersampled by conventional transrectal ultrasound biopsy.

Assessment of whole TZ heterogeneity by spatially filtered textural analysis of routinely acquired multiparametric MRI images can discriminate significant tumor without the need to predefine tumors and at no additional burden to patients. TZ containing significant tumors show reduced entropy on coarsely filtered early post contrast T1 and T2 weighted images and reduced kurtosis unfiltered ADC values.

In the future, this could augment radiological interpretation and facilitate computer-aided diagnosis.

2489

Luminal water imaging: a novel MRI method for prostate cancer diagnosis

Shirin Sabouri¹, Silvia Chang^{2,3}, Richard Savdie⁴, Jing Zhang⁵, Edward Jones⁶, Larry Goldenberg^{4,7}, and Piotr Kozlowski^{2,4,5,7}

¹*Physics and Astronomy, University of British Columbia, Vancouver, BC, Canada*, ²*Radiology, University of British Columbia, Vancouver, BC, Canada*, ³*Vancouver General Hospital, Vancouver, BC, Canada*, ⁴*Urologic Sciences, University of British Columbia, Vancouver, BC, Canada*, ⁵*UBC MRI Research Center, Vancouver, BC, Canada*, ⁶*Pathology, Vancouver General Hospital, Vancouver, BC, Canada*, ⁷*Vancouver Prostate Centre, Vancouver, BC, Canada*

MR multi-exponential T₂ mapping can be used for extracting valuable information about tissue composition in prostate. Using this technique, the fractional volume of the luminal space in the prostatic tissue can be determined. Since tissue composition and the amounts of lumen differ between normal and cancerous tissues, this technique can be applied for detection of prostatic tumors. We have investigated the suitability of using MR multi-exponential T₂ mapping for detection and staging of prostate cancer. We have acquired and analyzed MR images of 11 patients, and concluded that this technique is highly sensitive and specific in detection of prostatic tumors.

2490

Comparison of PIRADS v1.0 and v2.0 for MRI detection of prostate cancer: preliminary findings in patients with whole-mount histological workup

Josephin Otto¹, Alexander Schaudinn¹, Simone Mucha¹, Nicolas Linder¹, Nikita Gornov¹, Jens-Uwe Stolzenburg², Lars-Christian Horn³, Thomas Kahn¹, Michael Moche¹, and Harald Busse¹

Multiparametric MRI of the prostate has substantially improved the detection of clinically significant prostate cancer (PCa) and the confidence in benign and insignificant findings. The recent v2.0 update of the Prostate Imaging Reporting and Data System (PIRADS) has replaced the sum of individual MRI sequence scores (1-15 or 1-20) with a zone-dependent, dominant MRI sequence (DWI in the peripheral and T2W in the transition zone) with an overall score from 1-5. The aim of this preliminary study was the blinded comparison of both versions for the detection of PCa on the same patients using whole-mount histological workup as gold standard.

2491

B1+ Inhomogeneity Correction for Estimation of Pharmacokinetic Parameters through an Approximation Approach
Xinran Zhong^{1,2}, Novena Rangwala¹, Steven Raman¹, Daniel Margolis¹, Holden Wu^{1,2}, and Kyunghyun Sung^{1,2}

¹Radiological Sciences, University of California, Los Angeles, Los Angeles, CA, United States, ²Physics and Biology in Medicine, University of California, Los Angeles, Los Angeles, CA, United States

A simplified version of the B₁⁺ correction method using an approximation model was proposed for estimation of pharmacokinetic modeling parameters. The proposed method was evaluated in both simulation and *in vivo* DCE-MRI data, and was applied to DCE-MRI with 63 suspicious lesions from two MRI systems to investigate B₁⁺ induced errors in K^{trans}. Significant difference of estimated K^{trans} distributions was observed between two systems, showing it's necessary to perform B₁⁺ correction for DCE-MRI analysis between systems.

2492

Rapid pre-biopsy MRI in patients with a clinical suspicion of prostate cancer: results of a controlled prospective registered IMPROD-trial
Ivan Jambor¹, Peter Boström², Pekka Taimen¹, Esa Kähkönen², Markku Kallajoki², Tommi Kauko¹, Ileana Montoya¹, Otto Ettala², Harri Merisaari¹, Kari Syvänen², and Hannu Juhani Aronen¹

¹University of Turku, Turku, Finland, ²Turku University Hospital, Turku, Finland

In this prospective single institution registered clinical trial we aimed to evaluate the role of rapid pre-biopsy prostate MRI consisting of T2-weighted imaging and DWI, no endorectal coil, no iv contrast. The primary end point was the diagnostic accuracy of the models incorporating clinical variables, PSA, and MRI findings. In total 175 patients were enrolled and 161 were included in final analyses. Rapid pre-biopsy prostate MRI was shown to be an accurate tool for the management of patients with a clinical suspicion of prostate cancer.

2493

A Fast Method for Simultaneous ADC and T2 Mapping Using Spin Echo EPI Sequence
Minxiong Zhou^{1,2}, Xu Yan³, Ming Deng⁴, Zan Ke⁴, Xiangde Min⁴, Caixia Fu⁵, Hui Liu³, Alto Stemmer⁶, and Liang Wang⁴

¹Shanghai University of Medicine & Health Sciences, Shanghai, China, People's Republic of, ²Department of Radiology, Ruijin Hospital, Shanghai Jiao Tong University of Medicine, China, Shanghai, China, People's Republic of, ³MR Collaboration NE Asia, Siemens Healthcare, Shanghai, China, Shanghai, China, People's Republic of, ⁴Department of Radiology, Tongji Hospital, Tongji Medical College, Huazhong University of Science and Technology, Wuhan, China, People's Republic of, ⁵Siemens Shenzhen Magnetic Resonance Ltd, Shenzhen, China, People's Republic of, ⁶Siemens Healthcare, Erlangen, Germany

This study proposes a fast SE-EPI-based method to simultaneously acquire ADC and T2 maps using dataset with multiple b-values and multiple TE values, which can be acquired in around 3 minutes. This method was validated using a group of prostate data, showing that the T2 maps generated by the proposed method were comparable to those by a conventional TSE-based method. In addition, both T2 and ADC showed significant differences between prostate cancer and benign prostatic hyperplasia, indicating that joint usage of ADC and T2 mapping might potentially help in tumor differentiation in difficult cases in addition to ADC alone. Furthermore, this method is intrinsically free of registration and misalignment artifacts between ADC and T2 and can also be integrated with other diffusion models such as IVIM, DKI.

2494

Investigational PC-based tool for computer-aided evaluation of multiparametric MRI data of the prostate
Harald Busse¹, Josephin Otto¹, Alexander Schaudinn¹, Nicolas Linder¹, Nikita Garnov¹, Minh Do², Roman Ganzer², Jens-Uwe Stolzenburg², Lars-Christian Horn³, Thomas Kahn¹, and Michael Moche¹

¹Diagnostic and Interventional Radiology Department, Leipzig University Hospital, Leipzig, Germany, ²Urology Department, Leipzig University Hospital, Leipzig, Germany, ³Institute of Pathology, University of Leipzig, Leipzig, Germany

Multiparametric MRI (mpMRI) has been shown to improve detection, localization and characterization in patients with suspected prostate cancer (PCa). The Prostate Imaging Reporting and Data System (PIRADS) aims to establish corresponding technical parameters and simplify reporting. While computer-aided evaluation (CAE) technology is not required for prostate mpMRI interpretation, the current PIRADS guideline (v2) also states that CAE may improve workflow, provide quantitative perfusion data, enhance discrimination performance for less experienced radiologists and also facilitate integration of MRI data for some biopsy systems. The goal of this work was to demonstrate relevant features and benefits of an investigational PC-based CAE tool.

2495

Molecular Imaging and Targeting of Hypoxic Microenvironment
Balaji Krishnamachary¹, Louis Dore-Savard¹, Santosh Kumar Bharti¹, Flonne Wildes¹, Yelena Mironchik¹, and Zaver M Bhujwalla¹

¹Radiology, Johns Hopkins University, Baltimore, MD, United States

Hypoxic environments frequently exist in solid tumors and result in resistance to therapy and the evolution of a more lethal phenotype. Here, we have genetically engineered human prostate cancer PC-3 cells to report on hypoxia and also express yeast cytosine deaminase under the control of hypoxia response elements to convert the prodrug 5-fluorocytosine to 5-Fluorouracil. We also show that selective killing of hypoxic cells significantly reduces tumor growth.

2496

Texture analysis of equivocal Likert scored 3/5 peripheral zone prostate lesions on mpMRI

Aishah Azam¹, Dario Picone², Mrishta Brizmohun Appayya², Balaji Ganeshan³, Nikolaos Dikaios², Raymond Endozo³, Ashley Groves³, Hashim Ahmed⁴, and Shonit Punwani¹

¹University College London Hospital, London, United Kingdom, ²Centre for Medical Imaging, University College London, London, United Kingdom,

³Institute of Nuclear Medicine, University College London, London, United Kingdom, ⁴Division of Surgery, University College London Hospital, London, United Kingdom

Approximately 30% of multiparametricMRIs for peripheral zone prostate cancer are scored as "equivocal". Texture analysis was performed on 66 patients with "equivocal" mpMRIs using TexRad software to see if there were any particular textural differences between patients with significant cancer and non-significant disease on biopsy. We found average entropy on ADC sequences of the PZ is reduced in patients with significant cancer ($p=0.003$). Using an entropy threshold of <5.99 demonstrates a sensitivity of 0.88 and specificity is 0.60 for detecting significant PZ prostate cancer. Therefore, ADC entropy can help assess "equivocal" studies and enable selection of patients for biopsy and treatment.

2497

Histological validation of VERDICT cellularity map in a prostatectomy case

Joseph G Jacobs^{1,2}, Edward Johnston³, Alex Freeman⁴, Dominic Patel⁵, Manuel Rodriguez-Justo⁵, David Atkinson³, Shonit Punwani³, Gabriel Brostow², Daniel C Alexander^{1,2}, and Eleftheria Panagiotaki^{1,2}

¹Centre for Medical Image Computing, University College London, London, United Kingdom, ²Department of Computer Science, University College London, London, United Kingdom, ³Centre for Medical Imaging, University College London, London, United Kingdom, ⁴Department of Histopathology, University College London Hospitals NHS Foundation Trust (UCLH), University College London, London, United Kingdom,

⁵Department of Research Pathology, UCL Cancer Institute, University College London, London, United Kingdom

This study aims to validate the cellularity map produced by the VERDICT framework with histology. The VERDICT cellularity map is an indication of the number of cells present in each voxel in a diffusion-weighted MR (DW-MR) image. We attempt to validate this measure by comparing it with a cellularity map produced from a corresponding prostatectomy histological section. We find that the VERDICT cellularity map is able to differentiate between areas of tumour and benign tissue with statistical significance. This result demonstrates the potential of VERDICT as a method for non-invasive quantification of tumours.

2498

Effect of temporal resolution on diagnostic performance of DCE-MRI of the prostate

Ahmed Othman¹, Florian Falkner¹, Jakob Weiss¹, Stephan Kruck², Robert Grimm³, Petros Martirosian¹, Konstantin Nikolaou¹, and Mike Notohamiprodjo¹

¹Department of Diagnostic and Interventional Radiology, University Hospital Tübingen, Tübingen, Germany, ²Department of Urology, University Hospital Tübingen, Tübingen, Germany, ³Siemens Healthcare, Siemens Healthcare, Erlangen, Germany

In DCE-MRI of the prostate, a high temporal resolution (TR) is recommended. Nonetheless, no studies on the effects of TR on diagnostic accuracy of DCE-MRI of the prostate are available. In this study we examined the effect of TR of DCE-MRI on its diagnostic accuracy for detection of potentially malignant lesions. Our results indicate that TR>10s / timepoint leads to spurious perfusion estimates and therefore deteriorates the diagnostic accuracy for identification of potentially malignant prostate lesions.

2499

Utility of computed diffusion-weighted imaging for predicting aggressiveness of prostate cancer

Yuma Waseda¹, Soichiro Yoshida¹, Taro Takahara², Hiroshi Tanaka³, Minato Yokoyama¹, Junichiro Ishioka¹, Yoh Matsuoka¹, Noboru Numao¹, Kazutaka Saito¹, Yasuhisa Fujii¹, and Kazunori Kihara¹

¹Urology, Tokyo Medical and Dental University Graduate School, Tokyo, Japan, ²Biomedical Engineering, Tokai University School of Engineering, Kanagawa, Japan, ³Radiology, Ochanomizu Surugadai Clinic, Tokyo, Japan

Apparent diffusion coefficient (ADC) value is reported to reflect aggressiveness of prostate cancer (PCa). Yet ADC value depends on imaging protocols. To overcome the limitation, we developed a simple method to discriminate aggressive PCa using computed DWI (cDWI). We analyzed changes in cDWI signal of 51 PCa, that results from increasing b-value. At $b = 700 \text{ sec/mm}^2$, signal intensity in Gleason grade 4-5 was higher than that in normal, whereas in Gleason grade 3 cancer it was equal to or lower than that in normal (sensitivity/specificity: 97.0%/72.2%). Semi-quantitative analysis using DWI might be a simple method for discriminating aggressive PCa.

2500

Assessment of Kurtosis Model for Diffusion-Weighted Imaging and T1 Relaxation Time in the Rotating Frame of Prostate Cancer

Huiyan Li¹, Yingjie Mei², Queenie Chan³, and Yikai Xu¹

¹Department of Medical Imaging Center, Nanfang Hospital, Southern Medical University, Guangzhou, China, People's Republic of, ²Philips Healthcare, Guangzhou, China, People's Republic of, ³Philips Healthcare, HongKong, China, People's Republic of

Kurtosis model based on Gaussian distribution may be an appropriate condition in prostate. T1rho can detect slow molecular motions of tissue water or proton chemical exchange selectively, which may alter in prostate cancer (PCa). Parameters Dapp, Kapp and T1

relaxation time obtained from T1rho sequence and kurtosis model for DWI underwent statistic analysis between PCa and benign prostate hyperplasia (BPH) patients. Our study showed that Kapp and Dapp could be an effective parameter on PCa detection, while T1rho failed to differentiate PCa and BPH.

2501

To Assess Stretched-Exponential and Monoexponential Models for Diffusion-Weighted Imaging in Prostate Magnetic Resonance Imaging
Huiyan Li¹, Yingjie Mei², Queenie Chan³, and Yikai Xu¹

¹Department of Medical Imaging Center, Nanfang Hospital, Southern Medical University, Guangzhou, China, People's Republic of, ²Philips Healthcare, Guangzhou, China, People's Republic of, ³Philips Healthcare, HongKong, China, People's Republic of

DWI (diffusion weighted imaging) plays an important role in multiparametric MRI of prostate, and Stretched-exponential model (SEM) for DWI may better describe the diffusion-related signal decay than monoexponential model. Parameter DDC and α underwent statistic analysis between PCa and benign prostate hyperplasia (BPH) patients and correlation between ADC and DDC was also assessed. Our study shows SEM for DWI is feasible for prostate MRI examination. Parameter ADC and DDC had good correlations. However parameter α failed to distinguish PCa from BPH.

2502

Correlation of ADC and T2 measurements with Ki-67 labeling index in peripheral zone prostate cancer at 3.0 T
Liang Li¹, Yunfei Zha¹, Wei Gong¹, Dongjie Huang¹, and Dong Xing¹

¹Department of Radiology, Renmin Hospital of Wuhan University, Wuhan, China, People's Republic of

Assessment of tumor proliferation has been suggested as an important additional predictor of tumor behavior. The purpose of this study was to investigate the possible correlation between T2 imaging, diffusion weighted imaging (DWI), and Ki-67 labeling index in patients with newly diagnosed prostate tumor.

2503

Characterising Indeterminate Lesions (Likert 3/5) in the Peripheral Zone of the Prostate on Multi-parametric MRI
Mrishta Brizmohun Appayya¹, Harbir Singh Sidhu^{2,3}, Nikolaos Dikaios², Edward William Johnston^{2,3}, Lucy Simmons⁴, Alex Freeman⁵, Alex Kirkham³, Hashim Uddin Ahmed⁴, and Shonit Punwani^{2,3}

¹Department of Radiology, Erasme Hospital, Universite Libre de Bruxelles, Brussels, Belgium, ²Centre for Medical Imaging, University College of London, London, United Kingdom, ³Department of Radiology, University College London Hospital, London, United Kingdom, ⁴Division of Surgery and Interventional Science, University College London Hospital, London, United Kingdom, ⁵Department of Pathology, University College London Hospital, London, United Kingdom

Despite the strong potential of multi-parametric MRI (mpMRI) in prostate cancer detection, 37% of prostate mp-MRI are Likert-scored 3/5, which are indeterminate for the presence of significant cancer. In this study, we assessed whether quantitative analysis of PSA, gland volume, volume-adjusted PSA density, PIRADS rescore of Likert 3/5 lesions and qualitative prostate mpMRI descriptors could better characterise equivocal prostate lesions within the peripheral. We found that discontinuous signal changes on qualitative mpMRI were associated with clinically non-significant cancer; PIRADS rescore did not appropriately categorise patients with clinically significant cancer. Conversely, PSA density was the most statistically significant discriminator ($p=0.0040$).

2504

Using mathematical model to analyzing dynamic contrast enhanced MRI to distinguish between stromal benign prostatic hyperplasia and prostate cancer

Xiaobing Fan¹, Shiyang Wang¹, Milica Medved¹, Tatjana Antic², Serkan Guneysi¹, Gregory S Karczmar¹, and Aytekin Oto¹

¹Radiology, University of Chicago, Chicago, IL, United States, ²Pathology, University of Chicago, Chicago, IL, United States

Previous dynamic contrast enhanced (DCE) MRI studies demonstrated that stromal benign prostatic hyperplasia (BPH) nodules are difficult to differentiate from transition zone prostate cancer (PCa). Therefore, it is important to improve the accuracy of DCE-MRI to distinguish BPH from PCa. A total of 24 patients with biopsy confirmed PCa were enrolled in this study. DCE-MRI data were acquired at 3 T for a total of ~8.3 minutes. The relative signal enhancement curves for cancer (n=24) and BPH (n=19) were calculated and analyzed using an empirical mathematical model. The ratio of washout-rate/uptake-rate ($p<0.01$) was significantly smaller in BPH than in cancers.

2505

Reduced FOV arterial spin labeling based perfusion on prostate cancer
Jianxun Qu¹, Hairui Xiong², Bing Wu¹, and Junhai Zhang²

¹MR Research China, GE Healthcare, Beijing, China, People's Republic of, ²Department of Radiology, Huashan Hospital Affiliated to Fudan University, Shanghai, China, People's Republic of

In body perfusion measurement with arterial spin labeling technique, single shot acquisition was usually used, which suffers from susceptibility induced distortion. A straightforward way was to reduce readout echo train, which however lead to lower spatial resolution. In this work, we performed flow sensitive alternating inversion recovery (FAIR) with reduced FOV excitation to shorten echo train length while maintaining spatial resolution in prostate cancer perfusion imaging.

2506

Esophageal carcinoma: ex vivo high resolution MR imaging study compare with histopathological findings
Yi Wei^{1,2}, Shao-Cheng Zhu^{1,2}, Sen Wu^{1,2}, Da-Peng Shi^{1,2}, and Dan-Dan Zheng³

¹*Radiology, Zhengzhou University People's Hospital, Zhengzhou, China, People's Republic of*, ²*Henan Provincial People's Hospital, Zhengzhou, China, People's Republic of*, ³*GE Healthcare, MR Research China, Beijing, China, People's Republic of*

The prognosis of patients with esophageal carcinoma is heavily dependent on the histopathological staging of the carcinoma. However, the common examination modalities are extremely difficult to identify the preoperative staging. Magnetic resonance imaging (MRI) was reported to evaluate the esophageal layers invasion in vitro and demonstrated that high-resolution T2-weighted imaging can clearly depict 8 layers of the esophagus which can provide essential information of the carcinoma invasion. However, former studies were mostly carried on ultra-high-field scanner after formalin fixed within 24 hours ex vivo, which might cause the signal changes of the esophageal layers and carcinoma. In this study, an ex vivo experiment was conducted on 3.0T clinical scanner to prospectively establish the MRI signal characteristics of the normal esophageal wall without formalin fixation and to assess the diagnostic accuracy of high-resolution MR scanner for depicting the depth of esophageal wall invasion by making the correspondence with certain histopathological slice.

2507

In vivo Enzyme Activity Measurements with Hyperpolarized C13 Pyruvate in a Transgenic Tumor Mouse Model
Zihan Zhu^{1,2}, Peder E.Z. Larson¹, Hsin-Yu Chen^{1,2}, Peter J Shin¹, Robert A Bok¹, John Kurhanewicz¹, and Daniel B Vigneron¹

¹*Department of Radiology and Biomedical Imaging, University of California, San Francisco, San Francisco, CA, United States*, ²*UC Berkeley-UCSF Graduate Program in Bioengineering, UC Berkeley and UCSF, San Francisco, CA, United States*

Hyperpolarized ¹³C MRI has been an emerging tool for *in vivo* enzymatic activity assessment. In this study, two dynamic hyperpolarized ¹³C sequences were compared in the same animal for two sequential injections in a transgenic prostate tumor murine model. The results suggested that the dynamic fitted metabolic conversion rates acquired from the two approaches were highly correlated.

2508

Investigating Prostate Cancer Aggressiveness with Hyperpolarized 13C-Urea + 13C-Pyruvate Perfusion & Metabolic Imaging of Transgenic Primary and Metastatic Tumors
Hsin-Yu Chen¹, Peder E.Z. Larson^{1,2}, Robert A. Bok², Cornelius von Morze², Renuka Sriram², Romelyn Delos Santos², Justin Delos Santos², Jeremy W. Gordon², John Kurhanewicz^{1,2}, and Daniel B. Vigneron^{1,2}

¹*Graduate Program in Bioengineering, UCSF and UC Berkeley, University of California, San Francisco, San Francisco, CA, United States*,
²*Department of Radiology and Biomedical Imaging, University of California, San Francisco, San Francisco, CA, United States*

An unmet clinical need facing the management of prostate cancer is an accurate method for distinguishing aggressive prostate cancer from indolent disease. The project investigated the use of hyperpolarized (HP) ¹³C 3D CS-EPSI imaging of co-polarized ¹³C-urea + ¹³C-pyruvate to provide this distinction by simultaneously measuring metabolism and perfusion. Significantly higher pyruvate-to-lactate conversion rates, k_{PL} , ($P<0.00001$) and significantly ($P<0.004$) lower urea perfusion were detected in high-grade tumors compared to low-grade tumor. Lymph-node metastases demonstrated high metabolic conversion ($P>0.8$) and urea perfusion not significantly ($P>0.4$) different than high-grade primary tumor.

2509

The effects of noise on pharmacokinetic analysis of the apparent conversion of hyperpolarized pyruvate
Changyu SUN¹, Christopher M. Walker¹, and James A. Bankson¹

¹*Department of Imaging Physics, The University of Texas MD Anderson Cancer Center, Houston, TX, United States*

Effects of noise and bias in signal and different parameters in the kinetic model affects the reproducibility of the estimation of the apparent rate of conversion of hyperpolarized (HP) pyruvate into HP lactate (k_{PL}). The purpose of this study is to investigate the effect of signal to noise ratio for a pharmacokinetic model with two chemical and two physical compartments in estimating k_{PL} . We examine the k_{PL} estimated using the kinetic model by the simulated HP data with a variety of SNRs (10–50) by 95% confidence interval, mean and standard deviation. The results demonstrate that SNR affects the reproducibility of the estimation of k_{PL} by kinetic analysis and the reproducibility of k_{PL} estimated decreases quickly below an SNR threshold of ~25.

2510

Assessment of cHSA-PEO (2000)16-Gd in breast cancer xenografts on chicken chorioallantoic membrane @ 11.7T
Zhi Zuo^{1,2,3}, Tatiana Syrovets⁴, Tao Wang⁵, Yu-zhou Wu⁵, Felicitas Genze⁴, Alireza Abaei³, Ina Vernikouskaya², Wei-na Liu⁵